Expanding the scope of responsive polymeric nanostructures

By

Kay Elizabeth Beatrice Doncom

Submitted for the degree of Doctor of Philosophy

Department of Chemistry

March 2014

For James

Table of Contents

Chapter Two

Acknowledgements

Firstly I'd like to thank Rachel, my supervisor, for giving me the opportunity to work in her research group and whose supervision and support has been critical in the last three and a half years. Thank you for letting me follow my own ideas, and for giving me a prod in the right direction when I got a little lost. I am also grateful to the University of Warwick Postgraduate Research Scholarship for funding.

A massive thanks also goes to my parents, who have always supported and encouraged me. Now you can read this and find out exactly what it is I've been doing the last few years!

To the O'Reilly group, past and present, thanks for making each day fun and entertaining, and for all your advice.

A special thank you goes to Helen. You managed to make me laugh pretty much every day! Thank you for all the help you have given me with the chemistry, but particularly your constant encouragement, enthusiasm and supply of sweets have been invaluable over the course of this PhD and especially the last few months.

To my friends outside the chemistry bubble, thank you for your positivity and for helping me remember it's not the end of the world if an experiment fails.

Finally my biggest thank you is to James. Without you I am not sure I'd have stayed the course. You commiserated with me when things didn't go as planned, and celebrated when they went better than expected. You didn't complain (much) about having to do all the housework and you were always there when I got home. For this, and so much more, Thank You.

Declaration

This thesis is submitted to the University of Warwick in support of my application for the degree of Doctor of Philosophy. It has been composed by myself and has not been submitted in any previous application for any degree. The work presented (including data generated and data analysis) was carried out by the author except in the cases outlined below:

- Some previous work carried out by Dr Claire Hansell during her PhD is included in Chapter Three, section 3.2.1.
- The SAXS characterisation in Chapter Five was acquired and analysed by Dr Anaïs Pitto-Barry from Professor Rachel O'Reilly's group of the University of Warwick.

List of Publications

pH-switchable polymer nanostructures for controlled release. K. E. B. Doncom, C. F. Hansell, P. Theato and R. K. O'Reilly, *Polym. Chem*, 2012, **3**, 3007-3015

Synthesis of responsive polymers by RAFT polymerisation, and their self-assembly into morphology switching nanostrcutures, K. E. B. Doncom, C. F. Hansell, P. Theato and R. K. O'Reilly, *Abstracts of Papers, 245th ACS National Meeting and Exposition, New Orleans*, **2013**, PMSE-539

Tuning the micelle to unimer transition temperature of polysulfobetaines: complimentary SAXS and LS, K. E. B. Doncom, A. Pitto-Barry, H. Willcock, A. Lu, N. Kirby and Rachel K. O'Reilly, *Manuscript in preparation*

The synthesis and self-assembly of a multi-responsive triblock copolymer, K. E. B. Doncom, H. Willcock, R. K. O'Reilly, *Journal of Polym. Sci. Part A - submitted*

Abstract

This thesis focuses on expanding the scope of self-assembled polymeric nanostructures and their morphology transitions in response to a variety of applied stimuli.

Chapter One gives an introduction to the main concepts and techniques used throughout the thesis.

Chapter Two utilises a pH-deprotectable protected acid, incorporated into a diblock copolymer, in order to induce a morphology change in response to a change in pH. In addition, the effect of the hydrophilicity of the end group upon self-assembly is investigated.

Chapter Three investigates a reversible pH-responsive system to induce a reversible vesicle to micelle morphology transition. This was achieved *via* the synthesis of an activated ester polymeric scaffold and the post-polymerisation introduction of backbone and end group functionality. Different end groups are investigated, along with the effect the molecular weight of the polymer has on the speed of transition. In addition, the controlled release of a hydrophilic payload is demonstrated.

Chapter Four focuses on the incorporation of hydrophilic blocks, hydrophobic blocks or a combination of the two into sulfobetaine methacrylate containing polymers. The synthesis of these polymers by RAFT polymerisation is discussed and the polymers are thoroughly characterised by ^{1}H NMR spectroscopy, SEC, SLS and multi-angle DLS.

Chapter Five investigates the self-assembly and thermo-responsive behaviour of the polymers synthesised in Chapter Four. The subtle differences between the polymers and the effect of these differences on the responsive behaviour are highlighted. In addition the self-assembly of a thermo- pH- and CO_2- triply-responsive triblock copolymer is discussed.

Chapter Six investigates the synthesis and polymerisation behaviour of a sulfobetaine acrylate, in comparison to the sulfobetaine methacrylate observed in Chapter Four.

Abbreviations

δ	Chemical shift
θ	Scattering angle
λ	wavelength
λ_{em}	emission wavelength
λ_{ex}	excitation wavelength
τ	Relaxation time
τ_{fast}	Relaxation time for the fast mode
A_2	Second virial coefficient
ACVA	Azobis(4-cyanovaleric acid)
AIBN	2, 2'-Azobis(2-methylpropionitrile)
ATRP	Atom Transfer Radical Polymerisation
BCB	Brilliant cresyl blue
br	Broad (^{1} H NMR)
c	Concentration
cryo-TEM	Cryogenic transmission electron microscopy
CTA	Chain Transfer Agent
d	Doublet
D_{av}	Average diameter
DCM	Dichloromethane
dd	Doublet of doublets
DDMAT	2-(dodecylthiocarbonylthioylthio)-2-methylpropionic acid
DEAEMA	*N, N*-(diethylamino) ethyl methacrylate
DEAEMA	*N, N*-diethylacrylamide
DEGMA	Diethyleneglycol monomethyl ether methacrylate
D_h	Hydrodynamic diameter

DHP	Dihydropyran
DIPEA	*N, N*-(diisopropylamino) ethyl acrylate
DIPEMA	*N, N*-(diisopropylamino) ethyl methacrylate
DLS	Dynamic light scattering
$Đ_M$	dispersity
DMA	Dimethylacrylamide
DMAEMA	*N, N*-(dimethylamino) ethyl methacrylate
DMAPS	2-(methacryloyloxy)ethyl dimethyl-(3-sulfopropyl)ammonium hydroxide
DMF	*N, N*-dimethylformamide
DMSO	Dimethyl sulfoxide
dn/dc	Refractive index increment
DNA	Deoxyribonulceic acid
DP	Degree of polymerisation
D_t	Translational diffusion coefficient
*D*t, app	Apparent translational diffusion coefficient
equiv.	Equivalents
ESI	Electrospray ionisation
eV	Electron volts
FT-IR	Fourier transform infrared
GO	Graphene oxide
GTP	Group Transfer Polymerisation
HEMA	Hydroxymethylmethacrylate
HFIP	Hexafluroisopropanol
HRMS	High resolution mass spectrometry
I	Average scattered intensity
J	Coupling constant

K	Constant
k_B	Boltzmann constant
KPS	Potassium persulfate
LCST	Lower critical solution temperature
LPO	Lauroyl peroxide
m	Multiplet
m/z	Mass to charge ratio
MA	Methyl acrylate
MADIX	Macromolecular Design by Interchange of Xanthates
M_n	Number average molecular weight
mol%	Mole percent
M_w	Weight average molecular weight
MW	Molecular weight
MWCO	Molecular weight cut off
n	Refractive index
N_A	Avogadros number
NAM	*N*-acryloylmorpholoine
NIPAM	*N*-isopropylacrylamide
NMP	Nitroxide-Mediated Polymerisation
NMR	Nuclear Magnetic Resonance
p	Packing parameter
PAA	Poly(acrylic acid)
PEG	Poly(ethylene glycol) mono methylether acrylate
PEGMA	Poly(ethylene glycol) mono methylether methacrylate
PEO	Poly(ethylene oxide)
PFP	Pentafluorophenyl
PFPA	Pentafluorophenyl acrylate

PFPMA	Pentafluorophenyl methacrylate
PFPVB	Pentafluorophenyl 4-vinylbenzoate
pK_a	Acid dissociation constant
PLA	Polylactide
PMA	Poly(methyl acrylate)
PMMA	Poly(methyl methacrylate)
PNIPAM	Poly(N-isopropylacrylamide)
ppm	Parts per million
PS	Polystyrene
q	Quartet
q	Scattering vector
RAFT	Reversible Addition-Fragmentation chain Transfer
RDR	Reversible Deactivation Radical
R_g	Radius of gyration
R_h	Hydrodynamic radius
RI	Refractive index
R_θ	Rayleigh ratio
$R_{\theta, fast}$	Rayleigh ratio for the fast mode
s	Singlet
SAXS	Small Angle X-ray Scattering
SBA	2-(acryloyloxy) ethyl dimethyl-(3-sulfopropyl) ammonium hydroxide
SEC	Size exclusion chromatography
SLS	Static Light Scattering
t	Triplet
T	Temperature
t-BuA	*Tert*-butyl acrylate
TEA	Triethyl amine

TEGA	Triethylene glycol monomethyl ether acrylate
TEM	Transmission electron microscopy
TFA	Trifluoroacetic acid
T_g	Glass transition temperature
THF	Tetrahydrofuran
THPA	Tetrahydropyranyl acrylate
UA	Uranyl acetate
UCST	Upper critical solution temperature

Chapter One

Introduction

1.1 Polymers

Since the synthesis of the first synthetic polymer, Bakelite, just over 100 years ago, and the first explanation of the structure of polymers published by Staudinger a decade later,[1] academic and industrial interest in Polymer Science has greatly expanded. The scarcity of certain materials, such as silk, during times of conflict hastened the research into synthetic replacements, for example the work of Carothers *et al*. at DuPont into the development of Nylon. Since then polymers have become part of our everyday lives. The vast majority are synthesised for their bulk properties; it is only relatively more recently that achieving control over polymerisations has been investigated,[2] leading to the formation of a wide range of new polymer architectures and sophisticated uses on the nanoscale.

1.2 Radical Polymerisation

Radical polymerisation is a useful technique for the production of polymers, due to the requirement of relatively mild conditions and tolerance towards monomer functionality and trace impurities. In traditional polymerisation techniques, such as free radical polymerisation, all stages of the polymerisation occur at the same time,[3] thus chains formed early in the reaction when monomer concentration is high will result in polymers of high molecular weight. As the reaction proceeds the decreasing monomer concentration means chains formed later in the polymerisation will be of lower molecular weight. Thus, a free radical polymerisation proceeds with little control, resulting in polymers with broad dispersities and unpredictable molecular weights. Another disadvantage of conventional free radical polymerisation is the inability to produce block copolymers as there are no living radicals left at the end of the polymerisation.[3] Polymers made by free radical polymerisation are therefore ill-suited for use in advanced material applications.

1.3 Living Radical Polymerisation

A living polymerisation is one from which chain termination and chain transfer reactions are eliminated.[4] The experimental criteria for whether a polymerisation can be considered living are as follows:[5, 6]

1. The rate of initiation is fast compared to the rate of propagation, and termination is prevented.
2. The number average molecular weight (M_n) and the number average degree of polymerisation (DP) have a linear relationship with conversion.
3. The polymerisation proceeds until all monomer is consumed and further addition of monomer results in further polymerisation.
4. The number of growing polymer chains is constant throughout the polymerisation and is independent of conversion.
5. Polymers with predictable molecular weights can be achieved by controlling the monomer to initiator ratio.
6. Polymers with narrow molecular weight distributions ($Đ_M$) are produced.
7. Sequential addition of monomers can produce block copolymers, meaning the chain end remains living after polymerisation.
8. Chain-end functionalised polymers are produced in quantitative yield.

True living polymerisation processes usually require stringent reaction conditions such as the use of ultra-pure and dry solvents and have little tolerance towards impurities.[7] These living polymerisation systems also suffer from intolerance towards certain monomer functionalities, limiting their use in the preparation of a wider range of functional block copolymers. Therefore the ability to impart living or controlled characteristics upon radical polymerisation is of great research interest.

1.4 Reversible Deactivation Radical Polymerisation

Reversible deactivation radical (RDR) polymerisation techniques, previously referred to as controlled radical polymerisation,[8] fulfil most of the conditions required for living polymerisation systems (see section 1.3) but have the advantage that they are synthetically easier to set up and have higher tolerance to functional groups in the monomer and impurities in the system.[9] The most common of these RDR polymerisation techniques are Atom Transfer Radical Polymerisation (ATRP),[10, 11] Nitroxide-Mediated Polymerisation (NMP)[9,12] and Reversible Addition-Fragmentation chain Transfer polymerisation (RAFT).[9, 10, 13, 14] All three of these processes are based on the concept of a single species mediating all parts of the polymerisation; *i.e*. initiation, chain transfer and termination, based on the iniferter concept of Otsu *et al.* over 30 years ago.[15, 16] Matyjaszewski *et al*. first introduced the concept of degenerative transfer in 1995.[11] These techniques impart control over the polymerisation through a reversible activation process that produces a small number of active propagating chains and a large number of dormant chains, meaning the polymer chains all grow at the same rate.[3, 17] This allows for the formation of polymers of controlled molecular weight, with narrow dispersities ($Đ_M$) and exhibiting pseudo-living characteristics, such as the ability to chain extend to form block copolymers.[12] It should be noted that termination reactions are not absent from RDR polymerisation techniques.

1.4.1 Reversible Addition-Fragmentation chain Transfer (RAFT)

Of the RDR polymerisation methods, RAFT has perhaps proved to be the most robust and versatile route and is applicable to the greatest variety of monomer classes,[9, 14] under a variety of conditions, including in aqueous media.[18-22] RAFT polymerisation produces polymers which have predictable molecular weights and narrow dispersities, usually $Đ_M \leq 1.2$.[23]

The CSIRO group in Australia first reported RAFT polymerisation in early 1998[14] and researchers in France developed a similar polymerisation technique later that year.[24] In France the polymerisation system was called Macromolecular Design by Interchange of

Xanthates (MADIX). MADIX and RAFT proceed *via* the same reaction mechanism but MADIX is mediated only by xanthates, whereas RAFT can be mediated by more general thiocarbonylthio chain transfer agents. Therefore the term RAFT is most commonly used to describe these polymerisations.

1.4.1.1 The mechanism of RAFT polymerisation

The generally accepted mechanism proposed for RAFT is shown in Scheme 1.1.[9, 25] The mechanism is similar to that of a free radical polymerisation but includes two important steps, pre-equilibrium (chain transfer) and the main equilibrium (chain equilibrium), mediated by the chain transfer agent. The presence of the chain transfer agent results in many of the chains remaining dormant, meaning there are only a small number of actively growing polymer chains. This minimises termination reactions and therefore the growth of each polymer chain remains well-controlled, retaining the α- and ω-end group functionalities present in the chain transfer agent.

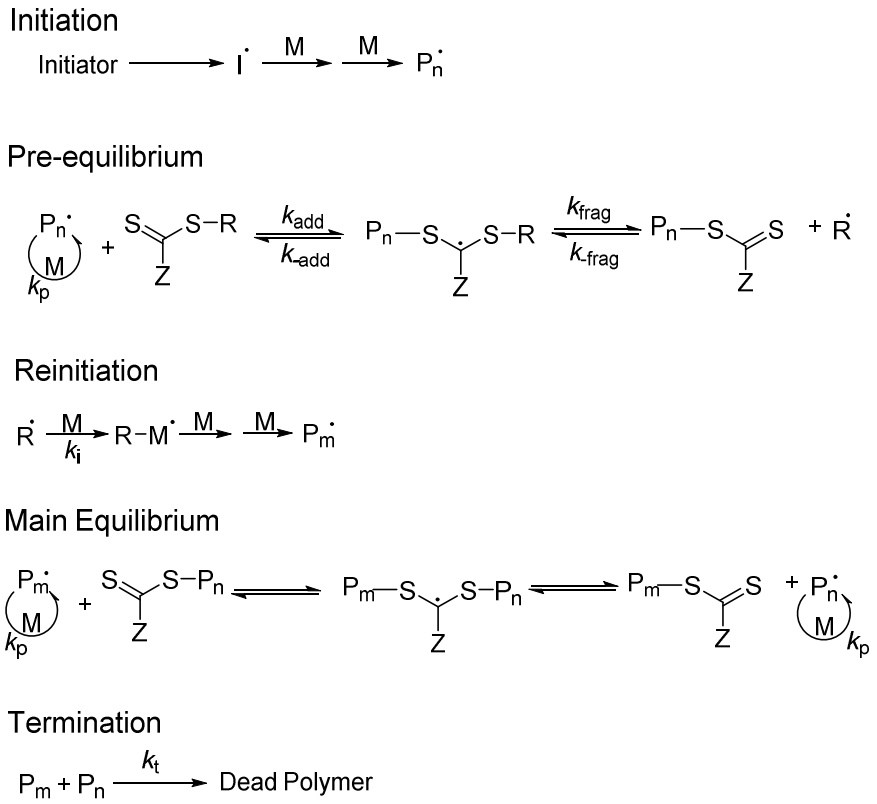

Scheme 1.1: The general mechanism of RAFT polymerisation[9]

The mechanism of RAFT polymerisation begins with initiation of an external free radical source, typically by the thermal decomposition of diazo compounds[23] (see Scheme 1.1). The radicals produced polymerise a small number of monomers units. These oligomeric radicals then react with the CTA (pre-equilibrium), ideally before chain propagation occurs. The intermediate formed can then fragment reversibly, releasing either the growing polymer chain ($P_n^{\cdot}$), or the re-initiating group, $R^{\cdot}$. This $R^{\cdot}$ then reinitiates polymerisation of free monomer to form a growing polymer chain ($P_m^{\cdot}$ or $P_n^{\cdot}$). These growing chains rapidly react with the CTA until all polymers are capped by CTA. The reaction then enters the main equilibrium and rapid exchange between the active chains and the thiocarbonylthio-capped dormant chains ensures that all polymer chains grow at a similar rate and termination steps are minimised.[9] The exact kinetics of RAFT polymerisations are complex and, along with what side reactions may be occurring, are still under discussion in the literature.[26, 27]

1.4.1.2 Choice of RAFT agent

A key aspect in a RAFT polymerisation is the design of the chain transfer agent; this can determine whether the polymerisation will yield polymers of predictable molecular weights and narrow dispersity whilst retaining the end group functionality. A generic description of a thiocarbonylthio RAFT agent is shown in Figure 1.1.[25]

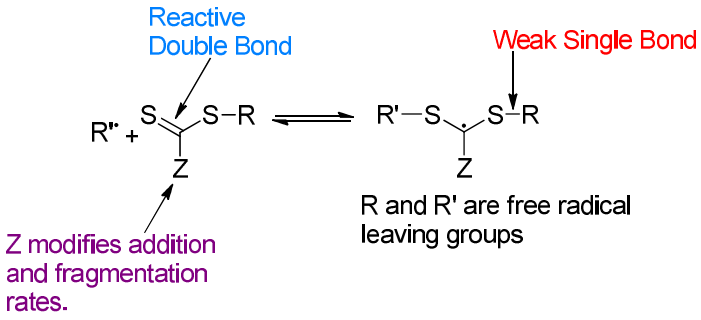

Figure 1.1: Thiocarbonylthio RAFT CTA[25]

The choice of the R and Z groups is important for determining both the addition and fragmentation rates, and therefore the effectiveness of the CTA. The Z group strongly influences the stability of the thiocarbonylthio intermediate radical, depending on its

electron donating or withdrawing behaviour. Electron withdrawing groups (CR'R'', SR') will increase the reactivity of the C=S bond toward radicals, as the intermediate will be more stabilised than the propagating radical and therefore formation of the intermediate is favoured. Electron donating groups (NR'R'', OR') have the opposite effect. The formation of the intermediate is not favoured as the reactivity of the C=S bond towards radicals is decreased.[28] Varying the Z groups leads to the four most common classes of CTA: dithioesters, trithiocarbonates, dithiocarbamates and xanthates (Figure 1.2).[29-31]

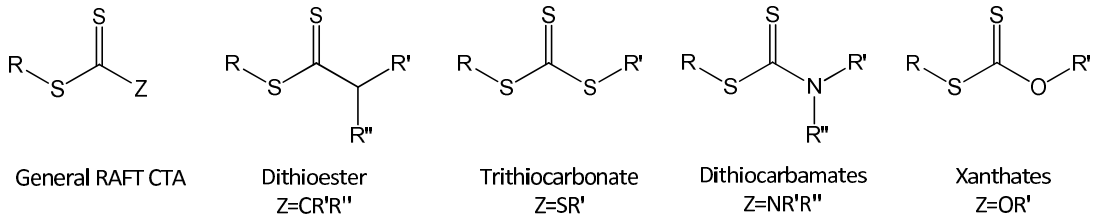

Figure 1.2: The different types of chain transfer agents that are used in RAFT polymerisation[29-31]

More activated monomers such as acrylics and methacrylics form more stable radicals and propagate more quickly, therefore requiring the use of more activated RAFT agents with higher chain transfer constants, such as trithiocarbonates (Z = SR'). Dithiobenzoates (Z = aryl) are also useful for more activated monomers but may show retardation in high concentrations and are more vulnerable to hydrolysis.[27, 32] When these RAFT agents are used in conjunction with less activated monomers, such as vinyl acetate, the polymerisation is inhibited or retarded as a result of the poor leaving groups the monomers form, leading to lower fragmentation rates. Less activated RAFT agents such as xanthates (Z = OR') and dithiocarbonates (Z = NR'R'') are effective for the polymerisation of less activated monomers that have unstable radicals, such as vinyl acetate. The Z groups are stabilising to favour the formation of the intermediate radical.[32] The use of these RAFT agents with more activated monomers would be ineffective due to the decreased reactivity of the C=S bond. Moad *et al*. proposed an order of Z group reactivity as shown in Figure 1.3.[9]

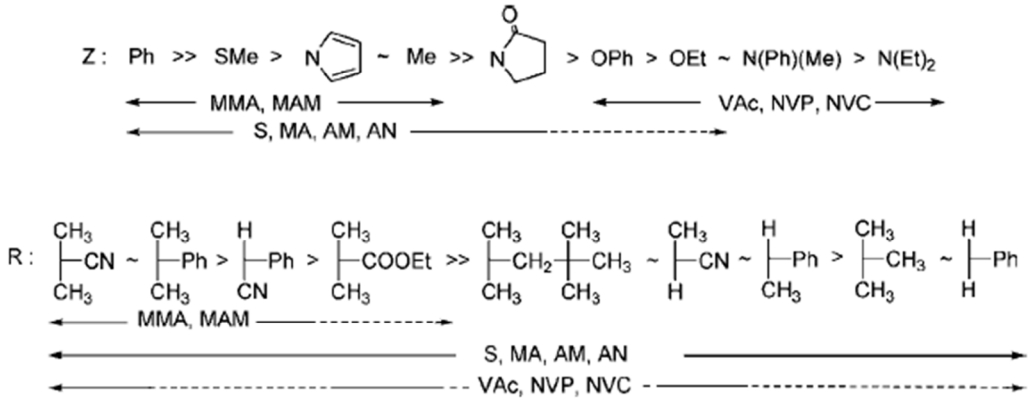

Figure 1.3: The order of reactivity of R and Z groups of RAFT agents. For the Z group, the fragmentation rate increases left to right. For the R group, the fragmentation rate decreases left to right. A dashed line indicates only partial control of the monomer with the group above[9]

The choice of R group is equally important as it is this that governs the pre-equilibrium. The R group should be a good homolytic leaving group with respect to the attacking radical and therefore should have as good radical stability as the monomer used, to ensure that fragmentation favours its release.[33] However, it should also be reactive enough to ensure efficient re-initiation of the monomer used. For example, the use of a benzylic R group with less activated monomers, such as vinyl acetate, would result in retardation, as the benzylic leaving group would be poor at reinitiating polymerisation.

1.5 Achieving functionality at the polymer chain ends

1.5.1 α-end group functionality

A key advantage of RAFT polymerisation methodology is the ability to introduce functionality into the RAFT agent through either the R (α) or Z (ω) group, allowing for ready access to functionalised polymers without the need for post polymerisation modification. Skey *et al*. synthesised a series of functional trithiocarbonate and xanthate chain transfer agents without the need for stringent reaction conditions and with simple purification procedures (see Scheme 1.2).[30] CTAs containing acid, alcohol and alkyne functionality on the R group were synthesised using commercially available thiols.

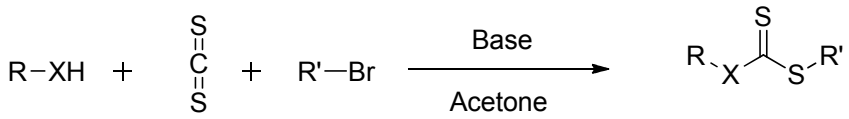

R, R' = alkyl or aryl

X = O, S or N

Scheme 1.2: The general synthetic route employed by Skey *et al.* to synthesise a range of RAFT agents[30]

Functionality at the α-end of the polymer can also be achieved post-polymerisation by the use of a CTA containing a reactive R-group functionality, such as an activated ester.[34, 35] Theato and co-workers synthesised an activated ester functionalised RAFT agent, pentafluorophenyl-[4-(phenylthiocarbonylthio)-4-cyano-valerate] (PFP-CTA) *via* the esterification of azobis(4-cyanovaleric acid) (see Scheme 1.3).[35]

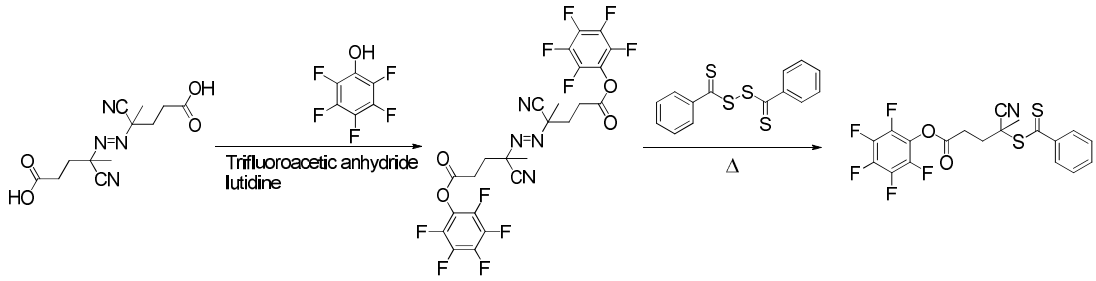

Scheme 1.3: Synthetic route to the PFP functionalised dithiobenzoate CTA reported by Theato and co-workers.[35]

This CTA was then used in the polymerisation of several different methacrylate monomers, including methyl methacrylate (MMA), diethyleneglycol monomethyl ether methacrylate (DEGMA) and lauryl methacrylate. Diblock copolymers were also formed and generally had dispersities ≤ 1.2. The dithiobenzoate chain end of the polymers was further functionalised by reaction of bis(pentafluorophenyl)azobis(4-cyanovalerate) to yield telechelic polymers with pentafluorophenyl (PFP) functionality at both ends.

Wilks *et al*. recently reported the use of a trithiocarbonate chain transfer agent bearing a PFP group.[34] The CTA was used for the polymerisation of *N*-isopropylacrylamide (NIPAM) and, after removal of the trithiocarbonate group with 2, 2'-azobis(2-methylpropionitrile) (AIBN) and lauroyl peroxide (LPO), the PFP group was substituted with 1-azido-3-aminopropane to

yield an alkyne functionalised CTA. This was then used to conjugate the polymer to DNA. The use of the activated ester was essential as initial studies using an alkyne terminated chain transfer agent showed considerable degradation of the alkyne functionality during the RAFT polymerisation.

1.5.2 ω-end group functionality

The living nature of RAFT causes the chain transfer agent to be retained on the majority of polymer chains, allowing for the synthesis of block copolymers. However, one potential disadvantage with the thiocarbonylthio end group is that it is highly coloured and potentially toxic. Therefore the removal or, more usefully, the modification of the end groups to form polymers with well-defined, functional end groups is attractive.[25, 36-41]

1.5.2.1 End group removal

There are two different ways to completely remove the RAFT end group. One method for desulphurisation is thermolysis.[42] The advantage of thermolysis is that it requires no additional chemicals and therefore reduces the steps required to purify the polymer, post removal.[37] Postma *et al*. synthesised polystyrene and poly(*n*-butyl acrylate) using a phthalimidomethyl functionalised CTA. The polymers were heated to 210 – 250 °C to cause end group elimination. In the case of polystyrene the end group was removed by concerted elimination to leave an unsaturated end group. Polymers of *n*-butyl acrylate underwent C-S bond homolysis to yield an *n*-butyl acrylate propagating radical that then could undergo intramolecular transfer or β scission. This resulted in lower molecular weight oligomers with either unsaturated or radical chain ends. The polymers that contained a radical at the chain end could couple to form higher molecular weight polymers (see Figure 1.4). A disadvantage of thermal elimination is that the polymer and any desired functionality must be stable at the high temperatures required.

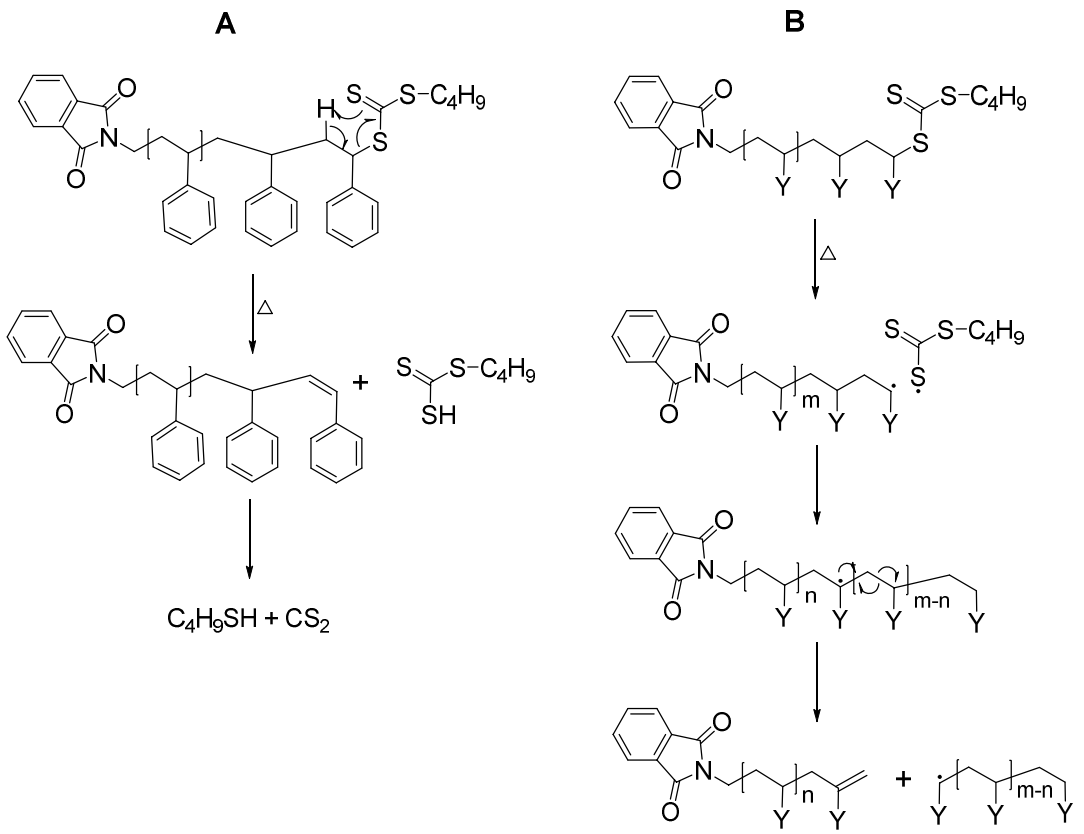

Figure 1.4: Mechanisms of end group removal by thermolysis (Y = $COO(CH_2)_4$)[42]

The other method for complete desulphurisation of the polymer is *via* radical induced end group removal.[37] A radical species that reacts with the thiocarbonylthio group of the CTA is used. The intermediate radical can then react with a trapping agent. The use of a hydrogen donor, such as a hypophosphite salt, leaves polymers with a terminal proton or the initiating radical species can be used in excess to react with the end group of the polymer.[43] Perrier *et al.* used an excess of AIBN in the removal of a dithiobenzoate RAFT group from polymethyl methacrylate (PMMA) to completely remove the end group.[40] However, this method of excess AIBN does not result in 100% end group removal when used with acrylate polymers. For such cases, using lauryl peroxide in conjunction with AIBN has proved to be more effective.[41]

1.5.2.2 End group modification

As discussed previously, functionality at the α-end of the polymer is usually achieved through the use of a functionalised chain transfer agent. Functionality at the ω-end of RAFT

synthesised polymers can be achieved by modification of the thiocarbonylthio group. One of the most common methods is to use a nucleophile, such as an amine, or a reducing agent, such as sodium borohydride, to reduce the thiocarbonylthio group to a thiol. This thiol can then be used in disulphide coupling or in a reaction with a Michael acceptor, such as an acrylate or maleimide.[36-38, 44-47] This method has been used in the post-polymerisation modification of polymers with a wide range of different functionalities, such as fluorescent groups[47] or biomolecules (see Figure 1.5).[46, 48]

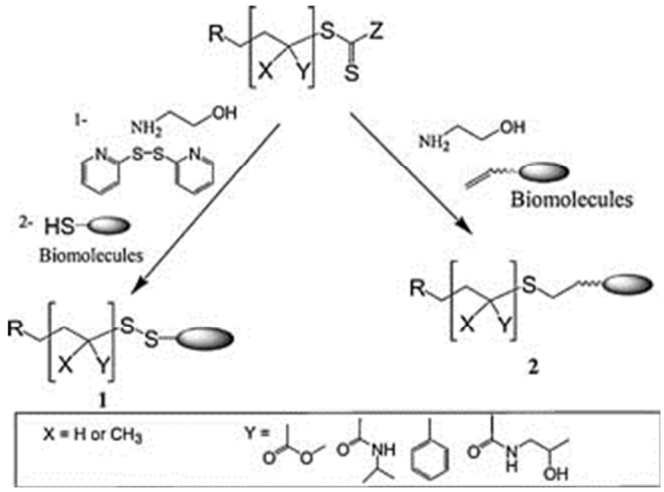

Figure 1.5: Modification of the ω-end of a polymer by aminolysis and thiolene reactions[46]

Spruell *et al*. developed a one-pot method for the reduction of the thiocarbonate group and subsequent Michael addition with an acrylate.[38] A polystyrene homopolymer was synthesised by RAFT polymerisation ($Đ_M$ = 1.08). Primary amines and sodium borohydride were investigated as a means of reducing the dithiobenzoate group. Monomodal SEC chromatograms were achieved by conducting the reaction in an inert atmosphere, with a Michael acceptor and sodium borohydride or tributyl phosphine as a reducing agent. Many different acrylates were investigated and the majority showed high (> 90%) functionalisation.

Boyer *et al*. utilised this strategy to functionalise homopolymers of pentafluorophenyl acrylate (PFPA) ($Đ_M \leq 1.2$) with amine functionalised sugars and modify the

trithiocarbonate end group with a biotin maleimide.[48] The end group modification was calculated to be over 95% from ^{1}H NMR spectroscopy.

1.6 Introducing functionality along the polymer backbone

Functionality along the backbone of the polymer can most often be achieved by polymerisation of the desired monomer, which contains that particular chemistry. Polymerisation techniques have become more sophisticated to allow for the use of a wide range of monomer functionalities. However it is still sometimes desirable to modify the polymer after synthesis, for example if the monomer functionality is unstable to the polymerisation conditions or causes the loss of control of the polymerisation, or if the aim is to create one scaffold polymer and then modify it to create a library of functional polymers.[49, 50] One method to modify the backbone of the polymer is to employ activated esters. Activated esters are those with good leaving groups and therefore have an enhanced reactivity to nucelophiles, such as primary amines, resulting in amide formation.[51] By incorporating these activated esters into monomers, it is possible to synthesise a polymer containing substitutable groups.

1.6.1 PFP activated Esters

An activated ester that has been used extensively is pentafluorophenyl acrylate (PFPA) and methacrylate (PFPMA). Both PFPA and PFPMA have been shown to be polymerisable by RAFT polymerisation methodology. Theato and co-workers synthesised homopolymers of PFPMA using two different dithiobenzoate chain transfer agents (CTAs) (see Figure 1.6).[52]

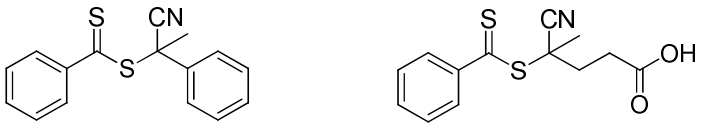

CTA 1 **CTA 2**

Figure 1.6: The structures of the two different CTAs employed in the polymerisation of PFPMA[52]

The homopolymers produced using **CTA 2** displayed narrower dispersities ($Đ_M \leq 1.13$) compared to those produced using **CTA 1** ($Đ_M \leq 1.3$), showing that **CTA 2** is a more

efficient chain transfer agent for the polymerisation of PFPMA. The homopolymers of PFPMA were then chain extended with either methyl methacrylate (MMA), *N*-acryloylmorpholine (NAM) or *N,N*-diethylacrylamide (DEA). The diblock copolymers containing **CTA 2** displayed narrower dispersities ($Đ_M \leq 1.30$) compared to those containing **CTA 1** ($Đ_M \leq 1.46$).[52]

The activated ester functionality can easily be substituted with primary amines.[35, 48-50, 52-56] Theato and co-workers investigated the relative reactivity of polymers of PFPMA and PFPA to various amines and alcohols.[50] PFPA and PFPMA homopolymers were synthesised by free radical polymerisation methods and the resulting polymers reacted with varying amines and alcohols. The reactions were performed in dry DMF at 50 °C. When PFPA and PFPMA homopolymers were reacted with hexylamine, the PFPA homopolymer was substituted with 99% conversion whereas only 65% of the backbone of the PFPMA homopolymer had been substituted. This shows that PFPA has a higher level of reactivity than PFPMA towards primary amines. In the case of a primary alcohol a base, triethylamine (TEA), was required in order to activate the alcohol and allow substitution. Only 30% of the PFPA homopolymer reacted when one equivalent of the alcohol and base were used but when seven equivalents were used 60% substitution was acheived. In both cases there was 0% conversion of the PFPMA backbone.

The same group have also demonstrated that poly(pentafluorophenyl 4-vinyl-benzoate) (polyPFPVB) displays a higher reactivity towards alcohols and amines than PFPMA.[55] The differing reactivity was exploited to synthesise block copolymers with orthogonal reactivity.[55] Block copolymers of PFPVB and PFPMA were synthesised by RAFT polymerisation using cumyldithiobenzoate as the CTA. The block copolymers had narrow dispersities ($Đ_M \leq 1.21$). The PFPMA had been shown to have no reactivity towards aromatic amines and so reaction of the block copolymer with aniline resulted in 100% conversion of the PFPVB block, leaving the PFPMA block unchanged. The substitution reactions were confirmed by the disappearance in the ^{19}F NMR spectrum of the peaks

relating to the PFPVB groups. The PFPMA groups were then reacted with isopropylamine and again this reaction proceeded to 100% substitution.[55]

Boyer *et al*. exploited the reactivity of PFPA in order to synthesise glycopolymers whilst avoiding the lengthy purification procedures required in the synthesis of sugar containing monomers.[57] A series of homopolymers of PFPA were prepared by RAFT polymerisation with 3-(benzylsulfanylthiocarbonylsulfanyl)-propionic acid (BSPA) as the chain transfer agent. The resulting homopolymers ranged in molecular weight from 4 kDa to 17 kDa and all had $Đ_M \leq 1.20$. The homopolymers were then dissolved in DMF and a solution of either $_D$-glucosamine or $_D$-galactosamine in DMF/water mixture (50/50 vol%) containing TEA slowly added. 100% conversion was seen for all polymers in under one hour. The successful substitution was observed by ^{19}F NMR spectroscopy, ^{1}H NMR spectroscopy and IR spectrometry. The physical properties of the polymers after substitution were also notably different. The hydrophobic PFPA homopolymers became water-soluble after substitution with the sugar.

1.7 Self-assembly of polymers

The controlled nature of RDR polymerisation techniques, such as NMP, ATRP and RAFT allows for the formation of block copolymers, with good control over their molecular weights and compositions, leading to a wide range of possible polymer architectures (see Figure 1.7).[58]

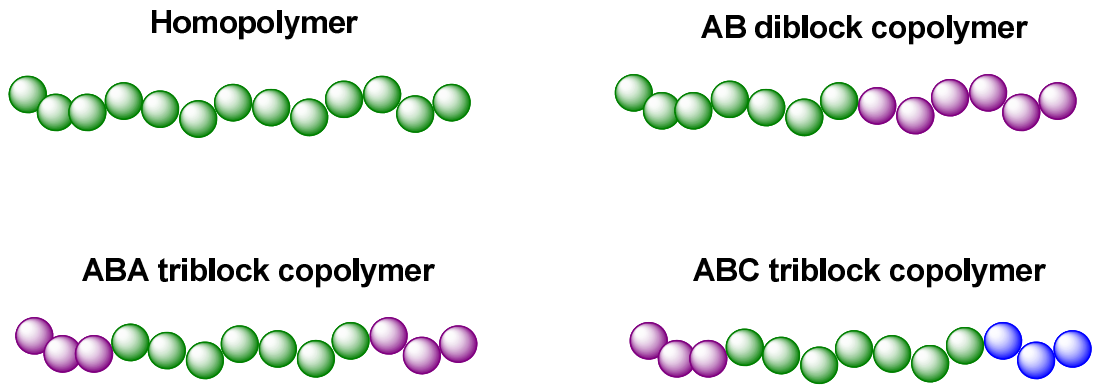

Figure 1.7: A few of the possible polymer architectures that can be synthesised using RDR polymerisation techniques

The simplest example of a linear block copolymer is an AB diblock copolymer, formed from two chemically different monomers. Amphiphilic diblock copolymers are formed when the two polymer blocks have opposite solubilities in water. These amphiphilic block copolymers will undergo self-assembly in aqueous media in order to minimise the energetically unfavourable repulsive interactions between the hydrophobic block and the surrounding water.[58, 59] There is a wide variety of different morphologies possible with the most commonly adopted structures being spherical micelles,[58] cylindrical micelles[60] and vesicles.[61] The structure adopted is determined by the chemical composition of the blocks and their relative lengths (*i.e.* the amphiphilic balance).[59] These factors affect the inherent curvature of the polymer chain and how it packs together in a self-assembled structure. The morphology a specific polymer will adopt in solution can be predicted by calculating the packing parameter;

$$p = \frac{v}{a_o l_c}$$

where v is the volume of the hydrophobic section, a_o is the contact area of the head group and l_c is the length of the hydrophobic section. In general spherical micelles are formed for $p \leq ⅓$, cylindrical micelles are formed when $⅓ \leq p \geq ½$ and when $½ \leq p \geq 1$ vesicles are formed (see Figure 1.8).[59, 63]

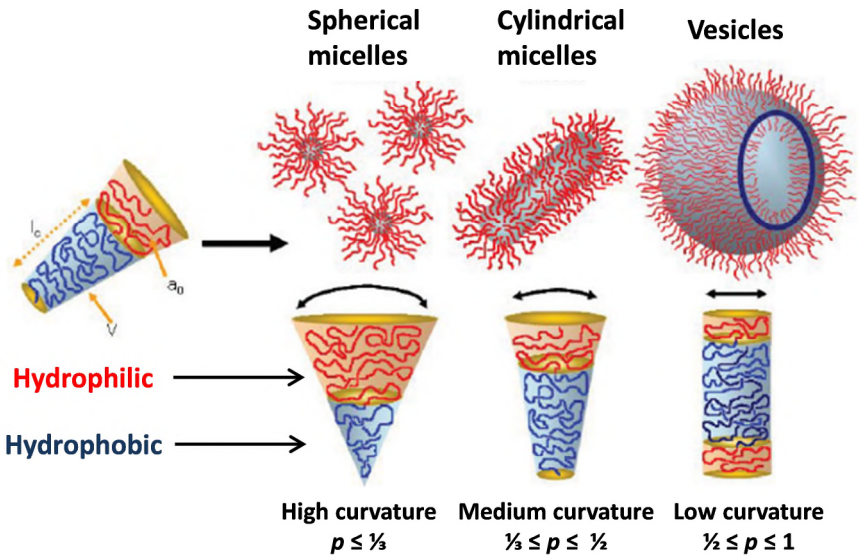

Figure 1.8: Schematic representation of the effect of the amphiphilic balance on the inherent curvature of the polymer and therefore the morphology adopted in solution[59]

Micelles have much higher surface curvature than vesicles and tend to form when the volume of the hydrophilic block is equal to, or slightly greater than, the volume of the hydrophobic block. Vesicles have a much lower surface curvature and tend to form when the volume of the hydrophobic fraction is greater than that of the hydrophilic.[64] Eisenberg and Discher have also proposed a simplified method for predicting the morphology adopted by polymers, dependent upon the weight fraction (*f*) of their hydrophilic block.[61, 65] For polymers with $f > 50\%$, micelles are predicted to form, for $f = 40\text{-}50\%$ cylinders are formed, and for $f = 25\text{-}40\%$, vesicles should be formed. However, the molecular weights of the polymers that these rules have been shown to apply to are low (< 20 kDa).

However, in practice the packing parameter is rarely calculated prior to synthesis and self-assembly of the polymer as other factors such as solvent composition or method of self-assembly can affect the final morphology.[61, 66] Eisenberg showed that for block copolymers of polystyrene (PS) and poly(acrylic acid) (PAA) where the PS block is much longer than the PAA block, PS_{310}-*b*-PAA_{52}, the actual morphology achieved was dependent upon the solvent composition and the copolymer concentration in the solvent (see Figure 1.9).[61]

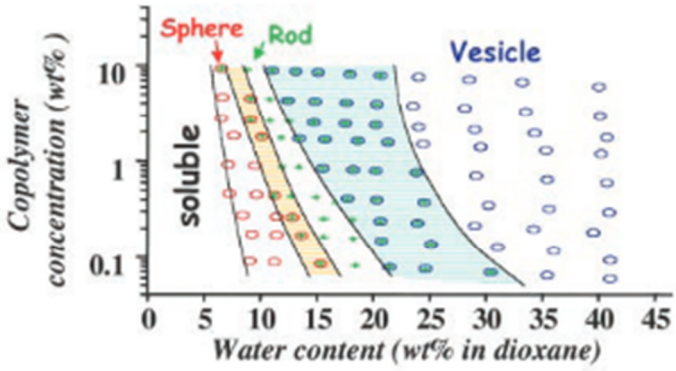

Figure 1.9: Phase diagram for PS_{310}-*b*-PAA_{52} showing the different morphologies achieved dependent upon the solvent composition and the copolymer concentration[61]

1.8 Responsive polymers

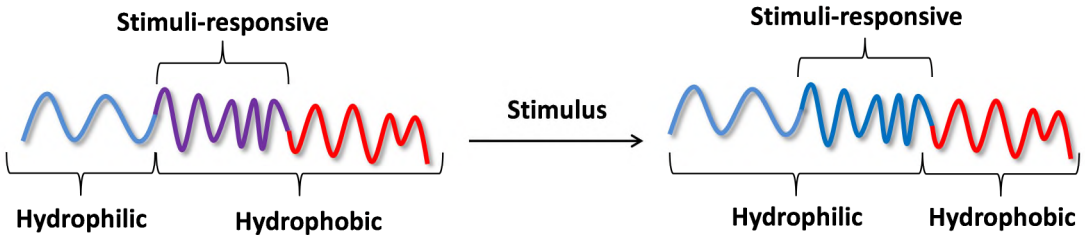

Figure 1.10: Schematic showing how incorporating a responsive block into a block copolymer can cause a change in the amphiphilic balance of the polymer upon application of the stimulus

Stimuli-responsive polymers are interesting as a result of their propensity to undergo a phase transition in response to a particular stimulus (see Figure 1.10).[64] By incorporating these types of polymers into block copolymers a change in the amphiphilic balance of the overall polymer can occur upon application of the particular stimulus. If drastic enough, this change in hydrophilicity can result in the polymer adopting a different morphology. Such polymers that self-assemble and switch morphology in response to a particular stimulus have potential uses in areas such as drug delivery and nanoreactors.[67-70] Stimuli which have been investigated within the literature include, but are not limited to, temperature,[71-74] pH[67, 75] carbon dioxide[76] and light.[74, 77]

1.8.1 pH-responsive polymers

There are many different examples of pH-responsive polymers and for a more thorough account the reader is directed to several reviews on the subject.[67, 75, 78, 79] There are two different ways that pH can cause a hydrophilicity change in a polymer. Either the application of a pH change can cause a reversible change within the polymer, *i.e.* the protonation of amine units to render them hydrophilic,[44, 80, 81] or can cause an irreversible chemical change of the polymer structure.[60, 82, 83]

This permanent chemical modification of the polymer can be utilised in the synthesis of amphiphilic diblock copolymers that would otherwise prove difficult to directly synthesise or for ease of characterisation.[61, 82-85] Petzetakis *et al*. have synthesised diblock copolymers

of polylactide and poly(acrylic acid) through ring opening metathesis polymerisation of the lactide, followed by RAFT polymerisation of a protected acid, tetrahydropyranyl acrylate (THPA). The THPA block was then deprotected, with acetic acid and heating, to form poly(acrylic acid) (PAA).[60] This amphiphilic polymer was then self-assembled in water. It was observed that if the core block was comprised of enantiomerically pure homochiral polylactide, cylinders were formed, but if the core of the structures contained amorphous atactic polylactide, then spherical micelles were formed (see Figure 1.11). This difference in morphology achieved was a result of the crystallinity of the enantiomerically pure lactide core, whereas the racemic mixture was unable to crystallise.

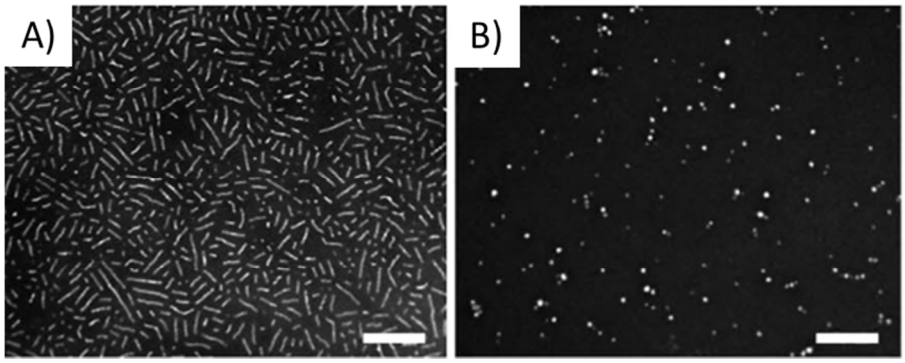

Figure 1.11: A) cylinders formed from enantiomerically pure PLA-*b*-PAA, B) micelles formed from a racemic mixture of PLA-*b*-PAA[60]

Wooley and co-workers have also used protected acids to synthesise amphiphilic block copolymers bearing Click-reactive functional groups at the α-terminus.[86] Firstly NMP was used to synthesise block copolymers of *tert*-butyl acrylate (*t*-BuA) and styrene (PS) using a chloromethyl-substituted alkoxyamine NMP initiator. The *t*-BuA groups were then removed using trifluoroacetic acid (TFA) to yield α-functionalised amphiphilic diblock copolymers (see Scheme 1.4). These polymers were then used to form micelles with a functionalised surface by reacting the chloromethyl functionality at the end of the functionalised polymer with sodium azide. The azide functionality was incompatible with the chemistry needed to remove the *t*-BuA groups, hence the need for post-polymerisation end group functionalisation.

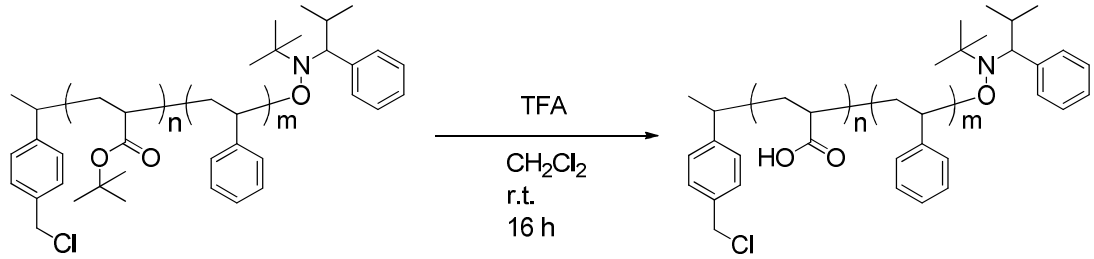

Scheme 1.4: Deprotection of the *t*-BuA groups of the chloromethyl functionalised diblock copolymers to form the amphiphilic diblock copolymers[86]

Alkyne end functionalised polymers were also synthesised by RAFT polymerisation but utilising THPA, instead of *t*-BuA. This new approach was required as a result of the incompatibility of the alkyne functionality with the harsh conditions required to deprotect the *t*-BuA groups, and the poor control afforded by NMP over the polymerisation of THPA. These polymers were self-assembled into micelles in a similar manner to the azide functionalised polymers.[86] Hoogenboom *et al*. have also demonstrated deprotection techniques using 1-ethoxyethyl acrylate in order to synthesise block copolymers of poly(acrylic acid).[85]

Whilst these pH-deprotectable monomers are useful precursors in the synthesis of otherwise challenging amphiphiles, a reversible pH response is arguably more useful. One class of functional group to exhibit a reversible pH response is tertiary amines. Below its pK_a the tertiary amine will be protonated and at pH values above the pK_a, the amine functionality will be deprotonated. This can cause a change in the hydrophilicity of the polymer and its amphiphilic balance. pH-responsive polymers have been utilised in morphology transitions such as (dis)assembly of a micelle[87-93] or vesicle,[81, 94-96] transition between two self-assembled structures such as a micelle and a vesicle[44] or even single chain assembly.[97] Cross-linking of the self-assembled structures can prevent complete disassembly upon the pH change, often resulting in swellable nanoparticles.[98-102]

Lee and co-workers synthesised homopolymers of 2-(diisopropylamino) ethyl methacrylate (DIPEMA) by RAFT polymerisation with low dispersity ($Đ_M$ < 1.2).[92] These homopolymers were then used as macroCTAs in the chain extension with poly(ethylene glycol) methyl

ether methacrylate (PEGMA) to form amphiphilic diblock copolymers ($Đ_M \geq 1.40$) with varying lengths of hydrophilic or hydrophobic block. The diblock copolymers were dissolved in acidic water (below the pK_a) and unimers were formed. Upon increasing the pH of the polymer solution, self-assembly occurred at *ca*. pH 6.7, as the DIPEMA block became deprotonated and hydrophobic, thereby causing micelles with D_h *ca*. 25 - 30 nm to form, as observed by DLS analysis (see Figure 1.12). This showed a unimer to micelle morphology transition with increasing pH. However the authors did not investigate the reversibility of this transition.[92] Peng *et al*. have utilised a similar responsive system for the controlled release of hydrophobic payloads.[103]

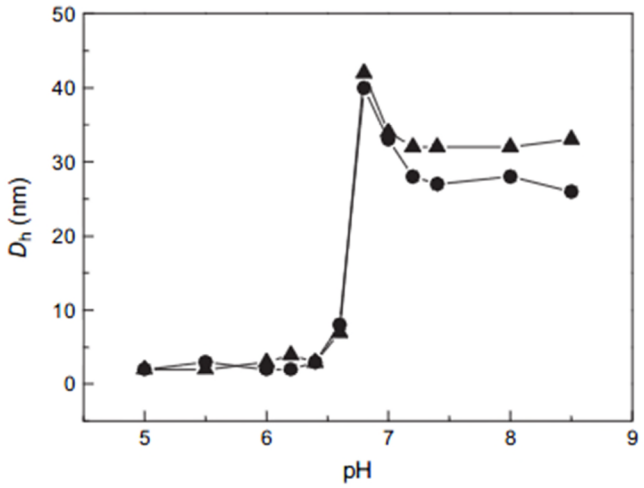

Figure 1.12: Size change with pH observed by DLS analysis for DIPEMA$_{31}$-*b*-PEGMA$_{29}$ (circles) and DIPEMA$_{31}$-*b*-PEGMA$_{62}$ (triangles)[92]

McCormick and co-workers synthesised a pH-responsive triblock copolymer consisting of a poly(ethylene oxide) (PEO) block, poly(*N*-(3-aminopropyl) methacrylamide) (PAPMA) block and the pH-responsive block DIPEMA by RAFT polymerisation.[101] At acidic pH, the polymer is unimerically dissolved in solution with D_h < 10 nm. Increasing the pH of the polymer solution to above pH 6 caused micelles with a DIPEMA core to form. The size of the micelles could be tuned by the length of the DIPEMA block. For example, a PEO$_{46}$-*b*-PAPMA$_{21}$-*b*-DIPEMA$_{36}$ triblock formed micelles with a D_h = 20 nm. A PEO$_{46}$-*b*-PAPMA$_{21}$-*b*-DIPEMA$_{101}$ formed micelles with D_h = 80 nm.

Cross-linking of the PAPMA shells, followed by lowering the pH to below 5, resulted in swollen micelles. The swollen size is also dependent upon the length of the DIPEMA block. The cross linked micelles formed from PEO_{46}-*b*-$PAPMA_{21}$-*b*-$DIPEMA_{36}$ swelled from 46 nm at pH 8.1 to 82 nm at pH 3.3. The shell cross-linked micelles formed from the longer PEO_{46}-*b*-$PAPMA_{21}$-*b*-$DIPEMA_{101}$ triblock swelled from 95 nm at pH 7.4 to 215 nm at pH 2.9.

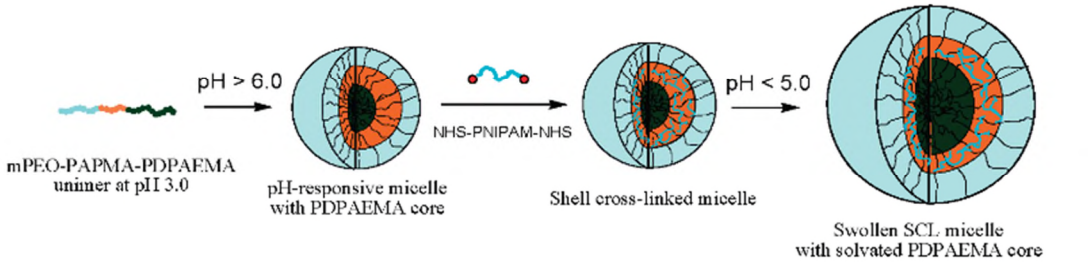

Figure 1.13: The PEO-*b*-PAMA-*b*-DIPEMA triblocks copolymers assemble into micelles with a DIPEMA core. Shell cross-linking and then lowering the pH results in the micelles swelling[101]

A schizophrenic block copolymer, a term coined by Armes and co-workers, is one that can self-assemble in aqueous media in the absence of any organic solvents to form two distinct assemblies and the hydrophilicity of the separate blocks can be tuned by subtle changes in the solution pH, temperature or ionic strength.[104] Liu and Armes synthesised a schizophrenic diblock copolymer of poly(*N, N*-(diethylamino)ethyl methacrylate) (DEAEMA) and poly(4-vinyl benzoic acid) (VBA) by ATRP.[105] The DEAEMA block becomes insoluble at pH values greater than *ca*. 7.1 and the VBA block becomes soluble at pH values greater than 6.2. The polymer assembled in pH 2 water to form micelles with VBA core (D_h = 36 nm). At pH values between 6.6 and 8.3 the polymer precipitated. However, upon raising the pH of the solution to 10 the polymer self-assembled to form micelles with a DEAEMA core and VBA corona (D_h = 35 nm) (see Figure 1.14). This self-assembly behaviour was found to be fully reversible.

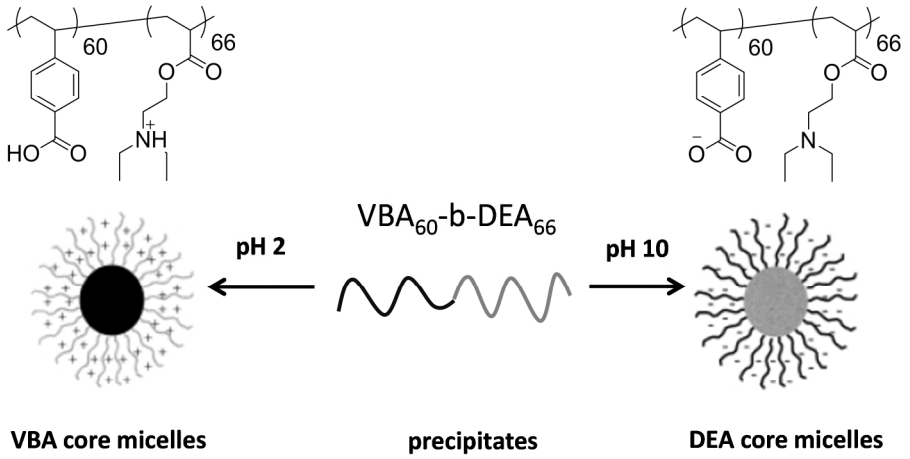

Figure 1.14: Chemical structure of the VBA-*b*-DEAEMA diblock at pH 2 and pH 10 and the schizophrenic micellisation behaviour in solution[105]

One widely studied potential use for pH-responsive polymers is in targeted drug delivery and controlled release of payloads.[67, 78, 79, 103, 106-110] Chen and Du utilised vesicles formed from block copolymers consisting of a hydrophilic block of poly(ethylene oxide) (PEO) attached to a statistical block of DEAEMA and (2-tetrahydrofuranyloxy)ethyl methacrylate (TMA).[109] The vesicles were loaded with an anticancer drug, DOX-HCl, and release of the drug could be achieved by lowering the pH to pH 4 (see Figure 1.15). The incorporation of the TMA into the polymer rendered the vesicles sensitive to ultrasound, allowing for another trigger for drug release from within the polymer.

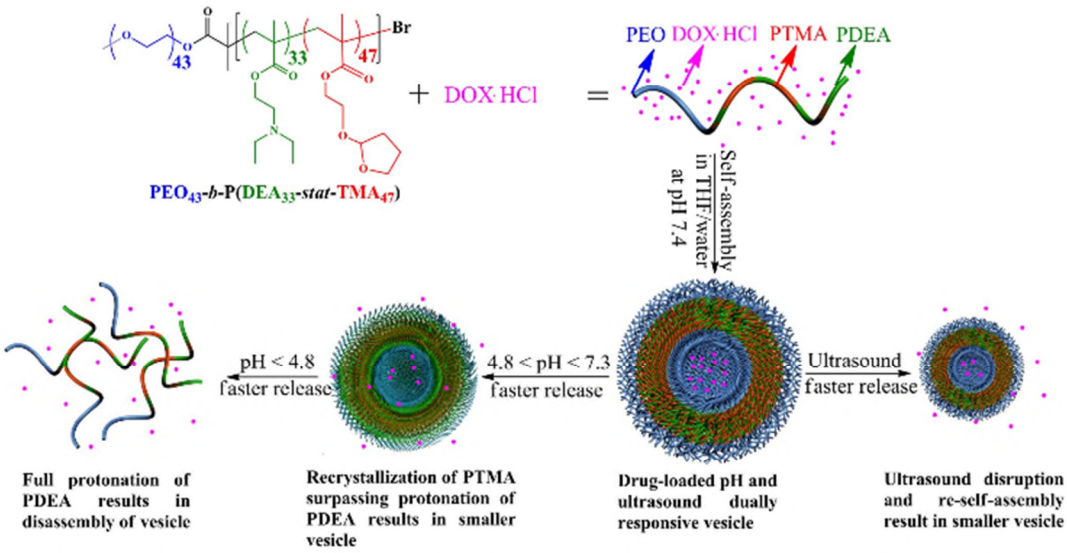

Figure 1.15: Schematic showing the formation of DOX-HCl loaded vesicles and the subsequent drug release in response to a change in pH[109]

Alexander and co-workers have exploited a similar vesicle to unimer morphology transition to release DNA.[108] A RAFT triblock of hydrophilic PEO, pH-responsive imidazole block and a hydrophilic glycerol methacrylate (GMA) block was self-assembled into vesicles in the presence of DNA at pH 7.4 (see Figure 1.16). Adjusting the pH to 5.0 resulted in release of the DNA as the vesicles dissociated. Attachment of a ligand to the polymer chain end resulted in cellular uptake and this, along with the non-toxicity of the polymers, shows the potential of these systems for targeted delivery of DNA in the human body.

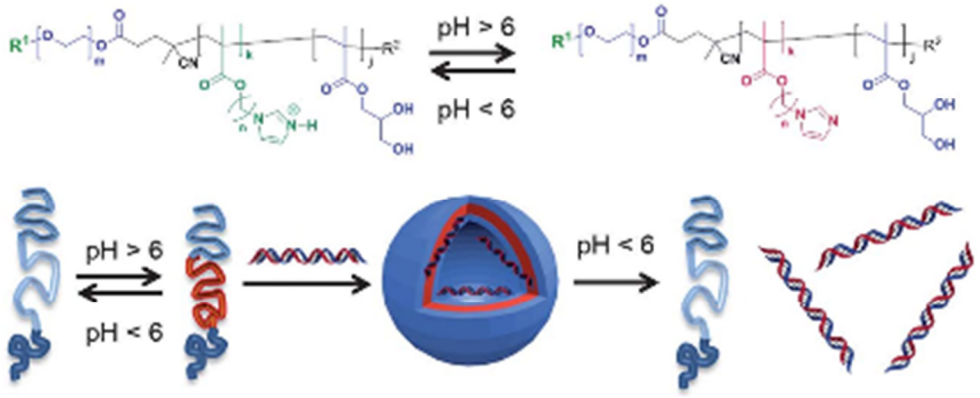

Figure 1.16: Schematic showing the structure of the triblock copolymer and the self-assembly behaviour[108]

1.8.2 Temperature responsive polymers

Polymers which respond to temperature by undergoing a hydrophilicity change, so-called thermo-responsive polymers, come in two distinct classes; those which display a lower critical solution temperature (LCST) and those which display an upper critical solution temperature (UCST). LCST polymers become insoluble upon heating and UCST polymers, the reverse. The phase behaviour of a simple thermo-responsive polymer can be depicted by a bimodal (coexistence) curve. Temperature is plotted against concentration and the bimodal (coexistence) curve line depicts the temperature at which the phase separation begins.[111] The actual LCST or UCST is defined as being the intersection of the spinodal and bimodal (coexistence) curves (see Figure 1.17).[71] The spinodal curve is the boundary where absolute phase separation occurs.[4]

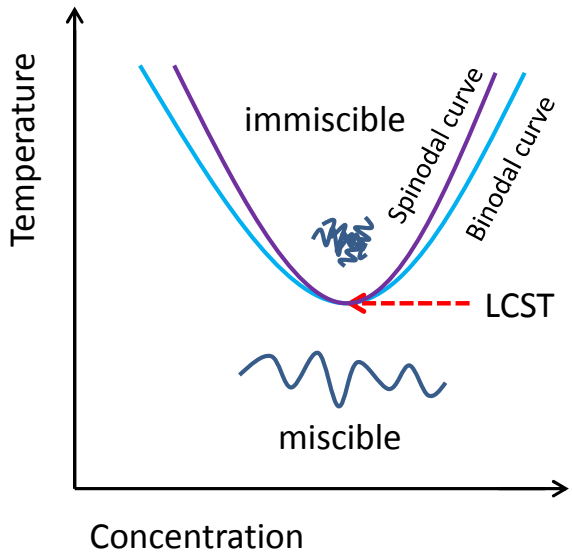

Figure 1.17: Depiction of a phase diagram showing the LCST as the intersection of the bimodal and spinodal curves

In practice the LCST is rarely measured and instead a cloud point is reported. The cloud point is the temperature at which a macroscopic phase separation occurs at a particular concentration (see Figure 1.18). The cloud point and LCST may be similar, as in the case of NIPAM, whose phase separation temperature varies very little over a range of concentration and molecular weight (this will be discussed further in the following section).[112, 113] However, for other polymers, the cloud point is highly dependent upon such factors.[21]

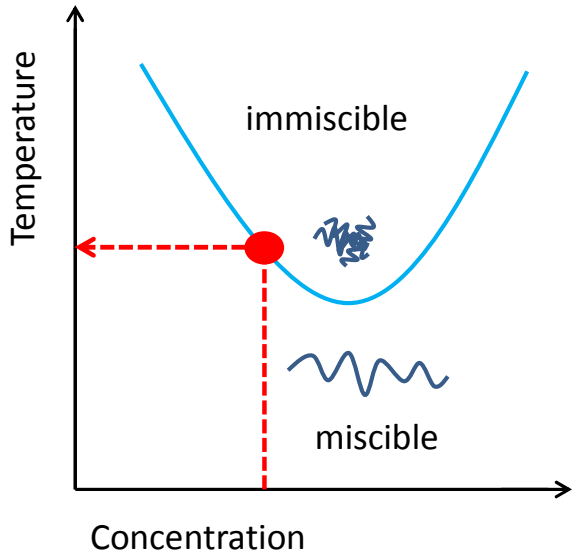

Figure 1.18: The cloud point, shown by the red circle, is the temperature at which macroscopic precipitation occurs at a given concentration. Here an LCST cloud point is shown

Polymers can also display more complex phase behaviour in water, such as having both an LSCT and a UCST (see Figure 1.19).

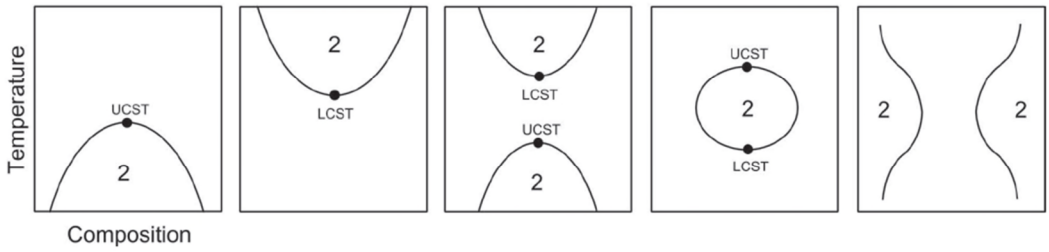

Figure 1.19: Different phase behaviour is possible as depicted by the phase diagrams shown here[111]

1.8.2.1 LCST polymers

As previously mentioned, LCST polymers undergo a phase transition from being soluble to insoluble upon heating. One of the most commonly studied LCST type polymers is PNIPAM.[72] At high molecular weights, the LCST of PNIPAM is largely independent of the polymer concentration, dispersity or end group structure.[113] Furyk *et al*. synthesised a 213 kDa PNIPAM homopolymer by free radical polymerisation and the LCST was found to be 30.22 °C. This was then fractionated into samples with different molecular weights by selective precipitation. The LCST cloud point for a sample with a molecular weight of 18 kDa had only increased by 0.6 °C.[113] Increasing the concentration from 10 mg mL^{-1} to 100 mg mL^{-1} induced only a 0.2 °C increase in cloud point.

At smaller molecular weights the cloud point of PNIPAM has been reported to change with concentration, but this is often attributed to be a consequence of end group effects. Xiu *et al*. synthesised low molecular weight PNIPAM by ATRP. The 2.8 kDa polymer displayed a cloud point of 43 °C but increasing the molecular weight to 26.5 kDa decreased the cloud point to 33.3 °C.[114] A later report by the same group showed that increasing the hydrophobicity of the end group caused the cloud point of PNIPAM to decrease, at a given molecular weight.[115] Polymer concentration can also have an effect on the LCST cloud point of low molecular weight homopolymers of PNIPAM, especially when coupled with end

group effects.[116, 117] This end group effect on the cloud point of other polymers displaying LCSTs has also been reported.[118]

The LCST of PNIPAM in water is entropy-driven. It arises from the disruption of the dynamic arrangement of hydrogen bonds between water molecules by the non-polar polymer.[119] The water molecules can hydrogen bond to the polar parts of the PNIPAM polymer, but must reorder themselves around the non-polar parts, resulting in a decrease in the entropy of the system (negative ΔS) (see Figure 1.20).[112]

$$\Delta G = \Delta H - T\Delta S$$

The equation for Gibbs free energy (ΔG) of a system is given above. The enthalpic term (ΔH) of the Gibbs free energy is exothermic as a result of the formation of hydrogen bonds upon initial dissolution, but as the temperature increases the entropic effect becomes dominant. At a certain temperature ΔG becomes positive, resulting in phase separation of the polymer.

Figure 1.20: Images showing the ordering of the water molecules around the PNIPAM polymer below the LCST cloud point, resulting in a dissolved polymer, and the macroscopic precipitation that occurs upon heating above the LCST cloud point of the polymer[120]

Many other polymers display LCST behaviour and for more information the reader is directed to several reviews on this topic.[67, 71, 73, 121, 122] Inclusion of these thermo-responsive polymers into amphiphilic block copolymer systems can result in a change in the amphiphilic balance of the polymer, and therefore affect the morphology adopted upon self-assembly. Grubbs and co-workers have investigated a system using a thermo-responsive ABC triblock copolymer, consisting of PNIPAM as a thermo-responsive block positioned

between a low T_g hydrophobic poly(isoprene) block and a permanently hydrophilic poly(ethylene oxide) block.[123] The polymer self-assembled into micelles below the LCST cloud point of the PNIPAM block but upon heating the micelle solution to 65 °C a micelle to vesicle transition occured. The time taken for this morphology change was in the order of weeks.

Moughton *et al*. synthesised a diblock copolymer consisting of equal length blocks of PNIPAM and *t*-BuA. The CTA used in the RAFT polymerisation of this diblock copolymer contained a quaternary amine functionality, thereby providing a permanently hydrophilic head group.[124] The polymer was self-assembled into water below the LCST cloud point of the PNIPAM and micelles were formed, as evidenced by DLS and TEM analysis. Upon heating the micelle solution to above the LCST cloud point of the PNIPAM, a micelle to vesicle morphology transition was achieved. However, the solution required heating to 60 °C for over seven days to afford the morphology change. By increasing the length of the PNIPAM block, and using a hydrophobic block with a lower T_g, polymethyl acrylate (PMA), the speed of the micelle to vesicle morphology transition increased and the polymer solution only required heating to 60 °C for 23 hours to induce the transition (see Figure 1.21).[125] The transition was shown to be reversible as upon cooling to room temperature, the vesicles reformed into micelles.

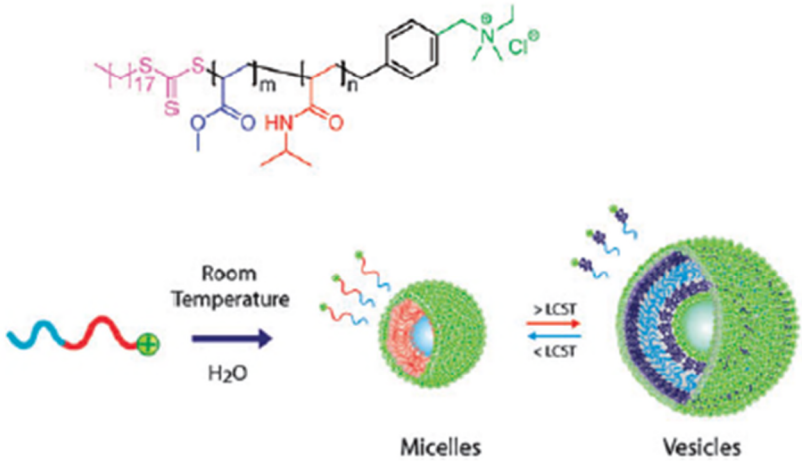

Figure 1.21: Showing the structure of the diblock copolymer and the reversible morphology transition from vesicle to micelle with temperature[125]

These examples all exhibit relatively long heating periods to afford a morphology transition. Jiang and co-workers synthesised a NIPAM homopolymer with a hydrophilic acid group at one end and a hydrophobic hydrocarbon (C_{12}) chain at the other. The polymer self-assembled to form micelles with a hydrocarbon core and a micelle to vesicle transition could be induced in 30 minutes when heated at 37 °C.[126] The authors suggest that the retardation seen in Grubbs' and Moughton's examples is a result of hydrophobicity of the micellar core restricting chain movement.

1.8.2.2 UCST polymers

The majority of examples of thermo-responsive polymers deal with those that display LCST behaviour. For example, in a recent review on thermo-responsive polymers by Sumerlin and co-workers, 57 examples of LCST type polymers are reported, but only five that display UCST behaviour.[73] UCST polymers are ones that undergo a phase transition from insoluble to soluble upon heating. Unlike LCST, which is entropy driven, the UCST can be considered to be enthalpy driven.[111, 127] Below the UCST the polymer-polymer and solvent-solvent interactions are stronger than polymer-solvent interactions. Increasing the temperature breaks these interactions and, hence, the polymer becomes soluble.[127] Additionally, UCST polymers can be subdivided into those that rely on hydrogen bonding (HB-UCST), such as poly(uracilacrylate) and those that rely on coulombic interaction (C-UCST), such as zwitterionic polymers (see Figure 1.22).[127]

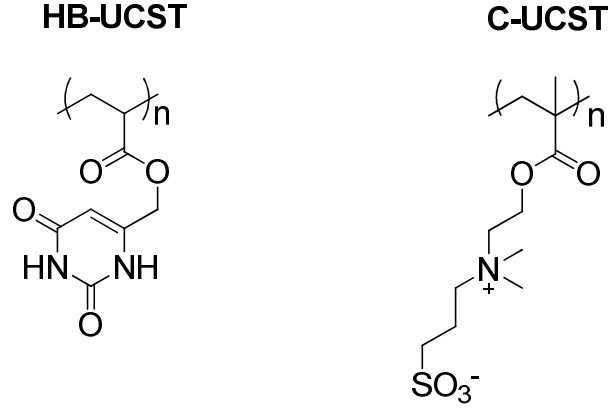

Figure 1.22: An example of a hydrogen bonding UCST (HB-UCST) polymer, poly(uracilacrylate) and a zwitterionic UCST polymer that relays on coulombic interactions (C-UCST)[127]

Other UCST polymers that rely on thermally reversible hydrogen bonding include poly(*N*-acryloylglycinamide) (PNAGA)[128, 129], poly(*N*-acryloylasparginimide)[130], proline-based copolymers[131] and copolymers of polyacrylamide and polyacrylonitrile. As with LCST polymers, the chain ends can have an effect upon UCST behaviour. PNAGA was polymerised by RAFT polymerisation with cyanomethyldodecyl trithiocarbonate as the CTA. At molecular weights between 15-35 kDa, the UCST cloud point is almost independent of molecular weight, but below 15 kDa the UCST cloud point increased with decreasing molecular weight (9 °C at 15.7 kDa to 22 °C at 3.7 kDa). This is a result of the hydrophobic end group having a greater effect on the smaller polymers and therefore an increase in the cloud point.[132] It has also been noted that the presence of ionic groups can suppress the UCST behaviour of PNAGA.[133]

Polymeric sulfobetaines are a class of zwitterionic polymers in which the cationic and anionic functional groups are located on the same monomer unit.[134] These polymers can undergo different types of self-association, such as intrachain or interchain aggregation (see Figure 1.23), leading to salt-responsive and thermo-responsive behaviour.[111]

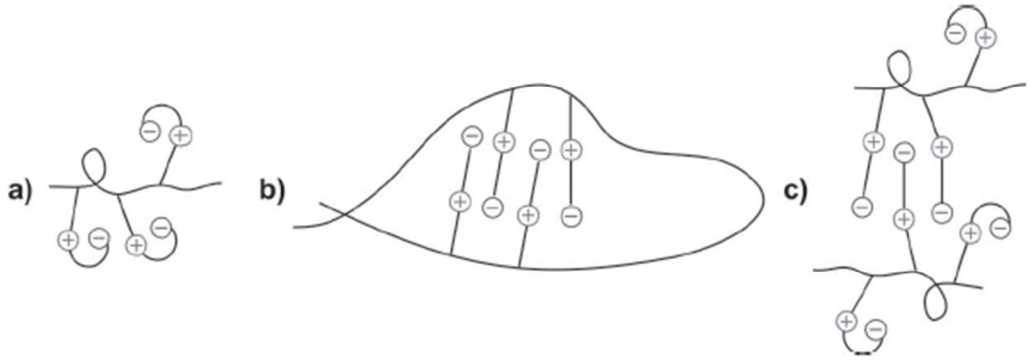

Figure 1.23: The different types of interaction that zwitterionic polymers can undergo, a) intragroup, b) intrachain and c) interchain[111]

Some sulfobetaines display UCST behaviour based on coulombic interactions.[111, 135-139] These polymers often become soluble upon the addition of salt, which can suppress the UCST behaviour by breaking up the ionic bonds.[134, 140-143] Sulfobetaines have been polymerised by both free radical polymerisation[143-146] and by RDR methods, such as

RAFT.[21, 140, 147-152] Another method of sulfobetaine synthesis is to firstly synthesise a tertiary amine containing polymer and then modify post-polymerisation with 1, 3-propane sultone, to introduce the sulfobetaine functionality (see Scheme 1.5).[151-154]

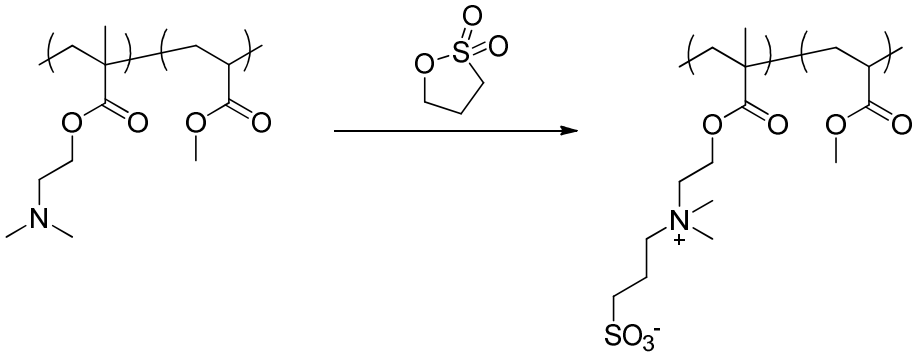

Scheme 1.5: The modification of a tertiary amine containing polymer by 1, 3-propane sultone to yield a sulfobetaine[151]

The UCST cloud point of sulfobetaines is dependent upon the polymer molecular weight and the concentration of polymer in solution.[21, 137, 150, 155] Willcock *et al*. investigated the effect of these two variables upon the cloud point displayed by homopolymers of [2-(methacryloyloxy) ethyl] dimethyl-(3-sulfopropyl) ammonium hydroxide (DMAPS).[21] A range of linear homopolymers of DMAPS from 5 kDa to 500 kDa were synthesised by RAFT polymerisation. The 5 kDa and 20 kDa homopolymers did not display UCST cloud points at a concentration of 1 mg mL^{-1} and the cloud point increased from 11 °C for the 50 kDa to 43 °C for the 500 kDa homopolymer. Similarly increasing the concentration of the polymer in solution increased the cloud point observed. Incorporation of 5 mol% of PEGMA, copolymerised with the DMAPS, suppressed the UCST behaviour as no cloud points were observed. Interestingly, when branched polymers of DMAPS were synthesised, cloud points were not observed, even for the largest of the polymers, until very concentrated samples (50 mg mL^{-1}) were used. The authors reported this to be a result of shorter DMAPS chains solubilising the otherwise collapsed DMAPS particles. Incorporation of PEGMA into the branched DMAPS polymers eliminated the cloud point altogether, which was attributed to the hydrophilic PEG shell preventing aggregation.[21]

Thermo-responsive block copolymers of sulfobetaines have also been synthesised.[135, 149, 150, 156-159] Laschewsky and co-workers synthesised diblock copolymers of PNIPAM and 3-(*N*-(3-methacrylamidopropyl)-*N,N*,dimethyl) aminopropane sultone (SPP) by RAFT polymerisation.[150] The polymers exhibited double thermoresponsivity as a result of the LCST phase transition of the PNIPAM block and the UCST phase transition of the SPP block. The diblock copolymers self-assembled into different morphologies across the temperature range. Below the UCST cloud point of the SPP block, micelles with a SPP core were formed. The polymer was molecularly dissolved between the UCST cloud point and the LCST cloud point, and above the LCST cloud point micelles with a PNIPAM core were formed (see Figure 1.24).The PNIPAM block length was kept constant at 95 units and the SPP block length was either 33 units or 180 units. The shorter SPP block lead to a lower UCST cloud point of 8.6 °C and an LCST cloud point of 31.5 °C. The longer SPP block had a similar LCST cloud point at 31.4 °C but the UCST cloud point was increased to 18.4 °C. This shows that the UCST of the SPP block is dependent upon the molecular weight of the zwitterionic block. No size information for the assemblies was provided, as they were characterised by ^{1}H NMR spectroscopy.

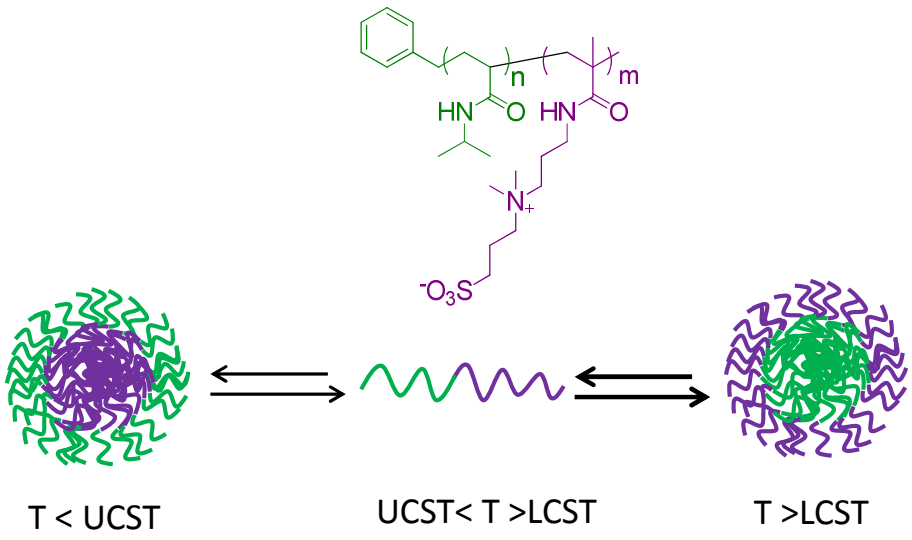

Figure 1.24: The structure of the PNIPAM-b-SPP diblock and the different morphologies presumed at different temperatures[150]

Recently Ning *et al*. synthesised homopolymers and hydrogels of SPP by free radical polymerisation, with a cross-linker in the case of the hydrogels.[160] Both the hydrogels and solutions of the homopolymer displayed UCST behaviour. The cloud point was concentration dependant, but did not display a linear increase. The cloud point increased from 2 °C at 2.5 mg mL^{-1} to 30 °C at a polymer concentration of 10 mg mL^{-1}. Between 10 – 100 mg mL^{-1}, the cloud point only increased by a further 10 °C.

The hydrogels formed were found to have a lower cloud point than the equivalent aqueous homopolymer and decreased with increasing cross-linker concentration. The cross-linked gels could be dissolved by dilution with aqueous NaCl solution or by dilution and then heating to above the UCST for 24 hours (see Figure 1.25).

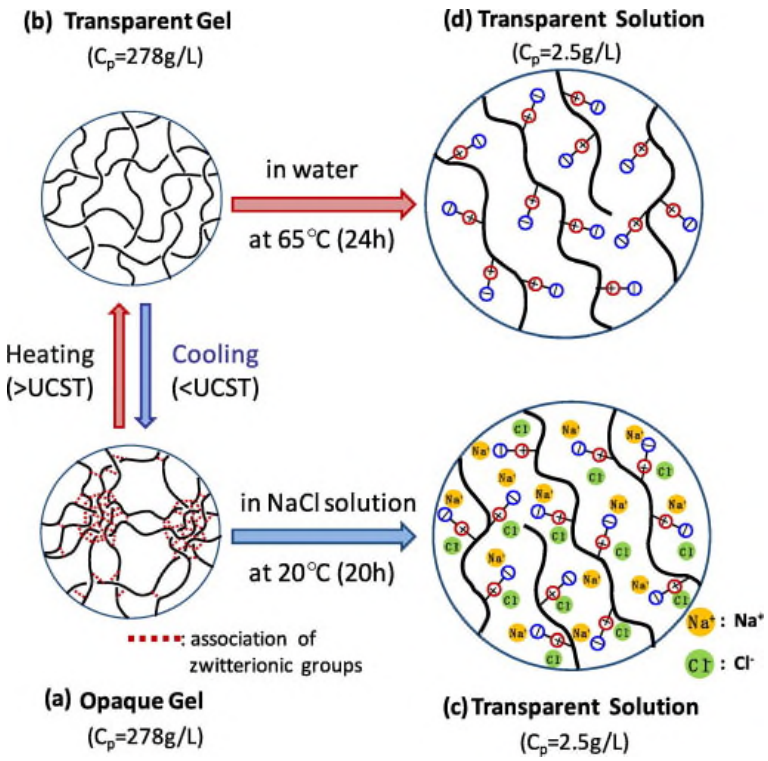

Figure 1.25: Schematic representation of the various physical states of the SPP hydrogels. A) opaque gel below the UCST, b) transparent gel upon heating above the UCST, c) transparent solution after dissolution into NaCl solution, d) transparent solution after dilution and heating to 65 °C for 24 hours[160]

The UCST of polymers can be tuned by incorporation of a hydrophilic or hydrophobic monomer.[21, 139, 158, 161-163] Seuring and Agarwal demonstrated this by the copolymerisation of acrylamide with varying amounts of acrylonitrile.[161] Polyacrylamide as a homopolymer has

not been known to display UCST behaviour. However, copolymerisation of hydrophobic acrylonitrile with the acrylamide introduced a UCST. Moreover, the UCST cloud point could be tuned by varying the amounts of acrylonitrile added. Incorporating 7.6 mol% of acrylonitrile into the copolymer introduced a cloud point of 6.4 °C. Increasing this to 16.9 mol% increased the cloud point to 56.7 °C.

The increase of the cloud point with increasing hydrophobic content can be explained by consideration of the Gibbs free energy. The UCST of acrylamide relies on thermally reversible hydrogen bonds. Polymers dissolve in a solvent when the Gibbs free energy of the system (ΔG) is negative. Polymer solutions show a UCST when both the enthalpy and entropy terms (ΔH and ΔS) are positive. Therefore the UCST can be considered the point at which $\Delta G = 0$ and $T = \Delta H/\Delta S$. To increase the UCST (T), either the enthalpy term can be increased or the entropy term can be decreased. So the addition of hydrophobic moieties causes the water molecules to order themselves around the hydrophobic parts of the polymer chain, and hence ΔS decreases, leading to a higher UCST.[161]

Woodfield *et al*. have also demonstrated this increase in UCST cloud point with hydrophobic modification of a sulfobetaine polymer.[139] They synthesised a homopolymer of the activated ester PFPA and substituted it with a sulfobetaine amine, 3-((3-aminopropyl) dimethylammonio) propane-1-sulfonate (ADPS) and a hydrophobic amine. The post-polymerisation modification method was necessary because of the limited solubility of sulfobetaines and therefore the synthetic challenges associated with the incorporation of hydrophobic monomers. Pentylamine, benzylamine and dodecylamine were investigated to determine the effect of the different hydrophobicities on the UCST. Interestingly, incorporation of the pentylamine increased the solubility of the copolymer (*i.e*. lowered the cloud point). Incorporation of 34 mol% of dodecylamine rendered the copolymer insoluble. Increasing incorporation of benzylamine increased the UCST cloud point of the copolymer, from 7.2 °C at 5 mol% to 82.4 °C at 65 mol% incorporation (see Figure 1.26).

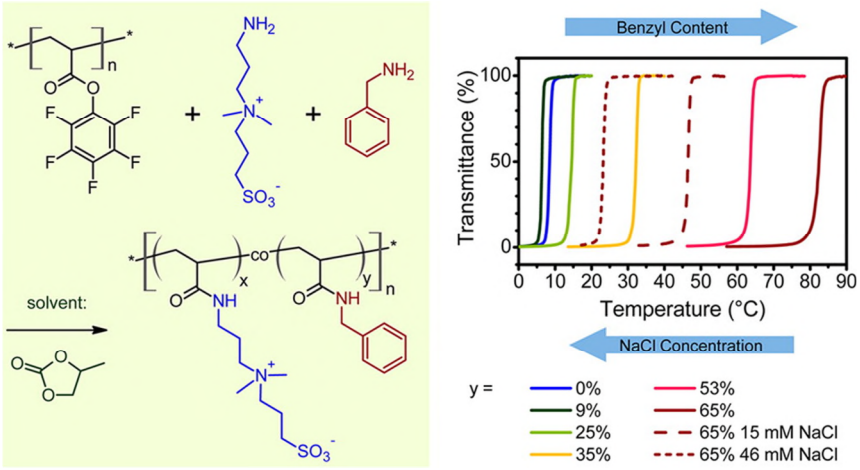

Figure 1.26: Increasing the mol% of benzylamine incorporated into the copolymer increased the UCST observed[139]

The increased solubility with increasing pentylamine incorporation was unusual and could not be explained by self-assembly of the pentylamine groups, as ^{1}H NMR spectroscopy and DLS analysis provided no evidence for micellisation. The authors rationalised it as a result of the higher rotational entropy of the alkyl chain compared to the benzyl ring, and stabilisation of higher energy gauche transformations in solutions. This would result in an increase in entropy upon dissolution of the copolymer, and therefore a lower UCST cloud point compared to the benzyl amine functionalised copolymer.

1.8.3 CO_2-responsive polymers

One stimulus that has recently garnered a lot of attention is carbon dioxide.[76, 164] CO_2 is an interesting stimulus because it is biocompatible and also possesses good membrane permeability.[165] An advantage is that repeated applications do not accumulate by-products, whereas repeatedly changing the pH of a system by additions of acid or base may cause salts to accumulate, which may contaminate the system.[76] Polymers that respond to CO_2 are also of interest due to the potential to use these polymers to trap the gas.[166] Global emissions of CO_2 have risen greatly in the last 40 years or so.[167] Considering that CO_2 is a key contributor to the greenhouse effect,[168] the ability to utilise or trap these emissions are of great interest.

One way that CO_2- responsive polymers can react with CO_2 is by the formation of zwitterionic compounds (see Scheme 1.6).[166, 169] Endo *et al.* synthesised a polymer of

4-(1, 4, 5, 6-tetrahydropyrimide-1-yl) methylsytrene (THPS) by free radical polymerisation.[166] When a solution of this polymer in DMF was bubbled with carbon dioxide for one hour at room temperature, 73% of the amidine moieties fixed CO_2. The fixing efficiency was determined by the weight increase of the reaction mixture.

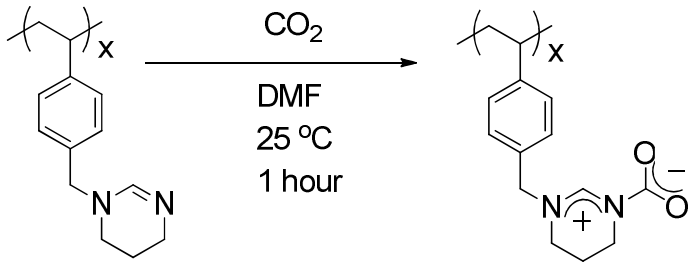

Scheme 1.6: The formation of the zwitterionic polymer formed upon poly(THPS) reacting with CO_2[166]

A copolymer of THPS and *N*-vinylacetamide (NVA) was also synthesised by free radical polymerisation and cast as a film. Exposure to CO_2 at 25 °C for 500 minutes resulted in a fixing efficiency of 25%. Increasing the temperature increased the fixing efficiency (27% at 35 °C and 34% at 45 °C) as a result of higher rates of diffusion of carbon dioxide through the film. Heating the film to 95 °C released the carbon dioxide. The authors demonstrated that the fixing efficiency was not affected over three cycles.[166]

Carbon dioxide can also react with neutral amidine or amine containing polymers and render them charged.[165, 170-173] One area where this has been exploited is in the synthesis of "breathing" vesicles.[165, 171, 172] Yan *et al*. synthesised a diblock copolymer of poly(ethylene oxide) (PEO) and (*N*-amidino) dodecyl acrylamide (PAD) with narrow dispersity ($Đ_M$ = 1.14) *via* ATRP (see Scheme 1.7).[165]

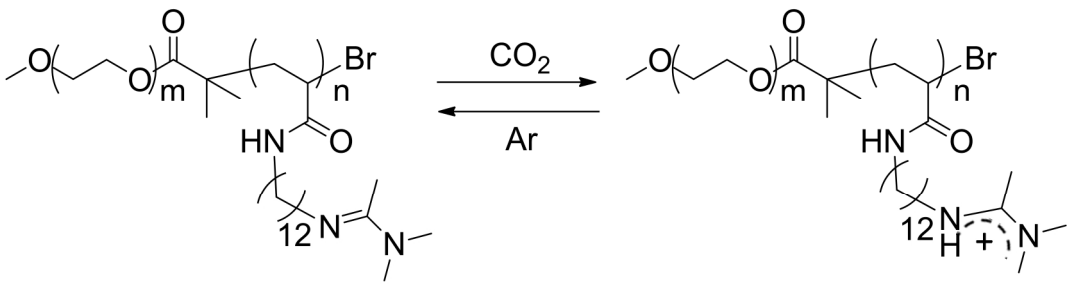

Scheme 1.7: The diblock copolymer of PEO-*b*-PAD synthesised by ATRP and its reversible hydrophilicity change in response to CO_2[165]

The polymers self-assembled in water to form vesicles, evidenced by TEM (D_{av} = 110 nm) and DLS (D_h = 119 nm). The wall thickness of the vesicles was measured to be 22.5 nm from TEM. After treatment with CO_2 for 20 minutes the size of the vesicles had increased to 241 nm measured by DLS and 205 nm by TEM (see Figure 1.27). The wall thickness had decreased to 12.5 nm. This is a result of the protonation of the PAD block.

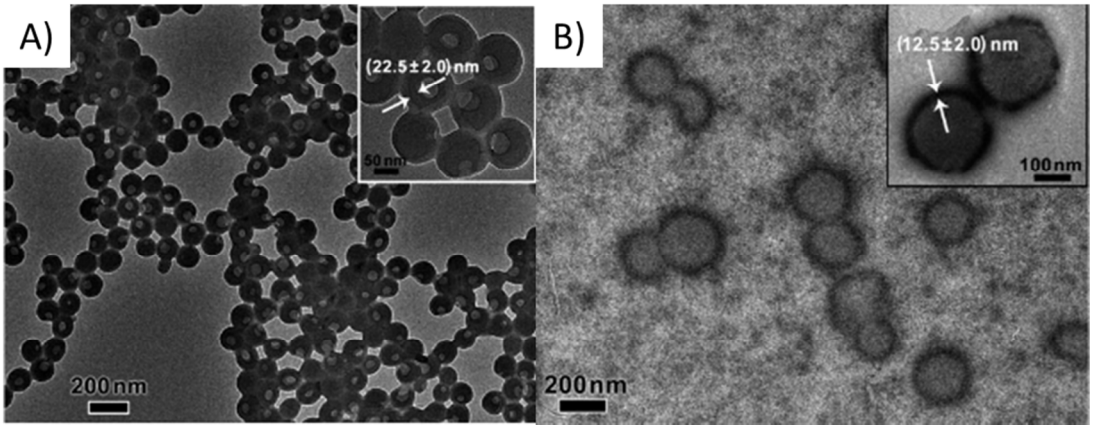

Figure 1.27: TEM images of the PEO-*b*-PAD vesicles A) before treatment with CO_2 and B) after treatment with CO_2

Analysis of the vesicles by SLS before and after treatment with carbon dioxide, shows that the aggregation number does not significantly change, thereby eliminating the possibility of vesicle fusion as an explanation for the size increase observed. However, the authors noted that should the PAD block be completely protonated, the polymer would be completely hydrophilic and therefore unimers would be formed. Zeta potential measurements confirmed that only 41% of the PAD units are protonated after CO_2 treatment. The vesicles could be returned to their original size by treatment with argon. The vesicles were shown to release Rhodamine B from within their central water pools in response to CO_2. The amount of Rhodamine B released could be increased by alternating treatment with CO_2 and argon, as a result of the expansion and retraction movement of the vesicle.[165]

Zhao and co-workers showed a vesicle to unimer transition in response to carbon dioxide.[172] A block copolymer consisting of a relatively short hydrophilic *N, N'*-dimethylacrylamide (PDMA) block and a longer *N, N'*-(diethylamino)ethyl methacrylate (PDEAEMA) block

was synthesised by RAFT polymerisation. Self-assembly in water by nano-precipitation formed vesicles (D_h *ca*. 300 nm). Upon injection of 18 mol% of CO_2 into solution, the vesicles dissociated into unimers, evidenced by an increase in transmittance through the solution and a decrease in size to *ca*. 10 nm observed by DLS. The PDEAEMA block was calculated to be 50% protonated at this concentration of carbon dioxide. Lower mol% of carbon dioxide caused swelling of the vesicles (D_h = 720 nm at 13 mol% CO_2), indicating that the vesicles firstly swell before complete dissociation. Purging the unimeric solution with argon removed the CO_2 but the vesicles were not reformed and precipitation of the polymer was observed.

Cross-linking the PDEAEMA block by incorporation of coumarin methacrylate (CM) followed by photodimerisation, allowed "breathing" vesicles to be formed. Treatment with carbon dioxide resulted in the vesicle swelling and the degree of swelling could be controlled by the cross-linking density.[172] 5 mol% of CM was incorporated into the PDEAEMA block and the percentage of photodimerisation controlled by the length of UV irradiation. 90% photodimerised polymers showed a much reduced swelling than polymers that were only 30% dimerised.

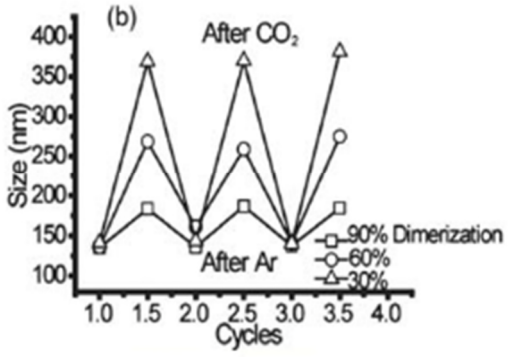

Figure 1.28: The amount of swelling of PDMA-*b*-(PDEAEMA-*co*-PCM) vesicles is controlled by the percentage of coumarin units that were crosslinked[172]

Transitions between other morphologies upon treatment of CO_2 are also possible. Zhao and Yan synthesised a series of triblocks copolymers, consisting of hydrophilic PEO,

hydrophobic PS and PDEAEMA by ATRP.[170] By varying the length of the middle PS block whilst keeping the PEO and PDEAEMA block length constant, spherical micelles, worm-like micelles or vesicles could be formed upon self-assembly into water. In all cases, the PDEAEMA block was situated in the core (see Figure 1.29).

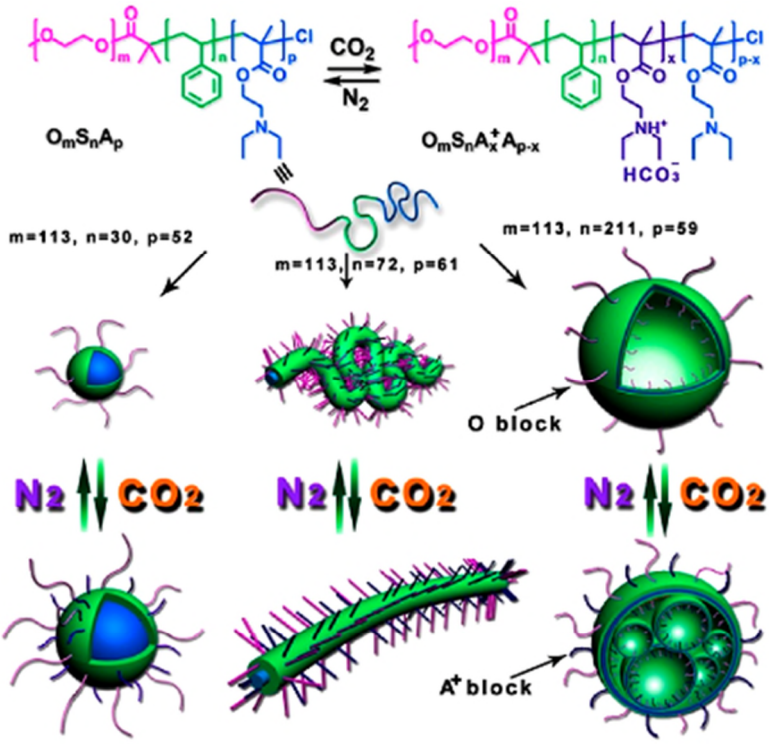

Figure 1.29: Figure showing the morphologies adopted by the series of PEO-*b*-PS-*b*-PDEAEMA triblocks and the morphology deformation upon exposure to CO_2[170]

Purging a solution of spherical micelles with CO_2 for ten minutes resulted in a size increase from 24 nm to 34 nm, as evidenced by TEM analysis. 30 minutes of bubbling with carbon dioxide resulted in micelles with an average size of 67 nm observed in TEM. The size increase was almost linear with the length of time of carbon dioxide treatment.

The worm-like micelles that formed were observed by TEM to have a large number of curling/curving sites, but after 30 minutes of CO_2 exposure the flexible worms had transformed into rigid nanowires (see Figure 1.30).

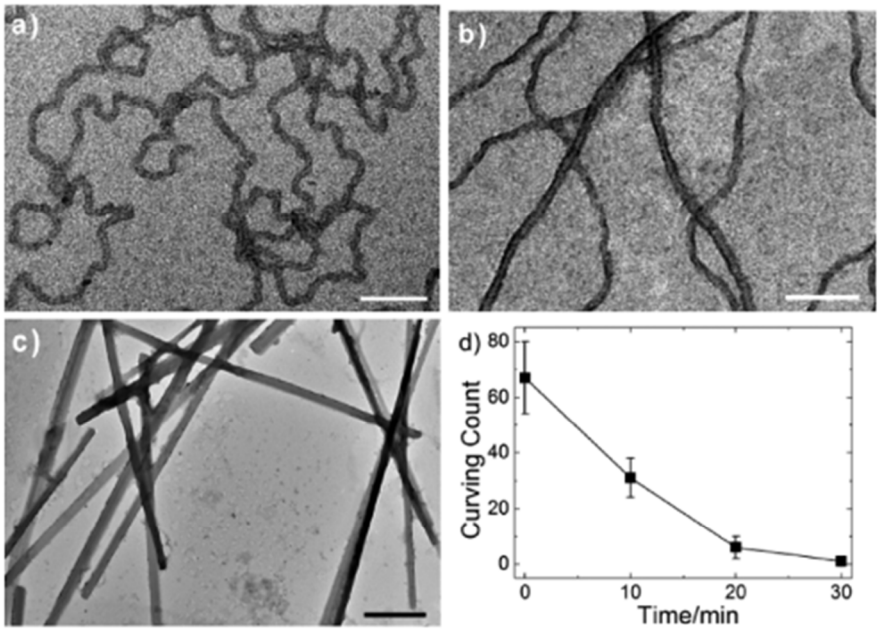

Figure 1.30: TEM images of worm-like micelles of PEO-*b*-PS-*b*-PDEAEMA after a) no exposure to CO_2, b) after 15 minutes exposure to CO_2, c) after 30 minutes of exposure to CO_2 and d) the number of curving sites observed in TEM images after different time lengths of CO_2 exposure[170]

The self-assembled vesicles were also found to undergo a deformation in response to CO_2. The size of the structures did not change upon bubbling with CO_2, but the vesicles appeared to have smaller sacs situated within them. All the shape changes were reversible upon bubbling the polymer solutions with nitrogen.

CO_2-responsive polymers can also be used to tune the LCST cloud points of thermo-responsive polymers.[173, 174] Theato and co-workers synthesised a series of doubly-responsive copolymers by firstly synthesising a homopolymer of PFPA by RAFT.[173] Three different copolymers (**PI** – **PIII**) were then made by substituting the PFP groups with functional primary amines. **PI** contained isopropyl amine (NIPAM) and 3-*N, N*-(dimethylamino) propylamine (DMPA), **PII** contained NIPAM and $_L$-arginine and **PIII** contained cyclopropylamine (CPA) and $_L$-arginine (see Figure 1.31).

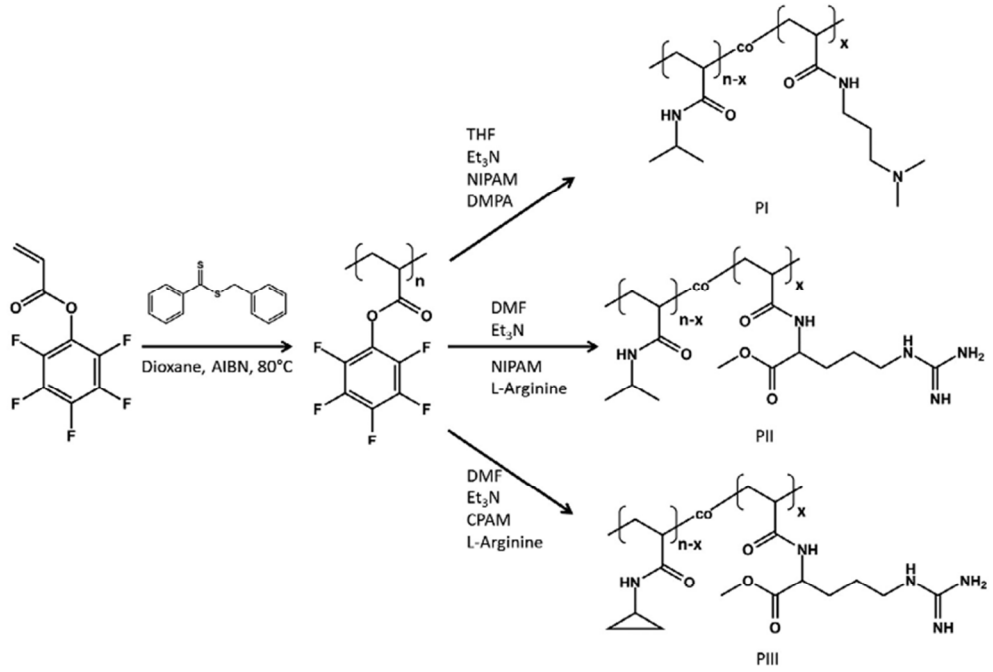

Figure 1.31: The different polymers synthesised by reacting a PFP homopolymer with various amines[173]

The LCST cloud point of **PI** was determined to be 44.8 °C, which is higher that than seen for homopolymers of PNIPAM (31 °C). The LCST cloud point of a PNIPAM homopolymer was shown to be unaffected by bubbling with CO_2 but the cloud point of **PI** increased to 51.1 °C after 25 minutes of purging with CO_2. Purging the solution with argon resulted in the cloud point decreasing to that observed before CO_2 exposure. **PII** was not soluble in water, indicating that incorporation of the $_L$-arginine had dramatically decreased the LCST cloud point of the NIPAM block. **PIII** had the opposite response to CO_2 than **PI**. After exposure to CO_2 the cloud point was reduced from 54.7 °C to 39.9 °C (see Figure 1.32).

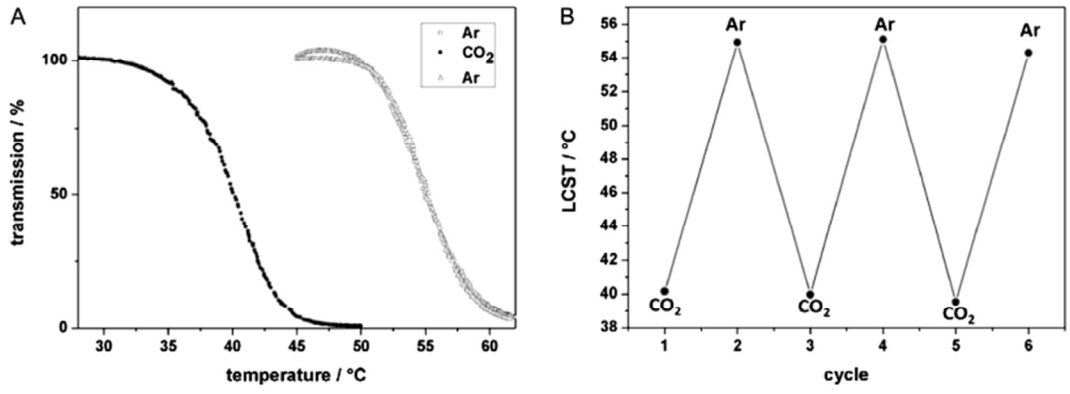

Figure 1.32: The change in LCST cloud point for copolymer 3 after bubbling with carbon dioxide or argon[173]

1.8.4 Multi-responsive polymers

Combining two or more responsive blocks into one polymer yields multi stimuli-responsive polymers. There are different effects seen when combining multiple responsive blocks into one polymer. One possibility is that application of one stimulus will result in the response from both groups. This occurs when one stimulus is applied and the respective group responds, in itself creating the stimulus that the second group is responsive to.[175] For example, Uchiyama *et al*. synthesised a copolymer consisting of *N, N*-dimethylaminopropyl acrylamide (DMAPAM), *N*-*t*-butyl acrylamide (NTBAM) and a benzofuran containing moiety (DBD-AE) (see Figure 1.33).[176]

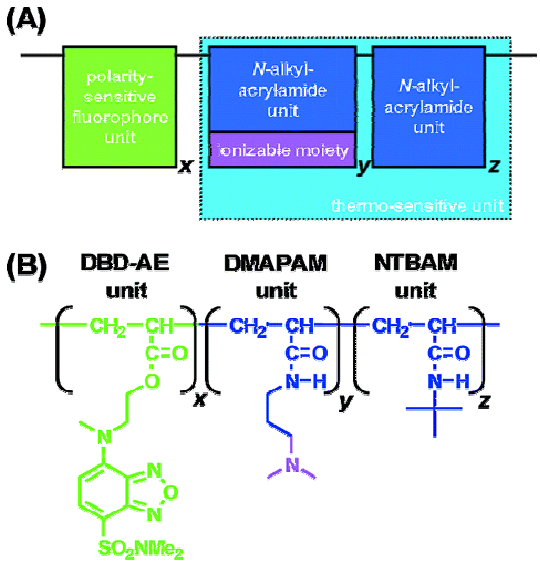

Figure 1.33: The structure of the thermo-responsive copolymer bearing the benzofuran group[176]

The NTBAM is thermo-responsive and displays LCST behaviour. The fluorescence response of the benzofuran is affected by the surrounding environment and is higher in a nonpolar medium. Heating a solution of the polymer resulted in a significant increase in the fluorescence intensity of the polymer, along with a change in the emission wavelength, showing that the microenvironment around the benzofuranyl groups had become more hydrophobic as the NTBAM units had become hydrophobic and collapsed. The DMAPAM units were required in order to retain the solubility of the polymer above its LCST cloud

point. Therefore this shows an example of applying one stimulus (heat) which causes the polymer to become more hydrophobic and consequently, the benzofuran fluoresces.

More commonly, stimulating one group does not affect the other, and therefore these polymers can be considered to have orthogonal functionality.[175] Examples of combined stimuli are temperature-light,[49, 74, 177] temperature-pH,[100, 178-182] and temperature-CO_2.[183] There are also some examples of triply responsive polymers.[184-187]

McCormick and co-workers synthesised diblock copolymers of DEAEMA and *N*-isopropylacrylamide (NIPAM) by aqueous RAFT polymerisation.[188] Two different polymers with the same DEAEMA block lengths but different lengths of NIPAM were investigated (52.5 wt% NIPAM and 70.8 wt% NIPAM). Both polymers were found to respond to temperature and pH, but the morphologies formed were different, depending on the NIPAM block length (see Figure 1.34).

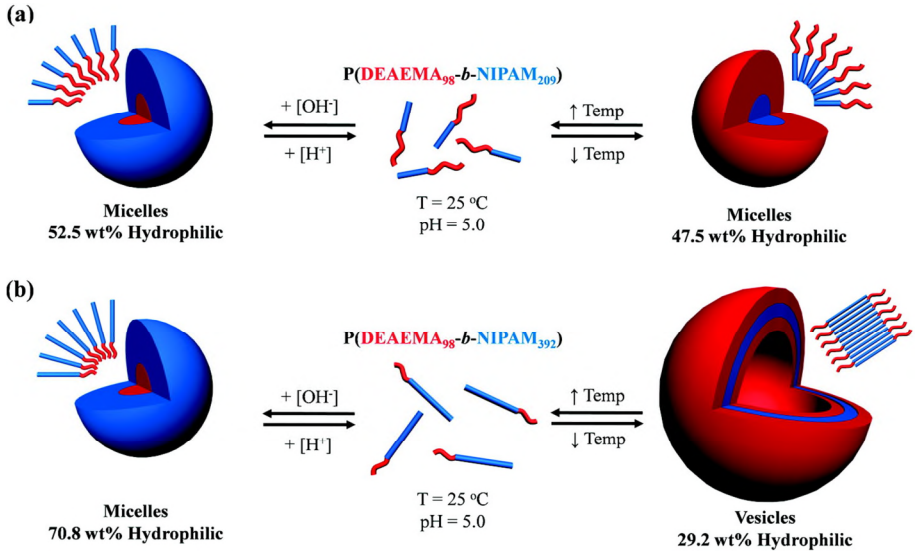

Figure 1.34: Schematic of the morphology transition of the diblock copolymers of DEAEMA-*b*-NIPAM in response to temperature and pH, a) 52.5 wt% NIPAM, b) 70.8 wt% NIPAM

At pH 5 and 25 °C (below the pK_a of the DEAEMA block and the LCST cloud point of the NIPAM block) both polymers were molecularly dissolved in solution. Upon raising the pH to above the pK_a of the DEAEMA block, micelles with a DEAEMA core were formed for both polymers. The longer diblock copolymer formed slightly larger micelles (42 nm

compared to 50 nm). When the temperature was raised to above the LCST cloud point of the NIPAM block (keeping the solution pH at 5.0 so the DEAEMA block remained protonated), the shorter block copolymer (52.5 wt% NIPAM) formed micelles with a NIPAM core. The longer diblock (70.8 wt% NIPAM) formed vesicles.[188]

Dong *et al*. reported the synthesis of a copolymer and subsequent self-assembly into a micelle bearing a photoresponsive shell and a pH- and thermo-responsive core.[187] *N, N*-dimethylamino ethyl methacrylate (DMAEMA) was synthesised by ATRP and partially quaternised using a bromo-functionalised pyrene, to yield the triply responsive polymer. The LCST cloud point for the pyrene functionalised polymer was measured to be 54 °C. The polymer was self-assembled in water to form micelles with a pyrene shell and DMAEMA core (D_h = 130 nm). Irradiation with UV light caused micelle dissociation (D_h = 6.2 nm), whilst heating to above the LCST of the DMAEMA block caused the micelles to shrink. Lowering the pH of the micelle solution to pH 3 caused some micelle dissociation and some micelle swelling, evidenced by two peaks observed in DLS analysis (D_h = 7.2 and 148 nm). Raising the pH to pH 10 caused two populations to form, one corresponding to the shrunken micelles (D_h = 44 nm), and a much larger peak (D_h = 550 nm) corresponding to micelle aggregation (see Figure 1.35).

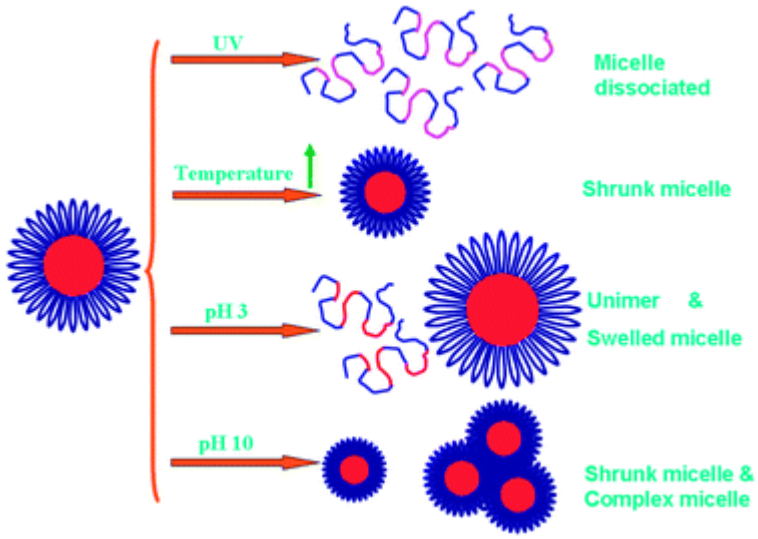

Figure 1.35: Schematic showing the change in size of the micelle in response to different stimuli[187]

1.9 Conclusions

This Chapter has introduced the key aspects of RAFT polymerisation and the importance of this technique in the synthesis of well-defined block copolymers for self-assembly applications. Some of the different procedures for introducing functionality into the polymer, both along the backbone and at the chain ends, have been discussed. The self-assembly of amphiphilic copolymers into different morphologies and the effect that altering the amphiphilic balance by using responsive polymers has on the morphology adopted has been introduced. Several different stimuli that will be investigated within this thesis have been briefly reviewed.

1.10 Aims of the Thesis

Our research interest focuses on the synthesis of well-defined stimuli-responsive polymers and their incorporation into self-assembling polymeric systems. We propose that application of a chosen stimulus can allow for some control over the morphology adopted by the polymers in aqueous solution. The potential application of these sophisticated structures in areas such as drug delivery or nanoreactors has heightened the interest in this research area.

This Thesis aims to broaden the current knowledge of stimuli-responsive polymers, discussed in this Chapter, by utilising novel, or little explored, monomers. We aim to synthesise well-defined amphiphilic block copolymers from these responsive-monomers by a combination of Reversible Addition Fragmentation chain Transfer (RAFT) polymerisation and post-polymerisation modification techniques in order to achieve the desired polymer architecture. We will use a range of different stimuli, from the more commonly utilised temperature and pH, to the relatively new area of carbon dioxide responsive polymers, to afford a hydrophilicity change within the polymer and achieve a change in the morphology of the nanostructure in solution. We aim to achieve different morphology transitions, such that encapsulation and release of both hydrophilic and hydrophobic payloads are possible.

1.11 References

1. H. Staudinger, *Ber. Dtsch. Chem. Ges.*, 1920, 53, 1073-1085.
2. M. Szwarc, *Nature*, 1956, 178, 1168-1169.
3. D. Colombani, *Prog. Polym. Sci.*, 1997, 22, 1649-1720.
4. IUPAC, *Compendium of Chemical Terminology (the "Gold Book")*, Blackwell Scientific Publications, Oxford, 2 edn., 1997.
5. R. P. Quirk and B. Lee, *Polym. Int.*, 1992, 27, 359-367.
6. M. Szwarc, *J. Polym. Sci., Part A: Polym. Chem.*, 1998, 36, IX-XV.
7. C. J. Hawker and K. L. Wooley, *Science*, 2005, 309, 1200-1205.
8. A. D. Jenkins, R. D. Jones and G. Moad, *Pure Appl. Chem.*, 2010, 82, 483-491.
9. G. Moad, E. Rizzardo and S. Thang, *Acc. Chem. Res.*, 2008, 41, 1133-1142.
10. W. A. Braunecker and K. Matyjaszewski, *Prog. Polym. Sci.*, 2007, 32, 93-146.
11. K. Matyjaszewski, S. Gaynor and J.-S. Wang, *Macromolecules*, 1995, 28, 2093-2095.
12. C. J. Hawker, A. W. Bosman and E. Harth, *Chem. Rev.*, 2001, 101, 3661-3688.
13. G. Moad, *Aust. J. Chem.*, 2006, 59, 661-662.
14. J. Chiefari, Y. Chong, F. Ercole, J. Krstina, J. Jeffery, T. Le, R. Mayadunne, G. Meijs, C. Moad and G. Moad, *Macromolecules*, 1998, 31, 5559-5562.
15. T. Otsu and M. Yoshida, *Makromol. Chem. Rapid. Commun.*, 1982, 3, 127-132.
16. T. Otsu, M. Yoshida and T. Tazaki, *Makromol. Chem. Rapid. Commun.*, 1982, 3, 133-140.
17. A. Goto and T. Fukuda, *Prog. Polym. Sci.*, 2004, 29, 329-385.
18. X. Wang, S. Li, Y. Su, F. Huo and W. Zhang, *J. Polym. Sci., Part A: Polym. Chem.*, 2013, 51, 2188-2198.
19. B. S. Sumerlin, M. S. Donovan, Y. Mitsukami, A. B. Lowe and C. L. McCormick, *Macromolecules*, 2001, 34, 6561-6564.
20. C. L. McCormick and A. B. Lowe, *Acc. Chem. Res.*, 2004, 37, 312-325.
21. H. Willcock, A. Lu, C. F. Hansell, E. Chapman, I. R. Collins and R. K. O'Reilly, *Polym. Chem.*, 2014, 5, 1023-1030.
22. S. Kessel, N. P. Truong, Z. Jia and M. J. Monteiro, *J. Polym. Sci., Part A: Polym. Chem.*, 2012, 50, 4879-4887.
23. D. J. Keddie, *Chem. Soc. Rev.*, 2014, 43, 496-505.
24. P. C. D. Charmot, D. Michelet, S. Z. Zard, T. Biadatti, *Chem. Abstr.*, 1999, 130, 82018.
25. G. Moad, Y. Chong, A. Postma, E. Rizzardo and S. Thang, *Polymer*, 2005, 46, 8458-8468.

26. C. Barner-Kowollik, M. Buback, B. Charleux, M. L. Coote, M. Drache, T. Fukuda, A. Goto, B. Klumperman, A. B. Lowe, J. B. McLeary, G. Moad, M. J. Monteiro, R. D. Sanderson, M. P. Tonge and P. Vana, *J. Polym. Sci., Part A: Polym. Chem.*, 2006, 44, 5809-5831.
27. G. Moad, *Macromol. Chem. Phys.*, 2014, 215, 9-26.
28. J. Chiefari, R. T. A. Mayadunne, C. L. Moad, G. Moad, E. Rizzardo, A. Postma and S. H. Thang, *Macromolecules*, 2003, 36, 2273-2283.
29. R. Mayadunne, E. Rizzardo, J. Chiefari, Y. Chong, G. Moad and S. Thang, *Macromolecules*, 1999, 32, 6977-6980.
30. J. Skey and R. K. O'Reilly, *Chem. Commun.*, 2008, 2008, 4183-4185.
31. M. R. Wood, D. J. Duncalf, S. P. Rannard and S. Perrier, *Org. Lett.*, 2006, 8, 553-556.
32. G. Moad, Rizzardo, E., Thang, S., *Material Matters*, 2010, 5, 2-4.
33. G. Moad, E. Rizzardo and S. H. Thang, *Aust. J. Chem.*, 2005, 58, 379-410.
34. T. R. Wilks, J. Bath, J. W. de Vries, J. E. Raymond, A. Herrmann, A. J. Turberfield and R. K. O'Reilly, *ACS Nano*, 2013, 7, 8561-8572.
35. P. J. Roth, K. T. Wiss, R. Zentel and P. Theato, *Macromolecules*, 2008, 41, 8513-8519.
36. C. Boyer, A. Granville, T. P. Davis and V. Bulmus, *J. Polym. Sci., Part A: Polym. Chem.*, 2009, 47, 3773-3794.
37. H. Willcock and R. K. O'Reilly, *Polym. Chem.*, 2010, 1, 149-157.
38. J. M. Spruell, B. A. Levy, A. Sutherland, W. R. Dichtel, J. Y. Cheng, J. F. Stoddart and A. Nelson, *J. Polym. Sci., Part A: Polym. Chem.*, 2009, 47, 346-356.
39. S. Perrier and P. Takolpuckdee, *J. Polym. Sci., Part A: Polym. Chem.*, 2005, 43, 5347-5393.
40. S. Perrier, P. Takolpuckdee and C. A. Mars, *Macromolecules*, 2005, 38, 2033-2036.
41. M. Chen, G. Moad and E. Rizzardo, *J. Polym. Sci., Part A: Polym. Chem.*, 2009, 47, 6704-6714.
42. A. Postma, T. P. Davis, G. Moad and M. S. O'Shea, *Macromolecules*, 2005, 38, 5371-5374.
43. Y. K. Chong, G. Moad, E. Rizzardo and S. H. Thang, *Macromolecules*, 2007, 40, 4446-4455.
44. K. E. B. Doncom, C. F. Hansell, P. Theato and R. K. O'Reilly, *Polym. Chem.*, 2012, 3, 3007-3015.
45. M. Deletre and G. Levesque, *Macromolecules*, 1990, 23, 4733-4741.
46. C. Boyer, V. Bulmus and T. P. Davis, *Macromol. Rapid Commun.*, 2009, 30, 493-497.

47. A. W. York, C. W. Scales, F. Huang and C. L. McCormick, *Biomacromolecules*, 2007, 8, 2337-2341.
48. C. Boyer and T. P. Davis, *Chem. Commun.*, 2009, 6029-6031.
49. F. D. Jochum and P. Theato, *Macromolecules*, 2009, 42, 5941-5945.
50. M. Eberhardt, R. Mruk, R. Zentel and P. Theato, *Eur. Polym. J.*, 2005, 41, 1569-1575.
51. K. A. Günay, P. Theato and H. A. Klok, *J. Polym. Sci., Part A: Polym. Chem.*, 2013, 51, 1-28.
52. M. Eberhardt and P. Théato, *Macromol. Rapid Commun.*, 2005, 26, 1488-1493.
53. P. Theato, *J. Polym. Sci., Part A: Polym. Chem.*, 2008, 46, 6677-6687.
54. J. Seo, P. Schattling, T. Lang, F. Jochum, K. Nilles, P. Theato and K. Char, *Langmuir*, 2009, 26, 1830-1836.
55. K. Nilles and P. Theato, *J. Polym. Sci., Part A: Polym. Chem.*, 2010, 48, 3683-3692.
56. P. Theato and H.-A. Klok, eds., *Functional Polymers by Post-Polymerization Modification. Concepts, Guidelines, and Applications*, Wiley-VCH, Weinhelm, 2012.
57. C. Boyer, A. Granville, T. P. Davis and V. Bulmus, *Journal of Polymer Science, Part A: Polymer Chemistry*, 2009, 47, 3773-3794.
58. G. Riess, *Prog. Polym. Sci.*, 2003, 28, 1107-1170.
59. A. Blanazs, S. P. Armes and A. J. Ryan, *Macromol. Rapid Commun.*, 2009, 30, 267-277.
60. N. Petzetakis, A. P. Dove and R. K. O'Reilly, *Chem. Sci.*, 2011, 2, 955-960.
61. D. E. Discher and A. Eisenberg, *Science*, 2002, 297, 967-973.
62. Y. Mai and A. Eisenberg, *Chem. Soc. Rev.*, 2012, 41, 5969-5985.
63. J. Israelachvili, *Intermolecular and Surface Forces*, Academic Press, London, 2nd edn., 1991.
64. R. B. Grubbs and Z. Sun, *Chem. Soc. Rev.*, 2013, 42, 7436-7445.
65. D. E. Discher and F. Ahmed, in *Annu. Rev. Biomed. Eng.*, Annual Reviews, Palo Alto, 2006, vol. 8, pp. 323-341.
66. T. Nicolai, O. Colombani and C. Chassenieux, *Soft Matter*, 2010, 6, 3111-3118.
67. D. Schmaljohann, *Adv. Drug Deliver. Rev.*, 2006, 58, 1655-1670.
68. S. Mura, J. Nicolas and P. Couvreur, *Nature Mater.*, 2013, 12, 991-1003.
69. O. Onaca, R. Enea, D. W. Hughes and W. Meier, *Macromol. Biosci.*, 2009, 9, 129-139.
70. Q. Zhang, N. Re Ko and J. Kwon Oh, *Chem. Commun.*, 2012, 48, 7542-7552.
71. M. I. Gibson and R. K. O'Reilly, *Chem. Soc. Rev.*, 2013, 42, 7204-7213.
72. R. Liu, M. Fraylich and B. Saunders, *Colloid. Polym. Sci.*, 2009, 287, 627-643.

73. D. Roy, W. L. A. Brooks and B. S. Sumerlin, *Chem. Soc. Rev.*, 2013, 42, 7214-7243.
74. F. D. Jochum and P. Theato, *Chem. Soc. Rev.*, 2013, 42, 7468-7483.
75. S. Dai, P. Ravi and K. C. Tam, *Soft Matter*, 2008, 4, 435-449.
76. S. Lin and P. Theato, *Macromol. Rapid Commun.*, 2013, 34, 1118-1133.
77. S. Dai, P. Ravi and K. C. Tam, *Soft Matter*, 2009, 5, 2513-2533.
78. K. Huh, H. Kang, Y. Lee and Y. Bae, *Macromol. Res.*, 2012, 20, 224-233.
79. M. H. A. H. Almeida, P. Lobao, *J. Appl. Pharm. Sci.*, 2012, 2, 1-10.
80. J. P. Salvage, S. F. Rose, G. J. Phillips, G. W. Hanlon, A. W. Lloyd, I. Y. Ma, S. P. Armes, N. C. Billingham and A. L. Lewis, *J. Controlled Release*, 2005, 104, 259-270.
81. J. Du, Y. Tang, A. L. Lewis and S. P. Armes, *J. Am. Chem. Soc.*, 2005, 127, 17982-17983.
82. N. Petzetakis, D. Walker, A. P. Dove and R. K. O'Reilly, *Soft Matter*, 2012, 8, 7408-7414.
83. N. Petzetakis, M. P. Robin, J. P. Patterson, E. G. Kelley, P. Cotanda, P. H. H. Bomans, N. A. J. M. Sommerdijk, A. P. Dove, T. H. Epps and R. K. O'Reilly, *ACS Nano*, 2013, 7, 1120-1128.
84. S. Dai, P. Ravi, K. C. Tam, B. W. Mao and L. H. Gan, *Langmuir*, 2003, 19, 5175-5177.
85. R. Hoogenboom, U. S. Schubert, W. Van Camp and F. E. Du Prez, *Macromolecules*, 2005, 38, 7653-7659.
86. R. K. O'Reilly, M. J. Joralemon, C. J. Hawker and K. L. Wooley, *J. Polym. Sci., Part A: Polym. Chem.*, 2006, 44, 5203-5217.
87. S. Yu, C. He, J. Ding, Y. Cheng, W. Song, X. Zhuang and X. Chen, *Soft Matter*, 2013, 9, 2637-2645.
88. B. Khorsand and J. K. Oh, *J. Polym. Sci., Part A: Polym. Chem.*, 2013, 51, 1620-1629.
89. B. Kim, E. Lee, Y. Kim, S. Park, G. Khang and D. Lee, *Adv. Funct. Mater.*, 2013, 23, 5091-5097.
90. H. T. T. Duong, C. P. Marquis, M. Whittaker, T. P. Davis and C. Boyer, *Macromolecules*, 2011, 44, 8008-8019.
91. S. S. Naik, J. G. Ray and D. A. Savin, *Langmuir*, 2011, 27, 7231-7240.
92. Y. Q. Hu, M. S. Kim, B. S. Kim and D. S. Lee, *Polymer*, 2007, 48, 3437-3443.
93. J. Fan, F. Zeng, S. Wu and X. Wang, *Biomacromolecules*, 2012, 13, 4126-4137.
94. S. W. Kang, Y. Li, J. H. Park and D. S. Lee, *Polymer*, 2013, 54, 102-110.
95. B. Surnar and M. Jayakannan, *Biomacromolecules*, 2013, 14, 4377-4387.

96. W. Zhang, J. He, Z. Liu, P. Ni and X. Zhu, *J. Polym. Sci., Part A: Polym. Chem.*, 2010, 48, 1079-1091.
97. A. Sanchez-Sanchez, D. A. Fulton and J. A. Pomposo, *Chem. Commun.*, 2014, 50, 1871-1874.
98. S. I. Ali, J. P. A. Heuts and A. M. van Herk, *Soft Matter*, 2011, 7, 5382-5390.
99. J. Yao, Y. Ruan, T. Zhai, J. Guan, G. Tang, H. Li and S. Dai, *Polymer*, 2011, 52, 3396-3404.
100. Z. Ge and S. Liu, *Macromol. Rapid Commun.*, 2013, 34, 922-930.
101. X. Xu, A. E. Smith, S. E. Kirkland and C. L. McCormick, *Macromolecules*, 2008, 41, 8429-8435.
102. L. He, E. S. Read, S. P. Armes and D. J. Adams, *Macromolecules*, 2007, 40, 4429-4438.
103. L.-Y. Y. C-L. Peng, T-Y. Luo, P-S. Lai, S-J. Yang, W-J. Lin, M-J. Shieh, *Nanotechnology*, 2010, 21, 155103-.
104. V. Bütün, S. Liu, J. V. M. Weaver, X. Bories-Azeau, Y. Cai and S. P. Armes, *React. Funct. Polym.*, 2006, 66, 157-165.
105. S. Liu and S. P. Armes, *Angew. Chem. Int. Ed.*, 2002, 41, 1413-1416.
106. Y. Liu, W. Wang, J. Yang, C. Zhou and J. Sun, *Asian J. Pharm. Sci.*, 2013, 8, 159-167.
107. S. Zhai, Y. Ma, Y. Chen, D. Li, J. Cao, Y. Liu, M. Cai, X. Xie, Y. Chen and X. Luo, *Polym. Chem.*, 2014, 5, 1285-1297.
108. T. Matini, N. Francini, A. Battocchio, S. G. Spain, G. Mantovani, M. J. Vicent, J. Sanchis, E. Gallon, F. Mastrotto, S. Salmaso, P. Caliceti and C. Alexander, *Polym. Chem.*, 2014, 5, 1626-1636.
109. W. Chen and J. Du, *Sci. Rep.*, 2013, 3.
110. C. Zheng, X. Yao and L. Qiu, *Macromol. Biosci.*, 2011, 11, 338-343.
111. J. Seuring and S. Agarwal, *Macromol. Rapid Commun.*, 2012, 33, 1898-1920.
112. H. G. Schild, *Prog. Polym. Sci.*, 1992, 17, 163-249.
113. S. Furyk, Y. Zhang, D. Ortiz-Acosta, P. S. Cremer and D. E. Bergbreiter, *J. Polym. Sci., Part A: Polym. Chem.*, 2006, 44, 1492-1501.
114. Y. Xia, X. Yin, N. A. D. Burke and H. D. H. Stöver, *Macromolecules*, 2005, 38, 5937-5943.
115. Y. Xia, N. A. D. Burke and H. D. H. Stöver, *Macromolecules*, 2006, 39, 2275-2283.
116. P. Kujawa, F. Segui, S. Shaban, C. Diab, Y. Okada, F. Tanaka and F. M. Winnik, *Macromolecules*, 2005, 39, 341-348.
117. P. Kujawa, F. Tanaka and F. M. Winnik, *Macromolecules*, 2006, 39, 3048-3055.

118. S. Jana, S. P. Rannard and A. I. Cooper, *Chem. Commun.*, 2007, DOI: 10.1039/B702067H, 2962-2964.
119. T. P. Silverstein, *J. Chem. Educ.*, 1998, 75, 116.
120. M. Okano and F. Winnick, *Material Matters*, 2010, 5.3, 56.
121. C. L. McCormick, B. S. Sumerlin, B. S. Lokitz and J. E. Stempka, *Soft Matter*, 2008, 4, 1760-1773.
122. Y. Morishima, *Angew. Chem. Int. Ed.*, 2007, 46, 1370-1372.
123. A. Sundararaman, T. Stephan and R. B. Grubbs, *J. Am. Chem. Soc.*, 2008, 130, 12264-12265.
124. A. O. Moughton and R. K. O'Reilly, *Chem. Commun.*, 2010, 46, 1091-1093.
125. A. O. Moughton, J. P. Patterson and R. K. O'Reilly, *Chem. Commun.*, 2011, 47, 355-357.
126. K. Wei, L. Su, G. Chen and M. Jiang, *Polymer*, 2011, 52, 3647-3654.
127. J. Seuring and S. Agarwal, *ACS Macro Lett.*, 2013, 2, 597-600.
128. H. C. Haas, R. D. Moreau and N. W. Schuler, *J. Polym. Sci., Part B: Polym. Phys.*, 1967, 5, 915-927.
129. J. Seuring and S. Agarwal, *Macromol. Chem. Phys.*, 2010, 211, 2109-2117.
130. S. Glatzel, A. Laschewsky and J.-F. o. Lutz, *Macromolecules*, 2010, 44, 413-415.
131. H. Mori, I. Kato, S. Saito and T. Endo, *Macromolecules*, 2009, 43, 1289-1298.
132. F. Liu, J. Seuring and S. Agarwal, *J. Polym. Sci., Part A: Polym. Chem.*, 2012, 50, 4920-4928.
133. J. Seuring, F. M. Bayer, K. Huber and S. Agarwal, *Macromolecules*, 2011, 45, 374-384.
134. A. B. Lowe and C. L. McCormick, *Chem. Rev.*, 2002, 102, 4177-4190.
135. F. Dai, P. Wang, Y. Wang, L. Tang, J. Yang, W. Liu, H. Li and G. Wang, *Polymer*, 2008, 49, 5322-5328.
136. P. Mary, D. D. Bendejacq, M. P. Labeau and P. Dupuis, *J. Phys. Chem. B*, 2007, 111, 7767-7777.
137. D. N. Schulz, D. G. Peiffer, P. K. Agarwal, J. Larabee, J. J. Kaladas, L. Soni, B. Handwerker and R. T. Garner, *Polymer*, 1986, 27, 1734-1742.
138. A. Takahashi, K. Hamai, Y. Okada and S. Sakohara, *Polymer*, 2011, 52, 3791-3799.
139. P. A. Woodfield, Y. Zhu, Y. Pei and P. J. Roth, *Macromolecules*, 2014, 47, 750-762.
140. B. Yu, A. B. Lowe and K. Ishihara, *Biomacromolecules*, 2009, 10, 950-958.
141. J. C. Salamone, W. Volksen, A. P. Olson and S. C. Israel, *Polymer*, 1978, 19, 1157-1162.
142. V. M. Monroy Soto and J. C. Galin, *Polymer*, 1984, 25, 121-128.
143. R. Hart and D. Timmerman, *J. Polym. Sci.*, 1958, 28, 638-640.

144. W. F. Lee and C. C. Tsai, *Polymer*, 1994, 35, 2210-2217.
145. C. L. McCormick and L. C. Salazar, *Polymer*, 1992, 33, 4617-4624.
146. H. Wang, T. Hirano, M. Seno and T. Sato, *Eur. Polym. J.*, 2003, 39, 2107-2114.
147. D. Wang, T. Wu, X. Wan, X. Wang and S. Liu, *Langmuir*, 2007, 23, 11866-11874.
148. M. S. Donovan, B. S. Sumerlin, A. B. Lowe and C. L. McCormick, *Macromolecules*, 2002, 35, 8663-8666.
149. M. S. Donovan, A. B. Lowe, T. A. Sanford and C. L. McCormick, *J. Polym. Sci., Part A: Polym. Chem.*, 2003, 41, 1262-1281.
150. M. Arotçaréna, B. Heise, S. Ishaya and A. Laschewsky, *J. Am. Chem. Soc.*, 2002, 124, 3787-3793.
151. Z. Tuzar, H. Pospisil, J. Plestil, A. B. Lowe, F. L. Baines, N. C. Billingham and S. P. Armes, *Macromolecules*, 1997, 30, 2509-2512.
152. A. B. Lowe, N. C. Billingham and S. P. Armes, *Macromolecules*, 1999, 32, 2141-2148.
153. V. Butun, C. E. Bennett, M. Vamvakaki, A. B. Lowe, N. C. Billingham and S. P. Armes, *J. Mater. Chem.*, 1997, 7, 1693-1695.
154. A. B. Lowe, N. C. Billingham and S. P. Armes, *Chem. Commun.*, 1996, DOI: 10.1039/cc9960001555, 1555-1556.
155. M. Noh, Y. Mok, D. Nakayama, S. Jang, S. Lee, T. Kim and Y. Lee, *Polymer*, 2013, 54, 5338-5344.
156. Y. J. Che, Y. Tan, J. Cao and G. Y. Xu, *J. Macromol. Sci., Phys.*, 2010, 49, 695-710.
157. Y. J. Shih, Y. Chang, A. Deratani and D. Quemener, *Biomacromolecules*, 2012, 13, 2849-2858.
158. Z. Dong, J. Mao, D. Wang, M. Yang, W. Wang, S. Bo and X. Ji, *Macromol. Chem. Phys.*, 2014, 215, 111-120.
159. J. Virtanen, M. Arotçaréna, B. Heise, S. Ishaya, A. Laschewsky and H. Tenhu, *Langmuir*, 2002, 18, 5360-5365.
160. J. Ning, K. Kubota, G. Li and K. Haraguchi, *React. Funct. Polym.*, 2013, 73, 969-978.
161. J. Seuring and S. Agarwal, *Macromolecules*, 2012, 45, 3910-3918.
162. H.-Y. Tian, J.-J. Yan, D. Wang, C. Gu, Y.-Z. You and X.-S. Chen, *Macromol. Rapid Commun.*, 2011, 32, 660-664.
163. Y. Su, M. Dan, X. Xiao, X. Wang and W. Zhang, *J. Polym. Sci., Part A: Polym. Chem.*, 2013, 51, 4399-4412.
164. J. Y. Quek, T. P. Davis and A. B. Lowe, *Chem. Soc. Rev.*, 2013, 42, 7326-7334.
165. Q. Yan, R. Zhou, C. Fu, H. Zhang, Y. Yin and J. Yuan, *Angew. Chem. Int. Ed.*, 2011, 50, 4923-4927.

166. T. Endo, D. Nagai, T. Monma, H. Yamaguchi and B. Ochiai, *Macromolecules*, 2004, 37, 2007-2009.
167. N. Stern, *Stern Review: The Economics of Climate Change*, Cambridge University Press, Cambridge, 2006.
168. M. Z. Jacobson, *Energy Environ. Sci.*, 2009, 2, 148-173.
169. H. Zhou, W.-Z. Zhang, Y.-M. Wang, J.-P. Qu and X.-B. Lu, *Macromolecules*, 2009, 42, 5419-5421.
170. Q. Yan and Y. Zhao, *J. Am. Chem. Soc.*, 2013, 135, 16300-16303.
171. Q. Yan, J. Wang, Y. Yin and J. Yuan, *Angew. Chem. Int. Ed.*, 2013, 52, 5070-5073.
172. B. Yan, D. Han, O. Boissiere, P. Ayotte and Y. Zhao, *Soft Matter*, 2013, 9, 2011-2016.
173. P. Schattling, I. Pollmann and P. Theato, *React. Funct. Polym.*, 2014, 75, 16-21.
174. D. Han, X. Tong, O. Boissière and Y. Zhao, *ACS Macro Lett.*, 2011, 1, 57-61.
175. P. Schattling, F. D. Jochum and P. Theato, *Polym. Chem.*, 2014, 5, 25-36.
176. S. Uchiyama, N. Kawai, A. P. de Silva and K. Iwai, *J. Am. Chem. Soc.*, 2004, 126, 3032-3033.
177. F. D. Jochum and P. Theato, *Chem. Commun.*, 2010, 46, 6717-6719.
178. C. Chang, H. Wei, J. Feng, Z.-C. Wang, X.-J. Wu, D.-Q. Wu, S.-X. Cheng, X.-Z. Zhang and R.-X. Zhuo, *Macromolecules*, 2009, 42, 4838-4844.
179. J. Mao, S. Bo and X. Ji, *Langmuir*, 2011, 27, 7385-7391.
180. S. Medel, J. Manuel García, L. Garrido, I. Quijada-Garrido and R. París, *J. Polym. Sci., Part A: Polym. Chem.*, 2011, 49, 690-700.
181. Z.-Y. Qiao, R. Ji, X.-N. Huang, F.-S. Du, R. Zhang, D.-H. Liang and Z.-C. Li, *Biomacromolecules*, 2013, 14, 1555-1563.
182. N. Suchao-in, S. Chirachanchai and S. Perrier, *Polymer*, 2009, 50, 4151-4158.
183. Y. Cai, W. Shen, R. Wang, W. B. Krantz, A. G. Fane and X. Hu, *Chem. Commun.*, 2013, 49, 8377-8379.
184. D. S. Achilleos and M. Vamvakaki, *Macromolecules*, 2010, 43, 7073-7081.
185. A. Klaikherd, C. Nagamani and S. Thayumanavan, *J. Am. Chem. Soc.*, 2009, 131, 4830-4838.
186. D. Roy, J. Cambre and B. Sumerlin, *Chem. Commun.*, 2009, 2009, 2106-2108.
187. J. Dong, Y. Wang, J. Zhang, X. Zhan, S. Zhu, H. Yang and G. Wang, *Soft Matter*, 2013, 9, 370-373.
188. A. E. Smith, X. Xu, S. E. Kirkland-York, D. A. Savin and C. L. McCormick, *Macromolecules*, 2010, 43, 1210-1217.

Chapter Two

The self-assembly and morphology transition of THP-protected polymers

2.1 Introduction

Since the advent of controlled radical polymerisation techniques, the synthesis of well-defined block copolymers has been relatively straight-forward. Block copolymers that consist of quite chemically different, often immiscible, blocks can be synthesised, which can self-assemble, either in bulk, or in solution.[1, 2]

Amphiphilic block copolymers consist of at least one block that is hydrophilic and at least one block that is hydrophobic. Therefore these polymers will undergo self-assembly in aqueous media in order to minimise the unfavourable interactions between the hydrophobic block and the surrounding water.[3] The morphology adopted upon self-assembly is dependent upon the packing parameter, p.

$$p = \frac{v}{a_o l_c}$$

where v is the volume of the hydrophobic section, a_o is the contact area of the head group and l_c is the length of the hydrophobic section. In general spherical micelles are formed for $p \leq ⅓$, cylindrical micelles are formed when $⅓ \leq p \geq ½$ and when $½ \leq p \geq 1$ vesicles are formed.[4]

Stimuli-responsive polymers are ones which undergo a change in hydrophilicity (*i.e.* they become either more hydrophilic or more hydrophobic) in response to an external stimulus.[5] The application of the stimulus causes a change in the overall amphiphilic balance (the hydrophilic: hydrophobic ratio) of the polymer chain and, if severe enough, can cause a change in the packing parameter and hence the morphology adopted in solution.

There are two ways to cause this change in amphiphilic balance. One method is to change the physical environment of the polymer, for example, changing the concentration of the polymer in solution,[6] or by the addition of salts and additives which promote the solubility of one block over the other.[7, 8] The other way is to cause a change within the polymer itself, either reversibly or irreversibly.

Two of the most commonly studied stimuli are temperature[5, 9-15] and pH.[16-18] Within this chapter pH as a stimulus to induce a morphology change is explored. The application of pH as a stimulus can cause a reversible change within the polymer, *i.e.* the protonation of amine units to render them hydrophilic,[19-21] or can cause an irreversible chemical change, for example, the deprotection of hydrophobic tetrahydropyranyl acrylate (THPA) to form hydrophilic acrylic acid (see Scheme 2.1).[22-24] THPA can be deprotected either thermally or through the use of acetic acid.[22-24] As the deprotection is acid catalysed, it can be considered to be self-catalytic, as once it starts to deprotect, the acrylic acid formed catalyses futher deprotection.

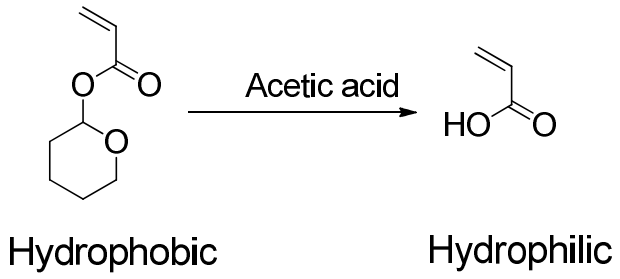

Scheme 2.1: The deprotection of THPA with acetic acid to give acrylic acid

In several examples by Petzetakis *et al.*[22-24] THPA was used during the synthesis of polylactide-polyTHPA acid block copolymers and then deprotected to form polylactide-poly(acrylic acid) block copolymers, which self-assemble in cylinders *via* crystallisation-driven self-assembly.

In another example, Klaikherd *et al.* investigated a system that involved multi stimuli-responsive blocks in which THP-protected 2-(hydroxyethyl) methacrylate (HEMA) was the pH-responsive block and NIPAM was utilised as the temperature responsive block (see Figure 2.1). These two blocks were joined by a redox sensitive disulfide linker and upon self-assembly, below the LCST cloud point of the NIPAM, micelles were observed to form with a THP core and NIPAM corona.

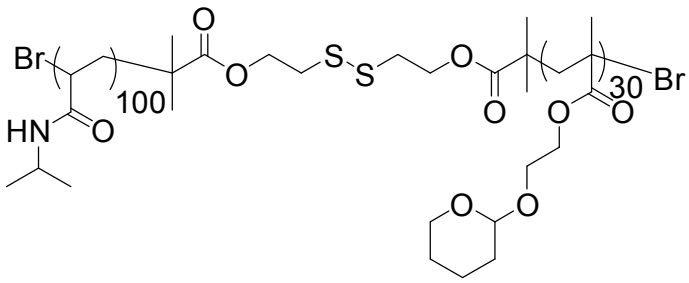

Figure 2.1: The multi-responsive triblock synthesised by Klaikherd *et al.*[25]

Upon lowering the pH, the THP-protected HEMA deprotected to leave hydrophilic HEMA, rendering the entire polymer water soluble and so a micelle to unimer morphology transition was observed.[25] This morphology transition was utilised to release the hydrophobic dye, Nile Red, from within the micelles in response to this change in pH. The polymer could also be made to precipitate out of solution by increasing the temperature to above the LCST of the NIPAM. Cleavage of the redox sensitive linker with a mild reducing agent, resulted in the formation of the constituent homopolymers and therefore dissociation of the micelles (see Figure 2.2).

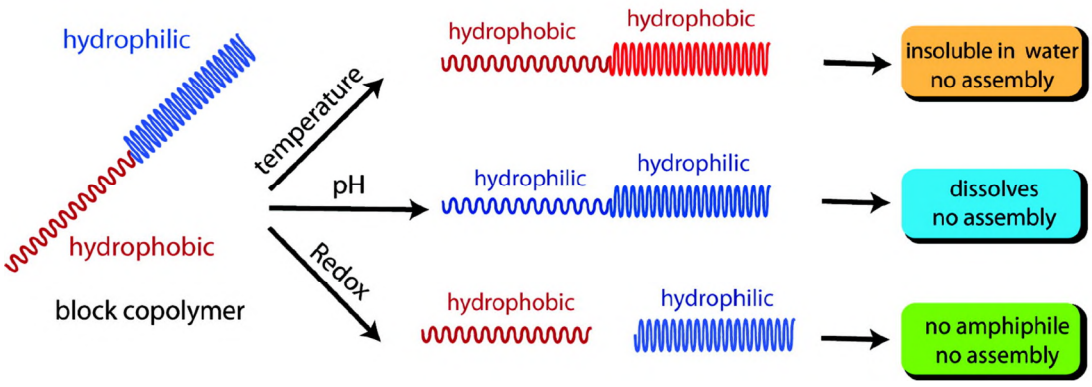

Figure 2.2: Schematic showing the amphiphilic diblock copolymer and the effect of the three different stimuli[25]

As shown in the previous example, the disruption of a self-assembled structure can be exploited by the encapsulation and release of cargo and there are many examples of hydrophobic cargo being released from a micelle in response to a stimulus.[26-28] Polymeric vesicles on the other hand have an inherent central water pool within the vesicle, which

allows for the encapsulation and delivery of hydrophilic payloads.[28, 29] There are relatively few examples of vesicles which undergo a morphology transition to a micelle in response to pH.[30] Eisenberg and co-workers prepared a triblock copolymer consisting of poly(acrylic acid), polystyrene and poly(4-vinyl pyridine) which self-assembled in DMF/THF/H_2O mixtures. At pH 1 the polymers formed vesicles but between pH 3 – 11 solid aggregates were formed.

Herein we report the synthesis of diblock copolymers consisting of a hydrophilic head group, a pH-deprotectable THPA block and a hydrophobic MA block (see Figure 2.3). Two different hydrophilic head groups are investigated; a positively charged quaternary amine head group and a neutral triethyleneglycol head group. The self-assembly behaviour of the polymers is investigated by DLS and TEM. The pH-response of the polymers is demonstrated by treatment with acetic acid to deprotect the THPA and the subsequent vesicle to micelle morphology transition analysed by DLS and TEM.

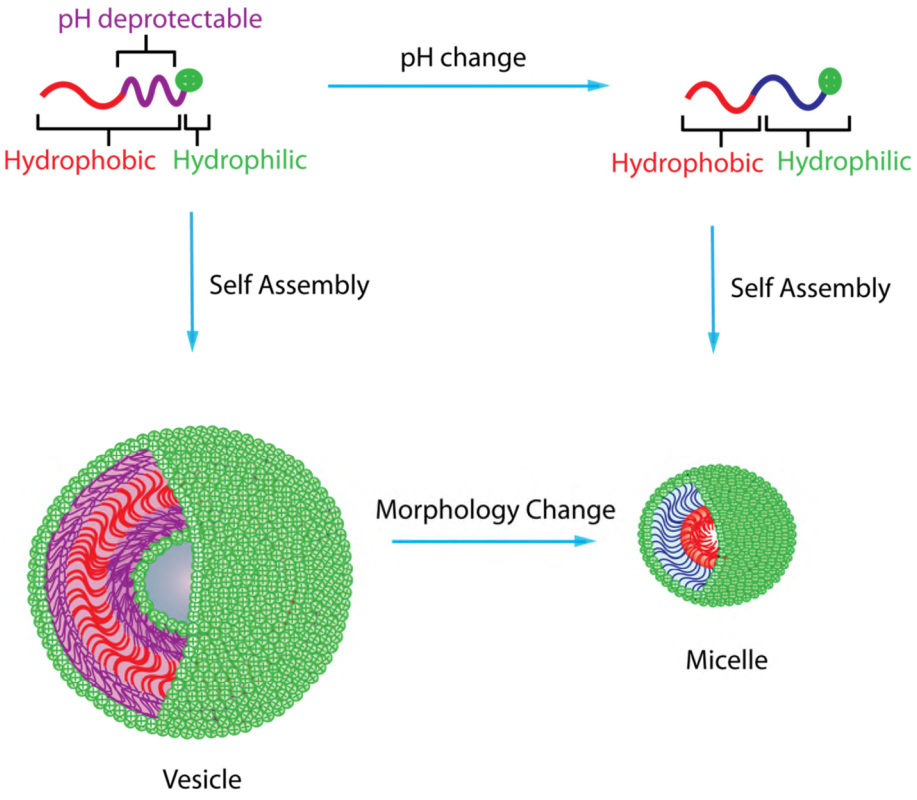

Figure 2.3: Schematic representation of the deprotection of the THP-functionalised polymer and the resultant change in morphology expected

2.2 Results and Discussion

2.2.1 Synthesis of quaternary amine charged CTA, 2.01

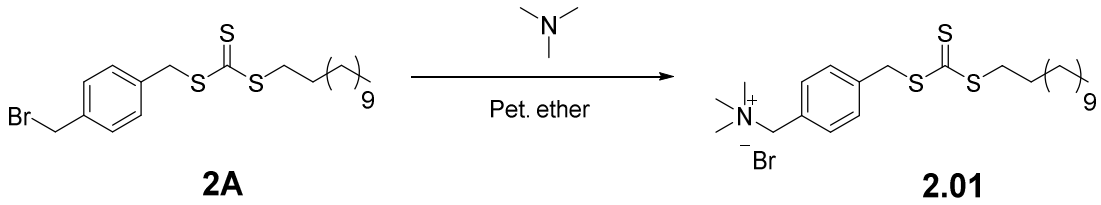

2A **2.01**

Scheme 2.2: Synthetic route to CTA 2.01

A novel chain transfer agent (CTA) containing a charged quaternary amine functionality was achieved by reacting a previously synthesised bromine functionalised CTA (**CTA 2A**)[31] with trimethylamine in petroleum ether with the resulting yellow precipitate, **2.01**, being collected by filtration. The CTA was characterised by ^{1}H NMR spectroscopy (Figure 2.4) and the conversion from the bromine functionalised CTA to the charged quaternary amine functionality was observed by the appearance of peak **a** at 3.2 ppm relating to the protons of the charged amine end ($(CH_3)_3N^+$). Signal **b**, corresponding to the CH_2 protons between the bromine and aromatic ring, shifts from 4.47 ppm to 5.06 ppm upon substitution. The lack of any residual signal at 4.47 ppm indicates complete conversion to the quaternary amine functionalised CTA. The signals **j**, **b** and **d**, at 0.88, 5.06 and 7.4 ppm respectively, integrate correctly with respect to each other, confirming that both ends of the CTA are present after reaction. The peak at 3.2 ppm corresponds to the protons of the charged amine end group (9H, **a**) and also the CH_2 next to the trithiocarbonate group (2H, **f**). Integration of this peak (*ca*. 11) indicates that the trithiocarbonate group has been unaffected by the reaction.

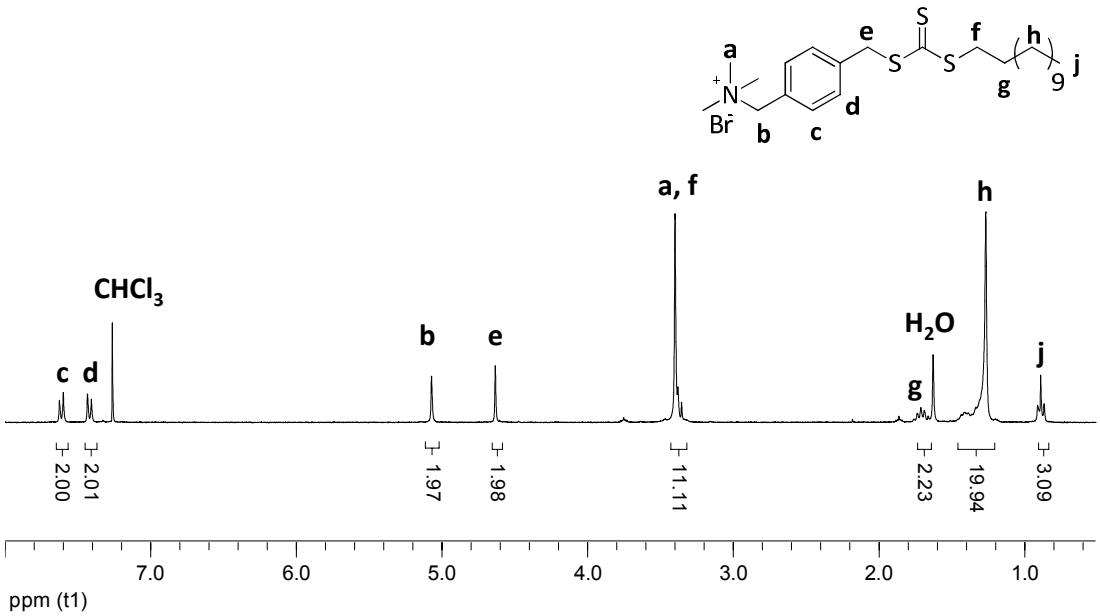

Figure 2.4: ^{1}H NMR spectrum of 2.01 in $CDCl_3$ with assignments shown, recorded at 25 °C and 400 MHz

2.2.2 Polymerisation of THPA with 2.01

THPA was synthesised as described in the literature.[32] Acrylic acid and dihydropyran (1: 2 ratio) were placed in an oven dried RBF under an inert atmosphere. Poly(4-vinyl pyridine HCl) was added as a catalyst for the reaction and phenothiazine as a radical inhibitor to prevent polymerisation. The solution was heated to 65 °C for 16 hours, allowed to cool and then sodium carbonate and calcium hydroxide added. The product was purified by vacuum distillation. The pure product was stored in the freezer to prevent deprotection.

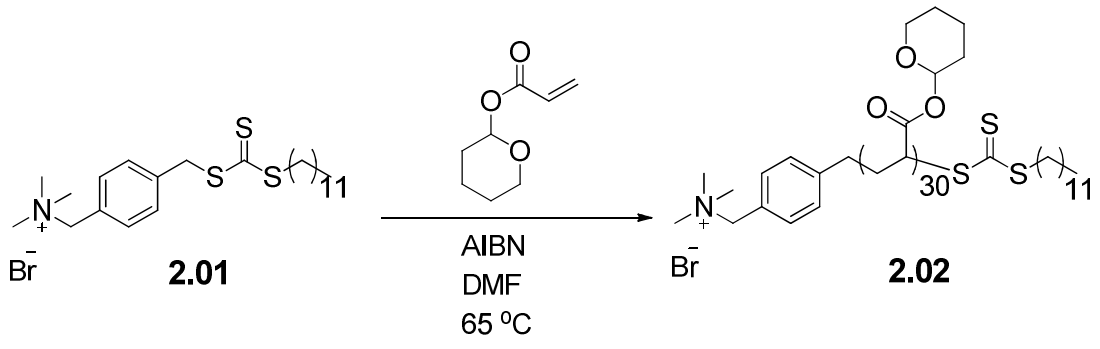

Scheme 2.3: The synthesis of homopolymer 2.02 using CTA 2.01

The RAFT agent, **2.01**, was then used to polymerise THPA in order to form the acid deprotectable block bearing a terminal hydrophilic functionality, **2.02**, M_n (^{1}H NMR) = 5.0

kDa, M_n (DMF SEC) = 4.8 kDa, $Đ_M$ = 1.08 (see Scheme 2.3). The narrow dispersity observed by SEC analysis shows that the polymerisation proceeded with good control. The UV trace of the SEC at 309 nm is in good agreement with the RI trace showing that the trithiocarbonate group has been retained throughout the polymerisation (see Figure 2.5).

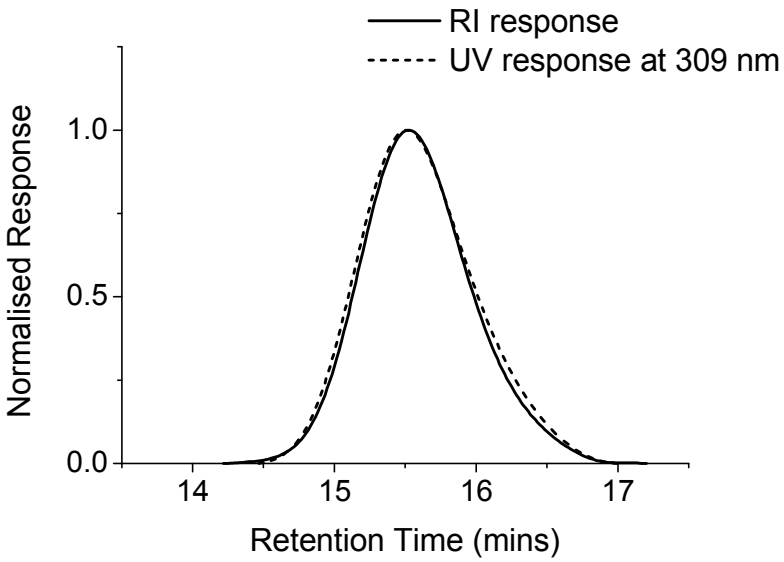

Figure 2.5: DMF SEC chromatograms showing refractive index and UV absorbance at 309 nm of homopolymer 2.02

Analysis of the polymer by ^{1}H NMR spectroscopy shows the presence of both end groups of the CTA (see Figure 2.6). The peaks at 0.9 ppm, 4.9 ppm and 7.5 ppm correspond to the terminal methyl group of the dodecyl chain (**p**), the protons adjacent to the quaternary amine (**b**) and the protons from the aromatic ring (**d**), respectively. The peak at 3.3 ppm integrates to *ca.* 11, showing the presence of both the protons adjacent to the trithiocarbonate (2H, **m**) and the methyl groups on the charged amine (9H, **a**). All the end group signals integrate well with respect to each other. Integration of these end group signals relative to the polymer peaks at 3.7ppm (**j**), 3.8 ppm (**j**) and 5.9 ppm (**e**) give a degree of polymerisation of 30. This agrees well with the expected value from the conversion NMR spectroscopy, again showing that the polymerisation proceeds with good control.

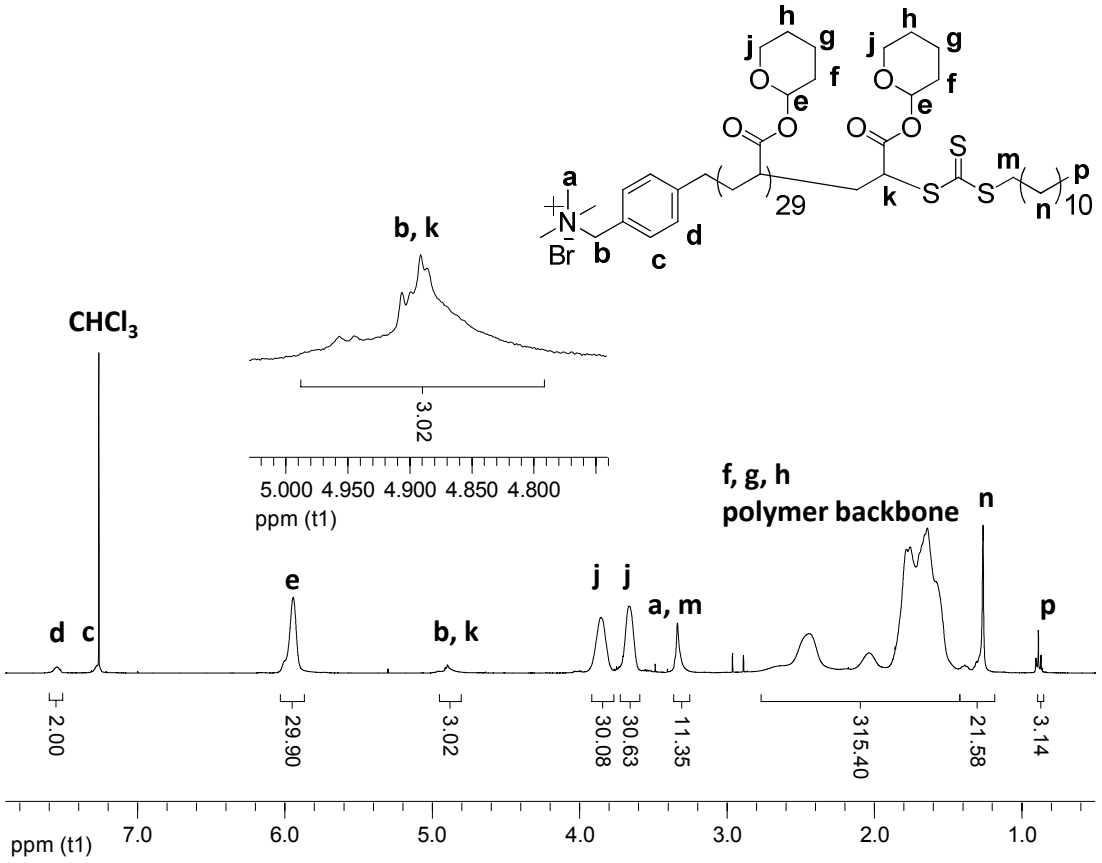

Figure 2.6: ^{1}H NMR spectrum of homopolymer 2.02 in $CDCl_3$ with assignments shown, recorded at 25 °C and 400 MHz

Analysis of the polymer in DMSO confirms that there has been no significant deprotection of the THPA backbone during polymerisation (see Figure 2.7). There is no acid proton peak observed between 10 – 13 ppm and no peaks relating to the by-product of deprotection, dihydropyran (DHP).

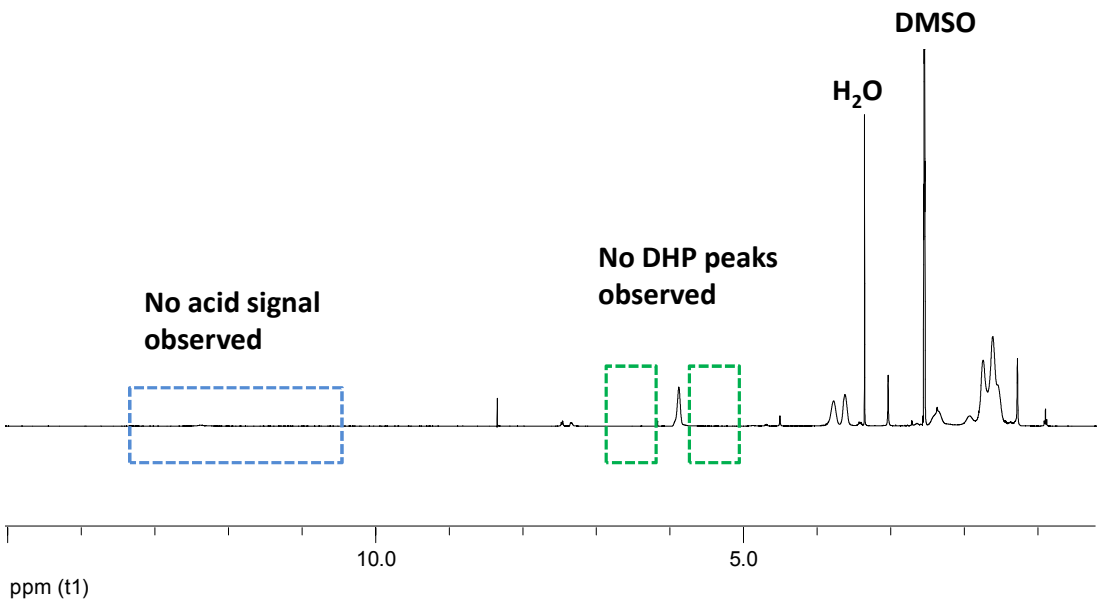

Figure 2.7: ^{1}H NMR spectrum of homopolymer 2.02 in DMSO, recorded at 25 °C and 400 MHz, confirming that no deprotection of the polymer occurred during polymerisation

In order to be able to compare the effect that different block lengths have on the self-assembly properties of the polymers, a longer homopolymer of THPA was synthesised using CTA **2.01**. A homopolymer with 37 THPA units, **2.03**, was synthesised, M_n (^{1}H NMR) = 6.3 kDa, M_n (DMF SEC) = 7.3 kDa, $Đ_M$ = 1.17. Due to issues with deprotection of the polymer, which will be discussed in a later section, another slightly shorter block length was also synthesised in order to complete the self-assembly studies. This homopolymer, **2.04**, was 25 THPA units in length, M_n (^{1}H NMR) = 4.4 kDa, M_n (DMF SEC) = 4.6 kDa, $Đ_M$ = 1.10.

2.2.3 Synthesis of charged diblock copolymers

The homopolymer was chain extended with methyl acrylate to form a diblock copolymer with a positively charged tertiary amine end group, **2.05**, M_n (^{1}H NMR) = 8.2 kDa, M_n (DMF SEC) = 8.5 kDa, $Đ_M$ = 1.07. Again, the narrow dispersity seen by SEC analysis shows that the polymerisation proceeds with good control. The efficient chain extension of the homopolymer can be seen in Figure 2.8.

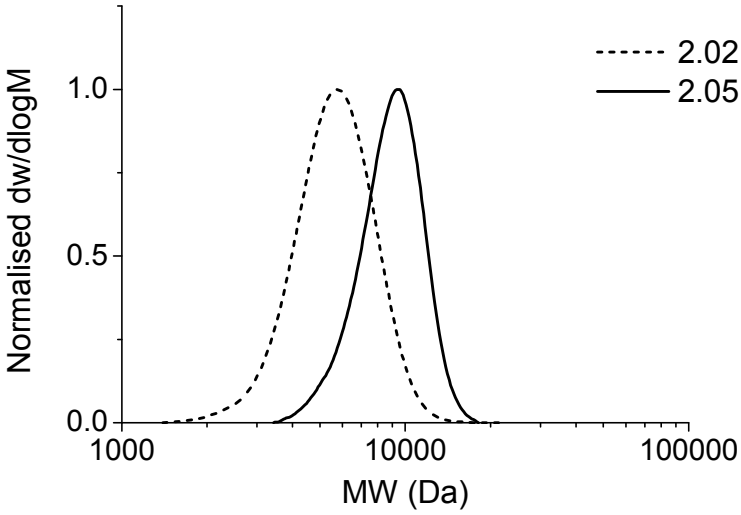

Figure 2.8 : DMF SEC chromatograms showing the shift to higher MW upon chain extension of homopolymer 2.02 to diblock copolymer 2.05

The retention of both the R and Z groups of the RAFT agent is shown by ^{1}H NMR spectroscopy (see Figure 2.9). The protons relating to the aromatic ring (**d**), the CH_2 between the $N^{+}(CH_3)_3$ and the aromatic ring (**b**) and the terminal CH_3 of the dodecyl chain (**q**) can clearly be seen at 7.54 ppm, 4.88 ppm and 0.87 ppm respectively and integrate well to each other. Integration of the methyl acrylate OCH_3 side chain (**k**) with respect to the end groups signals of the polymer (**d**, **b**, **a**, **n**) give a degree of polymerisation of 35 for the methyl acrylate block. The peak at 3.3 ppm integrates to *ca*. 11, corresponding to the methyl groups of the quaternary amine (9H, **a**) and the protons adjacent to the trithiocarbonate group (2H, **n**). The hydrophilicity the quaternary amine functionality provides is important in directing self-assembly as will be discussed later.

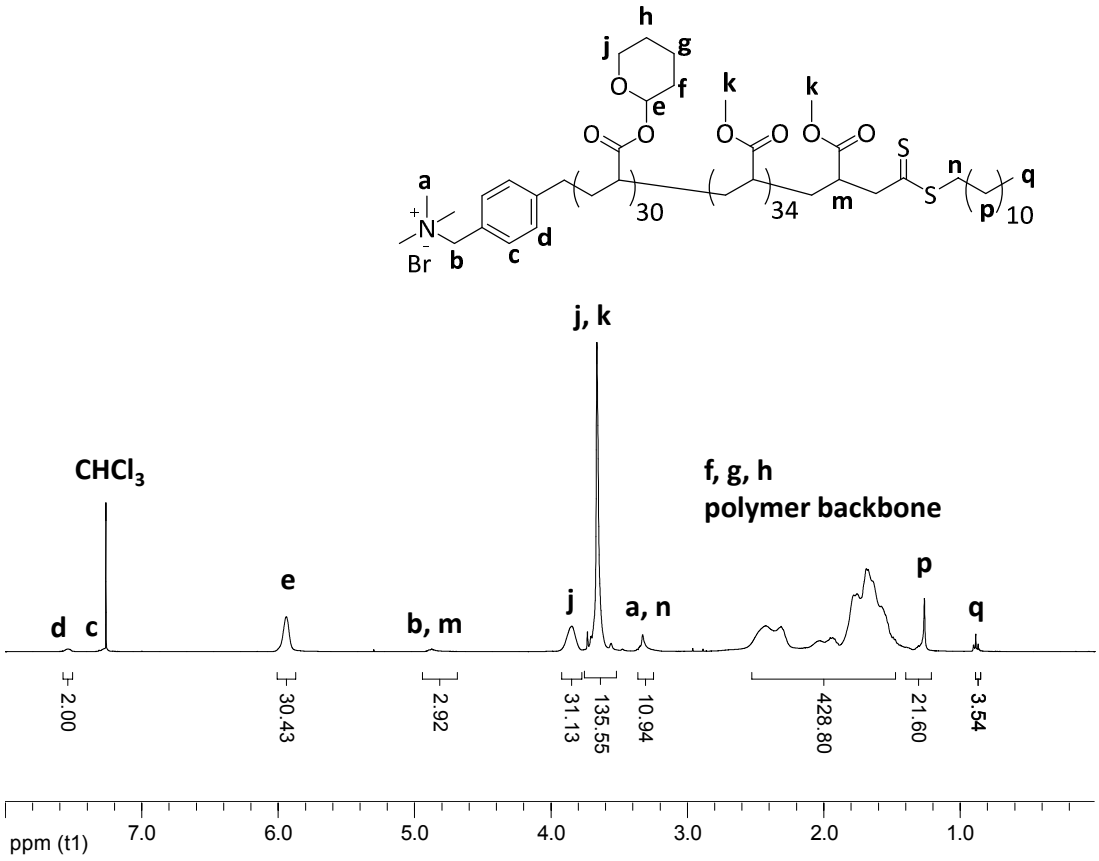

Figure 2.9: ^{1}H NMR spectrum of diblock copolymer 2.05 in $CDCl_3$, with assignments shown, recorded at 25 °C and 400 MHz

The other two THPA homopolymers, **2.03** and **2.04**, were also chain extended with methyl acrylate to form two quaternary amine functionalised diblock copolymers, **2.06** and **2.07** respectively. The polymers were analysed in a similar manner to **2.02**. Diblock copolymer **2.06** has a THPA block length of 37 and an MA block length of 33, M_n (^{1}H NMR) = 8.9 kDa, M_n (DMF SEC) = 8.8 kDa, $Đ_M$ = 1.12. Diblock copolymer **2.07** is overall a shorter polymer, with a THPA block length of 25 and an MA block length of 17, M_n (^{1}H NMR) = 5.9 kDa, M_n (DMF SEC) = 6.9 kDa, $Đ_M$ = 1.12.

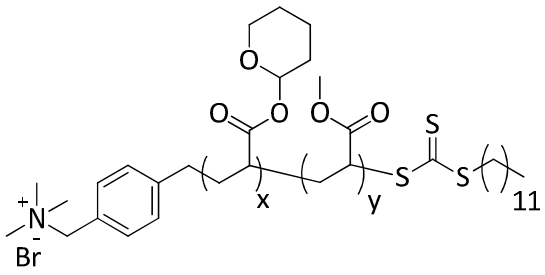

2.05; x = 30, y = 35

2.06; x = 37, y = 33

2.07; x = 25, y = 17

Figure 2.10: The structure of the quaternary amine end functionalised diblock copolymers 2.05, 2.06 and 2.07, and their respective block lengths

2.2.4 Synthesis of TEG-functionalised CTA, 2.08

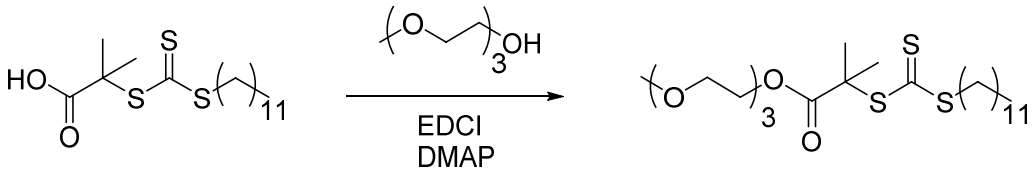

Scheme 2.4: Synthesis of triethyleneglycol functionalised DDMAT, 2.08

In order to be able to study how the hydrophilic end group can affect self-assembly a different amphiphilic CTA was investigated. This CTA bears no charge but instead derives its hydrophilicity from a triethyleneglycol (TEG) functionality. The novel trithiocarbonate chain transfer agent, **2.08**, was synthesised by reacting DDMAT with TEG monomethylether in the presence of EDCI with DMAP as a catalyst (see Scheme 2.4). The yellow solution obtained was purified by column chromatography and the yellow oil collected was determined to be pure by ^{1}H NMR spectroscopy (see Figure 2.11). The peak at 3.2 ppm (**g**) shows that the trithiocarbonate group is still present after modification and integrates correctly when compared to the peaks **a-e** that relate to the TEG. The CH_2 next to the OH (**e**) in the starting material has shifted from *ca.* 3.6 ppm to 4.25 ppm in the modified CTA, showing that the TEG monomethylether has reacted. Mass spectrometry of the product shows only one main peak *m/z* 533.1 ($M+Na^+$).

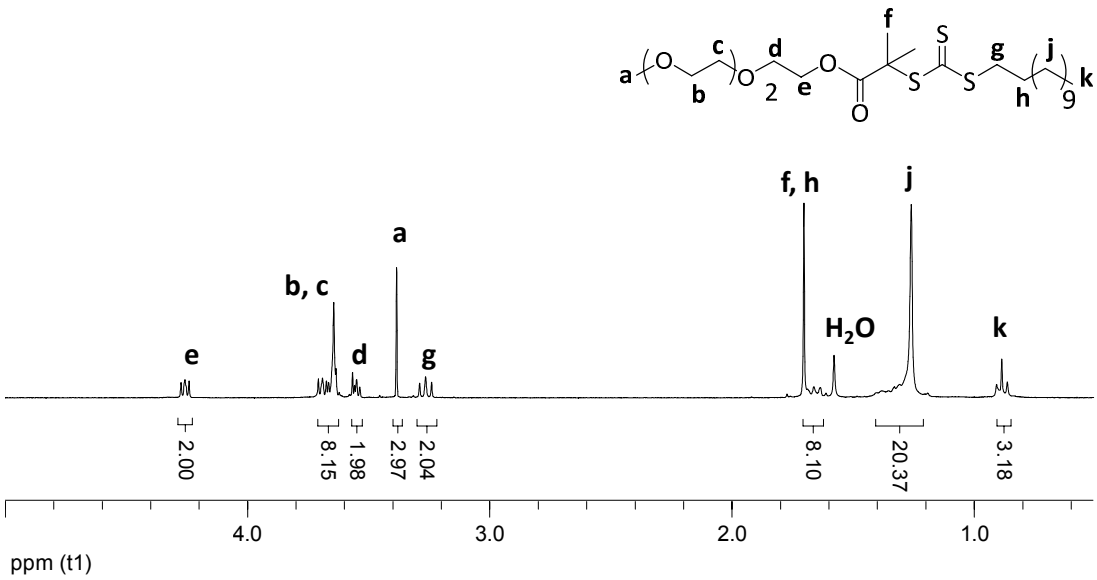

Figure 2.11: ^{1}H NMR spectrum of TEG modified RAFT agent, 2.08, in $CDCl_3$, recorded at 25 °C and 400 MHz. The $CHCl_3$ peak (7.26 ppm) is not shown

2.2.5 Polymerisation of THPA with TEG-functionalised CTA

The RAFT agent, **2.08**, was used in the polymerisation of tetrahydropyranyl acrylate in order to form the acid deprotectable block bearing a terminal hydrophilic functionality, **2.09**, M_n (^{1}H NMR) = 5.2 kDa, M_n (DMF SEC) = 3.0 kDa, $Đ_M$ = 1.12. The narrow dispersity seen by SEC analysis shows that the polymerisation proceeded with good control. The UV trace of the SEC at 309 nm is in good agreement with the RI trace showing that the trithiocarbonate group has been retained (see Figure 2.12).

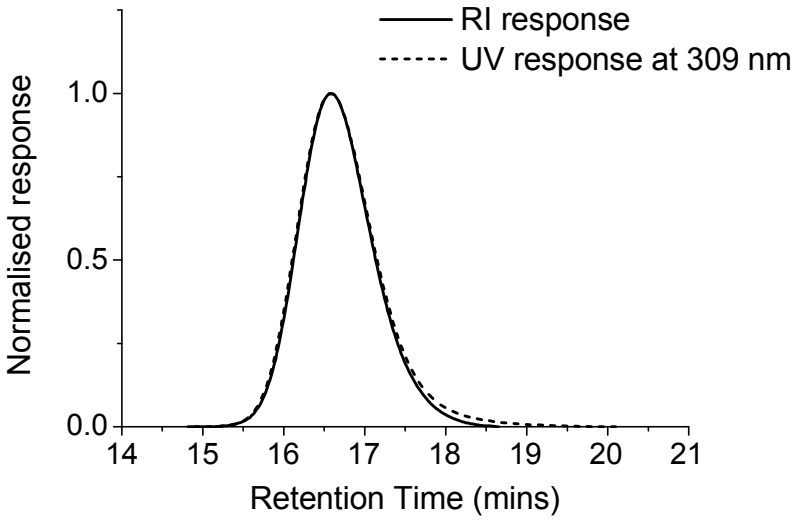

Figure 2.12: DMF SEC chromatograms showing refractive index and UV absorbance at 309 nm of homopolymer 2.09

Analysis of the polymer by ^{1}H NMR spectroscopy shows the presence of both end groups of the CTA (see Figure 2.13), as demonstrated by signals **a**, **p** and **e** at 3.3 and 4.2 ppm, which correspond to the terminal methyl group of the TEG (3H) and the CH_2 next to the trithiocarbonate group (2H) and to the CH_2 of the TEG next to the carbonyl. The end group signals integrate well with respect to each other. Integration of these end group signals relative to the polymer peaks, **m** and **g**, at 3.7, 3.8 and 5.9 ppm give a degree of polymerisation of 33. This agrees well with the expected value from the conversion ^{1}H NMR spectroscopy, again showing that the polymerisation proceeds with good control.

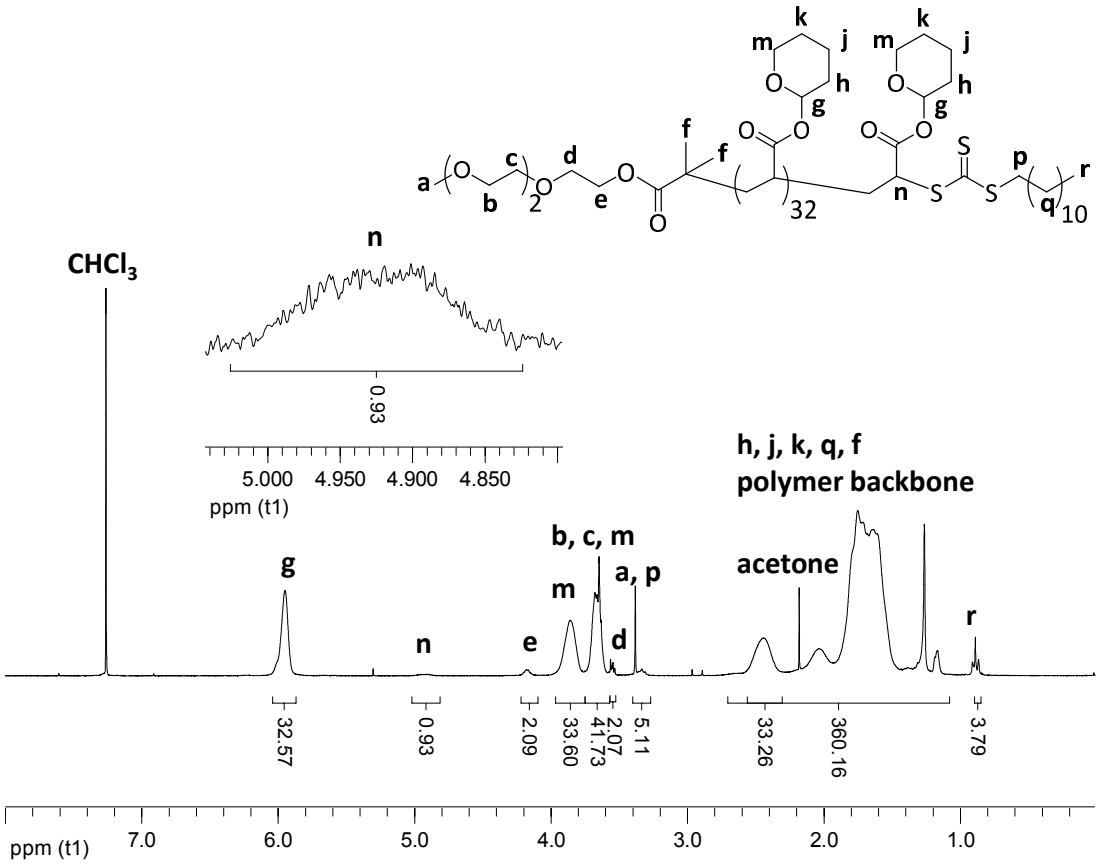

Figure 2.13: ^{1}H NMR spectrum of homopolymer 2.09 in $CDCl_3$ with assignments shown, recorded at 25 °C and 400 MHz

Analysis of **2.09** in DMSO confirms that the polymer has not deprotected during the polymerisation or purification procedures (see Figure 2.14). There is no acid signal at *ca*. 10 – 13 ppm. The by-product of the deprotection, DHP, is also not observed in the ^{1}H NMR spectrum, further confirming that no deprotection has occurred.

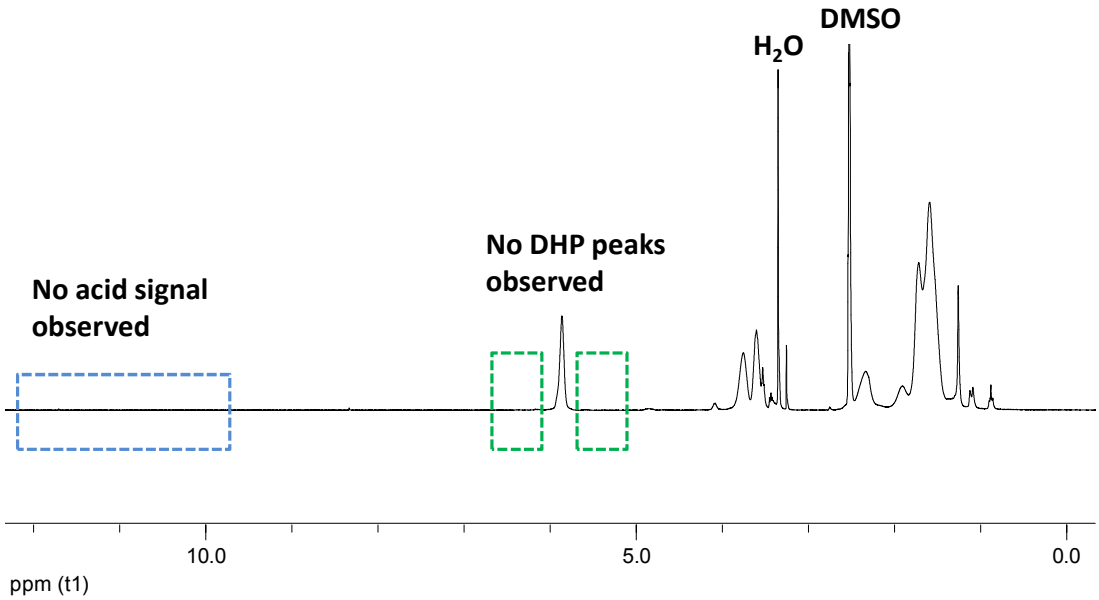

Figure 2.14: ^{1}H NMR spectrum of 2.09 in DMSO showing that no deprotection occurred during polymerisation, evidenced by the lack of an acid peak between 10 – 13 ppm and the lack of DHP signals at *ca*. 4.6 and 6.3 ppm. Spectrum recorded at 25 °C and 400 MHz

In order to directly compare the effects of the different end groups of the polymers, another triethylene glycol functionalised homopolymer, **2.10**, with 25 THPA units was synthesised, M_n (^{1}H NMR) = 4.2 kDa, M_n (DMF SEC) = 3.1 kDa, $Đ_M$ = 1.09. This homopolymer has the same block length as **2.04**, which bears the quaternary amine functionality. The polymer was analysed in the same manner as **2.09**.

2.2.6 Synthesis of TEG-functionalised diblocks

Methyl acrylate was then grown from the TEG functionalised homopolymer, **2.09**, in order to form the TEG functionalised pH deprotectable diblock copolymer **2.11**, M_n (^{1}H NMR) = 8.0 kDa, M_n (DMF SEC) = 6.0 kDa, $Đ_M$ = 1.14. The shift to higher molecular weight can be observed in the SEC trace, showing the chain extension (see Figure 2.15). There is a small amount of tailing seen in the diblock copolymer **2.11**, as a result of some inefficient chain extension.

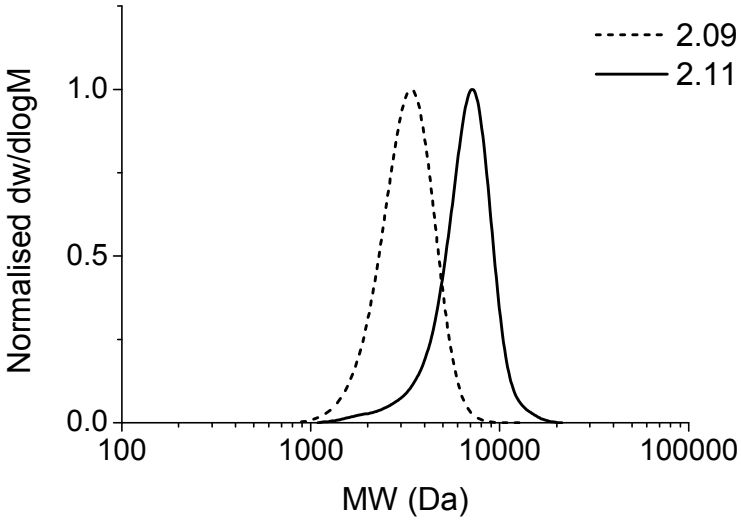

Figure 2.15: DMF SEC chromatograms showing increase in MW upon chain extension of homopolymer 2.09 to diblock copolymer 2.11

Analysis by ^{1}H NMR spectroscopy shows the presence of both the R and the Z group of the CTA (see Figure 2.16). The peak at 4.2 ppm (**e**) corresponds to the CH_2 of the TEG next to the ester functionality and the peak at 3.3 ppm (**a, q**) corresponds to the protons adjacent to the trithiocarbonate and to the terminal methyl group from the TEG functionality. These peaks integrate correctly relative to each other and when compared to the polymer peak at 3.6 ppm (**b, c, m**) give a degree of polymerisation of the methyl acrylate block of 30. Analysis of the same polymer in DMSO confirms that no deprotection of the THPA units has occurred during the chain extension. There is no peak between 10 – 13 ppm that would correspond to the acid functionality of acrylic acid and there are no signals that relate to the by-product of deprotection, DHP (see Figure 2.17).

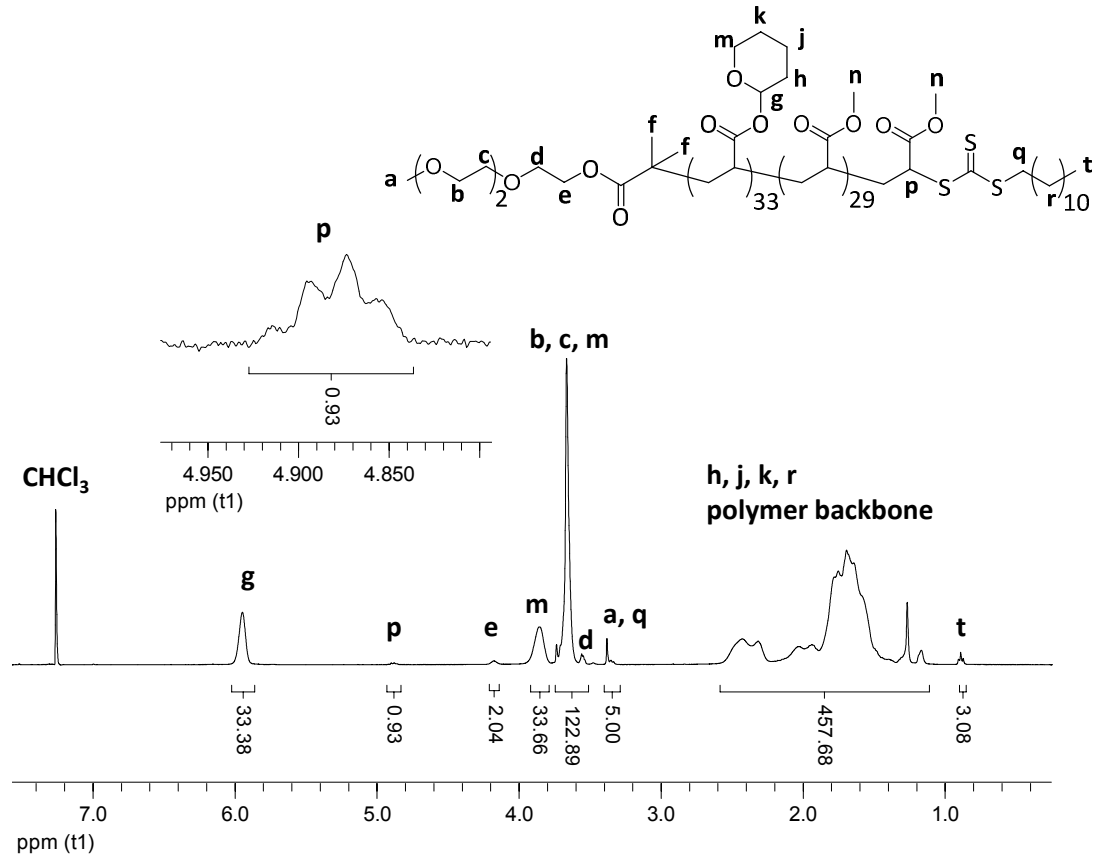

Figure 2.16: ^{1}H NMR spectrum of diblock copolymer 2.11 in $CDCl_3$, with assignments shown, recorded at 25 °C and 400 MHz

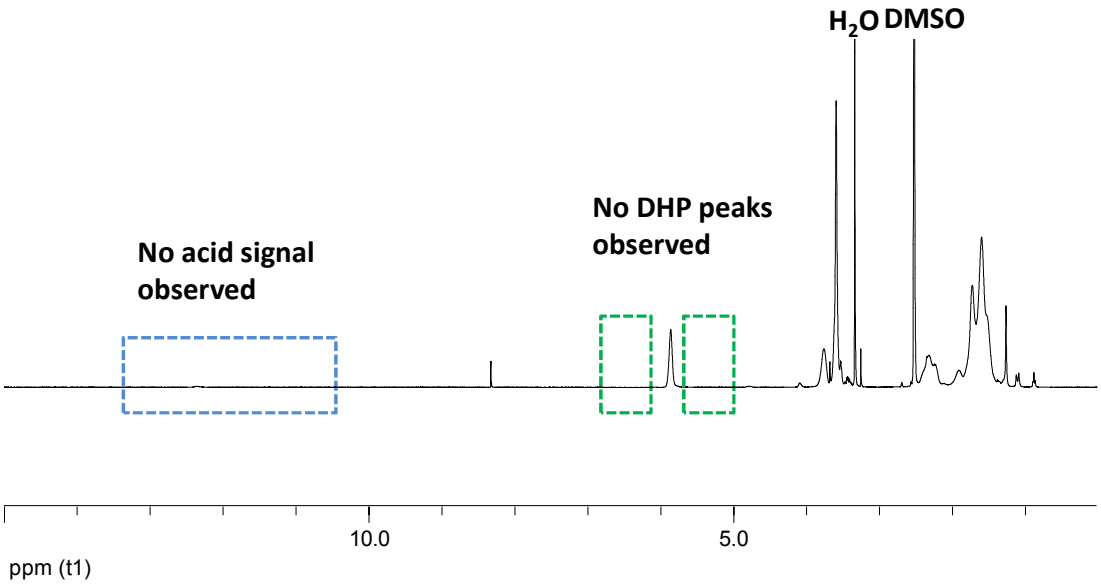

Figure 2.17: ^{1}H NMR spectrum of 2.11 in DMSO showing no deprotection has occurred during the chain extension. The spectrum was recorded at 25 °C and 400 MHz

The shorter TEG functionalised homopolymer, **2.10**, was used as a macroCTA in the polymerisation of MA to form diblock copolymer, **2.12**, with a MA block length of 16, M_n (^{1}H NMR) = 5.6 kDa, M_n (DMF SEC) = 5.2 kDa, $Đ_M$ = 1.07. This polymer has very comparable block lengths to the diblock copolymer, **2.07**, which bears a charged tertiary amine end group. This will allow for direct comparison of the effect that the hydrophilic functionality has upon self-assembly. The polymers were all stored as a dry solid below 0 °C as deprotection started to occur when stored at room temperature, as will be discussed in a later section.

2.2.7 Self-assembly of the quaternary amine functionalised polymers

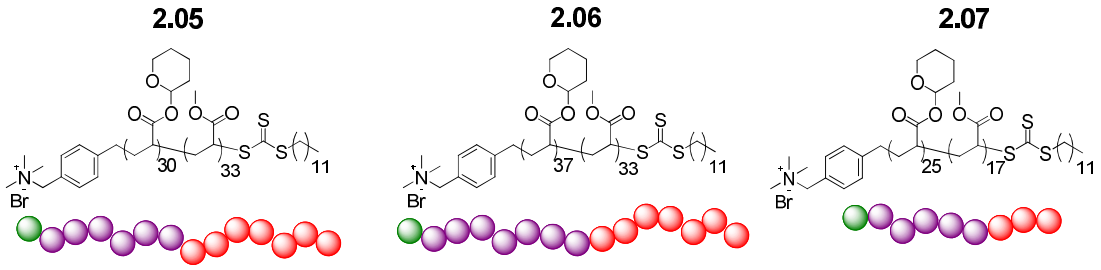

Figure 2.18: Structure of the three quaternary amine functionalised diblock copolymers, 2.05, 2.06, 2.07

It is expected that self-assembly of the triblock copolymers in their THP-protected state (see Figure 2.18) will result in vesicle formation, since the entire polymer chain is hydrophobic and therefore self-assembly is directed by the hydrophilic quaternary amine end group. In order to assess the best method by which to self-assemble the polymers several different self-assembly methods were investigated. Firstly the solvent switch method was attempted. The diblock copolymer, **2.05**, which has a THPA and MA block length of 30 and 35, respectively, was dissolved in THF (a good solvent for both blocks) at a concentration of 0.5 mg mL^{-1}. 18.2 MΩ cm^{-1} water was added at a rate of 0.6 mL min^{-1} so the overall concentration of polymer was 0.25 mg mL^{-1}. The resulting solution was cloudy and precipitate formed during dialysis. Therefore it was decided that this was not a viable method for self-assembling **2.05**.

Another method reported in the literature for vesicle formation is *via* thin film formation.[30] In this method the polymer, **2.05**, was dissolved in THF and the solvent then slowly removed *in vacuo* to leave a thin film of the polymer layering the walls of the vessel. 18.2 MΩ cm^{-1} water was added to reach a polymer concentration of 0.25 mg mL^{-1} and the solution stirred in a water bath set to 30 °C for five days. After this time not all the film appeared to have disappeared from the walls of the vessel. Analysis of the transparent solution by DLS showed there to be two populations, one population with a D_h by intensity of 124 nm, which is in the size range expected for vesicles, and a much smaller population with a D_h of 34 nm (see Figure 2.19). This smaller population suggests that some of the polymer has started to deprotect and is forming micelles rather than vesicles. This may be due to the extended time required in order to solubilise the thin film, as some polymer coating remained in the vessel after five days.

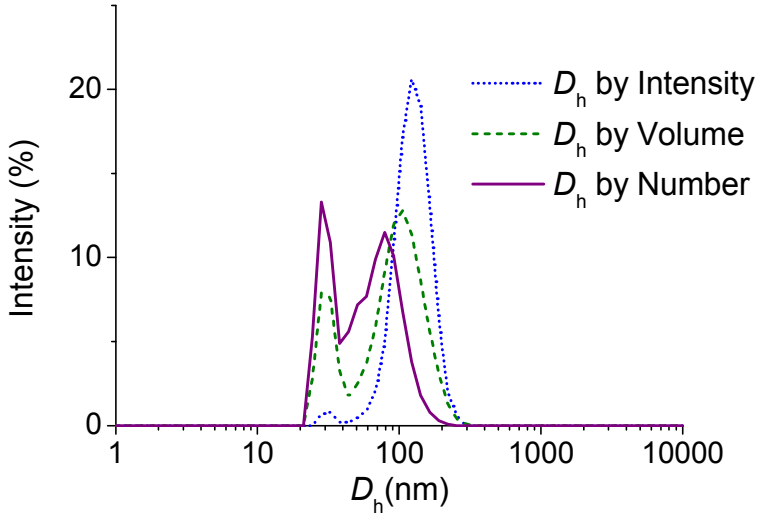

Figure 2.19: DLS traces of 2.05 after attempted self-assembly by thin film formation

The last method investigated for vesicle formation was direct dissolution. Due to fluctuations of the laboratory temperature it was decided to assemble the polymer, **2.05**, at 30 °C in order to eliminate any effects of these fluctuations. The polymer was stirred in 18.2 MΩ cm^{-1} water at 30 °C at a concentration of 0.25 mg mL^{-1}. After stirring for three days the polymer had self-assembled and a transparent solution was obtained. This solution was

analysed by DLS and a population with D_h by number of 130 ± 2 nm with a $Đ$ of 0.11 was observed.

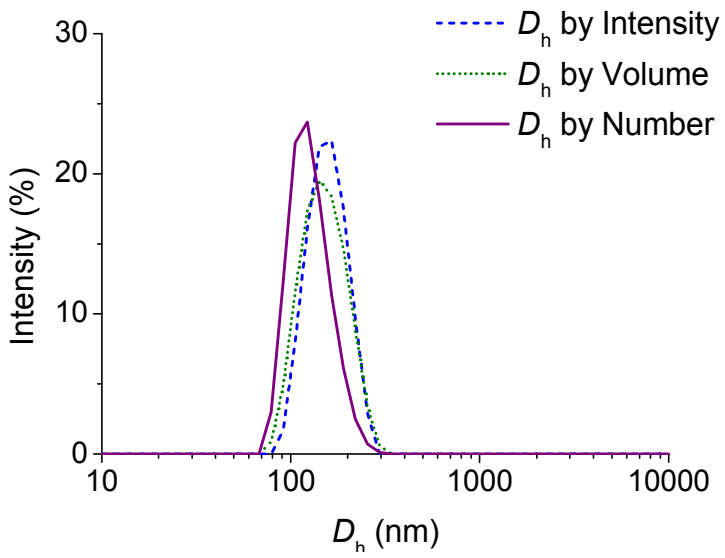

Figure 2.20: DLS traces for 2.05 after self-assembly by direct dissolution at 30 °C

This solution was analysed by TEM. A sample was made by drop deposition of the solution onto a formvar grid and then allowing to dry. Upon staining with uranyl acetate solution, spherical structures with a D_h of 136 ± 23 nm were observed (see Figure 2.21). The edges of these structures did not appear to be completely smooth. Uranyl acetate is an acidic stain (pH *ca.* 4.5) and increased lengths of staining time caused more micelles to be observed, clustered around the vesicles. Therefore it appears that the acidic nature of the stain is causing the vesicles to start to deprotect upon the grid and micelles to form (see Figure 2.22)

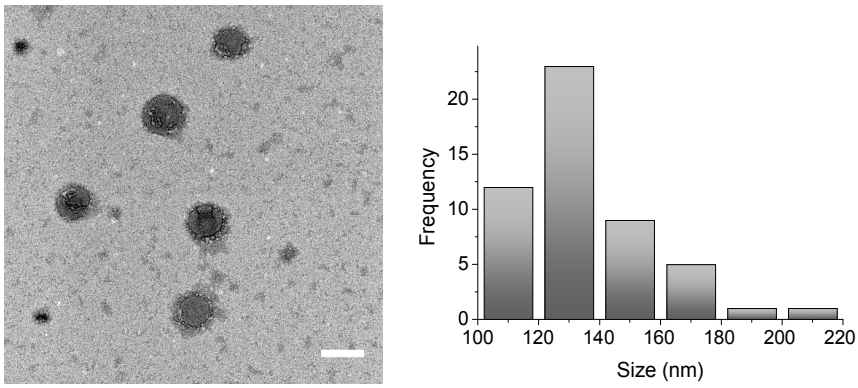

Figure 2.21: TEM image of a solution of 2.05 at 0.25 mg mL^{-1} stained with uranyl acetate for 15 seconds, scale bar = 200 nm, and distribution of sizes observed

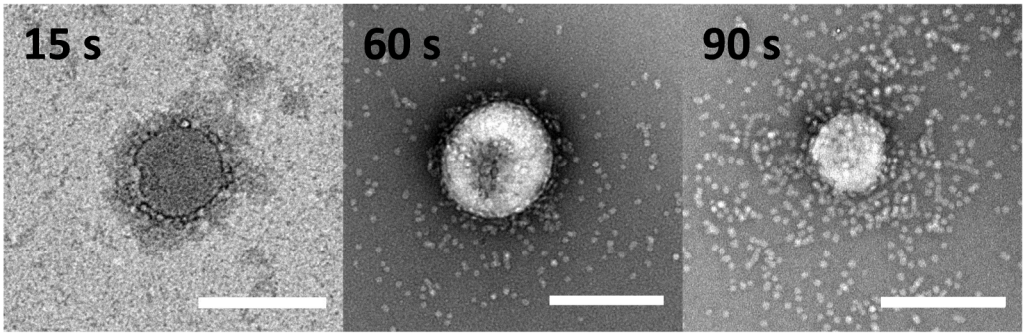

Figure 2.22: TEM images of a solution of 2.05 stained with uranyl acetate for different lengths of time, scale bar = 200 nm in all cases

In order to further prove that these structures were vesicles, a sample was analysed by cryo-TEM. Cryo-TEM is a method of imaging the assembled structures whilst frozen in solution, meaning that drying effects are avoided and the use of problematic stains is unnecessary. Spherical structures with a clear bilayer were observed, showing that the polymer is assembling to form vesicles (see Figure 2.23). The vesicles were easily damaged by the electron beam and this coupled with the low concentration of the sample meant that few aggregations were observed. This vesicular morphology is as expected due to the small hydrophilic end group directing self-assembly.

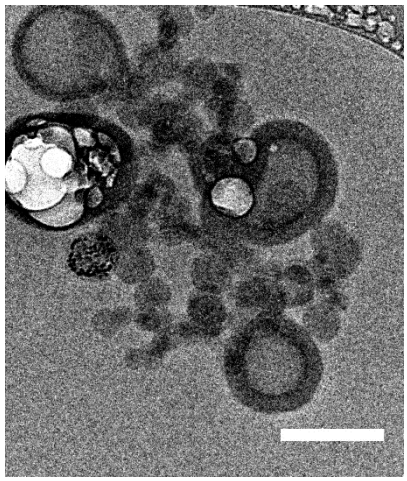

Figure 2.23: Cryo-TEM image of vesicles of 2.05 at 0.25 mg mL^{-1}, scale bar = 200 nm

The slightly longer quaternary amine functionalised block copolymer **2.06**, which has a THPA block length of 37 and a MA block length of 33, was self-assembled by direct dissolution at 30 °C at a concentration of 0.25 mg mL^{-1}. After three days of stirring there

was still precipitate present, indicating that the polymer had not self-assembled. The solution continued to be stirred for a further three days but the precipitate remained. This could be due to the hydrophobic portion of the polymer reaching a critical length, after which the solitary charge on the end of the RAFT agent is not sufficient to induce self-assembly and the polymer remains insoluble.

2.2.8 Self-assembly of the TEG functionalised polymers

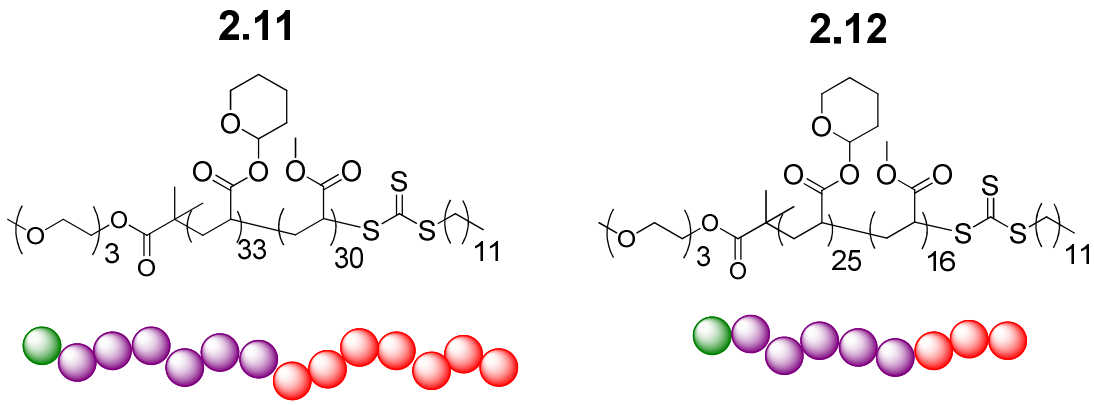

Figure 2.24: Structures of the TEG functionalised diblock copolymers 2.11 and 2.12

The self-assembly of the TEG functionalised diblock copolymer **2.11** was attempted by direct dissolution at 30 °C at a concentration of 0.25 mg mL^{-1} as this method proved to be the best for the quaternary amine functionalised polymers, **2.05** and **2.07**. However, after three days of stirring there was precipitate remaining in the vial, indicating that self-assembly had not occurred. The solution was left stirring for a further three days but precipitate remained in the vial.

Solvent switch was also employed as an alternative method of self-assembly. The polymer was dissolved in THF at a concentration of 0.5 mg mL^{-1} and an equal volume of water added slowly to induce self-assembly. However, the solution went very cloudy and upon dialysis the polymer precipitated. It was therefore decided that the TEG functionality was not hydrophilic enough to direct self-assembly in the case of polymer **2.11**. This may be related to the length of the THPA block, as seen in polymer **2.07**.

Therefore the self-assembly of the shorter diblock copolymer, **2.12**, was investigated. The block lengths of **2.12** are almost identical to that of **2.07** and so any effect upon self-assembly is related to the different end group functionalities (see Figure 2.25)**.**

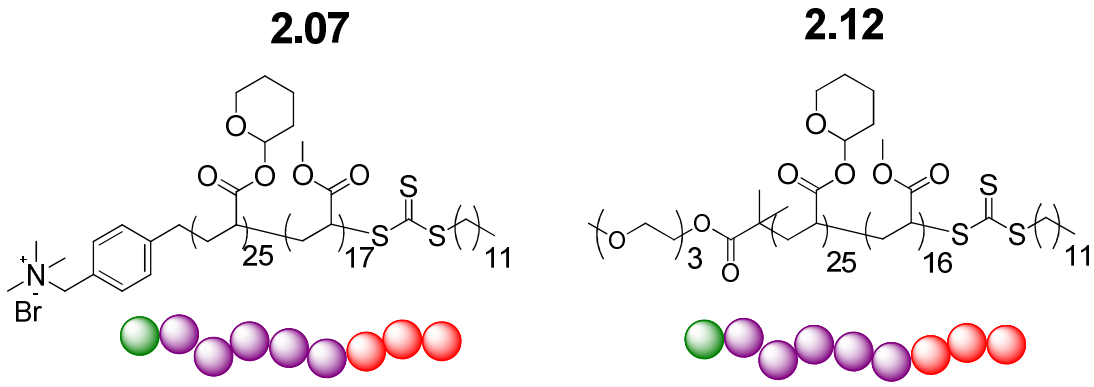

Figure 2.25: The structures of 2.07 and 2.12 with near identical block lengths but bearing different end group functionality

Polymer **2.07** was self-assembled by direct dissolution at 0.25 mg mL^{-1} and 30 °C to form structures with a D_h of 99 ± 4 nm. Therefore it would be expected that **2.12** would also be short enough to undergo self-assembly. **2.12** was assembled by direct dissolution at 30 °C at a concentration of 0.25 mg mL^{-1} but after three days precipitate remained in the vial. The solution was analysed by DLS to determine whether any of the polymer had self-assembled. The results were not stable for each run and varied in size between measurements (see Figure 2.26). The correlation coefficient was also low, meaning that the solution is too dilute and the measurements are not good quality. Therefore it would appear that the TEG functionality is not hydrophilic enough to induce self-assembly, even with shorter hydrophobic block lengths.

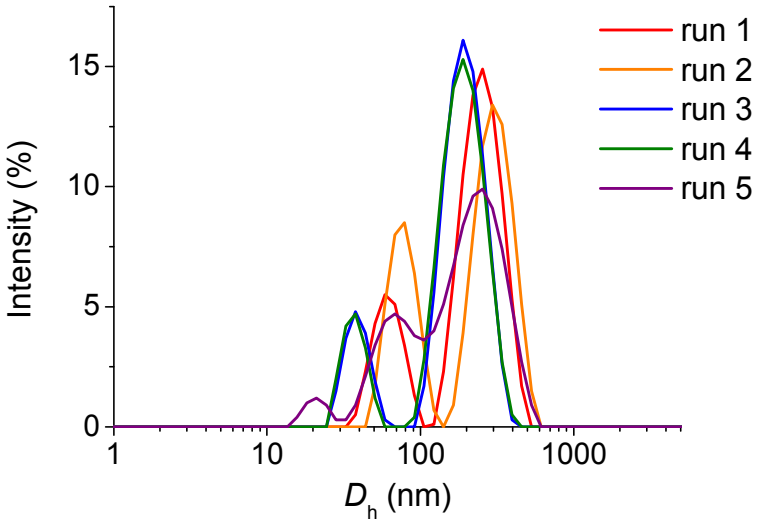

Figure 2.26: The variable D_h from DLS analysis of 2.12 after attempts at self-assembly at 0.25 mg mL^{-1} by direct dissolution at 30 °C

2.2.9 Concentration dependant morphology

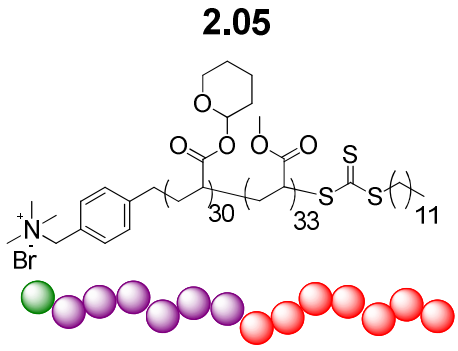

Figure 2.27: The structure of quaternary amine functionalised diblock copolymer 2.05

In order to determine whether the concentration at which the polymer was assembled affects the morphology adopted, the polymer that displayed the best self-assembly properties, **2.05** (see Figure 2.27), was assembled by direct dissolution at 30 °C, at concentrations of 1 and 2 mg mL^{-1}. These solutions were then analysed by DLS and TEM. For the solution at 1 mg mL^{-1}, the DLS results showed that there appeared to be two populations and the sizes varied between each measurement (see Figure 2.28). This solution was also analysed by cryo TEM and lamellar type structures can be seen (see Figure 2.29). This may be due to vesicle-like structures forming and aggregating.

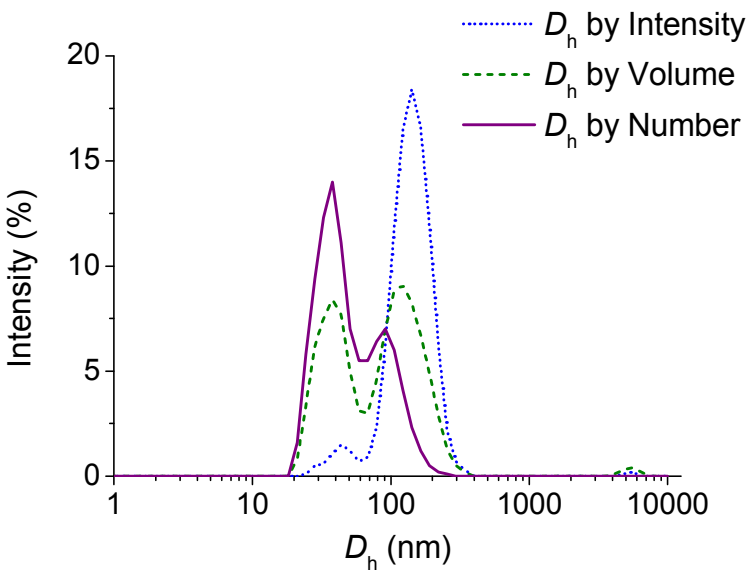

Figure 2.28: DLS traces of diblock copolymer 2.05 self-assembled by direct dissolution at 30 °C at a concentration of 1 mg mL^{-1}

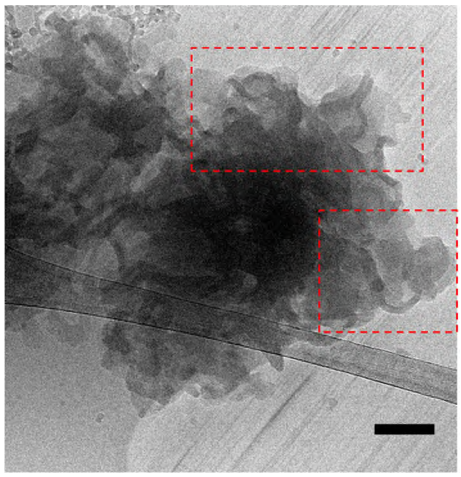

Figure 2.29: Cryo-TEM image of 2.05 self-assembled by direct dissolution at 1 mg mL^{-1}, scale bar = 200 nm. Lamellar type structures can be seen (highlighted)

The solution of **2.05** that was self-assembled at 2 mg mL^{-1} was also analysed by DLS and cryo TEM. The DLS results varied between measurements. Upon analysis by cryo-TEM, long strings of micelles could be seen (see Figure 2.31).

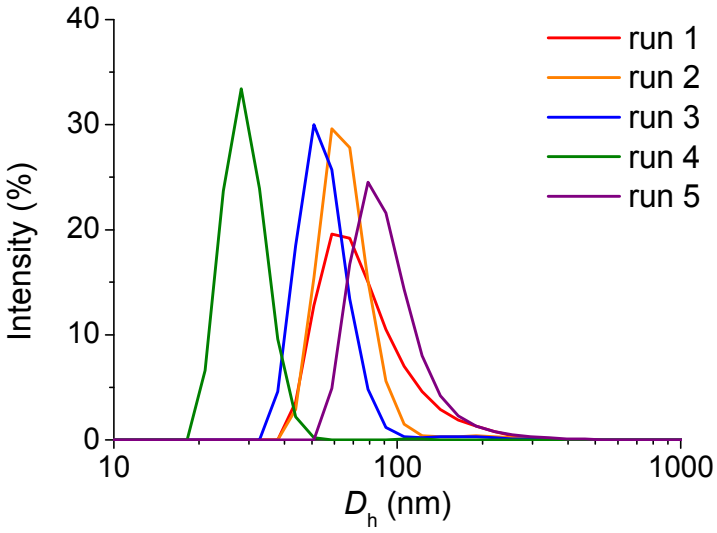

Figure 2.30: DLS traces of 2.05 self-assembled by direct dissolution at 30 °C at a concentration of 2 mg mL^{-1}

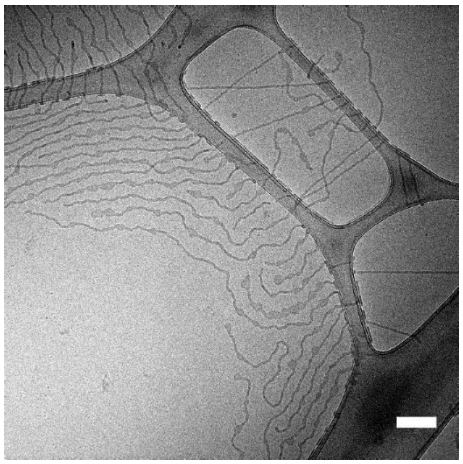

Figure 2.31: Cryo-TEM image of 2.05 self-assembled by direct dissolution at 30 °C at a concentration of 2 mg mL^{-1}, scale bar = 200 nm

These differences in morphology could be due to the polymer being assembled at different concentrations, as seen in previous examples within the literature.[6] Another possible cause for the difference in morphology could be due to different rates of deprotection of the polymer in solution. Since the deprotection of the THPA units can be acid-catalysed, and acrylic acid is formed after deprotection, it can be considered to be self-catalysing. Attempts were made to follow the deprotection by IR spectroscopy in solution but the solutions proved too dilute to be able to distinguish peaks. Following the deprotection by ^{1}H NMR

spectroscopy also proved too challenging, as for ^{1}H NMR spectroscopy the polymer needs to be in solution and three days of stirring were required before self-assembly occurred, by which point the different morphologies had formed. As the aim of this work was to target vesicles, no further exploration of the concentration effect upon morphology achieved was explored. However, these results are interesting and demonstrate the impact that slight variations in assembly conditions can have upon the adopted morphology of polymers in solution.

2.2.10 Deprotection of the polymer

Tetrahydropyran acrylate is a protected acid which can be deprotected either thermally or by an acid-catalysed reaction.[22-24] Upon deprotection the hydrophobic tetrahydropyranyl side chains degrade to form hydrophilic acrylic acid, releasing dihydropyran. In order to induce a vesicle to micelle morphology transition a vesicle solution of **2.05** at 0.25 mg mL^{-1} was heated at 65 °C overnight, with 1 equivalent of glacial acetic acid per THPA side chain. This resulted in the polymer precipitating, as the poly(acrylic acid) block is insoluble in acidic solution. In order to allow the deprotected polymer to self-assemble the solution was basified with NaOH solution until it was approximately pH 8. This solution was then stirred overnight to allow the self-assembled morphologies to stabilise. Based on the almost equal ratio of hydrophobic to hydrophilic blocks, the expected morphology for the deprotected polymer would be micelles. Analysis by DLS showed particles with a D_h of 19 ± 1 nm (Figure 2.32). Some larger structures are visible in the size by intensity, possibly caused by some vesicles remaining in solution or the micelles aggregating due to the polyelectrolyte effect.[33] Analysis of this solution by TEM shows populations of micelles with a D_h of 22 ± 4 nm (see Figure 2.33)

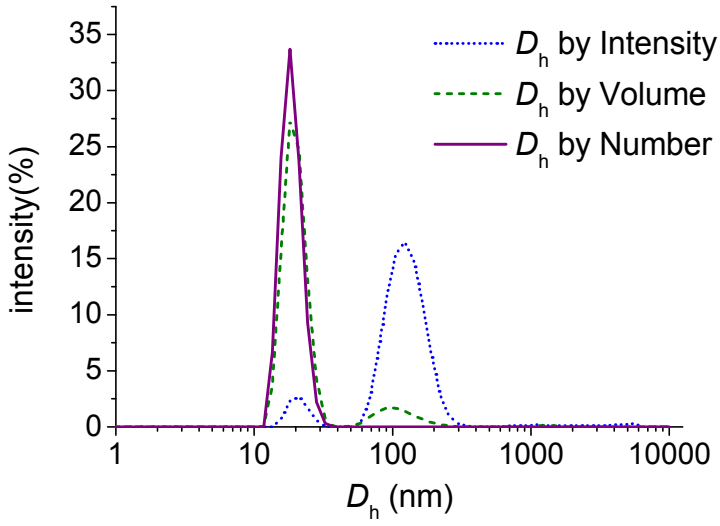

Figure 2.32: DLS traces of self-assembled diblock copolymer 2.05 at 0.25 mg mL^{-1} after deprotection with acetic acid

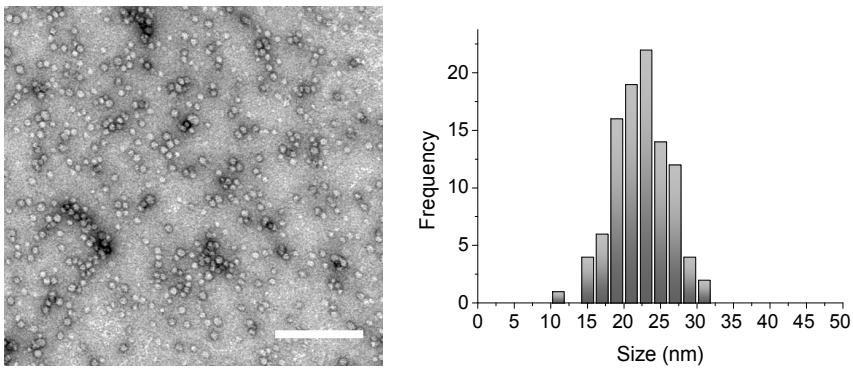

Figure 2.33: TEM image of micelles formed after deprotection of 2.05 with acetic acid, stained with uranyl acetate, scale bar = 200 nm, and the distribution of sizes observed

2.2.11 Limitations of THPA

The vesicle to micelle transition of the THPA block copolymers proceeds well as the deprotection requires relatively mild conditions and is self-catalysed. However, this ease of deprotection can prove to be a problem. It was noted that some of the polymers of THPA appeared to change from being fluffy powders to glassy polymers when stored for more than a week at 4 °C. A sample of **2.07** in DMSO was analysed over time by ^{1}H NMR spectroscopy and it showed considerable deprotection after three weeks of storage. The ^{1}H NMR spectra in Figure 2.34 show that the peaks at 7.37 and 7.50 ppm, which relate to the

aromatic protons, remain unchanged, as do the peaks at 3.06 and 0.88 ppm, which relate to the methyl groups on the charged quaternary amine and the terminal methyl group of the dodecyl chain, respectively. This shows that the CTA end groups are not degrading during storage. The peaks highlighted by the blue boxes are used to determine the deprotection. The peak at 5.91 ppm, corresponding to the THPA side chain, decreases over time and a broad peak at 12.5 ppm appears. This new peak is due to the formation of poly(acrylic acid).

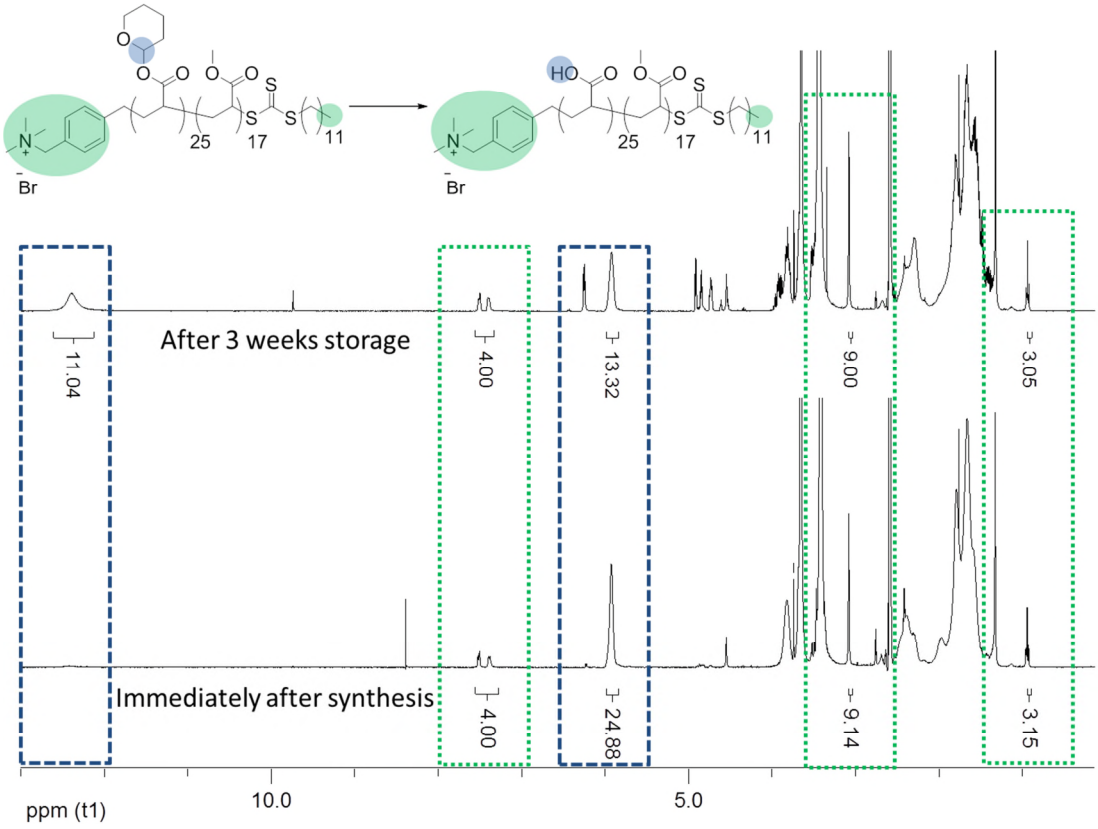

Figure 2.34: ^{1}H NMR spectra of 2.07 in DMSO immediately after synthesis (bottom) and after three weeks storage (top), showing the deprotection. The green boxes show the protons which remain unchanged and the blue boxes show the protons used to calculate the degree of deprotection. Spectra were recorded at 25 °C and 400 MHz.

Analysis of the polymer by IR spectroscopy also shows considerable deprotection. The appearance of the large broad peak at 3000 – 3500 cm^{-1} is representative of the OH acid group. The peak at 1731 cm^{-1} caused by the C=O of the ester in THPA has shifted to 1708 cm^{-1}, showing the transformation to an acid (see Figure 2.35).

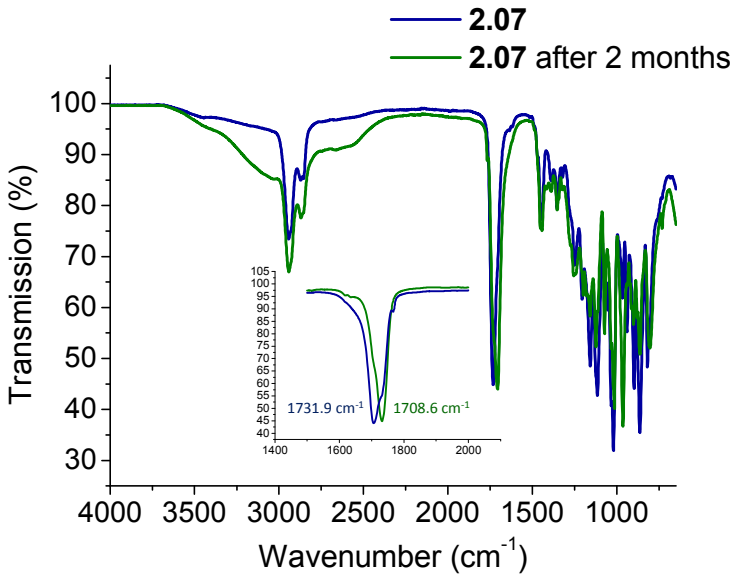

Figure 2.35: IR spectra of 2.07 immediately after synthesis (blue) and after 2 months storage (green), showing the deprotection that occurs upon storage

In order to test to see how stable the self-assembled vesicles are in aqueous solution, the polymer **2.07** was self-assembled by direct dissolution in water at 30 °C at a concentration of 0.25 mg mL^{-1}. After stirring for three days the polymer had self-assembled and the size was analysed by DLS. The solution continued to be analysed by DLS for several days and the change in size over time monitored (see Figure 2.36). Initially the size remained stable at *ca*. 98 nm, but after six days of stirring a smaller population with D_h = 45 ± 9 nm was also observed by DLS analysis. Analysis on the 7th day shows only the smaller population present. After 9 days stirring a small amount of salt was added to the solution in order to break up any aggregates caused by the polyelectrolyte effect and the size stabilised at 28 ± 1 nm. Therefore self-assembled solutions of these THPA polymers appear to have a very short shelf life.

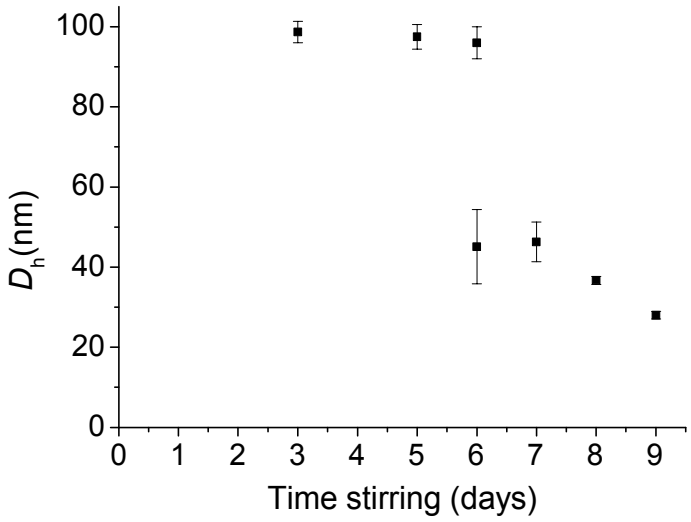

Figure 2.36: Size by number from DLS analysis of a self-assembled solution of diblock copolymer 2.07 at 0.25 mg mL^{-1} with time

Since the polymers deprotect in acidic solution, **2.07** was also self-assembled in pH 8.5 buffer at a concentration of 0.25 mg mL^{-1}. After 6 days of stirring at 30 °C there was still precipitate present in the vial. After several weeks of stirring the polymer had self-assembled and analysis by DLS shows a population with a $D_h = 31 \pm 3$ nm. This size is suggestive of micelle formation and therefore shows that the THP units can still deprotect in basic buffer to form micelles.

The original goal in targeting the vesicle to micelle transition was to be able to utilise the transition by releasing a hydrophilic substance from within the central water pool of the vesicle. Several attempts were made at this. Polymer **2.05** was self-assembled by solvent switch in the presence of the hydrophilic dye brilliant cresyl blue (BCB). This was not successful as a result of the precipitation of the polymer seen upon dialysis, as explained previously. The second attempt at encapsulating the hydrophilic dye within the vesicles was by direct dissolution of **2.05** in the presence of BCB.

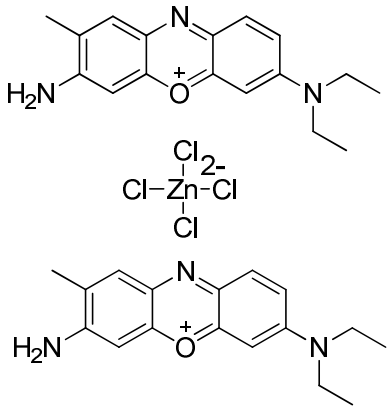

Figure 2.37: The structure of Brilliant Cresyl Blue

Polymer **2.05** was stirred at a concentration of 0.25 mg mL^{-1} at 30 °C in the presence of BCB at a concentration of 1 mg mL^{-1}. After three days of stirring the polymer had self-assembled as there was no visible precipitate in the polymer solution. The vesicle solution was dialysed in order to remove any dye that had not been trapped within the central water pool of the vesicles. However the polymer was seen to precipitate in the dialysis bag. Coupling the difficulty in self-assembling with the poor stability of the vesicles in water and the short shelf life of the polymer, both in solution and in a dry state, it was decided that future encapsulation and release attempts were futile. Therefore we shifted our attention to a different pH-responsive polymer system.

2.3 Conclusions

The pH deprotectable monomer THPA was utilised due to its ability to undergo a change in hydrophobicity in response to deprotection with acetic acid. By incorporating the monomer into a diblock copolymer bearing hydrophilic end group functionality, morphology switching structures were obtained. Two different hydrophilic end groups were investigated, a charged quaternary amine end group and a triethylene glycol end group. Different methods for self-assembly of the diblock copolymers were investigated and it was found that for the quaternary amine functionalised polymer direct dissolution at a low concentration (0.25 mg mL^{-1}), coupled with heating at 30 °C, achieved the formation of vesicles. These vesicles were then treated with acetic acid in order to deprotect the THP functionalities and form acrylic acid. Upon basifying the solution micelles were formed, showing the vesicle to micelle transformation.

The diblock copolymers that incorporated the triethylene glycol end group were found to not self-assemble under any of the conditions tried. This is due to the reduced hydrophilicity the triethylene glycol group provides compared to that of the charged quaternary amine.

The stability of the THPA units was investigated, both in the dry state and when assembled in solution. Analysis by ^{1}H NMR spectroscopy showed that the dried polymer would undergo deprotection when stored, even at low temperatures (4 °C). Analysis by DLS of the vesicle solution showed that the vesicles were stable for up to 5 days, after which point the size decreased as the THPA block started to deprotect. The unwanted deprotection of the THPA units is enhanced by the deprotection reaction being acid catalysed, and an acid being the product of the reaction.

2.4 Experimental

2.4.1 Materials

2,2'-Azobis(2-methylpropionitrile) (AIBN) was recrystallised from methanol and stored in the dark at 4 °C. Methyl acrylate (MA) was distilled over CaH_2 and stored at 4 °C. Tetrahydropyran acrylate (THPA) was synthesised as in literature[32] and stored at -7 °C. All other materials were used as received from Sigma-Aldrich Co. Tetrahydrofuran (THF) and *N, N*-dimethylformamide (DMF) were used as received from Fisher Scientific unless stated otherwise. Dry DMF was used as received from Sigma-Aldrich Co. Dialysis tubing was supplied by Medicell with a molecular weight cut off of 3.5 kDa.

2.4.2 Characterisation

^{1}H NMR spectroscopy and ^{13}C NMR spectroscopy were obtained at 400 and 125 MHz respectively with a Bruker DPX-400 spectrometer in $CDCl_3$ or DMSO unless otherwise stated. Chemical shifts are reported in parts per million (ppm) and referenced to the residual solvent peak ($CDCl_3$ ^{1}H: δ = 7.26 ppm, ^{13}C: δ = 77.16 ppm, DMSO ^{1}H δ = 2.50 ppm).

SEC data was obtained using HPLC grade DMF with 2% LiBr with a flow rate of 1 mL min^{-1}, on a set of two PLgel 5µm Mixed-D columns with a guard column. SEC data was analysed using Cirrus Software based on polymethylmethacrylate (PMMA) standards. Infrared spectroscopy was recorded on a Perkin-Elmer Spectrum 100 FT-IR ATR unit. Mass spectra were recorded on a Bruker Esquire 2000 ESI spectrometer.

Dynamic Light Scattering (DLS) analysis was performed on a Malvern Zetasizer Nano ZS instrument operating at 25 °C with a 4 mW He-Ne 633 nm laser module. Measurements were made at an angle of 173° (back scattering) and results were analysed using Malvern DTS 5.02. All determinations were made in triplicate unless otherwise stated (with 10 measurements recorded for each run).

TEM samples were prepared by placing an oxygen-plasma treated, carbon coated copper grid film side down onto a droplet of the solution to be analysed. After two minutes the excess liquid was blotted with filter paper and the grid allowed to dry. The sample was then stained using a 1% uranyl acetate solution for 30 seconds (unless otherwise stated), blotted with filter paper to remove excess liquid and the grid allowed to dry. Samples were analysed with a TEM microscope (JEOL TEM-1200 or JEOL TEM-2011), operating at 200 kV.

2.4.3 Synthesis of CTA 2.01

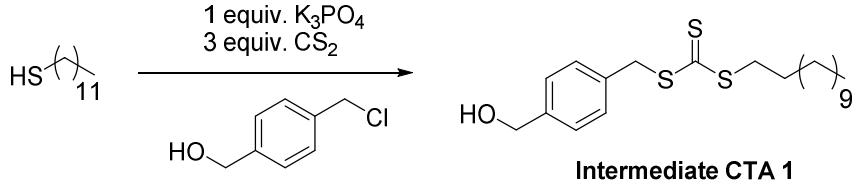

Scheme 2.5: Synthetic route to intermediate CTA 1

The quaternary amine functionalized CTA was synthesized in a three step procedure. Firstly dodecylsulfanyl ([4-(hydroxymethyl) phenyl] methylsulfanyl) methanethione was synthesized as previously reported.[22] Dodecanethiol (1 g, 4.9 mmol) was added to a stirred suspension of potassium phosphate (1.04 g, 4.9 mmol) in acetone (10 mL) and the reaction mixture was stirred for ten minutes. Carbon disulfide (1.12 g, 14.7 mmol) was added and the solution turned yellow. The solution was stirred for 1 hour 20 minutes, at which point 4-(chloromethyl) benzyl alcohol (0.77 g, 4.9 mmol) was added. The reaction mixture was then stirred at room temperature for a further 19 hours. The reaction mixture was then filtered and all volatiles removed under reduced pressure. The crude product was purified by dissolving in DCM (20 mL) and washing with hydrochloric acid (20 mL), water (3 x 20 mL) and saturated brine solution (3 x 20 mL). The organic layer was dried over magnesium sulphate, filtered and washed with dichloromethane and cold hexane to remove the last traces of dodecanethiol, to give intermediate CTA **1** as a yellow solid (1.7 g, 87%). IR spectroscopy (ν_{max}/cm^{-1}): 3360 (O-H), 2957 (alkane C-H), 2916 (alkane C-H), 2850 (alkane C-H), 1614 (aromatic C=C), 1512 (aromatic C=C), 1485 (aromatic C=C), 1061 (thiocarbonyl S=C). ^{1}H

NMR spectroscopy ($CDCl_3$, 400 MHz): δ (ppm): 0.88 (t, 3H, $^3J_{H\text{-}H}$=9 Hz, $(CH_2)_9CH_3$), 1.2-1.45 (m, 18H, $(CH_2)_9CH_3$), 1.7 (m, 2H, $SCSSCH_2CH_2$), 3.37 (t, 2H, $^3J_{H\text{-}H}$=9.8 Hz, $SCSSCH_2CH_2$), 4.61 (s, 2H, $ArCH_2SCSS$), 4.68 (d, 2H, $J_{H\text{-}H}$=7.6 Hz, $HOCH_2Ar$), 7.33 (m, 4H, Ar*H*). ^{13}C NMR spectroscopy ($CDCl_3$, 500 MHz): δ (ppm): 14.1, 22.7, 28.0, 28.9, 29.1, 29.4, 29.5, 29.6, 29.7, 31.9, 37.1, 41, 65, 127.3, 129.5, 134.6, 140.4, 223.7.

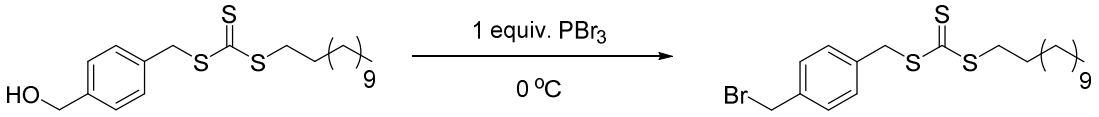

Intermediate CTA 2

Scheme 2.6: Synthetic route to intermediate CTA 2 from intermediate CTA 1

The next step in the procedure involved the bromination of the alcohol functionality.[31] Intermediate **CTA 1** (1.5 g, 3.8 mmol) was dissolved in diethyl ether/DMF (10:1 v/v, 55 mL total volume) under nitrogen. This was placed in an ice bath and phosphorous tribromide (0.36 mL, 3.8 mmol) was added drop wise. After stirring in ice for 1 hour, the reaction was allowed to come to room temperature and stirred for a further two hours. The crude product was washed with sodium hydrogen carbonate solution (3 x 50 mL), water (3 x 50 mL) and saturated brine (3 x 50 mL), dried over magnesium sulphate, filtered and the solvent removed under reduced pressure. The crude product was purified *via* flash column chromatography on silica gel using 9:1 petroleum ether: ethyl acetate as the eluent, giving intermediate **CTA 2** as a yellow solid (1.37 g, 79%). IR spectroscopy (ν_{max}/cm^{-1}): 2956 (alkane C-H), 2916 (alkane C-H), 2849 (alkane C-H), 1469 (aromatic C=C), 1060 (thiocarbonyl S=C). ^1H NMR spectroscopy ($CDCl_3$, 400 MHz): δ (ppm): 0.88 (t, 3H, $^3J_{H\text{-}H}$ = 9 Hz, $(CH_2)_9CH_3$), 1.2-1.45 (m, 18H, $(CH_2)_9CH_3$), 1.7 (m, 2H, $SCSSCH_2CH_2$), 3.37 (t, 2H, $^3J_{H\text{-}H}$ = 9.8 Hz, $SCSSCH_2CH_2$), 4.47 (s, 2H, $ArCH_2SCSS$), 4.60 (d, 2H, $^3J_{H\text{-}H}$ = 7.6 Hz, $HOCH_2Ar$), 7.33 (m, 4H, Ar*H*). ^{13}C NMR spectroscopy ($CDCl_3$, 500 MHz): δ (ppm): 14.2, 22.7, 28.0, 28.9, 29.1, 29.4, 29.5, 29.6, 29.7, 31.9, 33.0, 37.1, 40.8, 129.4, 129.7, 135.7, 137.3, 223.5.

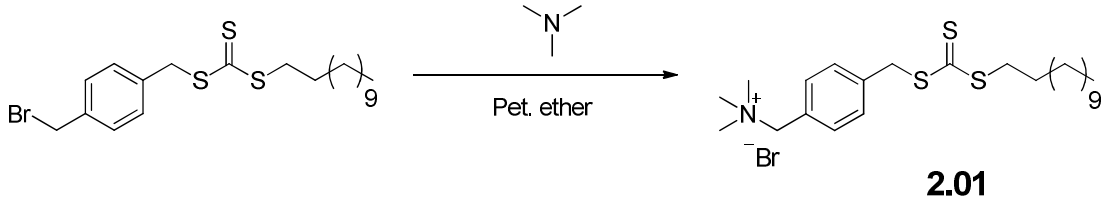

2.01

Scheme 2.7: Synthetic route to 2.01 from intermediate CTA 2

Intermediate **CTA 2** (1 g, 2.2 mmol) was dissolved in petroleum ether (50 mL) under nitrogen. Trimethylamine (1M in THF, 10.8 mL, 10.8 mmol) was added slowly and the reaction stirred at room temperature for 19 hours before the precipitated product was isolated by vacuum filtration, washed with petroleum ether (3 x 30 mL) and dried *in vacuo* to give **2.01** as a bright yellow solid (0.86 g, 91%). IR spectroscopy (ν_{max}/cm^{-1}): 3010 (aromatic C-H), 2955 (alkane C-H), 2919 (alkane C-H), 2850 (alkane C-H), 1614 (aromatic C=C), 1512 (aromatic C=C), 1485 (aromatic C=C), 1467 (aromatic C=C), 1060 (thiocarbonyl S=C). ^{1}H NMR spectroscopy ($CDCl_3$, 400 MHz): δ (ppm): 0.88 (t, 3H, $^3J_{H\text{-}H}$ = 9 Hz, $(CH_2)_9CH_3$), 1.2-1.45 (m, 18H, $(CH_2)_9CH_3$), 1.7 (m, 2H, $SCSSCH_2CH_2$), 3.39 (m, 11H, , $SCSSCH_2CH_2$ and $(CH_3)_3N$), 4.63 (s, 2H, $ArCH_2SCSS$), 5.05 (d, 2H, $^3J_{H\text{-}H}$ = 7.6 Hz, $HOCH_2Ar$), 7.40 (d, 2H, $^3J_{H\text{-}H}$ = 7.6 Hz, $(CH)_2CCH_2S$), 7.61 (d, 2H, $^3J_{H\text{-}H}$ = 8 Hz, $(CH_3)_3NCH_2C(CH)_2$). ^{13}C NMR spectroscopy ($CDCl_3$, 500 MHz): δ (ppm): 14.1, 22.7, 28.0, 28.96, 29.1, 29.3, 29.5, 29.6, 29.6, 29.57, 29.6, 31.9, 37.3, 40.3, 52.7, 68.3, 126.8, 130, 133.4, 138.8, 223. LR-ESI-MS found: 440.2 $(M)^+$ $C_{24}H_{42}NS_3$, 381.1 $C_{21}H_{33}S_3$. HR-ESI $C_{24}H_{42}NS_3$ $(M)^+$ 440.2474 (calcd), 440.2478 (found).

2.4.4 Synthesis of quaternary end group functionalised PTHPA

A typical polymerisation of THPA with the charged CTA **2.01** is detailed below. To achieve the different block lengths of the different homopolymers **2.02**, **2.03** and **2.04**, different equivalents of THPA monomer, relative to the CTA, were used. **2.01** (83.1 mg, 0.16 mmol), THPA (2.0 g, 12.8 mmol) and AIBN (2.6 mg, 0.02 mmol) were dissolved in dry DMF (4 mL, 2: 1 w: v compared to monomer) and placed in an oven dried ampoule with a stirrer bar,

under the flow of nitrogen. The solution was degassed at least three times by successive *freeze-pump-thaw* techniques and released to and sealed under nitrogen. The polymerisation mixture was then heated at 65 °C for 1 hour 10 minutes. The polymerisation mixture was cooled to stop the reaction and the resulting polymer purified by precipitation into diethyl ether (300 mL) once and hexanes (300 mL) twice to afford chain end functionalised homopolymer, **2.02**, M_n (^{1}H NMR) = 5.0 kDa, M_n (DMF SEC) = 5.3 kDa, $Đ_M$ = 1.11. IR spectroscopy (ν_{max}/cm^{-1}): 2940 (alkane C-H), 2868 (alkane C-H), 1732 (ester C=O), 1443 (aromatic C=C), 1020 (thiocarbonyl S=C). ^{1}H NMR spectroscopy ($CDCl_3$, 400 MHz): δ (ppm): 0.85 (t, 3H, $^3J_{H-H}$ = 6.8 Hz, $(CH_2)_9CH_3$ of CTA end group), 1.21-1.40 (m, 20H,$CH_2(CH_2)_{10}CH_3$ in CTA), 1.41-2.72 (br m, C*H* and CH_2 in polymer backbone and THPA side chain), 3.34 (m, 11H, $(CH_3)_3N^+$ and $SCSSCH_2(CH_2)_{11}CH_3$), 3.61-3.90 (br d, 58H, OCH_2CH_2 in THPA side chain), 4.91 (br m, 2H, $(CH_3)_3NCH_2Ar$), 5.93 (br s, 29H, OC*H*O THPA side chain), 7.27 (br s, 2H, Ar*H*), 7.54 (br s, 2H, Ar*H*).

Homopolymer **2.03**, M_n (^{1}H NMR) = 6.3 kDa, M_n (DMF SEC) = 7.3 kDa, $Đ_M$ = 1.16. ^{1}H NMR spectroscopy ($CDCl_3$, 400 MHz): δ (ppm): 0.88 (t, 3H, $^3J_{H-H}$ = 6.7 Hz, $(CH_2)_9CH_3$ of CTA end group), 1.23-1.40 (m, 20H,$CH_2(CH_2)_{10}CH_3$ in CTA), 1.43-2.60 (br m, C*H* and CH_2 in polymer backbone and THPA side chain), 3.32 (m, 11H, $(CH_3)_3N^+$ and $SCSSCH_2(CH_2)_{11}CH_3$), 3.57-3.95 (br d, 74H, OCH_2CH_2 in THPA side chain), 4.88 (br m, 2H, $(CH_3)_3NCH_2Ar$), 5.95-6.05 (br s, 37H, OC*H*O THPA side chain), 7.27 (br s, 2H, Ar*H*), 7.54 (br s, 2H, Ar*H*).

Homopolymer **2.04**, M_n (^{1}H NMR) = 4.4 kDa, M_n (DMF SEC) = 4.6 kDa, $Đ_M$ = 1.10. ^{1}H NMR spectroscopy ($CDCl_3$, 400 MHz): δ (ppm): 0.86 (t, 3H, $^3J_{H-H}$ = 6.7 Hz, $(CH_2)_9CH_3$ of CTA end group), 1.20-1.40 (m, 20H,$CH_2(CH_2)_{10}CH_3$ in CTA), 1.41-2.70 (br m, C*H* and CH_2 in polymer backbone and THPA side chain), 3.31 (m, 11H, $(CH_3)_3N^+$ and $SCSSCH_2(CH_2)_{11}CH_3$), 3.58-3.91 (br d, 74H, OCH_2CH_2 in THPA side chain), 4.87 (br m, 2H, $(CH_3)_3NCH_2Ar$), 5.86-6.02 (br s, 37H, OC*H*O THPA side chain), 7.27 (br s, 2H, Ar*H*), 7.53 (br s, 2H, Ar*H*).

2.4.5 Synthesis of quaternary end group functionalised diblock copolymer

The typical conditions for the chain extension of the quaternary amine functionalised PTHPA homopolymer with MA are detailed below. To achieve the different MA block lengths in **2.05**, **2.06** and **2.07**, different equivalents of MA were used. **2.05** (0.2 g, 0.04 mmol), MA (0.13 g, 1.45 mmol), and AIBN (1.2 mg, 0.008 mmol) were dissolved in dry DMF (0.5 mL) and placed in an oven dried ampoule with a stirrer bar, under the flow of nitrogen. The ampoule was degassed at least three times and released to and sealed under nitrogen. The polymerisation mixture was then heated at 65 °C for 2 hours. The polymerisation mixture was rapidly cooled by submerging the vessel in liquid nitrogen to stop the reaction and the resulting polymer purified by precipitation into hexanes (3 x 300 mL) to afford chain end functionalised diblock copolymer, **2.05**, M_n (^{1}H NMR) = 7.6 kDa, M_n (DMF SEC) = 10.5 kDa, $Đ_M$ = 1.12. IR spectroscopy (ν_{max}/cm^{-1}): 2940 (alkane C-H), 2868 (alkane C-H), 1732 (ester C=O), 1443 (aromatic C=C), 1020 (thiocarbonyl S=C). ^{1}H NMR spectroscopy (CDCl3, 400 MHz): δ (ppm): 0.87 (t, 3H, $^3J_{H-H}$ = 6.8 Hz, CH_2CH_3 of CTA end group), 1.21-1.30 (m, 20H, $CH_2(CH_2)_{10}CH_3$ of CTA end group), 1.31-2.50 (br m, C*H* and CH_2 in polymer backbone and THPA side chain), 3.33 (m, 11H, $(CH_3)_3N^+$ and $SC{=}SSCH_2(CH_2)_{11}CH_3$), 3.61-3.90 (br m, 150H, OCH_2CH_2 in THPA side chain and OCH_3 in MA side chain), 4.89 (br m, 2H, $(CH_3)_3NCH_2Ar$), 5.90-6.04 (br s, 30H, OC*H*O THPA side chain), 7.27 (br m, 2H, Ar*H* in CTA head group), 7.54 (br m, 2H, Ar*H* in CTA head group).

Diblock copolymer **2.06,** M_n (^{1}H NMR) = 8.9 kDa, M_n (DMF SEC) = 8.8 kDa, $Đ_M$ = 1.12. ^{1}H NMR spectroscopy (CDCl3, 400 MHz): δ (ppm): 0.87 (t, 3H, $^3J_{H-H}$ = 6.8 Hz, CH_2CH_3 of CTA end group), 1.21-1.30 (m, 20H, $CH_2(CH_2)_{10}CH_3$ of CTA end group), 1.31-2.50 (br m, C*H* and CH_2 in polymer backbone and THPA side chain), 3.33 (m, 11H, $(CH_3)_3N^+$ and $SC{=}SSCH_2(CH_2)_{11}CH_3$), 3.61-3.90 (br m, 161H, OCH_2CH_2 in THPA side chain and OCH_3 in MA side chain), 4.89 (br m, 2H, $(CH_3)_3NCH_2Ar$), 5.84-6.04 (br s, 37H, OC*H*O THPA side chain), 7.27 (br m, 2H, Ar*H* in CTA), 7.54 (br m, 2H, Ar*H* in CTA).

Diblock copolymer **2.07,** M_n (^{1}H NMR) = 5.9 kDa, M_n (DMF SEC) = 6.9 kDa, $Đ_M$ = 1.12. ^{1}H NMR spectroscopy (CDCl3, 400 MHz): δ (ppm): 0.88 (t, 3H, $^3J_{H\text{-}H}$ = 6.8 Hz, CH_2CH_3 of CTA end group), 1.20-1.38 (m, 20H, $CH_2(CH_2)_{10}CH_3$ of CTA end group), 1.38-2.60 (br m, C*H* and CH_2 in polymer backbone and THPA side chain), 3.33 (m, 11H, $(CH_3)_3N^+$ and $SC{=}SSCH_2(CH_2)_{11}CH_3$), 3.58-3.94 (br m, 95H, OCH_2CH_2 in THPA side chain and OCH_3 in MA side chain), 4.89 (br m, 2H, $(CH_3)_3NCH_2Ar$), 5.86-6.02 (br s, 25H, OC*H*O THPA side chain), 7.27 (br m, 2H, Ar*H* in CTA), 7.54 (br m, 2H, Ar*H*).

2.4.6 Synthesis of TEG functionalised CTA

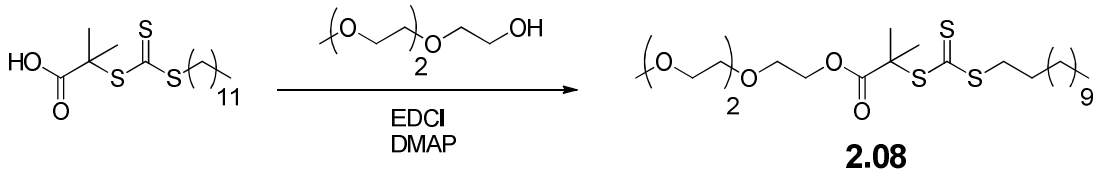

2.08

Scheme 2.8: Synthetic route to TEG functionalised CTA 2.08

DDMAT (1 g, 2.7 mmol) was stirred in DCM (10 mL) that had been purged with nitrogen. EDCI (0.58 g, 3.01 mmol), DMAP (0.17 g, 1.37 mmol) and triethyleneglycol momomethylether (0.49 g, 3.01 mmol) were added. The solution was stirred at room temperature overnight. 50 mL DCM was added and the organic solution washed with water. The organic layer was collected and washed with brine and then dried over magnesium sulphate. The crude product was columned in 2: 1 petroleum ether: ethyl acetate and the pure product collected and dried to yield **2.08** as a yellow oil. IR spectroscopy (ν_{max}/cm^{-1}): 2922 (alkane C-H), 2853 (alkane C-H), 1734 (ester C=O), 1465 (C-H alkane bend), 1257 (C-O ester), 1113 (C-O ester), 1066 (thiocarbonyl S=C). ^{1}H NMR spectroscopy ($CDCl_3$, 400 MHz): δ (ppm): 0.88 (t, 3H, $^3J_{H\text{-}H}$ = 6.68 Hz, $(CH_2)_9CH_3$), 1.22-1.40 (m, 18H, $(CH_2)_9CH_3$), 1.62-1.72 (m, 8H, $SCSSCH_2CH_2$ and $SCSSC(CH_3)_2COO$), 3.26 (t, 2H, $^3J_{H\text{-}H}$ = 7.44 Hz, $SCSSCH_2CH_2$), 3.38 (s, 3H, $CH_3OCH_2CH_2$), 3.55 (m, 2H,OCH_2CH_2OCO), 3.61-3.71 (m, 8H, $(OCH_2CH_2O)_2$), 4.26 (d, 2H, $^3J_{H\text{-}H}$ = 4.95 Hz, OCH_2CH_2OCO). ^{13}C NMR spectroscopy ($CDCl_3$, 500 MHz): δ (ppm): 14.1, 22.7, 25.3, 27.8, 28.9, 29.1, 29.3, 29.6, 55.9, 59.1, 65.1,

67.1, 68.8, 70.6, 71.9, 223.0 HR-ESI $C_{24}H_{46}O_5S_3$ $(M)^+$ 510.2507 (calcd), $(M+Na)^+$ 533.25 (found).

2.4.7 Synthesis of the TEG functionalised homopolymer

The general technique for the polymerisation of THPA with the TEG functionalised CTA, **2.08**, is detailed below. To achieve the shorter block length fewer equivalents of THPA were used in the polymerisation. **2.08** (81.7 mg, 0.16 mmol), THPA (1.0 g, 6.4 mmol) and AIBN (2.6 mg, 0.02 mmol) were dissolved in dry DMF (1 mL, 1: 1 w: v compared to monomer) and placed in an oven dried ampoule with a stirrer bar, under the flow of nitrogen. The solution was degassed at least three times by successive *freeze-pump-thaw* techniques and released to and sealed under nitrogen. The polymerisation mixture was then heated at 65 °C for one hour, then cooled to stop the reaction and the resulting polymer purified by precipitation into diethyl ether (300 mL) once and hexanes (300 mL) twice to afford chain end functionalised homopolymer, **2.09**, M_n (^{1}H NMR) = 5.2 kDa, M_n (DMF SEC) = 3.0 kDa, $Đ_M$ = 1.12. ^{1}H NMR spectroscopy (CDCl3, 400 MHz): δ (ppm): 0.88 (t, 3H, $^3J_{H\text{-}H}$ = 6.8 Hz, CH_2CH_3 of CTA end group), 1.02-2.70 (br m, $CH_2(CH_2)_{10}CH_3$ of CTA end group, C*H* and CH_2 in polymer backbone and THPA side chain), 3.33 (m, 5H, $CH_3OCH_2CH_2$ from TEG functionality and $SC{=}SSCH_2(CH_2)_{11}CH_3$), 3.54 (br m, 2H, OCH_2CH_2OCO in TEG functionality), 3.57-3.75 (br m, 41H, $OCHHCH_2$ in THPA side chain and OCH_2CH_2O from TEG functionality), 3.75-3.96 (br s, 34H, $OCHHCH_2$ in THPA side chain), 4.17 (br m, 2H, OCH_2CH_2OCO in TEG functionality), 5.87-6.05 (br s, 34H, OC*H*O THPA side chain).

Homopolymer **2.10**, M_n (^{1}H NMR) = 4.2 kDa, M_n (DMF SEC) = 3.1 kDa, $Đ_M$ = 1.09. ^{1}H NMR spectroscopy (CDCl3, 400 MHz): δ (ppm): 0.88 (t, 3H, $^3J_{H\text{-}H}$ = 6.8 Hz, CH_2CH_3 of CTA end group), 1.02-2.70 (br m, $CH_2(CH_2)_{10}CH_3$ of CTA end group, C*H* and CH_2 in polymer backbone and THPA side chain), 3.34 (m, 5H, $CH_3OCH_2CH_2$ from TEG functionality and $SC{=}SSCH_2(CH_2)_{11}CH_3$), 3.54 (br m, 2H, OCH_2CH_2OCO in TEG functionality), 3.58-3.75 (br m, 41H, $OCHHCH_2$ in THPA side chain and OCH_2CH_2O from

TEG functionality), 3.75-3.98 (br s, 34H, OCH*H*CH_2 in THPA side chain), 4.18 (br m, 2H, OCH_2CH_2OCO in TEG functionality), 5.87-6.06 (br s, 34H, OC*H*O THPA side chain).

2.4.8 Synthesis of the TEG functionalised diblock copolymer

The general technique for the chain extension of the TEG functionalised PTHPA homopolymer with MA is detailed below. To achieve the shorter block length fewer equivalents of MA were used in the polymerisation. **2.09** (0.2 g, 0.04 mmol), MA (0.12 g, 1.5 mmol) and AIBN (1.2 mg, 0.007 mmol) were dissolved in dry DMF (0.5 mL) and placed in an oven dried ampoule with a stirrer bar, under the flow of nitrogen. The solution was degassed at least three times by successive *freeze-pump-thaw* techniques and released to and sealed under nitrogen. The polymerisation mixture was then heated at 65 °C for 1 hour 30 minutes. The polymerisation mixture was cooled to stop the reaction and the resulting polymer purified by precipitation into diethyl ether (300 mL) once and hexanes (300 mL) twice to afford chain end functionalised diblock copolymer, **2.11**, M_n (^{1}H NMR) = 8.0 kDa, M_n (DMF SEC) = 6.0 kDa, $Đ_M$ = 1.14. ^{1}H NMR spectroscopy (CDCl3, 400 MHz): δ (ppm): 0.88 (t, 3H, $^3J_{H\text{-}H}$ = 6.8 Hz, CH_2CH_3 of CTA end group), 1.02-2.70 (br m, $CH_2(CH_2)_{10}CH_3$ of CTA end group, C*H* and CH_2 in polymer backbone and THPA side chain), 3.34 (m, 5H, $CH_3OCH_2CH_2$ from TEG functionality and SC=SSC$H_2(CH_2)_{11}CH_3$), 3.54 (br m, 2H, OCH_2CH_2OCO in TEG functionality), 3.60-3.78 (br m, 120H, OC*H*HCH_2 in THPA side chain, OCH_2CH_2O from TEG functionality, and OCH_3 from MA side chain), 3.78-3.94 (br s, 34H, OCH*H*CH_2 in THPA side chain), 4.18 (br m, 2H, OCH_2CH_2OCO in TEG functionality), 5.88-6.02 (br s, 34H, OC*H*O THPA side chain).

Diblock copolymer **2.12**, M_n (^{1}H NMR) = 5.6 kDa, M_n (DMF SEC) = 5.2 kDa, $Đ_M$ = 1.07. ^{1}H NMR spectroscopy (CDCl3, 400 MHz): δ (ppm): 0.88 (t, 3H, $^3J_{H\text{-}H}$ = 6.8 Hz, CH_2CH_3 of CTA end group), 1.02-2.70 (br m, $CH_2(CH_2)_{10}CH_3$ of CTA end group, C*H* and CH_2 in polymer backbone and THPA side chain), 3.34 (m, 5H, $CH_3OCH_2CH_2$ from TEG functionality and SC=SSC$H_2(CH_2)_{11}CH_3$), 3.55 (br m, 2H, OCH_2CH_2OCO in TEG functionality), 3.58-3.76 (br m, 80H, OC*H*HCH_2 in THPA side chain and OCH_2CH_2O from

TEG functionality), 3.76-3.94 (br s, 24H, OCH*H*CH_2 in THPA side chain), 4.18 (br m, 2H, OCH_2CH_2OCO in TEG functionality), 5.86-6.04 (br s, 24H, OC*H*O THPA side chain).

2.4.9 Self-assembly techniques

Solvent switch

The polymer was dissolved in THF at a concentration of 0.5 mg mL^{-1} and an equal volume of water slowly added at a rate of 0.6 mL min^{-1}, with stirring. The solution was then transferred to a dialysis bag (MWCO 3.5 kDa) and dialysed against 18.2 MΩ cm^{-1} water, incorporating at least six water changes.

Thin film formation

The polymer was dissolved in THF in a round bottom flask at a concentration of 0.25 mgmL^{-1}. After stirring for one hour, the solvent was slowly removed *in vacuo* with rotation of the flask. This left a thin film of polymer coating the sides of the flask. 18.2 MΩ cm^{-1} water was then added to a concentration of 0.25 mg mL^{-1} and then solution stirred at 30 °C for three days.

Direct dissolution

The polymer was stirred in 18.2 MΩ cm^{-1} water at a concentration of 0.25 mg mL^{-1} in an oil bath maintained at 30 °C for three days.

2.4.10 Deprotection of the polymer

A solution of self-assembled polymer at 0.25 mg mL^{-1} was stirred overnight with acetic acid (1 equivalent per THPA unit) with heating to 65 °C. The solution was then cooled to room temperature and the pH of the solution adjusted to neutral in order to analyse the assemblies by DLS and TEM.

2.5 References

1. G. Riess, *Prog. Polym. Sci.*, 2003, 28, 1107-1170.
2. Y. Mai and A. Eisenberg, *Chem. Soc. Rev.*, 2012, 41, 5969-5985.
3. A. Blanazs, S. P. Armes and A. J. Ryan, *Macromol. Rapid Commun.*, 2009, 30, 267-277.
4. J. Israelachvili, *Intermolecular and Surface Forces*, Academic Press, London, 2nd edn., 1991.
5. R. B. Grubbs and Z. Sun, *Chem. Soc. Rev.*, 2013, 42, 7436-7445.
6. S. Y. Kim, K. E. Lee, S. S. Han and B. Jeong, *J. Phys. Chem. B*, 2008, 112, 7420-7423.
7. D. Wang, T. Wu, X. Wan, X. Wang and S. Liu, *Langmuir*, 2007, 23, 11866-11874.
8. M. d. R. Rodriguez-Hidalgo, C. Soto-Figueroa and L. Vicente, *Soft Matter*, 2013, 9, 5762-5770.
9. M. I. Gibson and R. K. O'Reilly, *Chem. Soc. Rev.*, 2013, 42, 7204-7213.
10. D. Roy, W. L. A. Brooks and B. S. Sumerlin, *Chem. Soc. Rev.*, 2013, 42, 7214-7243.
11. J. Seuring and S. Agarwal, *Macromol. Rapid Commun.*, 2012, 33, 1898-1920.
12. J. Seuring and S. Agarwal, *ACS Macro Lett.*, 2013, 2, 597-600.
13. S. Dai, P. Ravi and K. C. Tam, *Soft Matter*, 2009, 5, 2513-2533.
14. R. Liu, M. Fraylich and B. Saunders, *Colloid. Polym. Sci.*, 2009, 287, 627-643.
15. Y. Morishima, *Angew. Chem. Int. Ed.*, 2007, 46, 1370-1372.
16. D. Schmaljohann, *Adv. Drug Deliver. Rev.*, 2006, 58, 1655-1670.
17. S. Dai, P. Ravi and K. C. Tam, *Soft Matter*, 2008, 4, 435-449.
18. P. Theato, B. S. Sumerlin, R. K. O'Reilly and T. H. Epps III, *Chem. Soc. Rev.*, 2013, 42, 7055-7056.
19. J. P. Salvage, S. F. Rose, G. J. Phillips, G. W. Hanlon, A. W. Lloyd, I. Y. Ma, S. P. Armes, N. C. Billingham and A. L. Lewis, *J. Controlled Release*, 2005, 104, 259-270.
20. K. E. B. Doncom, C. F. Hansell, P. Theato and R. K. O'Reilly, *Polym. Chem.*, 2012, 3, 3007-3015.
21. J. Du, Y. Tang, A. L. Lewis and S. P. Armes, *J. Am. Chem. Soc.*, 2005, 127, 17982-17983.
22. N. Petzetakis, A. P. Dove and R. K. O'Reilly, *Chem. Sci.*, 2011, 2, 955-960.
23. N. Petzetakis, D. Walker, A. P. Dove and R. K. O'Reilly, *Soft Matter*, 2012, 8, 7408-7414.

24. N. Petzetakis, M. P. Robin, J. P. Patterson, E. G. Kelley, P. Cotanda, P. H. H. Bomans, N. A. J. M. Sommerdijk, A. P. Dove, T. H. Epps and R. K. O'Reilly, *ACS Nano*, 2013, 7, 1120-1128.
25. A. Klaikherd, C. Nagamani and S. Thayumanavan, *J. Am. Chem. Soc.*, 2009, 131, 4830-4838.
26. C. Boyer, V. Bulmus, T. P. Davis, V. Ladmiral, J. Liu and S. Perrier, *Chem. Rev.*, 2009, 109, 5402-5436.
27. Q. Zhang, N. Re Ko and J. Kwon Oh, *Chem. Commun.*, 2012, 48, 7542-7552.
28. S. Mura, J. Nicolas and P. Couvreur, *Nature Mater.*, 2013, 12, 991-1003.
29. O. Onaca, R. Enea, D. W. Hughes and W. Meier, *Macromol. Biosci.*, 2009, 9, 129-139.
30. J. Du and R. K. O'Reilly, *Soft Matter*, 2009, 5, 3544-3561.
31. M. P. Robin, M. W. Jones, D. M. Haddleton and R. K. O'Reilly, *ACS Macro Lett.*, 2011, 1, 222-226.
32. P. Vana, *Macromol. Symp.*, 2007, 248, 71-81.
33. W. Schärtl, *Light Scattering from Polymer Solutions and Nanoparticle Dispersions*, Springer-Verlag Berlin Heidelberg, Berlin, 2007.

Chapter Three

The synthesis of pH-responsive polymers *via* an activated ester scaffold and their self-assembly and responsive behaviour

3.1 Introduction

Amphiphilic block copolymers, which contain both a hydrophilic block and a hydrophobic block, will self-assemble in water in order to minimise the unfavourable interactions between the hydrophobic block and the surrounding water.[1] There are many possible morphologies that the amphiphilic polymer can adopt upon self-assembly. These range from the conventional spherical micelles,[2] rods,[3] cylindrical micelles[4] and vesicles,[5-7] to the more exotic hamburger micelles[8] and Janus particle micelles.[9, 10] The morphology adopted by the polymer is related to the amphiphilic balance of the polymer chain, or the ratio of the hydrophilic block to the hydrophobic block. This ratio affects the packing of the polymer chains, and therefore the surface curvature of the self-assembled structure. As discussed by Blanazs *et al.* a dimensionless factor known as the packing parameter, *p*, can be used to predict the morphology a particular block copolymer will adopt when self-assembled, based upon the amphiphilic balance of the block copolymer (see Figure 3.1).[1] Micelles have a much higher surface curvature than vesicles and tend to be formed when the volume of the hydrophilic fraction is larger than the hydrophobic fraction, and vesicles tend to be formed when the opposite is true.[11] Therefore, changing the length of the hydrophilic block will cause a change in the packing parameter and in the morphology formed upon self-assembly.

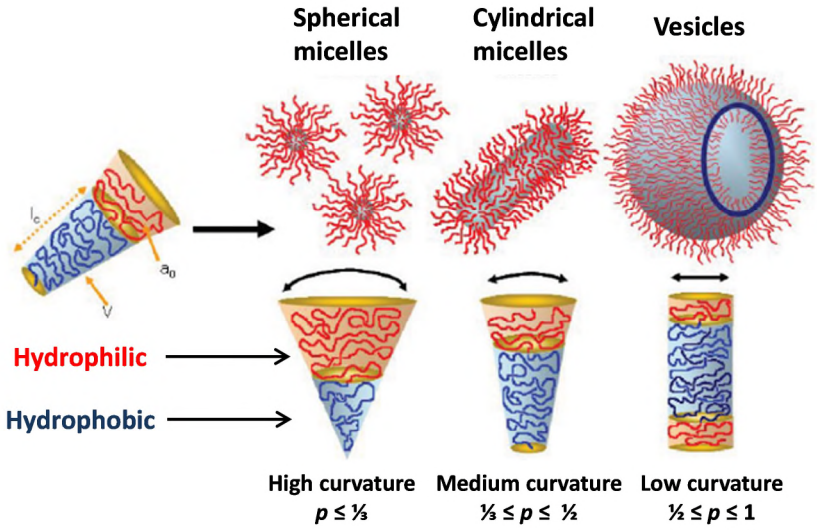

Figure 3.1: Schematic representation of the effect of the amphiphilic balance on the surface curvature of the diblock copolymer and therefore the morphology adopted in solution[1]

Stimuli-responsive polymers are ones that undergo a phase transition in response to a particular stimulus.[11] Their incorporation into self-assembling block copolymers can result in a change in the amphiphilic balance of the overall polymer upon application of the particular stimulus. If drastic enough, this change in hydrophilicity can result in the polymer adopting a different morphology. Stimuli which have been investigated within the literature include, but are not limited to, temperature,[12-15] pH[16, 17] and light.[15, 18] He *et al*. synthesised linear and branched copolymers of PEGMA-*b*-DMAEMA and PEGMA-*b*-DEAEMA by ATRP in THF.[19] The linear PEGMA was firstly homo-polymerised, followed by chain extension with the relevant tertiary amine and, in the case of the branched copolymers, a bifunctional monomer, ethyleneglycol dimethacrylate (EGDMA). The polymer solutions were dialysed against acidic (pH 3.7) water, from which solutions of different pH values were prepared. The solutions of linear and branched copolymers at varying pHs were analysed by DLS. No particles were observed to have formed in the solutions of linear polymers below pH 7, and poorly defined aggregates were detected at pH 9.8. The branched polymers formed particles between 200 – 250 nm between pH 3.7 – 7.0 and displayed a decrease in size at higher pH values. For the PEGMA-*b*-DMAEMA branched copolymers the size decrease occurred at pH 7.5 and for the PEGMA-*b*-DEAEMA branched copolymers the size decreased at pH 6.5. The decrease in size is due to the tertiary amine units becoming deprotonated and therefore hydrophobic and the branched polymers which contained higher proportions of the tertiary amine monomer underwent a greater decrease in size with pH.[19] The benefit of using amine containing polymers to yield a pH-response is that typically the change in hydrophilicity is reversible.

Controlled radical polymerisation techniques such as Atom Transfer Radical Polymerisation (ATRP),[20] Nitroxide Mediated Polymerisation (NMP)[21] and Reversible Addition Fragmentation chain Transfer (RAFT) polymerisation provide a facile route to the synthesis of these amphiphilic polymers as they allow the formation of polymers with controlled architecture.[22] Of these techniques, RAFT polymerisation displays the highest tolerance for

functional groups on the monomer units.[22] However, for cases where the chosen functionality (namely nucelophiles) impedes the polymerisation an alternative approach is the use of a scaffold polymer, *via* the use of an activated ester.[23] Pentafluorophenyl acrylate (PFPA) has been shown to be readily polymerisable *via* RAFT polymerisation techniques and is quantitatively substituted with primary amines and alcohols.[23-29]

Functionality at the chain ends is also an important consideration in the self-assembly process. At the α chain end this can be introduced by selecting the chain transfer agent (CTA) that bears that functionality on the R group (see Figure 3.2).[30]

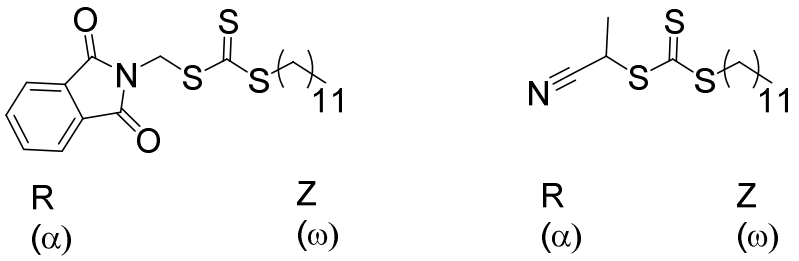

Figure 3.2: Two examples of CTAs with functional R groups[30]

Functionality can also be achieved post-polymerisation by the use of a chain transfer agent that contains an activated ester. Wilks *et al.* used a CTA bearing a terminal PFP ester group (see Figure 3.3) in order to firstly polymerise NIPAM and then substitute the PFP group with 1-azido-3-aminopropane to afford PNIPAM with a terminal azide group (see Figure 3.3). This then allowed for conjugation to DNA.[31]

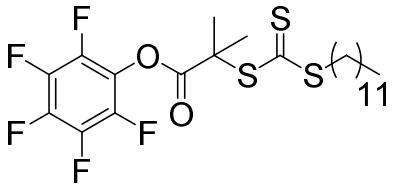

Figure 3.3: The structure of the PFP functionalised CTA used by Wilks *et al*.[31]

Moughton *et al*. synthesised a diblock copolymer consisting of a charged quaternary ammonium end group, the thermo-responsive block PNIPAM and the hydrophobic block PMA by RAFT polymerisation. Below the LCST cloud point of the PNIPAM micelles with

a D_h = 19 nm were formed. Heating the self-assembled solution to above the LCST of the PNIPAM block formed vesicles with a D_h = 147 nm, as the PNIPAM block became hydrophobic and only the charged end group directed self-assembly. This morphology transition was shown to be reversible, however the transition from micelle to vesicle required heating well above the LCST of the PNIPAM for 23 hours.[32]

Functionality at the ω chain end can be achieved by post-polymerisation modification. The RAFT end group can be removed by several methods to leave a proton, or reduced to a thiol *via* aminolysis.[33] This thiol can then be reacted with an acrylate *via* a Michael addition in order to add on the desired functionality.[34-36] Combinations of post-polymerisation modification techniques can be used to add functionality to both the backbone and the end group of the polymer. Boyer *et al.* synthesised a series of homopolymers of PFPA by RAFT polymerisation and all polymers had $Đ_M \leq 1.2$. A one-pot two-step method was employed to substitute the PFPA backbone with either D-glucosamine or D-galactosamine and then end group modify with a biotin modified maleimide.[37]

The monomer chosen to be investigated within this chapter, 2-(*N, N*-diisopropylamino) ethylene acrylate (DIPEA, Figure 3.4), was chosen since it has been largely unexplored within the literature and the methacrylate version, 2-(*N, N*-diisopropylamino) ethylene methacrylate (DIPEMA) has been reported to be more stable as a polymer than the ethyl- and methylamine versions.[38]

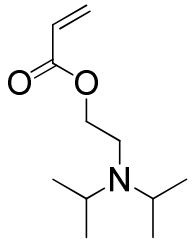

Figure 3.4: The structure of the monomer, 2-(*N, N*-diisopropylamino) ethylene acrylate (DIPEA)

The pK_a of the homopolymer of the methacrylate version of this monomer was reported to be *ca*. 6.3, rendering it hydrophobic at neutral pH.[39] The methyl- and ethylamine version are

reported to have higher pK_as which cause them to be hydrophilic at neutral pH.[40] The methacrylate version of the monomer, 2-(*N,N*-diisopropylamino)ethyl methacrylate (DIPEMA), has been polymerised by ATRP[38, 41, 42] and RAFT previously, although in the case of RAFT polymerisation the formation of diblock copolymers led to a loss of control, shown by broad dispersities ($Đ_M$ > 1.4).[43-45] Armes and coworkers investigated the pH-responsive behaviour of a block copolymer consisting of a short block of hydrophilic 2-(methacryloyloxy) ethyl phosphorylcholine (MPC) and a longer pH-responsive block of DIPEMA synthesised by ATRP. The polymer dissolved in acidic water (*ca*. pH 2.0) and unimers were formed, but as the pH was raised with NaOH to pH 6.0, the DIPEMA block became deprotonated and therefore hydrophobic and vesicles with a D_h = 160 nm were formed. TEM analysis confirms the presence of the vesicles.[46]

Lee and coworkers synthesised block copolymers of DIPEMA and PEGMA by RAFT polymerisation. The DIPEMA block was synthesised first and the homopolymers had fairly narrow dispersities ($Đ_M \leq 1.21$), but chain extension with PEGMA led to dispersities of 1.40 – 1.46. At low pH values no particles were observed in solution but as the pH increased to above 6.7, micelles were observed by DLS analysis.[45]

To the best of our knowledge there are no reported cases of the acrylate monomer being polymerised by RAFT methodology.

3.2 Results and Discussion

The aim of the project was to synthesise a diblock copolymer that bears a permanently hydrophilic end group, a pH-responsive block and a permanently hydrophobic block. By altering the pH of the self-assembled polymer solution, the amphiphilic balance of the diblock copolymer would change as the pH-responsive block became either hydrophobic or hydrophilic. If the change in the amphiphilic balance is great enough it will cause a change in the morphology that the self-assembled polymer adopted in solution. When the pH-responsive block is hydrophobic, self-assembly will only be directed by the hydrophilic end group and therefore vesicles will be formed. Conversely, when the pH-responsive block is hydrophilic the block ratios suggest that micelles will be formed. By using a tertiary amine functionalised monomer to form the pH-responsive block, the hydrophilicity change will be reversible and therefore repeated transitions between different morphologies of the self-assembled polymer would be possible. By targeting a vesicle to micelle morphology transition, the central water pool of the vesicle could be exploited in the encapsulation and controlled release of hydrophilic payloads (see Figure 3.5).

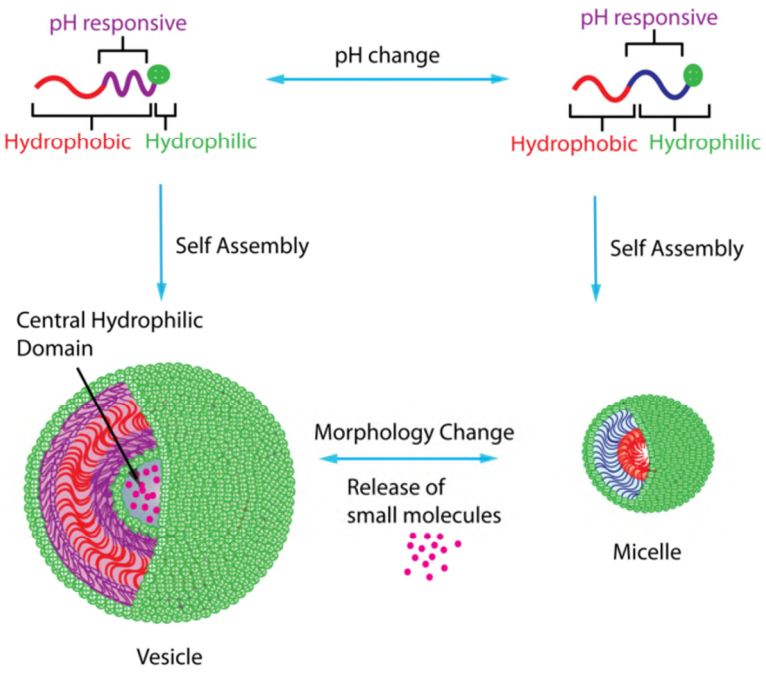

Figure 3.5: Schematic showing the aim of synthesising a pH-responsive diblock copolymer consisting of a hydrophilic end group, a reversibly pH-responsive block and a hydrophobic block to achieve a vesicle to micelle morphology transition in response to a change in pH

3.2.1 Attempts to polymerise DIPEA

Previous work within the group, carried out by Dr Claire Hansell during the first year of her PhD (but not included in her thesis), had focused on attempting to polymerise the monomer, 2-(*N, N*- diisopropylamino) ethylene acrylate (DIPEA) but had yielded little success. Several different CTAs were investigated (see Figure 3.6). The polymerisations proceeded to low conversions and extended reaction times did not improve the conversion. The resulting polymers had broad dispersities when analysed by SEC (see Table 3.1). The results of some attempted polymerisations are shown below.

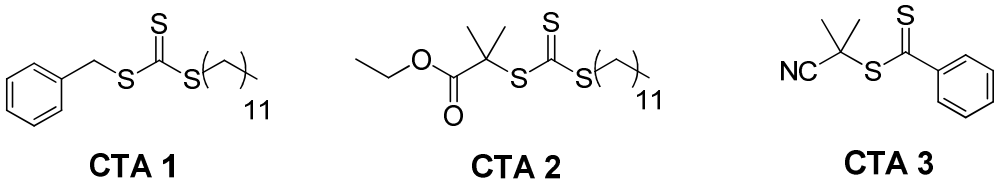

Figure 3.6: The CTAs used in the attempted polymerisations of DIPEA

Table 3.1: Different conditions tried in the attempts to polymerise the monomer DIPEA by RAFT polymerisation

Entry	CTA	[M]	[AIBN] w.r.t [CTA]	Solvent[a]	Temp (°C)	Time (h)	Conv (%)	$M_{n,\,SEC}$[b] (kDa)	$Đ_M$[b]
1	**1**	60	0.1	DMF	80	24	0	-	-
2	**1**	60	0.1	DMF	80	48	0	-	-
3	**1**	60	0.2	DMF	90	20	0	-	-
4	**1**	60	0.2	DMF	90	44	0	-	-
5	**2**	60	0.1	DMF	80	20	0	-	-
6	**2**	60	0.2	dioxane	70	25	35	2.5	1.32
7	**2**	60	0.2	*bulk*	70	25	41	2.9	2.23
8	**2**	100	0.2	dioxane	70	23	21	2.1	1.33
9	**2**	60	0.3	dioxane	70	23	40	3.0	1.35
10	**2**	60	0.3	dioxane	70	22	38		
11	**2**	60	0.5	dioxane	70	24	57	3.3	1.44
12	**2**	60	0.2	toluene	70	24	25		
13	**2**	60	0.2	dioxane*	70	24	33	2.1	1.43
14	**3**	100	0.3	DMF	90	21	24		

[a] Monomer : solvent 1: 1 w/v
***** Monomer: solvent 3: 1 w/v
[b] THF SEC, PMMA standards

The kinetics of one of the polymerisations with **CTA 2** were followed and shows the conversion stops at *ca.* 40% despite prolonged reaction times.

Table 3.2: Kinetics of polymerisation with CTA 2 with [M]:[2]:[AIBN] = 60:1:0.3 at 70°C in dioxane

Time (h)	Conversion (%)
1	22
2	30
3	36
4	36
5	37
6	36
8	37
22	39
47	39

As a result of the low conversions and the rather broad dispsersities of the resulting polymers, it was decided to follow an alternative synthetic route.

3.2.2 Attempts to polymerise PFPA

Since the direct polymerisation of the desired monomer DIPEA had already proved to be unsuccessful, an alternative route was required. Therefore it was decided to synthesise a scaffold polymer consisting of a hydrophilic end group, a block that could be easily substituted to bear the desired functionality, and a permanently hydrophobic block. The activated ester pentafluorophenyl acrylate was evaluated to be a good choice as a substitutable block as it has been polymerised by RAFT methodologies before and is readily substituted with primary amines or alcohols.[23-29] A CTA with charged quaternary amine functionality was employed in order to provide the hydrophilic end group (**CTA 4**). The synthesis and characterisation of this CTA is described in Chapter Two (compound **2.01**). The polymerisations using **CTA 4** were not well controlled, as evidenced by the broad dispersities seen in SEC analysis and often multiple peaks. This may be a result of using DMF as a polymerisation solvent, required because of the limited solubility of the CTA 4 in standard solvents. DMF degrades to form amines upon heating, so it is possible that during the polymerisation the DMF was forming amines which were reacting with the PFPA. Once

this CTA was deemed unsuitable, our attentions focused on **CTA 5**, a precursor to **CTA 4**, with the idea that removing the charge would promote the solubility of the CTA and therefore improve the polymerisation control. The charge would then be introduced by post-polymerisation modification of the bromine group. The synthesis of **CTA 5** has previously been reported.[47] The CTAs explored are shown below, and the results from the PFPA polymerisations given in Table 3.3.

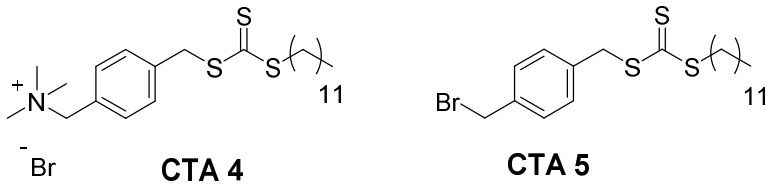

Figure 3.7: The different RAFT CTAs used in the polymerisation attempts of PFPA

Table 3.3: Different polymerisation conditions for the homopolymerisation of PFPA

Exp. Number	CTA	Solvent	Temp (°C)	Time (h)	Conversion (%)	$M_{n,\ NMR}$ (kDa)	$Đ_M$
1	**4**	$CHCl_3$	65	15.5	92	19.7	1.35 THF
2	**4**	$CHCl_3$	65	2.5	12	2.01	-
3	**4**	$CHCl_3$	65	8.25	49	9.2	1.69
4	**4**	$CHCl_3$	65	22.5	86	23.0	2.08
5	**4**	$CHCl_3$	80	2.5	60	-	-
6	**4**	dioxane	80	2.5	73	39.3	2.38
7	**4**	DMF	80	1	38	7.6	-
8	**4**	DMF	80	2.5	42	7.9	1.98
9	**4**	DMSO	80	3	0	-	-
10	**5**	dioxane	65	15.5	99	14.2	1.27
11	**5**	dioxane	65	5	88	13.5	1.29
12	**5**	dioxane	65	3.5	80	22.5	1.32
13	**5**	dry dioxane	65	2	50	14.7	1.23

CTA 5, the bromine end-capped trithiocarbonate, was more promising than **CTA 4**. The polymers produced using this CTA had backbone lengths that matched those predicted from conversion and relatively narrow dispersities. As PFPA is known to react with amines, its reactivity under the conditions used for end group modification was investigated. Entry **11** from the above table was reacted with trimethylamine (TMA), in THF, in order to form the quaternary amine functionality. After stirring overnight a precipitate had formed. This

precipitate was separated by filtration and upon analysis by ^{19}F NMR spectroscopy in DMSO there were no peaks observed, meaning that the PFP groups had been displaced (see Figure 3.8).

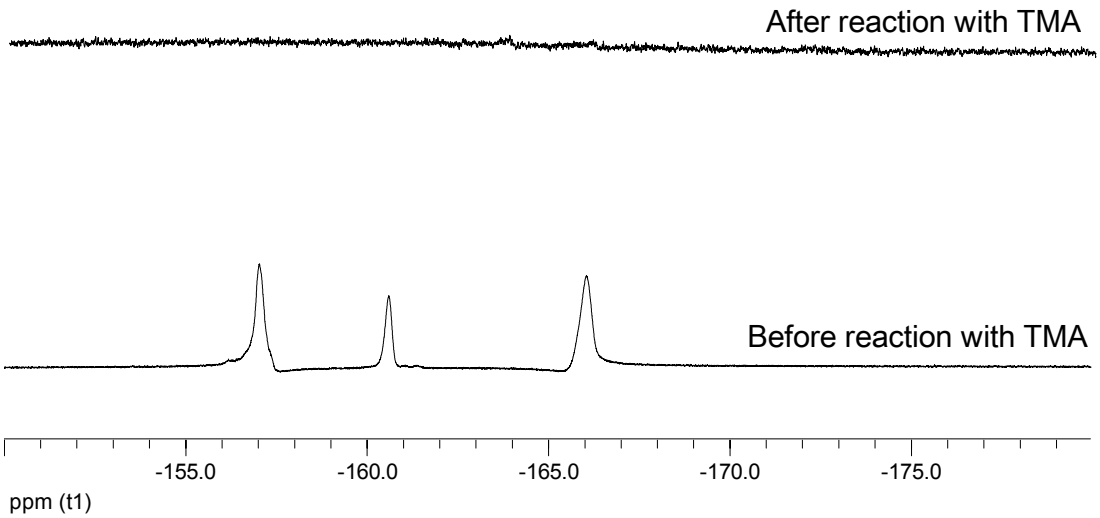

Figure 3.8: ^{19}F NMR spectra of polymer 11 in DMSO before (bottom) and after (top) reaction with TMA showing that the TMA reacts with the PFP groups on the backbone. The spectra were recorded at 25 °C and 300 MHz

Analysis by ^{1}H NMR spectroscopy also showed the disappearance of the characteristic peak at 3.1 ppm, relating to the C*H* of the PFP backbone. Additionally, the polymer **11** became water soluble after reaction with TMA, further suggesting that the TMA had reacted with the PFP groups to form a cationic polymer of quaternary amines (see Scheme 3.1). Therefore due to the ability of the tertiary amine to react with PFPA, this strategy was unsuitable.

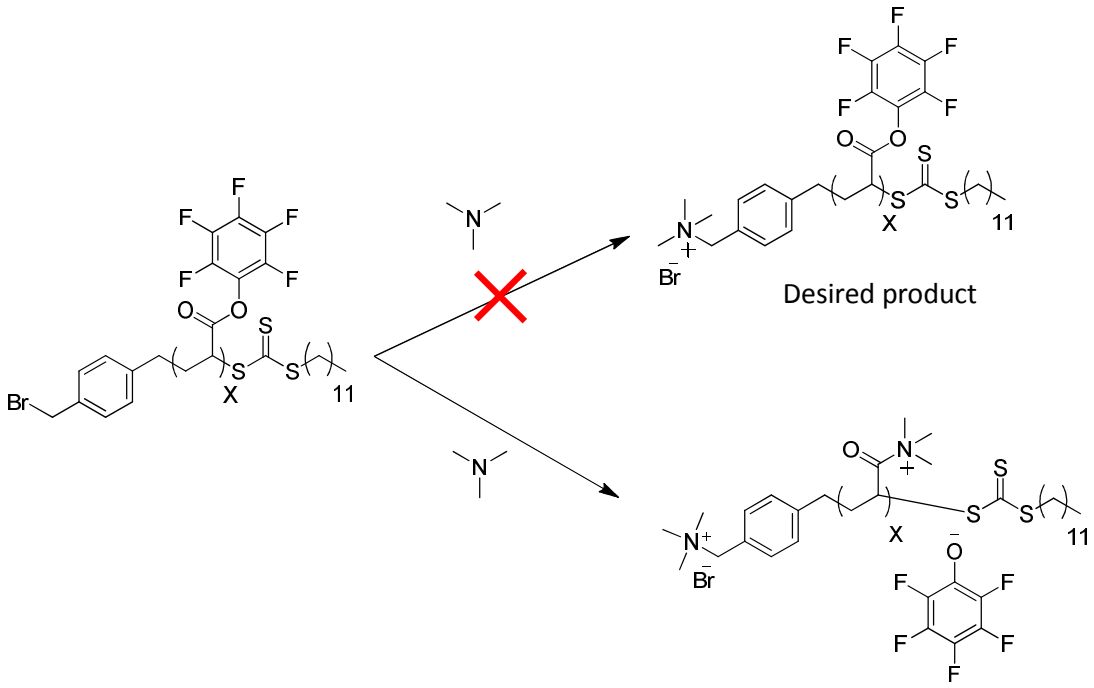

Scheme 3.1: Reaction of polymer 11 with TMA, showing the desired product (top) and the reaction of the TMA with the PFP side chains (bottom)

The alternative to this route would be to firstly modify the backbone of the polymer by reaction of the primary amine, without affecting the end group chemistry, and then to introduce the hydrophilic end group by reaction of the bromine functionality with TMA. In order to test whether the primary amine would react with the bromine end group, a small molecule test reaction using benzyl bromide as an analogue for the CTA was stirred overnight with isopropylamine, a primary amine, in THF. A white precipitate was observed to form and analysis of this precipitate by ^{1}H NMR spectroscopy showed the peak relating to the CH_2 next to the bromine had shifted from 4.51 ppm in the starting material, benzyl bromide, to 4.13 ppm after the reaction. This shows that the primary amine has reacted with the benzyl bromide. Mass spectroscopy of the precipitate also revealed two products with M^+ 150.2 and 240.2. A mass of 150.2 relates to the amine reacting with one benzyl bromide and a mass of 240.2 relates to the primary amine reacting with two benzyl bromides, as shown in Scheme 3.2. Therefore this strategy was also unsuitable as the primary amine used to modify the PFP backbone would also react with the bromine end group.

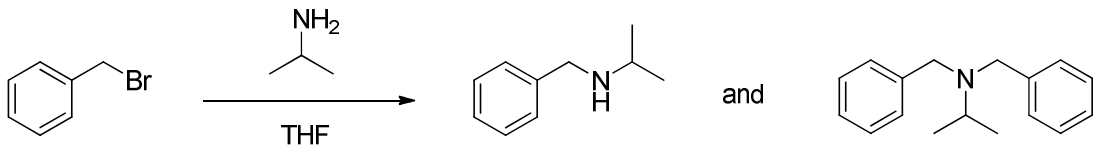

Scheme 3.2: The two products formed after the test reaction of benzyl bromide and isopropylamine, showing that the primary amine reacts with the bromine group of the benzyl bromide

Since functionality within the CTA seemed to interfere with the PFPA polymerisation and modification of **CTA 5** post-polymerisation proved unsuitable, it was decided to firstly polymerise the hydrophobic block and then chain extend with the PFPA to form a scaffold diblock copolymer. This was then followed by post-polymerisation modification of the backbone and reaction of the ω end of the CTA in order to introduce the hydrophilic functionality (see Figure 3.9). Two different hydrophilic end groups were investigated, a positively charged quaternary ammonium cation and a triethylene glycol (TEG) end group.

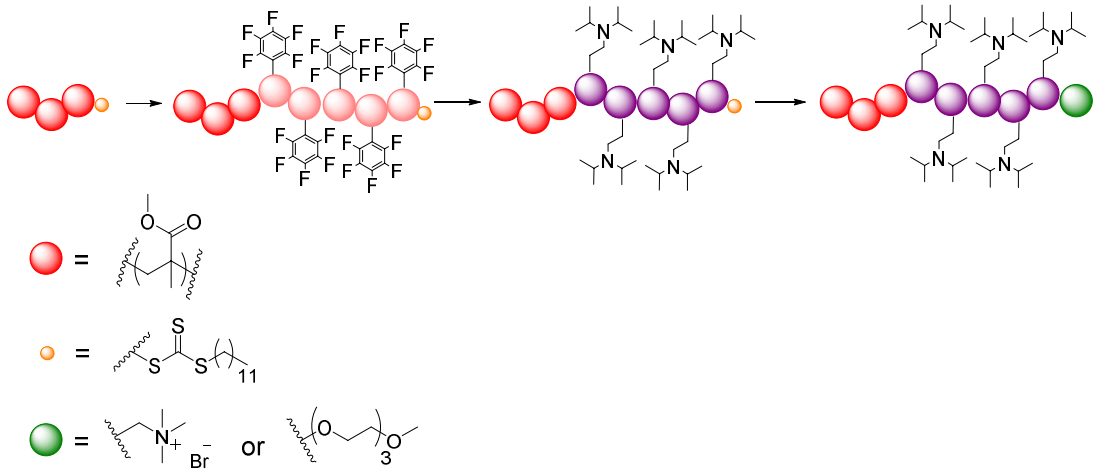

Figure 3.9: Schematic showing the route to the pH-responsive polymers, *via* an activated ester scaffold, followed by modification of the backbone and functionalisation of the ω end of the CTA to introduce the hydrophilicity

3.2.3 Synthesis of the scaffold polymer

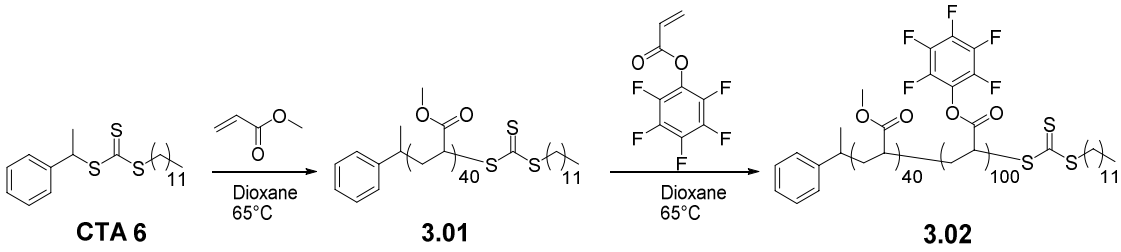

Scheme 3.3: Synthesis of homopolymer 3.01 using CTA 6 and subsequent chain extension with PFPA to form diblock copolymer 3.02

The first step in synthesising the scaffold polymer was to polymerise MA using a previously reported CTA [48] (**CTA 6**), to form a hydrophobic block, **3.01**, M_n (^{1}H NMR) = 3.8 kDa, M_n (DMF SEC) 2.5 kDa and $Đ_M$ = 1.06 (see Scheme 3.3). Analysis of the polymer by ^{1}H NMR spectroscopy shows the presence of both end groups (see Figure 3.10). The signals **a** and **c** at 7.2 ppm correspond to the protons from the benzene ring. The signals **h** at 3.4 ppm and **k** at 0.9 ppm correspond to the CH_2 next to the trithiocarbonate and the terminal methyl group of the dodecyl chain, respectively. All the end group signals integrate correctly with respect to each other, showing that both the R and the Z groups of the CTA have been retained throughout the polymerisation. Integration of these end group signals relative to the polymer peaks **e** and **g** at 3.7 ppm and 2.3 ppm give a degree of polymerisation of 40. This DP matches well with that predicted from conversion and along with the narrow dispersity seen in SEC analysis, shows that the polymerisation proceeded with good control.

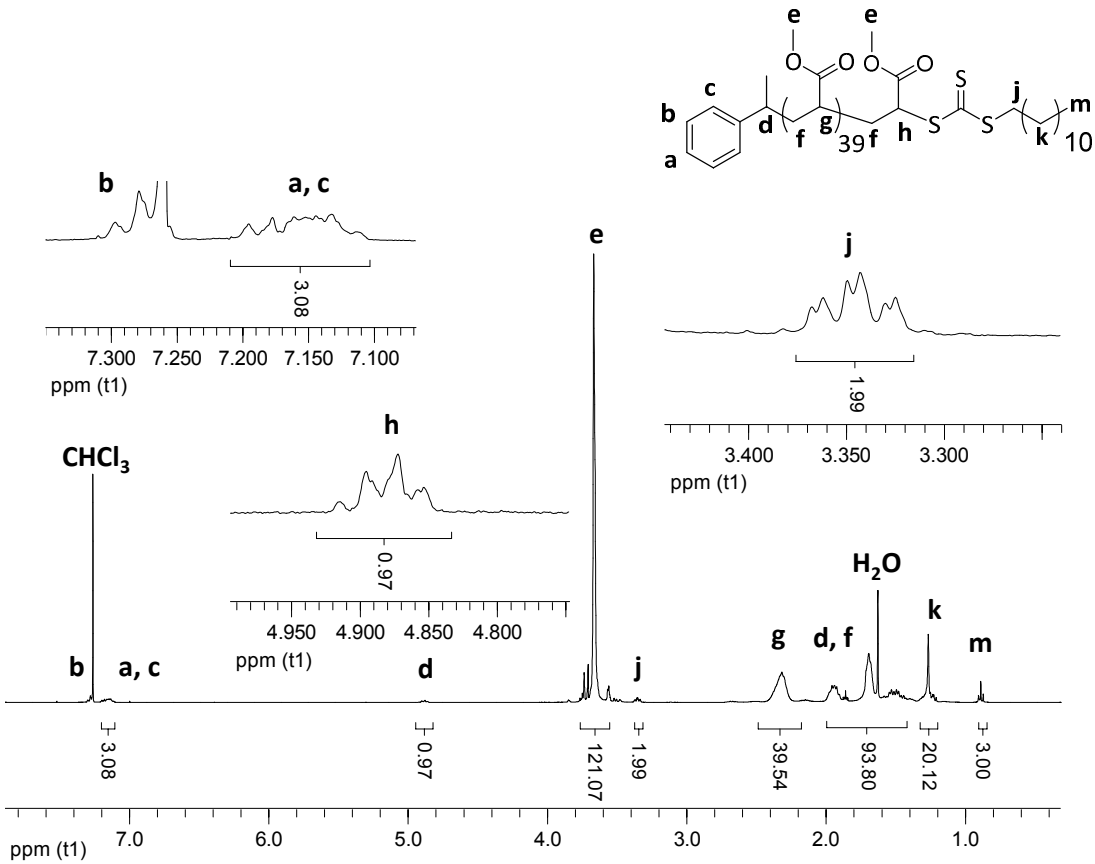

Figure 3.10: ^{1}H NMR spectrum of homopolymer 3.01 in $CDCl_3$ with assignments shown, recorded at 25 °C and 400 MHz

The next step in synthesising the scaffold polymer was to chain-extend **3.01** with PFPA. The polymerisation was carried out in 1,4-dioxane to yield the yellow polymer, **3.02**, M_n (^{1}H NMR) = 27.5 kDa, M_n (DMF SEC) = 7.7 kDa and $Đ_M$ = 1.29. Again the end group signals of the CTA were visible by ^{1}H NMR spectroscopy (see Figure 3.11). Integration of the signals of the benzene ring (**a** and **c**) and the CH_2 next to the trithiocarbonate (**k**), at 7.15 ppm and 3.37 ppm respectively, relative to the polymer peak, **j**, at 3.15 ppm give a DP of 100 for the activated ester block. This matched well with the conversion from both ^{1}H and ^{19}F NMR spectroscopies.

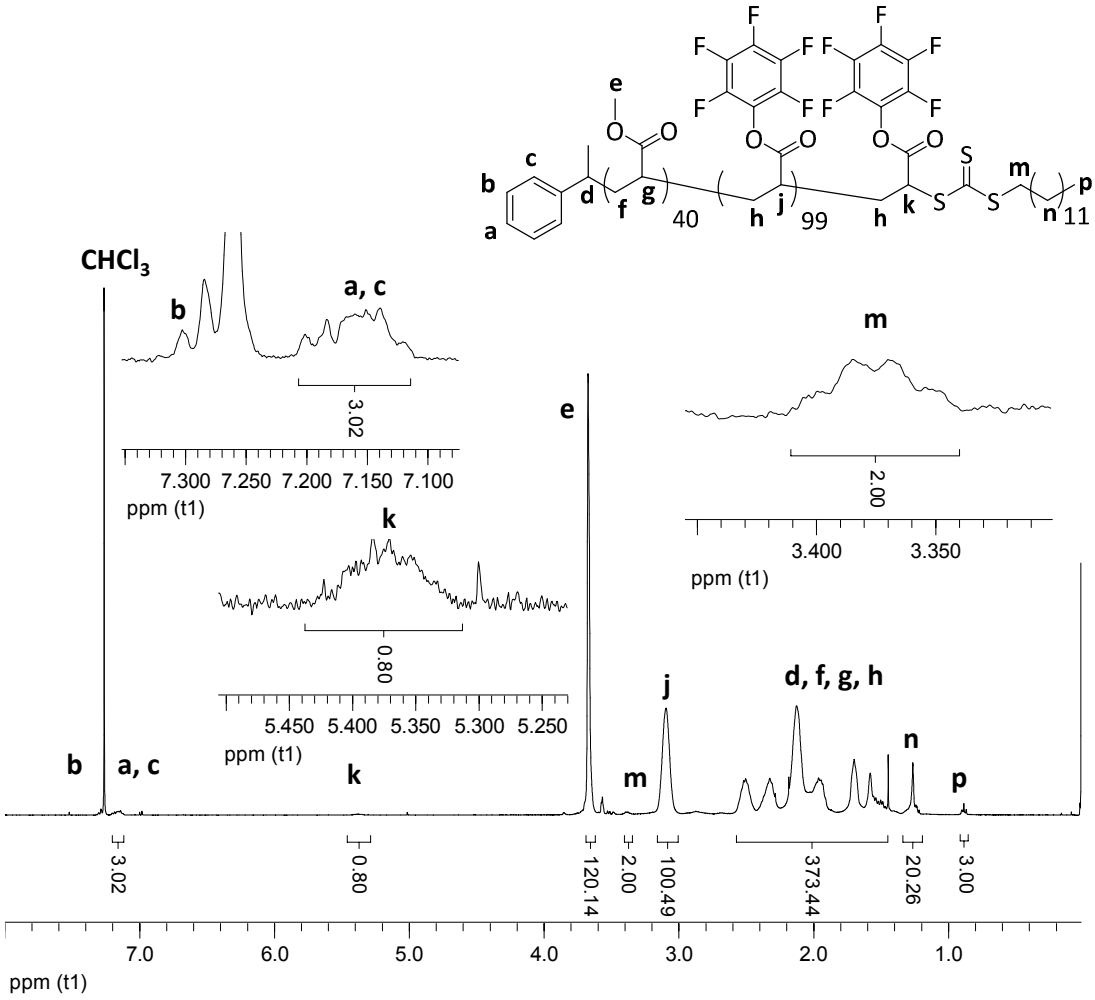

Figure 3.11: ^{1}H NMR spectrum of diblock copolymer 3.02 in $CDCl_3$ with assignments shown, recorded at 25 °C and 400 MHz

The chain extension can also be seen by the shift in MW in the SEC traces (see Figure 3.12).

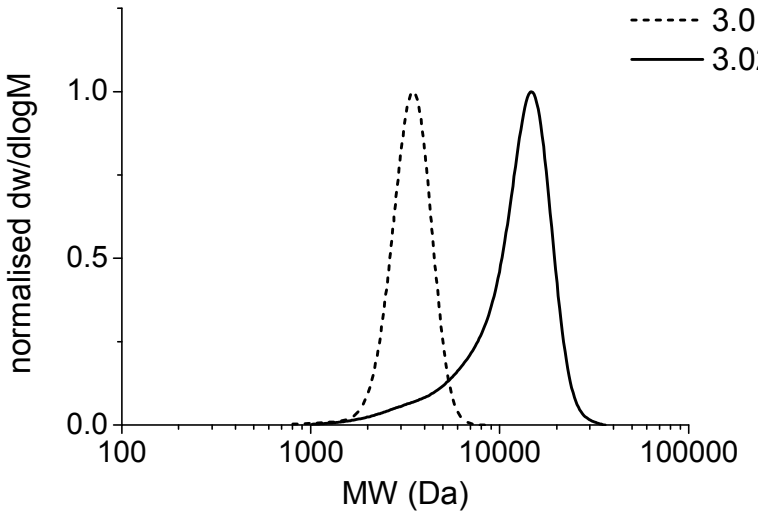

Figure 3.12: DMF SEC chromatograms showing shift in MW upon chain extension from homopolymer 3.01 to diblock copolymer 3.02

3.2.4 Synthesis of the charged quaternary ammonium end group, 3.03

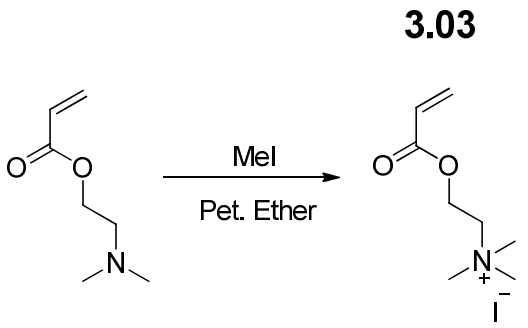

Scheme 3.4: Synthesis of charged acrylate, 3.03

The charged quaternary ammonium acrylate was synthesised by reacting *N, N*-(dimethylamino) ethyl acrylate with methyl iodide in petroleum ether (see Scheme 3.4). The product precipitated as a white solid and was collected by filtration and dried *in vacuo*. The ^{1}H NMR spectrum shows the pure product (see Figure 3.13).

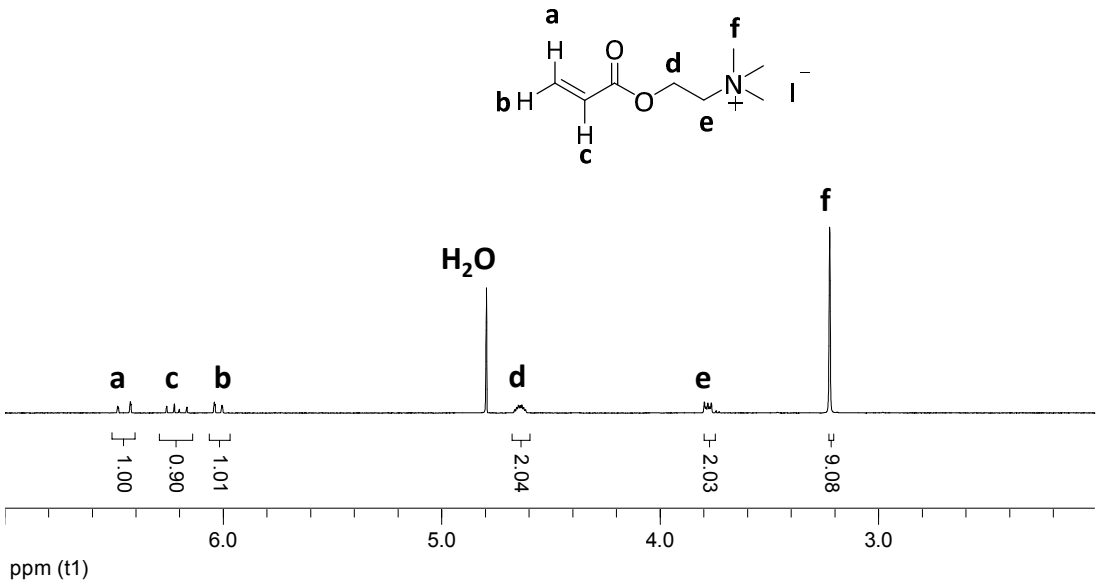

Figure 3.13: ^{1}H NMR spectrum of 3.03 in D_2O with assignments shown, recorded at 25 °C and 400 MHz

3.2.5 Substitution and end group modification of the scaffold polymer

In order to form the desired pH-responsive diblock copolymer from this scaffold polymer, both the backbone of the polymer and the CTA end group must be functionalised. This was done using post-polymerisation modification chemistries. The backbone modification was achieved using the well-studied displacement of PFP with primary amines,[15, 23-25, 36] and the

end group modification consisted of aminolysis with a primary amine to reduce the trithiocarbonate to a thiol and then Michael-addition of the thiol with an acrylate.[33-36] Two different hydrophilic end groups were explored thereby allowing for the direct comparison of the effect that different end groups have on the self-assembly, whilst keeping the polymer backbone identical. The two end groups investigated were a positively charged quaternary amine functionalised end group, **3.03**, and an uncharged triethyleneglycol acrylate (TEGA) end group.

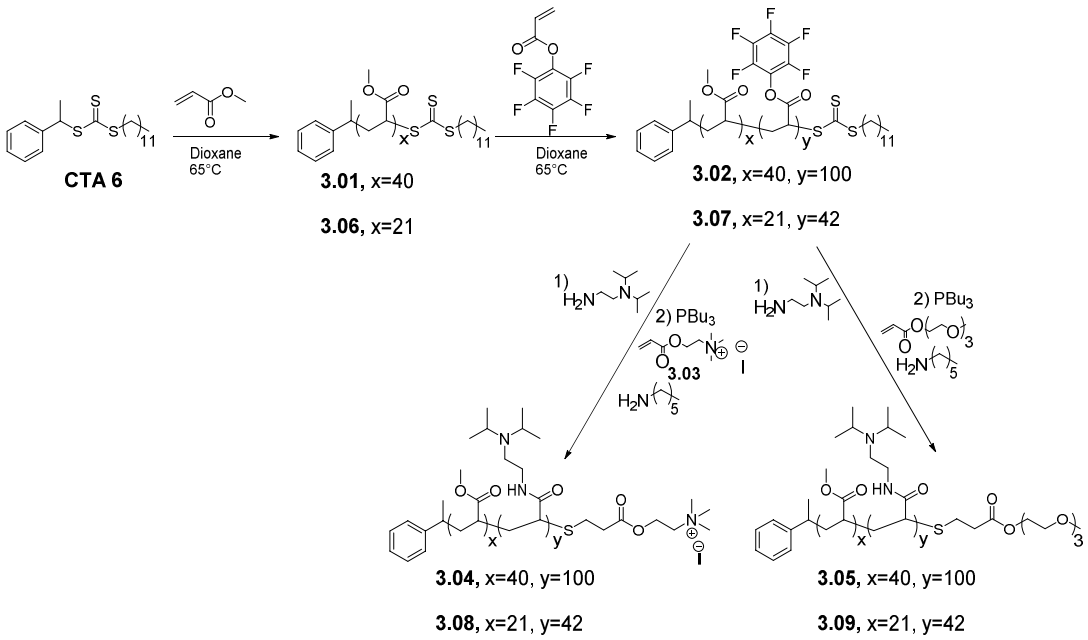

Scheme 3.5: Synthetic route to polymers 3.01-3.09

The modifications were carried out in a one-pot, two-step method. Firstly the polymer **3.02** was dissolved in DMF at a concentration of 150 mg mL^{-1}. Since it has been shown that removal of oxygen prevents disulphide coupling,[35] the solution was degassed by successive *freeze-pump-thaw* cycles. The primary amine bearing the desired functionality, 2-(*N, N*-diisopropylamino) ethylamine, was dissolved in DMF in a separate ampoule and also degassed. The amine solution was then transferred to the polymer solution with 1.5 equivalents of amine per PFPA unit. This excess would allow for complete conversion of the PFPA groups. This solution was stirred overnight. The conversion of all the ester groups was confirmed by ^{19}F NMR spectroscopy. The disappearance of the broad polymer signals at -

153.2 ppm, -156.7 ppm and -162.2 ppm and appearance of sharp pentafluorophenol signals at -170.0 ppm and -172.8 ppm were observed, indicating the complete conversion of the activated ester groups. After dialysis no peaks can be seen in the ^{19}F NMR showing that all the PFPA salts had been removed by dialysis.

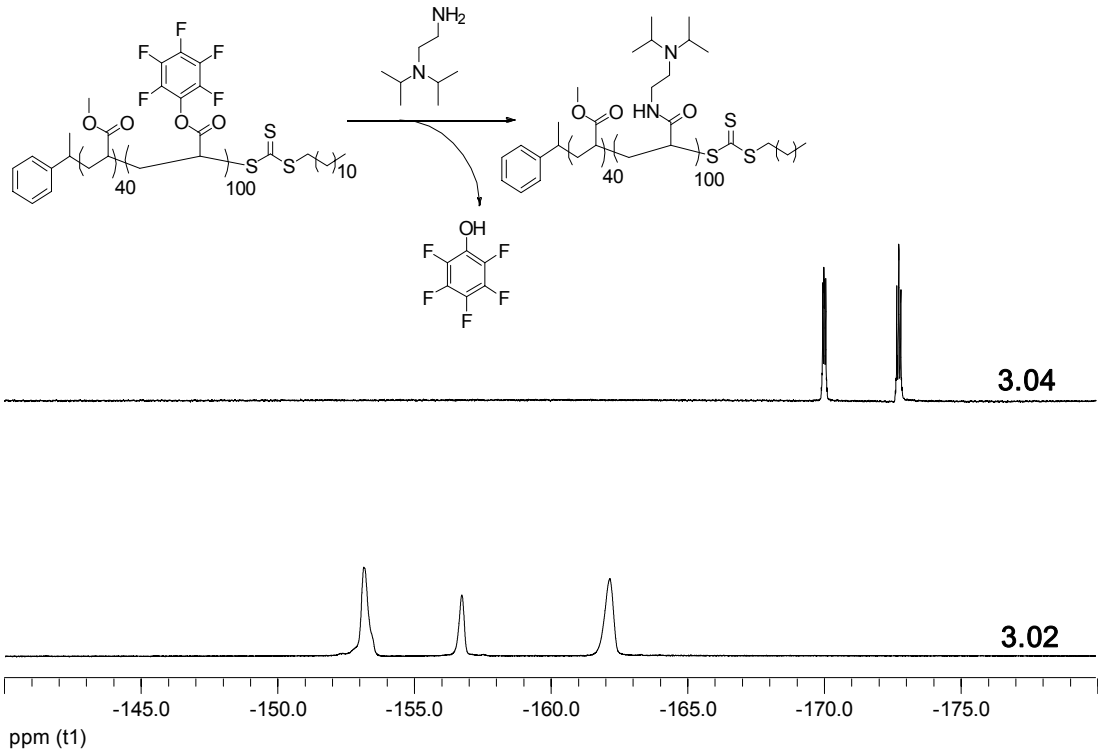

Figure 3.14: ^{19}F NMR spectra of polymers 3.02 and 3.03, recorded at 25 °C and 300 MHz, showing the disappearance of the broad polymer peaks and the appearance of the sharp pentafluorophenol peaks upon substitution. Two of the expected three pentafluorophenol peaks are seen, the third is expected at -185 ppm, which is out of range of the spectrometer.

The second step involved the subsequent addition of hexylamine, the primary amine used to reduce the trithiocarbonate to a thiol, the desired hydrophilic end group, and PBu_3, a reducing agent, which was present to prevent any disulphide coupling from occurring. This was done by dissolving the PBu_3 and desired monomer in DMF and separately degassing before transferring into the polymer solution. A solution of degassed hexylamine in DMF was then added and the solution left to stir overnight. Immediately after addition of the hexylamine the yellow colour of the solution disappeared. The removal of the end group was monitored by the loss of the 309 nm UV trace from DMF SEC analysis (see Figure 3.15). This shows the removal of the trithiocarbonate group. The SEC chromatograms also show

the shift in molecular weight upon substitution. The polymers were purified by dialysis against acidic and then basic water followed by lyophilisation, to yield polymers **3.04** and **3.05** as powdery solids in good yield.

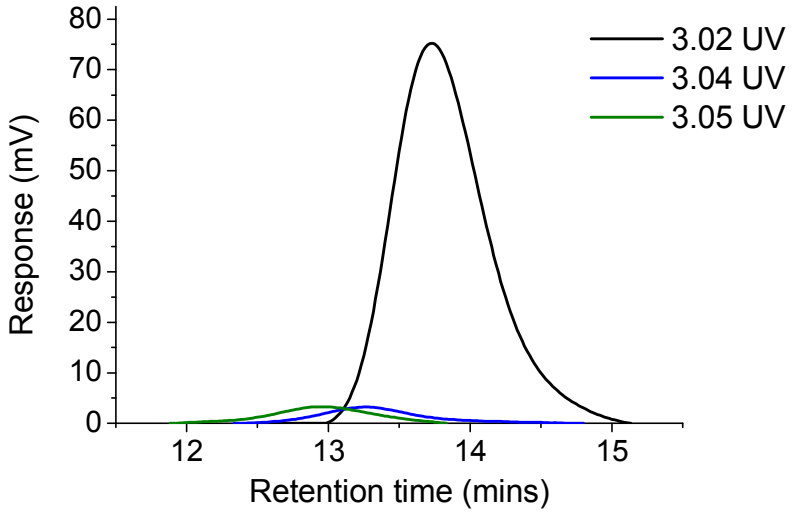

Figure 3.15: DMF SEC chromatograms showing the loss of absorbance at 309 nm upon end group modification from 3.02 to form the quaternary amine functionalised 3.04 and TEG functionalised 3.05

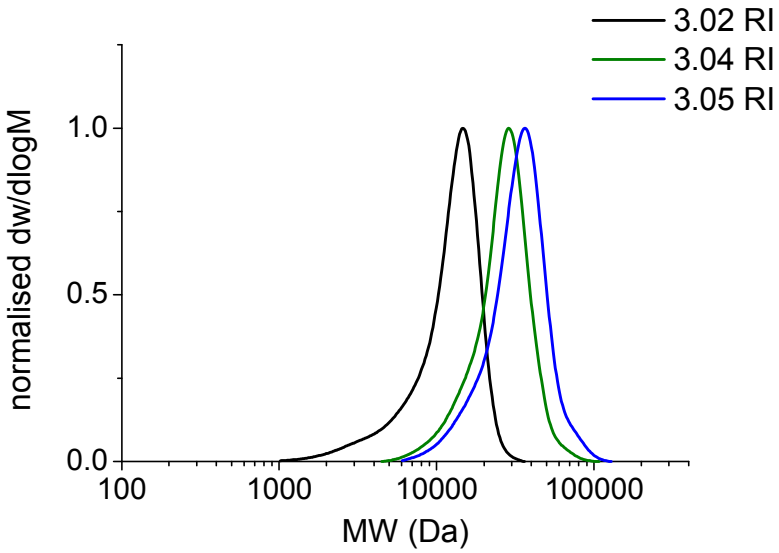

Figure 3.16: DMF SEC RI chromatograms showing the shift in molecular weight upon substitution of 3.02 to form the quaternary amine functionalised 3.04 and TEG functionalised 3.05

Polymer **3.04** bears the charged quaternary amine end group, M_n (^{1}H NMR) = 23.9 kDa M_n (DMF SEC) = 23.1 kDa and $Đ_M$ = 1.19. The full substitution of the PFPA block with the

N, N-diisopropylethyl amine was again confirmed by the appearance of new signals at 1.0 ppm, 2.6 ppm and 3.0 – 3.3 ppm in the ^{1}H NMR spectrum, relating to the NCH(CH_3)$_2$, NC*H*(CH_3)$_2$, and NHCH_2CH_2 respectively. These peaks integrate as expected when set against known signals, such as the methyl acrylate side chain signals, which are not affected by the substitution or end group modification processes. The incorporation of the end group was observed by ^{1}H NMR spectroscopy and the appearance of new signals at 4.50 ppm and 2.80 ppm for the CH_2 next to the thioester and the CH_2 next to the charged tertiary amine respectively confirmed the successful end group modification (see Figure 3.17).

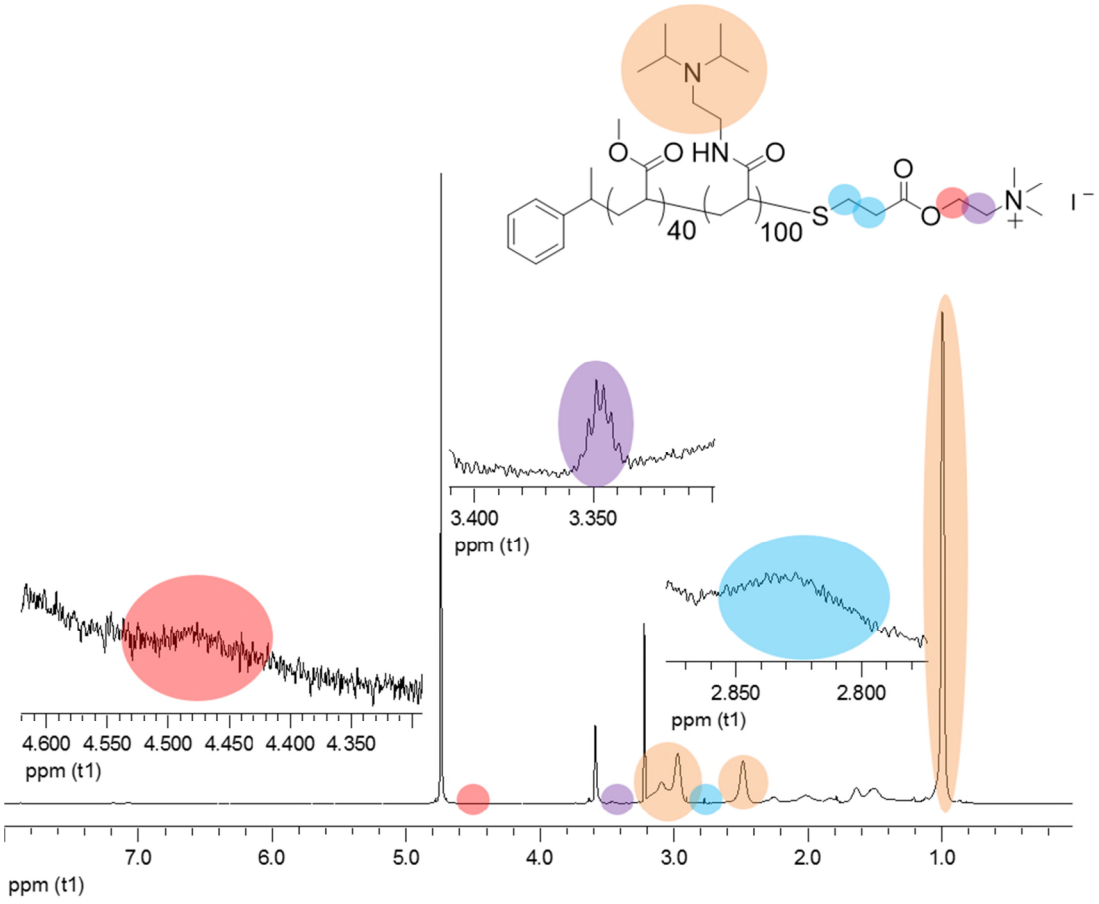

Figure 3.17: ^{1}H NMR spectrum of diblock copolymer 3.04 in MeOD showing the new signals relating to the polymer peaks and the incorporated end group. The spectrum was recorded at 25 °C and 400 MHz

Polymer **3.05** bears the triethylene glycol (TEG) end group, M_n (^{1}H NMR) = 23.9 kDa, M_n (DMF SEC) = 21.5 kDa and $Đ_M$ = 1.21. Again the substitution of the backbone with the pH-responsive functionality was confirmed by ^{1}H NMR spectroscopic analysis and the appearance of the peaks at 3.20 ppm, 3.60 ppm and 3.80 ppm. The incorporation of the end

group functionality was also confirmed by ^{1}H NMR spectroscopy with the CH_3 signal of the TEGA end group clearly observable at 3.7 ppm as is the signal at 4.18 ppm relating to the CH_2 next to the carbonyl group (see Figure 3.18).

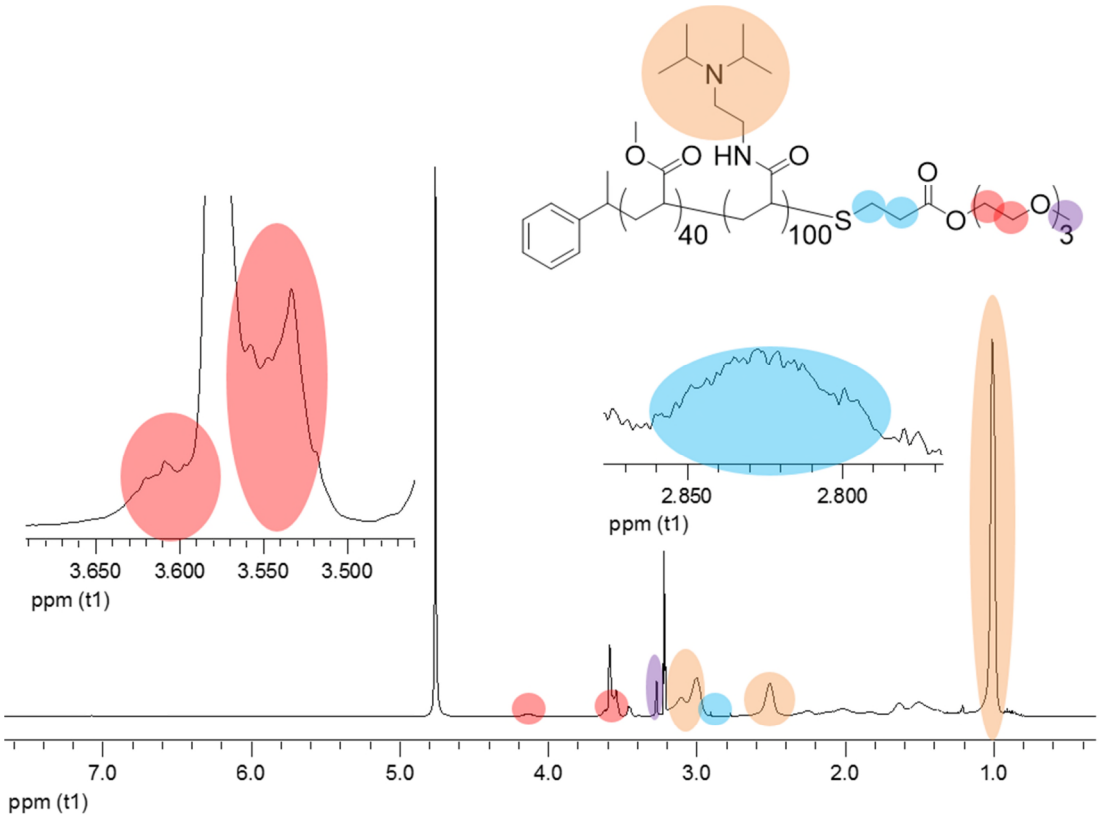

Figure 3.18: ^{1}H NMR spectrum of diblock copolymer 3.05 in MeOD showing the key signals relating to the substituted backbone and the incorporated end group of the polymer. The spectrum was recorded at 25 °C and 400 MHz

The substitution of the backbone PFP groups was also confirmed by IR spectroscopy. The PFPA C=O ester stretch at 1783 cm^{-1} disappeared and was replaced by a C=O stretch at 1646 cm^{-1}, relating to the amide group formed, with the MA ester stretch at 1737 cm^{-1} remaining unchanged (see Figure 3.19).

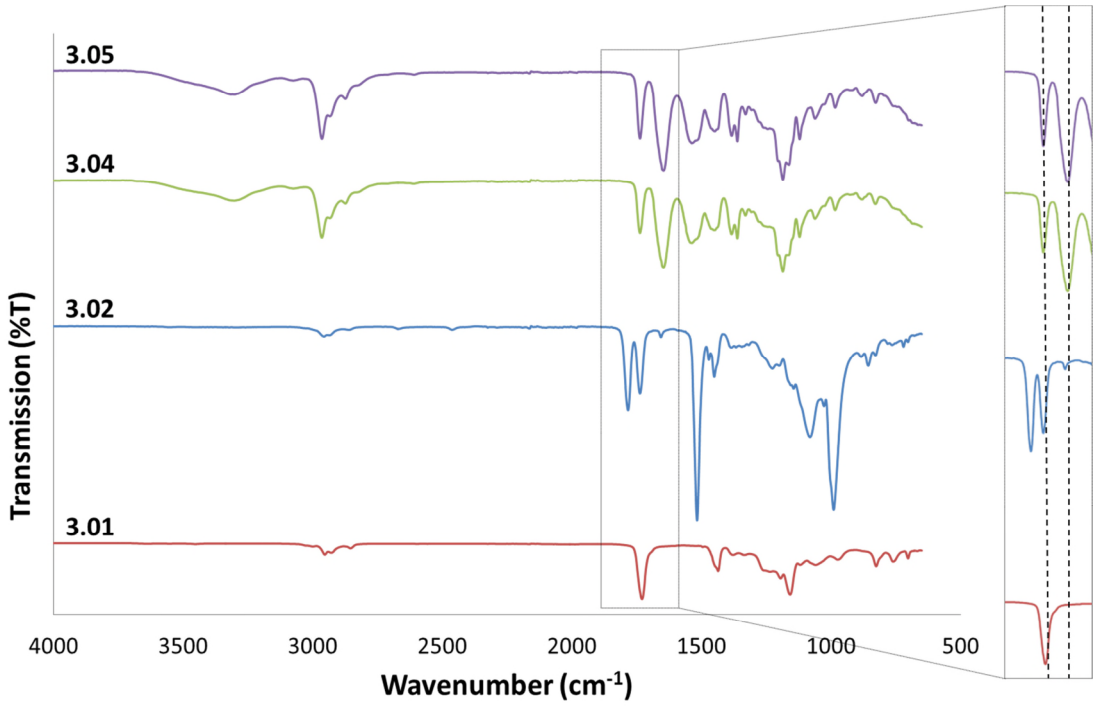

Figure 3.19: IR spectra of 3.01, 3.02, 3.04 and 3.05, showing the disappearance of the ester stretch relating to the PFPA (3.02) and the appearance of an amide stretch relating to the substituted group (3.04 and 3.05) whilst the MA ester stretch (3.01) remains unchanged

3.2.6 Self-assembly and pH-responsive behaviour of the polymers

The self-assembly behaviour of the end group modified polymers was investigated. Firstly, polymer **3.04** was self-assembled by the solvent switch method. The polymer was dissolved in DMF at a concentration of 0.5 mg mL^{-1} and then water was slowly added until a concentration of 0.25 mg mL^{-1} was reached. The solution was then dialysed extensively to remove the DMF. After dialysis the solution was slightly turbid and had a final concentration of 0.16 mg mL^{-1} and a final pH of 7.4. The pK_a of the polymer was calculated by titration to be 5.96. Therefore, at this pH, the pH-responsive block should be mainly deprotonated and therefore hydrophobic. Based upon the relative block ratios of the hydrophilic and hydrophobic segments of the polymer these structures were expected to be vesicles and DLS analysis reveals the presence of large structures with a D_h of 340 ± 31 nm. These assemblies were further characterised by TEM and after staining with uranyl acetate structures with a D_h of 353 ± 41 nm were observed (see Figure 3.20).

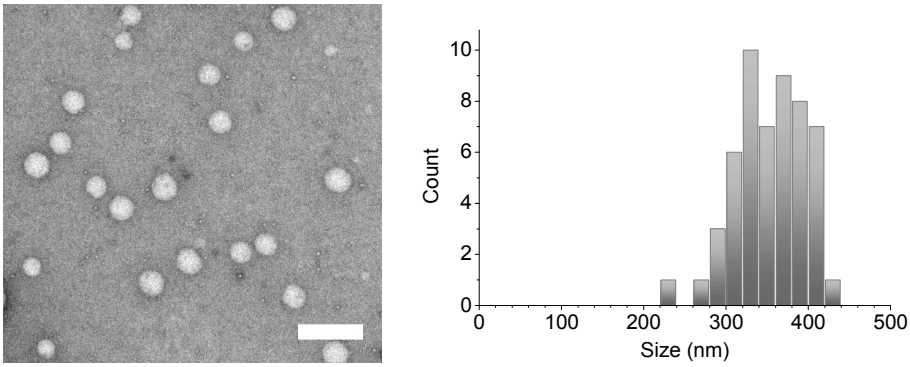

Figure 3.20: TEM image of assemblies of 3.04 stained with uranyl acetate, scale bar = 1 µm, and the distribution of sizes observed

Due to the amine functionality within the polymer it should be possible to protonate the pH-responsive block causing the block to become hydrophilic, and induce a change in the morphology of the self-assembled structures (see Figure 3.21).

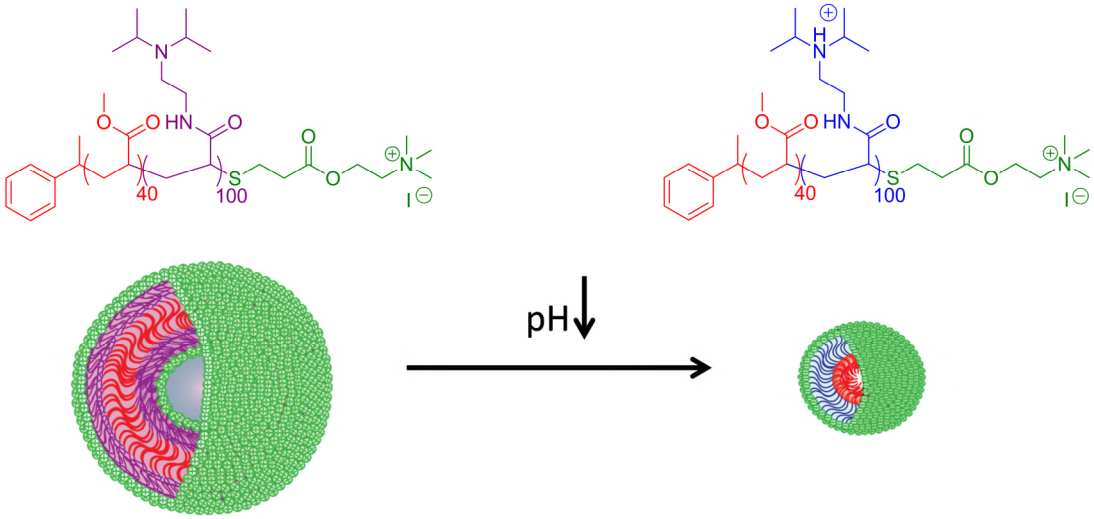

Figure 3.21: Schematic showing the protonation of the pH-responsive blocks as the pH is lowered and the expected morphology change

To test this, a solution of the self-assembled polymer bearing the charged quaternary ammonium end group, **3.04**, (0.16 mg mL^{-1}) was treated with diluted HCl solution (*ca.* 0.2 mL) to adjust the pH from 7.4 to 1.75. This pH value is well below the pK_a of the polymer therefore it can be considered that all the amine groups are protonated. This renders the block hydrophilic and so based upon the new hydrophilic to hydrophobic block ratios, it can be expected that micelles will form. Immediately upon addition of the acid the turbidity of

the solution disappeared and after stirring overnight the solution was analysed by DLS (see Figure 3.22). Structures with a D_h = 36 ± 3 nm were observed. This solution was then analysed by TEM and micelles with an average size of 32 ± 4 nm were observed, confirming that the morphology had switched from a vesicle to a micelle upon lowering the pH (see Figure 3.23). Since such a small volume of acid was used the concentration was effectively unchanged.

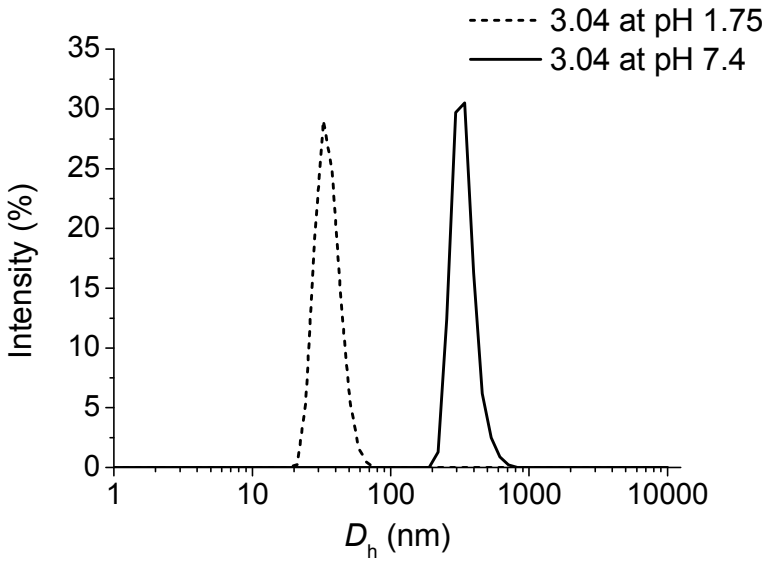

Figure 3.22: DLS traces of a solution of 3.04 at 0.16 mg mL^{-1} , showing the decrease in D_h as the pH is lowered from 7.4 to 1.75

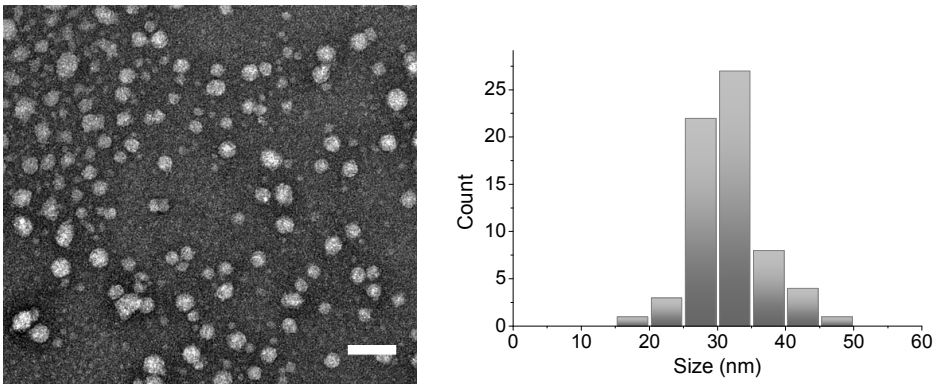

Figure 3.23: TEM image of micelles of a solution of 3.04 with a concentration of 0.16 mg mL^{-1} at pH 1.75, stained with uranyl acetate, scale bar = 200 nm, and the distribution of sizes observed

The assembly and pH-responsive behaviour of **3.05**, which bears the TEGA functionality, was also investigated. Polymer **3.05** was self-assembled in the same manner as **3.04** *via*

solvent switch and dialysis. The final solution after exhaustive dialysis had a concentration of 0.12 mg mL^{-1} of and a pH of 7.8. Again, this pH means that the majority of the pH-responsive block will be deprotonated and therefore hydrophobic. The solution was analysed by DLS and assemblies with a D_h of 191 ± 8 nm were observed. The difference in size between these assemblies of **3.05** and those of **3.04** (340 nm) can be attributed to the difference in the hydrophilic end group of the polymer, since the backbone is identical in the two polymers. The packing parameter, *p*, determines the morphology that the polymer will adopt upon self-assembly and is related to the length of the hydrophilic and hydrophobic fractions.

$$p = \frac{v}{a_o l_c}$$

In the above equation, v is the volume of the hydrophobic section, a_o is the contact area of the head group and l_c is the length of the hydrophobic section. Therefore changing the hydrophilic head group has an impact upon *p*, and the curvature of the assemblies. Polymer **3.04** bears the positively charged quaternary amine end group functionality and this has resulted in larger assemblies, with a lower surface curvature. Polymer **3.05** bears the neutral TEG end group functionality this has resulted in the formation of smaller vesicles with a higher surface curvature.

A sample of this self-assembled solution of **3.05** was analysed by TEM. After staining with uranyl acetate, a population with an average size of 126 ± 30 nm could be observed (see Figure 3.24).

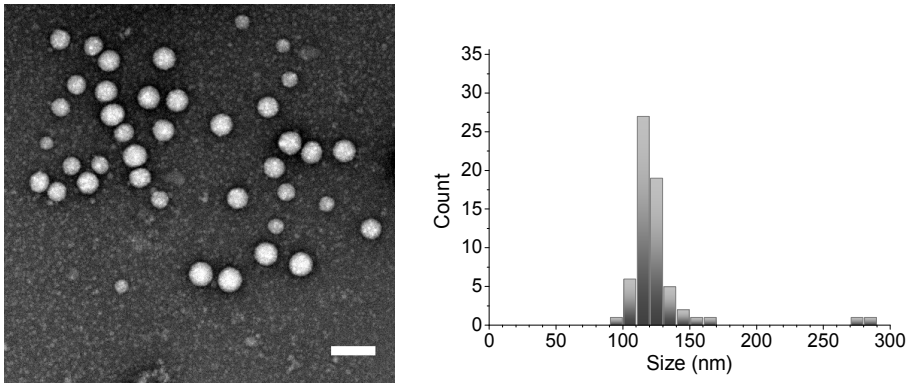

Figure 3.24: TEM of a solution of 3.05 at 0.12 mg mL^{-1} at a pH of 7.8 stained with uranyl acetate, scale bar = 200 nm, and the distribution of sizes observed

The pH-responsive behaviour of **3.05** was also investigated. Again, diluted HCl was added to a solution of **3.05** to reduce the pH from 7.8 to 3.7, resulting in the protonation of the pH-responsive block. After stirring overnight, analysis by DLS shows that micelles with a D_h = 45 ± 3 nm have formed (see Figure 3.25) and these were confirmed by TEM analysis. Upon staining with uranyl acetate, micelles with an average size of 35 ± 5 nm were observed (see Figure 3.26).

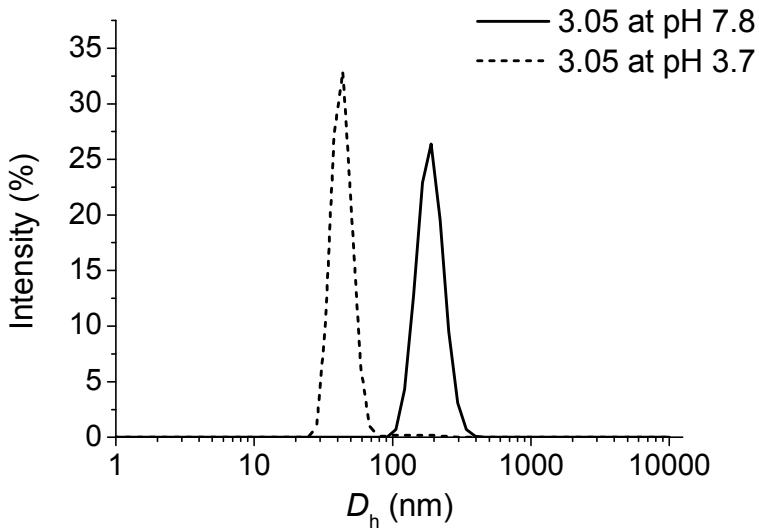

Figure 3.25: DLS traces showing the decrease in D_h of 3.05 with a decrease in pH from 7.8 to 3.7

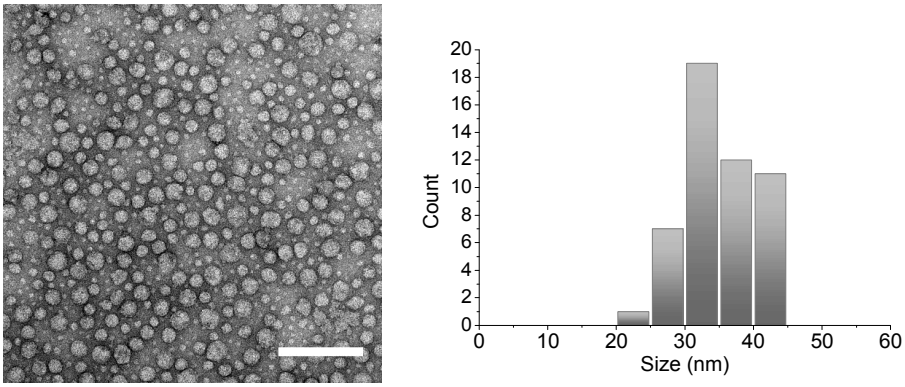

Figure 3.26: TEM of a self-assembled solution of 3.05 at 0.12 mg mL^{-1} at a pH of 3.7 stained with uranyl acetate, scale bar = 200 nm, and the distribution of sizes observed

3.2.7 Encapsulation and release experiments

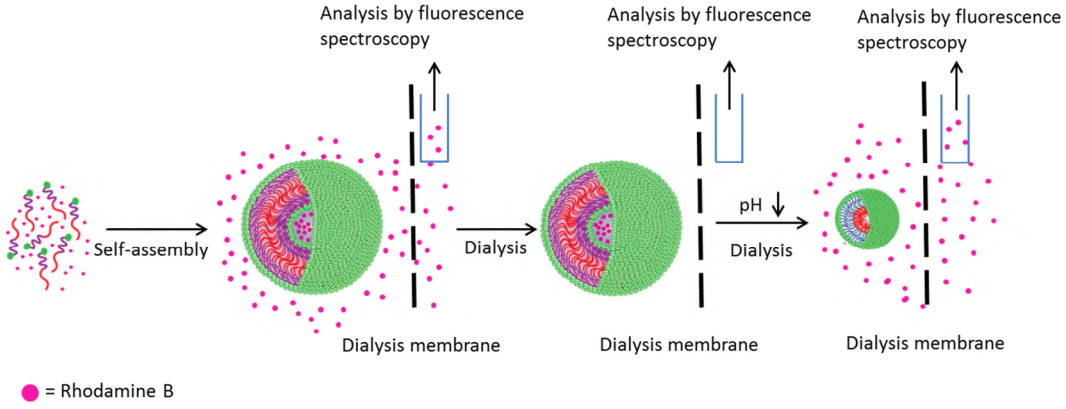

Figure 3.27: Schematic representation of the method used for encapsulating Rhodamine B within the central water pool of the vesicle and releasing it in response to a drop in pH

Vesicles, by their very nature, have a central water pool within their structure. This can be exploited to encapsulate a hydrophilic molecule and in the case of the above polymers, release it in response to a change in pH. To test this polymer **3.05** was assembled in the presence of Rhodamine B; a hydrophilic fluorescent dye with λ_{em} = 550 nm and λ_{ex} = 575 nm. Polymer **3.05** was dissolved in DMF at a concentration of 0.5 mg mL^{-1} and Rhodamine B was added to a concentration of 0.8 mg mL^{-1}. Water was then added slowly until the polymer concentration reached 0.25 mg mL^{-1}. The solution was then dialysed against 200 mL water. The dialysis water was tested for fluorescence at each water change and during the first few water changes there was a large response as any non-encapsulated Rhodamine B dialysed out of the polymer solution. After two consecutive water samples in which no

fluorescence was detected, it was decided that no significant amounts of dye were being removed from the polymer system and therefore any Rhodamine B that remains within the polymer solution must be encapsulated within the central water pool of the vesicles. The polymer solution was removed from inside the dialysis bag and the pH recorded as 7.0. The sample at this point was analysed by fluorescence spectroscopy and a significant fluorescence response detected, showing that indeed the vesicles had trapped Rhodamine B (see Figure 3.28).

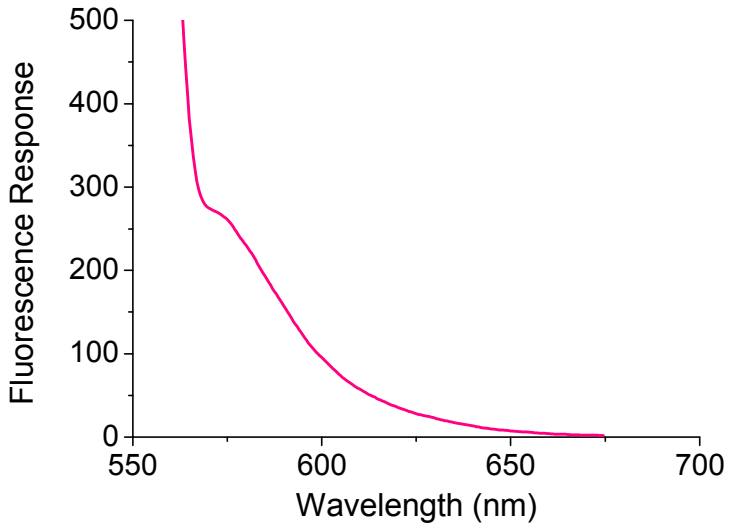

Figure 3.28: Fluorescence recorded (λ_{ex} = 550 nm, λ_{em} = 575 nm) for the self-assembled sample of 3.05 before the pH was adjusted showing that Rhodamine B had been encapsulated within the central water pools of the vesicles

The pH of the polymer solution was then dropped to pH 2.5 using diluted HCl and after stirring overnight the solution was again dialysed against water. The dialysis water was tested for fluorescence and a response was detected. Figure 3.29 shows the lack of a signal in the dialysis water before the polymer solution was acidified and then the response in the dialysis water after the acidic polymer solution was dialysed. In both cases the sample was excited at λ = 550 nm and the emission at λ = 575 nm recorded.

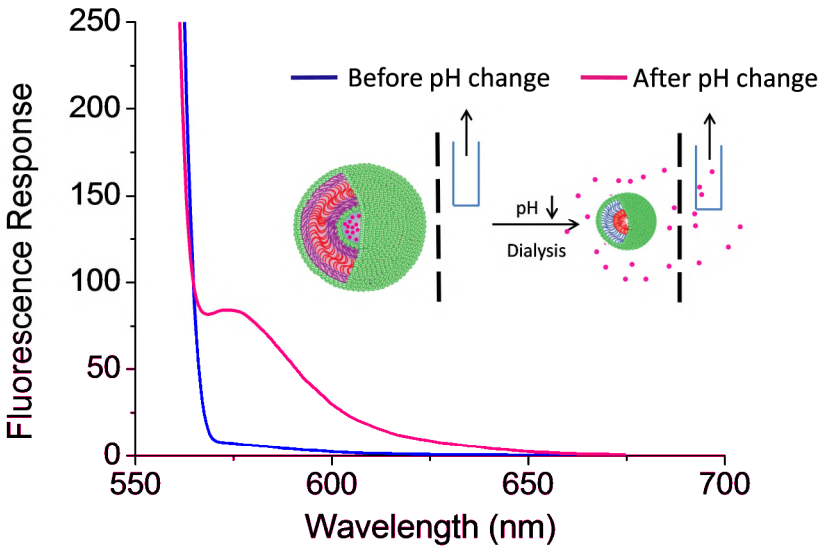

Figure 3.29: Fluorescence spectra recorded at λ_{ex} = 550 nm, λ_{em} = 575 nm for the dialysis water before the pH of the polymer solution was dropped (blue line) and after the pH had been dropped and again dialysed (pink line)

3.2.8 Speeding up the morphology transition

Since both of the previous polymers require stirring overnight after addition of the acid, to allow the assemblies to stabilise, it was decided that a smaller overall polymer may provide a faster morphology switch. Therefore, using the same CTA as for **3.02**, a homopolymer of MA was synthesised, **3.06,** M_n (^{1}H NMR) = 2.1 kDa, M_n (DMF SEC) = 2.57, $Đ_M$ = 1.11. The DP of the MA block was determined to be 21 by ^{1}H NMR spectroscopy, in the same manner as for **3.01**. This was then chain extended with PFPA, as before, to yield a smaller scaffold polymer, **3.07**, M_n (^{1}H NMR) = 11.8 kDa, M_n (DMF SEC) = 8.71, $Đ_M$ = 1.13. This scaffold polymer has an activated ester block length of 42, as determined by ^{1}H NMR spectroscopy, using known integrations of the CTA end groups, in the same manner as described for **3.02**.

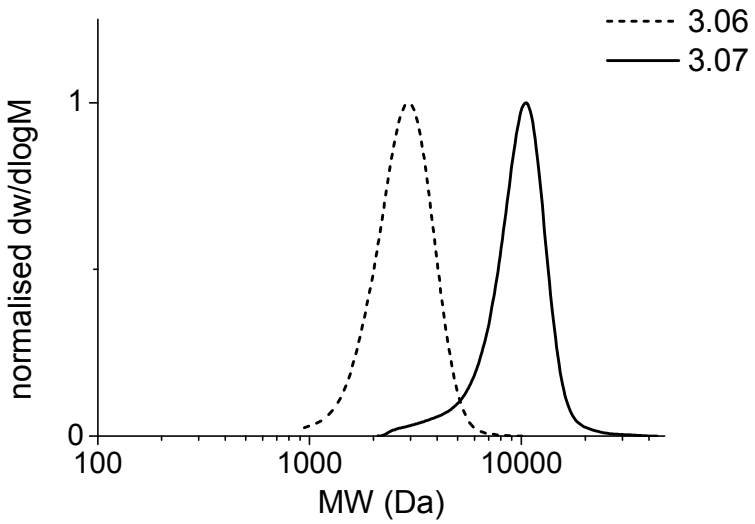

Figure 3.30: DMF SEC chromatograms showing the shift in molecular weight upon the chain extension of homopolymer 3.06 to form diblock copolymer 3.07

This scaffold polymer was then substituted and end group modified as before, to yield two polymers. Polymer **3.08** bears the charged quaternary amine end group, M_n (^{1}H NMR) = 10.4 kDa, M_n (DMF SEC) = 14.2 kDa, $Đ_M$ = 1.14. The substitution of the backbone was confirmed by the disappearance of the broad polymer peaks in the ^{19}F NMR spectrum and the appearance of the sharp peaks relating to pentafluorophenol. The incorporation of the end group was demonstrated again by the appearance of new peaks in the ^{1}H NMR spectrum, as for **3.04**. Polymer **3.09** bears the TEG end group and the successful backbone substitution was confirmed by ^{19}F NMR spectroscopy. The end group modification was confirmed by the appearance of peaks at 2.8 and 3.4 ppm in the ^{1}H NMR spectrum which correspond to the SCH_2CH_2COO protons and the terminal OCH_3 on the TEG functionality respectively (see Figure 3.31). The end group modification was also confirmed by IR spectroscopy (see Figure 3.32).

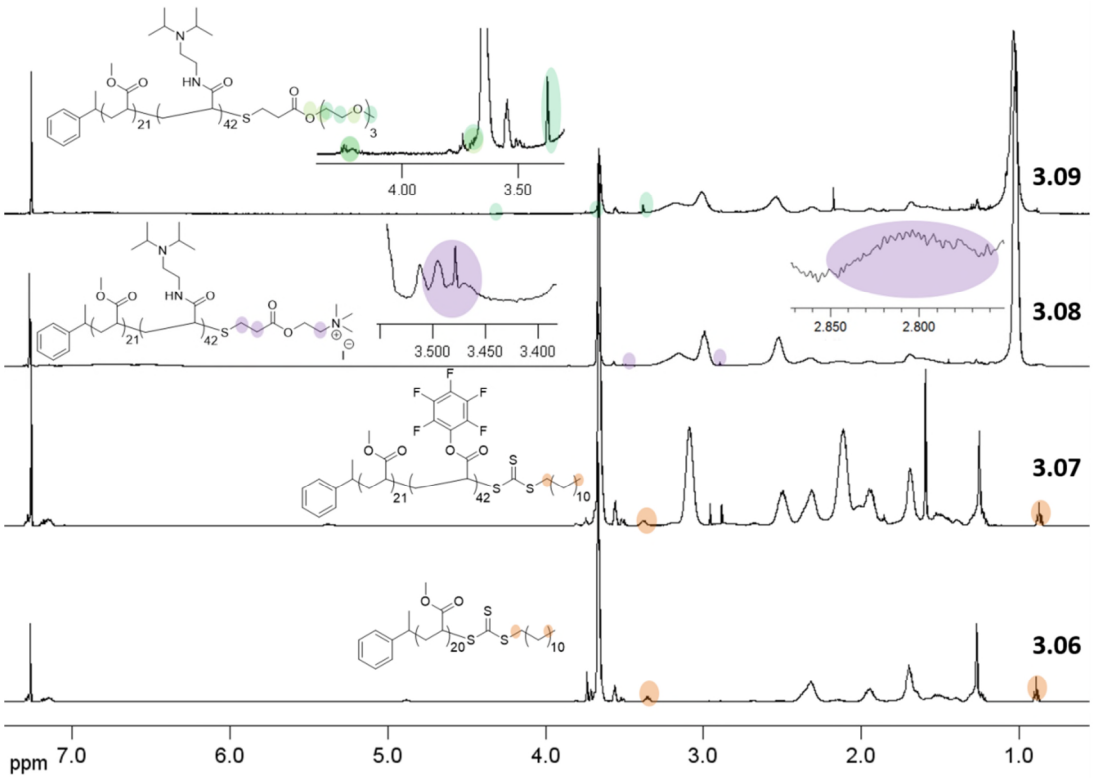

Figure 3.31: ^{1}H NMR spectra of 3.06, 3.07, 3.08 and 3.09 in $CDCl_3$ with key end group peaks highlighted. Spectra were recorded at 25 °C and 400 MHz

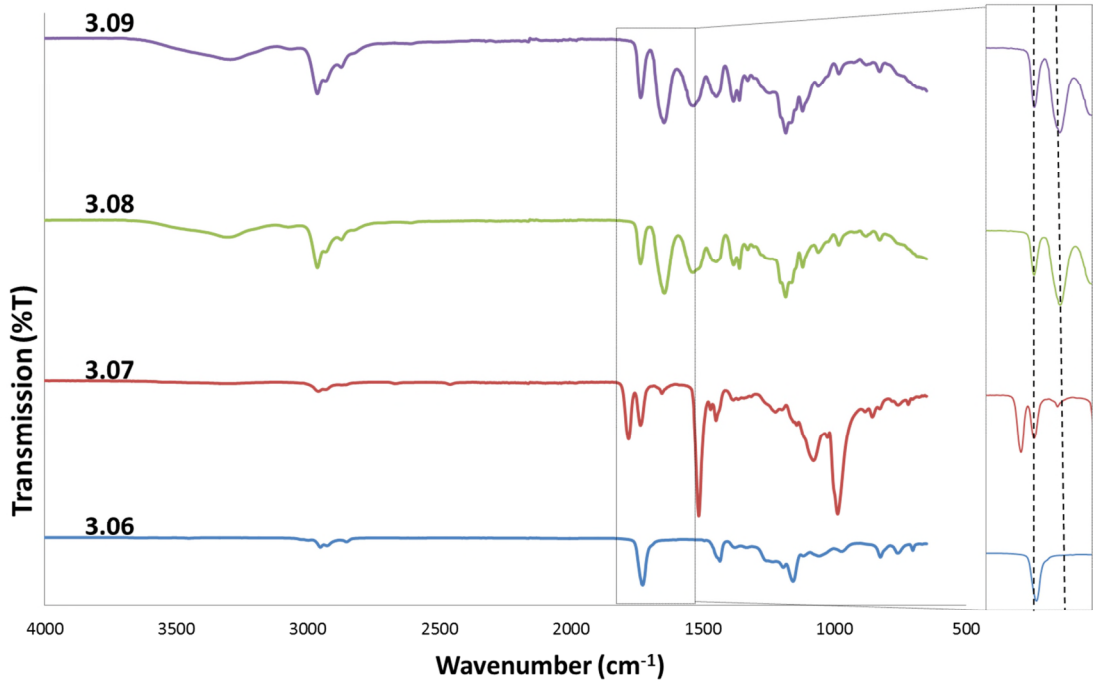

Figure 3.32: IR spectra of 3.06, 3.07, 3.08 and 3.09, showing the shift of the C=O ester stretch for PFPA (3.07) to a C=O amide stretch (3.08 and 3.09) upon substitution, whilst the C=O ester stretch for MA (3.06) remains the same.

3.2.9 Self-assembly behaviour of the smaller block copolymers

Due to the smaller overall block lengths of these polymers it was decided to self-assemble them by direct dissolution into acidic water, in order to avoid the use of organic solvents and exhaustive dialysis. Firstly polymer **3.08** was directly dissolved into pH 2.25 water at a concentration of 0.25 mg mL^{-1}. At this pH, the amine groups will be protonated and therefore it is predicted that micelles will form. Analysis by DLS shows a population with D_h = 37 ± 4 nm. The presence of spherical micelles was confirmed by TEM analysis, which, after staining with uranyl acetate, showed the micelles had an average size of 36 ± 5 nm (see Figure 3.33).

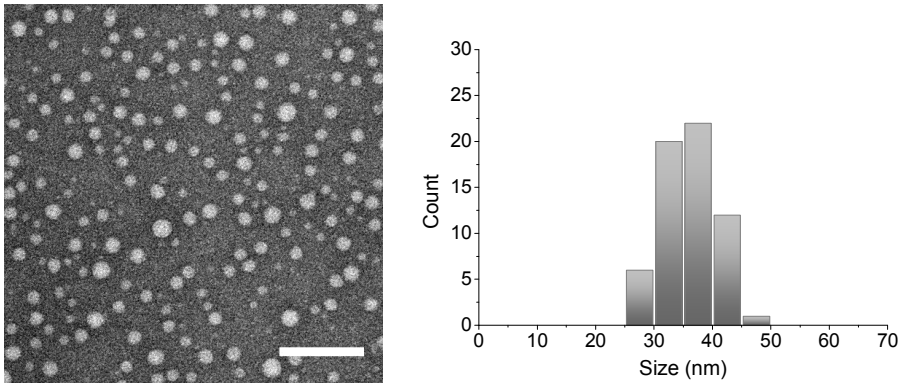

Figure 3.33: TEM image, stained with uranyl acetate, showing the presence of micelles of 3.08 at pH 2.25, scale bar = 200 nm, and the distribution of sizes observed

Diluted NaOH was added to this solution to raise the pH to above the pK_a of the polymer. Approximately 0.2 mL of diluted NaOH was added to increase the pH to 8.5 and resulted in the solution turning slightly turbid. Upon analysis by DLS vesicles with a D_h of 97 ± 6 nm could be observed. Again, TEM was employed to image the particle and after staining with uranyl acetate a population with an average size of 102 ± 19 nm could be observed (see Figure 3.34).

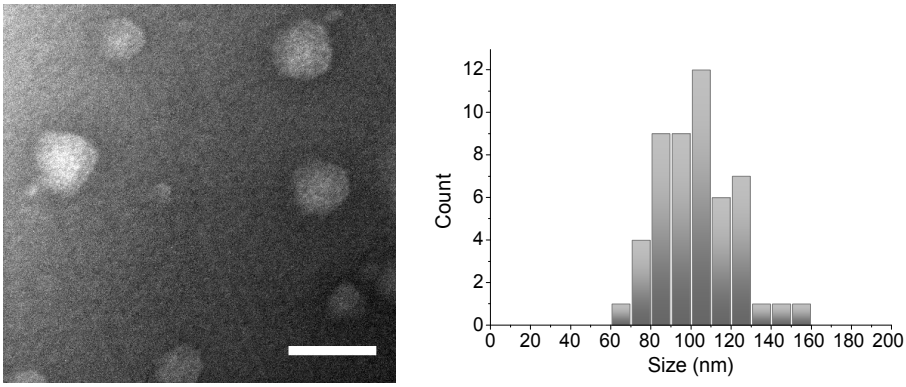

Figure 3.34: TEM image, of vesicles formed from 3.08 at pH 8.5, stained with uranyl acetate, scale bar = 200 nm, and the distribution of sizes observed

The reversibility of this morphology change was demonstrated by cycling the pH between *ca.* pH 3.0 and *ca.* pH 8.5, with the size being recorded by DLS after each pH change. As can be seen from the graph below (Figure 3.35) the size change in response to pH is both reversible and repeatable, with the sizes at each pH staying fairly constant at each cycle. The time taken for the morphologies to stabilise after addition of either acid or base was only 10 minutes, showing that the smaller polymer chain has indeed afforded a faster morphology switch.

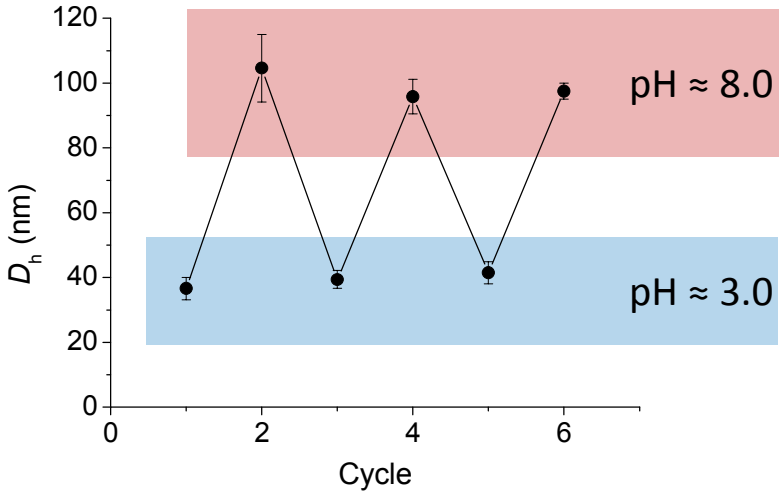

Figure 3.35: Graph showing the switching behaviour of 3.08 is fully repeatable and reversible

Polymer **3.09** was assembled in the same way as **3.08**, by direct dissolution into pH 2.25 water. The solution was analysed by DLS and micelles with a D_h = 37 ± 5 nm were

observed. The solution was then analysed by TEM and, after staining with uranyl acetate, micelles with an average size of 28 ± 5 nm were obtained (see Figure 3.36).

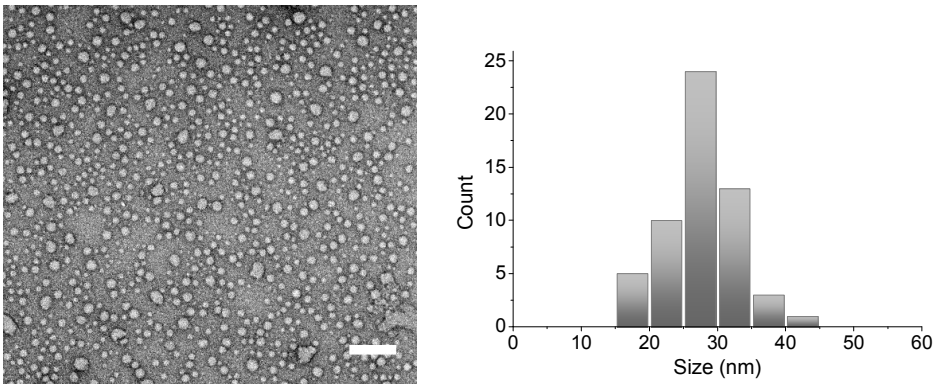

Figure 3.36: TEM image of micelles of 3.09 at pH 2.25, stained with uranyl acetate, scale bar = 200 nm, and the distribution of sizes observed

The pH was then raised by addition of *ca*. 0.2 mL of diluted NaOH solution to a pH of 8.5 and the size measured again by DLS. The size had increased to 122 ± 6 nm and analysis by TEM confirmed the presence of a population with an average size of 123 ± 27 nm (see Figure 3.37).

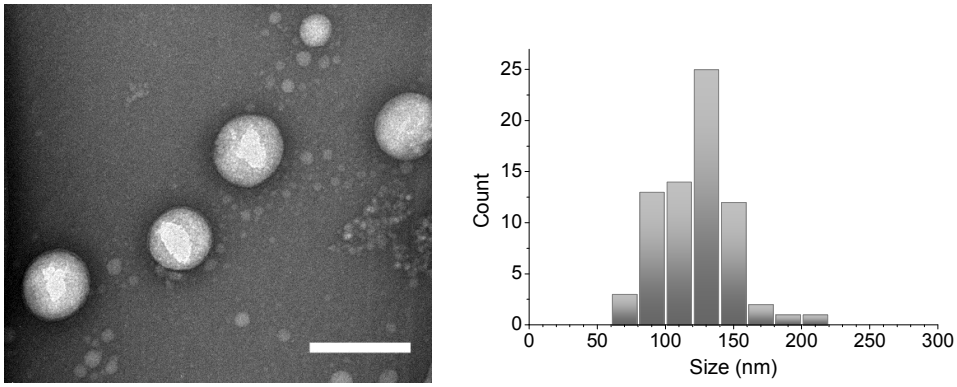

Figure 3.37: TEM image of 3.09 at pH 8.5 stained with uranyl acetate, scale bar = 200 nm, and the distribution of sizes observed

The size change was shown to be fully reversible and repeatable on changing the pH. The pH was cycled between *ca*. pH 3.0 and *ca.* pH 8.0 and again the sizes stayed fairly constant between cycles at each pH (see Figure 3.38).

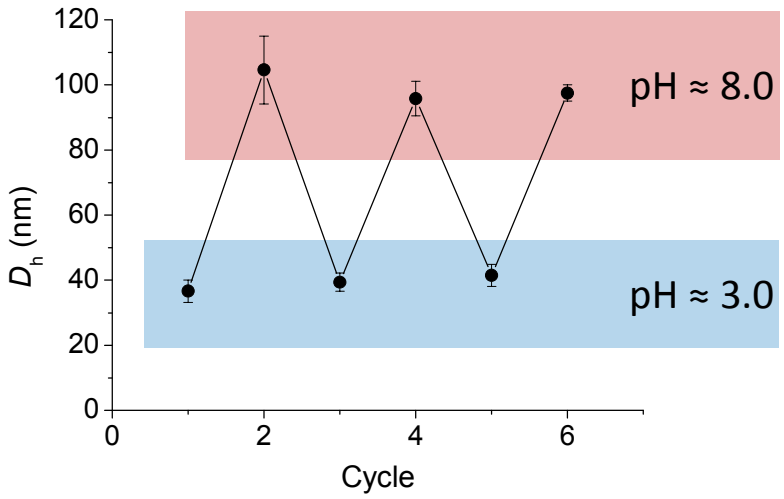

Figure 3.38: Graph showing that the size change of 3.09 with pH is fully repeatable and reversible

3.2.10 Encapsulation and release studies

The ability of the smaller block copolymers to encapsulate and release the hydrophilic dye, Rhodamine B, was explored. Two different self-assembly techniques were used for the encapsulation of the dye; direct dissolution in basic water in the presence of Rhodamine B, and solvent switch from DMF into water in the presence of Rhodamine B.

3.2.10.1 Encapsulation by direct dissolution

Polymer **3.09**, bearing the TEG end group, was assembled by direct dissolution in the presence of Rhodamine B. A solution of **3.09** and Rhodamine B, both at 0.5 mg mL^{-1}, in water with a pH of 8.0 was stirred at 30 °C for three days. The gentle heating was intended to facilitate self-assembly of the polymer in basic water. After three days the polymer solution was dialysed against water to remove any non-encapsulated Rhodamine B. Samples were removed at every water change and tested for fluorescence as described for **3.05.** After two consecutive water samples with no fluorescence emission, the polymer solution was removed from the dialysis bag. The pH was recorded as 7.2 and the sample showed a fluorescence response at λ = 575 nm, showing that the polymer solution contained Rhodamine B, trapped within the central water pools of the vesicles (see Figure 3.39).

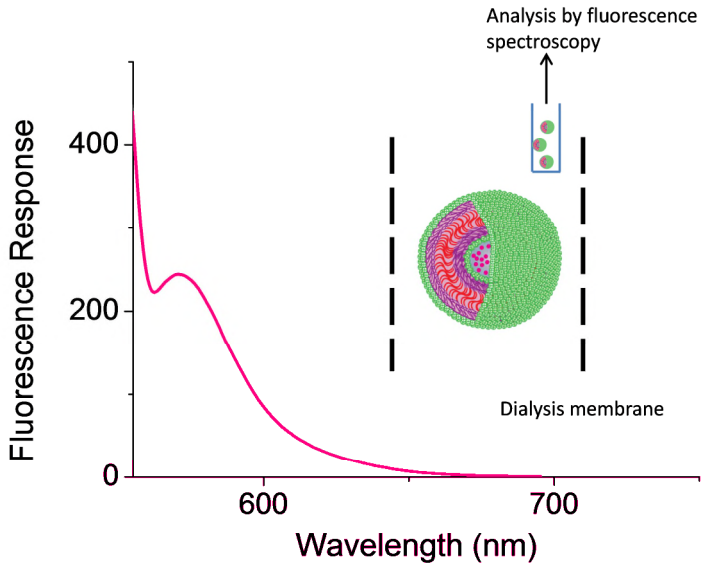

Figure 3.39: Fluorescence recorded (λ_{ex} = 550 nm, λ_{em} = 575 nm) for the self-assembled sample of 3.09 before the pH was adjusted showing that Rhodamine B had been encapsulated within the central water pools of the vesicles

The pH of the solution was dropped to 2.9 and the solution dialysed again against water. Testing of this dialysis water revealed a very small fluorescence emission at λ = 575 nm, showing that Rhodamine B was released from within the central water pools of the vesicles. The smaller response may be a result of the lower concentration used (see Figure 3.40).

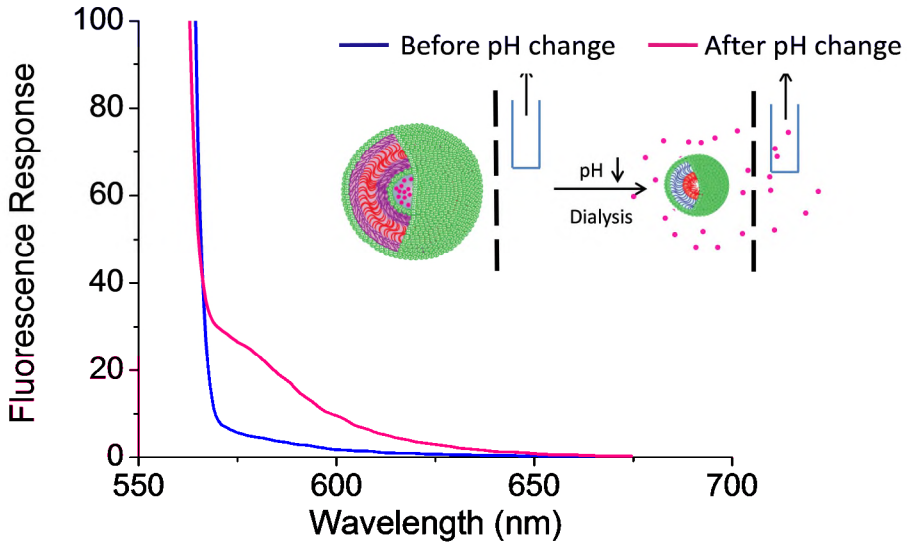

Figure 3.40: Fluorescence recorded (λ_{ex} = 550 nm, λ_{em} = 575 nm) of the dialysis water before the pH of 3.09 was changed (blue line) and after it was adjusted and the sample again dialysed (pink line)

3.2.10.2 Encapsulation by solvent switch

Polymer **3.08** was also self-assembled in the presence of Rhodamine B. Polymer **3.08** was dissolved in DMF at a concentration of 2 mg mL^{-1} and Rhodamine B added to a concentration of 0.8 mg mL^{-1}. Water was then added until the polymer was at a concentration of 1.0 mg mL^{-1} and then the solution was dialysed to remove the DMF and any non-encapsulated Rhodamine B. Therefore after each change of the dialysis water, the fluorescence was tested, as described in the previous section. The first few water changes had considerable fluorescence responses, as the Rhodamine B was removed into the dialysis water. After two water changes where there was no fluorescence response recorded it can be considered that any Rhodamine B detected in the polymer solution is trapped within the central water pools of the vesicles. The solution was then removed from the dialysis bag and the pH lowered from pH 7.46 to pH 2.5. After this pH change the solution was placed back inside the dialysis bag and dialysed against water. Again, the water was tested for fluorescence after several hours and a fluorescence response at λ = 575 nm detected (see Figure 3.41). This shows that Rhodamine B had been encapsulated within the central water pools of the vesicle and released in response to a change in pH.

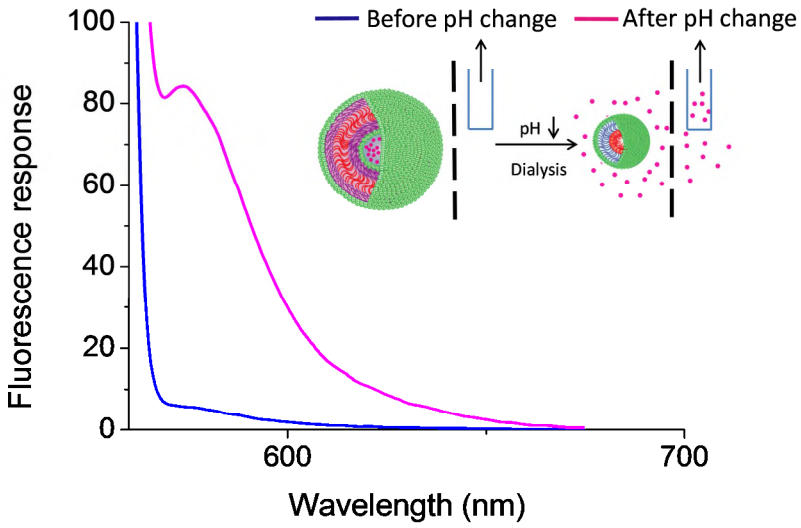

Figure 3.41: Fluorescence spectra showing the lack of a fluorescence response at λ_{ex} = 575 nm (when excited at 550 nm) before the pH of the solution was adjusted (blue line) and the fluorescence response detected after the pH of the solution was adjusted (pink line)

3.3 Conclusions

In this chapter we have explored the pH-responsive behaviour of 2-(*N, N*-diisopropylamino) ethyl containing polymers. Previous attempts to polymerise the acrylate monomer, 2-(*N, N*-diisopropylamino) ethyl acrylate were unsuccessful, with low conversions and broad dispersities. Initial attempts to polymerise the PFPA using a quaternary amine functionalised CTA were unsuccessful. Therefore a scaffold polymer consisting of the hydrophobic block MA and the substitutable block PFPA was synthesised. A one-pot two-step method was employed to substitute the backbone of the scaffold and end group modify the polymer to attach the hydrophilic functionality.

Two end groups were investigated, one bearing a charged quaternary amine functionality and the other bearing a TEG group. Self-assembled structures from both polymers underwent a reversible morphology change in response to a change in pH, as confirmed by DLS and TEM. Using a smaller scaffold polymer increased the rate of the morphology transition and was demonstrated to be fully reversible and repeatable. The encapsulation and release of a hydrophilic payload was demonstrated.

3.4 Experimental

3.4.1 Materials

N,N-dimethylformamide (DMF 99.9%), 1,4-dioxane, *N, N*-diisopropylethlenediamine and all other chemicals were used as received from Aldrich and Tokyo Chemical Industry unless otherwise stated. AIBN [2, 2'-azobis(2-methylpropionitrile)] was recrystallised twice from methanol and stored in the dark at 4°C. Methylacrylate was passed over a short column of alumina immediately prior to use in order to remove the inhibitor. Pentafluorophenyl acrylate was synthesised according to literature procedures.[24] Triethylene glycol methyl ether acrylate was synthesised according to literature procedures.[49]

3.4.2 Characterisation

Nuclear magnetic resonance (NMR) experiments were performed on a Bruker 400 FT-NMR spectrometer operating at 400 MHz (^{1}H) ,300 MHz (^{19}F) or 125 MHz (^{13}C) using deuterated solvents. Chemical shifts are reported in parts per million relative to $CHCl_3$ (7.26 ppm for ^{1}H and 77.0 ppm for ^{13}C) or MeOH (4.84 ppm for ^{1}H and 49.05 ppm for ^{13}C). Extended ^{1}H and ^{13}C NMR spectra were recorded on a 500 FT-NMR spectrometer operating at 500 MHz, all at 25°C.

Size exclusion chromatography (SEC) measurements were obtained in either HPLC grade $CHCl_3$ or DMF containing 0.1M $NH_4BF_4$with a flow rate of 1 mL min^{-1}, on a set of two Pgel 5μm Mixed D columns plus a guard column. Cirrus GPC software was used to analyse the data using polymethylmethacrylate (PMMA) standards.

Hydrodynamic diameters (D_h) and size distributions of the self-assembled structures in aqueous solutions were determined by dynamic light scattering (DLS). The DLS instrumentation consisted of a Malvern ZetasizerNanoS instrument operating at 25°C with a 4 mW He-Ne 633 nm laser module. Measurements were made at a detection angle of 173° (back scattering) and Malvern DTS software was utilised to analyse the data. All measurements were run at least three times with at least 10 runs per measurement.

TEM measurements were made by drop deposition of 4 μL solution onto an argon plasma treated carbon-coated copper grid. Analysis was performed on a JEOL TEM 2011 operating at 200 keV. Number average particle diameters (D_{av}) were generated from the analysis of a minimum of 50 particles from at least 3 different micrographs.

Fluorescence measurements were recorded on a Perkin Elmer LS 55 spectrometer. Infrared spectrometry was recorded on a Perkin Elmer Spectrum 100 FT-IR ATR unit. Mass spectra were recorded on a Bruker Esquire 2000 ESI spectrometer. Elemental analysis was performed by Warwick Analytical Service.

Dialysis tubing was purchased from Spectrum labs with a molecular weight cut off 3.5 kDa.

3.4.3 Formation of the MA homopolymers, 3.01 and 3.06

MA (3 g, 34.5 mmol, 40 equiv.), **CTA 7**[48] (0.3334 g, 0.87 mmol) and AIBN (14.3 mg, 0.087 mmol, 0.1 equiv) were dissolved in 1, 4-dioxane (2: 1 volume compared to monomer) and placed in an oven dried ampoule under the flow of nitrogen with a stirrer bar. The ampoule was degassed at least three times and released to and sealed under nitrogen. The polymerisation mixture was then heated at 65 °C for 1 hour 35 minutes to afford **3.01**. The polymer was purified by precipitation into a stirred solution of cold MeOH: H_2O (10: 1) three times, followed by dissolution in THF, drying over anhydrous $MgSO_4$, removal of the THF and drying *in vacuo* to yield a yellow oily polymer, **3.01**, M_n (^{1}H NMR) = 3.8 kDa, M_n ($CHCl_3$ SEC) = 2.6 kDa, $Đ_M$ = 1.07. ^{1}H NMR (400 MHz, $CDCl_3$): δ (ppm): 0.88 (t, $^3J_{H\text{-}H}$ = 6.8 Hz, CH_2CH_3 3H, of CTA end group), 1.20-1.38 (br m, 20H, $(CH_2)_{10}CH_3$of CTA end group), 1.40-2.10 (br m, 80H, $CHCH_2$ of polymer backbone), 2.24-2.40 (br s, 40H, $CHCH_2$ of polymer backbone, 3.34 (t, $^3J_{H\text{-}H}$ = 7.41 Hz, 2H, $SCSSCH_2$ of CTA end group), 3.60-3.70 (br s, 120H, OCH_3 of PMA side chain), 4.88 (q, $^3J_{H\text{-}H}$ = 7.60 Hz, 1H, CH_2CHS of polymer backbone), 7.12-7.28 (m, 5H, Ar*H* in CTA end group). ^{13}C NMR (125 MHz, $CDCl_3$): δ (ppm): 14.1, 21.8, 22.2, 22.4, 22.5, 22.6, 23.0, 27.8, 28.9, 29.0, 29.3, 29.4, 29.5, 29.6, 31.9, 34.1, 36.0, 37.5, 41.1, 41.3, 50.0, 50.4, 50.5, 51.7, 52.9, 126.2, 126.9, 128.4, 146.2, 170.4,

174.2, 174.8, 175.6, 175.8, 221.4. FTIR υ_{max}/ cm^{-1} 2953 and 2854 (alkane C-H stretch), 1729 (C=O ester stretch), 1435 and 1378 (C=C aromatic stretch), 1194 and 1157 (C-N stretch).

Polymer **3.06** was synthesised in a similar manner. M_n (^{1}H NMR) = 2.1 kDa, M_n (DMF SEC) = 2.6 kDa, $Đ_M$ = 1.11. ^{1}H NMR (400 MHz, $CDCl_3$): δ (ppm): 0.88 (t, $^3J_{H-H}$ = 7.35 Hz, 3H, CH_2CH_3 of CTA end group), 1.18-1.38 (br m, 20H, $(CH_2)_{10}CH_3$of CTA end group), 1.40-2.10 (br m, 40H, $CHCH_2$ of polymer backbone), 2.24-2.40 (br s, 20H, $CHCH_2$ of polymer backbone), 3.34 (t, 2H, $SCSSCH_2$ of CTA end group), 3.60-3.70 (br s, 60H, OCH_3 of PMA side chain), 4.88 (q, $^3J_{H-H}$ = 7.45 Hz, 1H, CH_2CHS of polymer backbone), 7.12-7.28 (m, 5H, Ar*H* in CTA end group). ^{13}C NMR (125 MHz, $CDCl_3$): δ (ppm): 14.1, 21.7, 22.2, 22.4, 22.6, 23.0, 27.7, 28.8, 29.0, 29.3, 29.4, 29.5, 29.6, 31.9, 34.0, 36.0, 37.5, 41.1, 41.3, 50.4, 50.5, 51.7, 52.9, 126.2, 126.9, 128.4, 146.2, 170.4, 174.2, 174.3, 175.6, 175.8, 221.4. FTIR υ_{max}/ cm^{-1} 2953 and 2854 (alkane C-H stretch), 1729 (C=O ester stretch), 1435 and 1378 (C=C aromatic stretch).

3.4.4 Formation of the scaffold diblock copolymers, 3.02 and 3.07

PFPA (1.5 g, 6.3 mmol, 45 equiv.), homopolymer **3.01** (0.33 g, 0.16 mmol) and AIBN (5.1 mg, 0.031 mmol, 0.2 equiv.) were dissolved in 1, 4-dioxane (1: 1 volume compared to monomer) and placed in an oven dried ampoule under the flow of nitrogen with a stirrer bar. The ampoule was degassed at least three times and released to and sealed under nitrogen. The polymerisation mixture was then heated at 65 °C for 1 hour 50 minutes to afford diblock copolymer, **3.02**. The polymer was purified by precipitation into cold hexanes three times and dried *in vacuo* to yield a yellow powder. M_n (^{1}H NMR) = 27.5 kDa, M_n ($CHCl_3$ SEC) = 7.7 kDa, $Đ_M$ = 1.29. ^{1}H NMR (400 MHz, $CDCl_3$): δ (ppm): 0.88 (t, $^3J_{H-H}$ = 6.84 Hz, 3H, CH_2CH_3 of CTA end group), 1.20-1.38 (br m, 20H, $(CH_2)_{10}CH_3$of CTA end group), 1.40-2.40 (br m, 280H, $CHCH_2$ of polymer backbone), 2.40-2.50 (br s, 40H, $CHCH_2$ of polymer backbone, 3.0-3.15 (br s, 100H, $CHCH_2$ of polymer backbone), 3.34 (m, 2H, $SCSSCH_2$ of CTA end group), 3.60-3.70 (br s, 120H, OCH_3 of PMA side chain), 7.12-7.28 (m, 5H, Ar*H* in CTA end group). ^{13}C NMR (125 MHz, $CDCl_3$): δ (ppm): 14.0, 22.7, 25.6, 28.9, 29.0,

29.3, 29.4, 29.5, 29.6, 30.3, 32.8, 32.9, 33.0, 36.2, 39.9, 41.1, 41.3, 51.7, 124.4, 126.2, 126.9, 127.0, 128.4, 136.7, 138.8, 138.9, 139.9, 140.0, 140.8, 141.9, 142.0, 169.7, 169.8, 170.0, 170.1, 174.9, 221.4. ^{19}F NMR (300MHz, $CDCl_3$): δ (ppm): -162.8 (br s, 2F, Ar*F* in polymer side chain), -157.3 (br s, 1F, Ar*F* in polymer side chain), -153.8 (br s, 2F, Ar*F* in polymer side chain). FTIR υ_{max}/ cm^{-1} 2956 (alkane C-H stretch), 1783 and 1737 (C=O ester stretch), 1517 and 1471 (C-F stretch), 1453 (C=C aromatic stretch).

Polymer **3.07** was synthesised in a similar manner. M_n (^{1}H NMR) = 11.8 kDa, M_n (DMF SEC) = 8.7 kDa, $Đ_M$ = 1.13. ^{1}H NMR (400 MHz, $CDCl_3$):): δ (ppm): 0.88 (t, $^3J_{H\text{-}H}$ = 6.84 Hz, 3H, CH_2CH_3 of CTA end group),), 1.20-1.38 (br m, 20H, $(CH_2)_{10}CH_3$of CTA end group), 1.40-2.40 (br m, 140H, $CHCH_2$ of polymer backbone), 2.40-2.50 (br s, 20H, $CHCH_2$ of polymer backbone, 3.0-3.15 (br s, 50H, $CHCH_2$ of polymer backbone), 3.34 (m, 2H, $SCSSCH_2$ of CTA end group), 3.60-3.70 (br s, 60H, OCH_3 of PMA side chain), 7.12-7.28 (m, 5H, Ar*H* in CTA end group). ^{19}F NMR (300MHz, $CDCl_3$): δ (ppm): -162.8 (br s, 2F, Ar*F* in polymer side chain), -157.3 (br s, 1F, Ar*F* in polymer side chain), -153.8 (br s, 2F, Ar*F* in polymer side chain). ^{13}C NMR (125 MHz, $CDCl_3$): δ (ppm): 14.1, 22.7, 28.9, 29.1, 29.4, 29.6, 34.7, 36.1, 40.0, 41.3, 51.7, 124.4, 126.3, 127.0, 128.5, 136.9, 138.9, 139.9, 140.8, 141.9, 142.0, 169.4, 169.7, 169.8, 170.1, 174.9, 221.4. FTIR υ_{max}/ cm^{-1} 2955 (alkane C-H stretch), 1783 and 1737 (C=O ester stretch), 1516 and 1471 (C-F stretch), 1450 (C=C aromatic stretch).

3.4.5 Synthesis of the charged tertiary amine acrylate, 3.03

N, N- (Dimethylamino) ethyl acrylate (DMAEA) (5 mL, 1 equiv.) was dissolved in petroleum ether (100 mL). Methyl iodide (20.5 mL, 10 equiv.) was added and left to stir for 1 hour. The solution was then filtered and the solid dried to give a white solid. ^{1}H NMR spectroscopy (400 MHz, D_2O): δ (ppm): 3.11 (s, 9H, $N^+(CH_3)_3$), 3.67 (m, 2H,CH_2CH_2N), 4.53 (m, 2H, $COOCH_2$), 5.92 (dd, 1H,$^2J_{H\text{-}H}$ = 1.2 Hz, $^3J_{H\text{-}H}$ = 14.0 Hz, CHH=CH), 6.11 (m, 1H, CHH=C*H*), 6.35 (dd, 1H,$^2J_{H\text{-}H}$ = 1.2 Hz, $^3J_{H\text{-}H}$ = 23.2 Hz, CH*H*=CH). ^{13}C NMR (125 MHz, D_2O): δ (ppm): 54.6, 59.1, 66.1, 128.8, 132.9. FTIR υ_{max}/ cm^{-1} 3020 (alkene C-H

stretch), 3002 and 2949 (alkane C-H stretch), (1731 C=O acrylate stretch), 1621 (C=C alkene stretch), 1267 and 1278 (C-O stretch), 1061 (C-N stretch).

3.4.6 Substitution of the PFPA and end group modification

The substitution of the PFPA scaffold and subsequent end group modification proceeds via a one pot, two step method, the general procedure for which is as follows.

The diblock copolymer (**3.02** or **3.07**) was dissolved in DMF at a concentration of 150 mg mL^{-1} and placed in an oven dried ampoule. The ampoule was degassed at least three times and released to and sealed under nitrogen. In a separate oven dried ampoule *N, N* diisopropylethylenediamine (1.5 equiv. per PFPA) was dissolved in DMF and the ampoule was degassed three times and released to and sealed under nitrogen. The amine solution was transferred to the polymer solution using air sensitive techniques and was stirred at room temperature overnight. ^{19}F NMR spectroscopy was used to confirm the full modification of pentafluorophenyl groups. The desired end group acrylate (100 equiv.) and PBu_3 (20 equiv.) were dissolved in DMF and placed in an oven dried ampoule. The ampoule was degassed three times and released to and sealed under nitrogen. This solution was transferred to the polymer solution using air sensitive techniques. The solution was stirred for 10 minutes. Hexylamine (20 equiv.) was dissolved in DMF and placed in an oven dried ampoule. The ampoule was degassed three times and released to and sealed under nitrogen. The hexylamine solution was transferred to the polymer solution using air sensitive techniques and the polymer solution was then stirred overnight. The polymer was purified by exhaustive dialysis against water, incorporating both acidic and basic water changes. The polymer was recovered by lyophilisation to yield diblock copolymer **3.04**, **3.05**, **3.08** or **3.09**.

Polymer 3.04, M_n (^1H NMR) = 23.9 kDa, M_n (DMF SEC) = 23.1 kDa, $Đ_M$ = 1.19. ^1H NMR (400 MHz, MeOD): δ (ppm): 1.11-2.50 (br m, 420H, C*H*C*H*$_2$ of polymer backbone), 1.35-1.50 (br s, 1200H, N(CH(C*H*$_3$)$_2$)$_2$ of DIPEA side chain), 2.62 (m, 2H, SCH$_2$C*H*$_2$COO of end group), 2.90 (br m, 2H, SC*H*$_2$CH$_2$COO of end group), 3.16-3.40 (br s, 200H, NHCH$_2$C*H*$_2$N

of DIPEA side chain), 3.40-3.90 (br m, 520H, $NHCH_2CH_2N$ and $N(CH(CH_3)_2)_2$ of DIPEA side chain and OCH_3 of PMA side chain), 4.55 (m, 2H, $COOCH_2CH_2N$ of end group), 7.10-7.30 (m, 5H, Ar*H* of end group). ^{13}C NMR (125 MHz, MeOD): δ (ppm): 21.2, 35.9, 42.1, 42.7, 43.7, 46.0, 50.8, 52.4, 68.9, 128.2, 129.6, 176.7, 176.9. FTIR υ_{max}/ cm^{-1}: 3303 (N-H amide stretch), 2964 (alkane C-H stretch), 1737 (C=O ester stretch), 1646 (C=O amide stretch), 1536 (N-H amide bend), 1361 and 1185 (C-N stretch).

Polymer 3.05, M_n (^{1}H NMR) = 23.9 kDa, M_n (DMF SEC) = 23.1 kDa, $Đ_M$ = 1.19. ^{1}H NMR (400 MHz, $CDCl_3$): δ (ppm): 0.90-1.11 (br s, 1200H, $N(CH(CH_3)_2)_2$ of DIPEA side chain) 1.20 -2.40 (br m, 420H, $CHCH_2$ of polymer backbone), 2.40-2.50 (br s, 200H, $NHCH_2CH_2N$ of DIPEA side chain), 2.75 (m, 4H, SCH_2CH_2COO of end group), 2.90-3.20 (br m, 300H, $NHCH_2CH_2N$ and $N(CH(CH_3)_2)_2$ of DIPEA side chain), 3.39 (br s, 3H, OCH_3 of end group), 3.47-3.56 (m, 8H, $(OCH_2CH_2O)_2$ of end group), 3.60-3.69 (br s, 120H, OCH_3 of PMA side chain), 3.69-3.72 (m, 2H, $COOCH_2CH_2O$ of end group), 4.20-4.27 (m, 2H, $COOCH_2CH_2O$ of end group), 7.10-7.30 (m, 5H, Ar*H* of end group). ^{13}C NMR (125 MHz, $CDCl_3$): δ (ppm): 14.1, 20.8, 21.3, 23.1, 29.3, 29.6, 31.9, 32.1, 34.9, 35.0, 35.1, 40.0, 41.3, 42.7, 44.3, 45.3, 48.7, 51.7, 59.0, 63.8, 69.0, 69.1, 70.6, 71.9, 126.2, 126.9, 127.0, 128.4, 174.9. FTIR υ_{max}/ cm^{-1}: 3294 (N-H amide stretch), 2964 (alkane C-H stretch), 1737 (C=O ester stretch), 1648 (C=O amide stretch), 1536 (N-H amide bend), 1361 and 1185 (C-N stretch).

Polymer 3.08, M_n (^{1}H NMR) = 10.4 kDa, M_n (DMF SEC) = 14.2 kDa, $Đ_M$ = 1.14. ^{1}H NMR (400 MHz, MeOD): δ (ppm): 0.90-1.10 (br s, 500H, $N(CH(CH_3)_2)_2$ of DIPEA side chain) 1.20 -2.40 (br m, 210H, $CHCH_2$ of polymer backbone), 2.40-2.50 (br s, 100H, $NHCH_2CH_2N$ of DIPEA side chain), 2.68 (t, 2H, SCH_2CH_2COO of end group), 2.78 (br m, 2H, SCH_2CH_2COO of end group), 2.90-3.20 (br m, 200H, $NHCH_2CH_2N$ and $N(CH(CH_3)_2)_2$ of DIPEA side chain), 3.50-3.62 (br s, 63H, OCH_3 of PMA side chain), 4.55 (m, 2H,

COOC*H*$_2$CH$_2$N of end group), 7.10-7.30 (m, 5H, Ar*H* of end group). ^{13}C NMR (125 MHz, MeOD): δ (ppm): 21.2, 35.9, 42.2, 42.8, 46.0, 50.8, 52.5, 127.4, 128.2, 129.6, 176.6, 176.9. FTIR υ_{max}/ cm^{-1}: 3304 (N-H amide stretch), 2966 (alkane C-H stretch), 1737 (C=O ester stretch), 1646 (C=O amide stretch), 1533 (N-H amide bend), 1383 and 1185 (C-N stretch).

Polymer 3.09, M_n (^{1}H NMR) = 10.4 kDa, M_n (DMF SEC) = 14.9 kDa, $Đ_M$ = 1.11. ^{1}H NMR (400 MHz, $CDCl_3$): δ (ppm): 0.90-1.10 (br s, 500H, N(CH(C*H*$_3$)$_2$)$_2$ of DIPEA side chain) 1.20 -2.40 (br m, 210H, C*H*C*H*$_2$ of polymer backbone), 2.40-2.50 (br s, 100H, NHCH$_2$C*H*$_2$N of DIPEA side chain), 2.75 (m, 4H, SC*H*$_2$C*H*$_2$COO of end group), 2.90-3.20 (br m, 200H, NHCH$_2$C*H*$_2$N and N(CH(C*H*$_3$)$_2$)$_2$ of DIPEA side chain), 3.39 (br s, 3H, OC*H*$_3$ of end group), 3.47-3.56 (m, 8H, (OC*H*$_2$C*H*$_2$O)$_2$ of end group), 3.60-3.69 (br s, 63H, OC*H*$_3$ of PMA side chain), 3.69-3.72 (m, 2H, COOCH$_2$C*H*$_2$O of end group), 4.20-4.27 (m, 2H, COOC*H*$_2$CH$_2$O of end group), 7.10-7.30 (m, 5H, Ar*H* of end group). ^{13}C NMR (125 MHz, $CDCl_3$): δ (ppm): 14.1, 20.8, 21.3, 23.1, 29.3, 29.6, 31.9, 32.1, 34.9, 35.1, 40.0, 41.3, 42.7., 44.3, 45.3, 48.7, 51.7, 59.0, 63.8, 69.0, 69.1, 70.6, 71.9, 126.2, 126.9, 127.0, 128.4, 174.9. FTIR υ_{max}/ cm^{-1}: 3295 (N-H amide stretch), 2965 alkane (C-H stretch), 1737 (C=O ester stretch), 1647 (C=O amide stretch), 1535 (N-H amide bend), 1361 and 1185 (C-N stretch).

3.4.7 Self-Assembly techniques

3.4.7.1 Solvent Switch

A general procedure for solvent switch is given. The polymer was dissolved in DMF to a concentration double of the target concentration and stirred overnight. The same volume of 18.2 MΩ cm^{-1} water was added at 0.6 mL min^{-1}, after which the opaque solution was dialysed against 18.2 MΩ cm^{-1} water, incorporating at least 6 water changes. The final concentration of the self-assembled solution was calculated by measuring the final volume.

3.4.7.2 Direct Dissolution

The polymer was dissolved in acidic water (below pH 2.5) was stirred overnight. The reversibility of the responsive behaviour was tested by adjusting the pH until the solution became slightly pearlescent and then stirring to allow the particles to stabilise.

3.4.8 Release studies

The polymer was dissolved in DMF at a concentration double that desired, after which Rhodamine B was added at the stated concentration and the solution was stirred overnight. 18.2 MΩ cm^{-1} water was added at a speed of 0.6 mL min^{-1}. After addition the solution was dialysed against either 500 mL or 200 mL of 18.2 MΩ cm^{-1}. After leaving for at least 6 hours to allow the system to equilibrate, the dialysis water was tested for fluorescence at an excitation wavelength of 550 nm and the emission at 575 nm recorded. After two water changes where the system showed no fluorescence the solution was removed from the dialysis bag, the pH dropped to approximately 2.5 and then dialysed again. Again, the system was left to reach equilibrium and each time the water was changed and the fluorescence recorded.

3.5 References

1. A. Blanazs, S. P. Armes and A. J. Ryan, *Macromol. Rapid Commun.*, 2009, 30, 267-277.
2. G. Riess, *Prog. Polym. Sci.*, 2003, 28, 1107-1170.
3. Y. Mai and A. Eisenberg, *Macromolecules*, 2011, 44, 3179-3183.
4. N. Petzetakis, A. P. Dove and R. K. O'Reilly, *Chem. Sci.*, 2011, 2, 955-960.
5. F. Chécot, S. Lecommandoux, Y. Gnanou and H.-A. Klok, *Angew. Chem. Int. Ed.*, 2002, 41, 1339-1343.
6. F. Meng, Z. Zhong and J. Feijen, *Biomacromolecules*, 2009, 10, 197-209.
7. D. J. Adams, C. Kitchen, S. Adams, S. Furzeland, D. Atkins, P. Schuetz, C. M. Fernyhough, N. Tzokova, A. J. Ryan and M. F. Butler, *Soft Matter*, 2009, 5, 3086-3096.
8. Z. Li, M. A. Hillmyer and T. P. Lodge, *Macromolecules*, 2005, 39, 765-771.
9. R. Erhardt, A. Böker, H. Zettl, H. Kaya, W. Pyckhout-Hintzen, G. Krausch, V. Abetz and A. H. E. Müller, *Macromolecules*, 2001, 34, 1069-1075.
10. I. K. Voets, A. de Keizer, P. de Waard, P. M. Frederik, P. H. H. Bomans, H. Schmalz, A. Walther, S. M. King, F. A. M. Leermakers and M. A. Cohen Stuart, *Angew. Chem. Int. Ed.*, 2006, 45, 6673-6676.
11. R. B. Grubbs and Z. Sun, *Chem. Soc. Rev.*, 2013, 42, 7436-7445.
12. M. I. Gibson and R. K. O'Reilly, *Chem. Soc. Rev.*, 2013, 42, 7204-7213.
13. R. Liu, M. Fraylich and B. Saunders, *Colloid. Polym. Sci.*, 2009, 287, 627-643.
14. D. Roy, W. L. A. Brooks and B. S. Sumerlin, *Chem. Soc. Rev.*, 2013, 42, 7214-7243.
15. F. D. Jochum and P. Theato, *Chem. Soc. Rev.*, 2013, 42, 7468-7483.
16. S. Dai, P. Ravi and K. C. Tam, *Soft Matter*, 2008, 4, 435-449.
17. D. Schmaljohann, *Adv. Drug Deliver. Rev.*, 2006, 58, 1655-1670.
18. S. Dai, P. Ravi and K. C. Tam, *Soft Matter*, 2009, 5, 2513-2533.
19. T. He, F. Di Lena, K. C. Neo and C. L. L. Chai, *Soft Matter*, 2011, 7, 3358-3365.
20. W. A. Braunecker and K. Matyjaszewski, *Prog. Polym. Sci.*, 2007, 32, 93-146.
21. C. J. Hawker, A. W. Bosman and E. Harth, *Chem. Rev.*, 2001, 101, 3661-3688.
22. G. Moad, E. Rizzardo and S. Thang, *Acc. Chem. Res.*, 2008, 41, 1133-1142.
23. P. Theato and H.-A. Klok, eds., *Functional Polymers by Post-Polymerization Modification. Concepts, Guidelines, and Applications*, Wiley-VCH, Weinhelm, 2012.
24. M. Eberhardt, R. Mruk, R. Zentel and P. Theato, *Eur. Polym. J.*, 2005, 41, 1569-1575.

25. F. D. Jochum and P. Theato, *Macromolecules*, 2009, 42, 5941-5945.
26. M. Eberhardt and P. Théato, *Macromol. Rapid Commun.*, 2005, 26, 1488-1493.
27. P. Theato, *J. Polym. Sci., Part A: Polym. Chem.*, 2008, 46, 6677-6687.
28. J. Seo, P. Schattling, T. Lang, F. Jochum, K. Nilles, P. Theato and K. Char, *Langmuir*, 2009, 26, 1830-1836.
29. K. Nilles and P. Theato, *J. Polym. Sci., Part A: Polym. Chem.*, 2010, 48, 3683-3692.
30. J. Skey and R. K. O'Reilly, *Chem. Commun.*, 2008, 2008, 4183-4185.
31. T. R. Wilks, J. Bath, J. W. de Vries, J. E. Raymond, A. Herrmann, A. J. Turberfield and R. K. O'Reilly, *ACS Nano*, 2013, 7, 8561-8572.
32. A. O. Moughton, J. P. Patterson and R. K. O'Reilly, *Chem. Commun.*, 2011, 47, 355-357.
33. H. Willcock and R. K. O'Reilly, *Polym. Chem.*, 2010, 1, 149-157.
34. C. Boyer, A. Granville, T. P. Davis and V. Bulmus, *J. Polym. Sci., Part A: Polym. Chem.*, 2009, 47, 3773-3794.
35. J. M. Spruell, B. A. Levy, A. Sutherland, W. R. Dichtel, J. Y. Cheng, J. F. Stoddart and A. Nelson, *J. Polym. Sci., Part A: Polym. Chem.*, 2009, 47, 346-356.
36. K. A. Günay, P. Theato and H. A. Klok, *J. Polym. Sci., Part A: Polym. Chem.*, 2013, 51, 1-28.
37. C. Boyer and T. P. Davis, *Chem. Commun.*, 2009, 6029-6031.
38. J. P. Salvage, S. F. Rose, G. J. Phillips, G. W. Hanlon, A. W. Lloyd, I. Y. Ma, S. P. Armes, N. C. Billingham and A. L. Lewis, *J. Controlled Release*, 2005, 104, 259-270.
39. X. Bories-Azeau, S. P. Armes and H. J. W. van den Haak, *Macromolecules*, 2004, 37, 2348-2352.
40. V. Bütün, S. P. Armes and N. C. Billingham, *Polymer*, 2001, 42, 5993-6008.
41. E. S. Read, K. L. Thompson and S. P. Armes, *Polym. Chem.*, 2010, 1, 221-230.
42. F. C. Giacomelli, P. Stepanek, C. Giacomelli, V. Schmidt, E. Jager, A. Jager and K. Ulbrich, *Soft Matter*, 2011, 7, 9316-9325.
43. X. Xu, A. E. Smith, S. E. Kirkland and C. L. McCormick, *Macromolecules*, 2008, 41, 8429-8435.
44. L. He, E. S. Read, S. P. Armes and D. J. Adams, *Macromolecules*, 2007, 40, 4429-4438.
45. Y. Q. Hu, M. S. Kim, B. S. Kim and D. S. Lee, *Polymer*, 2007, 48, 3437-3443.
46. J. Du, Y. Tang, A. L. Lewis and S. P. Armes, *J. Am. Chem. Soc.*, 2005, 127, 17982-17983.
47. M. P. Robin, M. W. Jones, D. M. Haddleton and R. K. O'Reilly, *ACS Macro Lett.*, 2011, 1, 222-226.

48. A. Lu, T. P. Smart, T. H. Epps, D. A. Longbottom and R. K. O'Reilly, *Macromolecules*, 2011, 44, 7233-7241.

49. J.-H. Ryu, R. Roy, J. Ventura and S. Thayumanavan, *Langmuir*, 2010, 26, 7086-7092.

Chapter Four

Synthesis of sulfobetaine methacrylate containing block copolymers by RAFT polymerisation

4.1 Introduction

Polymeric betaines are a class of zwitterionic polymers in which the cationic and anionic functional groups are located on the same monomer unit.[1] Since their discovery in the 1950's these polymers are known to be salt responsive and are often insoluble in pure water at room temperature but become soluble upon addition of salt.[1-5] Betaines can also be categorised further into phosphobetaines[6], carboxybetaines[7] and sulfobetaines[5], which differ in the chemical nature of the groups that form the cationic and anionic functionalities.

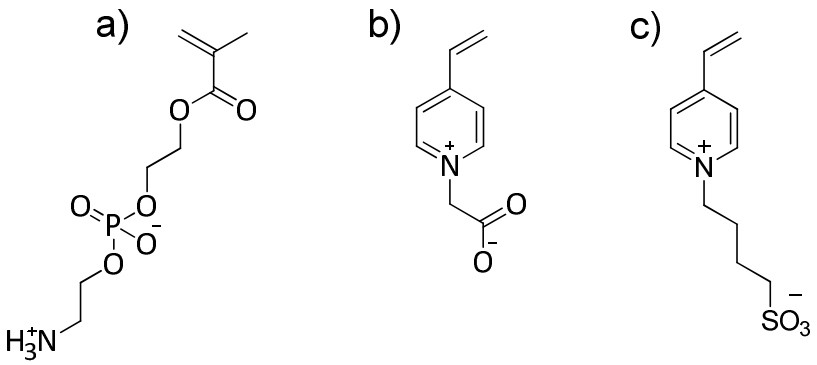

Figure 4.1: The first examples of a) phosphobetaine[6], b) carboxybetaine[7] c) sulfobetaine[5]

Sulfo- and phosphobetaines have been shown to be biocompatible[8-12] and have also been shown to reduce bacterial adhesion and protein fouling.[9] In the first report detailing the synthesis of polysulfobetaines it is mentioned that the butyl sulfobetaine of poly(4-vinypyridine) (c, shown in Figure 4.1) is insoluble in water across the entire pH range but becomes soluble upon the addition of salts, such as NaCl.[5]

Polymeric sulfobetaines are generally synthesised in two ways. Either the sulfobetaine monomer can be directly polymerised, or the corresponding tertiary amino-methacrylate monomer can be polymerised and the sulfonate group introduced post polymerisation by reaction with 1, 3-propane sultone.[13-16] One advantage of the second route is that the polymer before modification is soluble in organic solvents and this can facilitate the synthesis of block copolymers, for example. Additionally, the betainisation reaction is simple and quantitative. A disadvantage of this route is that the chemical required to modify the polymer chain, 1,3-propane sultone, is extremely toxic.

Armes and coworkers have exploited this method to synthesise homo-and block copolymers containing polysulfobetaines.[13-17] They have also shown the betainisation reaction to be selective.[13] Block copolymers consisting of DMAEMA and a related tertiary amine methacrylate, either 2-(diethylamino) ethyl methacrylate (DEAEMA), 2-(diisopropylamino) ethyl methacrylate (DIPEMA) or 2-(*N*-morpholino)ethyl methacrylate (MEMA), were synthesised by group transfer polymerisation (GTP). All polymers were shown to have narrow dispersity ($Đ_M \leq 1.15$). The polymers were then betainised by reacting with 1,3-propane sultone in THF at 25 °C. By keeping reaction times to between 16 and 24 hours they were able to selectively betainise only the DMAEMA group in each block copolymer.

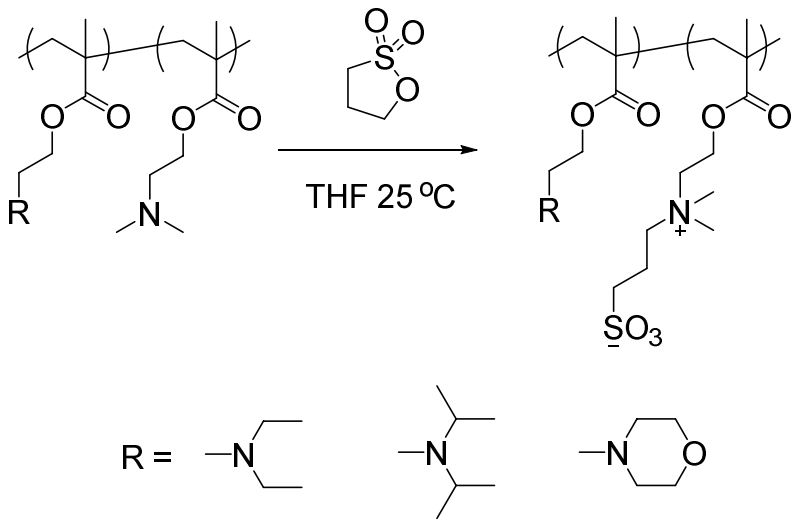

Scheme 4.1: Scheme showing the selective betainisation of DMAEMA residues in tertiary amine block copolymers[13]

The DEAEMA and MEMA blocks would undergo betainisation if the reaction was allowed to proceed for 48 – 72 hours or if the reaction proceeded under reflux. The DPAEMA blocks remained unreacted after 96 hours of refluxing in THF. The DMAEMA blocks were shown to be at least 88% betainised by elemental microanalysis. The betainised DMAEMA-*b*-DEAEMA and betainised DMAEMA-*b*-DPAEMA block copolymers underwent self-assembly in water to form micelles with a D_h *ca*. 20 nm. The addition of acid to solutions of these micelles caused dissolution to unimers. The betainised DMAEMA-*b*-MEMA block copolymer formed micelles when heated to 70 °C.[13]

Recently Roth and coworkers have described the post-polymerisation modification of an activated ester precursor polymer.[18] A homopolymer of pentafluorophenyl acrylate (PFPA) was synthesised by RAFT polymerisation ($Đ_M$ = 1.40) and then a sulfobetaine containing primary amine was used to substitute the PFP groups. Propylene carbonate was employed as a solvent due to hydrolysis of the PFP groups in water and the limited solubility of the sulfobetaine primary amine. The dispersity of the sulfobetaine polymer remained unchanged after substitution. Copolymers containing sulfobetaine and various hydrophobic groups were also synthesised by the addition of both the sulfobetaine amine and either pentylamine or benzylamine.

Betaine monomers have been shown to be polymerisable by RAFT, both as homopolymers and as block copolymers.[2, 15, 16, 19-23] The advantage of directly polymerising the monomer is that the polymerisation can be carried out in salt solution, avoiding the use of organic solvents and eliminating the need to use toxic 1,3-propane sultone.

Although the synthesis of homopolymers and diblock copolymers has been demonstrated several times, there are limited examples of triblock copolymers containing sulfobetaines in which the betaine block is directly polymerised, rather than formed from the post-polymerisation modification with a 1,3-propane sultone. Donovan *et al.* investigated the synthesis of di- and tri-block copolymers containing sulfobetaines using RAFT polymerisation. Linear dimethylacrylamide (DMA) homopolymers were synthesised bearing dithioester functionality at either just the ω-end or at both the α- and ω-ends (see Figure 4.2). These linear homopolymers were then used as macroCTAs in a chain extension with a methylacrylamido sulfobetaine, 3-[2-(*N*-methylacrylamido)-ethyldimethylammonio] propane sulfonate (MAEDAPS).[19]

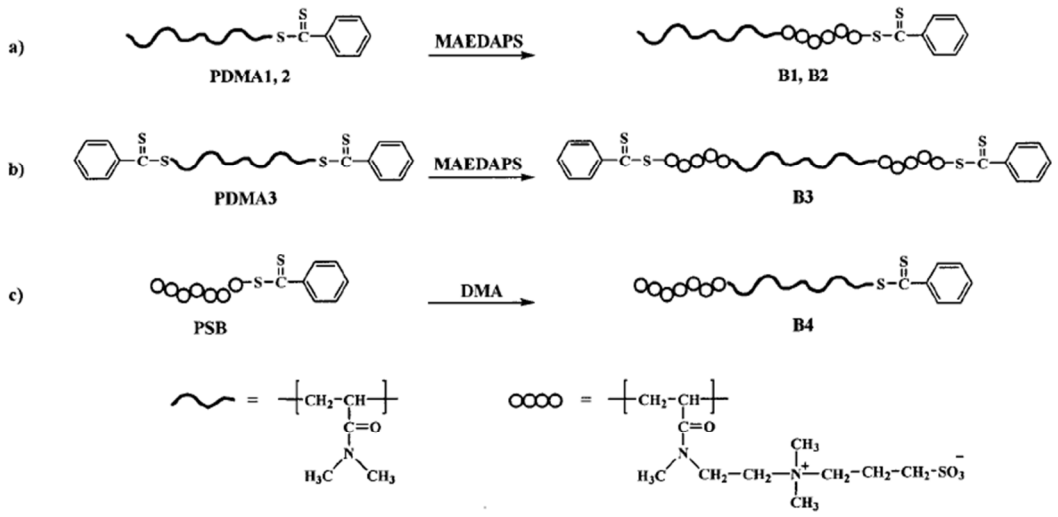

Figure 4.2: Examples of di- and triblock copolymers synthesised by Donovan *et al*[19]

Although these polymers were synthesised by RAFT polymerisation, the dispersities of the blocks formed were rather broad, with the diblocks displaying dispersities between 1.34 and 1.41 when analysed by SEC in 80/20 *v/v* 0.5 M NaBr solution and acetonitrile. The triblock polymer had a large dispersity of 1.81.[19]

The majority of sulfobetaine containing block copolymers, synthesised by the direct polymerisation of the betaine monomer, contain a hydrophilic block. Examples of sulfobetaine block copolymers include polymerisation with *N*-(morpholino)ethyl methacrylate,[20, 24] *N*-isopropylacrylamide,[21] and *N, N*-dimethylacrylamide[19]. The synthesis of sulfobetaine block copolymers containing a hydrophobic block is synthetically more challenging because of the limited solubility of sulfobetaine polymers in organic solvents.[25] To the best of our knowledge there are no reported examples of block copolymers containing a hydrophobic block and sulfobetaine block synthesised by RAFT polymerisation, without the use of post-polymerisation betainisation reactions. These polymers are of interest due to the thermo-responsive properties of the sulfobetaine block and therefore potentially interesting self-assembly behaviour of the block copolymers.

4.3 Results and Discussion

Sulfobetaines are an interesting class of polymers as some have been shown to display UCST cloud points.[18, 26-29] In order to explore the thermo-responsive behaviour of polysulfobetaines when incorporated in self-assembled structures a collection of sulfobetaine containing block copolymers were synthesised by RAFT polymerisation. A methacrylate sulfobetaine, 2-(methacryloyloxy)ethyl dimethyl-(3-sulfopropyl)ammonium hydroxide (DMAPS), was chosen as the cloud points at various molecular weights have previously been reported,[22] but its incorporation into block copolymers remains largely unexplored. Here, this monomer was incorporated into block copolymers with either permanently hydrophilic fractions, permanently hydrophobic fractions, or both. The synthesis of a triply-responsive sulfobetaine containing block copolymer is also reported. The self-assembly and responsive behaviour of these polymers are the subject of Chapter Five.

4.3.1 Synthesis of hydrophilic PEGMA homopolymer, 4.01

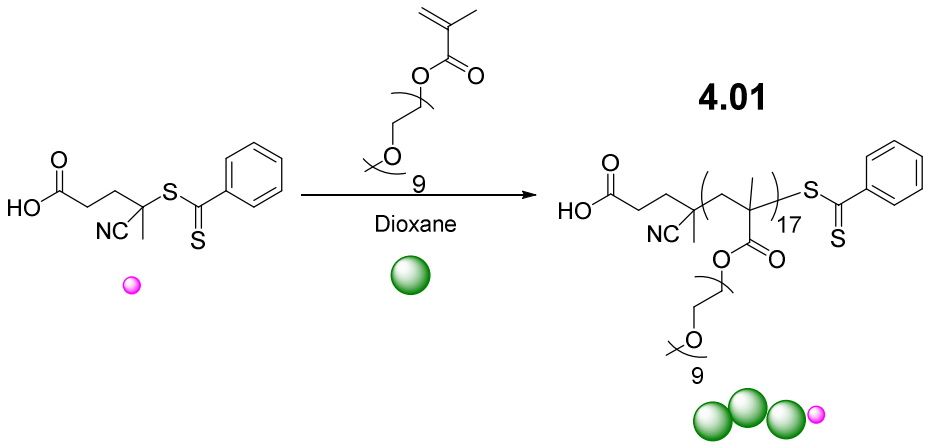

Scheme 4.2: The homopolymerisation of the PEGMA with CPTA to form 4.01

The first step was to synthesise the permanently hydrophilic block (see Scheme 4.2). For this the monomer polyethylene glycol monomethyl ether methacrylate (PEGMA) was chosen as it is often used as a hydrophilic block and is likely to be unaffected by the addition of salt. The polymerisation was carried out in 1,4-dioxane using 4-cyano-4-(phenylcarbonothioylthio) pentanoic acid (CPTA) as the chain transfer agent. The polymer was purified by dialysis and collected by lyophilisation to give the hydrophilic

homopolymer **4.01** as a yellow oil, M_n (^{1}H NMR) = 8.2 kDa, M_n (DMF SEC) = 10.1 kDa, $Đ_M$ = 1.08. Analysis by ^{1}H NMR spectroscopy (see Figure 4.3) gave a degree of polymerisation of 17 by comparison of the signal **a** at 2.49 ppm (from the CH_2 next to the carboxylic acid functionality on the chain transfer agent) to the polymer peaks at 3.4, 3.7 and 4.2 ppm (see Figure 4.3). The peaks **j**, **m** and **k** from the aromatic ring can be clearly seen at 7.60, 7.77 and 8.01 ppm showing that the dithiobenzoate functionality has been retained. The narrow dispersity seen in the SEC shows that the polymerisation proceeded with good control. In order to check that the polymer remains hydrophilic over the temperature range required the absorbance of the solution at 500 nm was measured between 6 and 70 °C and no cloud point was observed, indicating that it remains hydrophilic across this temperature range.

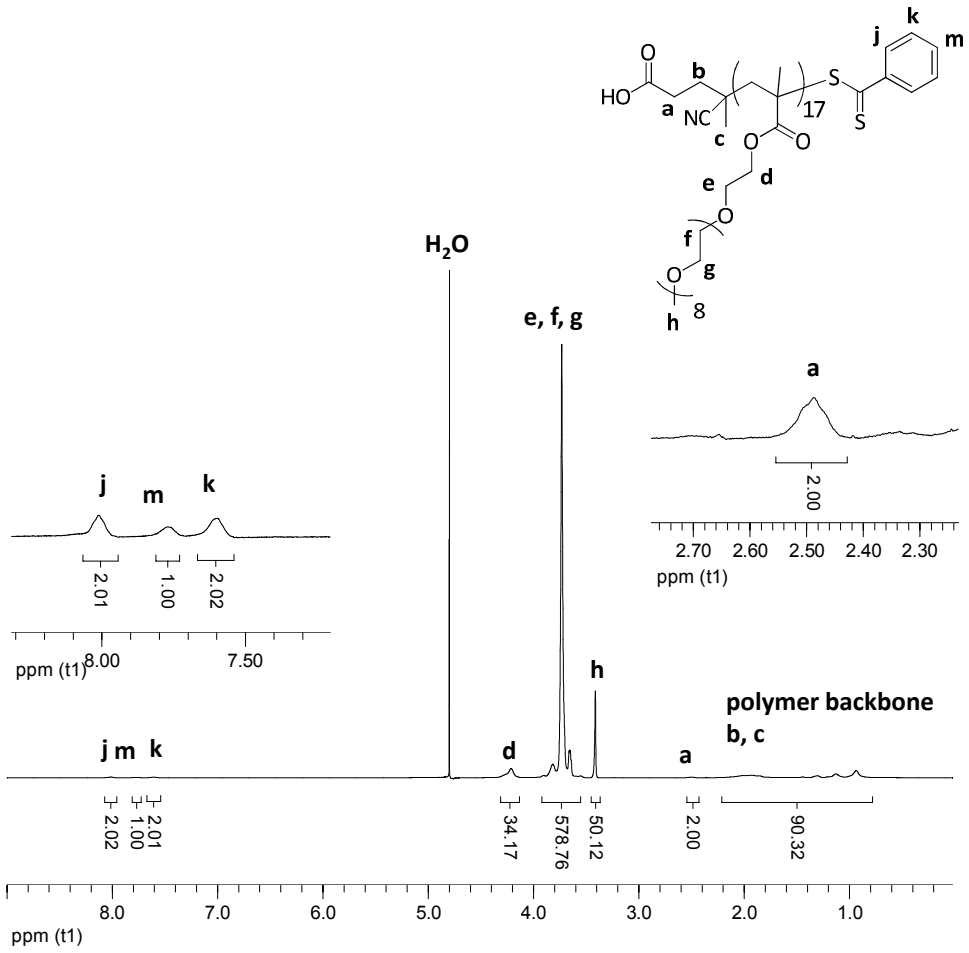

Figure 4.3: ^{1}H NMR spectrum with assignment for the hydrophilic homopolymer 4.01 in D_2O, recorded at 25 °C and 400 MHz

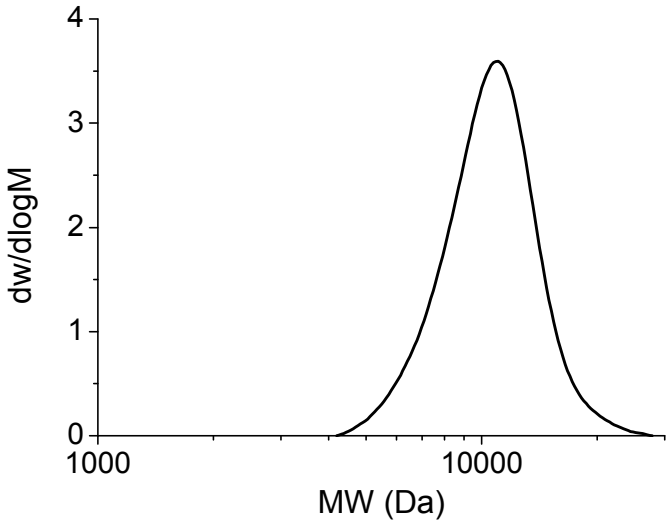

Figure 4.4: DMF SEC chromatogram of homopolymer 4.01

4.3.2 Synthesis of PEGMA-*b*-DMAPS diblock copolymer, 4.02

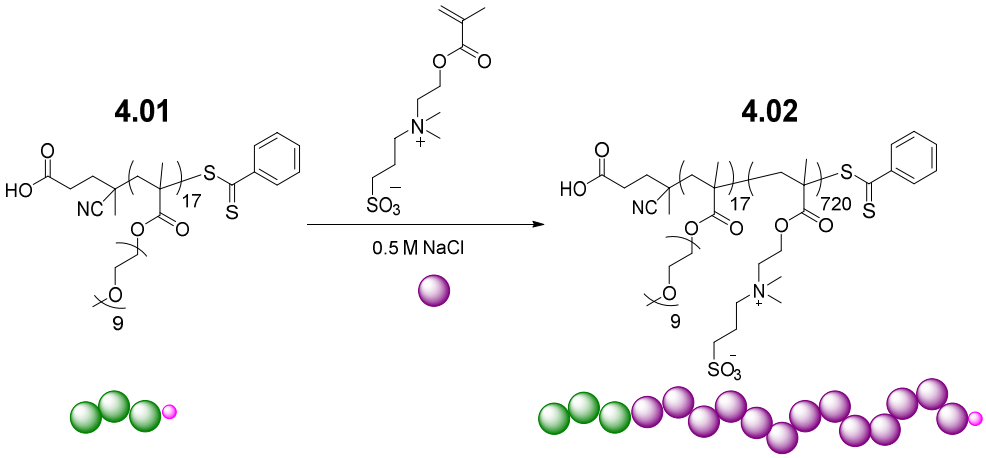

Scheme 4.3: Synthetic route to the diblock copolymer 4.02

The hydrophilic homopolymer **4.01** was chain extended with DMAPS in order to form the responsive diblock copolymer **4.02** (see Scheme 4.3).The chain extension of the homopolymer **4.01** with the sulfobetaine monomer, DMAPS was carried out in 0.5 M NaCl solution in order to fully solubilise both the betaine monomer and the resulting polymer.[3, 28] The polymer was purified by dialysis, and lyophilisation yielded the diblock copolymer **4.02** as a pale pink solid, M_n (^{1}H NMR) = 209 kDa, M_n (Aqueous SEC) = 106.4 kDa, $Đ_M$ = 1.16. The discrepancy between the M_n calculated by ^{1}H NMR spectroscopy and the M_n calculated by aqueous SEC is a result of the difference in the D_h of the diblock, **4.02**, and of the linear

PEO standards used to calibrate the aqueous SEC as a result of the difference in functionality of the two polymers. The length of the DMAPS block was calculated by comparison of the PEG groups (**d**, **e**, **f**) with the new signals at 2.4 (**m**), 3.1 (**n**) and 3.4 (**j**) ppm (see Figure 4.5). The degree of polymerisation was determined to be 720, which compares well with that predicted by conversion ^{1}H NMR spectroscopy. The dispersity of 1.16 observed in aqueous SEC is within the range found in the literature of examples of DMAPS being polymerised by RAFT[2, 23, 30, 31] and shows that the polymerisation proceeded with good control (Figure 4.6).

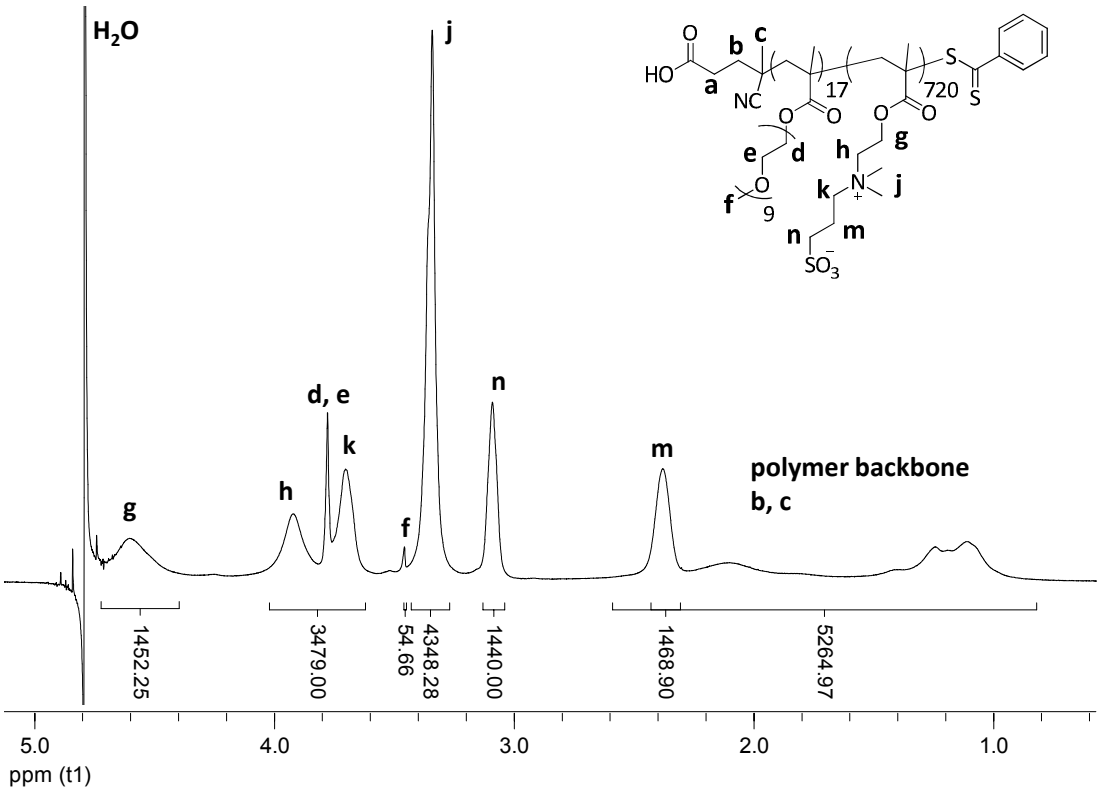

Figure 4.5: ^{1}H NMR spectrum of 4.02 in 0.5 M NaCl in D_2O, recorded at 25 °C and 400 MHz

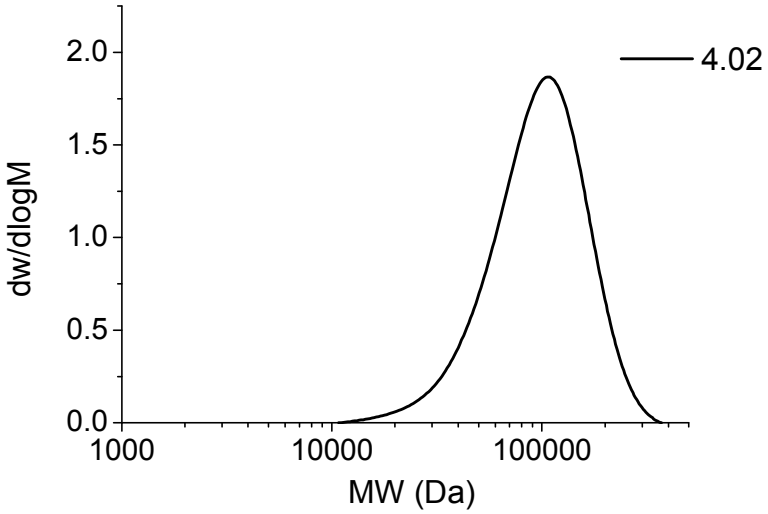

Figure 4.6: Aqueous SEC chromatogram of thermo-responsive diblock 4.02

4.3.3 Synthesis of PEGMA-*b*-DMAPS-*b*-PEGMA triblocks

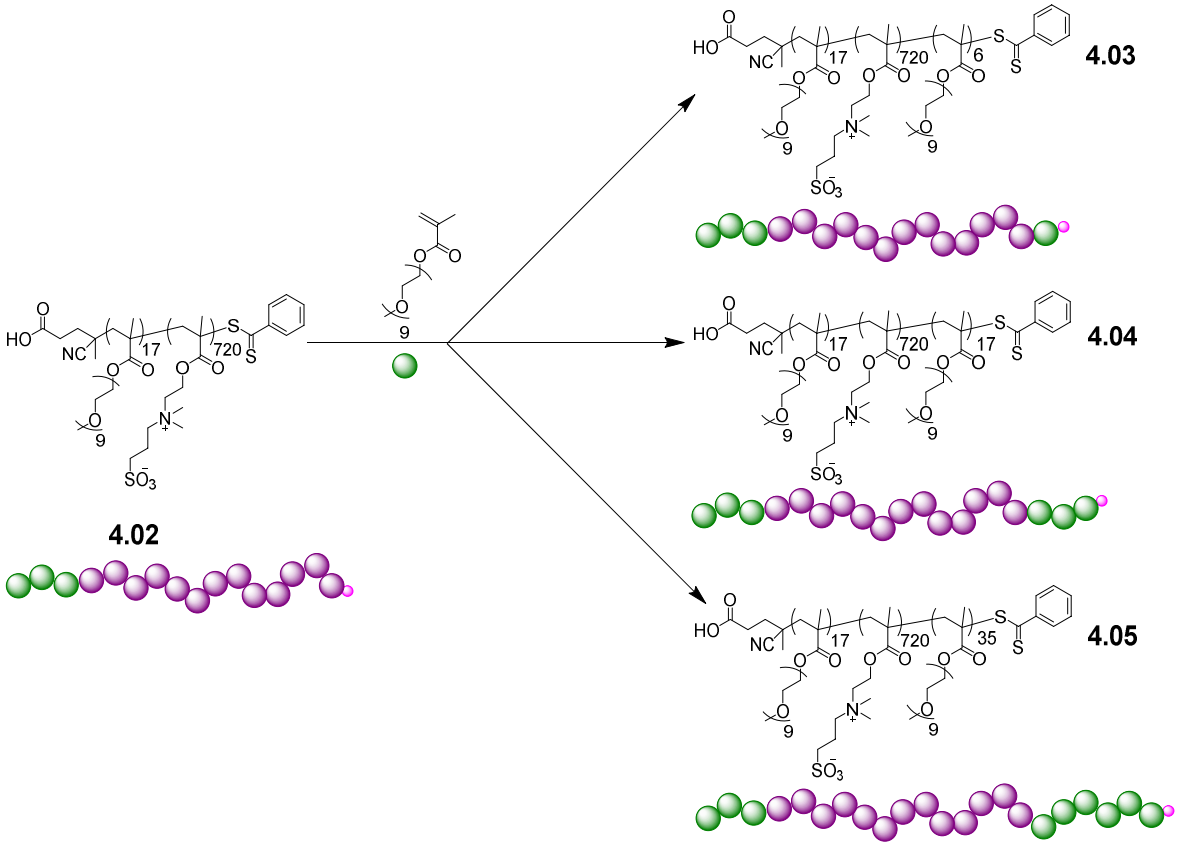

Scheme 4.4: Schematic showing the chain extension of diblock copolymer 4.02 to the ABA triblock copolymers 4.03, 4.04 and 4.05

Diblock copolymer **4.02** was chain extended with varying amounts of PEGMA in order to synthesise a series of triblock copolymers that differ only in the length of the third block. The polymerisations were again carried out in 0.5 M NaCl solution and the polymers purified after polymerisation by exhaustive dialysis against water. The dialysis tubing used had a molecular weight cut off of 12 – 14 kDa, which would have allowed any short homopolymers of PEGMA produced to be removed. The ABA triblock copolymers were recovered by lyophilisation to yield **4.03**, **4.04** and **4.05**.

4.03 (M_n (^{1}H NMR) = 211.9 kDa, M_n (Aqueous SEC) = 103.8 kDa, $Đ_M$ = 1.18) was determined to have a third block of 6 PEGMA units by comparing the integration of the peaks at 3.6 – 4.1 ppm before and after chain extension. These peaks correspond to 4H of the DMAPS side chain (**h** and **k**) and also to the signals from both PEG blocks (see Figure

4.7). Keeping the integration of peak **n** the same between **4.02** and **4.03** and subtracting the contribution from the DMAPS and the initial PEG block (**d** and **e**) the length of the third block can be calculated. Analysis by aqueous SEC gives $Đ_M$ = 1.18, which is significantly lower than that reported by Donovan *et al*. for sulfobetaine containing triblock copolymers.[19]

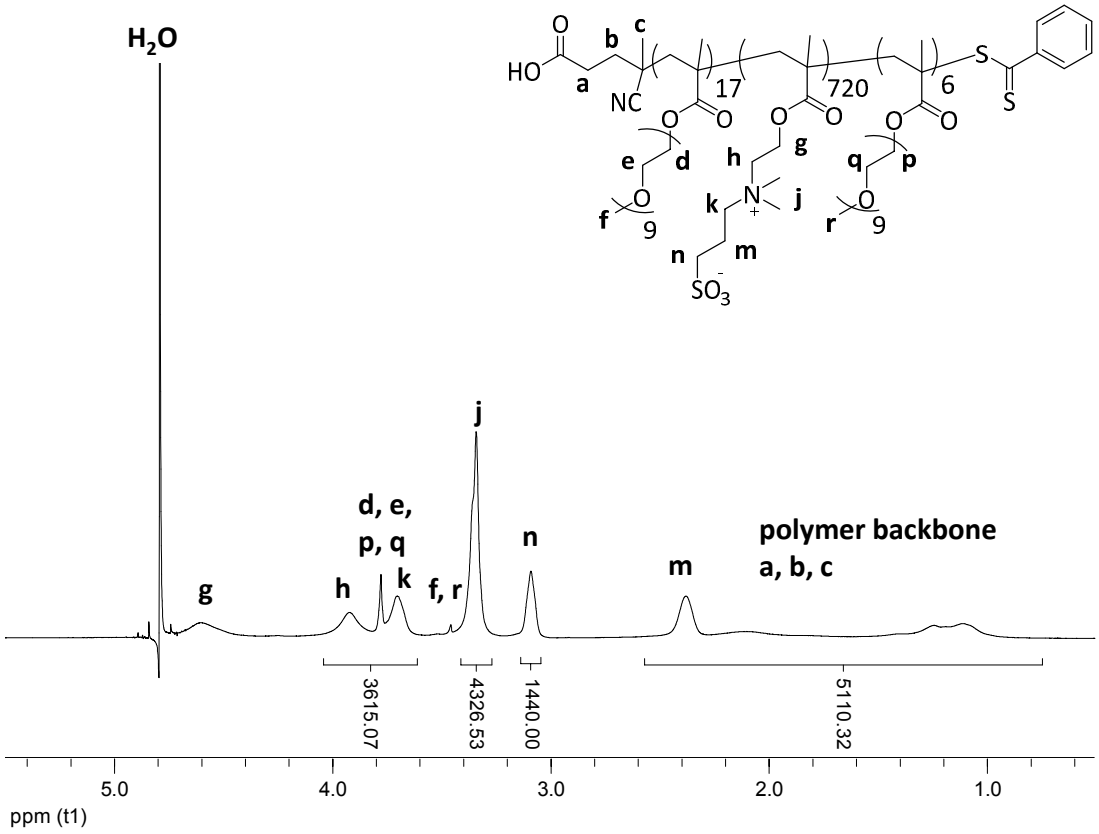

Figure 4.7: ^{1}H NMR spectrum of triblock copolymer 4.03 in 0.5 M NaCl in D_2O, with peaks assigned, recorded at 25 °C and 400 MHz

4.04 (M_n (^{1}H NMR) = 217.2 kDa, M_n (Aqueous SEC) = 101.2 kDa, $Đ_M$ = 1.20) was determined to have a third block length of 17 in the same way as for **4.03**, making it a completely symmetrical ABA triblock.

4.05 (M_n (^{1}H NMR) = 225.8 kDa, M_n (Aqueous SEC) = 95.2 kDa, $Đ_M$ = 1.22) was determined to have a third block length of 35 from analysis of the ^{1}H NMR spectrum in the same manner as described for **4.03** and **4.04**.

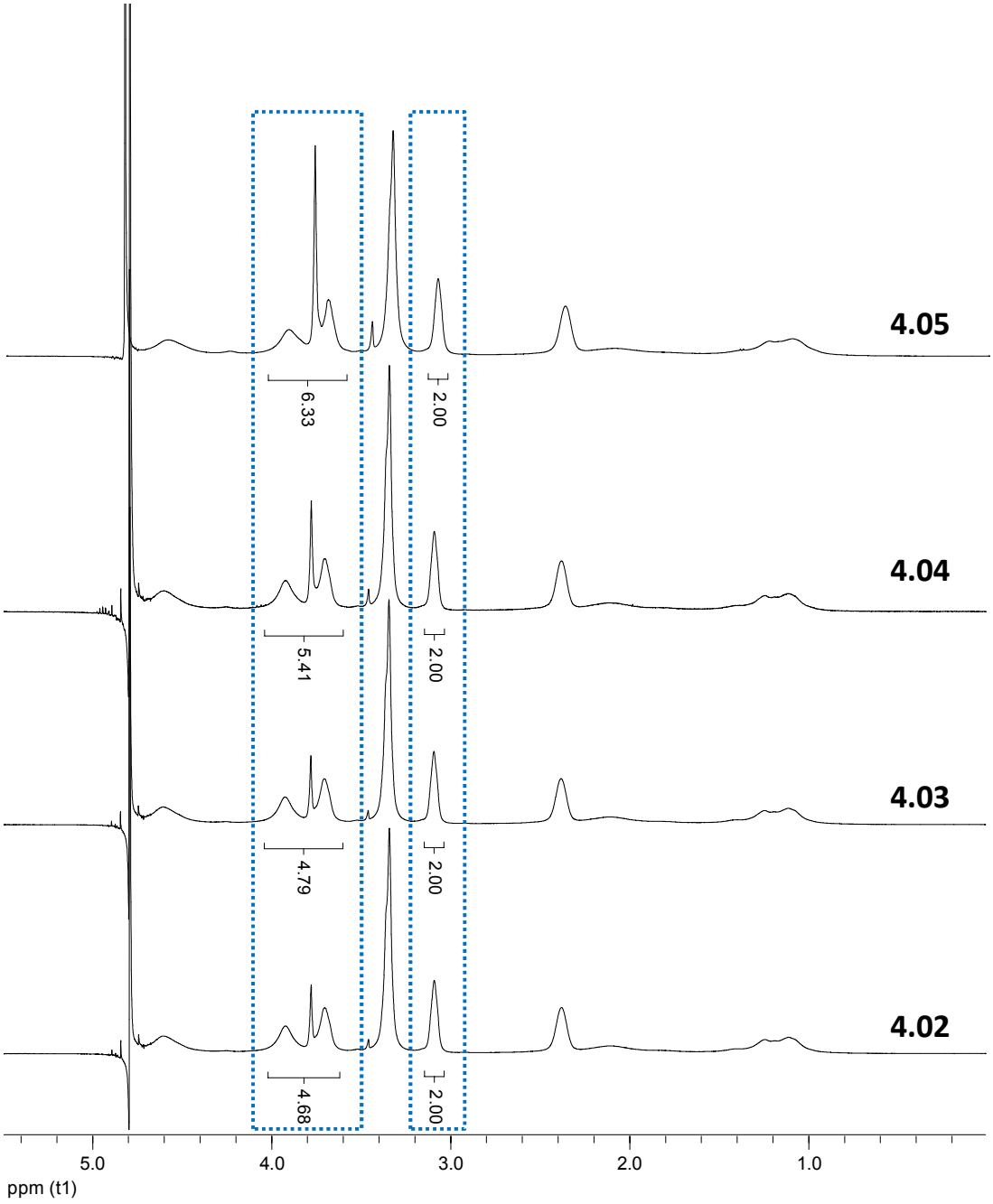

Figure 4.8: ^{1}H NMR spectra of 4.02, 4.03, 4.04 and 4.05 in 0.5 M NaCl in D_2O showing the increase of the integration of the PEG block. The areas used to calculate the DP of the PEG block are highlighted. Spectra were recorded at 25 °C and 400 MHz

Comparison of the aqueous SEC chromatograms shows small shifts to longer retention times as the block length of the PEGMA increases (see Figure 4.9). This is unexpected as a longer retention time usually relates to a lower molecular weight. Therefore the apparent molecular weight of the triblocks from SEC analysis decreases as the length of the third block is

increased, as can be seen by the increase of the M_n calculated by ^{1}H NMR spectroscopy and the decrease of the M_n calculated from aqueous SEC (see Table 4.1).

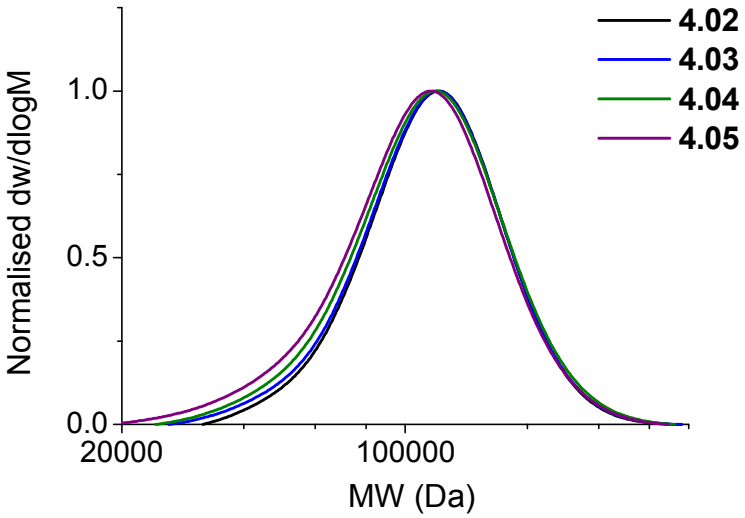

Figure 4.9: Aqueous SEC chromatograms showing the increase in tailing and slight shift to a lower apparent molecular weight as the length of the third block increases

Table 4.1: Molecular weight data for diblock copolymer 4.02 and the triblock copolymers 4.03, 4.04 and 4.05

Polymer	M_n (^{1}H NMR) (kDa)	M_n (Aqueous SEC) (kDa)	$Đ_M$
4.02	209.0	106.4	1.16
4.03	211.9	103.8	1.18
4.04	217.2	101.2	1.20
4.05	225.8	95.2	1.22

There is no free PEGMA homopolymer observed in the SEC chromatograms. Therefore this shift to an apparent lower molecular weight upon chain extension could be a consequence of the PEGMA blocks interacting more with the SEC column than the DMAPS block. This explains why as the PEGMA fraction of the polymer increases the shift is more noticeable. The slight increase in tailing with the increase in PEGMA block length, as shown in the

small increase in dispersity from **4.03** to **4.05**, also suggests increased interactions with the aqueous SEC columns.

4.3.4 Calculation of *dn/dc* for the di- and triblock copolymers

The refractive index increment (*dn/dc*) was determined using a Shodex RI-101 deflection refractometer. A range of concentrations of polymer in 0.5 M NaCl solution from 0.5 mg mL^{-1} to 2 mg mL^{-1} were measured. The refractive index response for each concentration was plotted against the concentration and the *dn/dc* calculated using the following equation.

$$\frac{dn}{dc} = \frac{slope \times n^o}{K}$$

Where the slope is the gradient of the linear fit of the refractive index response *vs* the concentration, n^o is the refractive index of the solvent and *K* is the instrument constant. The *dn/dc* calculated for diblock copolymer **4.02** in 0.5 M NaCl was 0.13 mLg^{-1}.

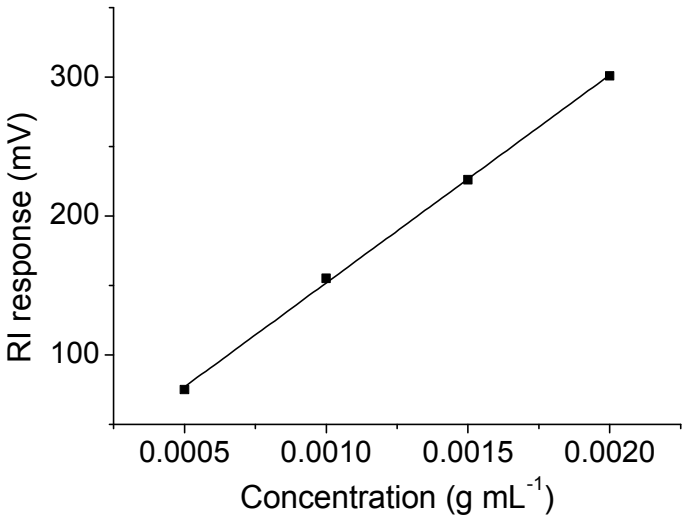

Figure 4.10: Plot of concentration *vs* RI response for 4.02. The *dn/dc* was calculated as 0.130 mL g^{-1} using the slope of the linear fit

The *dn/dc* was also calculated for triblock copolymers **4.03**, **4.04** and **4.05** in 0.5 M NaCl solution using the method described above. The calculated *dn/dc* values for the triblock copolymers are all very similar and are displayed in Table 4.2.

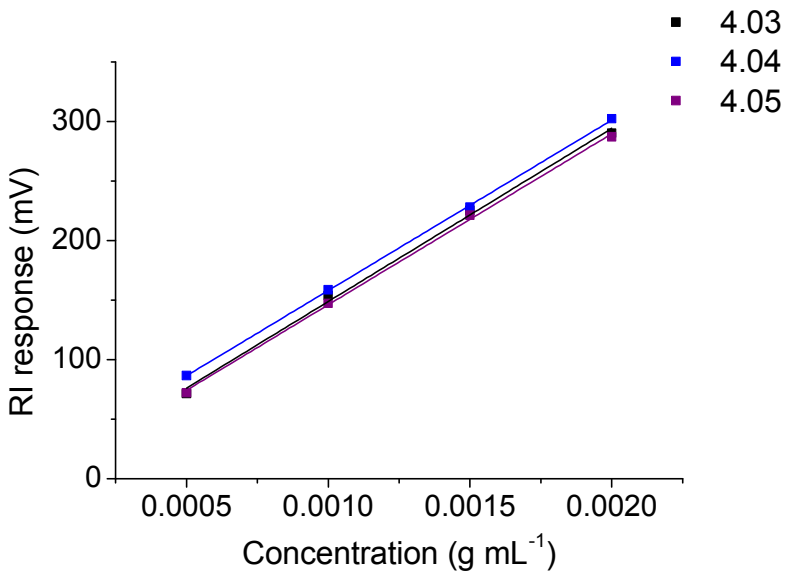

Figure 4.11: Plot of concentration *vs* RI response for 4.03.4.04 and 4.05. The *dn/dc* for each concentration was calculated using the slope of the linear fit

Table 4.2: Calculated *dn/dc* values for triblock copolymers 4.03, 4.04 and 4.05 in 0.5 M NaCl solution

Polymer	*dn/dc (mL g^{-1})*
4.03	0.126
4.04	0.124
4.05	0.125

4.3.5 Analysis of the di- and triblock copolymers by SLS

In order to obtain the absolute molecular weight the di- and triblock copolymers were analysed simultaneously by SLS and DLS in 0.5 M NaCl. Concentrations between 0.5 and 2 mg mL^{-1} were measured at a minimum of 7 angles between 30 and 150°. The scattered intensity at each angle was measured for at least 100 s for each concentration and was then used to calculate the absolute molecular weight (M_w) and radius of gyration (R_g).

$$\frac{Kc}{R_{\theta,fast}} = \frac{1}{M_w}\left(1 + \frac{q^2 {R_g}^2}{3}\right) + 2A_2c \quad (1)$$

Where q is the scattering vector, A_2 is the second virial coefficient (related to polymer-polymer and polymer-solvent interactions), c is the polymer concentration, K is a constant

calculated according to equation 2 and R_θ is the Rayleigh ratio of the sample calculated using equation 3.

$$K = \frac{4\pi^2 n_{ref}{}^2 \left(dn/dc\right)^2}{\lambda^4 N_A} \quad (2)$$

Where n_{ref} is the refractive index of the reference (toluene), *dn/dc* is the calculated refractive index increment of the polymer solution, λ is the wavelength of the laser (= 632.8 nm) and N_A is Avogadro's number.

The dissolved polymers were found to exhibit two relaxation modes, as determined by analysing the correlation function achieved from multi-angle DLS. The two relaxation modes and their contribution to the total observed scattering were analysed and separated using REPES.[32] The concentration of the larger species contributing to the slow mode of relaxation was negligible and thus only scattering from the fast mode was used to determine M_w and R_g. The Rayleigh ratio for the fast mode ($R_{\theta, fast}$) was calculated as follows:

$$R_{\theta,fast} = \mathrm{A}_{fast}(q)\mathrm{R}_\theta = \frac{\mathrm{A}_{fast}}{A_{fast}+A_{slow}}(q)\frac{I_{sample}(q) - I_{solvent}(q)}{I_{reference}(q)}R_{reference} \quad (3)$$

where $\mathrm{A}_{fast}(q)$ is the scattered intensity contribution at a given angle from the fast mode of relaxation as determined by DLS, I_{sample}, $\mathrm{I}_{solvent}$ and $\mathrm{I}_{reference}$ are the scattered intensities by the sample, the solvent and the reference respectively (at a given angle, q), and $\mathrm{R}_{reference}$ is the Rayleigh ratio of the reference solvent, which in this case was toluene.

$Kc/R_{\theta, fast}$ was plotted against q^2 for each concentration and each plot was extrapolated to zero q. The extrapolated $Kc/R_{\theta, fast}$ was subsequently plotted against polymer concentration. The line was extrapolated to zero concentration and the inverse of the intercept yielded the absolute molecular weight.

For polymer **4.02** the molecular weight was determined to be 259 kDa (see Figure 4.12). This is higher than the M_n calculated by ^{1}H NMR spectroscopy (209 kDa) and the M_w obtained from aqueous SEC analysis (124 kDa). The M_w from SEC analysis is lower due to

the difference between the PEO calibrants used and the polymer **4.02**. The difference between the M_n calculated from ^{1}H NMR spectroscopy and the M_w obtained from SLS analysis is reasonable when errors are taken into account. The errors associated with SLS analysis are in the range 10 – 20%.[33, 34] The largest source of error in the SLS analysis is in the *dn/dc* value.

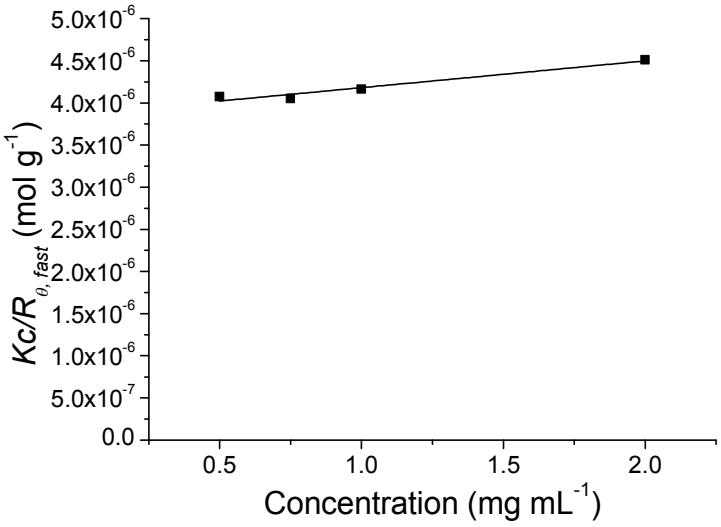

Figure 4.12: Plot of $Kc/R_{\theta, fast}$ *vs* concentration for 4.02. The M_w was calculated using the intercept of the linear fit to the SLS data and found to be 259 kDa

The triblock copolymers were also analysed in a similar manner and the absolute molecular weights calculated (see Table 4.3). For triblock copolymer **4.03** the molecular weight was determined to be 284 kDa. The M_w of **4.04** and **4.05** were found to be 317 kDa and 330 kDa, respectively (see Figure 4.13). Again, the molecular weights obtained by ^{1}H NMR spectroscopy and by SLS analysis compare reasonably well when the errors are accounted for.

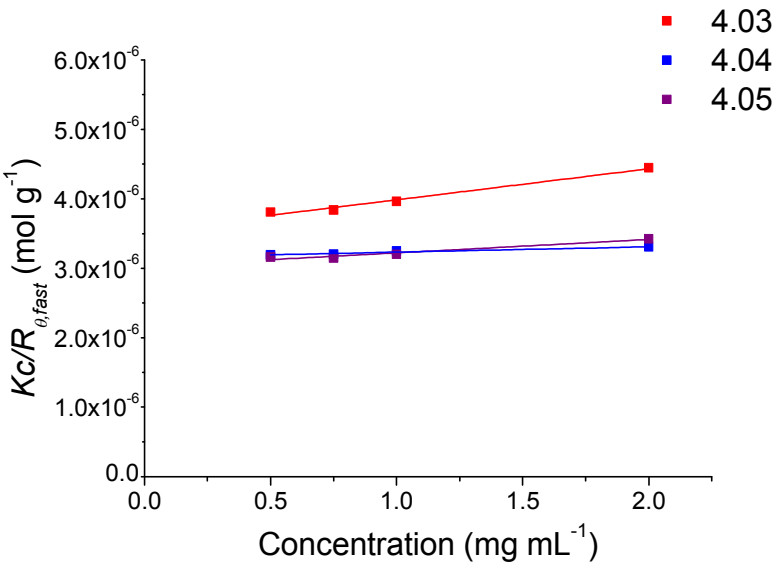

Figure 4.13: Plot of $Kc/R_{\theta, fast}$ *vs* concentration for triblock copolymers 4.03, 4.04 and 4.05. The M_w for each polymer was calculated using the intercept of the linear fit to the SLS data

Table 4.3: Summary of the molecular weights obtained from ^{1}H NMR spectroscopy and SLS analysis, and the dispersity calculated from SEC

Polymer	$M_{n, NMR}$ (kDa)	$M_{w, SEC}$ (kDa)	$Đ_M$
4.03	211.9	284	1.18
4.04	217.2	317	1.20
4.05	225.8	330	1.22

4.3.6 Synthesis of PEGMA-*b*-DMAPS-*b*-PMMA triblock, 4.06

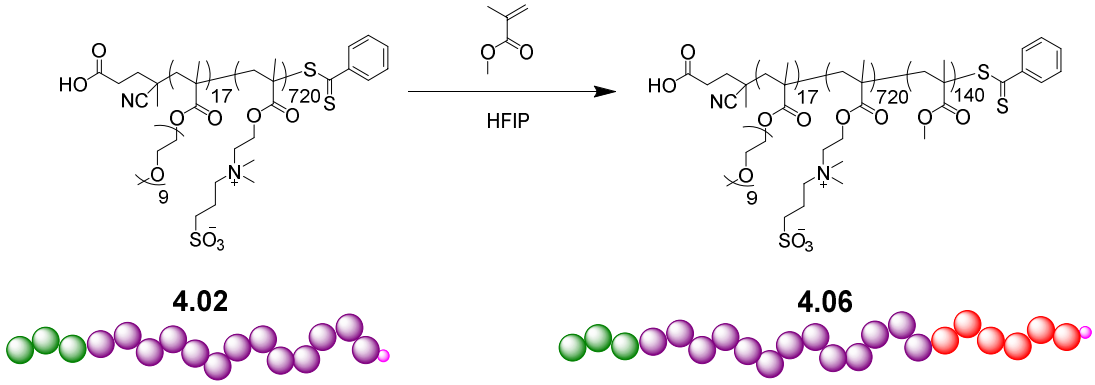

Scheme 4.5: Scheme showing the chain extension of diblock copolymer 4.02 with MMA in HFIP to form triblock copolymer 4.06

As a comparison to the ABA triblocks synthesised in the above section, an ABC triblock copolymer where C is a hydrophobic block was also synthesised (see Scheme 4.5). The hydrophobic block was chosen to be methyl methacrylate (MMA) as it has been used before it self-assembling systems and has a relatively low T_g. Sulfobetaines have limited solubility in many solvents. They are soluble in salt water and in some highly fluorinated solvents such as trifluoroethanol and hexafluoroisopropanol (HFIP).[14, 15, 35] Therefore the chain extension of **4.02** with MMA was performed in HFIP to ensure the solubility of both the monomer and the sulfobetaine containing diblock copolymer. A small amount of DMF was used as an internal standard to monitor conversion. The conversion was calculated by the relative integration of the vinyl peaks at 5.7 and 6.2 ppm to the DMF peak at 7.9 ppm, compared to those integrations in the sample taken at t = 0. The polymer was purified by precipitation into cold methanol to remove the MMA monomer to yield **4.06,** M_n (^{1}H NMR) = 228.2 kDa, M_n (HFIP SEC) = 148.2 kDa, $Đ_M$ = 1.52. The degree of polymerisation of the MMA block was calculated by ^{1}H NMR spectroscopy to be 113 (see Figure 4.14). The ^{1}H NMR spectroscopy was performed at 45 °C as the polymer is more soluble at increased temperatures and this improved the peak resolution. The peak at 3.0 -3.4 ppm corresponds to 8H from the DMAPS side chain (**f** and **j**). The MMA side chain signal (**k**) appears at 3.7 ppm and overlaps with the signals from the PEGMA side chain (**a** and **b**) and 4H from the

DMAPS side chain (**e** and **g**). Therefore by setting the peak at 3.0– 3.4 ppm to the correct integral value and then subtracting the known amounts for the PEGMA and the 4H from the DMAPS side chain the degree of polymerisation of the MMA block can be calculated. The length of 113 units is within a 10% error of that calculated from the conversion determined by ^{1}H NMR spectroscopy.

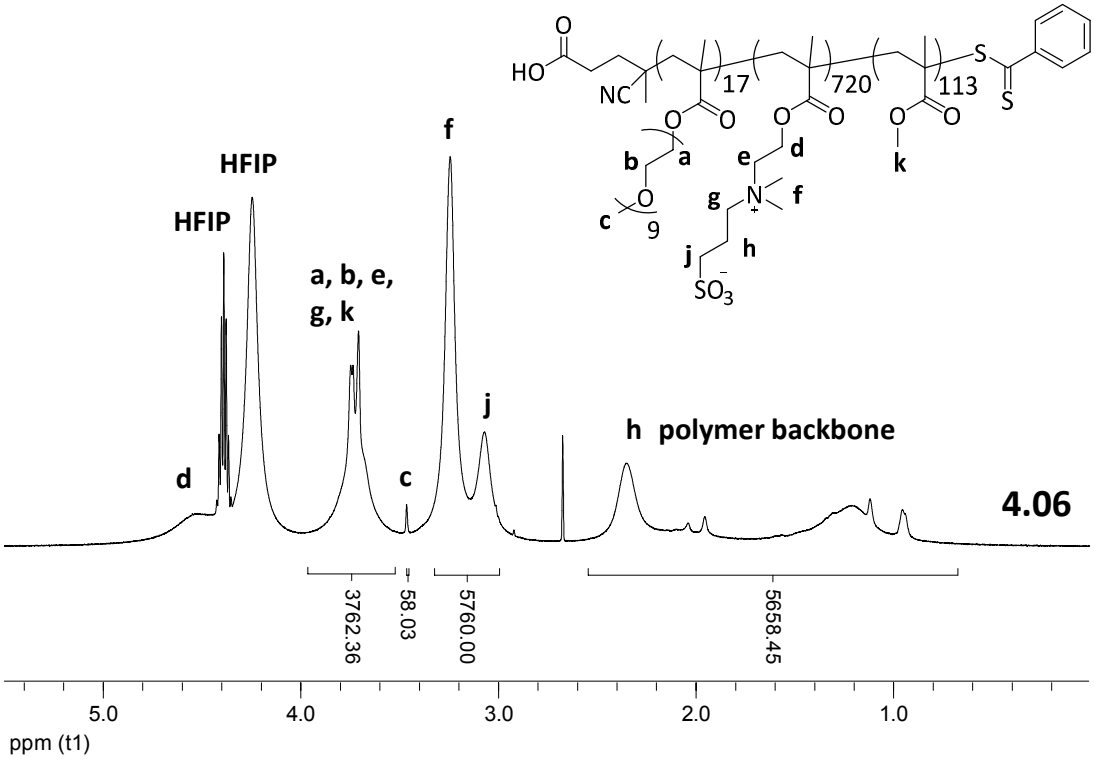

Figure 4.14: ^{1}H NMR spectrum of triblock 4.06 in HFIP with assignments shown. Spectrum was recorded at 45 °C and 500 MHz

The triblock copolymer was analysed by SEC using HFIP as a solvent. The M_n (HFIP SEC) is much smaller than that calculated by ^{1}H NMR spectroscopy (148.2 kDa *vs* 228.2 kDa respectively) and this is due to the difference between the composition of the polymer and the PMMA standards used to calibrate the SEC. The dispersity is quite broad ($Đ_M$ = 1.52) but analysis of the starting diblock copolymer, **4.02**, by HFIP SEC gives M_n (HFIP SEC) = 113.7 kDa, $Đ_M$ = 1.60. Analysis of this same polymer, **4.02**, by aqueous SEC gives a much narrower dispersity of 1.16. Therefore this increase in the dispersity is due to the difference in solvent and columns used for SEC analysis, and the broad dispersity for the triblock copolymer does not necessarily indicate a lack of control in the polymerisation. The shift to

a higher molecular weight shows the successful chain extension (see Figure 4.15). The *dn/dc* in HFIP could not be calculated as the solvent is incompatible with the refractometer instrument.

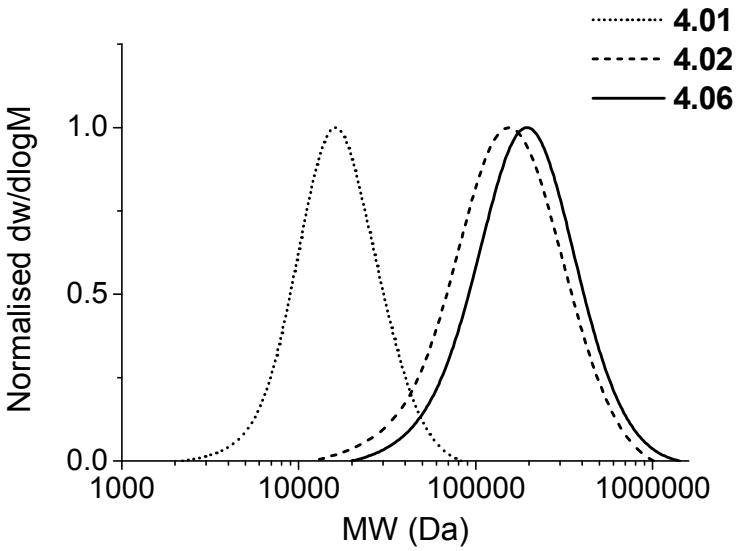

Figure 4.15: HFIP SEC chromatograms showing the shift in molecular weight from homopolymer 4.01 to diblock copolymer 4.02 and then to triblock copolymer 4.06

4.3.7 Synthesis of PEG-*b*-DMAPS-*b*-DEAEMA triblock

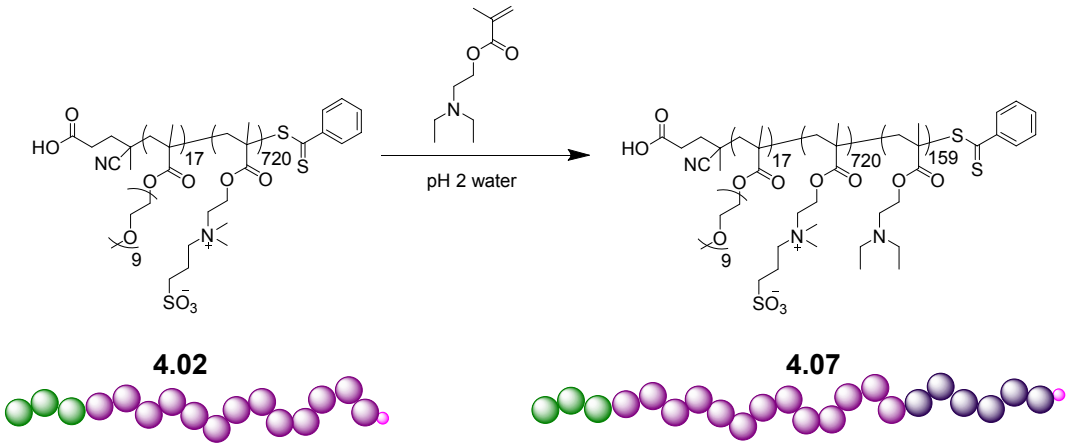

Scheme 4.6: Scheme showing the chain extension of 4.02 with DEAEMA in acidic water to form the triblock 4.07

A similar triblock but containing a pH- and CO_2-responsive group instead of a permanently hydrophobic block was synthesised by chain extending **4.02** with *N,N*-diethylamino ethyl methacrylate (DEAEMA). The polymerisation was carried out in acidic water (*ca*. pH = 2.5) to ensure the monomer was soluble. The initator, ACVA, is not soluble at acidic pH,

therefore potassium persulfate (KPS) was used as an initiator instead. The polymer was purified by dialysis and recovered by lyophilisation to yield **4.07**, M_n (^{1}H NMR) = 238.9 kDa, M_n (HFIP SEC) = 164.4 kDa, $Đ_M$ = 1.53. The degree of polymerisation of the pH-responsive block was calculated to be 159 by ^{1}H NMR spectroscopy (see Figure 4.16). The peak at 3.0 – 3.14 ppm corresponds to 2H from the DMAPS side chain (**j**). The signal at 3.3 – 3.5 ppm corresponds to the N(CH_2)$_2$ (**n**) from the DEAEMA block and the signal for the N^+(CH_3)$_2$ (**f**) from the DMAPS side chain. Therefore by subtracting the known value for the DMAPS the length of the pH-responsive block can be calculated. This can be confirmed by integration of the area between 3.5 and 4.0 ppm. This region corresponds to the PEG side chain signals (**a, b**), 4H from the DMAPS side chain (**e** and **g**) and to 2H from the DEAEMA side chain (**m**). Integration of the backbone area also gives a DP of 158, which compares well with that predicted from conversion.

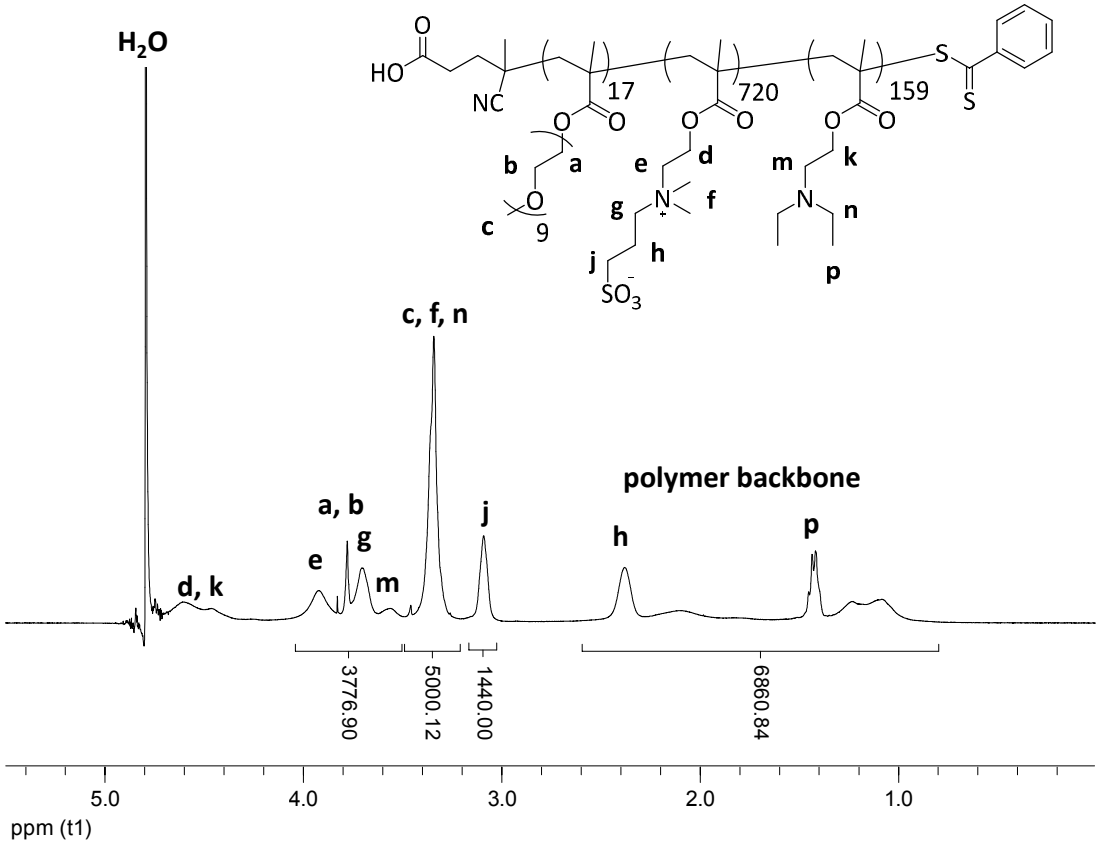

Figure 4.16: ^{1}H NMR spectrum of triblock copolymer 4.07 in acidic 0.5 M NaCl in D_2O, recorded at 25 °C and 400 MHz

Analysis of **4.07** by HFIP SEC shows a shift to higher molecular weight upon chain extension. Again, the dispersity ($Đ_M$ = 1.53) is quite high for RAFT polymerisations (typically ≤ 1.2)[36] but, as for **4.06**, analysis of the starting polymer, **4.02**, also displays a high dispersity ($Đ_M$ = 1.60) when analysed by HFIP SEC but a much lower dispersity ($Đ_M$ = 1.16) when analysed by aqueous SEC.

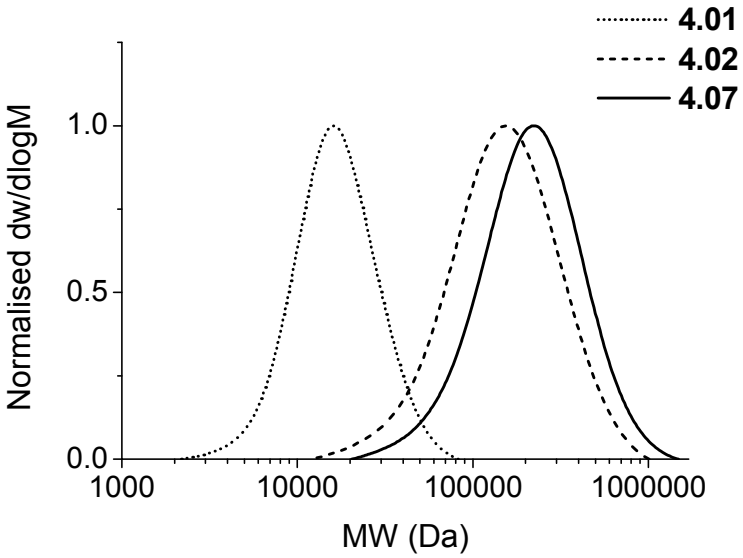

Figure 4.17: HFIP SEC chromatograms showing the shift in molecular weight upon forming triblock copolymer 4.07 from diblock copolymer 4.02

The triblock copolymer was analysed by SLS in order to determine the absolute molecular weight, as described for **4.02**. The polymer was dissolved in pH 3.5 0.5 M NaCl solution to ensure that the polymer was fully dissolved. The *dn/dc* was determined to be 0.121 mL g^{-1}.

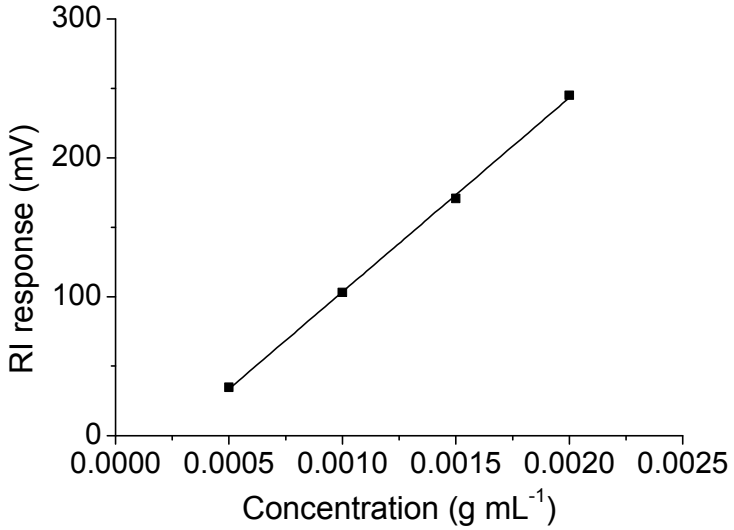

Figure 4.18 Plot of concentration *vs* RI response for triblock copolymer 4.07 in 0.5 M NaCl solution at pH 3.5. The *dn/dc* was calculated as 0.121 mL g^{-1} using the slope of the linear fit

$Kc/R_{\theta,\ fast}$ was plotted against q^2 for each concentration and each plot was extrapolated to zero q. The extrapolated $Kc/R_{\theta,\ fast}$ was subsequently plotted against polymer concentration. The line was extrapolated to zero concentration and the inverse of the intercept yielded the absolute molecular weight. For polymer **4.07** the M_w was determined to be 348 kDa. The M_n calculated from ^{1}H NMR spectroscopy is 238.9 kDa and these two values are in agreement when the errors in the SLS analysis and the dispersity of the polymer are accounted for.

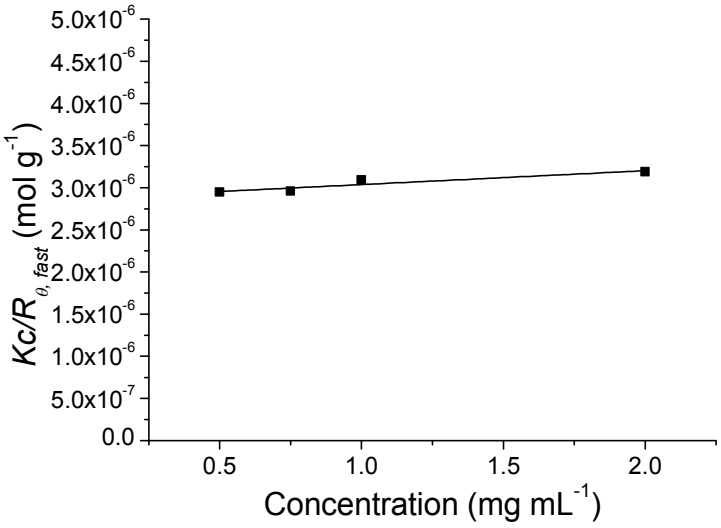

Figure 4.19 Plot of $Kc/R_{\theta,\ fast}$ *vs* concentration for 4.07. The M_w was calculated using the intercept of the linear fit to the SLS data and found to be 348 kDa

4.3.8 Synthesis of DMAPS homopolymers

Homopolymers of DMAPS were also synthesised by RAFT polymerisation. The polymerisation was carried out in 0.5 M NaCl to ensure the solubility of both the monomer and the growing polymer chain throughout the polymerisation. The CTA used was CPTA due to its solubility in water. The pH of the polymerisation mixture was adjusted to pH 7.0 using diluted NaOH in order to ensure both the CTA and the initiator were fully solubilised. After heating at 65 °C overnight the resulting polymer was purified by exhaustive dialysis against water and recovered by lyophilisation to yield **4.08**, M_n (^{1}H NMR) = 35.2 kDa, M_n (SEC) = 32.3 kDa, $Đ_M$ = 1.11. The degree of polymerisation of the DMAPS block was determined to be 125 from integration of the end group signals (**k**, **m** and **n**) between 7.50 – 8.10 ppm relative to the polymer peaks at 3.0 ppm (**f**) and 3.34 ppm (**j**). This matched well (within 10% error) with that predicted from conversion ^{1}H NMR spectroscopy.

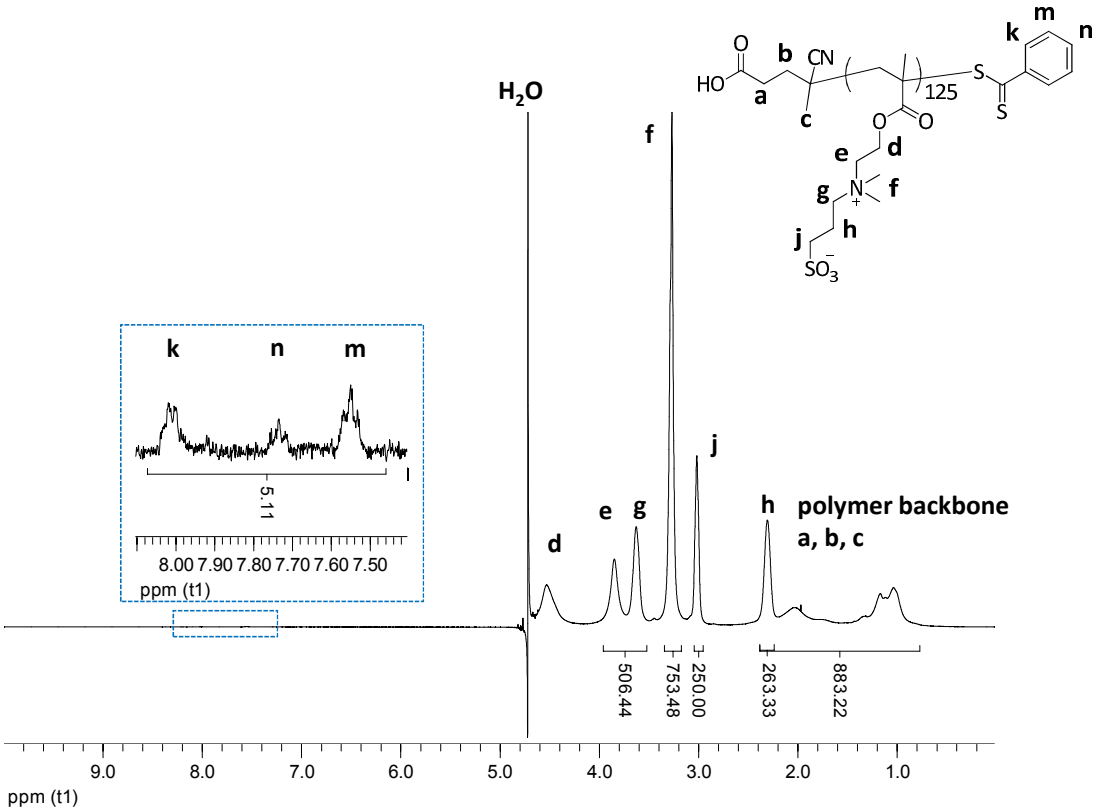

Figure 4.20: ^{1}H NMR spectrum of homopolymer 4.08 in 0.5 M NaCl in D_2O with assignments shown, recorded at 25 °C and 400 MHz

As a comparison to **4.08** a longer homopolymer of DMAPS was synthesised, in a similar manner, to form **4.09**, M_n (^{1}H NMR) = 111.6 kDa, M_n (SEC) = 59.7 kDa, $Đ_M$ = 1.09. This homopolymer has a DP of 400 as determined by conversion ^{1}H NMR spectroscopy (see Figure 4.21). In this longer block copolymer the CTA end groups were not visible by ^{1}H NMR spectroscopy due to the higher molecular weight of the polymer.

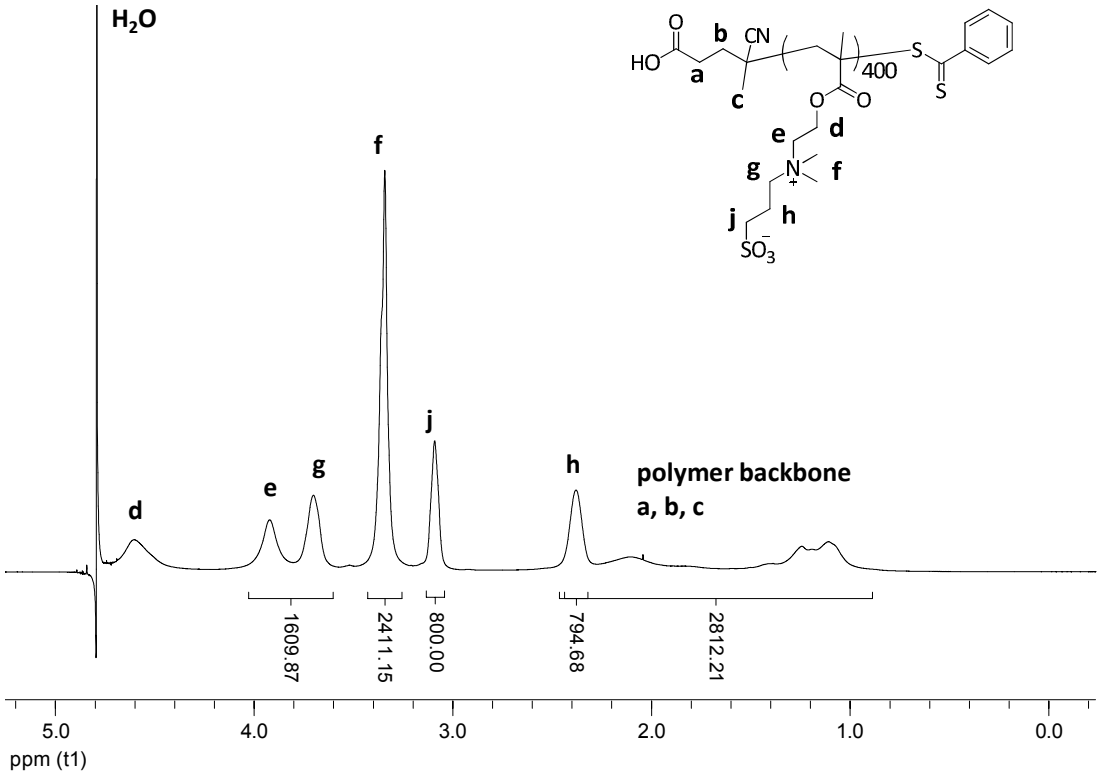

Figure 4.21: ^{1}H NMR spectrum of homopolymer 4.09 in 0.5 M NaCl in D_2O with assignments shown, recorded at 25 °C and 400 MHz

The *dn/dc* of **4.09** was determined as described previously and calculated to be 0.126 mL g^{-1}. Polymer **4.09** was analysed by simultaneous SLS and DLS measurements in order to calculate the absolute molecular weight of the polymer, as described for **4.02**.

$Kc/R_{\theta, fast}$ was plotted against q^2 for each concentration and each plot was extrapolated to zero q. The extrapolated $Kc/R_{\theta, fast}$ was subsequently plotted against polymer concentration. The line was extrapolated to zero concentration and the inverse of the intercept yielded the absolute molecular weight. The molecular weight was determined to be 136 kDa and is in good agreement with the M_n calculated from ^{1}H NMR spectroscopy (111.6 kDa).

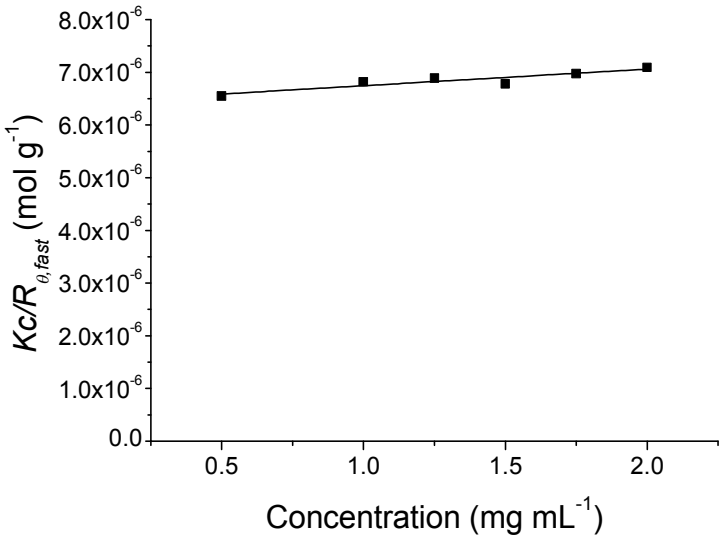

Figure 4.22: Plot of $Kc/R_{\theta, fast}$ *vs* concentration for 4.09. The M_w was calculated using the intercept of the linear fit to the SLS data and determined to be 136 kDa

4.3.9 Synthesis of DMAPS-*b*-PMMA diblocks

4.3.9.1 Emulsion Polymerisation

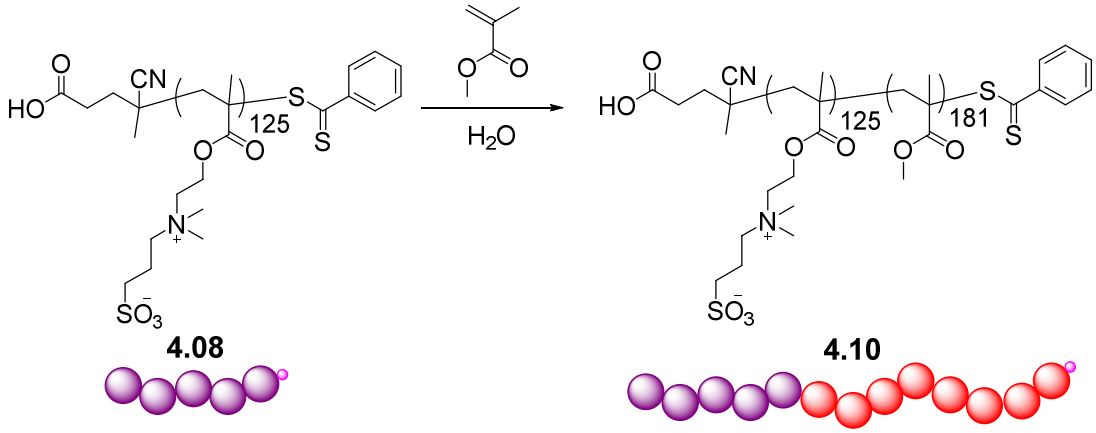

Scheme 4.7: The synthesis of diblock copolymer 4.10 by chain extension of homopolymer 4.08 with MMA by emulsion polymerisation

Amphiphilic block copolymers containing DMAPS have not been directly synthesised using the DMAPS monomer due to the limited solubility of the DMAPS homopolymer. Such block copolymers may have interesting self-assembly and thermo-responsive behaviour. Firstly **4.08** was chain extended with MMA in 0.5 M NaCl solution as an oil-in-water emulsion polymerisation. The macroCTA (**4.08)** and the initiator, AIBN, were stirred in 0.5 M NaCl, both at 1 wt%. The solution was degassed by purging with nitrogen for 30 minutes.

The monomer, MMA, was degassed in a separate vessel and then transferred to the reaction solution at 1 wt%. The solution was stirred vigorously and heated to 65 °C. After 20 hours the solution had turned opalescent which is indicative of particles having formed. The reaction was stopped and the polymer dialysed and recovered by lyophilisation. The recovered polymer was precipitated into hexanes and dried to yield **4.10**, M_n (^{1}H NMR) = 52.2 kDa, M_n (HFIP SEC) = 31.6 kDa, $Đ_M$ = 1.80. The dispersity observed in the HFIP SEC is broad, but the starting homopolymer, **4.08**, also displays a large dispersity when analysed by HFIP SEC (M_n (HFIP SEC) = 24.4 kDa, $Đ_M$ = 1.59) (see Figure 4.23). The same polymer when analysed by aqueous SEC displays a much lower dispersity (M_n (SEC) = 32.3 kDa, $Đ_M$ = 1.11) showing that again an artificially broad dispersity may be observed as a consequence of interactions between the HFIP SEC column and the polymer. The chromatogram of the absorbance at 309 nm overlays with the peak detected from refractive index showing that the RAFT end group has been retained throughout the polymerisation (see Figure 4.24). However there is some tailing observed in the SEC chromatogram of **4.10** indicating that the chain extension was not particularly efficient, possibly because of the use of water as a solvent and the insoluble nature of MMA in water.

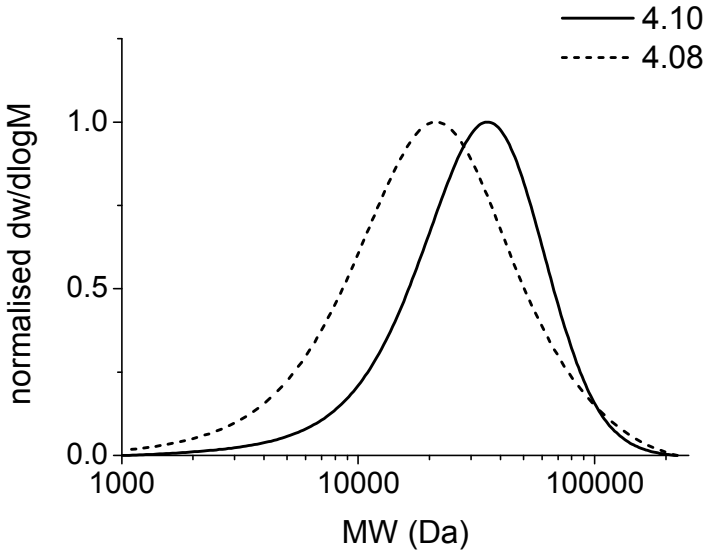

Figure 4.23: HFIP SEC chromatograms showing the chain extension from homopolymer 4.08 to diblock copolymer 4.10

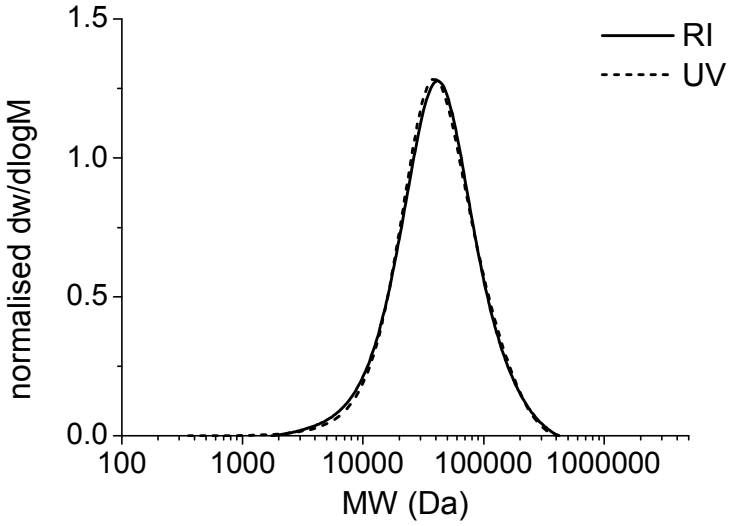

Figure 4.24: Normalised RI and UV at 309 nm chromatograms from HFIP SEC analysis of diblock copolymer 4.10 to show the retention of the RAFT end group

The length of the hydrophobic block was determined to be 181 units from ^{1}H NMR spectroscopy in deuterated HFIP. This was calculated by comparing the ^{1}H NMR spectra of the starting **4.08** and diblock copolymer **4.10** and integrating between set values (see Figure 4.25). The peak at 3.0 – 3.4 ppm integrates to 8H from the DMAPS side chain (**c** and **f**). The broad peak at 3.5 – 4.0 ppm corresponds to four other protons on the DMAPS side chain (**b** and **d**) and also to the three protons of the methyl group from the MA side chain (**g**). Therefore by setting the peak at 3.0 – 3.4 ppm to be the correct value, based on the known DP of the DMAPS block, the integration for the MA block can be calculated by subtracting the value for 4H of the DMAPS from the overall integration of the area between 3.5 – 4.0 ppm. Integration of the backbone area of the ^{1}H NMR gives DP = 194, which is within a 10% error of that calculated from the side chains (DP = 181).

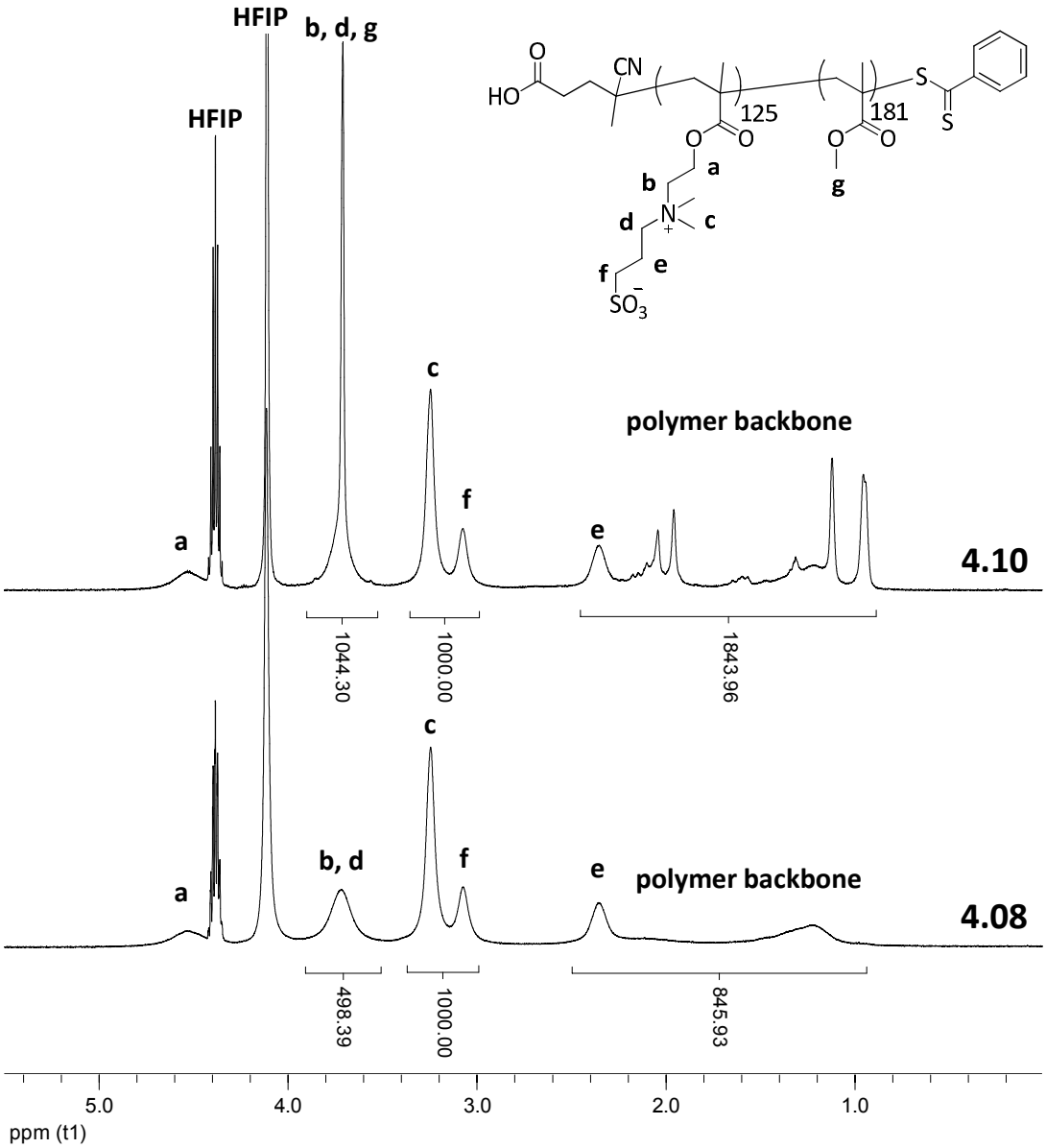

Figure 4.25: ^{1}H NMR spectra of homopolymer 4.08 and diblock copolymer 4.10 in HFIP-d2, showing the appearance of the MMA peak at 3.6 ppm and 0.9 ppm, recorded at 45 °C and 500 MHz

4.3.9.2 Polymerisation in HFIP

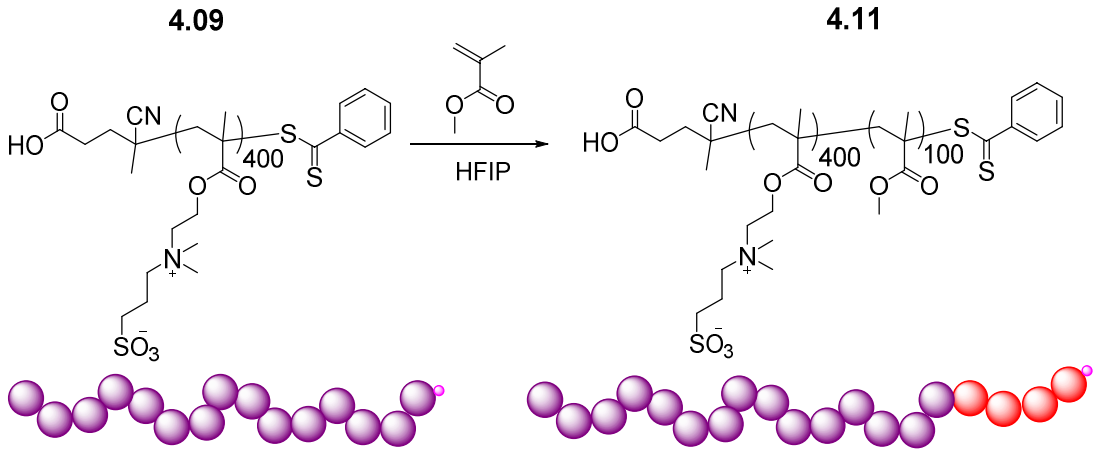

Scheme 4.8: The synthesis of diblock copolymer 4.11 by the chain extension of homopolymer 4.09 with MMA in HFIP

Polymer **4.09** was also chain extended with MMA to yield diblock copolymers. Instead of an emulsion polymerisation the chain extension polymerisation reaction was carried out in HFIP as both **4.09** and the monomer are soluble in this solvent. A small amount of DMF was added to act as a ^{1}H NMR spectroscopy standard. A sample was taken for ^{1}H NMR spectroscopy before the polymerisation began to be able to integrate the vinyl peaks to the DMF standard at t = 0. The reaction mixture was degassed *via* three *freeze-pump-thaw* cycles and heated at 65 °C for 17 hours. The conversion was calculated by the relative integration of the vinyl peaks at 5.7 and 6.2 ppm to the DMF peak at 7.9 ppm, compared to those integrations in the sample taken at t = 0. The polymer was purified by dialysis and recovered by lyophilisation to yield **4.11**, M_n (^{1}H NMR) = 121.7 kDa, M_n (HFIP SEC) = 73.1, $Đ_M$ = 1.34. In comparison to the starting polymer, **4.09** (M_n (HFIP SEC) = 52.5 kDa, $Đ_M$ = 1.51), HFIP SEC chromatogram shows a decrease in dispersity upon chain extension. The chain extension can be seen in the shift in the molecular weight of the HFIP SEC chromatogram of the starting polymer and the diblock copolymer (see Figure 4.26). There is significantly less tailing observed in the SEC chromatogram of **4.11** compared to that of **4.10** indicating that HFIP is a better solvent for the chain extension of polyDMAPS with MMA than 0.5 M NaCl solution.

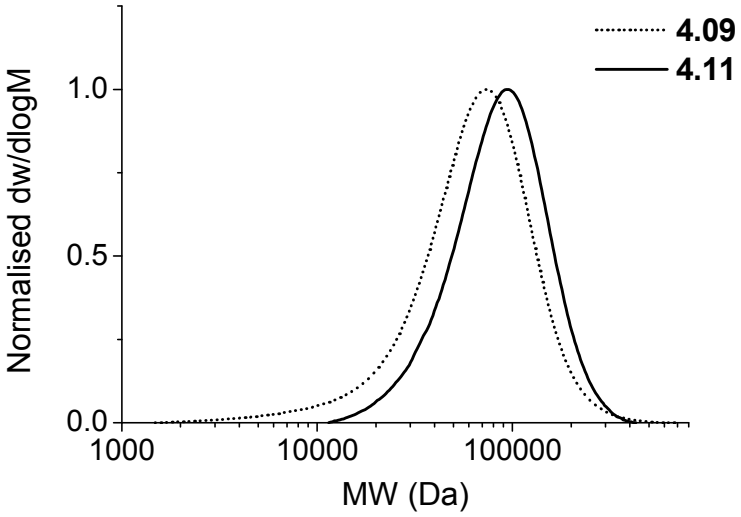

Figure 4.26: HFIP SEC chromatograms showing the shift in molecular weight upon chain extension from homopolymer 4.09 to diblock copolymer 4.11

The length of the MMA block was calculated by comparison of the starting homopolymer, **4.09**, and the diblock copolymer, **4.11** (see Figure 4.27). The peak between 3.0 – 3.4 ppm was set to be 3200 as it is equivalent to 8H from the DMAPS side chain (**c** and **a**) and the DP is known to be 400. The peak corresponding to the MMA side chain (**g**) appears at = 3.7 ppm and overlays with the signals corresponding to 4H of the DMAPS side chain (**b** and **d**). Integration of the area between 3.5 ppm and 4.0 ppm and subtraction of the known values for the DMAPS signals gives an MA block length of 100 units, which compares well with that predicted by conversion.

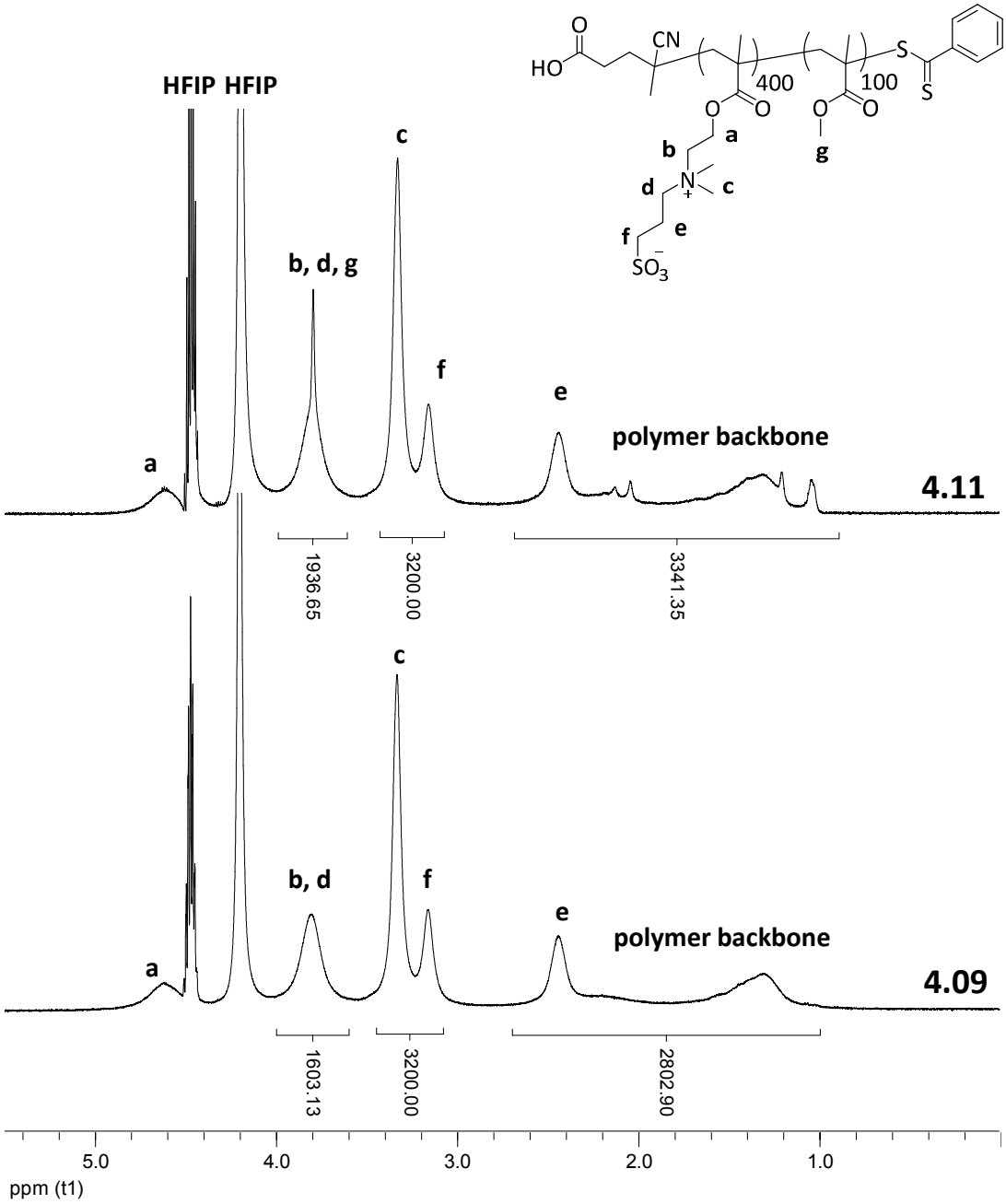

Figure 4.27: ^{1}H NMR spectra of homopolymer 4.09 and diblock copolymer 4.11 in HFIP at 45 °C, recorded at 500 MHz. The appearance of the signal relating to the MMA side chain is clearly visible at 3.7 ppm

4.4 Conclusions

The sulfobetaine, DMAPS, was utilised in synthesising a range of thermo-responsive di- and tri-block copolymers. Hydrophilic di- and triblock copolymers consisting of PEGMA and DMAPS were synthesised by aqueous RAFT polymerisation. The polymers displayed narrow dispersities and were lower than those previously reported.[19] The absolute molecular weight of the polymers was analysed using simultaneous SLS and DLS measurements.

Thermo-responsive diblock copolymers containing DMAPS and MMA were synthesised by either emulsion polymerisation in water or by using HFIP as the solvent. The polymer made by emulsion polymerisation displayed significant tailing in the HFIP SEC, whereas using HFIP as a solvent produced relatively narrow, well defined block copoylmers. ABC triblock copolymers, where A is the hydrophilic block, B is the thermo-responsive DMAPS block and C is a hydrophobic block were also synthesised using HFIP as a polymerisation solvent. These are the first examples of hydrophobic containing block copolymers of DMAPS synthesised by the direct polymerisation of the DMAPS monomer, rather than utilising post-polymerisation modification strategies.[14]

A triply responsive triblock copolymer of hydrophilic PEGMA, thermo-responsive DMAPS and pH- and CO_2-responsive DEAEMA was synthesised by RAFT polymerisation in acidic water. The resulting polymer displayed a relatively narrow dispersity in HFIP SEC.

4.5 Experimental

4.5.1 Materials

1,4-Dioxane, poly(ethylene glycol) methyl ether methacrylate (PEGMA), [2-(methacryloyloxy)ethyl]dimethyl-(3-sulfopropyl)ammonium hydroxide (DMAPS), methyl methacrylate (MMA), *N, N*- (diethylamino)ethyl methacrylate (DEAEMA), 4-cyano-4-(phenylcarbonothioylthio)pentanoic acid (CPTA) and 4, 4'- azobis(4-cyanopentanoic acid) (ACVA) were used as received from Aldrich and Fluka unless otherwise stated. AIBN [2, 2'- azobis(2-methylpropionitrile)] was recrystallised twice from methanol and stored in the dark at 4 °C. Hexafluoroisopropanol (HFIP) was obtained from Fluorochem and Apollo.

4.5.2 Characterisation

^{1}H Nuclear magnetic resonance (NMR) experiments were performed on a Bruker 400 FT-NMR spectrometer operating at 400 MHz using deuterated solvents. Chemical shifts are reported in parts per million relative to H_2O (4.79 ppm) or HFIP-d2 (4.4 ppm). Spectra were recorded at either 25 °C or 45 °C. Size exclusion chromatography (SEC) measurements were obtained in either HPLC grade DMF containing 0.1M NH_4BF_4 at a flow rate of 1 mL min^{-1}, on a set of two Pgel 5 μm Mixed D columns plus a guard column or in pH 8.2 phosphate buffer at a flow rate of 1 mL min^{-1}, on a set of one PL aquagel OH 50 and one PL aquagel mixed M plus a PL aquagel OH guard column. Cirrus SEC software was used to analyse the data using poly(methylmethacrylate) (PMMA) or poly(ethylene glycol) (PEG) standards.

dn/dc measurements were recorded on a Shodex RI-101 differential refractometer. 4 concentrations between 0.5 and 2 mg mL^{-1} were run. SLS and DLS measurements were recorded simultaneously on an ALV CGS3 spectrometer consisting of a 22 mW HeNe laser at λ = 632.8 nm. Measurements were carried out at 20 °C and recorded at 7 scattering angles between 20 and 150°. The scattering vector was defined as;

$$q = \frac{4\pi n}{\lambda\left[sin\frac{\theta}{2}\right]}$$

where n is the refractive index of the solvent. Concentrations between 0.1 and 2 mg.mL^{-1} were analysed for each sample. At least two measurements were run on each angle, each run for at least 100 seconds to determine the auto correlation function, $g_2(t)$, from DLS and the mean scattered intensity, I, from SLS. The resulting correlation functions were analysed using REPES programme.[32] The R_h for the fast mode was determined by plotting the apparent diffusion coefficient for each concentration, D_{fast}, against concentration and extrapolating to zero concentration. $Kc/R_{\theta, fast}$ *vs* q^2 was plotted and from this the molecular weight and R_g for the nanostructure were determined.

4.5.3 Synthesis of PEGMA homopolymer, 4.01

PEGMA (average M_n 480 Da) (1 g, 2.1 mmol, 20 equiv.), CPTA (29 mg, 0.1 mmol, 1 equiv.) and AIBN (1.7 mg, 0.01 mmol, 0.1 equiv.) were dissolved in 1, 4-dioxane (2:1 solvent: monomer) and placed in an oven dried ampoule under nitrogen flow with a stirrer bar. The polymerisation mixture was degassed with at least three *freeze-pump-thaw* cycles, released to and sealed under nitrogen. The reaction was subsequently submerged into an oil bath at 65 °C for 6 hours. The polymer was purified by dialysis against nanopure water (18.2 MΩ cm^{-1}) and recovered by lyophilisation yielding a pink oil, **4.01**, M_n (^{1}H NMR) = 8.2 kDa, M_n (DMF SEC) = 10.1 kDa, $Đ_M$ = 1.08. ^{1}H NMR spectroscopy (400 MHz, D_2O): δ (ppm): 0.70 – 1.30 (m, 51H, $CH_2C(CH_3)$ of polymer backbone), 1.60 – 2.20 (m, 34H, $CH_2C(CH_3)$), 2.35 – 2.45 (m, 2H, CH_2CH_2COOH), 3.30 – 3.36 (s, 51H, OCH_3 of polymer side chain), 3.40 – 3.86 (m, 578H, CH_2CH_2O of polymer side chain), 4.20 – 4.40 (br s, 34H, $COOCH_2CH_2O$ of polymer side chain), 7.46 – 7.58 (m, 2H, Ar ring of CTA), 7.64 – 7.74 (m, 1H, Ar ring of CTA), 7.88 – 7.98 (m, 2H, Ar ring of CTA).

4.5.4 Synthesis of PEG-*b*-PDMAPS diblock, 4.02

DMAPS (5 g, 18 mmol, 800 equiv.), homopolymer **4.01** (0.1 g, 0.02 mmol, 1 equiv.) and ACVA (1.2 mg, 0.005 mmol, 0.2 equiv.) were dissolved in 0.5 M NaCl solution (5:1 solvent: monomer w: v) and placed in an oven dried round-bottom flask under a flow of nitrogen with a stirrer bar. The solution was purged with nitrogen for 45 minutes and left under positive pressure of nitrogen. The polymerisation mixture was then heated at 65 °C for six hours. The polymer was purified by dialysis against 18.2 MΩ cm^{-1} water and recovered by lyophilisation yielding a pale pink solid polymer, **4.02,** M_n (^{1}H NMR) = 209.0 kDa, M_n (Aqueous SEC) = 106.4 kDa, $Đ_M$ = 1.16. ^{1}H NMR spectroscopy (400 MHz, 0.5 M NaCl in D_2O): δ (ppm): 0.9 – 1.5 (m, 2211H, $CH_2C(CH_3)$ of polymer backbone), 1.60 – 2.60 (m, 1474H, $CH_2C(CH_3)$ of polymer backbone), 2.30 – 2.50 (br s, 1440H, $CH_2CH_2SO_3^-$ of DMAPS side chain), 3.05 – 3.15 (br s, 1440H, $CH_2CH_2SO_3^-$ of DMAPS side chain), 3.26 – 3.40 (br s, 4320H, $N^+(CH_3)_2$ of DMAPS side chain), 3.45 – 3.46 (s, 50H, OCH_3 of PEGMA side chain), 3.60 – 3.72 (br s, 1440H, $N^+(CH_3)_2CH_2$ of DMAPS side chain), 3.72 – 3.81 (br m, 600H, CH_2CH_2O of PEGMA side chain), 3.81 – 4.30 (br s, 1440H, OCH_2CH_2N of DMAPS side chain), 4.40 – 4.70 (br s, 1440H, OCH_2CH_2N of DMAPS side chain). ^{13}C NMR spectroscopy (500 MHz, 0.5 M NaCl in D_2O): δ (ppm): 18.3, 18.5, 18.7, 44.8, 45.1, 47.5, 49.1, 49.3, 59.2, 62.0, 62.2, 63.4, 69.2, 69.7, 71.1, 177.5, 178.1, 221.7.

4.5.5 Synthesis of PEG-*b*-PDMAPS-*b*-PEG triblocks, 4.03, 4.04 and 4.05

The general procedure for the synthesis of the triblock copolymers is detailed below. In order to achieve the different block lengths seen in **4.03**, **4.04** and **4.05**, different relative equivalents of PEGMA were used. PEGMA (11 mg, 0.02 mmol, 20 equiv.), **4.02** (0.25 g, 0.001 mmol, 1 equiv.) and ACVA (0.04 mg, 0.0002 mmol, 0.2 equiv.) were dissolved in 0.5 M NaCl (5:1 solvent: **4.02**) and placed in an oven dried round-bottom flask with a stirrer bar. The solution was purged with nitrogen for 45 minutes and then placed in a preheated oil bath at 65 °C for 16 hours. The polymer was purified by dialysis and recovered by lyophilisation

to yield a very pale pink solid, **4.03**, M_n (^{1}H NMR) = 212 kDa, M_n (Aqueous SEC) = 103.8 kDa, $Đ_M$ = 1.18. ^{1}H NMR spectroscopy (400 MHz, 0.5 M NaCl in D_2O): δ = 0.9 – 1.5 (m, 2230H, $CH_2C(CH_3)$ of polymer backbone), 1.60 – 2.60 (m, 1486H, $CH_2C(CH_3)$ of polymer backbone), 2.30 – 2.50 (br s, 1440H, $CH_2CH_2SO_3^-$ of DMAPS side chain), 3.05 – 3.15 (br s, 1440H, $CH_2CH_2SO_3^-$ of DMAPS side chain), 3.26 – 3.40 (br s, 4320H, $N^+(CH_3)_2$ of DMAPS side chain), 3.45 – 3.46 (s, 69H, OCH_3 of PEGMA side chain), 3.60 – 4.10 (m, 3660H, $N^+(CH_3)_2CH_2$ of DMAPS side chain, CH_2CH_2O of PEGMA side chain and OCH_2CH_2N of DMAPS side chain), 4.40 – 4.70 (br s, 1440H, OCH_2CH_2N of DMAPS side chain). ^{13}C NMR spectroscopy (125 MHz, 0.5 M NaCl in D_2O): δ (ppm): 18.3, 18.5, 18.7, 44.8, 45.1, 47.5, 49.1, 49.3, 51.5, 52.1, 54.2, 59.1, 62.2, 63.4, 69.5, 69.7, 71.1, 177.4, 178.1, 205.1.

Triblock copolymer **4.04**, M_n (^{1}H NMR) = 217 kDa, M_n (Aqueous SEC) = 101.2 kDa, $Đ_M$ = 1.20. ^{1}H NMR spectroscopy (400 MHz, 0.5 M NaCl in D_2O): δ (ppm): 0.9 – 2.6 (br m, 5260H, $CH_2C(CH_3)$ of polymer backbone, $CH_2C(CH_3)$ of polymer backbone, $CH_2CH_2SO_3^-$ of DMAPS side chain), 3.05 – 3.15 (br s, 1440H, $CH_2CH_2SO_3^-$ of DMAPS side chain), 3.26 – 3.40 (br s, 4320H, $N^+(CH_3)_2$ of DMAPS side chain), 3.45 – 3.46 (s, 100H, OCH_3 of PEGMA side chain), 3.60 – 4.10 (m, 4020H, $N^+(CH_3)_2CH_2$ of DMAPS side chain, CH_2CH_2O of PEGMA side chain and OCH_2CH_2N of DMAPS side chain), 4.40 – 4.70 (br s, 1440H, OCH_2CH_2N of DMAPS side chain). ^{13}C NMR spectroscopy (125 MHz, 0.5 M NaCl in D_2O): δ (ppm): 7.94, 18.3, 18.5, 18.7, 45.0, 45.1, 47.2, 47.5, 49.2, 51.5, 51.8, 52.1, 54.2, 58.2, 62.2, 63.4, 69.5, 69.7, 71.1, 130.1, 177.4, 178.0, 205.0, 232.5.

Triblock copolymer **4.05**, M_n (^{1}H NMR) = 226 kDa, M_n (Aqueous SEC) = 95.2 kDa, $Đ_M$ = 1.22. ^{1}H NMR spectroscopy (400 MHz, 0.5 M NaCl in D_2O): δ (ppm): 0.9 – 2.6 (br m, 5309H, $CH_2C(CH_3)$ of polymer backbone, $CH_2C(CH_3)$ of polymer backbone, $CH_2CH_2SO_3^-$ of DMAPS side chain), 3.05 – 3.15 (br s, 1440H, $CH_2CH_2SO_3^-$ of DMAPS side chain), 3.26 – 3.40 (br s, 4320H, $N^+(CH_3)_2$ of DMAPS side chain), 3.45 – 3.46 (s, 160H, OCH_3 of PEGMA side chain), 3.60 – 4.10 (m, 4660H, $N^+(CH_3)_2CH_2$ of DMAPS side chain, CH_2CH_2O of PEGMA side chain and OCH_2CH_2N of DMAPS side chain), 4.40 – 4.70 (br s,

1440H, OCH_2CH$_2$N of DMAPS side chain). ^{13}C NMR spectroscopy (125 MHz, 0.5 M NaCl in D_2O): δ (ppm): 18.3, 18.5, 18.7, 45.0, 45.1, 47.0, 47.3, 49.2, 51.5, 51.8, 52.1, 54.3, 58.2, 62.2, 63.4, 69.5, 69.7, 71.1, 130.1, 177.4, 178.0, 205.2, 232.4.

4.5.6 Synthesis of PEG-*b*-PDMAPS-*b*-PMMA triblock, 4.06

Diblock copolymer **4.02** (0.25 g, 0.002 mmol, 1 equiv.) and MMA (0.009 g, 0.9 mmol, 400 equiv.) were dissolved in HFIP with a small amount of DMF as an internal ^{1}H NMR spectroscopy standard to monitor conversion. AIBN (0.07 mg, 0.0004 mmol, 0.2 equiv.) was added froma stock solution.The solution was placed in an oven dried ampoule and degassed *via* three successive *freeze-pump-thaw* cycles. The polymerisation mixture was heated at 65 °C for 20 hours and the polymer purified by precipitation into cold methanol to yield **4.06**, M_n (^{1}H NMR) = 228.2 kDa, M_n (HFIP SEC) = 148.2 kDa, $Đ_M$ = 1.52. ^{1}H NMR spectroscopy (400 MHz, HFIP): δ (ppm): 0.8 – 2.5 (m, 5658H, CH$_2$C(CH_3) of polymer backbone, CH_2C(CH$_3$) of polymer backbone, CH_2CH$_2$SO$_3^-$ of DMAPS side chain), 3.0 – 3.30 (m, 3200H, CH$_2$CH_2SO$_3^-$ of DMAPS side chain and N$^+$(CH_3)$_2$CH$_2$ of DMAPS side chain), 3.46 (s, 54H, OCH_3 of PEG side chain), 3.6 – 4.0 (br s, 3762H, N$^+$(CH$_3$)$_2$CH_2 of DMAPS side chain, OCH$_2$CH_2N of DMAPS side chain, OCH_2CH_2O of PEG side chain, OCH_3 of MMA side chain), 4.4 – 4.8 (br s, 1440H, OCH_2CH$_2$N of DMAPS side chain). ^{13}C NMR spectroscopy (125 MHz, HFIP): δ (ppm): 15.7, 17.7, 37.4, 44.6, 45.1, 51.8, 180.5.

4.5.7 Synthesis of PEG-*b*-PDMAPS-*b*-PDEAEMA triblock, 4.07

Diblock copolymer **4.02** (1 g, 0.005 mmol, 1 equiv.), DEAEMA (0.35 g, 1.88 mmol, 400 equiv.) and KPS (0.25 mg, 0.001 mmol, 0.2 equiv.) were dissolved in water. The pH was adjusted to *ca.* 2.3 to allow the monomer to dissolve. The solution was then degassed by bubbling with nitrogen for 40 minutes and then placed in a preheated oil bath at 65 °C for 16 hours. The polymer was purified by dialysis against acidic water and recovered by lyophilisation to yield a pale pink polymer, **4.07**, M_n (^{1}H NMR) = 238.9 kDa, M_n (HFIP SEC) = 164.4 kDa, $Đ_M$ = 1.53. ^{1}H NMR spectroscopy (400 MHz, 0.5 M NaCl in D_2O at pH 3): δ (ppm): 0.8 – 2.6 (br m, 6830H, CH$_2$C(CH_3) of polymer backbone, CH_2C(CH$_3$) of

polymer backbone,) $N(CH_2CH_3)_2$ of DEAEMA side chain and $CH_2CH_2SO_3^-$ of DMAPS side chain), 3.05 – 3.15 (br s, 1440H, $CH_2CH_2SO_3^-$ of DMAPS side chain), 3.26 – 3.45 (br s, 5000H, $N^+(CH_3)_2$ of DMAPS side chain, $N(CH_2CH_3)_2$ and OCH_3 of PEGMA side chain), 3.50 – 4.10 (m, 3776H, OCH_2CH_2N of DEAEMA side chain, $N^+(CH_3)_2CH_2$ of DMAPS side chain, CH_2CH_2O of PEGMA side chain, OCH_2CH_2N of DMAPS side chain), 4.40 – 4.70 (br m, 1758H, OCH_2CH_2N of DMAPS side chain, OCH_2CH_2N of DEAEMA side chain). ^{13}C NMR spectroscopy (125 MHz, 0.5 M NaCl in D_2O at pH 3): δ (ppm): 8.8, 18.5, 19.6, 45.0, 45.2, 47.5, 48.1, 48.2, 49.5, 51.6, 59.3, 62.2, 63.4, 69.7, 71.1, 177.4, 178.0, 178.6, 223.5.

4.5.8 Synthesis of DMAPS homopolymers, 4.08 and 4.09

The general procedure for the synthesis of the DMAPS homopolymers is detailed below. In order to achieve the different block lengths for **4.08** and **4.09**, the reaction was heated for different lengths of time. CPTA (10 mg, 0.004 mmol, 1 equiv.), DMAPS (5g, 17.9 mmol. 500 equiv.) and ACVA (2 mg, 0.001 mmol, 0.2 equiv.) were dissolved in 25 mL 0.5 M NaCl solution. The pH of the solution was adjusted to *ca*. pH 7 and then degassed by bubbling with nitrogen for 40 minutes. The polymerisation mixture was then heated to 65 °C for 2.5 hours. The conversion was calculated from the integration of the monomer signals at 5.7 and 6.1 ppm to the polymer peaks at 2.2, 2.9, 3.6 and 3.8 ppm. The polymer was purified by dialysis (MWCO 3.5 kDa) and recovered by lyophilisation to yield a pink polymer, **4.08**, M_n (^1H NMR) = 35.2 kDa, M_n (SEC) = 32.3 kDa, $Đ_M$ = 1.11. ^1H NMR spectroscopy (400 MHz, 0.5 M NaCl in D_2O): δ (ppm): 0.8 – 2.4 (m, 884H, $CH_2C(CH_3)$ of polymer backbone, $CH_2C(CH_3)$ of polymer backbone, $CH_2CH_2SO_3^-$ of DMAPS side chain), 3.05-3.14 (br s, 250H, $CH_2CH_2SO_3^-$ of DMAPS side chain), 3.20 – 3.30 (br s, 750H, $N^+(CH_3)_2$ of DMAPS side chain), 3.60 – 4.10 (m, 500H, $N^+(CH_3)_2CH_2$ of DMAPS side chain, OCH_2CH_2N of DMAPS side chain), 4.40 – 4.70 (br s, 250H, OCH_2CH_2N of DMAPS side chain), 7.50 – 8.10 (m, 5H Ar*H* of CTA). ^{13}C NMR spectroscopy (125 MHz, 0.5 M NaCl in D_2O): δ (ppm): 18.5, 18.9, 19.6, 45.1, 47.5, 51.6, 59.2, 62.4, 63.4, 177.5, 178.1, 222.9.

Homopolymer **4.09**, M_n (^{1}H NMR) = 111.6 kDa, M_n (SEC) = 59.7 kDa, $Đ_M$ = 1.09. ^{1}H NMR spectroscopy (400 MHz, 0.5 M NaCl in D_2O): δ (ppm): 0.8 – 2.4 (m, 2800H, $CH_2C(CH_3)$ of polymer backbone, $CH_2C(CH_3)$ of polymer backbone, $CH_2CH_2SO_3^-$ of DMAPS side chain), 3.05-3.14 (br s, 800H, $CH_2CH_2SO_3^-$ of DMAPS side chain), 3.20 – 3.30 (br s, 2400H, $N^+(CH_3)_2$ of DMAPS side chain), 3.60 – 4.10 (m, 1600H, $N^+(CH_3)_2CH_2$ of DMAPS side chain, OCH_2CH_2N of DMAPS side chain), 4.40 – 4.70 (br s, 800H, OCH_2CH_2N of DMAPS side chain). ^{13}C NMR spectroscopy (125 MHz, 0.5 M NaCl in D_2O): δ (ppm): 18.5, 44.9, 45.1, 47.5, 51.6, 59.2, 62.2, 63.4, 177.4, 177.9.

4.5.9 Synthesis of PDMAPS-b-PMMA diblock copolymers

4.5.9.1 Synthesis of 4.10 via emulsion polymerisation

4.08 (0.1 g, 0.003 mmol, 1 equiv.) and ACVA (1 mg, 0.0004 mmol, 0.1 equiv.) were dissolved in 10 mL 0.5 M NaCl solution. The solution was then purged with nitrogen for 1 hour. MMA was bubbled with nitrogen separately for ten minutes and then 104 μL (0.1 g, 1 mmol, 350 equiv.) was transferred to the polymer solution. The reaction was stirred vigorously and placed in a pre-heated oil bath at 65 °C for 16 hours, by which point the solution had turned opalescent. The polymer was purified by dialysis and recovered by lyophilisation to yield **4.10**, M_n (^{1}H NMR) = 52.2 kDa, M_n (HFIP SEC) = 31.6 kDa, $Đ_M$ = 1.80. ^{1}H NMR spectroscopy (400 MHz, HFIP): δ (ppm): 0.8 – 2.7 (m, 845H, $CH_2C(CH_3)$ of polymer backbone, $CH_2C(CH_3)$ of polymer backbone, $CH_2CH_2SO_3^-$ of DMAPS side chain), 3.0 – 3.40 (m, 1000H, $CH_2CH_2SO_3^-$ of DMAPS side chain and $N^+(CH_3)_2CH_2$ of DMAPS side chain), 3.6 – 4.0 (br s, 1050H, $N^+(CH_3)_2CH_2$ of DMAPS side chain, OCH_2CH_2N of DMAPS side chain, OCH_3 of MMA side chain), 4.4 – 4.8 (br s, 250H, OCH_2CH_2N of DMAPS side chain). ^{13}C NMR spectroscopy (125 MHz, HFIP): δ (ppm): 15.2, 17.2, 44.3, 44.7, 51.4, 179.5, 180.1, 180.5.

4.5.9.2 Synthesis of 4.11 in HFIP

4.09 (0.5 g, 0.005 mmol, 1 equiv.), MMA (0.1 g, 0.05 mmol, 200 equiv.) and AIBN (0.15 mg, 0.0005 mmol, 0.1 equiv.) were dissolved in HFIP with a small amount of DMF as an internal ^{1}H NMR spectroscopy standard. The solution was bubbled with nitrogen for 40 minutes and placed in a preheated oil bath at 65 °C. The polymer was purified by precipitation into methanol followed by dialysis (MWCO 12 – 14 kDa) and recovered by lyophilisation to yield **4.11**, M_n (^{1}H NMR) = 121.7 kDa, M_n (HFIP SEC) = 73.1, $Đ_M$ = 1.34. ^{1}H NMR spectroscopy (400 MHz, HFIP): δ (ppm): 0.8 – 2.7 (m, 3360H, $CH_2C(CH_3)$ of polymer backbone, $CH_2C(CH_3)$ of polymer backbone, $CH_2CH_2SO_3^-$ of DMAPS side chain), 3.0 – 3.40 (m, 3200H, $CH_2CH_2SO_3^-$ of DMAPS side chain and $N^+(CH_3)_2CH_2$ of DMAPS side chain), 3.6 – 4.0 (br s, 1936H, $N^+(CH_3)_2CH_2$ of DMAPS side chain, OCH_2CH_2N of DMAPS side chain, OCH_3 of MMA side chain), 4.4 – 4.8 (br s, 800H, OCH_2CH_2N of DMAPS side chain).

4.6 References

1. A. B. Lowe and C. L. McCormick, *Chem. Rev.*, 2002, **102**, 4177-4190.
2. B. Yu, A. B. Lowe and K. Ishihara, *Biomacromolecules*, 2009, **10**, 950-958.
3. J. C. Salamone, W. Volksen, A. P. Olson and S. C. Israel, *Polymer*, 1978, **19**, 1157-1162.
4. V. M. Monroy Soto and J. C. Galin, *Polymer*, 1984, **25**, 121-128.
5. R. Hart and D. Timmerman, *J. Polym. Sci.*, 1958, **28**, 638-640.
6. S. Nakai, T. Nakaya and M. Imoto, *Makromol. Chem.*, 1977, **178**, 2963-2967.
7. H. Ladenheim and H. Morawetz, *J. Polym. Sci.*, 1957, **26**, 251-254.
8. Y. J. Shih, Y. Chang, A. Deratani and D. Quemener, *Biomacromolecules*, 2012, **13**, 2849-2858.
9. S. L. West, J. P. Salvage, E. J. Lobb, S. P. Armes, N. C. Billingham, A. L. Lewis, G. W. Hanlon and A. W. Lloyd, *Biomaterials*, 2004, **25**, 1195-1204.
10. Y. Chang, S. C. Liao, A. Higuchi, R. C. Ruaan, C. W. Chu and W. Y. Chen, *Langmuir*, 2008, **24**, 5453-5458.
11. Y. Chang, S. H. Shu, Y. J. Shih, C. W. Chu, R. C. Ruaan and W. Y. Chen, *Langmuir*, 2009, **26**, 3522-3530.
12. Y. J. Shih and Y. Chang, *Langmuir*, 2010, **26**, 17286-17294.
13. V. Butun, C. E. Bennett, M. Vamvakaki, A. B. Lowe, N. C. Billingham and S. P. Armes, *J. Mater. Chem.*, 1997, **7**, 1693-1695.
14. A. B. Lowe, N. C. Billingham and S. P. Armes, *Chem. Commun.*, 1996, **0**, 1555-1556.
15. A. B. Lowe, N. C. Billingham and S. P. Armes, *Macromolecules*, 1999, **32**, 2141-2148.
16. Z. Tuzar, H. Pospisil, J. Plestil, A. B. Lowe, F. L. Baines, N. C. Billingham and S. P. Armes, *Macromolecules*, 1997, **30**, 2509-2512.
17. J. V. M. Weaver, S. P. Armes and V. Butun, *Chem. Commun.*, 2002, 2122-2123.
18. P. A. Woodfield, Y. Zhu, Y. Pei and P. J. Roth, *Macromolecules*, 2014, **47**, 750-762.
19. M. S. Donovan, A. B. Lowe, T. A. Sanford and C. L. McCormick, *J. Polym. Sci., Part A: Polym. Chem.*, 2003, **41**, 1262-1281.
20. D. Wang, T. Wu, X. Wan, X. Wang and S. Liu, *Langmuir*, 2007, **23**, 11866-11874.
21. M. Arotçaréna, B. Heise, S. Ishaya and A. Laschewsky, *J. Am. Chem. Soc.*, 2002, **124**, 3787-3793.
22. H. Willcock, A. Lu, C. F. Hansell, E. Chapman, I. R. Collins and R. K. O'Reilly, *Polym. Chem.*, 2014, **5**, 1023-1030.

23. M. S. Donovan, B. S. Sumerlin, A. B. Lowe and C. L. McCormick, *Macromolecules*, 2002, **35**, 8663-8666.
24. M. d. R. Rodriguez-Hidalgo, C. Soto-Figueroa and L. Vicente, *Soft Matter*, 2013, **9**, 5762-5770.
25. W. F. Lee and C. C. Tsai, *Polymer*, 1994, **35**, 2210-2217.
26. D. N. Schulz, D. G. Peiffer, P. K. Agarwal, J. Larabee, J. J. Kaladas, L. Soni, B. Handwerker and R. T. Garner, *Polymer*, 1986, **27**, 1734-1742.
27. J. Seuring and S. Agarwal, *Macromol. Rapid Commun.*, 2012, **33**, 1898-1920.
28. P. Mary, D. D. Bendejacq, M. P. Labeau and P. Dupuis, *J. Phys. Chem. B*, 2007, **111**, 7767-7777.
29. F. Polzer, J. Heigl, C. Schneider, M. Ballauff and O. V. Borisov, *Macromolecules*, 2011, **44**, 1654-1660.
30. C. L. McCormick and A. B. Lowe, *Acc. Chem. Res.*, 2004, **37**, 312-325.
31. H. Wang, T. Hirano, M. Seno and T. Sato, *Eur. Polym. J.*, 2003, **39**, 2107-2114.
32. J. Jakes, *Collect. Czech. Chem. Commun.*, 1995, **60**, 1781-1797.
33. O. Colombani, M. Ruppel, M. Burkhardt, M. Drechsler, M. Schumacher, M. Gradzielski, R. Schweins and A. H. E. Müller, *Macromolecules*, 2007, **40**, 4351-4362.
34. J. P. Patterson, M. P. Robin, C. Chassenieux, O. Colombani and R. K. O'Reilly, *Chem. Soc. Rev.*, 2014.
35. M. B. Huglin and M. A. Radwan, *Makromol. Chem.*, 1991, **192**, 2433-2445.
36. D. J. Keddie, *Chem. Soc. Rev.*, 2014, **43**, 496-505.

Chapter Five

Self-assembly and responsive behaviour of sulfobetaine methacrylate containing block copolymers

5.1 Introduction

Stimuli-responsive polymers are of great interest due to their ability to undergo a change in hydrophobicity in response to a change in an external stimulus. One stimulus that has been investigated often within the literature is temperature. Thermo-responsive polymers can be divided into two classes, those which exhibit a Lower Critical Solution Temperature (LCST) and those which exhibit an Upper Critical Solution Temperature (UCST). The LCST is the critical temperature below which the components of a mixture are miscible in all proportions and above which two or more phases are formed. The UCST is the critical temperature below which the components of a solution are immiscible and above which one phase is formed (see Figure 5.1).[1] Often the LCST or UCST cloud point is reported, that is, the temperature at which macroscopic precipitation occurs.[2] The cloud point can be dependent upon the molecular weight of the polymer and the concentration of the solution.[3]

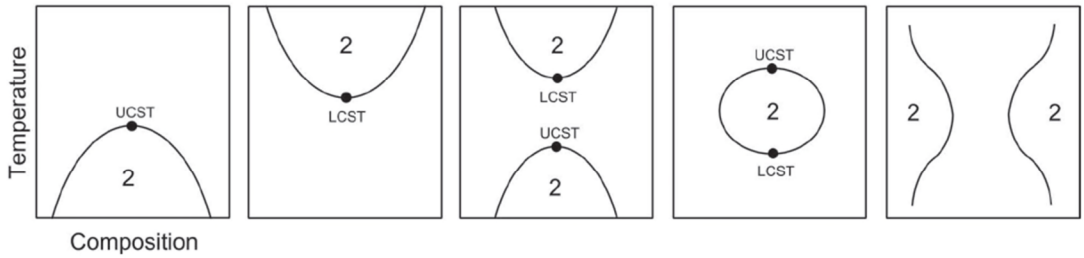

Figure 5.1: The different types of phase behaviour that polymer can display in solution. "2" denotes the two phase region[1]

LCST polymers have been widely studied within the literature and there are many examples of different polymers that display this behaviour.[2, 4-8] In contrast, reports of polymers exhibiting UCST type behaviour are far less common. In a recent review on thermo-responsive polymers 57 examples of LCST type polymers were given, compared to just 5 polymers that display UCST behaviour.[4]

One class of polymers which display UCST behaviour are betaines. Polymeric betaines are a class of zwitterionic polymers in which the cationic and anionic functional groups are located on the same monomer unit.[9] These polymers can undergo different types of self-

association, such as intrachain or interchain aggregation, leading to salt-responsive and thermo-responsive behaviour (see Figure 5.2).[1] These polymers are often insoluble in pure water at room temperature but become soluble upon addition of salt.[9-13] Betaines can be subdivided into three classes; sulfobetaines[13], phosphobetaines,[14] and carboxybetaines,[15] named for the group providing the negative charge.

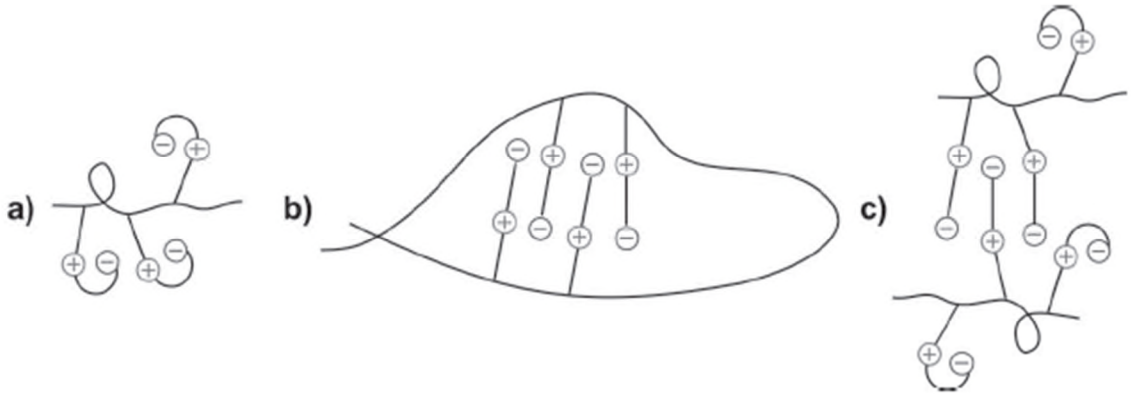

Figure 5.2: The different types of bonding that zwitterionic polymers can undergo, a) intragroup, b) intrachain, c) interchain[1]

The synthesis of polymeric betaines is discussed in Chapter Four. Betaine monomers have been shown to be polymerisable by Reversible Addition Fragmentation chain Transfer (RAFT) polymerisation, both as homopolymers and as block copolymers.[3, 10, 16-20]

Some sulfobetaine polymers display UCST behaviour with the UCST cloud point being related to the molecular weight of the polymer.[18, 21, 22] Unlike the LCST behaviour of polyNIPAM, the UCST behaviour of zwitterionic polymers can be considered to be enthalpy driven since the polymer-polymer and solvent-solvent coulombic interactions are much stronger than polymer-solvent interactions.[23]

Recently Willcock *et al.* investigated the differences in cloud point between linear homopolymers of the sulfobetaine monomer [2-(methacryloyloxy) ethyl] dimethyl-(3-sulfopropyl) ammonium hydroxide (DMAPS) and branched homopolymers of corresponding molecular weight. It was shown that at the same concentrations the cloud point of the branched DMAPS homopolymers was dramatically lower compared to that of

the linear DMAPS. For example a 100 kDa linear homopolymer of DMAPS displayed a cloud point of 23 °C at 1 mg mL^{-1} and 40 °C at 10 mg mL^{-1}. The branched 100 kDa DMAPS polymer did not display a cloud point at 1 mg mL^{-1} and at 10 mg mL^{-1} the cloud point was 33 °C. Addition of PEG as a comonomer into the branched particles eliminated the cloud point completely.[3]

To date there have been a limited number of examples of responsive block copolymers containing sulfobetaines. One response that has been exploited is the increased solubility of sulfobetaines in salt water rather than pure water.[9, 11, 12, 16, 17, 24] In one example from Donovan *et al*., several diblocks consisting of an *N*-methylacryamide sulfobetaine and dimethylacrylamide were synthesised by RAFT polymerisation and found to self-assemble into micelles in pure water but formed unimers upon dissolution into 0.5 M NaCl solution. The same paper reports the first example of a sulfobetaine containing triblock copolymer.[16]

There have been fewer examples that have looked at temperature as a stimulus for sulfobetaine containing copolymers.[18, 24-27] In an example by Che *et al*., random copolymers consisting of acrylamide and the sulfobetaine monomer, DMAPS, were synthesised by free radical polymerisation. The mole % of DMAPS present in the copolymers ranged from 10 to 25 %. These copolymers self-assembled in deionised water and the size of assemblies formed was found to be concentration dependant. As the concentration of copolymer in solution was increased from 0.1 to 1 mg mL^{-1}, the size of the assemblies decreased from *ca*. 50 nm to *ca*. 36 nm, until a minimum was achieved at 1 mg mL^{-1}. This initial decrease in size was explained by intra-chain interactions being more dominant at lower concentrations, leading to the shrinkage of individual polymer chains, and therefore a lower D_h. At concentrations higher than 1 mg mL^{-1} the size of the assemblies increased as inter-chain interactions were more prevalent, leading to inter-chain aggregation and so increasing the D_h.[24] An increase in the solution temperature from 25 °C to 60 °C resulted in an increase in D_h. This was rationalised as a decrease in the intrachain aggregation with increasing temperature and an increase in the interchain aggregation.

In a different example a schizophrenic block copolymer consisting of DMAPS and NIPAM was synthesised by Atom Transfer Radical Polymerisation ATRP. Cooling to below the UCST cloud point of the DMAPS block resulted in micelles with a hydrated NIPAM corona. At temperatures between the UCST cloud point of the polyDMAPS block and the LCST cloud point of the NIPAM block unimers were formed, and at temperatures above the LCST cloud point of the NIPAM, inverse micelles with the NIPAM block as the core and the DMAPS block as the hydrophilic corona were formed (see Figure 5.3).[26]

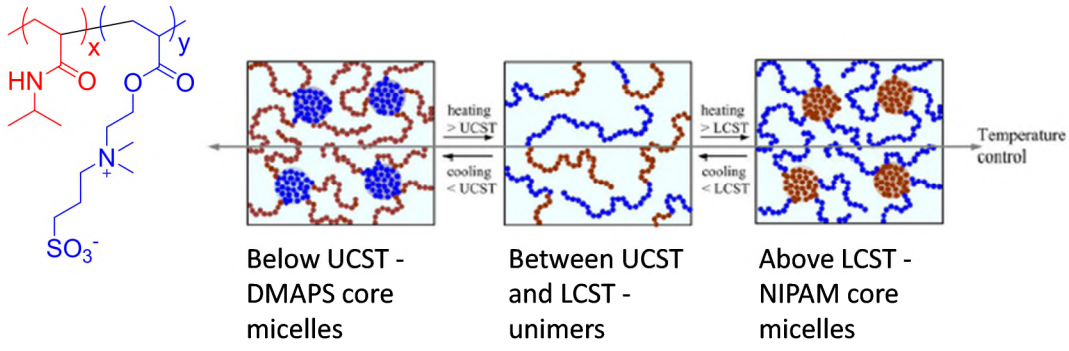

Figure 5.3: Figure depicting the schizophrenic thermo-responsive behaviour of a diblock copolymer of NIPAM and DMAPS and the different morphologies adopted at different temperatures[26]

A similar example utilises a diblock of a methacrylamido sulfobetaine and NIPAM synthesised by RAFT polymerisation. Since the sulfobetaine block displays UCST behaviour and the NIPAM block displays LCST behaviour, schizophrenic thermo-responsive behaviour was observed. By changing the temperature of the system the polymer was found to transition between a micelle, unimer and inverse micelle.[18]

5.2 Results and discussion

Chapter Four discussed the synthesis of sulfobetaine containing block copolymers. Herein we investigate the self-assembly and thermo-responsive behaviour of block copolymers containing the sulfobetaine monomer, DMAPS. This monomer was chosen as it has been shown to have UCST behaviour and be readily polymerised by RAFT.[3, 21, 24] The betaine-containing copolymers investigated contain hydrophilic blocks, hydrophobic blocks or both hydrophilic and hydrophobic blocks. In addition a triply responsive DMAPS-containing triblock copolymer is investigated.

5.2.1 Self-assembly behaviour of PEGMA-*b*-DMAPS diblock copolymer 4.02

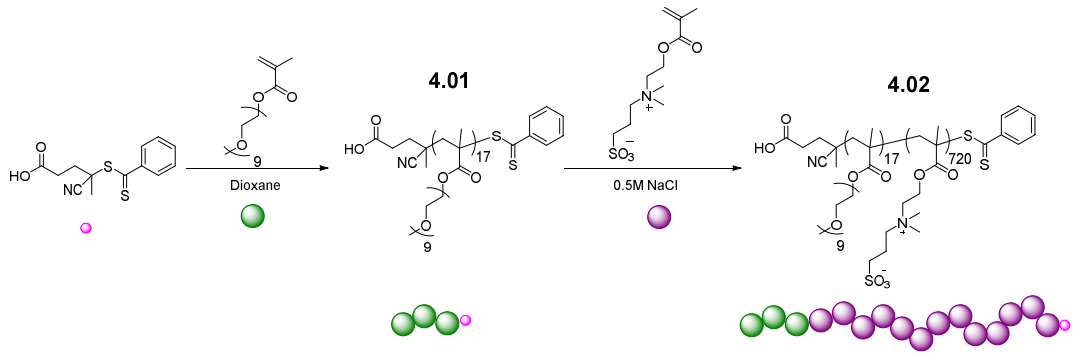

Scheme 5.1: Synthetic route to the diblock copolymer 4.02

A thermo-responsive diblock copolymer, **4.02** (M_n (^{1}H NMR) = 209 kDa, M_n (aqueous SEC) = 106.4 kDa, $Đ_M$ = 1.16) was synthesised by the RAFT chain extension from a PEGMA macro chain transfer agent (CTA) (**4.01**) with DMAPS in 0.5 M NaCl aqueous solution (see Scheme 5.1). Polymers of DMAPS have been shown to have increased solubility in salt solutions and display UCST type behaviour in salt-free aqueous media.[3, 20, 21, 24, 25, 28-30] The UCST cloud point of DMAPS is molecular weight dependant and so a block length of 720 DMAPS units was targeted as it has previously been reported that homopolymers of DMAPS of 200 kDa have a UCST cloud point of 26 °C at 1 mg mL^{-1}.[3] Therefore it is expected that below this temperature the DMAPS block of **4.02** will be hydrophobic and therefore self-assemble.

The self-assembly properties of the sulfobetaine containing diblock copolymer, **4.02**, were explored. Polymer **4.02** was self-assembled by direct dissolution into 0.5 M NaCl solution at 1 mg mL^{-1}. The use of the salt solution ensures that the DMAPS block is fully solubilised and therefore the polymer should exist as unimers in solution. Analysis by DLS gives a D_h of 18 ± 1 nm. Homopolymer **4.01** was also assembled by direct dissolution into water at 1 mg mL^{-1} and analysis of this solution shows a much smaller population where D_h = 5 ± 1 nm, showing that the increase in D_h of **4.02** is due to the increase in size of the polymer chains.

In order to investigate the self-assembly properties in salt-free water the polymer **4.02** was assembled by direct dissolution into 18.2 MΩ cm^{-1} water, at a concentration of 1 mg mL^{-1}. Analysis by DLS at 25 °C gives a population with a D_h of 74 ± 2 nm. This increase in size, compared to the polymer in salt solution, shows that the polymer has undergone self-assembly in a salt-free environment. The differences in size between **4.01**, **4.02** in 0.5 M NaCl and **4.02** in pure water at 25 °C can be seen in Figure 5.4.

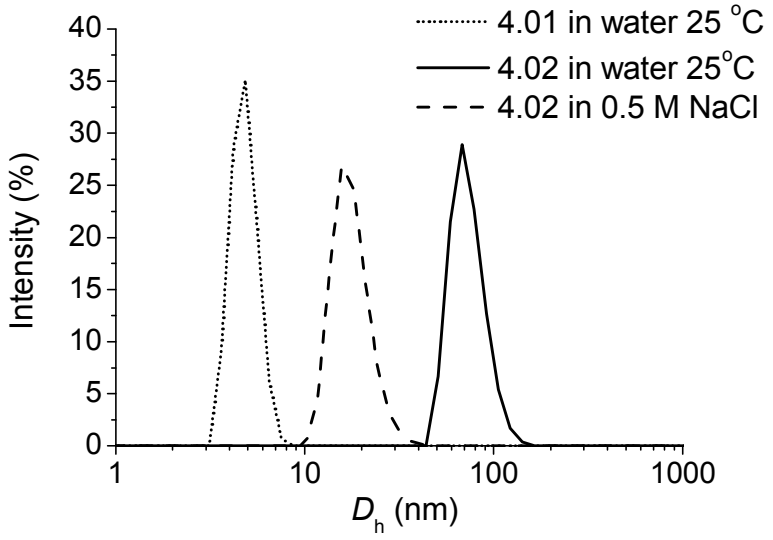

Figure 5.4: DLS traces showing the difference in D_h between the PEGMA homopolymer, 4.01, and the diblock, 4.02, in 0.5 M NaCl and in water

Analysis of these assemblies in water by dry-state TEM proved challenging. Several different methods of grid preparation were investigated. When 4 μL of sample at 1 mg mL^{-1}

were deposited onto the graphene oxide coated grids and left to dry only a film could be observed in TEM analysis. When, instead of allowing the sample to dry completely, most of the sample was removed after a short period of time (between 30 seconds – 2 minutes) by blotting, there was still a film present and relatively few micelles observed. When 4 μL of a solution of **4.02** at 0.1 mg mL^{-1} was deposited onto the grid and allowed to dry, spherical structures with an average diameter of 65 ± 8 nm were observed (see Figure 5.5). However, there was the presence of much smaller structures with an average diameter of 11 ± 2 nm (see Figure 5.6).

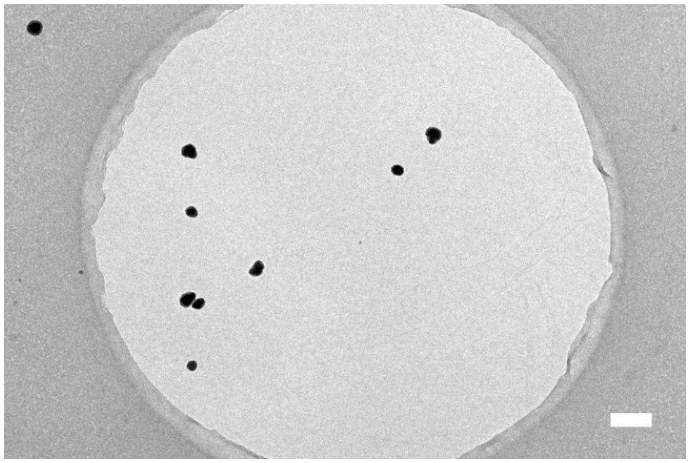

Figure 5.5: TEM image showing micelles formed from responsive diblock 4.02 below the transition temperature of the DMAPS block, scale bar = 200 nm, concentration = 0.1 mg mL^{-1}

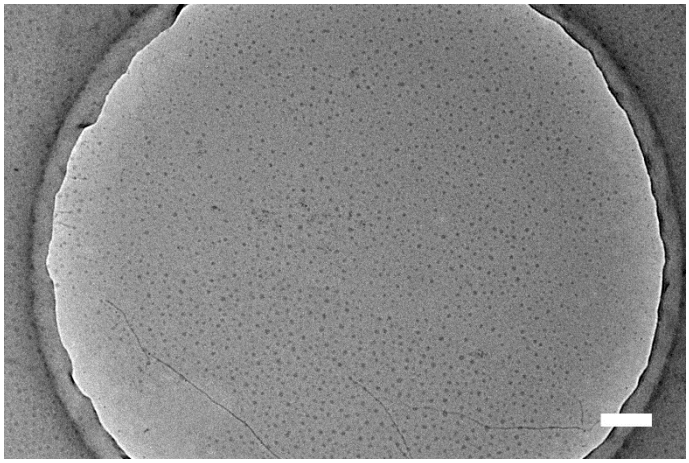

Figure 5.6: TEM image showing the smaller structures observed in a 0.1 mg mL^{-1} solution of 4.02, scale bar = 200 nm

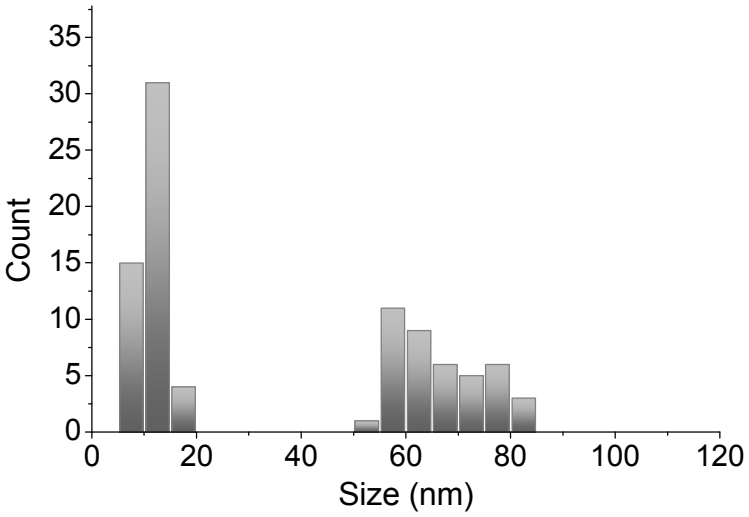

Figure 5.7: Distribution of sizes observed in TEM analysis of self-assembled 4.02 at 0.1 mg mL^{-1} showing the two populations

These smaller structures appear to be formed due to the dissociation of the self-assembled structures upon drying. The film observed at higher solution concentrations is most likely these smaller structures but the much higher concentration causes a film to be formed, rather than being able to individually image the particles. Even with varying the concentration of the sample used to make the TEM grids and the length of time before the sample was blotted off the grid, these smaller structures were always observed. Cryo-TEM allows for imaging of particles whilst frozen in solution and so avoids the drying process. Therefore this method may be advantageous in imaging the micelles without dissociation into the smaller structures. However as a result of on-going technical difficulties with the TEM instrumentation at this time we have not yet been able to utilise this method.

Based on the relative block lengths of the short hydrophilic PEGMA and the much longer thermo-responsive DMAPS block, it would be expected that below the UCST of the betaine, vesicles would be formed.[31-34] However, the sizes measured by DLS and morphology observed by TEM suggest that micelles are being formed, as based on the size of the unimers in salt solution, vesicles formed from this diblock copolymer would be expected to be much larger.

5.2.2 DLS and SLS characterisation of the self-assembled structures of 4.02

In order to further probe the morphology of the assembled structures, SLS and multi-angle DLS were utilised. The refractive index increment (*dn/dc*) was determined using a Shodex RI-101 deflection refractometer. A range of concentrations of polymer in 18.2 MΩ cm^{-1} water from 0.5 mg mL^{-1} to 2 mg mL^{-1} were measured. The refractive index response for each concentration was plotted against the concentration and the *dn/dc* calculated using the following equation.

$$\frac{dn}{dc} = \frac{slope \times n^o}{K}$$

Where the slope is the gradient of the linear fit of the refractive index response *vs* the concentration, n^o is the refractive index of the solvent and *K* is the instrument constant. The *dn/dc* was calculated for diblock copolymer **4.02** in water to be 0.127 mL g^{-1}.

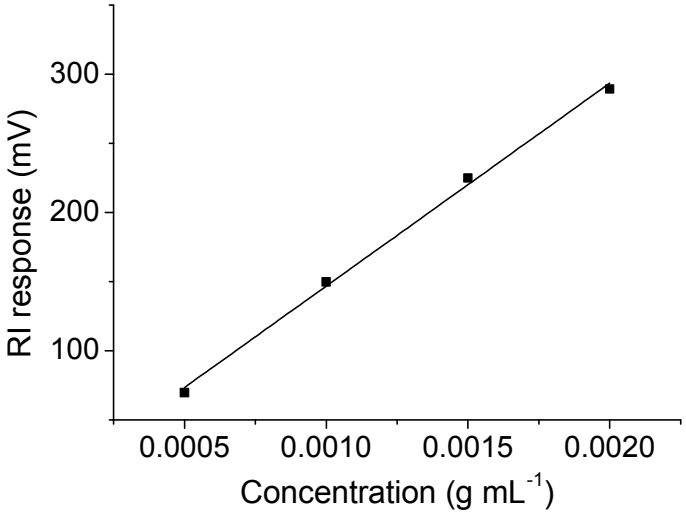

Figure 5.8 Plot of concentration *vs* RI response for diblock copolymer 4.02. The *dn/dc* was calculated as 0.127 mL g^{-1} using the slope of the linear fit

In order to determine the molecular weight, radius of gyration (R_g), aggregation number (N_{agg}) and hydrodynamic diameter (D_h) of the self-assembled nanostructures, solutions of **4.02** in water were analysed simultaneously by multi-angle DLS and SLS. Measurements were carried out on a multi-angle spectrometer, measured over 7 angles from 30 to 150° at a

range of concentrations between 0.5 – 2 mg mL^{-1}. The scattered intensity at each angle was measured for at least 100 s for each concentration and was then used to calculate the molecular weight (M_w) and radius of gyration (R_g).

$$\frac{Kc}{R_{\theta,fast}} = \frac{1}{M_w}\left(1 + \frac{q^2 {R_g}^2}{3}\right) + 2A_2c \quad (1)$$

where q is the scattering vector, A_2 is the second virial coefficient (related to polymer-polymer and polymer-solvent interactions), c is the polymer concentration, K is a constant calculated according to equation 2 and R_θ is the Rayleigh ratio of the sample calculated using equation 3.

$$K = \frac{4\pi^2 {n_{ref}}^2 \left(dn/dc\right)^2}{\lambda^4 N_A} \quad (2)$$

In equation 2 n_{ref} is the refractive index of the reference (toluene), dn/dc is the calculated refractive index increment of the polymer solution, λ is the wavelength of the laser (= 632.8 nm) and N_A is Avogadro's number.

As two modes of relaxation were observed for both assembled polymers in the correlation function, the resulting functions were analysed by REPES[35] in order to account for the fast and slow modes. The contribution of the slow mode to the total scattering intensity was found to be negligible and thus only scattering from the fast mode was used to determine M_w and R_g. The Rayleigh ratio for the fast mode ($R_{\theta,fast}$) was calculated as follows:

$$R_{\theta,fast} = A_{fast}(q)R_\theta = \frac{A_{fast}}{A_{fast}+A_{slow}}(q)\frac{I_{sample}(q) - I_{solvent}(q)}{I_{reference}(q)}R_{reference} \quad (3)$$

where $A_{fast}(q)$ is the scattered intensity contribution at a given angle from the fast mode of relaxation as determined by DLS, I_{sample}, $I_{solvent}$ and $I_{reference}$ are the scattered intensities by the sample, the solvent and the reference respectively at a given angle, q, and $R_{reference}$ is the Rayleigh ratio of the reference solvent, which in this case was toluene.

The inverse of the relaxation time for the fast mode divided by q^2 (τ_{fast}^{-1}/q^2) was plotted against the scattering vector squared (q^2) (see Figure 5.9). This was extrapolated to zero angle and the intercept yields the apparent diffusion coefficient. The apparent diffusion coefficient ($D_{t,\,app}$) can be related to the relaxation time by $D_{t,\,app}=(q^2\tau)^{-1}$.

The apparent diffusion coefficients were then plotted against polymer concentration and extrapolated to zero concentration to give the translational diffusion coefficient. Using the Stokes-Einstein equation yields the hydrodynamic diameter.

$$D_h = \frac{k_b T}{3\pi\eta D_t}$$

In the above equation, D_h is the hydrodynamic diameter, k_b is the Boltzmann's constant, T is the temperature (in K), η is the viscosity of the solvent and D_t is the translational diffusion coefficient.

Copolymer **4.02** in water at 1 mg mL^{-1} was found to have an apparent diffusion coefficient of 5.36 x 10^{-12} m^2 s^{-1} which corresponds to a hydrodynamic diameter of 90 nm (see Figure 5.9).

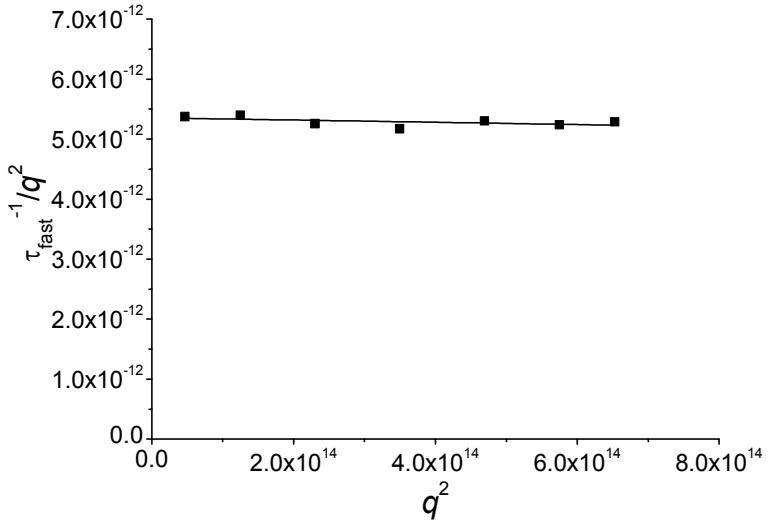

Figure 5.9: Plot of τ_{fast}^{-1}/q^2 *vs* q^2 for self-assembled micelles based on diblock copolymer 4.02 at 1 mg mL^{-1} in water, determined at 20 °C (D_h = 90 nm)

The diffusion coefficient for each concentration, apparent D_t, was plotted against concentration and the intercept of the linear fit, D_t, was found to be 4.98 x 10^{-12} m^2 s^{-1} which corresponds to a hydrodynamic diameter of 97 nm (see Figure 5.10). This size is slightly larger than that calculated for a solution of 1 mg mL^{-1} as it is slightly skewed by interactions between the particles at the higher concentrations.[36]

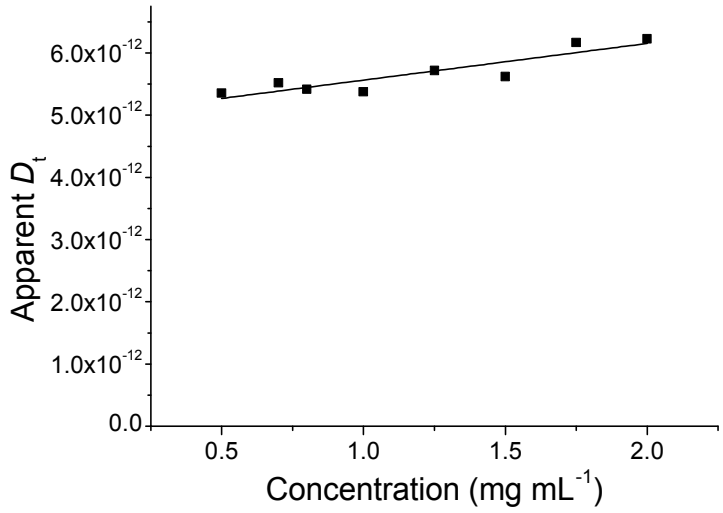

Figure 5.10: Plot of apparent *D*t *vs* concentration for diblock 4.02. The intercept gives the translational diffusion coefficient which is used to calculate the hydrodynamic diameter using the Stokes-Einstein equation, (D_h = 97 nm)

The self-assembled micelles from **4.02** were also analysed by SLS to determine the molecular weight, radius of gyration (R_g) and the aggregation number (N_{agg}) (equation 2). R_g can be determined for each concentration from the slope of $Kc/R_{\Theta,\ fast}$ *vs* q^2, and N_{agg} by comparing the molecular weight of the assembled structure to that of an individual polymer chain.[37] $Kc/R_{\Theta,\ fast}$ was plotted against q^2 for each concentration and each plot extrapolated to zero angle. The extrapolated $Kc/R_{\theta,\ fast}$ value was then plotted against concentration and extrapolated to zero concentration, which was used to determine the absolute molecular weight of the nanostructure (see Figure 5.11). The absolute molecular weight of the self-assembled structures of **4.02** was determined to be 28 MDa. This corresponds to an N_{agg} of 108 polymer chain per micelle, using an absolute molecular weight for an individual polymer chain of 259 kDa, as determined by SLS (Chapter 4).

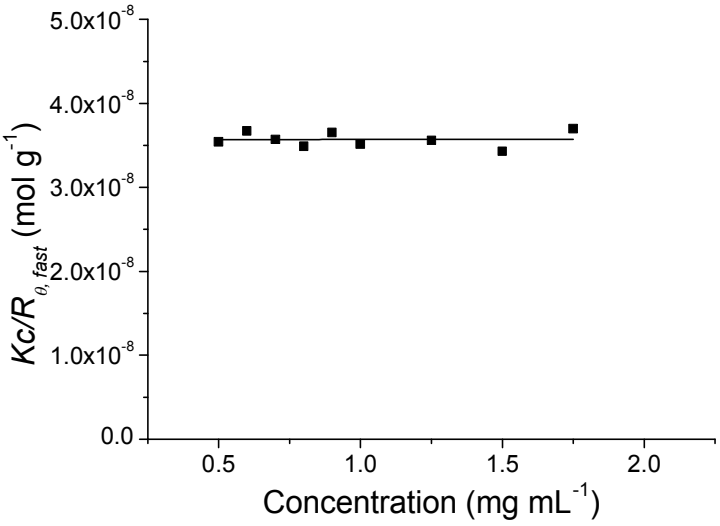

Figure 5.11: Plot of $Kc/R_{\theta, fast}$ *vs* concentration for self-assembled solutions of 4.02. The M_w of the micelles was calculated using the intercept of the linear fit to the SLS data and found to be 28 MDa

Due to attractive and repulsive forces between the particles at different concentrations the apparent R_g was used.[36] For a vesicular structure an R_g/R_h ratio of 1 is expected, whereas for a hard sphere a ratio of *ca*. 0.775 is instead expected.[38] The R_g/R_h ratio for **4.02** at 1 mg mL^{-1} was calculated to be 0.84. This suggests that the structures are not vesicular in nature and are closer in structure to hard spheres.

5.2.3 Thermo-responsive behaviour of self-assembled 4.02

A solution of **4.02** in 18.2 MΩ cm^{-1} water at 1 mg mL^{-1} was formed by direct dissolution of the polymer into the water at room temperature. This solution was then heated in the DLS instrument and the size measured every 2 °C from 4 to 50 °C, with 5 minutes of equilibration at each temperature. The size increased from *ca*. 80 nm to *ca*. 140 nm between 4 °C and 36 °C. At 38 °C the size decreased to *ca*. 15 nm (see Figure 5.12). It is interesting to note the swelling that the micelle undergoes before dissolution into unimers. The solution was allowed to cool to room temperature and then analysed a second time with the same heating procedure.

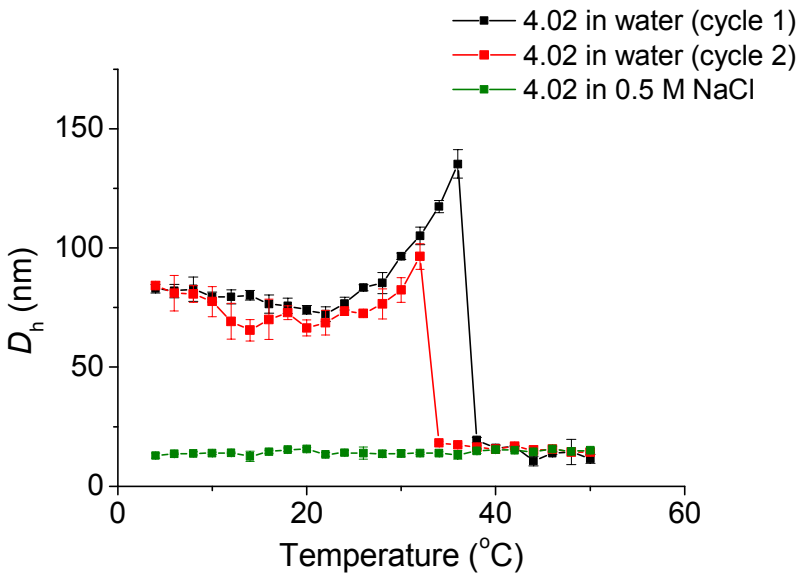

Figure 5.12: Graph showing the change in D_h with temperature for diblock copolymer 4.02 in water and in 0.5 M NaCl solution

During this second cycle the swelling before dissociation was much less pronounced. This can be rationalised by considering that direct dissolution into water below the transition temperature of the polymer will cause kinetically trapped micelles with a completely dehydrated core to form. Therefore as the micelle solution is heated initially and the hydrophobic DMAPS block starts to become hydrophilic, water will move to enter the core of the micelle, resulting in swelling. However, after the initial heating cycle the polymer will have been molecularly dissolved at the high temperatures and will form more thermodynamically favourable micelles upon cooling. Since the DMAPS block retains some hydrophilicity even at low temperatures (see section 5.2.4) there will be water present in the core of the reformed micelles. This explains the reduced swelling seen in the second heating cycle. The transition temperature is also altered between the two heating cycles. In the second cycle the micelle to unimer transition occurs at 34 °C. Therefore it was decided that the preferred way to self-assemble **4.02** to obtain reproducible results was by direct dissolution with gentle heating to aid dissolution and then allowing to cool to room temperature before analysis.

A solution of **4.02** dissolved in 0.5 M NaCl at 1 mg mL^{-1} was also analysed by DLS over the same temperature range. No size change was observed, showing that the addition of salt supresses the thermo-responsive behaviour of DMAPS (see Figure 5.12).

To confirm that the morphology adopted at higher temperatures is indeed unimers, the size of **4.02** at 50 °C was compared to that of the polymer in 0.5 M NaCl, as polyDMAPS is soluble in salt solution, and the similar sizes seen shows that unimers are being formed at higher temperatures (see Figure 5.13).

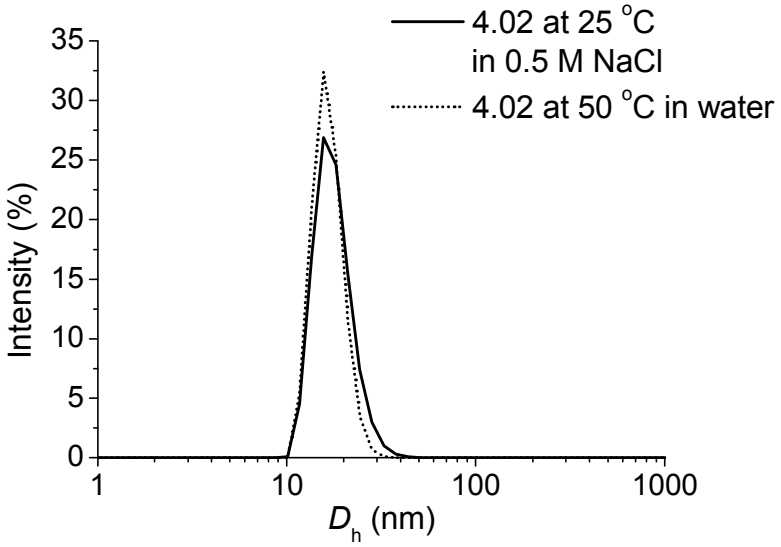

Figure 5.13: DLS traces showing the D_h of the polymeric unimers of diblock copolymer 4.02 in 0.5 M NaCl solution *vs* the D_h of the unimers at 50 °C

5.2.4 Studying the transition by variable temperature ^{1}H NMR spectroscopy

In order to investigate why the diblock copolymer forms micelles rather than the expected vesicles, variable temperature ^{1}H NMR spectroscopy was performed. A higher concentration of polymer solution was used to ensure reliable spectroscopic results were obtained. An ^{1}H NMR spectroscopy sample of **4.02** at 5 mg mL^{-1} was made in D_2O with an internal standard of DMF. The sample was analysed in the DLS to check that the micelles still undergo the micelle to unimer transition at this higher concentration (Figure 5.14).

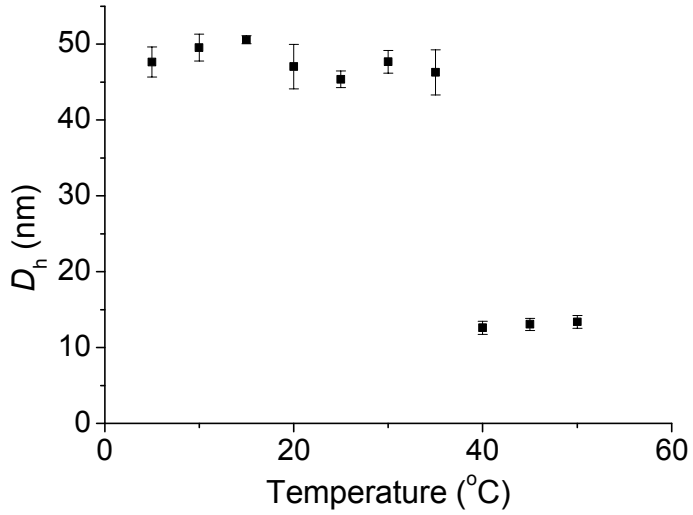

Figure 5.14: DLS analysis with temperature shows that diblock 4.02 still undergoes the micelle to unimer transition at 5 mg mL^{-1}

^{1}H NMR spectroscopy was performed at temperatures ranging from 5 to 65 °C with 10 °C increments. A small amount of DMF was used as an internal standard to allow calculation of the percentage hydrophilicity of the polymer. The COH peak of the DMF at 8.0 ppm was set at an integration of 1 and three separate peaks relating to the DMAPS block at 2.7, 3.7 and 4.1 ppm were integrated relative to this DMF peak (see Figure 5.15). The integration of each peak at the highest temperature was assumed to be 100% hydrophilic, *i.e*. all the DMAPS side chains are hydrated. The integrations of the same peaks at different temperatures were compared to these "100%" peaks to calculate the percentage solubilised and therefore hydrophilic present in the polymer at that temperature.

Figure 5.16 shows how the integrations of the DMAPS peaks change with temperature. The betaine block never becomes fully hydrophobic, even at temperatures of 5 °C approximately 30% of the block remains hydrophilic. Therefore the amphiphilic balance of the polymer is not directly proportional to the block lengths of the PEGMA and DMAPS.

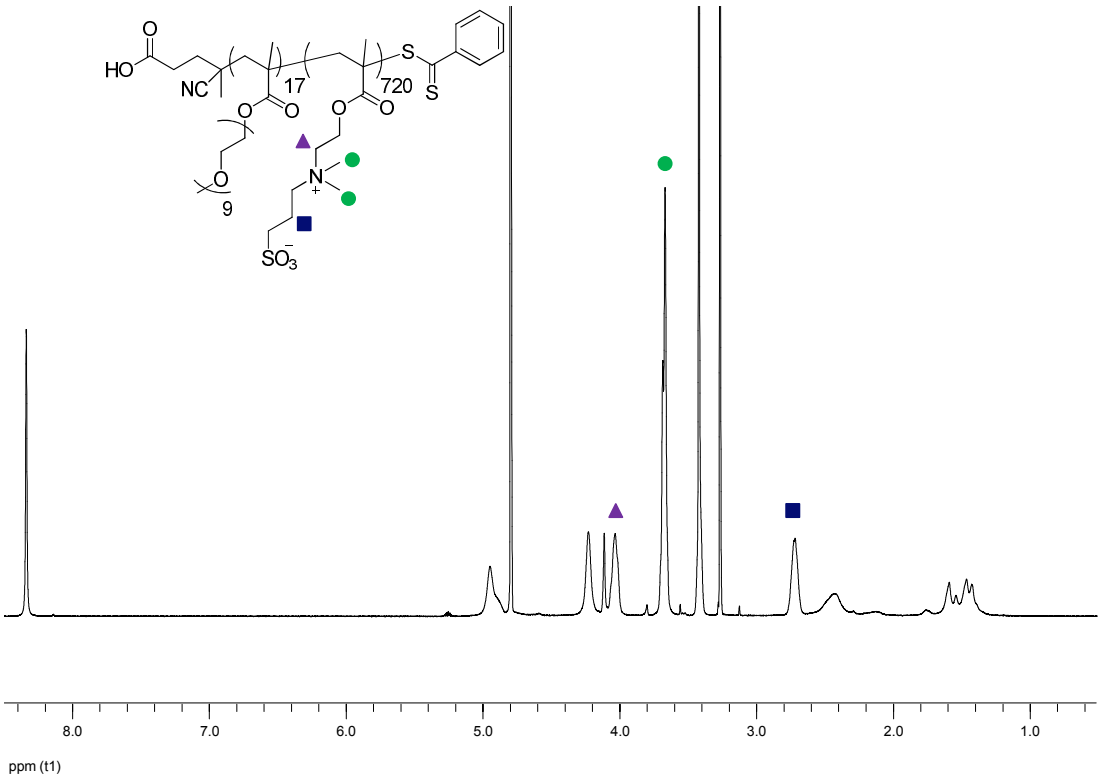

Figure 5.15: ^{1}H NMR spectrum of 4.02 in D_2O, showing the three DMAPS peaks used for calculating remaining hydrophilicity, recorded at 65 °C and 500 MHz

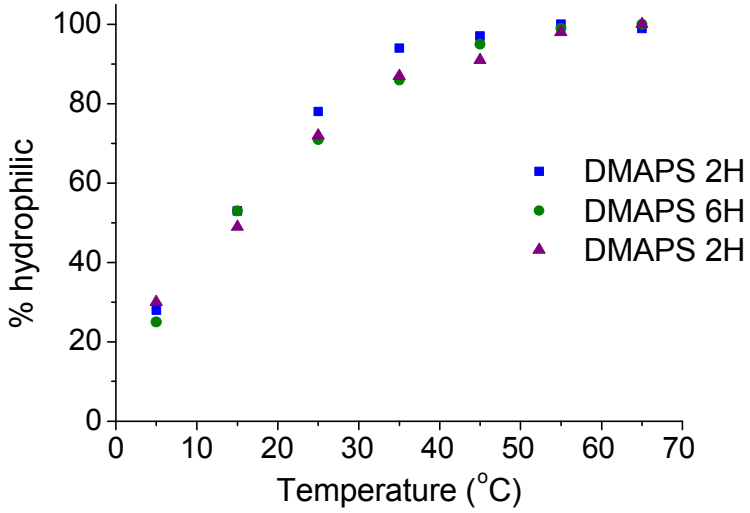

Figure 5.16: Graph showing how the % hydrophilicity of the DMAPS block of 4.02 changes with temperature

If the DMAPS block were fully hydrophobic, the weight fraction of the diblock copolymer **4.02** that is hydrophilic would be 3.75%. However, with 30% of the DMAPS retaining hydrophilicity, the hydrophilic weight fraction of the polymer is 37%. We propose that this

explains why micelles are formed, rather than vesicles. This is similar behaviour to that seen by Willcock *et al*. when comparing the cloud point of linear homopolymers of DMAPS and linear copolymers of PEGMA and DMAPS. Linear homopolymers of DMAPS between 50 and 500 kDa displayed UCST cloud points from 11 - 43 °C. Incorporation of 5 mol% PEGMA into similar sized polymers resulted fully soluble polymers with no cloud points being observed.[3]

5.2.5 Characterisation of 4.02 by SAXS

Small angle neutron scattering (SAXS) is a technique where the elastic scattering of X-rays by a sample are recorded at very low angles, providing information on the size and shape of nanoparticles.[36] SAXS analysis was carried out by Dr Anaïs Pitto-Barry at the Australian Synchrotron facility. Variable temperature SAXS studies were performed in order to further study the morphology of the diblock copolymer assemblies of **4.02** between 5 and 50 °C. A solution of **4.02** at 1 mg mL^{-1} in 18.2 MΩ cm^{-1} water was placed in a 1.5 mm diameter quartz capillary. The capillary was held in a temperature controlled sample holder and temperatures of 5, 10, 19, 24, 28, 32, 36, 40, 45 and 50 °C were reached. The sample was allowed to equilibrate for 10 minutes at each temperature before measurement. The measurements were collected at a sample to detector distance of 3.252 m to give a q range of 0.0015 to 0.07 $Å^{-1}$, where q is the scattering vector and is related to the scattering angle (2θ) and the photon wavelength (λ) by the following equation:

$$q = \frac{4\pi \sin(\theta)}{\lambda}$$

All patterns were normalised to fixed transmitted flux using a quantitative beamstop detector. The scattering from a blank (H_2O) was subtracted for each measurement. The two-dimensional SAXS images were converted in one-dimensional SAXS profile (*I(q) versus q*) by circular averaging, where *I(q)* is the scattering intensity. The functions used for the fitting from the NIST SANS analysis package were "Debye"[39] and "Core-Shell with Constant

Core/Shell Ratio" models.[40-42] ScatterBrain and Igor software were used to plot and analyse data. The scattering length density of the solvent and the monomers were calculated using the "Scattering Length Density Calculator" provided by NIST Center for Neutron Research Limits for *q* range were applied for the fitting from 0.002 to 0.05 $Å^{-1}$.[43]

A core-shell spherical micelle model was found to fit well up to 10 °C, giving the dimensions of an assembly with a core radius of 17-20 nm and a hydrated shell thickness of 6-10 nm. At 45 °C and above, a unimer model was found to fit well, with an R_g of *ca* 11 nm (see Figure 5.17). Between 19 and 36 °C, a linear combination of these two models suggested the coexistence of both unimers and micelles (see Table 5.1). The number of unimers in solution dramatically increases at 36 °C which correlates well with the transition temperature seen by DLS analysis. This coexistence of both micelles and unimers at may help explain the dissociation observed during TEM analysis of the assembled solutions (see section 5.2.1).

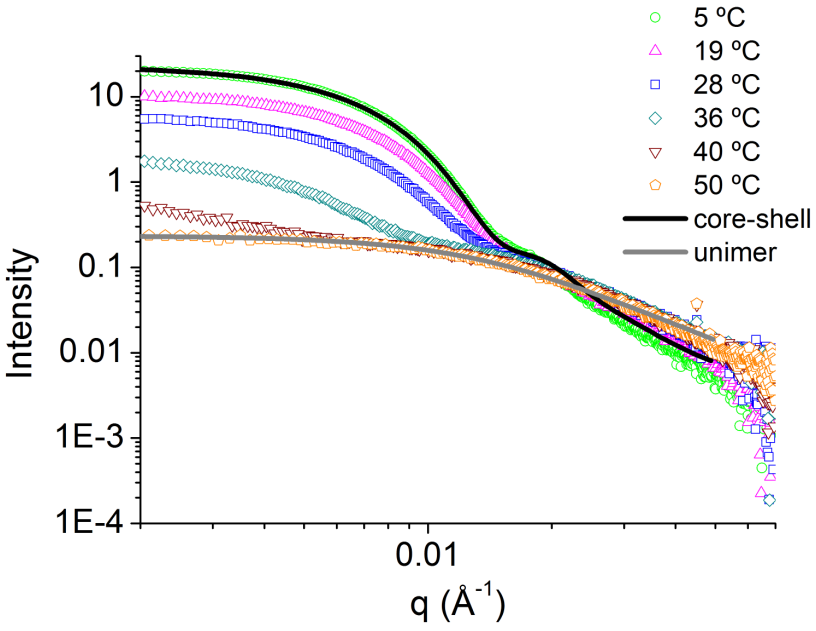

Figure 5.17: SAXS profiles and fits for a solution of 4.02 in water at 1 mg mL^{-1} between 5 and 50 °C

Table 5.1: Showing the morphologies present at each temperature and the ratio of micelles to unimers in a solution of 4.02 in water at 1 mg mL^{-1}as calculated by SAXS analysis

Temp. (°C)	Morphology (Ratio micelle:unimer)	Volume fraction (Ratio micelle:unimer ×10^4)	Number of micelles (/Vtot ×10^{10})
5	Micelles	27:0	344
10	Micelles	20:0	261
19	Micelles and unimers	1:337	129
24	Micelles and unimers	1:40	86
28	Micelles and unimers	1:423	182
32	Micelles and unimers	1:347	15
36	Micelles and unimers	1:3831	3
40	Micelles and unimers	1:4460	1
45	Unimers	0:2388	0
50	Unimers	0:2341	0

5.2.6 Closer examination of the micelle to unimer morphology transition

As the SAXS results suggest a combination of micelles and unimers close to the transition temperature, the size was again measured by DLS with heating. The equilibration time at each temperature was increased to 20 minutes. Figure 5.18 shows the D_h obtained from each of the 5 measurements across the transition range to show to appearance of two populations. At 30 °C all 5 measurements give D_h *ca*. 80 nm. At 32 °C three of the measurements show the larger population and two show unimers. As the temperature increases the unimeric population becomes dominant, so at 36 °C only one of the 5 measurements shows the larger population. This is in agreement with the results from SAXS analysis, shown in Table 5.1, which quantifies the ratio of the two populations.

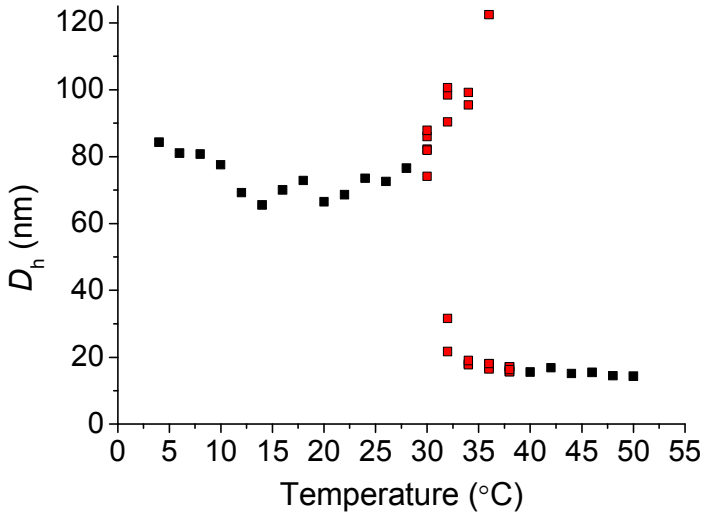

Figure 5.18: Graph showing the D_h of the two populations seen during the transition process of 4.02 (red fill) with all 5 measurements plotted. The average size is plotted for the other temperatures (black) for clarity.

5.2.7 Utilising the morphology transition of 4.02

The micelle to unimer transition can be utilised to encapsulate and release hydrophobic cargo in response to temperature. To test this, Nile Red (a hydrophobic dye) was encapsulated into the micelles by simply stirring, at 1 mg mL^{-1}, in a 1 mg mL^{-1} polymer micelle solution overnight. Excess Nile Red was removed by filtering through a 0.45 μm filter. The fluorescence of the micelle solution was monitored (λ_{ex} = 550nm, λ_{em} = 575 nm). To release the dye the micelle solution was heated at 36 °C for 5 minutes. The hot solution was then filtered to remove the released dye that precipitated and again the fluorescence response of the solution was measured. After heating and filtering there was a much smaller fluorescence response (see Figure 5.19). The colour change of the solution, from purple to colourless upon heating, was also easily observed (Figure 5.20).

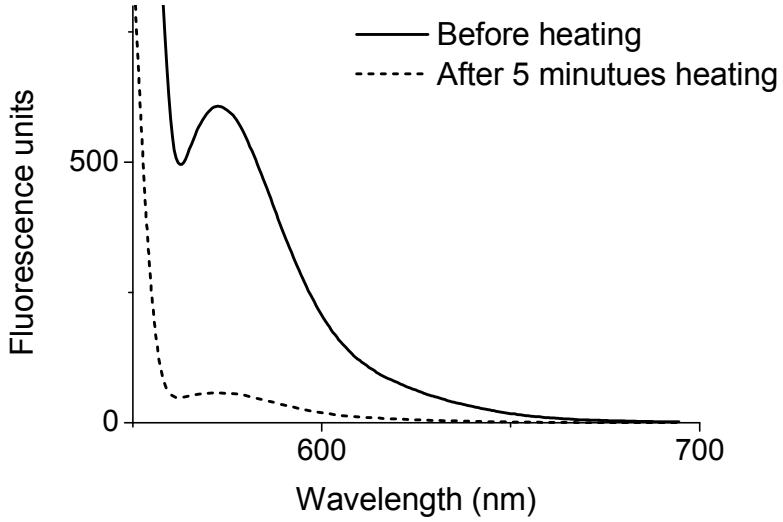

Figure 5.19: Graph showing the decrease in fluorescence after heating the micelle solution of 4.02 at 36 °C for 5 minutes

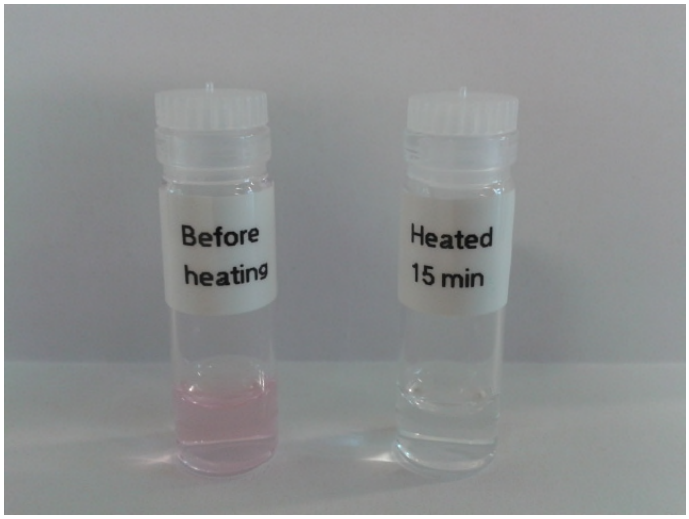

Figure 5.20: Left) encapsulated Nile Red in micelles of 4.02 Right) micelle solution after heating to unimers and removal of Nile Red by filtration

The solution was heated for an hour, with samples being removed and filtered every 15 minutes in order to see if the amount of dye released would increase, or whether a maximum level of release would be reached. As can be observed in Figure 5.21, the level of fluorescence decreases for the first 30 minutes, after which point the fluorescence response increases slightly. This could be attributed to the Nile Red becoming slightly more soluble in the polymer solution as it is heated for longer and therefore less being removed during filtration.

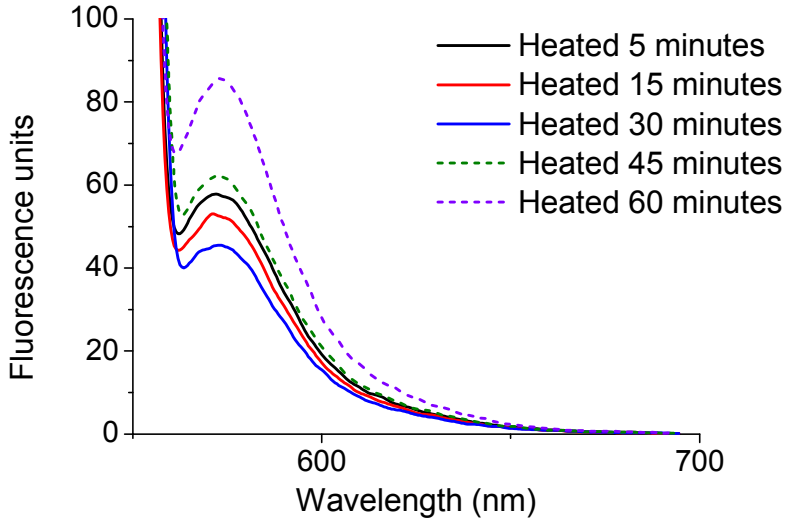

Figure 5.21: Graph showing how the length of time the micelle solution is heated for affects the residual amount of fluorescence

To ensure that the decrease in fluorescence was due to the Nile Red being released from the micelles and not due to the micelle solution being filtered multiple times, a further control experiment was carried out. The micelle solution was filtered twice without heating, and it can be seen that although the fluorescence response decreases slightly (due to loss of micelles onto the filter) the decrease is not significant (Figure 5.22).

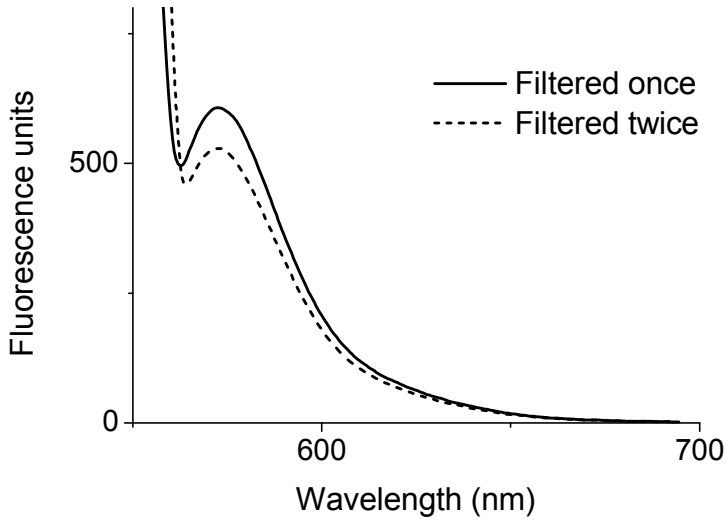

Figure 5.22: Graph showing the affect filtering the micelle solution (4.02) multiple times has on the fluorescence response

In order to investigate whether loading the micelles with Nile Red affects the transition from micelle to unimer, a solution of micelles of **4.02** at 1 mg mL^{-1} was stirred overnight with Nile Red. The solution was filtered and then the size change with temperature was analysed by DLS. It can be seen that the micelles are larger when loaded with Nile Red but the transition temperature remains unchanged (see Figure 5.23).

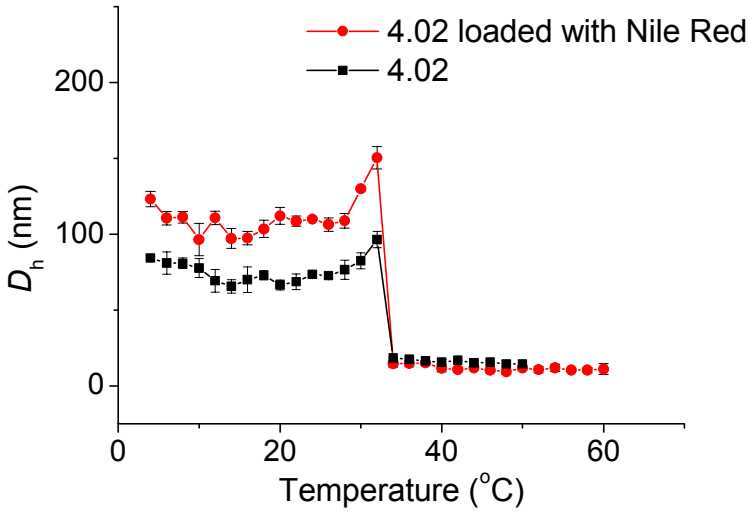

Figure 5.23: Comparison of the transition from micelle to unimer of self-assembled solutions of 4.02 with (red) and without (black) Nile Red

5.2.8 Self-assembly behaviour of PEGMA-*b*-DMAPS-*b*-PEGMA triblocks

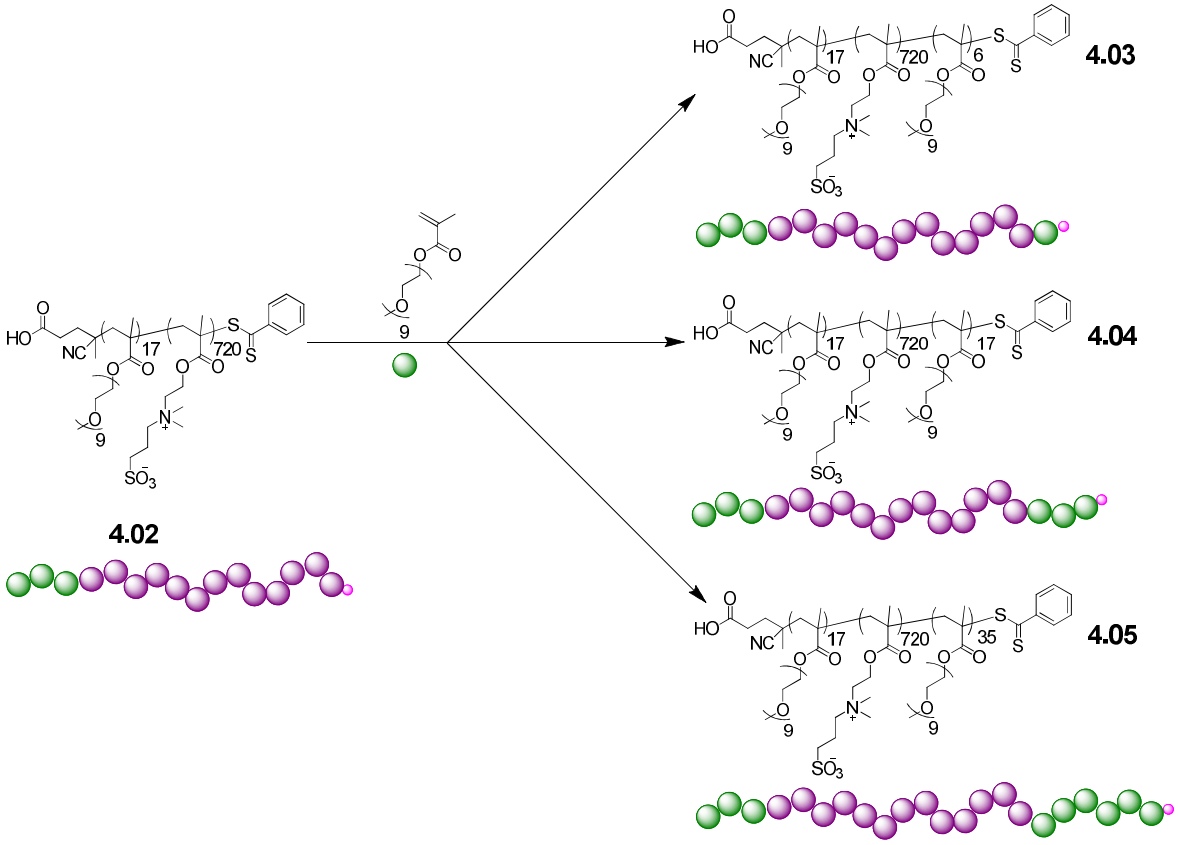

Scheme 5.2: Schematic showing the chain extension of 4.02 to the ABA triblock copolymers 4.03, 4.04 and 4.05

Sulfobetaine containing triblocks copolymers have barely been explored within the literature[16] and may provide some more interesting self-assembly properties. In order to investigate the effect that the addition of a third, hydrophilic, block has on the self-assembly and thermo-responsive properties of the polymer, a series of triblock copolymers were synthesised by chain extension of **4.02** with varying amounts of PEGMA to yield **4.03** with 6 PEGMA units making up the third block, M_n (^{1}H NMR) = 211.9 kDa, M_n (Aqueous SEC) = 103.8 kDa, $Đ_M$ = 1.18. **4.04**, with a third block length of 17 PEGMA units, M_n (^{1}H NMR) = 217.2 kDa, M_n (Aqueous SEC) = 101.2 kDa, $Đ_M$ = 1.20 and **4.05** bearing 35 PEGMA units as the third block, M_n (^{1}H NMR) = 225.8 kDa, M_n (Aqueous SEC) = 95.2 kDa, $Đ_M$ = 1.22.

5.2.8.1 Thermo-responsive behaviour of 4.03

Triblock copolymer **4.02** was self-assembled by direct dissolution into 18.2 MΩ cm^{-1} water at room temperature at a concentration of 1 mg mL^{-1}. Analysis by DLS at 25 °C shows a population with D_h = 88 ± 6 nm. The morphology of the polymer assemblies at varying temperature was studied by DLS. A solution at 1 mg mL^{-1} was analysed by DLS with heating from 4 °C to 50 °C with measurements being taken every 2 degrees. The structures remain a constant size (*ca* 86 nm) until 24 °C, at which point the size increases until the assemblies are *ca*. 200 nm at 38 °C. The micelle to unimer transition occurs at 40 °C. This is higher than that observed for the diblock copolymer **4.02** (34 °C) but the swelling behaviour is similar. As for **4.02**, the self-assembled solution of **4.03** was allowed to cool to room temperature and then reanalysed by DLS with heating. The second heat cycle shows little swelling and the micelle to unimer transition occurs at 36 °C (see Figure 5.24).

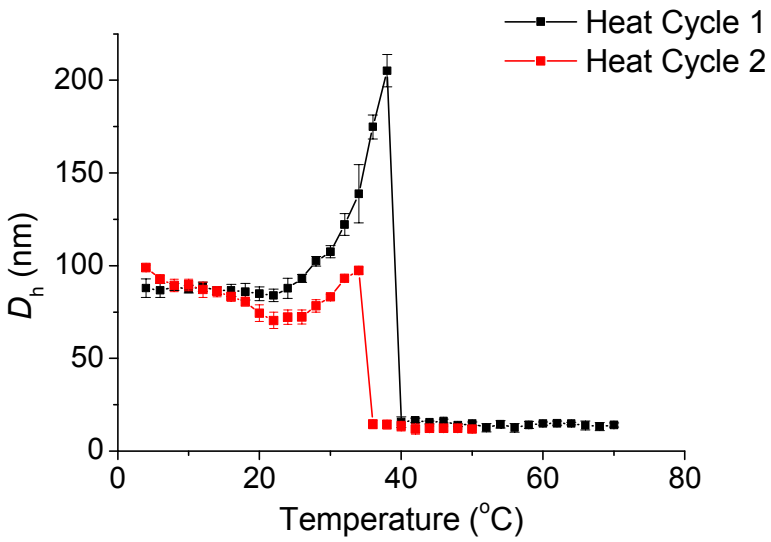

Figure 5.24 Graph showing change in D_h with temperature for the heating cycles 1 and 2 of triblock copolymer 4.03 in water at 1 mg mL^{-1}

Therefore once again the preferred method of self-assembly for these types of polymers is direct dissolution with gentle heating (*ca*. 40 °C). The heating causes the polymers to molecularly dissolve and therefore more thermodynamically favourable assemblies will form upon cooling, with the cores retaining some hydration, due to the DMAPS block not

becoming fully hydrophobic. Direct dissolution into water below the transition temperature of the polymer causes frozen structures to form, with dehydrated cores.

The two different self-assembly methods were investigated using SLS to investigate whether the molecular weight, radius of gyration (R_g) and the aggregation number (N_{agg}) change depending on the temperature at which self-assembly occurs.

A solution of **4.03** at 1 mg mL^{-1} which was assembled directly into water at room temperature was found to have a molecular weight (M_w) of 13.7 MDa, which relates to apparent N_{agg} of 47 and the R_g/R_h was calculated to be 0.68. The D_h measured by multi-angle DLS was 95 nm. The same solution was analysed by SLS after heating to 40 °C for 3 minutes and then cooling to room temperature (see Figure 5.25). Analysis by SLS gave a molecular weight of 23.3 MDa at 1 mg mL^{-1}. This relates to a N_{agg} of 81 polymer chains per micelle. In addition the R_g/R_h value at 1 mg mL^{-1} was 0.75 and the D_h = 74 nm. This decrease in hydrodynamic diameter with an increase in aggregation number suggests that after heating to unimers, micelles are formed that are closer to equilibrium and therefore the structures formed by direct dissolution at room temperature are more likely to be frozen aggregates.

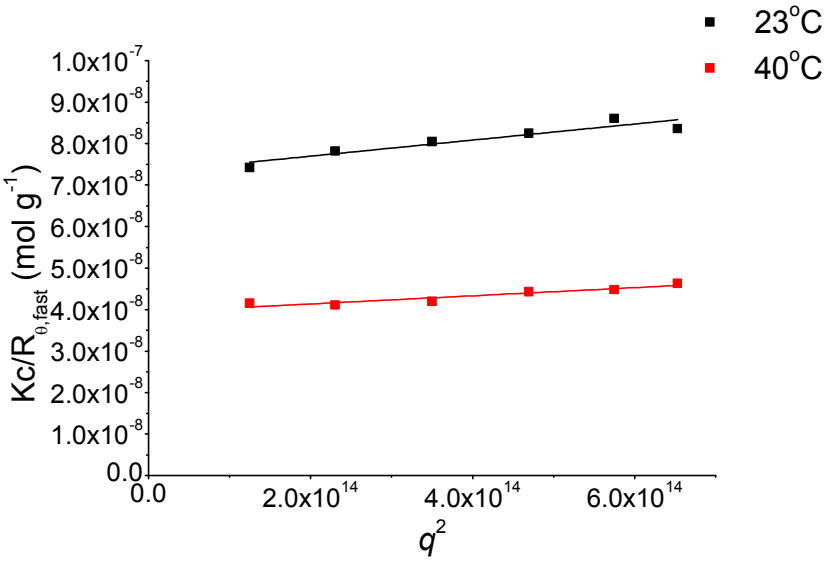

Figure 5.25 Plot of $Kc/R_{\theta, fast}$ *vs* q^2 for 1 mg mL^{-1} solutions of 4.03 assembled at either room temperature or at 40 °C. The M_w of the micelles was calculated using the inverse of the intercept

To investigate whether the micelles reform upon cooling, the size change during a cooling cycle was measured. A solution of **4.03** at 1 mg mL^{-1} was cooled from 60 °C to 4 °C with the size measured every 2 °C.The temperature at which the micelles reform is lower than that at which they dissociate, indeed they reform at 26 °C whereas they dissociate at 34 °C. The temperature at which they reform is the temperature at which the micelles start to swell slightly when heated. It is also interesting to note that the sizes of the micelles upon reforming (61 ± 5 nm) are smaller than that when they are formed by direct dissolution with gentle heating (76 ± 3 nm) (see Figure 5.26). This suggests that forming the micelles from molecularly dissolved unimers can form more stable particles, and the rate of cooling can affect the size of the particles obtained. Note that the cooling rate of the DLS is slower and more controlled than simply leaving the solution to cool on the bench.

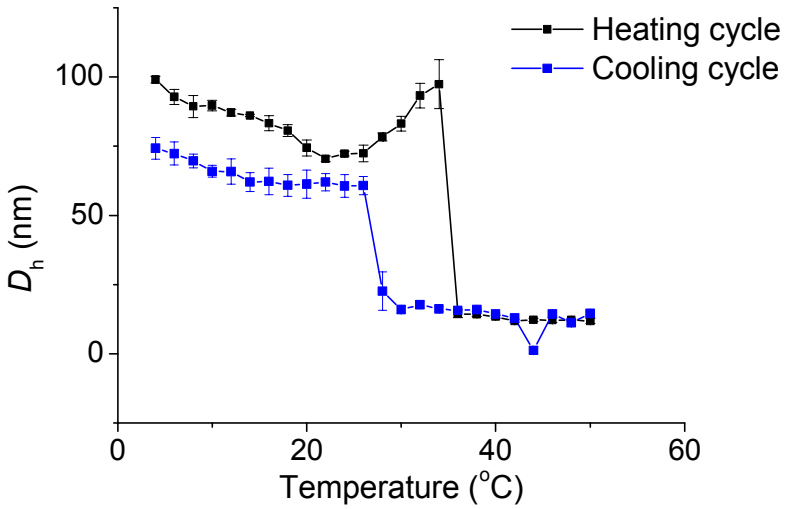

Figure 5.26: DLS graph showing the difference in the transition temperature of 4.03 upon heating or cooling

5.2.8.2 Tailoring the transition temperature by altering the length of the hydrophilic blocks

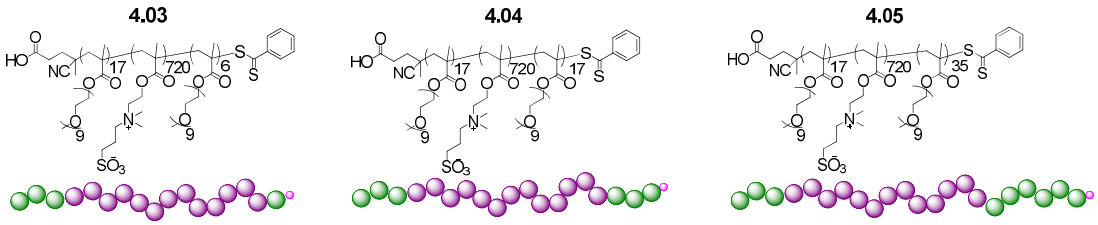

Figure 5.27: The structures of the three triblocks, 4.03. 4.04 and 4.05, with differing lengths of PEGMA

In order to investigate whether the temperature at which the micelle to unimer morphology transition occurs is modified by the PEGMA block length the two other triblock copolymers**,** **4.04** and **4.05** were analysed by DLS with heating. All solutions were at 1 mg mL^{-1} and were assembled at 40 °C. The size was measured by DLS from 4 °C to 50 °C every 2 °C with five minutes equilibration at each temperature.

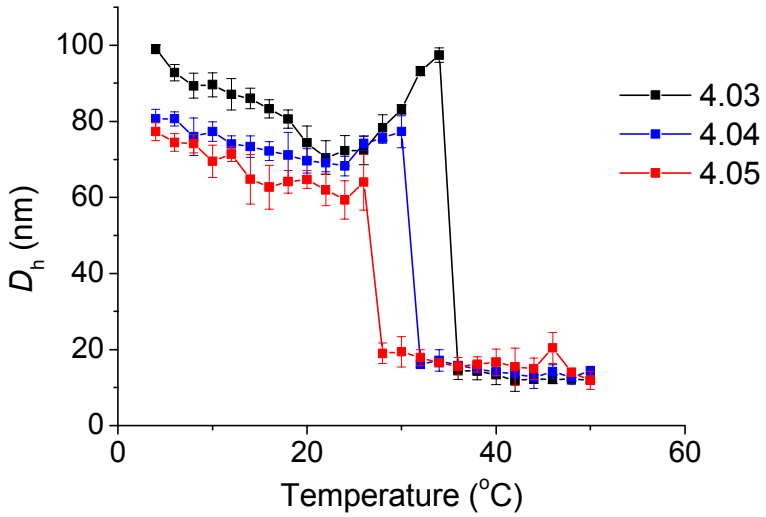

Figure 5.28: DLS results showing how the transition temperature decreases as the length of the third, PEGMA, block increases

As can be seen in Figure 5.28, the temperature at which this micelle to unimer morphology transition occurs is different for the different polymers. The transition temperature increases slightly from 34 to 36 °C between the diblock, **4.02** and the triblock **4.03**. This could be due to differences in packing between the diblock and the triblock but it is not a significant

increase. Then as the length of the hydrophilic block increases the transition temperature decreases (32 °C for **4.04** and 28 °C for **4.05**).

All the samples described above are at a concentration of 1 mg mL^{-1} and as the overall molecular weight of the polymer is increasing, the effective concentration of betaine in the self-assembled solutions is decreasing in solutions **4.02** to **4.05**. The UCST cloud point of betaines is concentration dependant and therefore it was necessary to check that the decrease in transition temperature between the three triblocks was not a result of this decrease in betaine concentration. A sample of **4.05** was made by direct dissolution at a concentration of 1.12 mg mL^{-1}, which is equivalent to 1 mg mL^{-1} of betaine in the solution. Triblock copolymer **4.05** was chosen as this is the largest of the three triblocks and therefore results in the largest difference between polymer concentration and effective betaine concentration. The sample was analysed by DLS between 4 and 50 °C, in the same manner as described for **4.03**. The temperature at which the transition occurs is the same in both the 1.12 mg mL^{-1} sample and in the 1 mg mL^{-1} sample (see Figure 5.29).

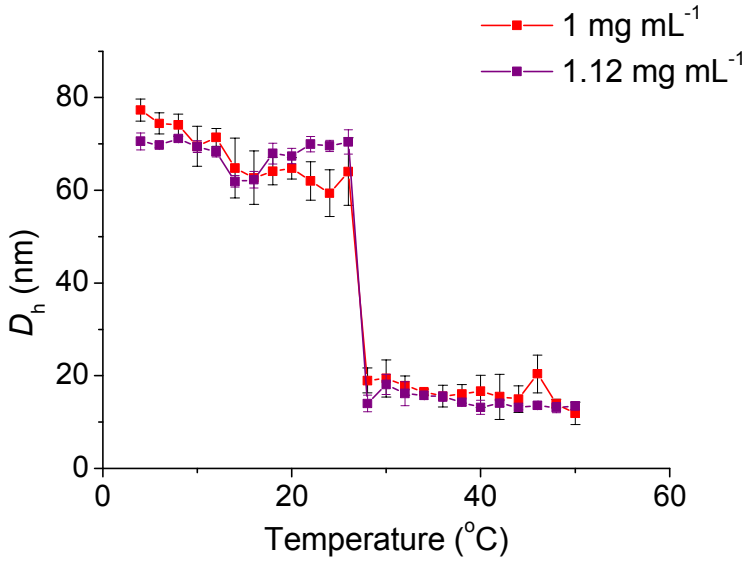

Figure 5.29: DLS results of self-assembled solutions of 4.05 at 1 mg mL^{-1} and 1.12 mg mL^{-1}, showing the same transition temperature

This confirms that the decrease in transition temperature across the triblock series is a result of the increased PEGMA length of the third block and not due to small decreases in betaine

concentration. This can be explained by the overall hydrophilicity of the polymer increasing as the length of the third block increases. Therefore it is expected that the dissolution of the micelles to unimers would occur at lower temperatures as the polymer becomes more hydrophilic. This shows that the transition temperature for these triblock systems can easily be altered by altering the length of the hydrophilic blocks.

5.2.8.3 Analysis of the self-assembled triblocks by DLS and SLS

The *dn/dc* values for the self-assembled triblocks in water were calculated using a Shodex RI-101 refractometer as described for diblock copolymer **4.02**. The *dn/dc* values for each triblock copolymer in water are listed in Table 5.2.

Table 5.2: Calculated *dn/dc* values for the triblock copolymers in 18.2 MΩ cm^{-1} water

Polymer	*dn/dc* (mL g^{-1})
4.03	0.125
4.04	0.125
4.05	0.128

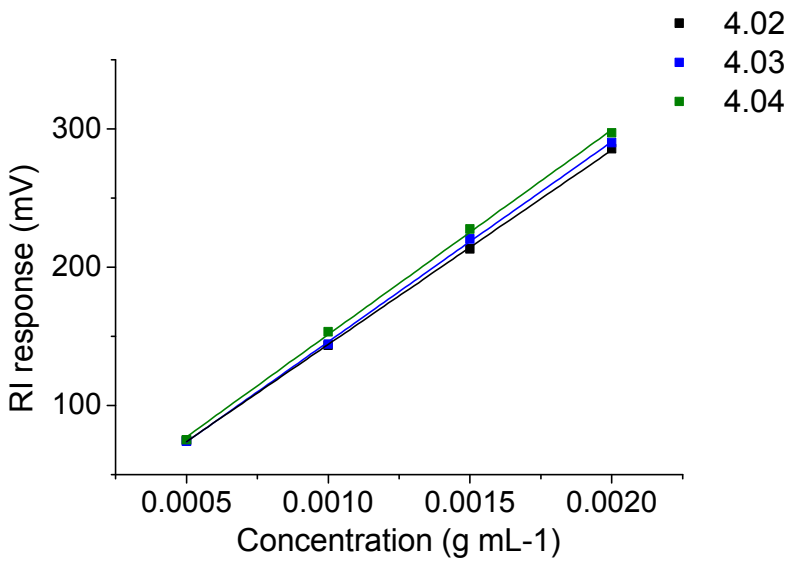

Figure 5.30: Plot of concentration *vs* RI response for 4.03, 4.04 and 4.05. The *dn/dc* was calculated using the slope of the linear fit

Polymer **4.03** was self-assembled in pure water by direct dissolution with gentle heating. The hydrodynamic diameter of **4.03** was analysed using multi-angle DLS, as for **4.02**. The inverse of the relaxation time for the fast mode divided by q^2 (τ_{fast}^{-1}/q^2) was plotted against the scattering vector squared (q^2) (see Figure 5.31). This was extrapolated to zero angle to yield the apparent diffusion coefficient. Copolymer **4.03** in water at 1 mg mL^{-1} was found to have an apparent diffusion coefficient of 6.54 x 10^{-12} m^2 s^{-1} which corresponds to an apparent hydrodynamic diameter of 73 nm.

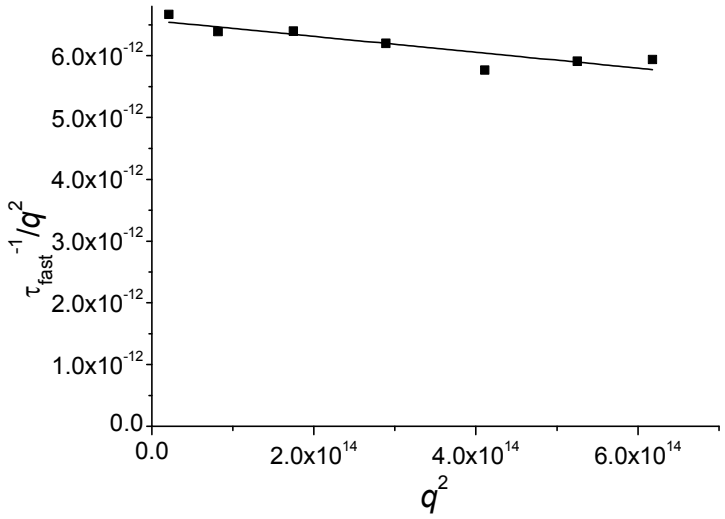

Figure 5.31: Plot of τ_{fast}^{-1}/q^2 *vs* q^2 for self-assembled micelles based on copolymer 4.03 at 1 mg mL^{-1} in water, determined at 20 °C (D_h = 73 nm)

Plotting the apparent diffusion coefficient for each concentration against concentration yields an intercept that relates to a translational diffusion coefficient (D_t) of 5.60 x 10^{-12} m^2 s^1 which corresponds to a hydrodynamic diameter of 85 nm. This is slightly higher than the D_h observed for a 1 mg mL^{-1} solution and is a result of interactions between the micelles at the higher concentrations and therefore skewing the data (see Figure 5.32).[36]

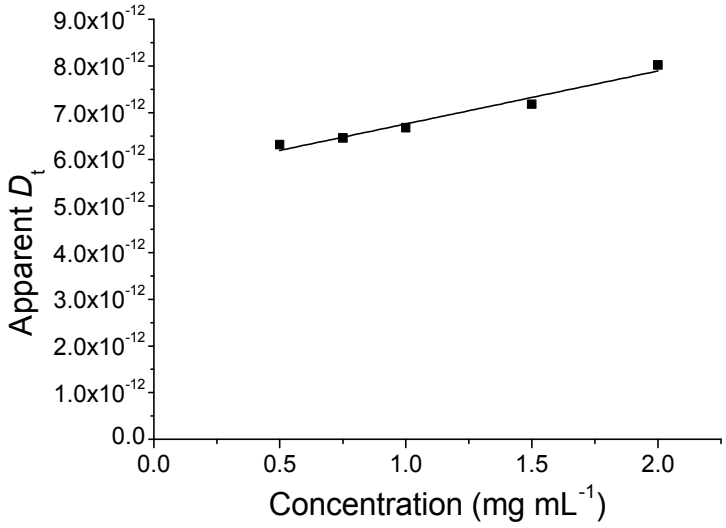

Figure 5.32: Plot of apparent D_t against concentration for triblocks copolymer 4.03. The intercept of this graph corresponds to a hydrodynamic diameter of 85 nm

The self-assembled micelles of **4.03** were also analysed by SLS to determine the molecular weight, radius of gyration (R_g) and the aggregation number (N_{agg}) as described for **4.02**. R_g can be determined for each concentration from the slope of $K_c/R_{\Theta, fast}$ *vs* q^2, and N_{agg} by comparing the molecular weight of the assembled structure to that of an individual polymer chain.[37] $K_c/R_{\theta, fast}$ was plotted against q^2 for each concentration and each plot extrapolated to zero angle. The extrapolated $K_c/R_{\theta, fast}$ value was then plotted against concentration and extrapolated to zero concentration, and the intercept was used to determine the absolute molecular weight of the nanostructure (see Figure 5.33). The absolute molecular weight of the self-assembled structures of **4.03** was determined to be 25 MDa. This corresponds to a N_{agg} of 86 polymer chains per micelle, using an absolute molecular weight for an individual polymer chain of 289 kDa, as determined by SLS (Chapter Four). For a vesicular structure an R_g/R_h ratio of 1 is expected, whereas for a hard sphere a ratio of about 0.775 is instead expected.[38] The R_g/R_h ratio for **4.03** at 1 mg mL^{-1} was calculated to be 0.75 suggesting that the self-assembled structures are micelles rather than vesicles.

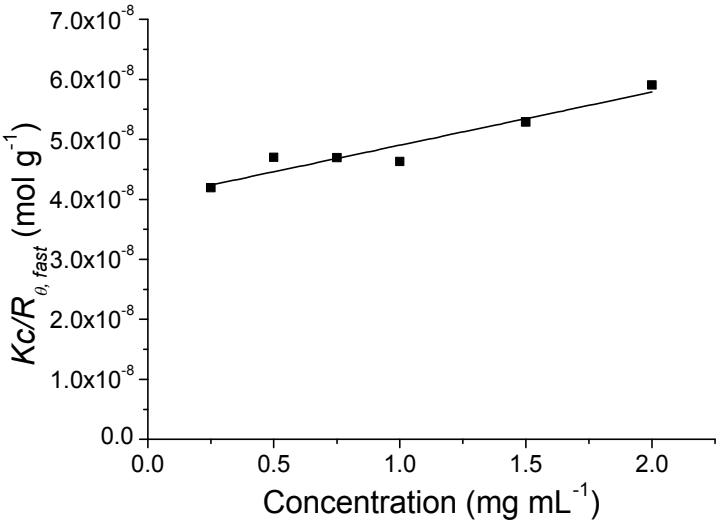

Figure 5.33: Plot of $Kc/R_{\theta, fast}$ *vs* concentration for self-assembled solutions of triblocks copolymer 4.03. The M_w was calculated using the intercept of the linear fit to the SLS data and found to be 25 MDa

Triblock copolymers **4.04** and **4.05** were also analysed in a similar manner by simultaneous SLS and multi-angle DLS in order to determine the molecular weight of the micelle, the aggregation number, hydrodynamic diameter and R_g/R_h value (see Appendix 1). The results are listed in Table 5.3.

Table 5.3: Summary of the analysis of the block copolymers by multi angle DLS and SLS

Polymer	$M_{w,\ micelles}$ (MDa)	N_{agg}	R_g/R_h[a]	D_h (nm)[b]	Transition Temp (°C)
4.02	28	103	0.84	76	34
4.03	25	86	0.75	73	36
4.04	24.3	77	0.89	73	32
4.05	17.9	54	0.81	75	28

[a] Determined at 1 mg mL^{-1}
[b] D_h at 1 mg mL^{-1} as determined by multi-angle DLS analysis

The R_g/R_h at 1 mg mL^{-1} for all triblocks is between 0.75 - 0.89, suggesting that the self-assembled structures are not vesicles and are micelles (see Table 5.3). For triblock copolymers **4.03** and **4.04** the molecular weight of the self-assembled micelles is similar (*ca.*

25 MDa), with aggregation numbers of 86 and 77 respectively. The molecular weight for the self-assembled micelles of **4.05** is smaller at 17.9 MDa. This decrease in molecular weight of the micelles leads to a lower aggregation number of 54. The aggregation number is decreasing across the three triblocks and is lower than seen in the diblock copolymer **4.02** (N_{agg} = 103). All measurements were performed at 20 °C and this decrease in aggregation number could be caused by the difference in overall hydrophilicity of the di- and triblock copolymers. The transition temperature of **4.05** is 28 °C compared to 34 °C for **4.02**. Therefore at 20 °C the micelles of **4.05** may be more dynamic than those of **4.02** and therefore have an increased amount of unimer exchange. This could lead to this lower aggregation number and molecular weight of the micelles.

5.2.9 Analysis of the morphology transition of 4.03 by SAXS

The temperature response of micelles of **4.03** was investigated from 5 to 50 °C by SAXS as described for diblock copolymer **4.02** and showed a micelle to unimer transition at *ca.* 36 °C. As for the diblock copolymer **4.02**, a core-shell spherical micelle model was found to fit well up to 10 °C and a unimer model was found to fit well at 36 °C and above. At temperatures in between the model suggests a mixture of micelle and unimers (see Table 5.4). The shell thickness observed for **4.03** (9.4 ± 1.4 nm at 5 °C) is thicker than that seen in **4.02** (from 6.2 ± 1.0 nm at 5 °C) while a decrease of the core radius is noticed (from 20.3 ± 1.0 nm in **4.02** to 15.1 ± 1.3 nm in **4.03** at 5 °C). The increase in the thickness of the shell can be explained by the presence of the third, hydrophilic PEG, block. The decrease in the core radius upon going from the diblock to the triblock could be explained by better packing in the ABA triblock, or by the higher hydrophilicity in the triblock. The incorporation of a hydrophilic monomer into homopolymers of DMAPS has been shown to decrease the cloud point of the polymer and therefore the presence of this second hydrophilic block could cause the DMAPS block to be more hydrophilic in the triblock than in the diblock at 20 °C.[3] This

increased hydrophilicity could explain the decrease in the core radius as less of the polymer is hydrophobic.

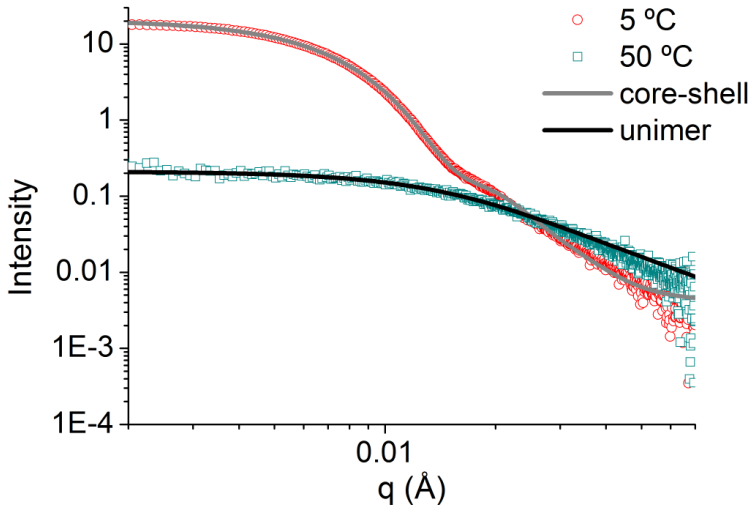

Figure 5.34: SAXS profiles and fits for triblocks copolymer 4.03 at 5 °C and 50 °C

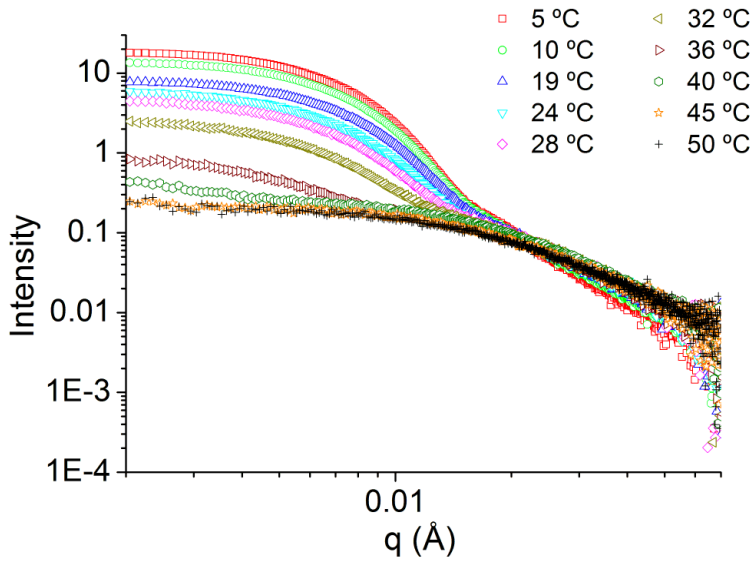

Figure 5.35: SAXS profiles for triblocks copolymer 4.03 at varying temperatures between 5 °C and 50 °C

Table 5.4: Morphologies present at each temperature and the ratio of micelles to unimers of 4.03 as calculated by SAXS analysis

Temperature (°C)	Morphology (Ratio micelle:unimer)	Volume fraction (Ratio micelle:unimer $\times 10^4$)	Number of micelles (/Vtot $\times 10^{10}$)
5	Micelles	25:0	398
10	Micelles	20:0	401
19	Micelles and unimers	1:311	145
24	Micelles and unimers	1:687	72
28	Micelles and unimers	1:1141	41
32	Micelles and unimers	1:1197	19
36	Micelles and unimers	1:7583	12
40	Unimers	0:2729	0
45	Unimers	0:2175	0
50	Unimers	0:2088	0

5.2.10 Encapsulation and release of hydrophobic dye from the micelles of 4.03

The encapsulation and release properties of the triblock copolymers were also investigated. A self-assembled solution of **4.03** at 1 mg mL^{-1} was stirred overnight with Nile Red at 1 mg mL^{-1}, filtered to remove any non-encapsulated dye, and then tested for fluorescence. The solution was then heated at 38 °C for 5 minutes, at which point a sample was removed, filtered and the fluorescence measured again (see Figure 5.36). As shown for **4.02** (Figure 5.19) the fluorescence response decreases significantly after heating as the Nile Red has been released from the micelles when dissociation occurs and therefore precipitates out and is removed by filtration.

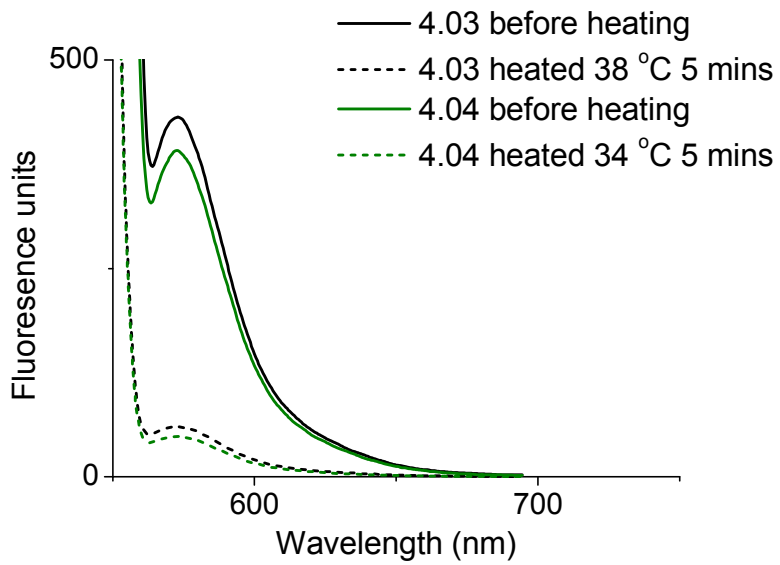

Figure 5.36: Graph showing the decrease in fluorescence after heating the micelle solution of 4.03 at 38 °C and 4.04 at 34 °C

Triblock copolymer **4.04** was also investigated in a similar manner and found to release Nile Red when heated to 34 °C (see Figure 5.36). The fluorescence responses of the two micelle solutions are similar, both before and after heating, showing that micelles of both **4.03** and **4.04** encapsulate and release similar amounts of Nile Red.

5.2.11 Self-assembly behaviour of PEGMA-*b*-DMAPS-*b*-PMMA, 4.06

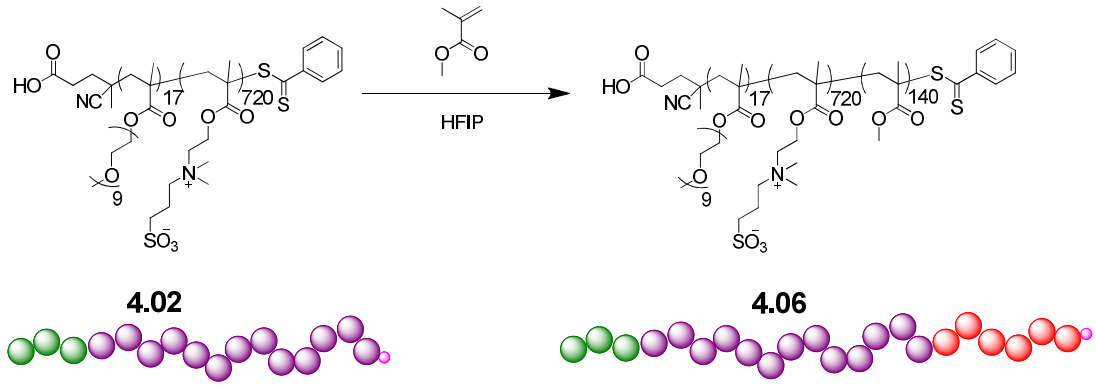

Scheme 5.3: Synthesis of triblock 4.03 by chain extension of diblock 4.02 with MMA in HFIP

As a comparison to the ABA triblocks discussed previously, and to investigate the difference that a hydrophobic rather than hydrophilic third block would have upon the self-assembly and thermo-responsive properties, an ABC type triblock copolymer was synthesised (see Scheme 5.3). Using a hydrophobic monomer to form the C block of the triblock copolymer should cause the amphiphilic balance of the polymer to change, as the hydrophobic section is longer, and therefore may potentially form vesicles. Diblock copolymer **4.02** was chain extended with methyl methacrylate in HFIP to yield **4.06**, M_n (^{1}H NMR) = 228.2 kDa, M_n (HFIP SEC) = 148.2 kDa, $Đ_M$ = 1.52. The broader dispersity seen by HFIP SEC analysis was discussed in Chapter Four.

Analysis of **4.06** at 1 mg mL^{-1} in 0.5 M NaCl solution by DLS shows a population with D_h = 119 ± 4 nm. Comparison of this to the size of diblock copolymer **4.02** in 0.5 M NaCl at 1 mg mL^{-1} (18 ± 1 nm), shows that the addition of the MMA block causes the polymer to self-assemble in salt, as expected (see Figure 5.37).

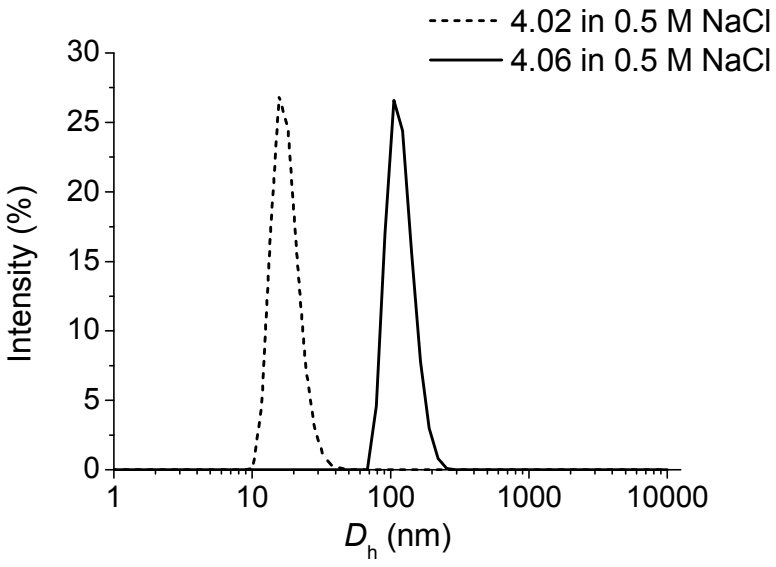

Figure 5.37: Comparison of the D_h from DLS for diblock 4.02 and triblocks 4.06 in 0.5 M NaCl shows that addition of the MMA block has resulted in self-assembly

As triblock copolymer **4.06** contains a hydrophobic block self-assembly *via* solvent switch was investigated, as this has previously been shown to give more uniform assemblies then direct dissolution.[44] Triblock copolymer **4.06** was dissolved in HFIP at a concentration of 2 mg mL^{-1} and 18.2 MΩ cm^{-1} water was slowly added until the polymer concentration reached 1 mg mL^{-1}. The solution was then dialysed against water to remove the HFIP. However, upon dialysis the polymer precipitated into the dialysis bag. Therefore it was decided to self-assemble the polymer by direct dissolution into 18.2 MΩ cm^{-1} water at 1 mg mL^{-1} with gentle heating to *ca*. 40 °C for a few minutes. Analysis by DLS at 25 °C shows a population with D_h = 82 ± 3 nm. This size suggests again that micelles not vesicles are being formed upon self-assembly, as for **4.02**.

The thermo-responsive behaviour of **4.06** was investigated by DLS analysis with heating. A 1 mg mL^{-1} self-assembled solution was heated from 5 °C to 65 °C with the size being recorded every 5 °C (see Figure 5.38).

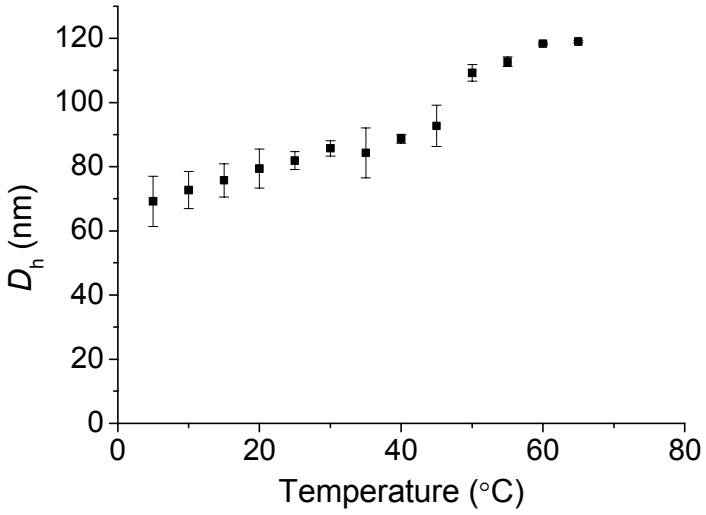

Figure 5.38: Graph showing the increase in D_h of triblocks 4.06 with temperature, as analysed by DLS

As can be seen in Figure 5.38, the size increases from 69 ± 8 nm at 5 °C to 119 ± 0.4 nm at 65 °C. This is due to the DMAPS block becoming more hydrophilic and therefore hydrated as the temperature increases. This shows that at 65 °C the DMAPS block is fully hydrated, as the sizes in salt (D_h = 119 ± 4 nm) and at 65 °C compare very well.

The observed increase in size with temperature is another indicator that vesicles have not been formed. It would be expected that vesicles would be larger than the size seen at 5 °C (69 nm) and that as the temperature increased and the DMAPS became hydrophilic, the vesicle would transition to a micelle. This would be observed by a decrease in size. Therefore it appears that the addition of the hydrophobic block has, perhaps surprisingly, not caused the polymers to self-assemble into vesicles.

Analysis of a 0.1 mg mL^{-1} solution of **4.06** by dry-state TEM on a graphene oxide support shows micelles with an average size of 43 ± 10 nm (see Figure 5.39). The size is smaller than that seen by DLS but this is expected as the TEM analysis is performed on a dried sample, whereas the micelles observed in DLS are hydrated in solution.[36]

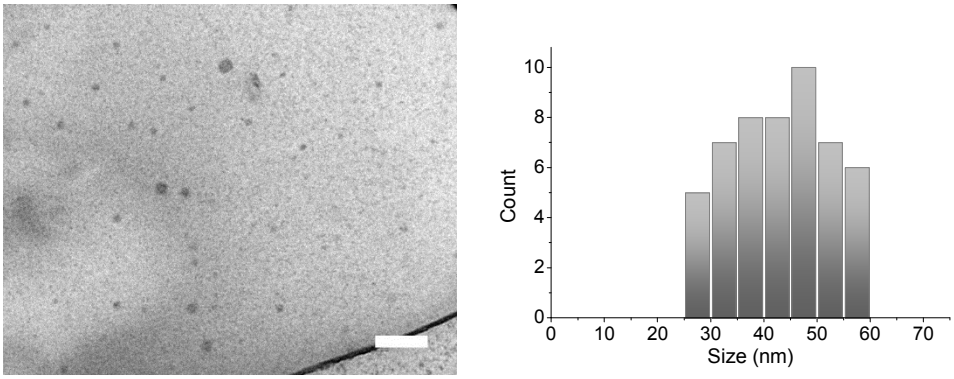

Figure 5.39: TEM image of micelles of 4.06 at 0.1 mg mL^{-1} using graphene oxide as a support, scale bar = 200 nm, and the distribution of sizes observed

5.2.12 Self-assembly behaviour of PEGMA-*b*-DMAPS-*b*-DEAEMA, 4.07

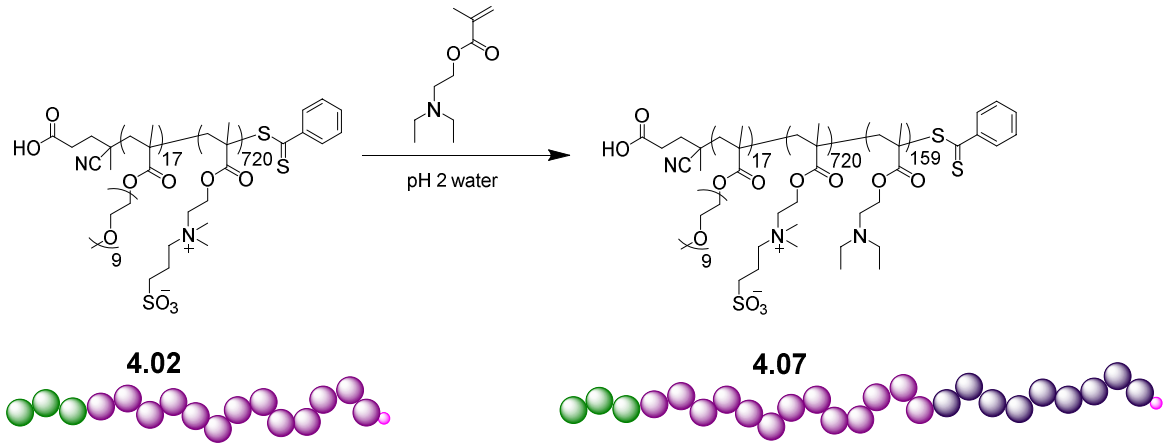

Scheme 5.4: The synthesis of a triply responsive triblock copolymer, 4.07, by the chain extension of diblock polymer 4.02 with DEAEMA

Another ABC triblock copolymer was synthesised by chain extending **4.02** with *N,N*-diethylamino ethyl methacrylate (DEAEMA) in acidic water. The increased hydrophobicity of DEAEMA may be sufficient to cause vesicle formation. Another consideration was the addition of a second responsive block. DEAEMA is both pH-[45] and CO_2-responsive[46] and therefore the triblock copolymer **4.07** is expected to be triply responsive to temperature, pH and CO_2.

5.2.12.1 pH-response of triblock copolymer 4.07

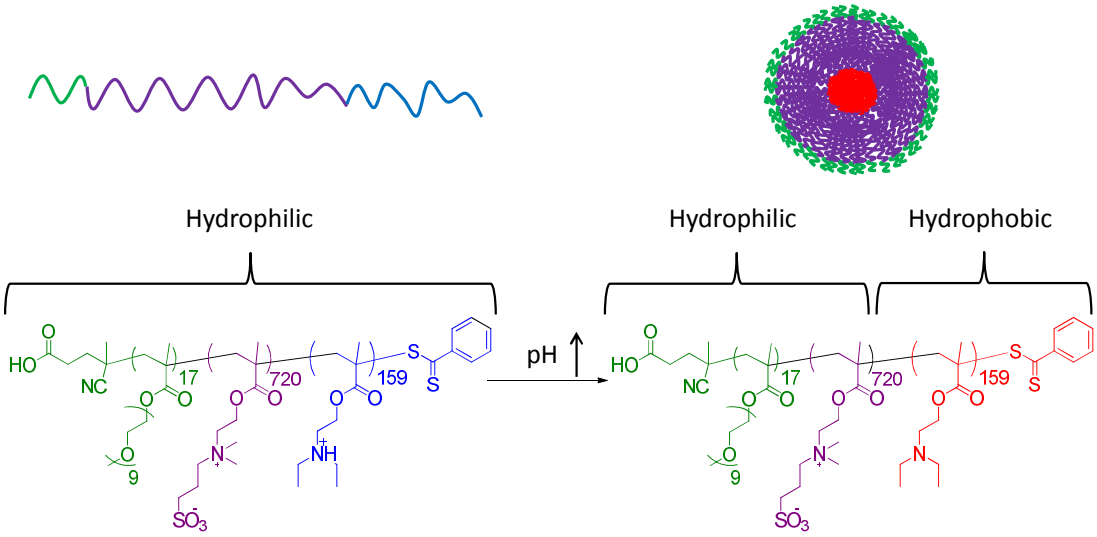

Figure 5.40: The unimer to micelle transition afforded by raising the pH of the 0.5 M NaCl solution to deprotonate the DEAEMA block

To test the pH-responsive behaviour **4.07** was self-assembled at 1 mg mL^{-1} in 0.5 M NaCl at a pH of 3.5. The use of the salt solution, together with the low pH, means that the polymer will be fully soluble, as the DMAPS block is soluble in the salt solution and the DEAEMA block will be protonated and therefore hydrophilic (see Figure 5.40). Analysis by DLS affords a D_h = 18 ± 1 nm for **4.07**. The pH of this solution was then adjusted to pH 9.5 using diluted NaOH solution (*ca.* 0.2 mL) and the solution reanalysed by DLS (see Figure 5.41). The size had increased to 57 ± 2 nm, as the DEAEMA block becomes deprotonated and therefore hydrophobic (see Figure 5.40). This shows that the polymer undergoes a unimer to micelle transition with increasing pH in 0.5 M NaCl solution.

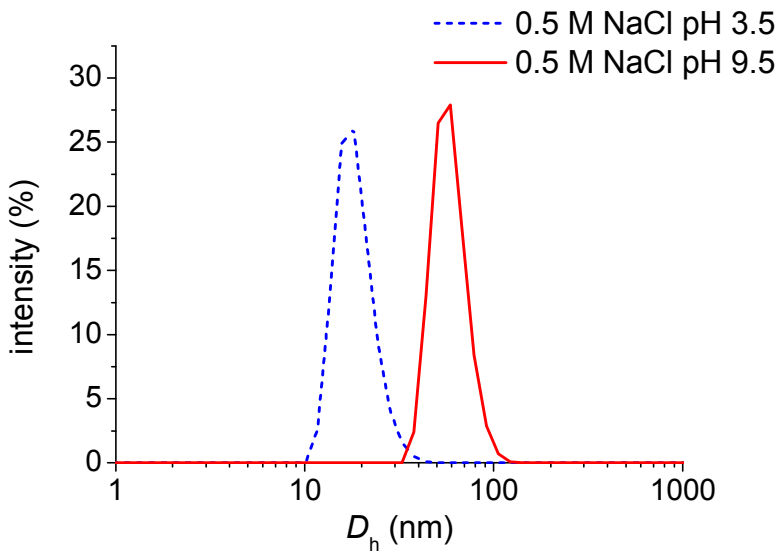

Figure 5.41: Comparison of D_h of triblock copolymer 4.07 in 0.5 M NaCl solution at pH 3.5 and pH 9.5, as analysed by DLS

5.2.12.2 Thermo-response of triblock copolymer 4.07 in acidic solution

In order to test the effect that pH had on the thermo-responsive properties of the polymer **4.07** was self-assembled into 18.2 MΩ cm^{-1} water at a concentration of 1 mg mL^{-1}. Immediately after direct dissolution the sizes were variable and not reproducible. However, after prolonged equilibration times, the solution had turned opalescent, indicating self-assembly. The pH of the solution was pH 5.6, and as the pK_a of polyDEAEMA has been reported to be *ca*. 7.3,[45, 47] at pH 5.6 the DEAEMA block is protonated and so hydrophilic. The pH of the solution is slightly acidic because during the purification procedure, the polymer was dialysed against acidic water but not neutralised before lyophilisation. The size by temperature was recorded by DLS between 4 °C and 60 °C with the temperature being measured every 2 °C (see Figure 5.42).

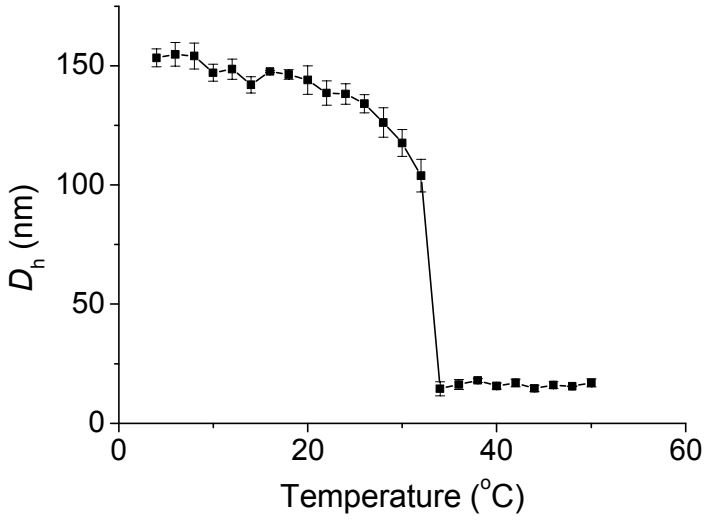

Figure 5.42: DLS analysis of D_h with temperature for a 1 mg mL^{-1} self-assembled solution of triblock copolymer 4.07 at pH 5.6

At 4 °C the size of the assembly is 153 ± 4 nm. This decreases slightly as the temperature increases to 26 °C (D_h = 134 ± 4 nm). The size then decreases more rapidly until D_h = 104 ± 7 nm at 32 °C. At 34 °C unimers are formed (D_h = 16 ± 2 nm). The sizes seen at the higher temperatures compare well with those seen in salt solution at pH 3.5 (18 ± 1 nm), confirming that they are unimers. The size of the assemblies at 20 °C (144 ± 6 nm) is much larger than the micelles formed from the PEGMA-*b*-DMAPS-*b*-PEGMA triblocks, **4.03** – **4.05**, therefore suggesting that the polymers may be self-assembling into vesicles.

In order to better understand the nature of the self-assembled structure of **4.07**, a sample at 1 mg mL^{-1} was analysed using SLS and multi-angle DLS, as described for triblock copolymers **4.03**, **4.04** and **4.05**. Firstly the *dn/dc* was determined, as described for **4.03** and was found to be 0.126 mL g^{-1}.

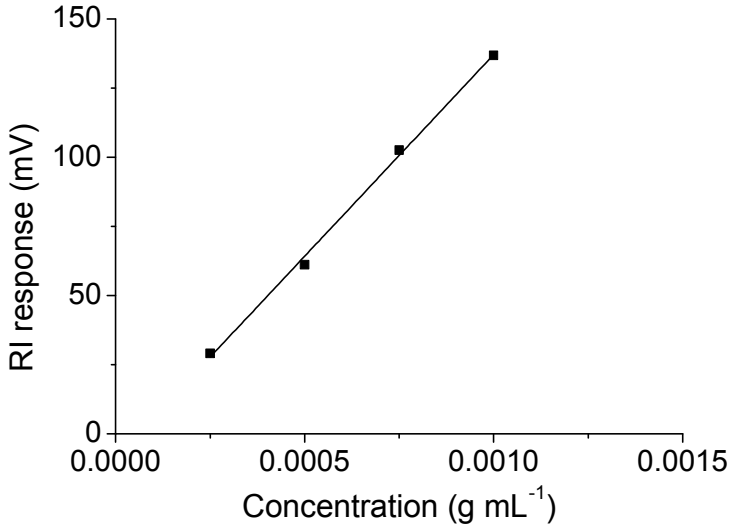

Figure 5.43: Plot of concentration *vs* RI response for 4.07. The *dn/dc* was calculated as 0.126 mL g^{-1} using the slope of the linear fit

$K_c/R_{\theta,\ fast}$ was plotted against q^2 and extrapolated to zero angle (see Figure 5.44). The molecular weight of the structure is determined from the inverse of the intercept, and R_g can be determined from the slope of $K_c/R_{\Theta,\ fast}$ *vs* q^2. The molecular weight for the structures at 1 mg mL^{-1} is 189 MDa. The R_g at 1 mg mL^{-1} is 87 nm.

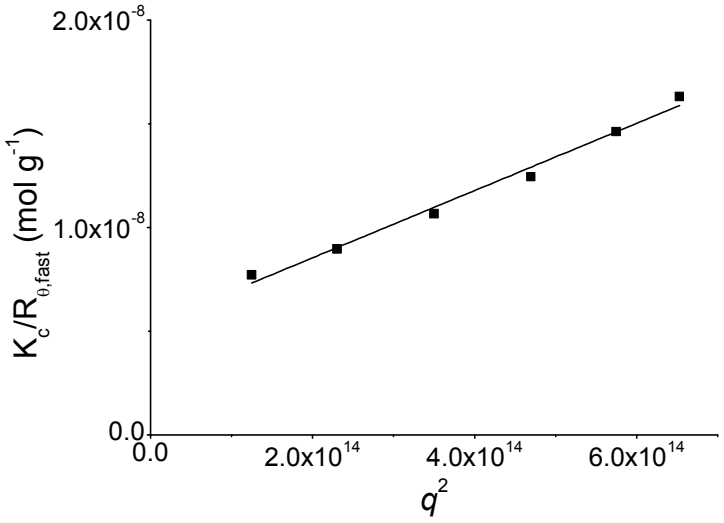

Figure 5.44 Plot of *Kc/R$_{\theta,\ fast}$ vs q^2* for self-assembled solutions of 4.07 at 1 mg mL^{-1}. The M_w of the structures was calculated using the intercept of the linear fit to the SLS data and found to be 189 MDa

The inverse of the relaxation time for the fast mode divided by q^2 (τ_{fast}^{-1}/q^2) was plotted against the scattering vector squared (q^2) (see Figure 5.45). This was extrapolated to zero

angle to yield the apparent diffusion coefficient. At 1 mg mL^{-1} the apparent diffusion coefficient is 2.57 x 10^{12} m^2 s^{-1} which corresponds to a hydrodynamic diameter of 166 nm.

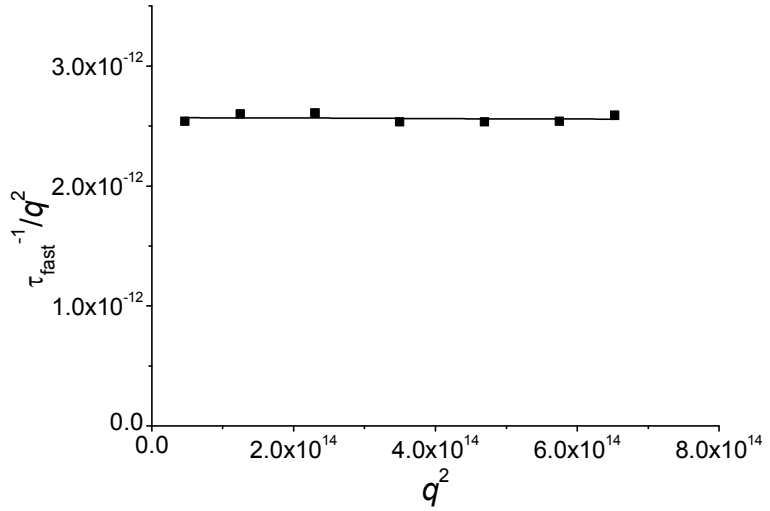

Figure 5.45 Plot of τ_{fast}^{-1}/q^2 *vs* q^2 for self-assembled micelles based on copolymer 4.07 at 1 mg mL^{-1} in water (pH 5.6), determined at 20 °C (D_h = 166 nm)

For a vesicular structure an R_g/R_h ratio of 1 is expected, whereas for a hard sphere a ratio of about 0.775 is instead expected.[38] Comparison of the R_h of 83 nm and the R_g of 87 nm equates to an apparent R_g/R_h at 1 mg mL^{-1} of 1.05. Therefore this value, along with the much higher molecular weight of these structures (189 MDa) than those seen for **4.03 – 4.05** (25 – 18 MDa) suggests that **4.07** is forming vesicles in solution at pH 5.6. The apparent aggregation numberof the assembly at 1 mg mL^{-1} can be calculated by comparing the molecular weight of the assembly with the molecular weight of one polymer chain. The absolute molecular weight of **4.07** calculated by SLS is 348 kDa (Chapter Four). Using this molecular weight an N_{agg} of 543 is obtained.

It is interesting to compare the morphologies of **4.05** and **4.07** that are adopted upon self-assembly. **4.05** is an ABA, PEGMA-*b*-DMAPS-*b*-PEGMA, triblock copolymer and it has been confirmed that micelles are formed below the transition temperature of the DMAPS block. **4.07** is an ABC triblock copolymer that has the same A and B blocks as **4.05** but

bears a longer, DEAEMA, C block. Upon self-assembly below the pK_a of the DEAEMA block vesicles are formed (see Figure 5.46).

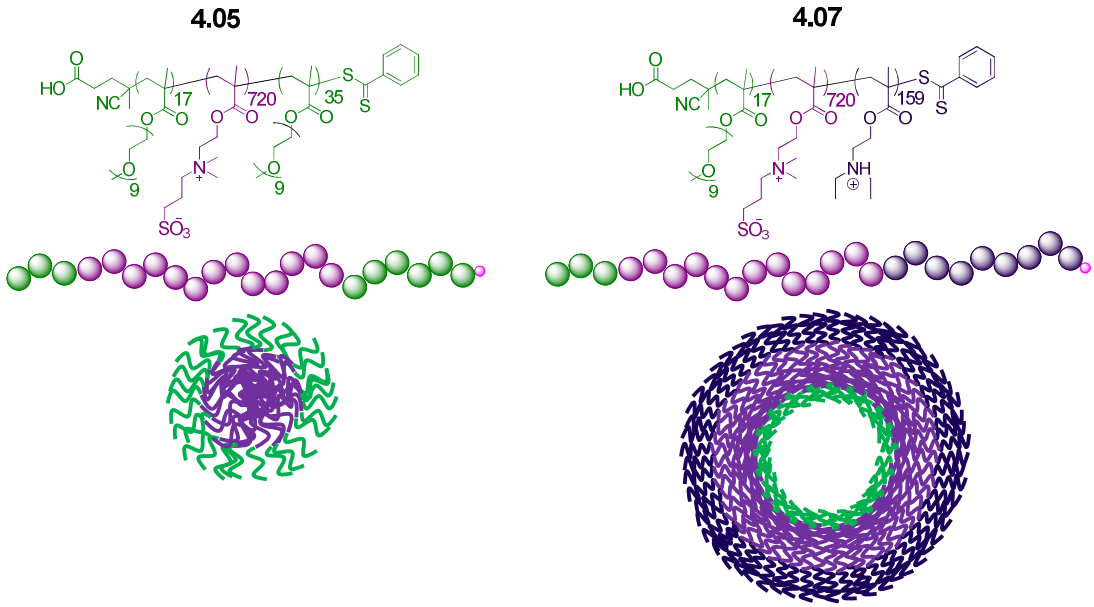

Figure 5.46: Structure of triblocks 4.05 and 4.07 and the morphologies they adopt upon self-assembly

The difference in the structures formed may be a consequence of the different chemical composition of the hydrophilic blocks. At low temperatures **4.05** may be expected to form a vesicle based on the long, hydrophobic, middle DMAPS block, bordered by two relatively short hydrophilic PEG blocks. However the DMAPS block does not become fully hydrophobic and therefore micelles are formed. However, ABC triblock copolymer **4.07** forms vesicles, which can be attributed to the phase separation between the two different hydrophilic blocks, as has been previously shown.[48] Similar systems have been studied previously by Meier and co-workers who synthesised triblock copolymers of poly(ethylene oxide) (PEO), poly(dimethyl siloxane) (DMS) and poly 2-(methyloxazoline) (MOXA). Different triblocks of varying lengths and composition were synthesised. The MOXA block was functionalised with a coumarin in order to study the arrangement of the polymers when self-assembled. Upon self-assembly vesicles were formed. Addition of Co^{2+} causes the fluorescence of coumarin to be quenched, if located on the outer walls of the vesicle. It was found that when the PEO and MOXA blocks were similar in length, vesicles with predominantly MOXA inner walls were formed. However, when the MOXA block was

significantly longer than the PEO block, the MOXA blocks predominantly were situated on the outer walls of the vesicle.[48]

As a result of the difference in block lengths between the PEGMA A block and the DEAEMA C block it would be interesting whether the vesicles have a predominantly PEG inner hydrophilic layer and a predominantly DEAEMA outer hydrophilic or *vice versa*.

5.2.12.3 Thermo-response of triblock copolymer 4.07 in basic solution

The pH of the solution was then adjusted to pH 9.5 using diluted NaOH solution. The higher pH causes the DEAEMA block to become deprotonated and therefore hydrophobic. The size with temperature was measured between 5 °C and 70 °C with the size being recorded every 5 °C (see Figure 5.47). The size is *ca*. 120 nm between 5 and 15 °C. Between 15 to 35 °C the size steadily decreases to *ca*. 60 nm.

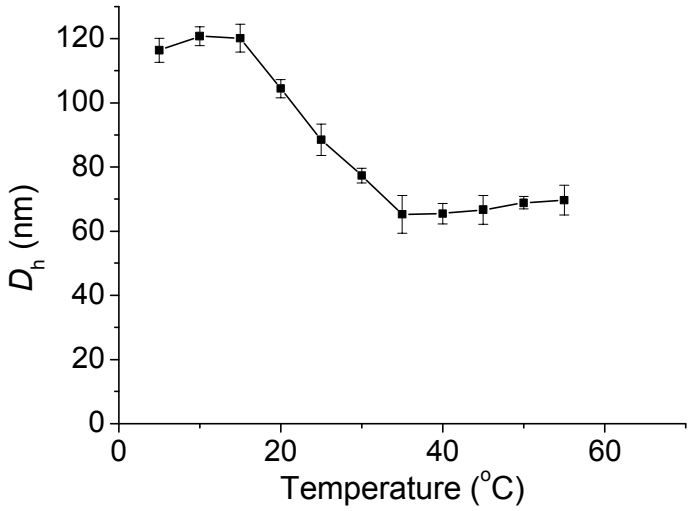

Figure 5.47: DLS results showing change in D_h with temperature for a self-assembled solution of triblock 4.07 at pH 9.5

The sizes formed at 40 °C (63 ± 1 nm) compare well to those seen in salt at pH 9.5 (57 ± 2 nm), suggesting that micelles are formed when the DMAPS block is hydrophilic as the DEAEMA block remains deprotonated, as expected (see Figure 5.48).

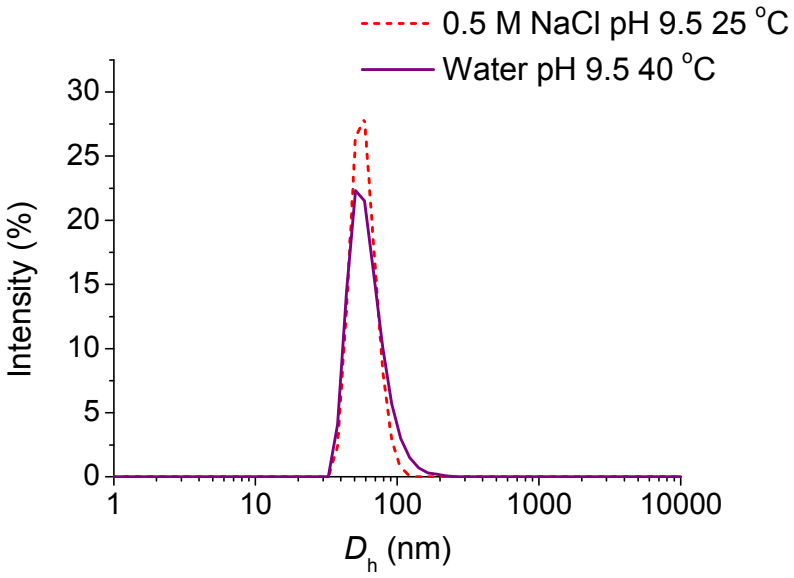

Figure 5.48: D_h of 4.07 in pH 9.5 water at 40 °C and in 0.5 M NaCl at pH 9.5 at 25 °C, determined by DLS

The morphology adopted at lower temperatures is less reproducible. The larger size of the assemblies, suggests that vesicles may be being formed at these temperatures. However, further analysis was not possible as the solution was unstable and precipitated upon standing, most likely a consequence of the hydrophobicity of the DEAEMA. The reproducibility of self-assembly at high pH is poor and further work is needed to determine the optimum self-assembly conditions.

The self-assembled solution of **4.07** at pH 9.5 was analysed by TEM on graphene oxide at 25 °C, before precipitation occurred. A population of micelles with an average size of 44 ± 7 nm was observed (see Figure 5.49).

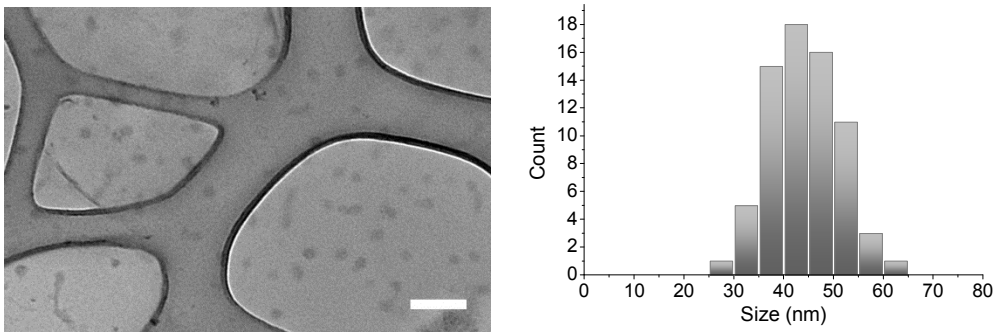

Figure 5.49: TEM of a self-assembled solution of 4.07 at pH 9.5 on a graphene oxide support, prepared at 25 °C with scale bar = 200 nm, and the distribution of sizes observed

In order to confirm that the polymer was chemically stable in the highly basic conditions an aqueous solution of **4.07** was stirred at pH 10 for a week. The polymer was then recovered by lyophilisation. Analysis by ^{1}H NMR spectroscopy confirmed that the polymer structure remained unaffected by the basic conditions (see Figure 5.50).

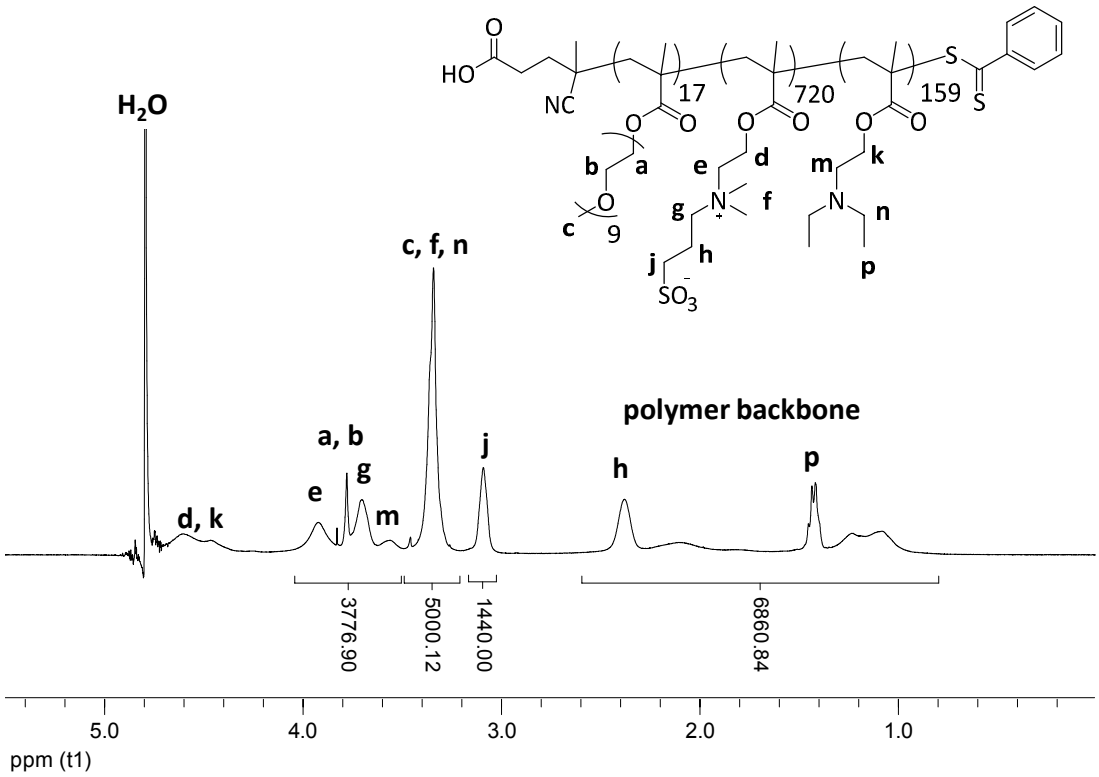

Figure 5.50: ^{1}H NMR spectrum of 4.07 in pH 2 0.5 M NaCl in D_2O after being stirred at pH 10 for a week. Spectrum was recorded at 25 °C and 500 MHz

5.2.12.4 CO_2-response of triblock copolymer 4.07

Tertiary amines have been shown to be CO_2-responsive.[46, 49] Zhao and co-workers have previously synthesised a block copolymer of DMAEMA and hydrophilic dimethylacrylamide (DMA) by RAFT polymerisation. The polymer self-assembled into vesicles in water and purging with CO_2 afforded a vesicle to unimer transition. However the transition was not reversible when the carbon dioxide was removed.[49] Therefore as the DEAEMA block is carbon dioxide responsive, it should be possible to afford a morphology change by purging a solution of **4.07** with CO_2 (see Scheme 5.5).

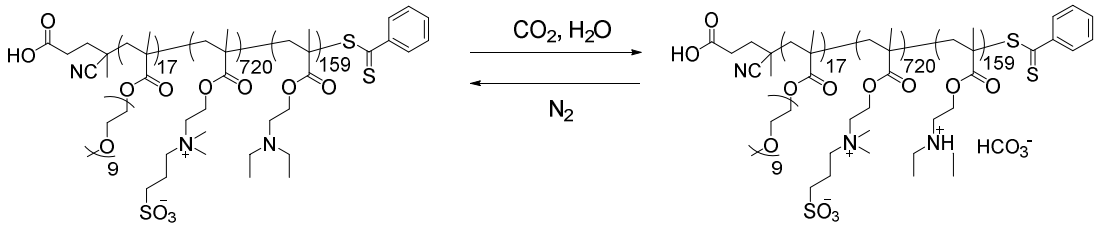

Scheme 5.5: Scheme showing the protonation of the DEAEMA block by purging with carbon dioxide in water, and the removal of the carbonic acid by purging with nitrogen

Triblock copolymer **4.07** was self-assembled in salt solution at pH 9.5. Analysis by DLS gives D_h = 57 ± 2 nm. This solution was then bubbled with CO_2 for 5 minutes with stirring. The solution was then analysed by DLS and the size found to have decreased to 19 ± 0.4 nm (see Figure 5.51).

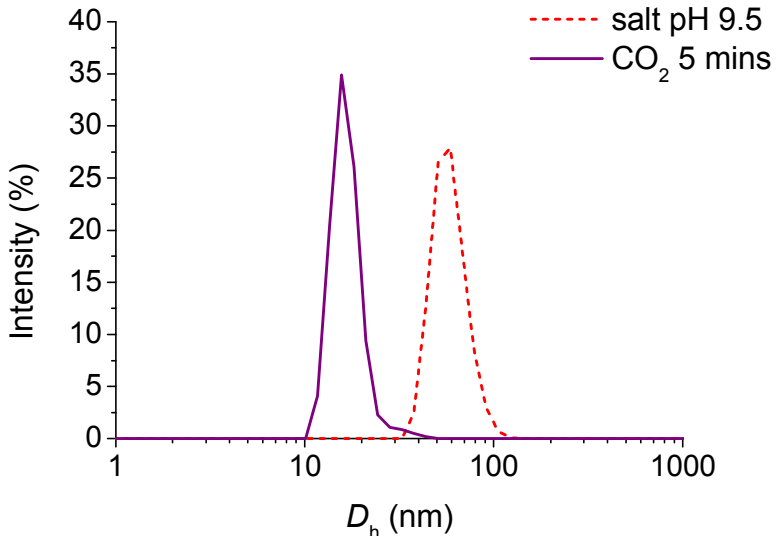

Figure 5.51: The change in D_h when a solution of 4.07 in 0.5 M NaCl at pH 9.5 was purged with CO_2 for 5 minutes

The size that is formed after purging with CO_2 is very similar to that observed when the polymer is dissolved in salt solution at pH 3.5 (see Figure 5.52). This shows that simply five minutes of purging with CO_2 causes a micelle to unimer transition.

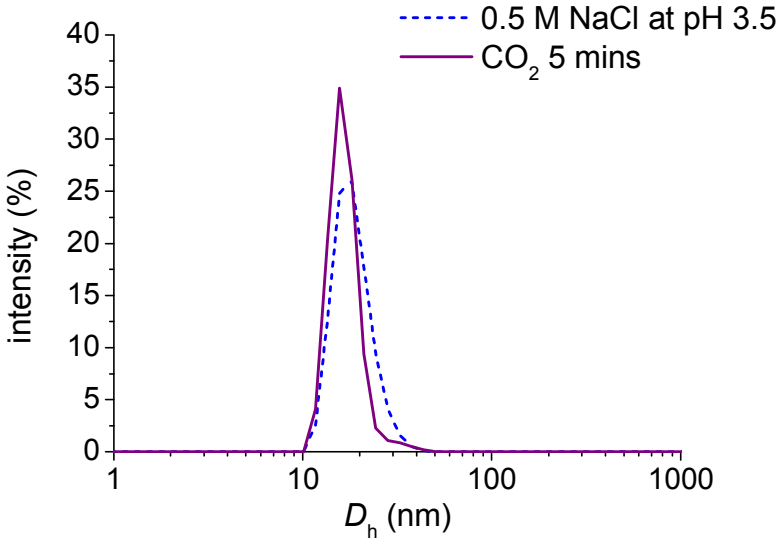

Figure 5.52: Comparison of DLS analysis of 4.07 in pH 9.5 0.5 M NaCl solution after purging for 5 minutes with CO_2 and in 0.5 M NaCl solution at pH 3.5

In order to test whether this transition from micelle to unimer is reversible, the same solution was then purged with nitrogen for 10 minutes. DLS analysis of the solution revealed the presence of a population with $D_h = 61 \pm 3$ nm (see Figure 5.53).

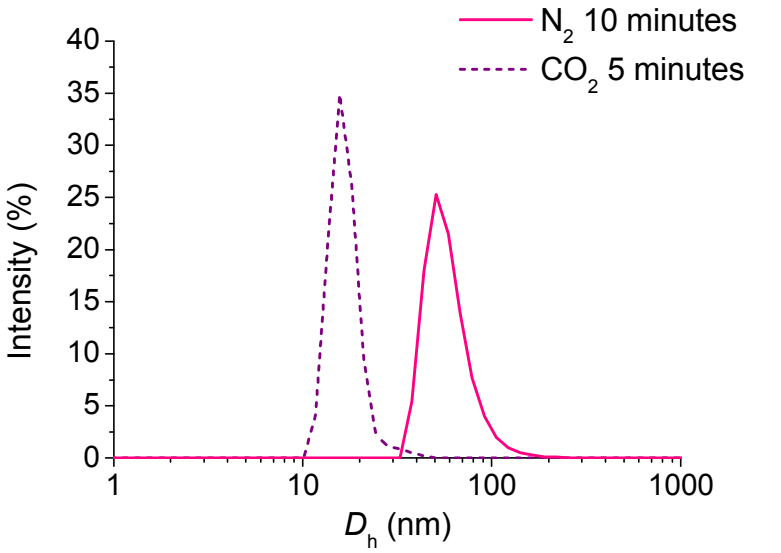

Figure 5.53: DLS analysis of the solution after purging with nitrogen for 10 minutes, showing the transition is reversible

Comparison of the size observed by DLS after purging with nitrogen and that observed in the solution at pH 9.5 shows that the unimer to micelle transition is reversible and the sizes obtained are reproducible (see Figure 5.54).

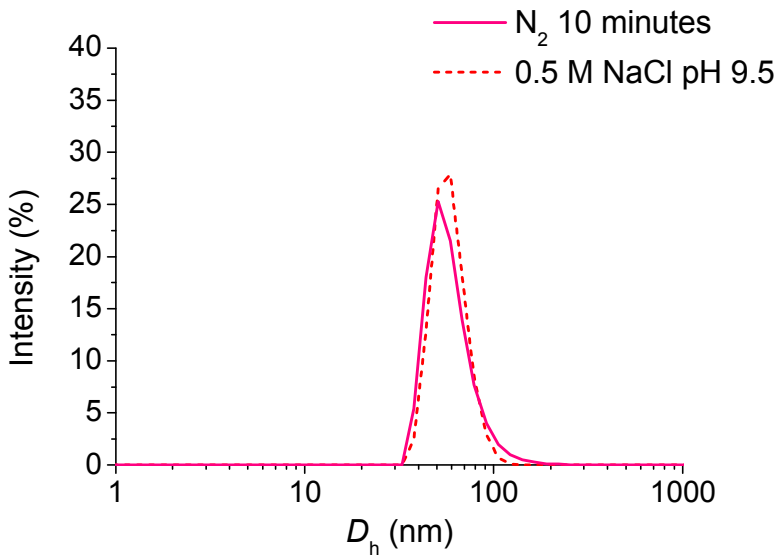

Figure 5.54: DLS analysis of the solution of 4.07 after purging with nitrogen and at pH 9.5 in 0.5 M NaCl solution, showing the reversible response

This demonstrates the responsive behaviour of the triblock copolymer **4.07** towards carbon dioxide and that the transition from micelle to unimer is reversible by bubbling with nitrogen.

5.2.12.5 CO_2-induced release of Nile Red from micelles of 4.07

As triblock copolymer **4.07** undergoes a micelle to unimer transition in response to CO_2, this can be utilised to encapsulate a hydrophobic payload within the hydrophobic core of the micelle and release it in response to CO_2. Polymer **4.07** was self-assembled in 0.5 M NaCl at 1 mg mL^{-1} and the pH adjusted to pH 9.5. This solution was then stirred with Nile Red for several hours and filtered to remove any non-encapsulated dye. The fluorescence was recorded and the sample was found to have a significant fluorescence response, showing that Nile Red had been encapsulated within the hydrophobic core of the micelles. The solution was then purged with CO_2 for 5 minutes and a sample removed and again filtered. After

purging the fluorescence response of the sample had decreased significantly, showing that the Nile Red had been released within 5 minutes of bubbling with CO_2 (see Figure 5.55).

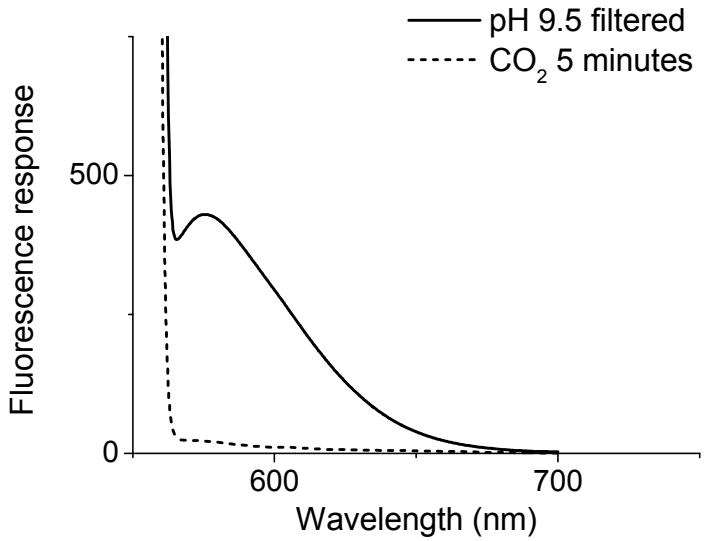

Figure 5.55: Plot of fluorescence response for micelles of 4.07 at pH 9.5 in 0.5 M NaCl before and after bubbling with CO_2

5.2.13 Self-assembly of DMAPS-*b*-PMMA diblocks

The addition of PEGMA to DMAPS polymers resulted in the overall hydrophilicity of the DMAPS increasing and therefore lowering the temperature at which the block becomes hydrophilic. In order to explore the effect purely a hydrophobic group has on the thermo-responsive behaviour of DMAPS, diblock copolymers were synthesised by the chain extension of DMAPS homopolymers with MMA. Diblock copolymer **4.10** (M_n (^{1}H NMR) = 52.2 kDa, M_n (HFIP SEC) = 31.6 kDa, $Đ_M$ = 1.80) was synthesised by the chain extension of a DMAPS homopolymer, **4.08**, (DP = 125) with MMA in water as an emulsion polymerisation. A discussion on the causes of the broader dispersity can be found in Chapter Four. This diblock copolymer bears a DMAPS block length of 125 and a hydrophobic block of 181 MMA units. The DMAPS homopolymer **4.08** displays no measurable UCST cloud point.

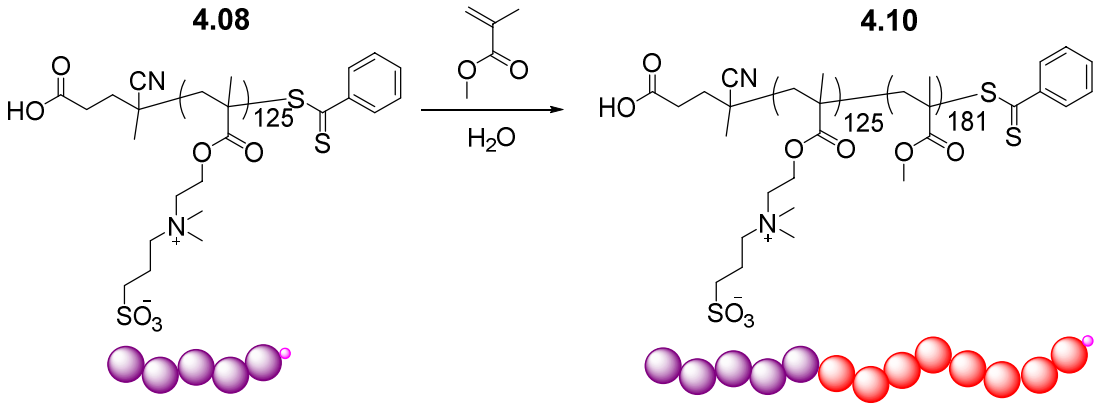

Scheme 5.6: The chain extension of DMAPS homopolymer 4.08 with MMA in water to form diblock copolymer 4.10

Since the diblock copolymer **4.11** contains a larger hydrophobic fraction, self-assembly *via* solvent switch was investigated. The polymer was dissolved in HFIP at a concentration of 2 mg mL^{-1} and then 18.2 MΩ cm^{-1} water was slowly added until the polymer concentration reached 1 mg mL^{-1}. The solution turned cloudy and then was dialysed against water to remove the HFIP. However during dialysis the polymer precipitated. Therefore this method of self-assembly was not successful. The diblock copolymer **4.11** was then self-assembled in water by direct dissolution at 1 mg mL^{-1}. Analysis by DLS gives a population with D_h = 98 ± 8 nm. The thermo-response of the diblock copolymer was measured by DLS with heating. A 1 mg mL^{-1} solution of the polymer in 18.2 MΩ cm^{-1} was measured by DLS from 5 °C to 65 °C with the size being measured every 5 °C. There was no significant size change across the temperature range (see Figure 5.56). This is not unexpected because of the smaller size of the DMAPS block. The homopolymer of DMAPS used to synthesise the diblock displays no UCST cloud point and so it can be considered to be hydrophilic across the temperature range. Therefore this block can be considered to be permanently hydrophilic and the diblock copolymer displays no thermo-responsive behaviour.

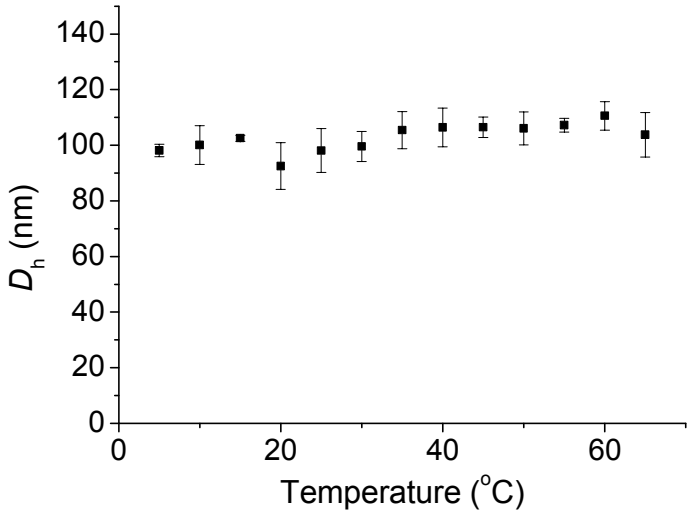

Figure 5.56: Plot of D_h *vs* temperature as measured by DLS analysis for a 1 mg mL^{-1} solution of diblock copolymer 4.10 in water

Analysis of this self-assembled solution by TEM showed the presence of spherical structures with an average size of 60 ± 10 nm (see Figure 5.57). This is smaller than that observed by DLS analysis but this is a result of the TEM analysis on a dried sample of the polymer and the DLS analysis is performed on the polymer in solution, when it is hydrated. Therefore as the polymer dried on the grid it collapses and a smaller size is observed.[36]

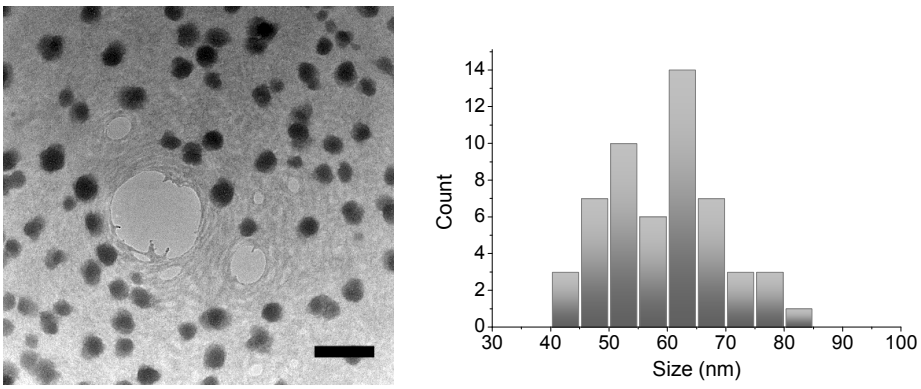

Figure 5.57: TEM image of micelles of 4.10 at 0.1 mg mL^{-1} on graphene oxide, scale bar = 200 nm, and the distribution of sizes observed

A similar diblock copolymer but having a longer DMAPS block length of 400 and a shorter MMA block length of 100 units was synthesised by the chain extension of the DMAPS

homopolymer **4.09** (M_n (^{1}H NMR) = 111.6 kDa, M_n (Aqueous SEC) = 59.7 kDa, $Đ_M$ = 1.09) in HFIP to yield **4.11** (M_n (^{1}H NMR) = 121.7 kDa, M_n (HFIP SEC) = 73.1, $Đ_M$ = 1.34).

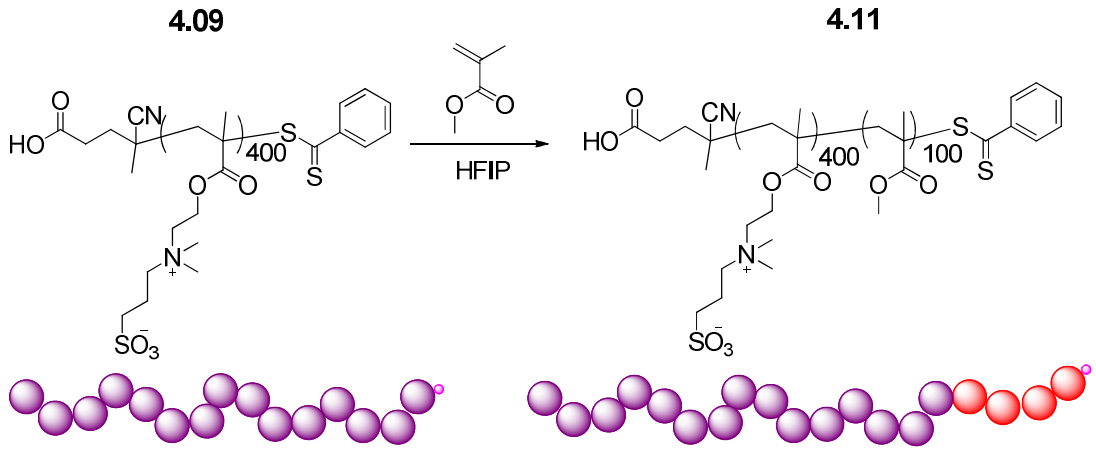

Scheme 5.7: Scheme showing the synthesis of diblock copolymer 4.11 by the chain extension of homopolymer 4.09 with MMA in HFIP

The macroCTA homopolymer of DMAPS, **4.09**, displayed a UCST cloud point of 19 °C at 1 mg mL^{-1}. It has been previously seen that incorporation of hydrophobic acrylonitrile into polymers of acrylamide causes an increase in the UCST cloud point displayed.[50] Therefore it may be expected that chain extending the DMAPS homopolymer with the hydrophobic MMA may cause an increase in the UCST cloud point. Diblock copolymer **4.11** was self-assembled by direct dissolution into water at a concentration of 1 mg mL^{-1}.The size of the structures at 25 °C was 67 ± 3 nm as observed by DLS analysis. The temperature response of the polymer was also investigated by DLS. The size was measured by DLS every 5 °C between 5 °C and 70 °C. The size can be seen to increase from 59 ± 2 nm at 5 °C to 81 ± 2 nm at 70 °C (see Figure 5.58). The MMA block is permanently hydrophobic and the DMAPS block is thermo-responsive, becoming more hydrophilic as the temperature increases. Based on the cloud point of the homopolymer **4.09** (19 °C) it would be expected that below this temperature the DMAPS would become completely hydrophobic and therefore precipitation would occur. However even at 5 °C there is an absence of precipitate and micelles are shown to be present by DLS analysis.

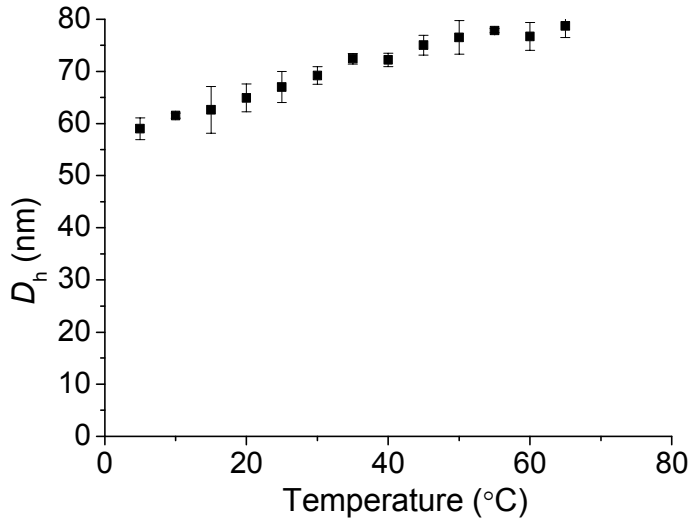

Figure 5.58: Plot of D_h *vs* temperature for a 1 mg mL^{-1} solution of diblock copolymer 4.11 in water

TEM analysis confirms the presence of micelles with an average size of 50 ± 12 nm (see Figure 5.59). As a consequence of particle aggregation and film formation in dry state TEM, the TEM sample was prepared by the freeze-drying method. 5 μL of a 0.1 mg mL^{-1} self-assembled solution of **4.11** was frozen onto a lacey carbon grid and the water then removed by lyophilisation. This method is not ideal due to the damage that can occur to the grid upon freezing. It was obvious to see the micelles on the grid bars, as there was little graphene oxide left on the grid after freezing.

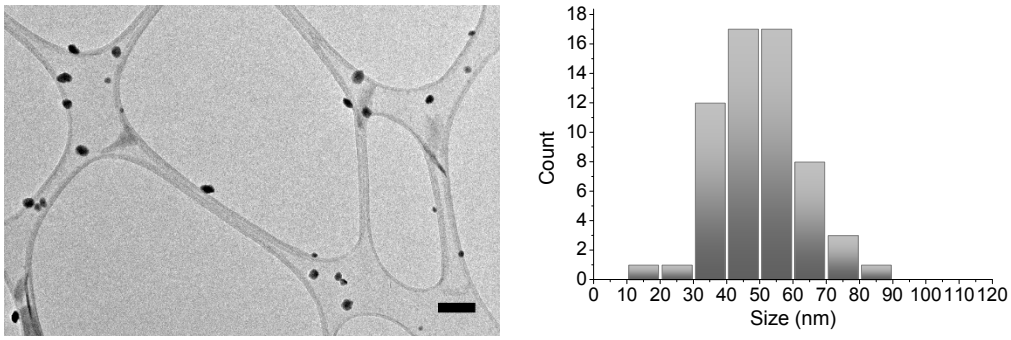

Figure 5.59: TEM of 4.11 at 0.1 mg mL^{-1} on graphene oxide, scale bar = 200 nm and the distribution of sizes observed

5.2.13.1 Investigation of the micelle swelling behaviour by ^{1}H NMR spectroscopy

In order to investigate why the polymers do not precipitate but remain self-assembled at such low temperatures, ^{1}H NMR spectroscopy experiments were performed at a range of temperatures between 5 °C and 65 °C, as described for **4.02**. A solution of **4.11** was made at 5 mg mL^{-1} in D_2O. ^{1}H NMR spectroscopy was performed at temperatures ranging from 5 to 65 °C every 10 °C. A small amount of DMF was used as an internal standard to help calculate the percentage hydrophilicity of the polymer. The COH peak of the DMF was set at an integration of 1 and three separate peaks relating to the DMAPS block were integrated relative to this DMF peak (see Figure 5.60). The integration of each peak at the highest temperature was assumed to be 100% hydrophilic, *i.e.* all the DMAPS side chains are hydrated. The integrations of the same peaks at different temperatures were compared to these "100%" peaks to calculate the percentage hydrophilicity present in the polymer at that temperature.

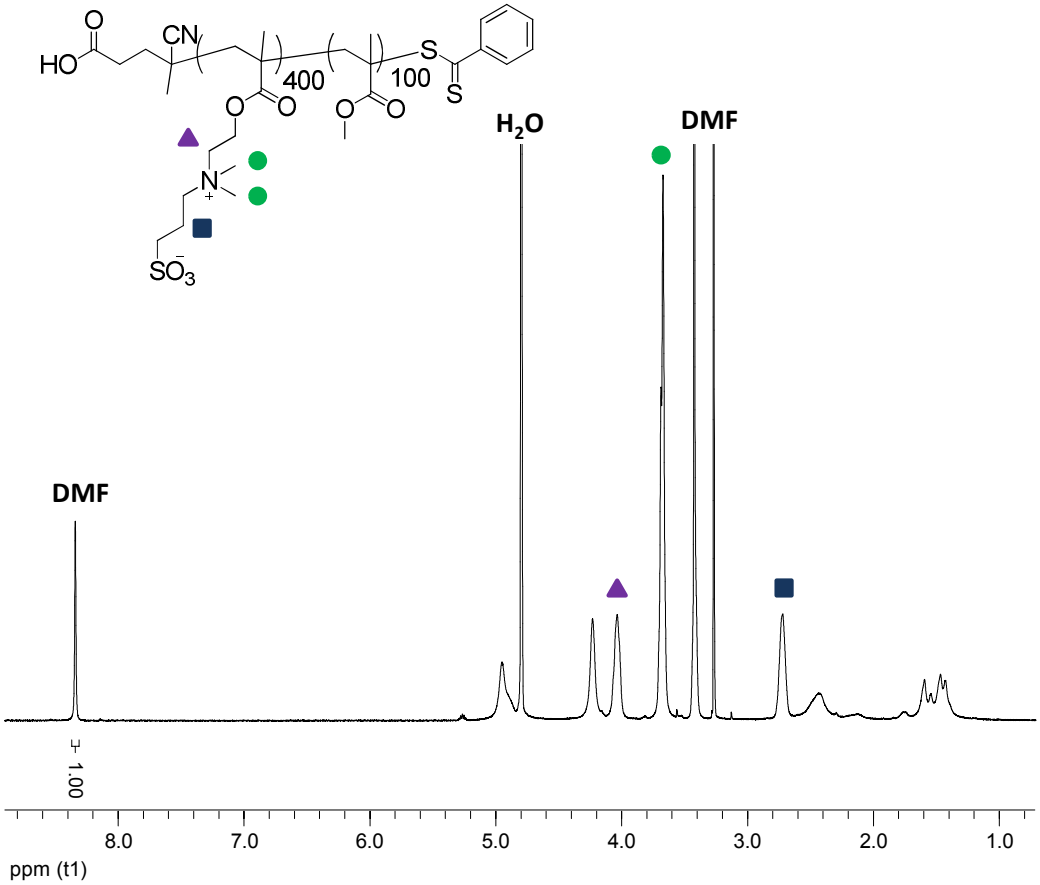

Figure 5.60: ^{1}H NMR spectrum of diblock copolymer 4.11 in D_2O, showing the three DMAPS peaks used for calculating remaining hydrophilicity, recorded at 65 °C and 500 MHz

Figure 5.61 shows how the integrations of the DMAPS peaks change with temperature. The betaine block never becomes fully hydrophobic, even at temperatures of 5 °C approximately 35 % of the block remains hydrophilic. The MMA block is not visible as it is not solvated.[51]

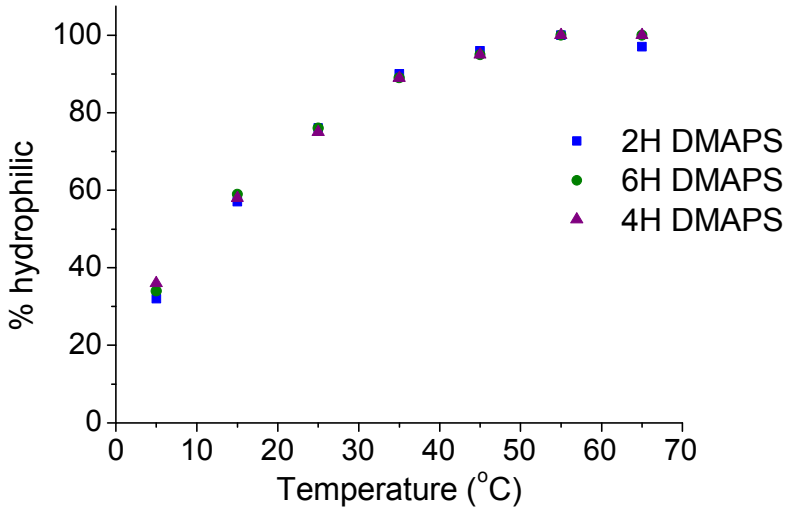

Figure 5.61 Graph showing how the % hydrophilicity of the DMAPS block of diblock 4.11 changes with temperature

This remaining hydrophilicity causes the polymers to stay self-assembled, even at temperatures well below the UCST cloud point of the DMAPS block. This is similar to that seen for **4.02** where the addition of the PEGMA causes the DMAPS block to retain some hydrophilicity. Therefore it appears that the incorporation of DMAPS into block copolymers affects the UCST cloud point behaviour, regardless of whether the other block is hydrophilic or hydrophobic.[2]

5.2.13.2 Investigation of the swelling behaviour of 4.11 by SLS

The *dn/dc* for **4.11** in water was calculated as described for **4.02** and found to be 0.125 mL g^{-1} (see Figure 5.62).

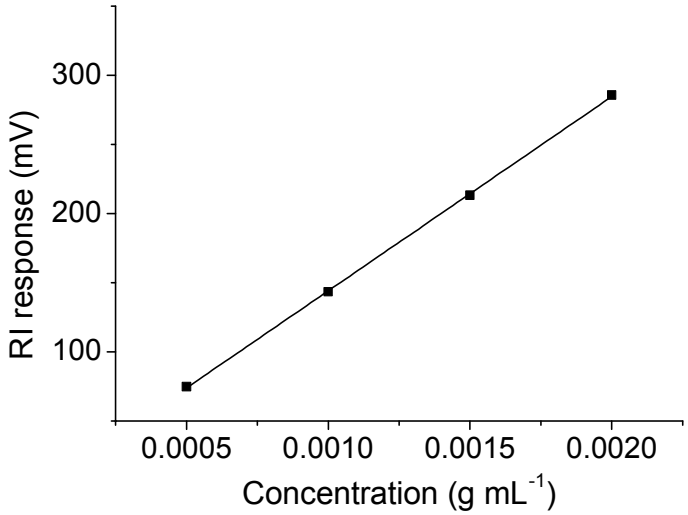

Figure 5.62: Plot showing the change in refractive index with concentration for 4.11 in water. The *dn/dc* was calculated to be 0.125 mL g^{-1} from the slope of the linear fit

Self-assembled solutions of **4.11** at concentrations between 0.5 and 2 mg mL^{-1} were analysed by SLS and multi-angle DLS at 20 °C and 60 °C, as described for **4.02**. The inverse of the relaxation time for the fast mode divided by q^2 (τ_{fast}^{-1}/q^2) was plotted against the scattering vector squared (q^2) (see Figure 5.63). This was extrapolated to zero angle to yield the apparent diffusion coefficient. Copolymer **4.11** in water at 1 mg mL^{-1} at 20 °C was found to have an apparent diffusion coefficient of 5.72 x 10^{-12} m^2 s^{-1} which corresponds to a hydrodynamic diameter of 74 nm. The sample was also measured at 60 °C and **4.11** at 1 mg mL^{-1} had an apparent diffusion coefficient of 1.25 x 10^{-11} m^2 s^{-1} which corresponds to a hydrodynamic diameter of 86 nm.

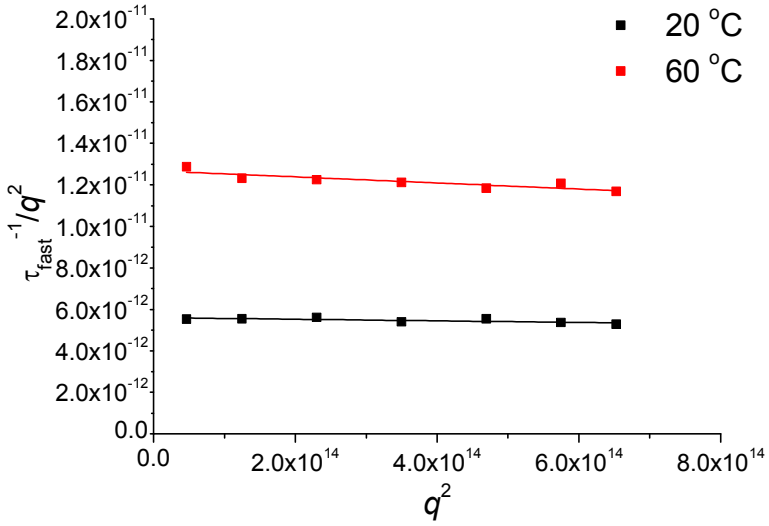

Figure 5.63: Plot of τ_{fast}^{-1}/q^2 *vs* q^2 for self-assembled micelles based on copolymer 4.11 at 1 mg mL^{-1} in water, determined at 20 °C (D_h = 74 nm) and at 60 °C (D_h = 86 nm)

Plotting the apparent diffusion coefficient for each concentration against concentration yields the translational diffusion coefficient. At 20 °C a D_t of 5.89 x 10^{-12} m^2 s^{-1} was obtained, which corresponds to a hydrodynamic diameter of 72 nm. At 60 °C the translational diffusion coefficient is 1.20 x 10^{-11} m^2 s^{-1} which corresponds to a hydrodynamic diameter of 87 nm (see Figure 5.64).

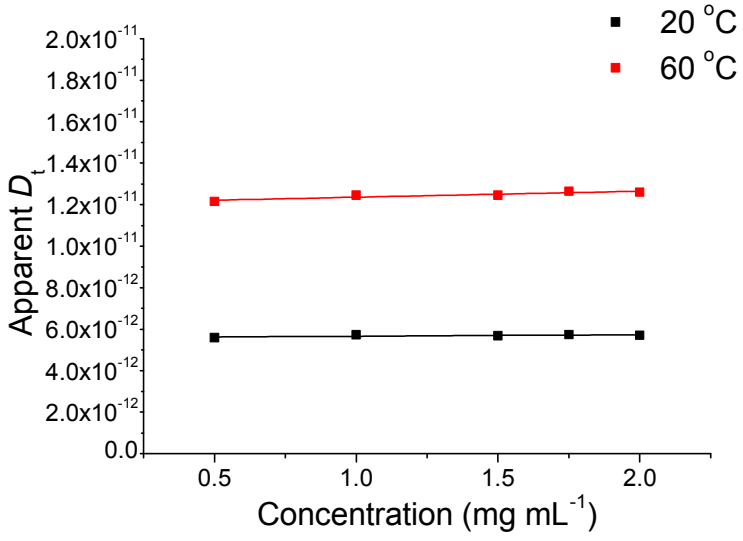

Figure 5.64: Plot of apparent D_t against concentration for diblock 4.11 at 20 °C and 60 °C. The intercepts of the linear fits correspond to the hydrodynamic diameters

$Kc/R_{\theta,\ fast}$ was plotted against q^2 for each concentration and each plot extrapolated to zero angle. The extrapolated $Kc/R_{\theta,\ fast}$ value was then plotted against concentration and extrapolated to zero concentration, which was used to determine the absolute molecular weight of the nanostructure at each temperature. The absolute molecular weight of the self-assembled structures of **4.11** was determined to be 27.5 MDa at 20 °C and 27.6 MDa at 60 °C. The R_g/R_h ratio at 20 °C was calculated to be 0.78 and at 60 °C was 0.71.

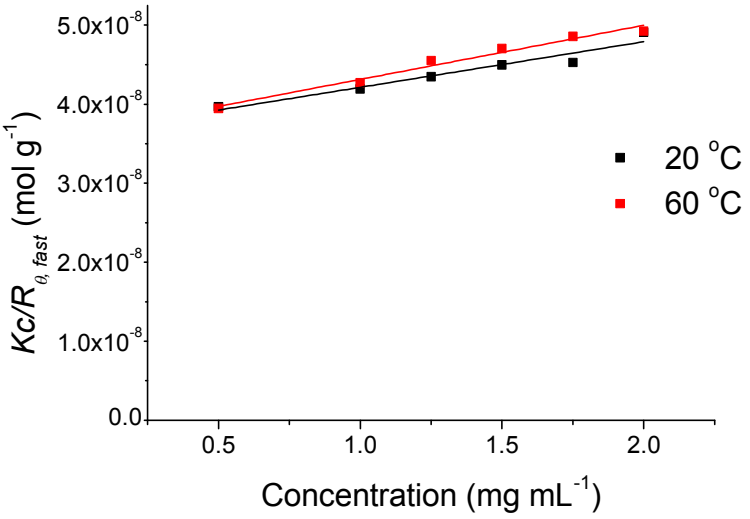

Figure 5.65: Plot of $Kc/R_{\theta,\ fast}$ *vs* concentration for self-assembled solutions of 4.11 at 20 °C and 60 °C. The M_w of the micelles was calculated using the intercept of the linear fit to the SLS data

The molecular weights of the micelles are very similar at 20 °C and 60 °C indicating that there has been no change in the aggregation number of the structures at the different temperatures. The difference in size is evident from the hydrodynamic diameters calculated (73 nm at 20 °C and 86 nm at 60 °C) and therefore this increase in size but not molecular weight confirms that the swelling seen is solely due to the hydration of the DMAPS block, as expected and not any difference in aggregation of the polymer chains.

5.2.13.3 Release of hydrophobic payloads from the swollen micelle

At lower temperatures the micelles formed by **4.11** are shrunken as the DMAPS block is mainly hydrophobic. This means that at low temperatures the hydrophobic core will be larger due to the permanently hydrophobic PMMA block and the hydrophobic portion of the DMAPS. At higher temperatures the DMAPS block becomes hydrophilic and hydrated and so the hydrophobic core of the micelles is smaller at elevated temperatures. Therefore it should be possible to encapsulate a hydrophobic payload within the core of the micelles at low temperatures and then release some of the payload at higher temperatures.

A 1 mg mL^{-1} solution of **4.11** was stirred overnight at 4 °C with Nile Red at 1 mg mL^{-1}. The solution was then filtered through a 0.45 μm nylon filter whilst cold in order to remove any non-encapsulated Nile Red and the sample tested for fluorescence (λ_{ex} = 550 nm, λ_{em} = 575 nm). There was a significant fluorescence response. The solution was then heated at 65 °C for 20 minutes, and then filtered whilst hot. The fluorescence response had significantly decreased, showing that some Nile Red had been released from the micelles upon heating (see Figure 5.66). This shows that even though the micelle remains intact throughout the temperature range, some Nile Red is released as the size of the hydrophobic core decreases.

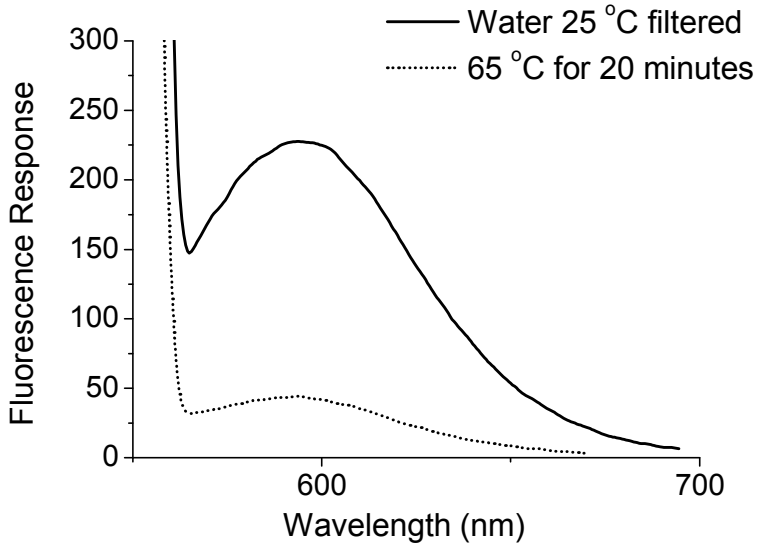

Figure 5.66: Plot of fluorescence of micelles of 4.11 loaded with Nile Red before and after heating at 65 °C for 20 minutes

5.3 Conclusion

In this Chapter a series of di-and triblock copolymers containing a thermo-responsive DMAPS block have been synthesised. Firstly, a series of PEGMA-*b*-DMAPS(-*b*-PEGMA) di- and triblock copolymers were investigated and were shown to self-assemble into micelles in water. All underwent a transition to unimers with heating and the transition temperature decreased as the overall hydrophilicity of the polymer increased. The assemblies were used to encapsulate and release a hydrophobic payload in response to temperature.

Triblock copolymers containing a hydrophilic block, DMAPS and a hydrophobic block were also investigated and shown to self-assemble into micelles in water. These micelles undergo a swelling with temperature. Replacing the permanently hydrophobic block with a responsive block, DEAEMA, allowed triply responsive polymers to be formed. This is the first example of a triply-responsive sulfobetaine containing polymer. The triblock copolymer self-assembled into vesicles at pH 5.6 and undewent a vesicle to unimer morphology transition with heating. Dissolution in acidic media and then increasing the pH resulted in a reversible unimer to micelle transition. The micelles could also be dissociated by purging with CO_2 and reformed upon purging with nitrogen. The CO_2-responsive nature of the micelles was utilised to encapsulate and release a hydrophobic payload.

Finally, the first examples of amphiphilic diblock copolymers directly synthesised from the sulfobetaine monomer, without post-polymerisation modification techniques, are demonstrated. Interestingly these diblock copolymers do not display a cloud point, unlike DMAPS homopolymers. Investigation by ^{1}H NMR spectroscopy shows that the DMAPS block does not become fully hydrophobic and hence the cloud point disappears.

5.4 Experimental

5.4.1 Materials

1,4-Dioxane, poly(ethylene glycol) methyl ether methacrylate (PEGMA), [2-(methacryloyloxy)ethyl]dimethyl-(3-sulfopropyl)ammonium hydroxide (DMAPS), 4-cyano-4-(phenylcarbonothioylthio)pentanoic acid (CPTA) and 4, 4'- azobis(4-cyanopentanoic acid) (ACVA) were used as received from Aldrich and Fluka unless otherwise stated. AIBN [2, 2'- azobis (2-methylpropionitrile)] was recrystallised twice from methanol and stored in the dark at 4 °C. Hexafluoroisopropanol (HFIP) was received from Fluorochem and Apollo.

5.4.2 Characterisation

^{1}H Nuclear magnetic resonance (NMR) experiments were performed on a Bruker 500 FT-NMR spectrometer operating at 500 MHz using deuterated solvents. Chemical shifts are reported in parts per million relative to H_20 (4.79 ppm).

Hydrodynamic diameters (D_h) and size distributions of the self-assembled structures in aqueous solutions were determined by dynamic light scattering (DLS). The DLS instrumentation consisted of a Malvern ZetasizerNanoS instrument operating at 25 °C (unless otherwise stated) with a 4 mW He-Ne 633 nm laser module. Measurements were made at a detection angle of 173° (back scattering) and Malvern DTS 6.20 software was utilised to analyse the data. All measurements were run at least three times with a minimum of 10 runs per measurement.

SLS and DLS measurements were recorded simultaneously on an ALV CGS3 spectrometer consisting of a 22 mW HeNe laser at λ = 632.8 nm. Measurements were carried out at two different temperatures, 20 and 50 °C, and recorded at least 7 scattering angles between 20 and 150°. The scattering vector was defined as

$$q = \frac{4\pi n}{\lambda\left[sin\frac{\theta}{2}\right]}$$

where n is the refractive index of the solvent. Concentrations between 0.1 and 2 mg.mL^{-1} were analysed for each sample. At least two measurements were run on each angle, each run for at least 100 seconds to determine the auto correlation function, $g_2(t)$, from DLS and the mean scattered intensity, I, from SLS. The resulting correlation functions were analysed using the REPES programme.[35] The R_h for the fast mode was determined by plotting the apparent diffusion coefficient for each concentration, D_{fast}, against concentration and extrapolating to zero concentration. $Kc/R_{\theta, fast}$ *vs* q^2 was plotted and from this the molecular weight and R_g for the nanostructure were determined. N_{agg} was determined by comparing the molecular weight of the assembled structures to the absolute molecular weight of the polymer.

The differential refractive index for the samples was calculated using a Shodex RI-101 refractometer. The refractive index response was plotted against concentration and the slope of the graph used to calculate the *dn/dc* using the following equation, where n^o is the refractive index of the solvent and K is the instrument constant.

$$\frac{dn}{dc} = \frac{slope \times n^o}{K}$$

TEM characterisation was carried out using lacy carbon grids that had been treated with graphene oxide (GO). GO solutions were synthesised as previously described.[52] One drop of GO solution was deposited onto an oxygen plasma treated lacy carbon copper grid and left to air dry. 4 μL of solution was deposited onto the grid and either left to dry completely or blotted off after a set period of time. Freeze dried samples were prepared by depositing a drop of solution onto a GO coated grid. This grid was then held inside a vial immersed in liquid nitrogen until frozen. The grid was then dried under vacuum. Analysis was performed on a JEOL 200FX microscope operating at 200 keV. Number average particle diameters (D_{av}) were generated from the analysis of a minimum of 50 particles from at least three

different micrographs. Fluorescence measurements were recorded on a Perkin Elmer LS 55 spectrometer. Dialysis tubing was purchased from Spectrum labs with molecular weight cut offs of 3.5 kDa and 12-14 kDa.

Small-angle X-ray scattering (SAXS) measurements were carried out on the SAXS/WAXS beamline at the Australian Synchrotron facility at photon energy of 8.2 keV. The samples were prepared in 18.2 MΩ cm^{-1} water and were run using 1.5 mm diameter quartz capillaries. Capillaries were held in a sample holder with temperature control achieved *via* a water bath connected to the sample holder. Temperatures of 5, 10, 19, 24, 28, 32, 36, 40, 45 and 50 °C were reached, and each sample was allowed to equilibrate for 5 minutes. The measurements were collected at a sample to detector distance of 3.252 m to give a q range of 0.0015 to 0.07 $Å^{-1}$, where q is the scattering vector and is related to the scattering angle (2θ) and the photon wavelength (λ) by the following equation:

$$q = \frac{4\pi sin(\theta)}{\lambda}$$

All patterns were normalised to fixed transmitted flux using a quantitative beamstop detector. The scattering from a blank (H_2O) was measured in the same location as sample collection and was subtracted for each measurement. The two-dimensional SAXS images were converted in one-dimensional SAXS profile (*I (q) versus q*) by circular averaging, where *I (q)* is the scattering intensity. The functions used for the fitting from the NIST SANS analysis package were "Debye"[39] and "Core-Shell with Constant Core/Shell Ratio" models.[40-42] ScatterBrain and Igor software were used to plot and analyse data. The scattering length density of the solvent and the monomers were calculated using the "Scattering Length Density Calculator" provided by NIST Center for Neutron Research Limits for q range were applied for the fitting from 0.002 to 0.05 $Å^{-1}$.[43]

5.4.3 Self-assembly of the polymers

5.4.3.1 Direct dissolution

Polymers were self-assembled by direct dissolution at 1 mg mL^{-1} in 18.2 MΩ cm^{-1} water. The solutions were gently heated (*ca.* 40 °C) to aid dissolution and then were allowed to cool to room temperature with stirring.

5.4.3.2 Solvent switch

The polymer was dissolved in HFIP at a concentration of 2 mg mL^{-1}. Water was added slowly until a concentration of 1 mg mL^{-1} was reached and the solution then dialysed to remove the HFIP.

5.4.4 Encapsulation and release studies

The encapsulations and release studies were performed in the same manner for both polymers **4.02**, **4.03**, **4.04**, **4.07** and **4.11**. The polymer was self-assembled at a concentration of 1 mg mL^{-1}. Nile Red was added at a concentration of 1 mg mL^{-1}. The solution was stirred overnight at 4 °C. Non encapsulated Nile Red was removed by filtration through a 0.45 μm Nylon filter. The fluorescence response was then recorded by exciting at λ_{ex} 550 nm and recording the emission at 575 nm. The micelle solution was then heated (36 °C for **4.02**, 38 °C for **4.03,** 34 °C for **4.04,** 65 °C for **4.11**) for 5 minutes. The solution was then filtered whilst hot to remove the precipitated Nile Red and the fluorescence again recorded at λ_{ex} 550 nm, λ_{em} 575 nm. In the case of **4.07**, the solution was bubbled with CO_2 for 5 minutes before filtering.

5.5 Appendix

Polymer **4.04** was self-assembled in pure water by direct dissolution with gentle heating. The hydrodynamic diameter of **4.04** was analysed using multi-angle DLS, as for **4.02**. The inverse of the relaxation time for the fast mode divided by q^2 (τ_{fast}^{-1}/q^2) was plotted against the scattering vector squared (q^2) (see Figure 5.67). This was extrapolated to zero angle to yield the apparent diffusion coefficient. Copolymer **4.04** in water at 1 mg mL^{-1} was found to have an apparent diffusion coefficient of 6.57 x 10^{-12} m^2 s^{-1} which corresponds to a hydrodynamic diameter of 73 nm.

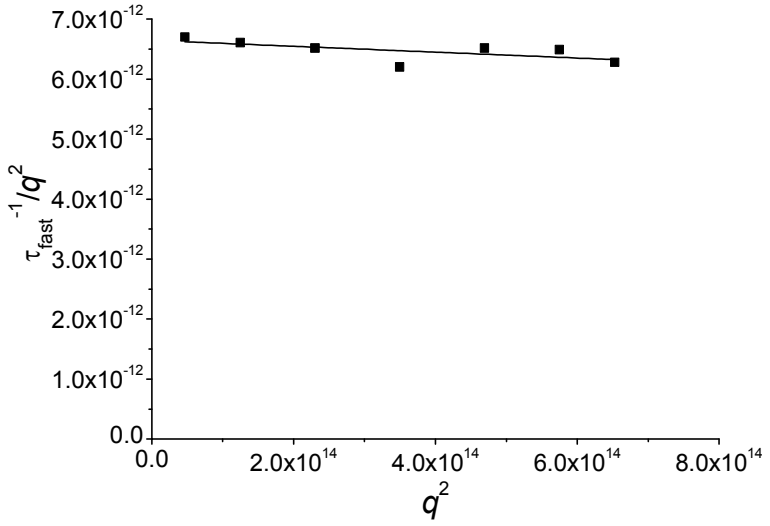

Figure 5.67: Plot of τ_{fast}^{-1}/q^2 *vs* q^2 for self-assembled micelles based on copolymer 4.04 at 1 mg mL^{-1} in water, determined at 20 °C (D_h = 73 nm)

Plotting the apparent diffusion coefficient for each concentration against concentration yields a translational diffusion coefficient of 5.88 x 10^{-12} m^2 s^{-1} which corresponds to a D_h of 82 nm (see Figure 5.68).

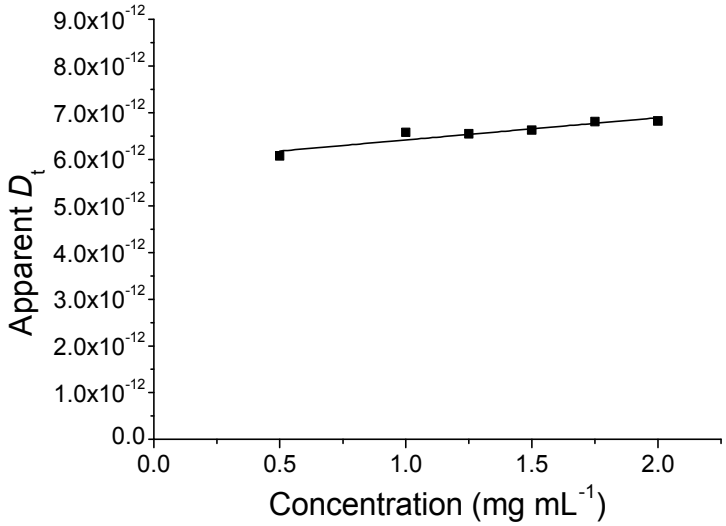

Figure 5.68: Plot of apparent D_t against concentration for triblock 4.04. The intercept of this graph corresponds to a D_h of 82 nm

The absolute molecular weight of the self-assembled structures of **4.04** was determined to be 24.3 MDa by SLS analysis, as described for **4.02** (see Figure 5.69**)**. This corresponds to a N_{agg} of 77 polymer chains per micelle, using an absolute molecular weight for an individual polymer chain of 317 kDa, as determined by SLS (Chapter Four). The R_g/R_h ratio for **4.04** at 1 mg mL^{-1} was calculated to be 0.89.

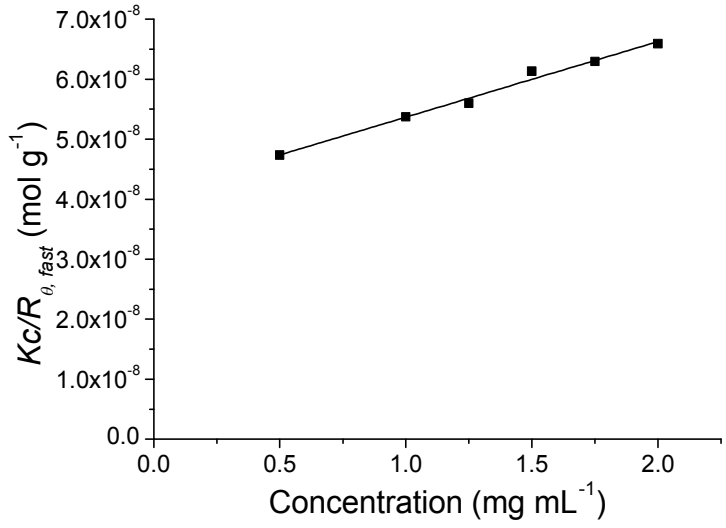

Figure 5.69: Plot of $Kc/R_{\theta, fast}$ *vs* concentration for self-assembled solutions of triblock copolymer 4.04. The M_w was calculated using the intercept of the linear fit to the SLS data and found to be 24.3 MDa

Triblock copolymer **4.05** was analysed in the same manner and was found to have an apparent diffusion coefficient of 6.44 x 10^{-12} m^2 s^{-1} at 1 mg mL^{-1} which corresponds to a hydrodynamic diameter of 75 nm (see Figure 5.70).

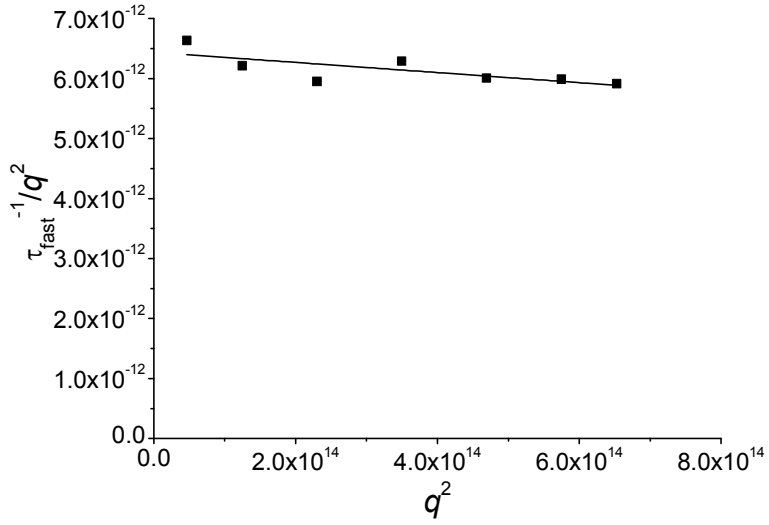

Figure 5.70: Plot of τ_{fast}^{-1}/q^2 *vs* q^2 for self-assembled micelles of triblocks copolymer 4.05 at 1 mg mL^{-1} in water, determined at 20 °C (D_h = 75 nm)

Plotting the apparent diffusion coefficient for each concentration against concentration yields a translational diffusion coefficient of 5.97 x 10^{-12} m^2 s^{-1} which corresponds to a hydrodynamic diameter of 80 nm (see Figure 5.71). Again this value is slightly higher than that observed at 1 mg mL^{-1} and is a result of interactions between the micelles at higher concentrations.

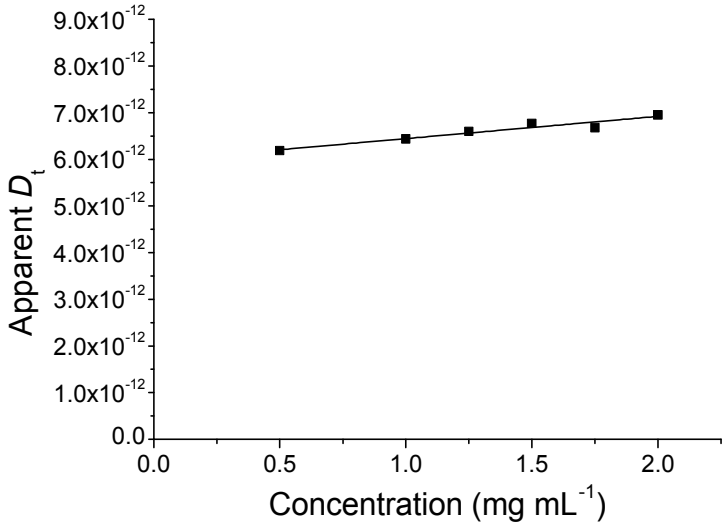

Figure 5.71: Plot of apparent D_t against concentration for triblock copolymer 4.05. The intercept of this graph corresponds to a D_h of 80 nm

The absolute molecular weight of the self-assembled structures of **4.04** was determined to be 17.9 MDa by SLS analysis, as described for **4.02**. This corresponds to a N_{agg} of 54 polymer chains per micelle, using an absolute molecular weight for an individual polymer chain of 330 kDa, as determined by SLS (Chapter Four). The R_g/R_h ratio for **4.04** at 1 mg mL^{-1} was calculated to be 0.81.

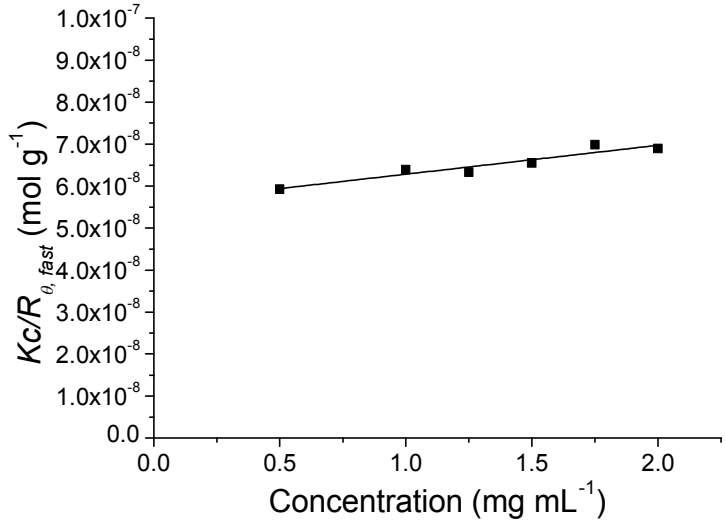

Figure 5.72: Plot of $Kc/R_{\theta, fast}$ *vs* concentration for self-assembled solutions of 4.05. The M_w was calculated using the intercept of the linear fit to the SLS data and found to be 17.9 MDa

5.6 References

1. J. Seuring and S. Agarwal, *Macromol. Rapid Commun.*, 2012, 33, 1898-1920.
2. M. I. Gibson and R. K. O'Reilly, *Chem. Soc. Rev.*, 2013, 42, 7204-7213.
3. H. Willcock, A. Lu, C. F. Hansell, E. Chapman, I. R. Collins and R. K. O'Reilly, *Polym. Chem.*, 2014, 5, 1023-1030.
4. D. Roy, W. L. A. Brooks and B. S. Sumerlin, *Chem. Soc. Rev.*, 2013, 42, 7214-7243.
5. L. Klouda and A. G. Mikos, *Eur. J. Pharm. Biopharm.*, 2008, 68, 34-45.
6. R. Liu, M. Fraylich and B. Saunders, *Colloid. Polym. Sci.*, 2009, 287, 627-643.
7. S. Dai, P. Ravi and K. C. Tam, *Soft Matter*, 2009, 5, 2513-2533.
8. F. D. Jochum and P. Theato, *Chem. Soc. Rev.*, 2013, 42, 7468-7483.
9. A. B. Lowe and C. L. McCormick, *Chem. Rev.*, 2002, 102, 4177-4190.
10. B. Yu, A. B. Lowe and K. Ishihara, *Biomacromolecules*, 2009, 10, 950-958.
11. J. C. Salamone, W. Volksen, A. P. Olson and S. C. Israel, *Polymer*, 1978, 19, 1157-1162.
12. V. M. Monroy Soto and J. C. Galin, *Polymer*, 1984, 25, 121-128.
13. R. Hart and D. Timmerman, *J. Polym. Sci.*, 1958, 28, 638-640.
14. S. Nakai, T. Nakaya and M. Imoto, *Makromol. Chem.*, 1977, 178, 2963-2967.
15. H. Ladenheim and H. Morawetz, *J. Polym. Sci.*, 1957, 26, 251-254.
16. M. S. Donovan, A. B. Lowe, T. A. Sanford and C. L. McCormick, *J. Polym. Sci., Part A: Polym. Chem.*, 2003, 41, 1262-1281.
17. D. Wang, T. Wu, X. Wan, X. Wang and S. Liu, *Langmuir*, 2007, 23, 11866-11874.
18. M. Arotçaréna, B. Heise, S. Ishaya and A. Laschewsky, *J. Am. Chem. Soc.*, 2002, 124, 3787-3793.
19. Z. Tuzar, H. Pospisil, J. Plestil, A. B. Lowe, F. L. Baines, N. C. Billingham and S. P. Armes, *Macromolecules*, 1997, 30, 2509-2512.
20. A. B. Lowe, N. C. Billingham and S. P. Armes, *Macromolecules*, 1999, 32, 2141-2148.
21. D. N. Schulz, D. G. Peiffer, P. K. Agarwal, J. Larabee, J. J. Kaladas, L. Soni, B. Handwerker and R. T. Garner, *Polymer*, 1986, 27, 1734-1742.
22. M. Noh, Y. Mok, D. Nakayama, S. Jang, S. Lee, T. Kim and Y. Lee, *Polymer*, 2013, 54, 5338-5344.
23. J. Seuring and S. Agarwal, *ACS Macro Lett.*, 2013, 2, 597-600.
24. Y. J. Che, Y. Tan, J. Cao and G. Y. Xu, *J. Macromol. Sci., Phys.*, 2010, 49, 695-710.
25. P. Mary, D. D. Bendejacq, M. P. Labeau and P. Dupuis, *J. Phys. Chem. B*, 2007, 111, 7767-7777.

26. Y. J. Shih, Y. Chang, A. Deratani and D. Quemener, *Biomacromolecules*, 2012, 13, 2849-2858.
27. L. Chen, Y. Honma, T. Mizutani, D. J. Liaw, J. P. Gong and Y. Osada, *Polymer*, 2000, 41, 141-147.
28. M. Kobayashi, Y. Terayama, M. Kikuchi and A. Takahara, *Soft Matter*, 2013, 9, 5138-5148.
29. J. Virtanen, M. Arotçaréna, B. Heise, S. Ishaya, A. Laschewsky and H. Tenhu, *Langmuir*, 2002, 18, 5360-5365.
30. F. Polzer, J. Heigl, C. Schneider, M. Ballauff and O. V. Borisov, *Macromolecules*, 2011, 44, 1654-1660.
31. A. Blanazs, S. P. Armes and A. J. Ryan, *Macromol. Rapid Commun.*, 2009, 30, 267-277.
32. A. A. Choucair, A. H. Kycia and A. Eisenberg, *Langmuir*, 2003, 19, 1001-1008.
33. D. J. Adams, M. F. Butler and A. C. Weaver, *Langmuir*, 2006, 22, 4534-4540.
34. T. Azzam and A. Eisenberg, *Angew. Chem. Int. Ed.*, 2006, 45, 7443-7447.
35. J. Jakes, *Collect. Czech. Chem. Commun.*, 1995, 60, 1781-1797.
36. J. P. Patterson, M. P. Robin, C. Chassenieux, O. Colombani and R. K. O'Reilly, *Chem. Soc. Rev.*, 2014, DOI: 10.1039/C3CS60454C.
37. J. P. Patterson, E. G. Kelley, R. P. Murphy, A. O. Moughton, M. P. Robin, A. Lu, O. Colombani, C. Chassenieux, D. Cheung, M. O. Sullivan, T. H. Epps and R. K. O'Reilly, *Macromolecules*, 2013, 46, 6319-6325.
38. W. Burchard, in *Light Scattering from Polymers*, Springer Berlin Heidelberg, 1983, vol. 48, ch. 1, pp. 1-124.
39. R. J. Roe, *Methods of X-ray and Neutron Scattering in Polymer Science*, Oxford University Press, 2000.
40. J. B. Hayter, in *Physics of Amphiphiles-Micelles, Vesicles, and Microemulsions*, ed. M. C. V. DeGiorgio, North-Holland Publishing Company, 1983, pp. 59-93.
41. S. T. Mudie, Australian Synchrotron, 1.15 edn., 2013.
42. J. A. C. S. Kline, 39, 895-900, *J. Appl. Crystallogr.*, 2006, 39, 895-900.
43. NIST SLD calculator, http://www.ncnr.nist.gov/resources/sldcalc.html.
44. G. Riess, *Prog. Polym. Sci.*, 2003, 28, 1107-1170.
45. V. Bütün, S. P. Armes and N. C. Billingham, *Polymer*, 2001, 42, 5993-6008.
46. S. Lin and P. Theato, *Macromol. Rapid Commun.*, 2013, 34, 1118-1133.
47. Y. Özcan, S. İde, U. Jeng, V. Bütün, Y. H. Lai and C. H. Su, *Mater. Chem. Phys.*, 2013, 138, 559-564.
48. R. Stoenescu and W. Meier, *Chem. Commun.*, 2002, DOI: 10.1039/B209352A, 3016-3017.

49. B. Yan, D. Han, O. Boissiere, P. Ayotte and Y. Zhao, *Soft Matter*, 2013, 9, 2011-2016.

50. J. Seuring and S. Agarwal, *Macromolecules*, 2012, 45, 3910-3918.

51. V. Butun, C. E. Bennett, M. Vamvakaki, A. B. Lowe, N. C. Billingham and S. P. Armes, *J. Mater. Chem.*, 1997, 7, 1693-1695.

52. N. R. Wilson, P. A. Pandey, R. Beanland, R. J. Young, I. A. Kinloch, L. Gong, Z. Liu, K. Suenaga, J. P. Rourke, S. J. York and J. Sloan, *ACS Nano*, 2009, 3, 2547-2556.

Chapter Six

Investigation into the synthesis of sulfobetaine acrylate containing polymers *via* RAFT polymerisation

6.1. Introduction

Betaines are a class of monomer that contain both a cationic group and an anionic group on the same moiety.[1] There are three types of betaines that differ in the chemical nature of the cationic and anionic functionality. These are phosphobetaines[2], carboxybetaines[3] and sulfobetaines.[4] Sulfo- and phosphobetaines have been shown to be biocompatible.[5-9] Many polymeric betaines are insoluble in pure water but become soluble upon the addition of salt, due to the anti-polyelectrolyte effect.[10-13] Some sulfobetaines also display an upper critical solution temperature (UCST).[14-16] There are several examples of the methacrylate sulfobetaine, 2-(methacryloyloxy) ethyl dimethyl-(3-sulfopropyl) ammonium hydroxide (DMAPS), being polymerised by controlled polymerisation techniques.[17-19] However the acrylate version, 2-(acryloyloxy) ethyl dimethyl-(3-sulfopropyl) ammonium hydroxide (SBA), has been largely ignored.

Yuan *et al.* synthesised monolithic columns for hydrophilic interaction chromatography by the free radical copolymerisation of SBA and a cross linker, *N,N'*– methylenebisacrylamide (MBA) in a water/methanol mixture within 100 μm capillaries (see Scheme 6.1). By varying the weight content of the cross linker, MBA, the permeability of the columns could be tuned. The columns showed an enhanced hydrophilicity when compared to those that contained DMAPS instead of SBA.[20]

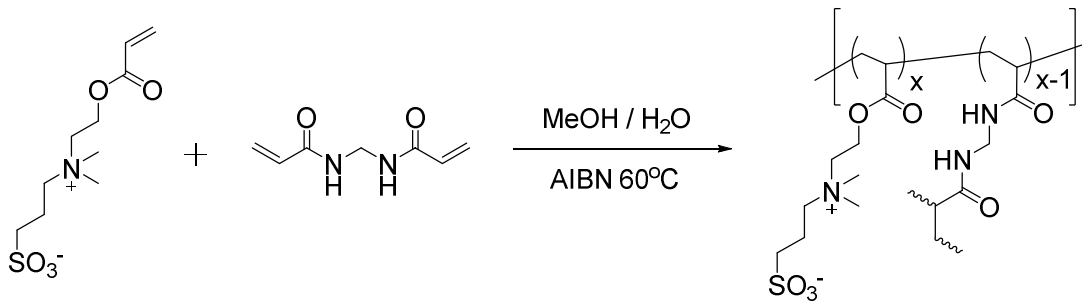

Scheme 6.1: Preparation of the monolithic column by free radical copolymerisation of SBA and MBA[20]

Laschewsky *et al*. reported the free radical polymerisation of another sulfobetaine acrylate monomer with a larger aliphatic spacer length between the acrylate group and the quaternary amine functionality (see Figure 6.1).[21] The solubility of the resulting polymer was

investigated and it was found to be insoluble in cold water (20 °C) but become soluble as the temperature of the water increased to 40 °C or upon the addition of 2% NaCl.

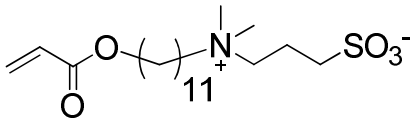

Figure 6.1: The structure of the sulfobetaine acrylate monomer investigated by Laschewsky *et al*[21]

Whilst there are many examples of the post-polymerisation modification of tertiary amine-containing methacrylate polymers with 1,3-propane sultone in order to afford the sulfobetaine functionality,[16, 22-28] this method has not been widely utilised in the synthesis of acrylate sulfobetaine polymers. In one example, Long and co-workers synthesised triblock copolymers consisting of styrene-*b*-(*n*-butyl acrylate-*co*-*N,N*-(dimethyl amino) ethyl acrylate)-*b*-styrene *via* RAFT polymerisation.[29] Firstly polystyrene (PS) was synthesised using a symmetrical trithiocarbonate as the chain transfer agent. The central amine-containing block was then inserted by using this styrene block as a macroCTA in the copolymerisation of *n*-butyl acrylate (*n*BA) and *N,N*-dimethylamino ethyl acrylate (DMAEA) (see Scheme 6.2). The DMAEA containing triblocks had dispersities between 1.39 and 1.44.

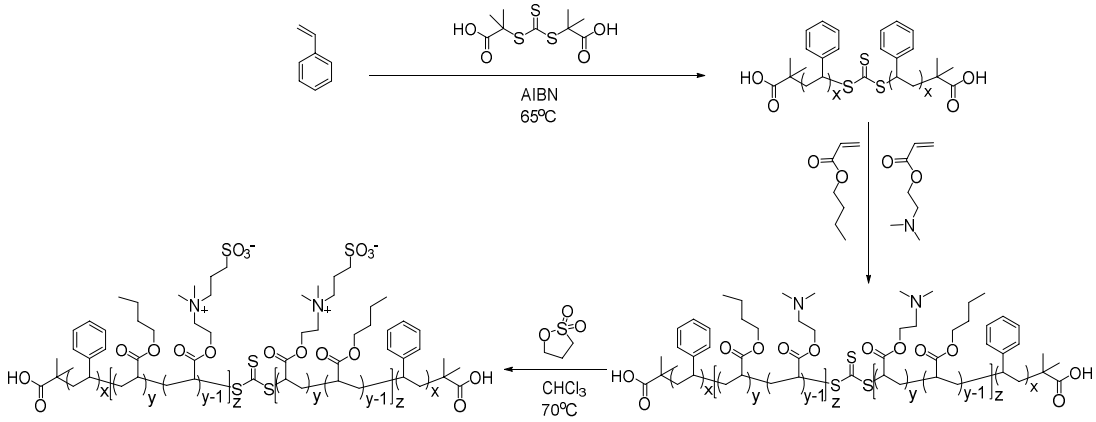

Scheme 6.2: Scheme showing the synthesis of the triblock PS-*b*-(*n*BA-*co*-DMAEA)-*b*-PS and the subsequent reaction with 1,3-propane sultone to afford the sulfobetaine containing triblock[29]

These triblocks were then functionalised with 1,3-propane sultone to yield the sulfobetaine containing triblocks (see Scheme 6.2). The full conversion of the DMAEA to the betaine

was confirmed by ^{1}H NMR spectroscopy. The swelling behaviour of these triblocks in ionic liquids was then investigated.

To the best of our knowledge there are no reports of the controlled polymerisation of sulfobetaine containing acrylates. These polymers are of interest because of their increased hydrophilicity compared to methacrylate sulfobetaines and their potential thermo-responsive properties.

6.2. Results and Discussion

In Chapter Four the synthesis of DMAPS containing polymers was discussed. In this chapter we will explore the synthesis of polymers containing the acrylate monomer, SBA.

6.1.1 Synthesis of the sulfobetaine acrylate monomer (SBA) 6.01

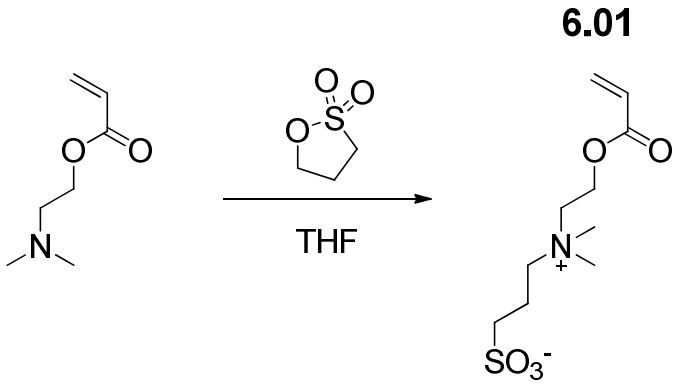

Scheme 6.3: Synthesis of SBA, 6.01

The sulfobetaine acrylate monomer, **6.01**, was synthesised in a similar manner to that described for the betainisation of *N,N*-dimethylaminoethyl methacrylate (DMAEMA) containing polymers.[26] The monomer, DMAEA, was dissolved in THF (1: 2 w: v). 1,3-propane sultone was dissolved in a small amount of THF and added slowly to the monomer solution (see Scheme 6.3). The reaction was stirred at room temperature for several hours, during which time a white precipitate formed. The precipitate was collected by filtration, washed with THF and dried under vacuum to yield **6.01** as a white solid. The product was confirmed to be pure by ^{1}H NMR spectroscopic analysis (see Figure 6.2). The appearance of new signals at 2.25 ppm (**g**), 2.96 ppm (**h**) and 3.54 ppm (**f**) show the reaction of the 1,3-propane sultone with DMAEA. There is no residual peak at 2.7 ppm that would correspond to the protons next to the sulphur group in the 1,3-propane sultone, meaning that no unreacted propane sultone remains.

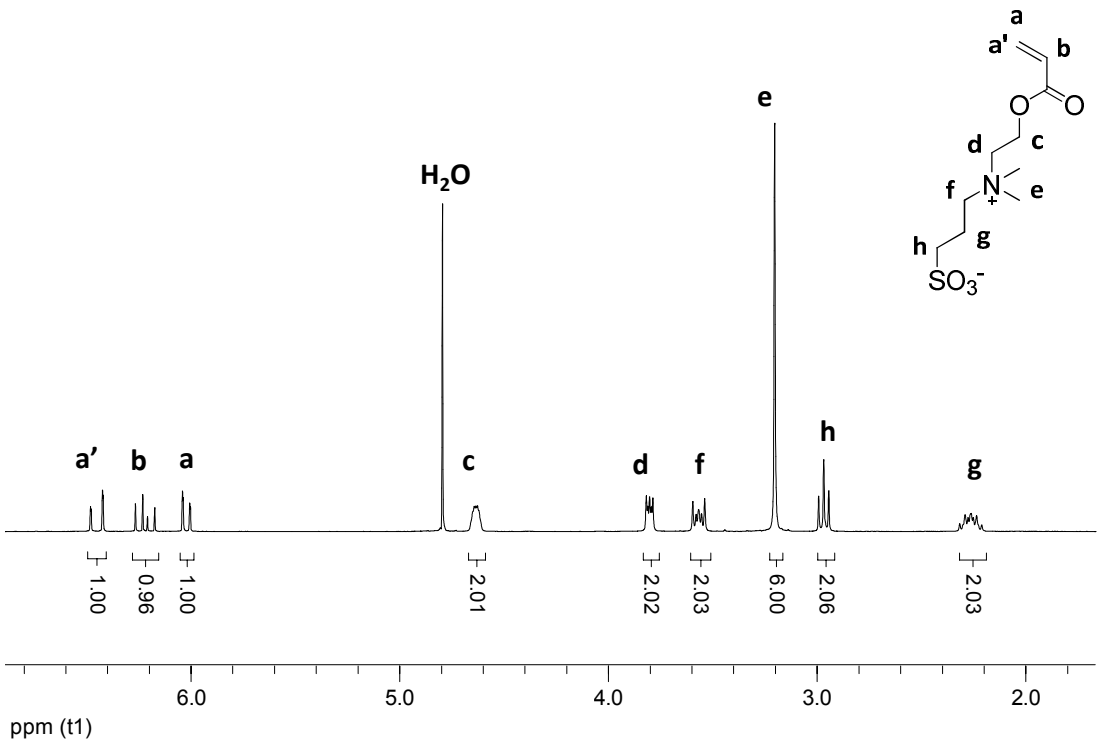

Figure 6.2: ^{1}H NMR spectrum of 6.01 in D_2O, with assignments shown, recorded at 25 °C and 400 MHz

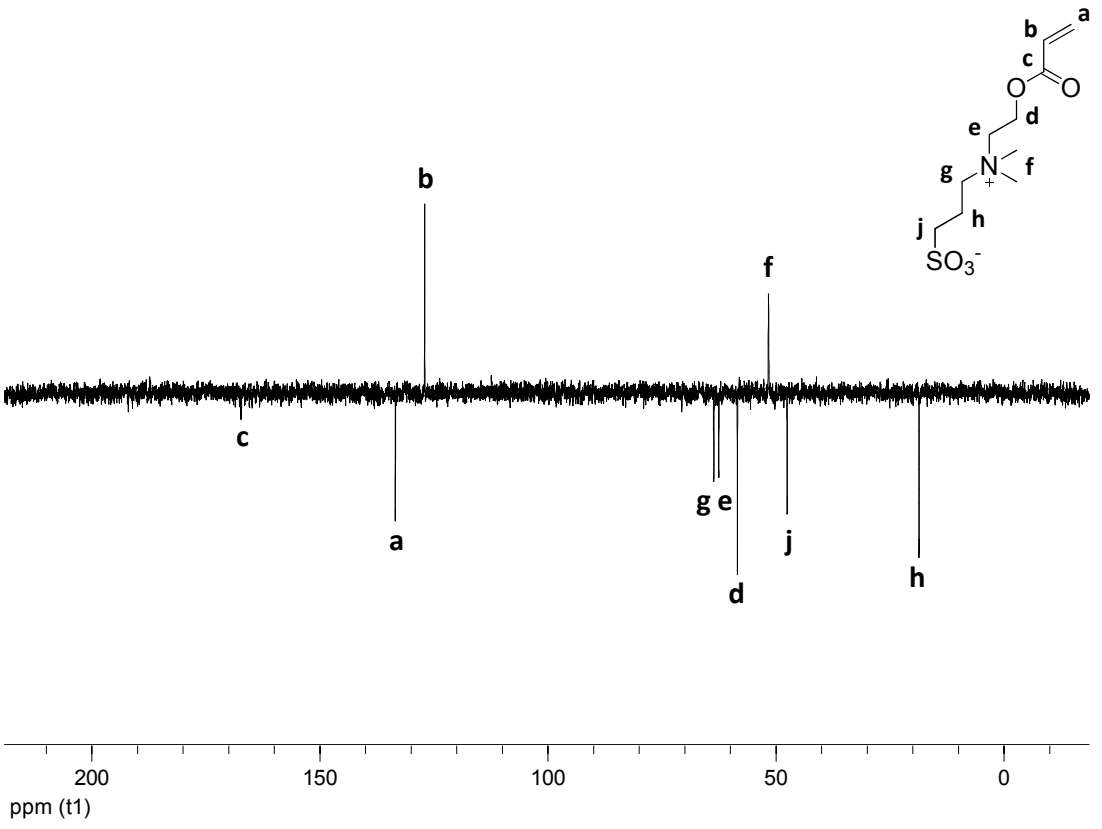

Figure 6.3: ^{13}C NMR spectrum of 6.01 in D_2O, recorded at 25 °C and 75 MHz, with assignments shown

6.1.2 Synthesis of PEG homopolymer 6.02

In Chapters Four and Five, the synthesis and self-assembly of PEGMA-*b*-DMAPS di-and triblock copolymers were explored. Our aim here was to explore similar systems containing the acrylate sulfobetaine. Therefore a homopolymer of poly((ethylene glycol) monomethyl ether acrylate) (PEG) was synthesised. Cyanomethyl dodecyl trithiocarbonate was used as the chain transfer agent (CTA) and the polymerisation was carried out using 1,4-dioxane as the solvent. The polymer was purified by dialysis against water (MWCO 1000 Da) and recovered by lyophilisation to yield **6.02** as a yellow oil, M_n (^{1}H NMR) = 10.4 kDa, M_n (DMF SEC) = 10.4 kDa, $Đ_M$ = 1.16. Analysis by ^{1}H NMR spectroscopy gives a degree of polymerisation of 21 by comparison of the triplet at 0.9 ppm (**k**) with the polymer peaks at 3.4 ppm (**f**), 3.5 ppm (**c**), 3.6 ppm (**d** and **e**) and 4.2 ppm (**b**) (see Figure 6.4). The protons of the dodecyl chain adjacent to the trithiocarbonate (**h**) appear under the peak corresponding to the terminal protons of the PEG side chains (**f**). The protons next to the cyano group of the CTA (**a**) appear under one of the PEG side chain peaks (**b**). The degree of polymerisation matches well with that predicted from conversion.

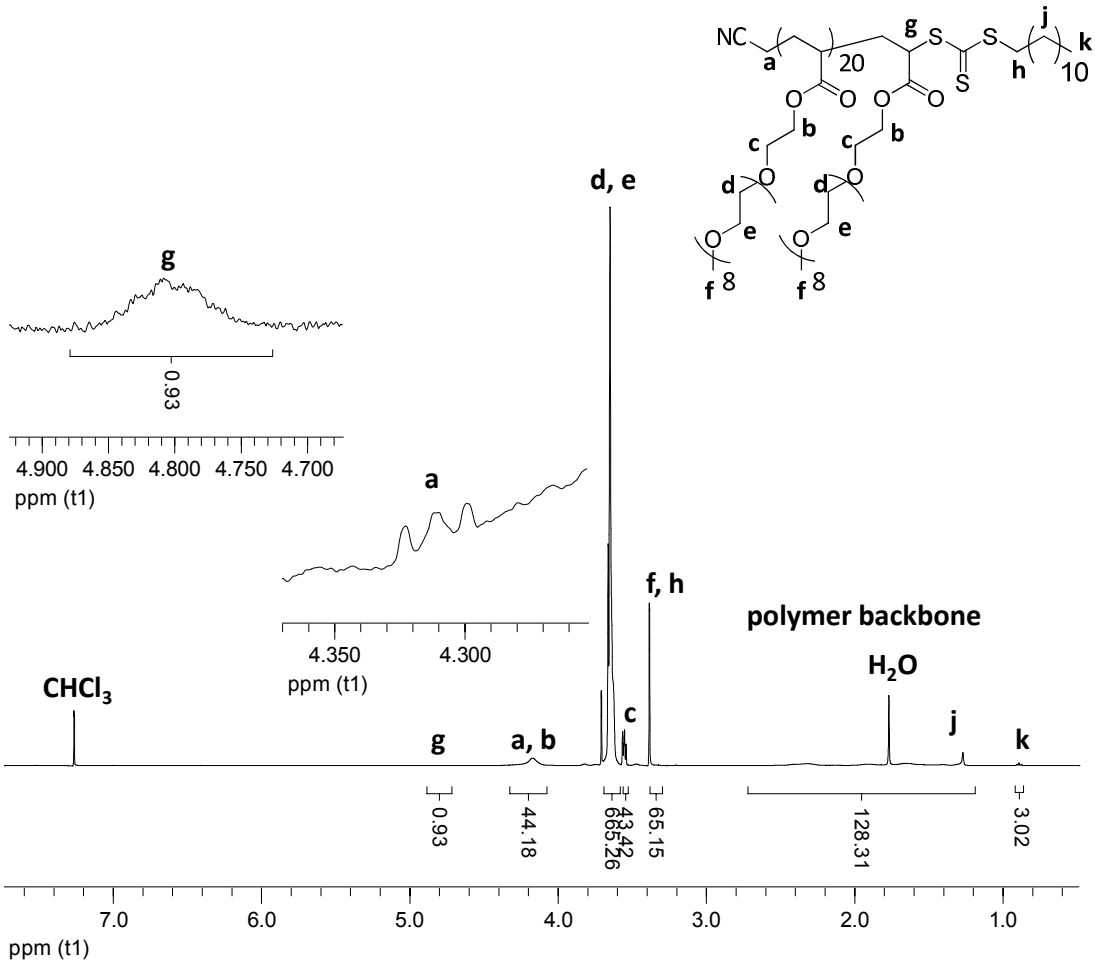

Figure 6.4: ^{1}H NMR spectrum of 6.02 in $CDCl_3$, recorded at 25 °C and 400 MHz, with assignments shown

The SEC trace of **6.02** has a narrow dispersity and shows that the polymerisation proceeded with good control (see Figure 6.5).

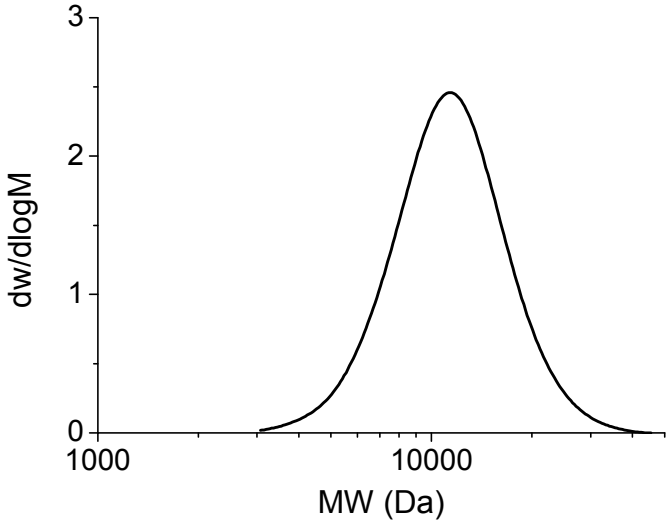

Figure 6.5: DMF SEC chromatogram of homopolymer 6.02

6.1.3 Synthesis of PEG-*b*-SBA acrylate diblock copolymers

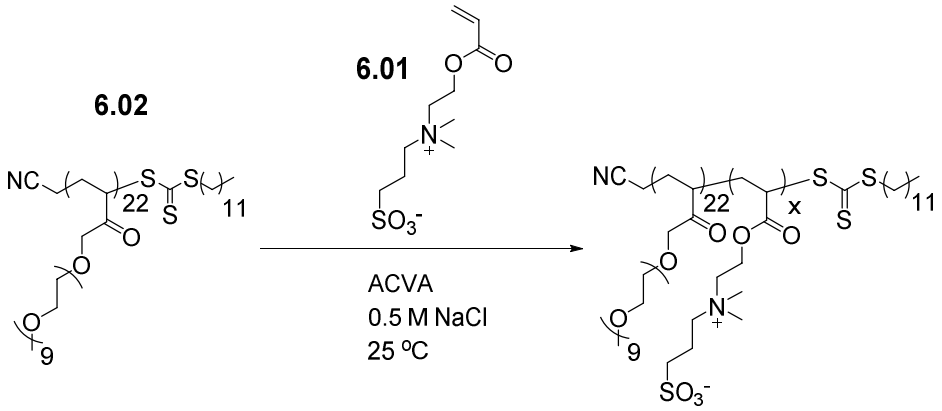

Scheme 6.4: The synthesis of PEG-*b*-SBA diblock copolymers by the chain extension of homopolymer 6.02 with monomer 6.01 in 0.5 M NaCl solution using 4,4'- azobis (4-cyanopentanoic acid) (ACVA) as the initiator

In order to compare the self-assembly and responsive properties of the methacrylate based copolymers discussed in Chapters Four and Five and the acrylate sulfobetaine discussed here, the PEG homopolymer **6.02** was chain extended with monomer **6.01** (see Scheme 6.4). The polymerisation was carried out in 0.5 M NaCl solution with 4,4'- azobis (4-cyanopentanoic acid) (ACVA) as the initiator (see Scheme 6.4). The polymerisation mixture was purged with nitrogen at room temperature for 60 minutes to remove oxygen, and during purging it was noticed that the mixture had become viscous. Therefore a sample (**6.03**) was removed, prior to heating, for analysis by ^{1}H NMR spectroscopy. This showed that there was *ca*. 55% conversion of the monomer, which accounted for the increased viscosity of the solution (see Figure 6.6).

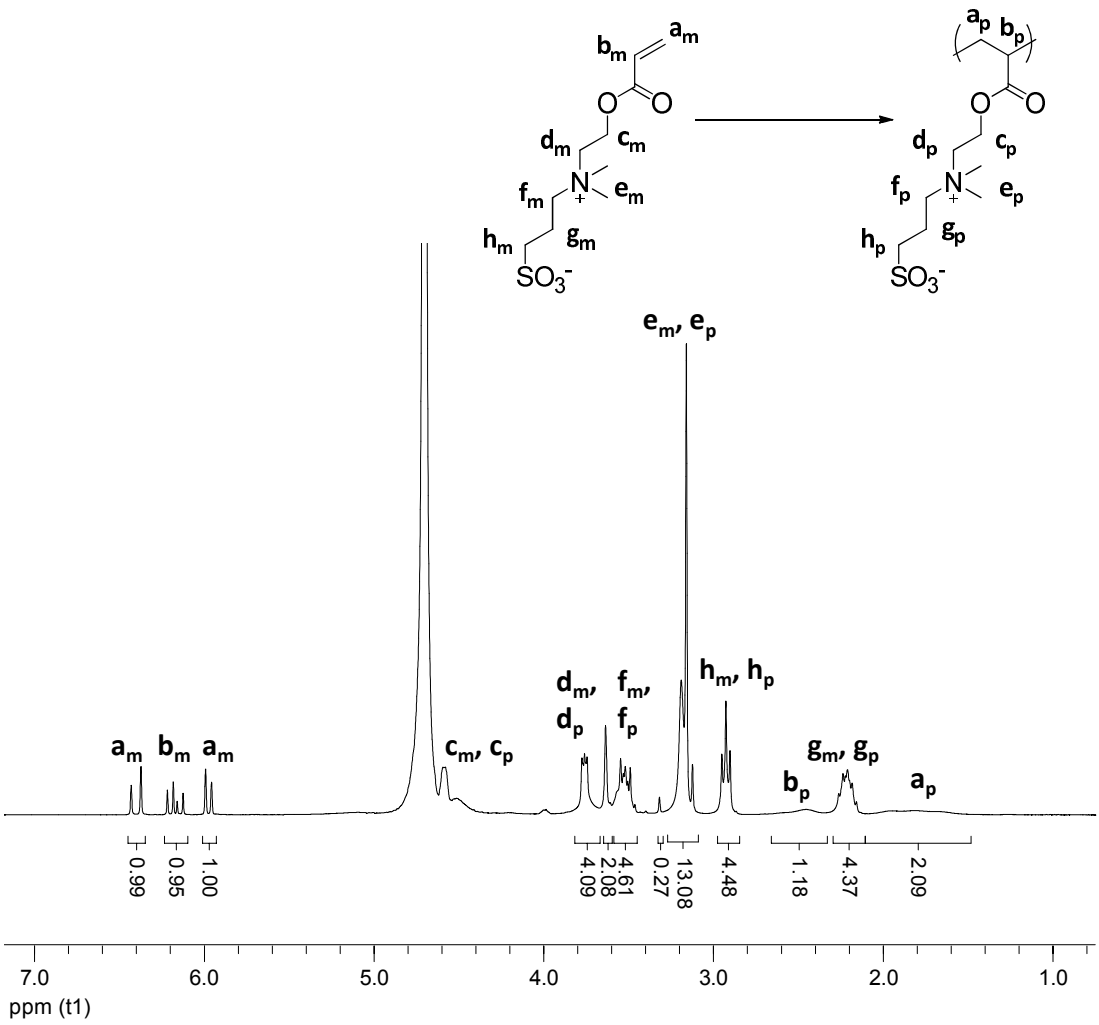

Figure 6.6: ^{1}H NMR of polymerisation mixture, 6.03, in 0.5 M NaCl in D_2O taken after purging for one hour, prior to heating, showing 55% conversion. The spectrum was recorded at 25 °C and 300 MHz.

The conversion was calculated using the equation

$$\%\, conversion = \frac{H_p}{H_p + H_m} \times 100$$

where H_p is the contribution of the protons from the polymer to the peak and H_m is the contribution from the monomer. In Figure 6.6 the vinyl peaks at 6.2, 6.3 and 6.5 ppm (**a_m** and **b_m**) were each set to a value of *ca.* 1. The polymer peak at 2.9 ppm (**h**) was integrated and the contribution from the monomer subtracted to leave the contribution from the polymer. This gives a value of 55% conversion. The other peaks at 3.2 ppm (**e**), 3.5 ppm (**f**) and 3.7 ppm (**d**) also confirm this degree of conversion.

A sample was also removed for analysis by aqueous SEC prior to the polymerisation mixture being heated. The SEC chromatogram shows there to be polymer present (see Figure 6.7). The peak extends above the higher calibration limit of the columns (500 kDa) and therefore the M_n obtained from SEC is likely to be artificially low. Even so, the M_n (Aqueous SEC) = 202 kDa is much higher than the theoretical M_n based on 55% conversion (109 kDa). As part of the trace lies outside the calibration limit, the dispersity from SEC ($Đ_M$ = 1.74) is not truly representative of the sample. Any polymers with a molecular weight higher than the calibration limit elute at the same point rather than being separated, and therefore it is expected that on a column set with a larger molecular weight range the dispersity would be greater.

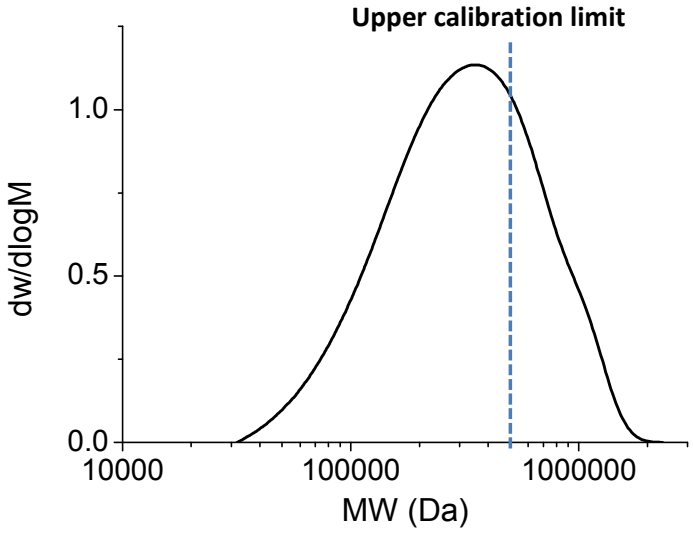

Figure 6.7: Aqueous SEC chromatogram of polymerisation mixture, 6.03, after bubbling for one hour, prior to heating. The upper calibration limit of the SEC columns shown by the dashed blue line

This polymerisation solution was then heated to 65 °C for 15 hours, purified by dialysis against water (MWCO 12 – 14 kDa) and recovered by lyophilisation to yield **6.03**, M_n (^{1}H NMR) = 186.8 kDa, M_n (aqueous SEC) = 106.1 kDa, $Đ_M$ = 2.64. Analysis by ^{1}H NMR spectroscopy gives a degree of polymerisation of 665 by comparison of the PEG signals (**a** and **b**) with the betaine signals at 3.0 ppm (**j**) and 3.3 ppm (**f**) (see Figure 6.8). This DP agrees well with that predicted from conversion.

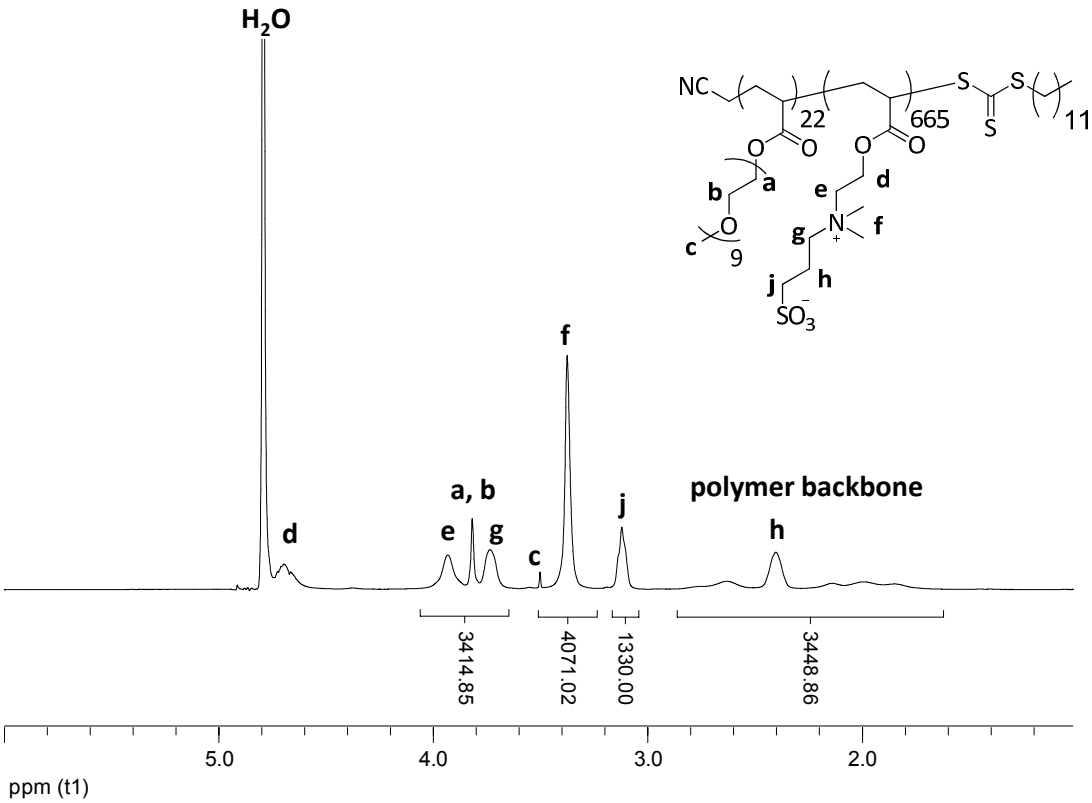

Figure 6.8: ^{1}H NMR spectrum of diblock copolymer 6.03 in 0.5 M NaCl D_2O with assignments shown, recorded at 25 °C and 400 MHz

However, unsurprisingly, analysis of the SEC chromatogram shows a broad polymer that excludes above the upper limits of the column. Comparison of the SEC chromatograms of **6.03** after purging but before heating, and after heating shows a larger lower molecular weight shoulder formed after heating (see Figure 6.9).

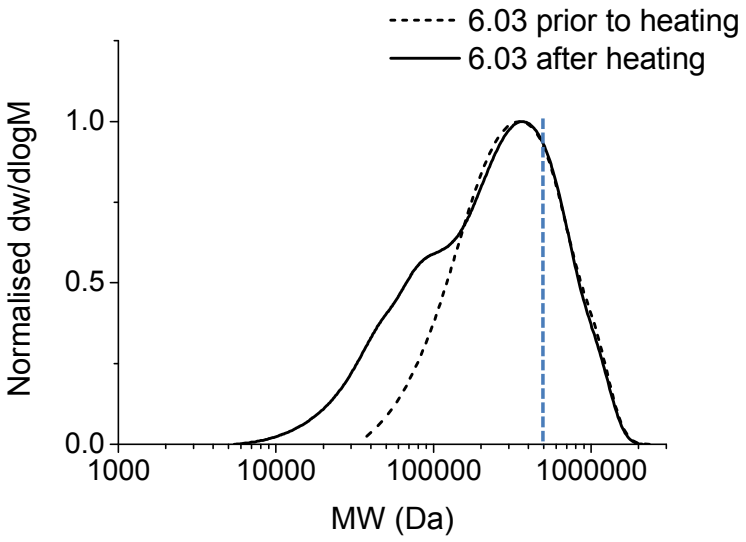

Figure 6.9: Aqueous SEC chromatograms of 6.03 after bubbling with nitrogen but prior to heating, and after heating. The dashed blue line represents the upper calibration limit

The higher molecular weight peak of the SEC trace appears to have a RAFT end group as it absorbs at 309 nm (see Figure 6.10), but the polymer formed when the solution is heated does not appear to contain a RAFT end group.

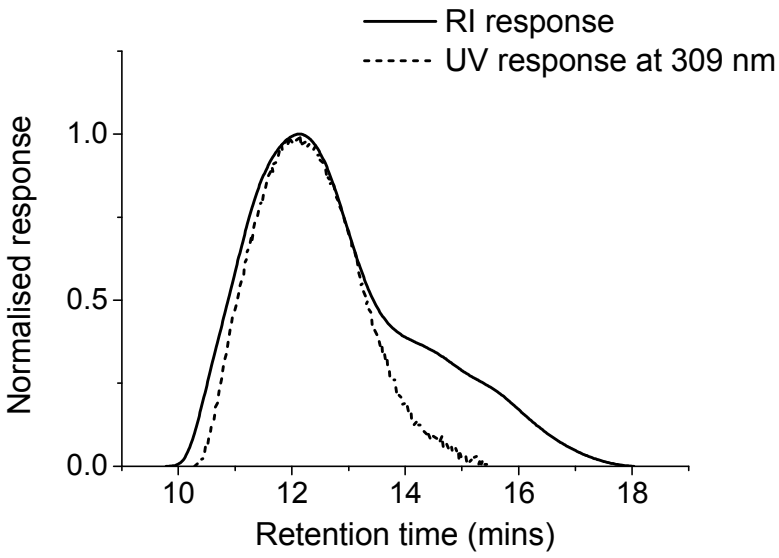

Figure 6.10: Aqueous SEC chromatograms showing the RI response and the UV response at 309 nm for diblock copolymer 6.03

This reaction was repeated several times with varying **6.02**:**6.01** (macroCTA: monomer) (see Table 6.1). The polymerisations were all bubbled with nitrogen and then heated to 65 °C for 15 hours. The resulting polymers were all analysed by aqueous SEC and showed uncontrolled polymers that excluded above the upper limit of the SEC columns (see Figure 6.11).

Table 6.1: Summary of the different polymerisation attempts of 6.01 using 6.02 as a macroCTA

Exp number	Equiv. 6.01 (*w.r.t.* 6.02)	Time purging (mins)	$M_{n,\ Theoretical}$ (kDa)[a]	$M_{n,\ SEC}$ (kDa)[b]	$Đ_M$[b]
6.04	300	40	63.6	99.2	1.88
6.05	500	60	106	132.6	1.90
6.06	750	80	186.8	106.1	2.64
6.07	1000	70	222.6	148.9	2.19
6.08	2000	60	434.6	112.9	2.74

[a] based on ^{1}H NMR conversion spectroscopy
[b] based on aqueous SEC analysis

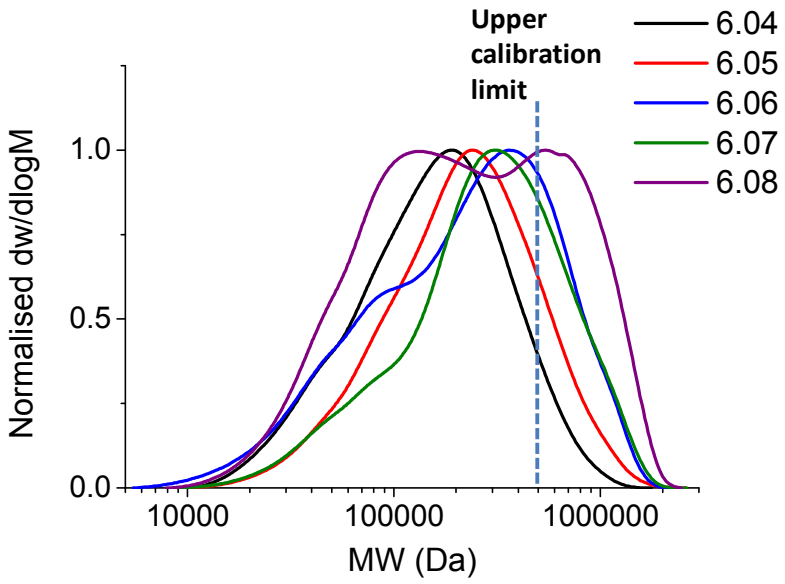

Figure 6.11: Aqueous SEC chromatograms for polymers 6.04 - 6.08, with the upper calibration limit of the columns highlighted by the dashed blue line

Polymer **6.08** shows a bimodal distribution. The absorbance at 309 nm for **6.08** was compared to the RI response (see Figure 6.12). The larger molecular weight peak appears to contain a RAFT end group as it has an absorbance at 309 nm, but the smaller molecular weight peak does not absorb at 309 nm, suggesting that the RAFT end group is not attached.

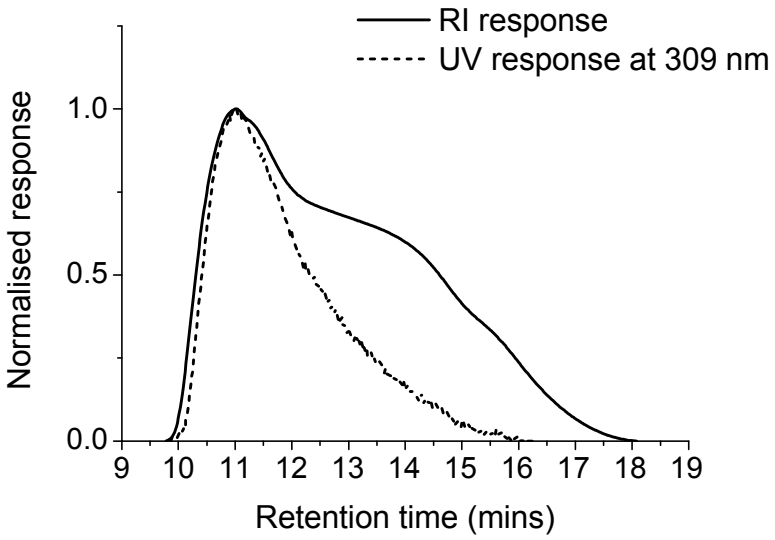

Figure 6.12: Aqueous SEC chromatograms for the RI response and the UV absorbance at 309 nm for 6.08

All of the polymerisations, 6.03 – 6.08 were uncontrolled, had high dispersities and excluded above the upper calibration limit of the column. As this was unexpected, when compared to the controlled nature of the DMAPS polymerisation (Chapter Four), the polymerisation of SBA was investigated further.

6.1.3.1 Effect of initiator upon polymerisation

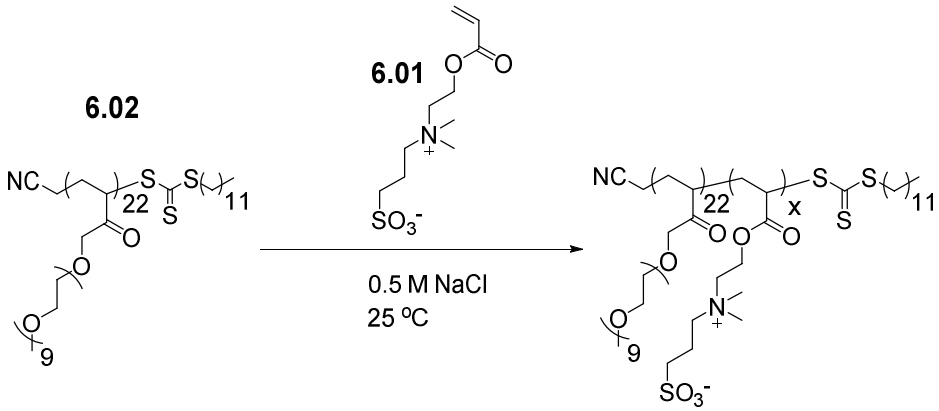

Scheme 6.5: Scheme showing the chain extension of 6.02 in the absence of initiator

The polymerisation occurring before the solution is heated is unexpected as the initiator is generally stable at room temperature and requires heating in order to initiate the polymerisation. The 10 hour half-life for ACVA in water is 69 °C and generally polymerisations are heated to this temperature for efficient initiation to occur. The same

polymerisation conditions as for **6.06** were used but no initiator was included (see Scheme 6.5). A sample was removed after 30 minutes of purging, before the initiator was added, and analysis by ^{1}H NMR spectroscopy shows there to be 48% conversion. A sample (**6.09**) was also analysed by aqueous SEC and shows the presence of polymer (M_n (Aqueous SEC) = 203.4 kDa, $Đ_M$ = 1.85), which again excludes above the upper limits of the column capacity (see Figure 6.13). This shows that the polymerisation is proceeding in the absence of the initiator and the resulting polymer is not controlled.

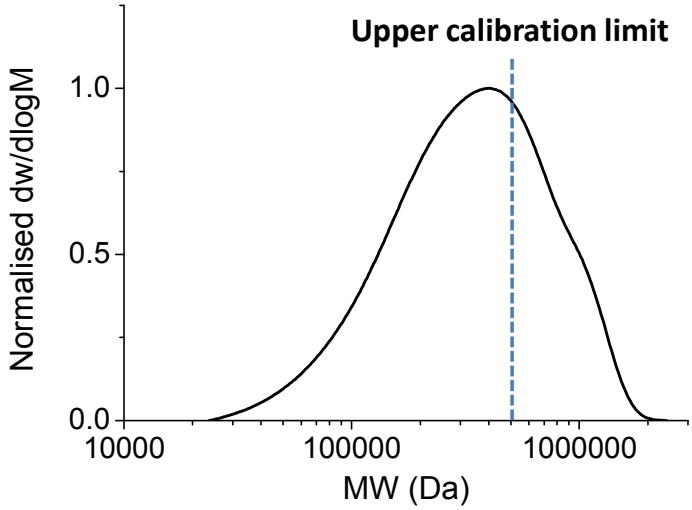

Figure 6.13: Aqueous SEC chromatogram for 6.09, showing that polymerisation has occurred during purging with nitrogen in the absence of an initiator. The upper calibration limit of the SEC columns is shown by the dashed blue line

6.1.3.2 Effect of temperature upon polymerisation

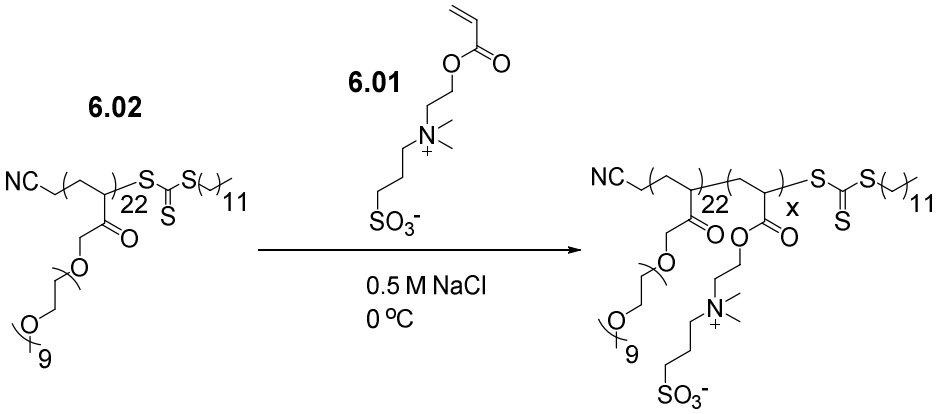

Scheme 6.6: The chain extension of 6.02 with monomer 6.01 was repeated but the degassing was carried out in an ice bath

To see the effect that temperature had on this unexpected polymerisation during purging with nitrogen, the monomer **6.01** and the macroCTA **6.02** were dissolved in 0.5 M NaCl solution. The initiator was not added (see Scheme 6.6). The solution was purged with nitrogen for 30 minutes whilst in an ice bath. A sample was taken and analysis by ^{1}H NMR spectroscopy showed that no significant conversion had occurred (≤ 7%). The purging was stopped and the solution was kept under a nitrogen atmosphere. A solution of degassed initiator was added and the reaction placed into a preheated oil bath at 65 °C for two hours. Analysis of the crude polymer (**6.10**) by SEC confirmed that the polymer the polymerisation had progressed to 93% conversion in an uncontrolled manner as the polymer had again excluded above the upper limits of the SEC column, M_n (Aqueous SEC) = 94.2 kDa, $Đ_M$ = 2.16 (see Figure 6.14).

This same reaction was repeated but after purging with nitrogen for 30 minutes the polymerisation mixture was removed from the ice bath and placed on the bench. A sample (**6.11**) was removed from this solution after a further 30 minutes and showed that 43% conversion had occurred (see Figure 6.15). Analysis by aqueous SEC also confirms the formation of polymer, M_n (Aqueous SEC) = 182.2 kDa, $Đ_M$ = 1.74 (see Figure 6.14). As the polymerisation had occurred when the sample was no longer being bubbled it can be concluded that it is not the mechanism of bubbling that induces the polymerisation.

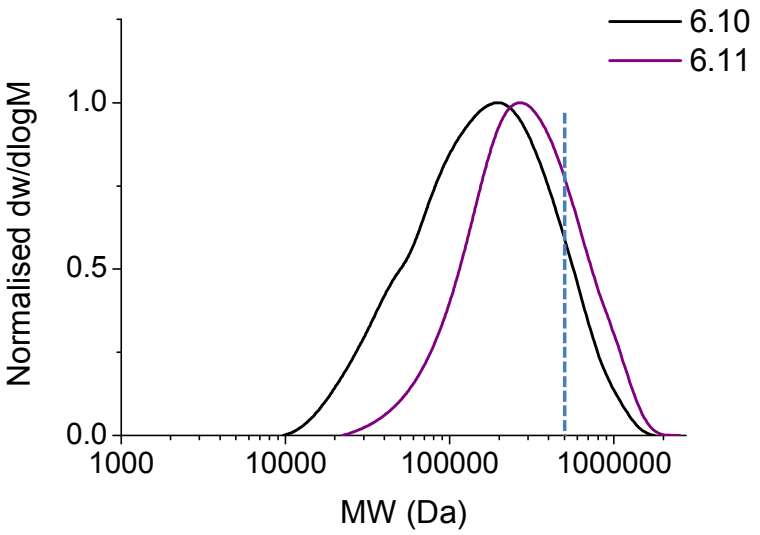

Figure 6.14: Aqueous SEC chromatograms of 6.10 and 6.11

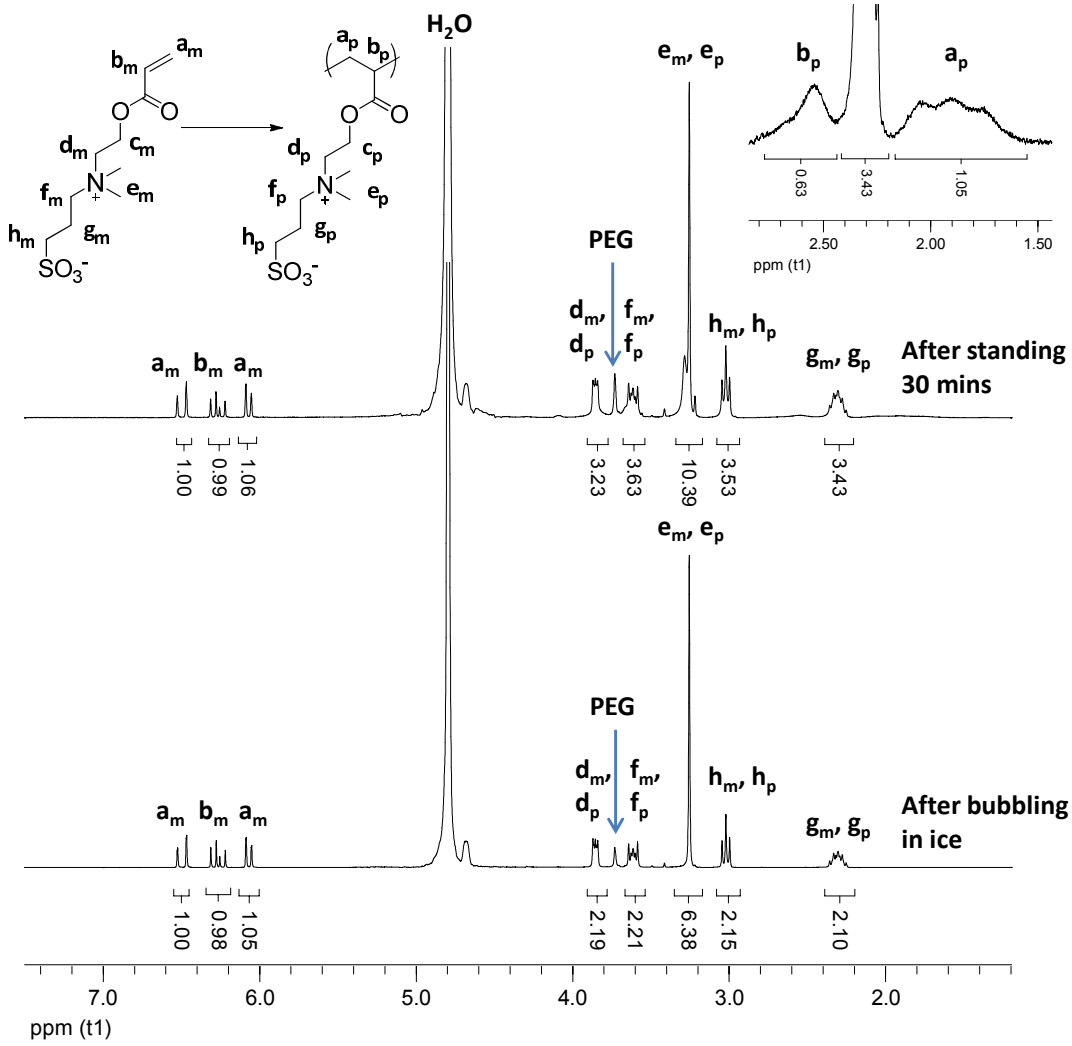

Figure 6.15: ^{1}H NMR spectra of 6.01 and 6.02 in 0.5 M NaCl in D_2O, degassed by bubbling with nitrogen whilst in an ice bath (bottom) and then after standing for 30 minutes at room temperature (top). Spectra recorded at 25 °C and 300 MHz.

6.1.3.3 Effect of the macroCTA 6.02 upon polymerisation

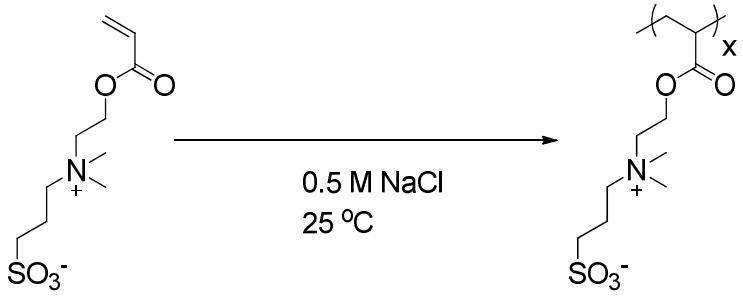

Scheme 6.7: Monomer 6.01 was dissolved in 0.5 M NaCl solution and purged with nitrogen to investigate the polymerisation behaviour

In order to investigate whether the presence of the macroCTA **6.02** had an effect upon the polymerisation, just the monomer, **6.01,** in 0.5 M NaCl solution was stirred at room temperature whilst purging with nitrogen (see Scheme 6.7). After 30 minutes of purging, analysis by ^{1}H NMR spectroscopy showed 15% conversion, and SEC analysis confirmed the formation of polymer. The reaction mixture was also quite viscous. Upon standing for 30 minutes under a nitrogen atmosphere the solution had gelled. Another sample was removed for analysis by ^{1}H NMR spectroscopy. The gel was difficult to dissolve and to filter so therefore was not analysed by SEC. ^{1}H NMR spectroscopy showed that 48% conversion had occurred, however this may not be accurate due to the difficulties with dissolving the polymer. The monomer may have dissolved more readily, thereby giving a smaller apparent conversion.

The gelling that occurred when just the monomer **6.01,** dissolved in 0.5 M NaCl solution, is bubbled with nitrogen behaviour is not seen when the macroCTA **6.02** is included in the reaction mixture. The solutions containing the homopolymer **6.02** became very viscous after bubbling but were still flowing and had not gelled as can be seen in Figure 6.16. This indicates that the chain transfer agent is offering some control over the polymerisation and the molecular weight of the polymer produced, resulting in a soluble polymer.

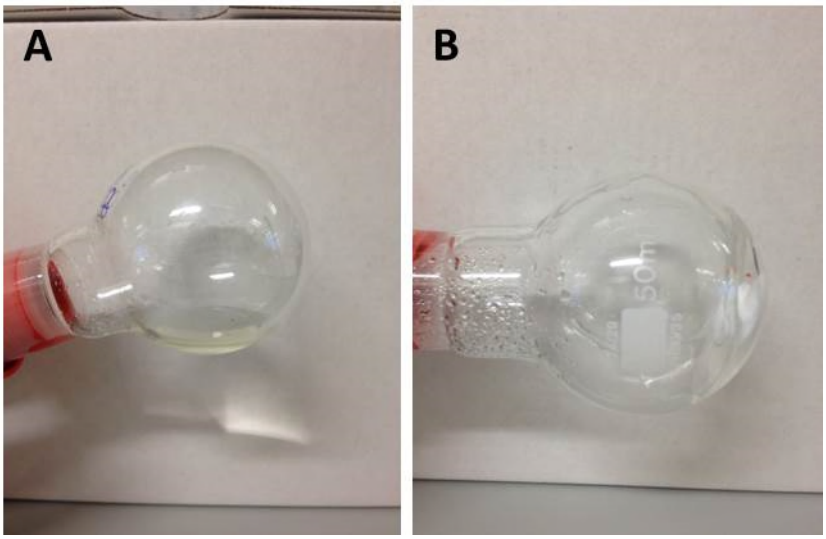

Figure 6.16: A) Photograph of the free flowing solution of 6.01 and 6.02 in 0.5 M NaCl after purging with N_2 for 30 minutes and standing for 30 minutes. B) Photograph of 6.02 in 0.5 M NaCl solution after purging with N_2 for 30 minutes and then standing for 30 minutes

The mechanism by which the monomer, **6.01**, is polymerising in the absence of any initiating species is still under investigation. A similar observation was made by Liaw and Lee in the 1990's.[30, 31] They observed that poly(DMAPS) and poly(SBA) can initiate the polymerisation of vinyl monomers. Poly(DMAPS) was dissolved in 0.5 M NaCl and a vinyl monomer (styrene (Sty), methyl methacrylate (MMA), vinyl acetate (VA) or acrylonitrile (AN)) added. The solution was degassed *via freeze-pump-thawing* and sealed under a high vacuum with no initiator included in the reaction mixture. The solution was then heated to 85 °C for three hours. After this time the conversion of the vinyl monomer was recorded using the difference in the mass of polymer after the reaction and the amount of poly(DMAPS) added to the reaction. In all cases there had been conversion of the vinyl monomer. Although the conversion was low (< 10%), it was significantly more than that observed when just the reaction was performed without the poly(DMAPS) (< 2%). The poly(SBA) caused higher levels of conversion than the poly(DMAPS). When the reaction was repeated but also included a radical scavenger no polymerisation was observed, showing that the process involves a radical mechanism. The authors concluded that the poly(betaine) (DMAPS or SBA) was initiating the polymerisation through the formation of hydrophobic areas in the aqueous solution and the incorporation of the hydrophobic monomers into these

areas.[31] The more hydrophobic monomers investigated (MMA and Sty) showed higher degrees of conversion than the more hydrophilic AN and VA. The double bond of the monomer is electron rich and therefore absorbs onto the quaternary amine of poly(betaine). The carboxyl group of the monomer is electron withdrawing and so the monomer may also absorb onto the sulfonate group of the betaine. The two absorbed monomers then form a charge transfer complex, followed by electron donation to produce a radical (see Scheme 6.8). Similar results have also been seen for carboxy- and phosphobetaines initiating the polymerisation of vinyl monomers.[32]

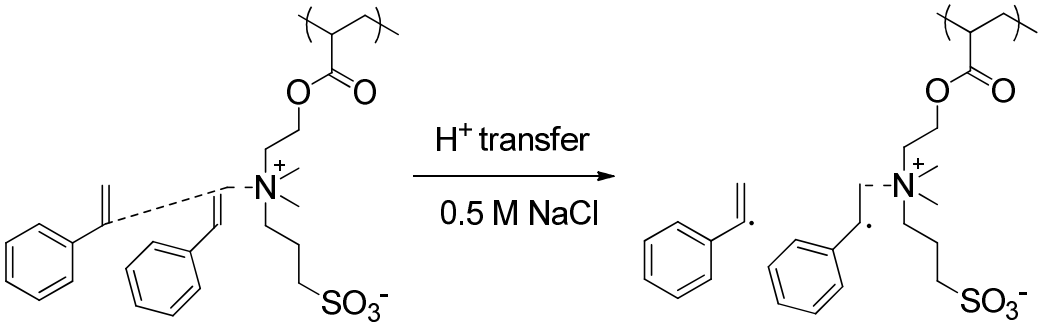

Scheme 6.8: The proposed mechanism by Liaw and Lee of the formation of radicals by the absorption of the double bond of the monomer to the quaternary carbon and the subsequent proton transfer to create radicals[31]

Although this may offer an insight into how polymerisation can be initiated in the presence of zwitterionic compounds, the conversions of the monomers reported were much lower than in our observations and the polymerisation solutions in these reports were heated to 85 °C.

6.1.4 Investigation into the auto-polymerisation of DMAPS

Chapters Four and Five focused on the synthesis and self-assembly of polymers containing the methacrylate version of SBA. The polymerisations were generally conducted in the same manner as described here but the polymers produced had narrow dispersities and predictable molecular weights, showing that the polymerisations were controlled. In order to investigate whether this auto-polymerisation behaviour is observed with the methacrylates, PEGMA homopolymer, **4.01**, DMAPS and ACVA were dissolved in 0.5 M NaCl solution, using the same conditions as for **6.03**. The pH of the solution was adjusted to pH 7 in order to

solubilise the initiator. The solution was then degassed by bubbling with nitrogen for 30 minutes. A sample was removed for analysis by ^{1}H NMR spectroscopy and no conversion was detected. The vinyl peaks at 5.8 and 6.1 ppm ($\mathbf{a_m}$), integrate correctly with respect to the other DMAPS peaks at 2.3 ppm ($\mathbf{g_m}$), 3.0 ppm ($\mathbf{h_m}$), 3.3 ppm ($\mathbf{e_m}$), 3.7 ppm (**fm**) and 3.9 ppm ($\mathbf{d_m}$), showing that no polymer had been formed. In the analogous acrylate reaction, **6.03**, there was 55% conversion after bubbling with nitrogen for the same time period. This confirms that the polymerisation of the methacrylate monomer, DMAPS, was not proceeding during the degassing stage, within the same time frame that the acrylate does.

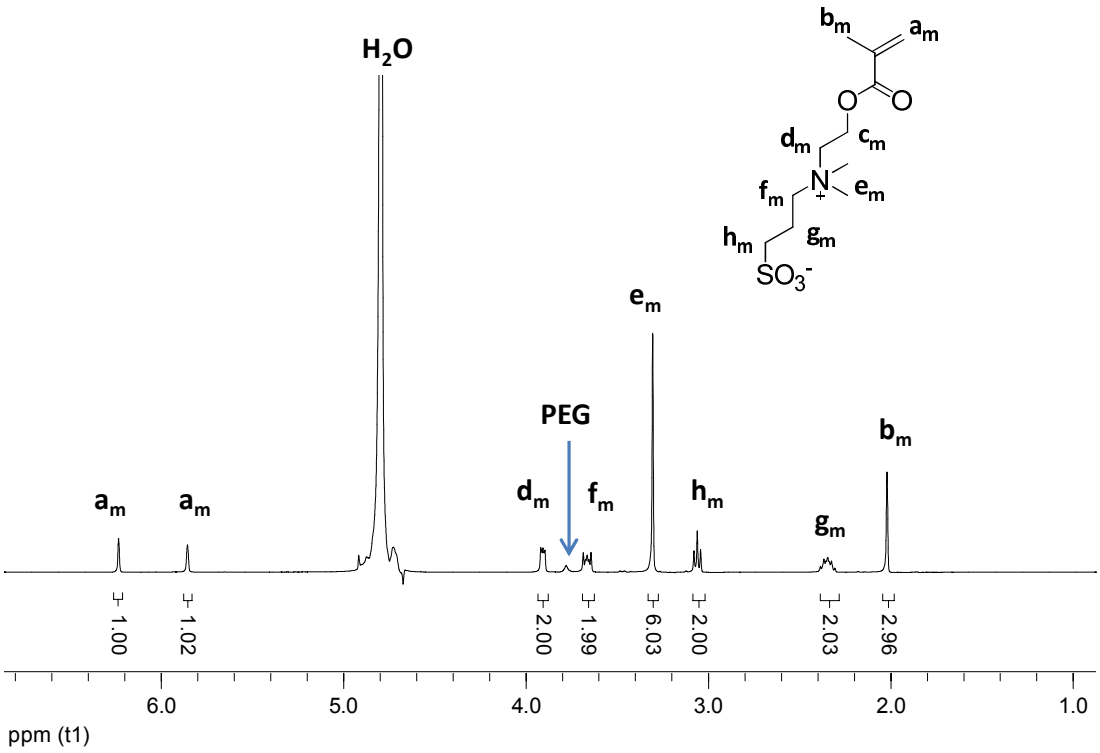

Figure 6.17: ^{1}H NMR spectrum of the polymerisation solution of DMAPS and PEG homopolymer 4.01 in 0.5 M NaCl in D_2O, showing that no conversion had occurred during the degassing stage

This difference may be due to the steric hindrance provided by the methyl group on the DMAPS. Liaw *et al*. investigated the free radical polymerisation of DMAPS and SBA in a foramide/dioxane mix at 30 °C, using AIBN as the initiator.[33] They found that for both monomers the rate of propagation was enhanced by the addition of NaCl at a concentration of 0.1 mol L^{-1} NaCl. The rate of initiation was not affected by the presence of the salt. The rate of propagation of DMAPS was 50% lower than that observed for the acrylate, SBA,

both in the presence and the absence of salt. The authors suggest this is a result of the increased steric hindrance of the methyl group on the α-carbon. This difference in propagation rates could explain why within 30 minutes of purging the acrylate monomer polymerised but the methacrylate did not.

6.1.5 Polymerisation of 6.01 in HFIP

In an attempt to synthesise well-controlled polymers containing the betaine acrylate we turned our attention to the use of a different solvent to explore if the polymerisation is more controlled. The limited solubility of polybetaines reduces the choice of polymerisation solvent to either 0.5 M NaCl or to highly polar fluorinated alcohols, such as hexafluoroisopropanol (HFIP).[34] Therefore the homopolymerisation of **6.01** in HFIP was investigated. Cyanomethyl dodecyl trithiocarbonate was used as the CTA and AIBN as the initiator. A 1: 3 (w/v) ratio of solvent to monomer was used. The solution was degassed *via* three *freeze-pump-thaw* cycles. After the third cycle an aliquot was removed for analysis by ^{1}H NMR spectroscopy. No conversion was detected. The polymerisation solution was then heated to 65 °C for 15 hours. A molecular weight of 280 kDa was targeted as DMAPS polymers of similar molecular weights have been shown to have UCST cloud points of *ca*. 26 °C at a concentration of 1 mg mL^{-1}.[19] The polymer was purified by dialysis to yield **6.12**, M_n (^{1}H NMR) = 238.5 kDa, M_n (Aqueous SEC) = 20.0 kDa, $Đ_M$ = 1.24 (see Figure 6.18). The degree of polymerisation based on conversion was calculated to be 900. The molecular weight obtained from aqueous SEC analysis is much lower than that from ^{1}H NMR spectroscopy; however this may be a result of the difference between the zwitterionic polymer and the linear PEG standards used to calibrate the SEC, as previously observed for the DMAPS homopolymers.[19] The lower dispersity and symmetrical shape of the chromatogram suggest that the polymerisation of SBA is more controlled in HFIP than in aqueous solution.

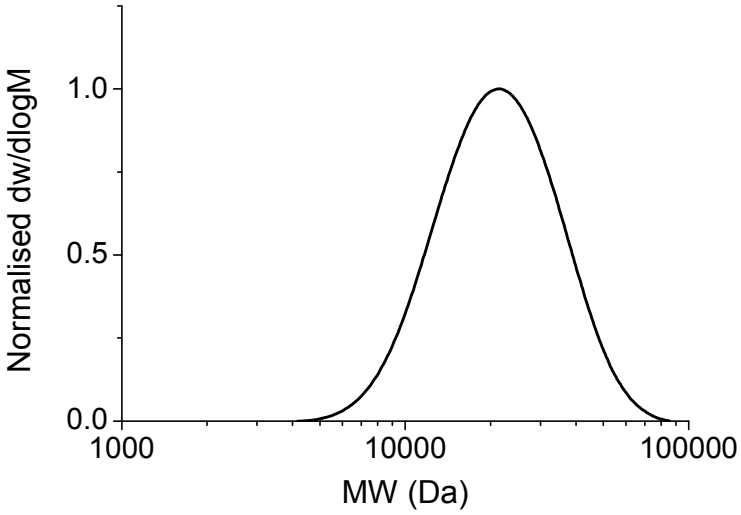

Figure 6.18: Aqueous SEC chromatogram of homopolymer 6.12, polymerised in HFIP

Homopolymer **6.12** was dissolved in 18.2 MΩ cm^{-1} water at a concentration of 1 mg mL^{-1}. Upon cooling to 4 °C the polymer remained soluble and no UCST cloud point was observed. A solution of **6.12** at a concentration of 10 mg mL^{-1} was also made and showed no UCST cloud point. This may be a result of the increased hydrophilicity of the SBA compared to the DMAPS.

6.1.6 Chain extension of 6.02 with 6.01 in HFIP

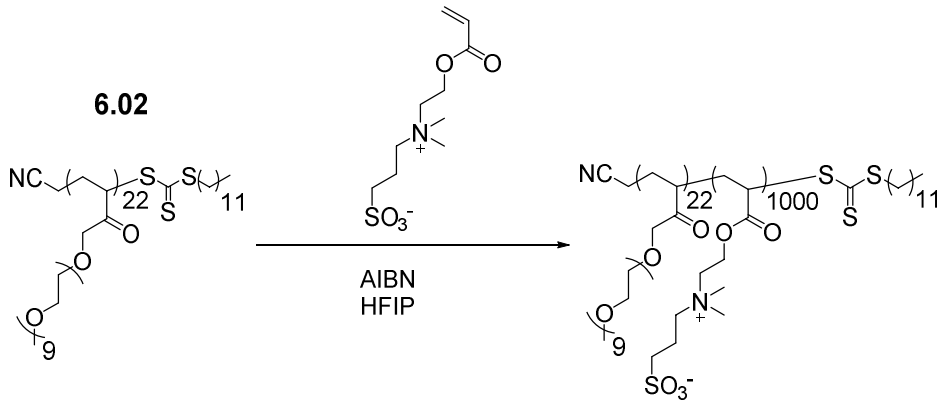

Scheme 6.9: The chain extension of homopolymer 6.02 with SBA performed in HFIP

Homopolymer **6.02** was chain extended with **6.01** in HFIP in order to form a diblock copolymer. AIBN was added as an initiator and the solution was degassed *via* three *freeze-pump-thaw* cycles (see Scheme 6.9). A sample was removed, prior to heating, for analysis

by ^{1}H NMR spectroscopy and no conversion was observed. The solution was then heated at 65 °C for 15 hours and the polymer purified by dialysis to yield **6.13**, M_n (^{1}H NMR) = 275.6 kDa, M_n (Aqueous SEC) = 22.4 kDa, $Đ_M$ = 1.29. Analysis by ^{1}H NMR spectroscopy gives a degree of polymerisation of 1000 by comparison of the PEG signals (**a** and **b**) with the betaine signals at 2.4 ppm (**h**), 3.0 ppm (**j**) and 3.3 ppm (**f**) (see Figure 6.19). This DP agrees well with that predicted from conversion.

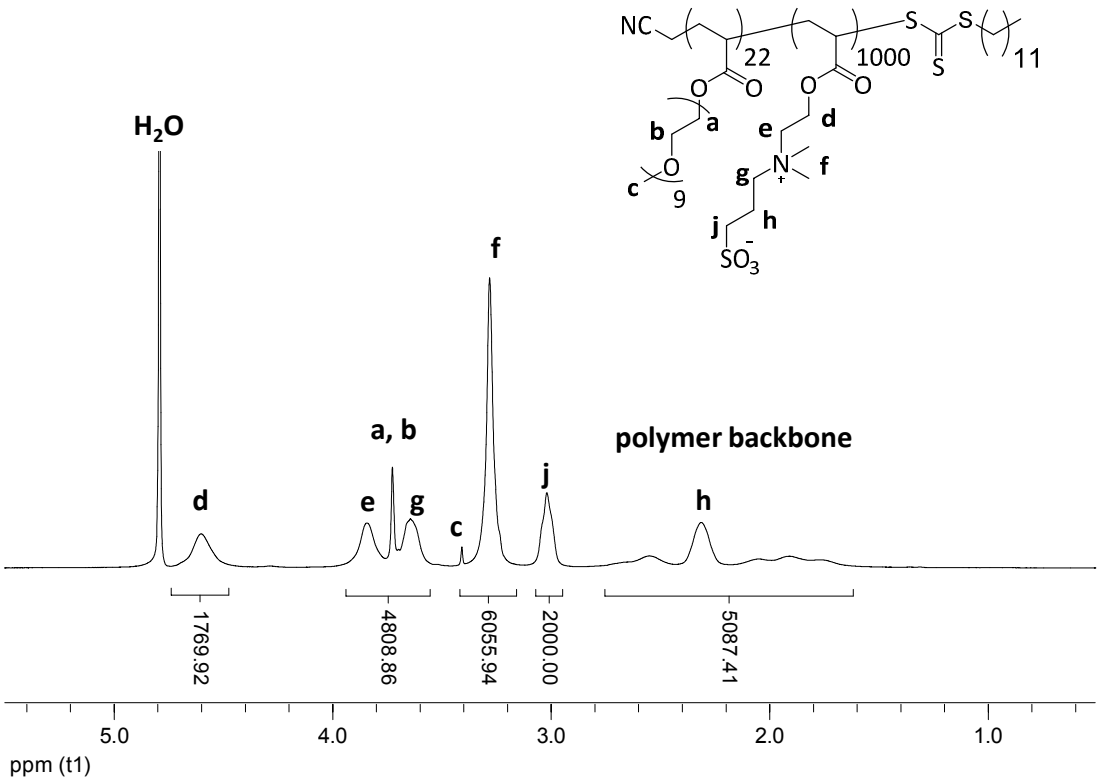

Figure 6.19: ^{1}H NMR spectrum of diblock copolymer 6.06 in 0.5 M NaCl in D_2O , with assignments shown, recorded at 25 °C and 400 MHz

The SEC chromatogram has a narrow dispersity (see Figure 6.20) and again has a lower molecular weight than that predicted by ^{1}H NMR spectroscopy, possibly as a result of the difference between the polymer and the PEG standards used in the SEC calibration.

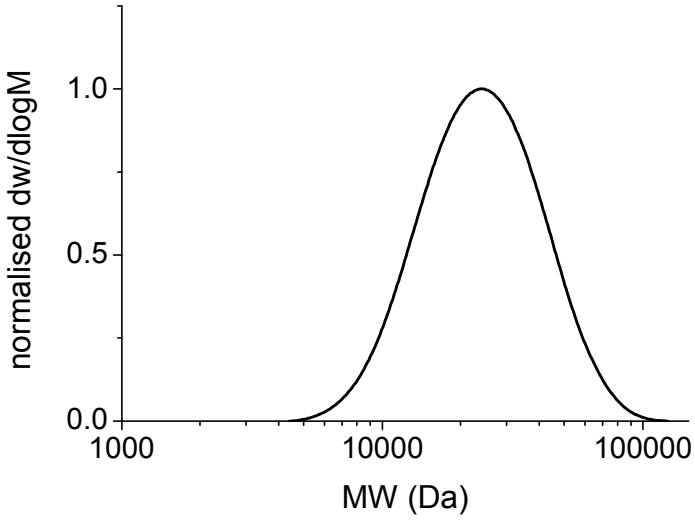

Figure 6.20: Aqueous SEC chromatogram for diblock copolymer 6.13, polymerised in HFIP

The diblock copolymer **6.13** was self-assembled in 18.2 MΩ cm^{-1} water by direct dissolution at a concentration of 1 mg mL^{-1}. Analysis by DLS shows that no self-assembly had occurred. Cooling the solution to 4 °C did not induce self-assembly. This may be a result of the decreased hydrophobicity of the SBA compared to the DMAPS.

6.3. Conclusions

The sulfobetaine acrylate monomer, [2-(acryloyloxy) ethyl] dimethyl-(3-sulfopropyl) ammonium hydroxide (SBA) was polymerised using a PEG homopolymer as a macroCTA. The polymerisations were uncontrolled and the resulting polymers had higher than predicted molecular weights and broad dispersities. It was found that the monomer was polymerising during the degassing process. This polymerisation occurred in the absence of an initiating species. Cooling the solution during degassing minimised the conversion but upon warming to room temperature the polymerisation proceeded in an uncontrolled manner. When no macroCTA was included in the polymerisation mixture the solution gelled completely, suggesting that the macroCTA may be offering some form of control over the polymerisation.

Polymerising in HFIP yielded polymers with narrower dispersities and controlled molecular weights. However the acrylate sulfobetaine polymers produced in this work do not self-assemble or display any thermo-responsive behaviour in water. This lack of thermo-responsive behaviour, coupled with the uncontrolled polymerisation in aqueous solution, may explain the lack of interest in this monomer in the literature.

6.4. Experimental

6.1.7 Materials

Poly(ethylene glycol) methyl ether acrylate (PEGA), cyanomethyl dodecyl trithiocarbonate (CTA), 1,3-propane sultone, *N,N* – (dimethylamine) ethyl acrylate (DMAEA) and 4, 4'-azobis (4-cyanopentanoic acid) (ACVA) were used as received from Aldrich and Fisher, unless otherwise stated. 2, 2'- azobis (2-methylpropionitrile) (AIBN)was recrystallised twice from methanol and stored in the dark at 4 °C. Hexafluoroisopropanol was received from FluoroChem and Apollo.

6.1.8 Characterisation

^{1}H Nuclear magnetic resonance (NMR) experiments were performed on a Bruker 400 FT-NMR spectrometer operating at 300 or 400 MHz using deuterated solvents. Chemical shifts are reported in parts per million relative to H_20 (4.79 ppm). Size exclusion chromatography (SEC) measurements were obtained in either HPLC grade DMF containing 0.1M NH_4BF_4 at a flow rate of 1 mL min^{-1}, on a set of Pgel 5 μm Mixed D columns plus a guard column or in pH 8.2 phosphate buffer at a flow rate of 1 mL min^{-1}, on a set of one PL aquagel OH 50 and one PL aquagel mixed M plus a PL aquagel OH guard column. Cirrus SEC software was used to analyse the data using poly(methylmethacrylate) (PMMA) or poly(ethylene glycol) (PEG) standards.

6.1.9 Synthesis of 6.01

DMAEA (11 g, 0.077 mol, 1.1 equiv.) was dissolved in THF (20 mL), placed in a round bottom flask in an ice bath. 1,3-propane sultone (8.5 g, 0.07 mol, 1 equiv.) was dissolved in THF (5 mL) and added drop wise to the stirred solution of monomer. The reaction was stirred for three hours at which point the white precipitate was collected by filtration, washed with THF and dried under vacuum to yield **6.01** as a white solid. ^{1}H NMR spectroscopy (400 MHz, 0.5 M NaCl in D_2O): δ (ppm):2.29 (m, 2H, $NCH_2C\mathit{H}_2CH_2S$), 3.01 (t, $^{3}J_{H\text{-}H}$ = 7.3 Hz, 2H, $NCH_2CH_2C\mathit{H}_2S$), 3.24 (s, 6H, $N^{+}(C\mathit{H}_3)_2$), 3.60 (m, 2H, $NC\mathit{H}_2CH_2CH_2S$), 3.84 (m, 2H,

OCH_2CH_2N), 4.67 (m, 2H, $COOCH_2$), 6.06 (dd, $^2J_{H\text{-}H}$ = 0.97 Hz, $^3J_{H\text{-}H}$ = 10.49 Hz, 1H, C*H*HCHCO), 6.25 (dd, 1H, $^3J_{H\text{-}H}$ = 10.47, 17.28 Hz, CHHC*H*CO), 6.49 (dd, $^2J_{H\text{-}H}$ = 0.99 Hz, $^3J_{H\text{-}H}$ = 17.27 Hz, 1H, CH*H*CHCO). ^{13}C NMR spectroscopy (75 MHz, 0.5 M NaCl in D_2O): δ (ppm):18.2, 47.2, 51.2, 58.1, 62.2, 63.3, 126.8, 133.2, 167.0

6.1.10 Synthesis of homopolymer 6.02

PEGA (average M_n 480 Da) (1 g, 2.1 mmol, 20 equiv.), CTA (29 mg, 0.1 mmol, 1 equiv.) and AIBN (1.7 mg, 0.01 mmol, 0.1 equiv.) were dissolved in 1,4-dioxane (2:1 solvent: monomer) and placed in an oven dried ampoule under nitrogen flow with a stirrer bar. The polymerisation mixture was degassed with at least three *freeze-pump-thaw* cycles, released to and sealed under nitrogen. The reaction was subsequently submerged into an oil bath at 65 °C for 6 hours. The polymer was purified by dialysis against 18.2 MΩ cm^{-1} water and recovered by lyophilisation yielding a yellow polymer as an oil, **6.02**, M_n (^{1}H NMR) = 10.4 kDa, M_n (DMF SEC) = 10.4 kDa, $Đ_M$ = 1.16. ^{1}H NMR spectroscopy (400 MHz, $CDCl_3$): δ (ppm):0.9 (m, 3H, $(CH_2)_{11}CH_3$ of CTA) 1.2 – 2.27 (m, 128H, CH_2CH of polymer backbone), 3.34 (s, 66H, OCH_3 of polymer side chain), 3.35 (m, 44H, $COOCH_2CH_2O$ of side chain, 3.7 (m, 665H, OCH_2CH_2O of polymer side chain), 4.0 – 4.3 (br s, 44H, $COOCH_2CH_2O$ of polymer side chain), 4.3 (m, 2H, $NCCH_2S$ of CTA), 4.8 (s, 1H, CH_2CHS).

6.1.11 Chain extension polymerisation of 6.02 with 6.01 in 0.5 M NaCl solution

In a typical polymerisation procedure, **6.02** (0.1 g, 0.01 mmol, 1 equiv.), **6.01** (2 g, 7.5 mmol, 750 equiv.) and ACVA (0.6 mg, 0.002 mmol, 0.2 equiv.) were dissolved in 10 mL 0.5 M NaCl solution. The pH was adjusted to pH 7 to solubilise the initiator. The solution was then degassed by bubbling with nitrogen for 30 minutes (unless otherwise stated). Samples were removed for analysis under the flow of nitrogen. The polymer was purified by dialysis and recovered by lyophilisation. Different block lengths were targeted by varying the equivalents of **6.01**.

6.1.12 Synthesis of 6.12 in HFIP

CTA (2.4 mg, 0.0075 mmol, 1 equiv.), **6.01** (2 g, 7.5 mmol, 1000 equiv.) were dissolved in 6 mL HFIP. AIBN (0.25 mg, 0.0015 mmol, 0.2 equiv.) was added from a stock solution. The solution was placed into an oven dried ampoule under the flow of nitrogen. The solution was degassed *via* three *freeze-pump-thaw* cycles and released to and sealed under nitrogen. Samples were removed for analysis under the flow of nitrogen. The polymerisation mixture was then placed in a pre-heated oil bath at 65 °C for 15 hours. The polymer was purified by dialysis against water and recovered by lyophilisation to yield **6.12**, M_n (^{1}H NMR) = 238.5 kDa, M_n (Aqueous SEC) = 20.0 kDa, $Đ_M$ = 1.24. ^{1}H NMR spectroscopy (400 MHz, 0.5M NaCl in D_2O): δ (ppm): 0.9 (m, 3H, $(CH_2)_{11}CH_3$ of CTA), 1.5 – 2.8 (m, 4500H, CH_2CH of polymer backbone, CH_2CH of polymer backbone, $CH_2CH_2SO_3^-$ of DMAPS side chain), 2.8 – 3.0 (br s, 1800H, $CH_2CH_2SO_3^-$ of DMAPS side chain), 3.0 – 3.3 (br s, 5400H, $N^+(CH_3)_2$ of DMAPS side chain), 3.4 – 3.9 (m, 3600H, $N^+(CH_3)_2CH_2$ of DMAPS side chain, OCH_2CH_2N of DMAPS side chain), 4.40 – 4.70 (br s, 1800H, OCH_2CH_2N of DMAPS side chain).

6.1.13 Synthesis of diblock copolymer 6.13 in HFIP

6.02 (75 mg, 0.0075 mmol, 1 equiv.), **6.01** (2 g, 7.5 mmol, 1000 equiv.) were dissolved in 6 mL HFIP. AIBN (0.25 mg, 0.0015 mmol, 0.2 equiv.) was added from a stock solution. The solution was placed into an oven dried ampoule under the flow of nitrogen. The solution was degassed *via* three *freeze-pump-thaw* cycles and released to and sealed under nitrogen. Samples were removed for analysis under a flow of nitrogen. The polymerisation mixture was then placed in a pre-heated oil bath at 65 °C for 15 hours. The polymer was purified by dialysis against water and recovered by lyophilisation to yield **6.13**, M_n (^{1}H NMR) = 275.6 kDa, M_n (Aqueous SEC) = 22.4 kDa, $Đ_M$ = 1.29. ^{1}H NMR spectroscopy (400 MHz, 0.5M NaCl in D_2O): δ (ppm): 0.9 (m, 3H, $(CH_2)_{11}CH_3$ of CTA), 1.5 – 2.8 (m, 5087H, CH_2CH of polymer backbone, CH_2CH of polymer backbone, $CH_2CH_2SO_3^-$ of DMAPS side chain), 2.8 – 3.0 (br s, 2000H, $CH_2CH_2SO_3^-$ of DMAPS side chain), 3.0 – 3.3 (br s, 6000H, $N^+(CH_3)_2$ of DMAPS side chain), 3.31 (s, 66H, OCH_3 of PEGMA side chain), 3.4 – 3.9 (m, 4800H,

$N^+(CH_3)_2CH_2$ of DMAPS side chain, OCH_2CH_2N of DMAPS side chain, OCH_2CH_2O of PEG side chain), 4.40 – 4.70 (br s, 2000H, OCH_2CH_2N of DMAPS side chain).

6.5. References

1. A. B. Lowe and C. L. McCormick, *Chem. Rev.*, 2002, 102, 4177-4190.
2. S. Nakai, T. Nakaya and M. Imoto, *Makromol. Chem.*, 1977, 178, 2963-2967.
3. H. Ladenheim and H. Morawetz, *J. Polym. Sci.*, 1957, 26, 251-254.
4. R. Hart and D. Timmerman, *J. Polym. Sci.*, 1958, 28, 638-640.
5. Y. Chang, S. H. Shu, Y. J. Shih, C. W. Chu, R. C. Ruaan and W. Y. Chen, *Langmuir*, 2009, 26, 3522-3530.
6. J. Du, Y. Tang, A. L. Lewis and S. P. Armes, *J. Am. Chem. Soc.*, 2005, 127, 17982-17983.
7. Y. J. Shih and Y. Chang, *Langmuir*, 2010, 26, 17286-17294.
8. Y. J. Shih, Y. Chang, A. Deratani and D. Quemener, *Biomacromolecules*, 2012, 13, 2849-2858.
9. S. L. West, J. P. Salvage, E. J. Lobb, S. P. Armes, N. C. Billingham, A. L. Lewis, G. W. Hanlon and A. W. Lloyd, *Biomaterials*, 2004, 25, 1195-1204.
10. Y. J. Che, Y. Tan, J. Cao and G. Y. Xu, *J. Macromol. Sci., Phys.*, 2010, 49, 695-710.
11. P. Mary, D. D. Bendejacq, M. P. Labeau and P. Dupuis, *J. Phys. Chem. B*, 2007, 111, 7767-7777.
12. M. d. R. Rodriguez-Hidalgo, C. Soto-Figueroa and L. Vicente, *Soft Matter*, 2013, 9, 5762-5770.
13. D. Wang, T. Wu, X. Wan, X. Wang and S. Liu, *Langmuir*, 2007, 23, 11866-11874.
14. M. Arotçaréna, B. Heise, S. Ishaya and A. Laschewsky, *J. Am. Chem. Soc.*, 2002, 124, 3787-3793.
15. D. N. Schulz, D. G. Peiffer, P. K. Agarwal, J. Larabee, J. J. Kaladas, L. Soni, B. Handwerker and R. T. Garner, *Polymer*, 1986, 27, 1734-1742.
16. M. Noh, Y. Mok, D. Nakayama, S. Jang, S. Lee, T. Kim and Y. Lee, *Polymer*, 2013, 54, 5338-5344.
17. M. S. Donovan, A. B. Lowe, T. A. Sanford and C. L. McCormick, *J. Polym. Sci., Part A: Polym. Chem.*, 2003, 41, 1262-1281.
18. M. S. Donovan, B. S. Sumerlin, A. B. Lowe and C. L. McCormick, *Macromolecules*, 2002, 35, 8663-8666.
19. H. Willcock, A. Lu, C. F. Hansell, E. Chapman, I. R. Collins and R. K. O'Reilly, *Polym. Chem.*, 2014, 5, 1023-1030.
20. G. Yuan, Y. Peng, Z. Liu, J. Hong, Y. Xiao, J. Guo, N. W. Smith, J. Crommen and Z. Jiang, *J. Chromatogr. A*, 2013, 1301, 88-97.
21. A. Laschewsky and I. Zerbe, *Polymer*, 1991, 32, 2070-2080.
22. V. Bütün, *Polymer*, 2003, 44, 7321-7334.

23. V. Butun, C. E. Bennett, M. Vamvakaki, A. B. Lowe, N. C. Billingham and S. P. Armes, *J. Mater. Chem.*, 1997, 7, 1693-1695.
24. I. Javakhishvili, K. Jankova and S. Hvilsted, *Polym. Chem.*, 2013, 4, 662-668.
25. A. B. Lowe, N. C. Billingham and S. P. Armes, *Macromolecules*, 1999, 32, 2141-2148.
26. A. B. Lowe, N. C. Billingham and S. P. Armes, *Chem. Commun.*, 1996, DOI: 10.1039/cc9960001555, 1555-1556.
27. Z. Tuzar, H. Pospisil, J. Plestil, A. B. Lowe, F. L. Baines, N. C. Billingham and S. P. Armes, *Macromolecules*, 1997, 30, 2509-2512.
28. J. V. M. Weaver, S. P. Armes and V. Butun, *Chem. Commun.*, 2002, DOI: 10.1039/B207251N, 2122-2123.
29. T. Wu, D. Wang, M. Zhang, J. R. Heflin, R. B. Moore and T. E. Long, *ACS Appl. Mater. Interfaces*, 2012, 4, 6552-6559.
30. D. J. Liaw and K. R. Lee, *J. Macromol. Sci., Part A: Pure Appl. Chem.*, 1990, 27, 875-895.
31. D. J. Liaw and K. R. Lee, *Polym. Int.*, 1993, 30, 381-386.
32. T. Ouchi, K. Nomoto, Y. Hosaka, M. Imoto, T. Nakaya and T. Iwamoto, *J. Macromol. Sci., Part A: Pure Appl. Chem.*, 1984, 21, 859-866.
33. D. J. Liaw, J. R. Lin and K. C. Chung, *J. Macromol. Sci., Part A: Pure Appl. Chem.*, 1993, 30, 51-58.
34. W. F. Lee and C. C. Tsai, *Polymer*, 1994, 35, 2210-2217.

Conclusions and Future Work

This work has focused on the responsive properties of a range of monomers and their incorporation into well-defined amphiphilic block copolymers by RAFT polymerisation. A range of different stimuli have been used in order to achieve control over the morphology adopted by the polymer in aqueous solution and afford transitions between different structures. Where possible, this morphology transition has been utilised in order to encapsulate and release a payload in a controlled manner.

The work in Chapter Two investigated the use of a pH-deprotectable monomer, tetrahydropyranyl acrylate (THPA) in order to synthesise hydrophobic block copolymers with hydrophilic end groups. Two different hydrophilic end groups were investigated, a charged quaternary amine and a neutral triethylene glycol. However, only the charged quaternary amine end group provided the hydrophilicity required to afford self-assembly. The deprotection of the polyTHPA in response to pH to form polyacrylic acid, and the associated hydrophilicity change, was utilised in a vesicle to micelle morphology transition. This work could be expanded upon to investigate the effect different hydrophilic end groups have upon self-assembly, however, the instability of the THPA, both in solution and in dried state remains a major challenge to potential applications of these structures.

Chapter Three again demonstrated a vesicle to micelle morphology transition, but by using a tertiary amine as the pH-responsive block a reversible transition, was afforded as demonstrated by the repeated cycling between pH 3 and pH 8 with no observed loss of control over the morphologies achieved. The direct synthesis of the block copolymers proved challenging, so an activated ester scaffold was synthesised, followed by post-polymerisation modification of the backbone and the end group to afford the pH-responsive block and the hydrophilicity required to drive self-assembly, respectively. This allowed the effect of two different end groups on the self-assembly behaviour to be studied. This route opens up the way to creating a library of responsive polymers that bear identical block

lengths and so allow for direct comparison between the that effect different responsive groups and different end groups have upon self-assembly. It would be interesting to expand on this work to investigate other responsive monomers that have proven to be difficult to directly polymerise.

The work in Chapter Four investigated the synthesis of sulfobetaine methacrylate containing block copolymers by RAFT polymerisation, incorporating both hydrophilic and hydrophobic blocks. There are relatively few examples of the controlled synthesis of such block copolymers in the literature. Whereas amphiphilic block copolymers have been made previously *via* post-polymerisation modification of a tertiary amine precursor,the direct polymerisation route utilised here avoids the use of the toxic chemical required for such a reaction. This chapter also reports the first examples of amphiphilic di- and tri-block copolymers synthesised by RAFT polymerisation of the sulfobetaine methacrylate monomer and the first triply-responsive sulfobetaine-containing triblock copolymer. Future efforts could focus on the controlled synthesis of more doubly- or triply-responsive sulfobetaine containing block copolymers with a view to their potentially interesting self-assembly behaviour.

Chapter Five investigated the self-assembly behaviour of the polymers produced in Chapter Four. The di- and tri-block polymers containing hydrophilic blocks underwent a micelle to unimer transition that was used to encapsulate and release a hydrophobic payload in response to temperature. The transition temperature could be tuned by altering the overall hydrophilicity of the polymer. Incorporating a hydrophobic block yielded swellable micelles. The thermo-responsive behaviour of the polysulfobetaine block was analysed by ^{1}H NMR spectroscopy, which showed that even at temperatures well below the UCST cloud point of the corresponding homopolymer, a significant proportion of hydrophilicity remained in the amphiphilic diblock copolymers. The chapter also demonstrated a triply-responsive triblock copolymer that responded to temperature, pH and carbon dioxide. Depending on the self-assembly conditions it was possible to either afford a micelle to

unimer, or a vesicle to unimer transition. Sulfobetaine methacrylate containing block copolymers provide interesting and potentially useful self-assembled morphologies. Their biocompatibility has been shown within the literature and therefore investigating the biocompatibility of these polymers would be interesting, as would further exploration into different combinations of stimuli.

Chapter Six investigated the RAFT polymerisation of the acrylate version of the sulfobetaine monomer utilised in Chapters Four and Five. The controlled polymerisation of this monomer has not been reported within the literature and our attempts proved challenging. The monomer undergoes auto-polymerisation in degassed aqueous solutions, in the absence of an initiator, at room temperature. The full explanation for this behaviour is not fully understood and therefore future work that focussed on understanding this polymerisation behaviour could prove enlightening and is currently under investigation within the group.